Quantifying subglacial roughness and its link to glacial geomorphology and ice speed

PHILIP WILLIAM PRESCOTT

Abstract

The shape of subglacial bed topography, termed its roughness, is a recognised control on basal ice-flow. Although glaciologists have observed patterns of variations in ice speed over beds with different roughness values, the strength of this relationship has rarely been quantified, and measurements of roughness are based on just a few methods. Moreover, the shape of topography can vary in a number of ways, but how this influences roughness and the quantification of roughness is largely unknown. This project investigates methods of measuring roughness, and how such measurements might be related to spatial patterns in ice speed in both contemporary and palaeo-settings. Roughness of ice-sheet beds has traditionally been summarised using spectral analysis. The first part of this projected was aimed at reviewing this method. The influence of the number of data points was explored by developing a new technique for re-digitising radio-echo sounding records, which remain the most extensive source of bed data from Antarctica. This yielded measurements with a resolution (c.250 m) eight-times higher than those used in previous work, and allowed assessment of roughness over short window lengths. Significantly, subjective decisions about, for example, the choice of window length can lead to differing results using spectral analysis. The second part of this project was, therefore, to identify and evaluate 36 alternative methods of quantifying roughness, many of which had never before been used to analyse subglacial beds. The project looked at the broader approach to quantifying roughness, exploring the benefits of 2D versus 3D techniques for investigating subglacial data. The relationship between roughness and ice speed was tested using these alternative techniques in isolation, but also in a combination. Indeed, the use of generalised linear models (GLMs) allowed the strength of this relationship to be quantified for the first time, and permitted the roughness variables most related to ice speed to be identified. Testing the agreement between patterns in roughness in ice speed for the Siple Coast showed a pattern of increasing ice speed as roughness decreased. Modelling revealed a 98% fit between ice speed and roughness for the MacAyeal Ice Stream indicating that roughness is a strong control on basal ice flow. It was revealed that the measures of roughness most related to ice speed were those that summarised changes in the vertical height of the surface, rather than the shape or wavelength of the features. It was also found that the lateral margin of the MacAyeal Ice Stream corresponds with an area of high bed roughness. Analysis of formerly glaciated areas of Britain showed that the size and frequency of subglacial bedforms influence parameter results as do subtle changes in the orientation of 2D profiles across bedform fields. It was demonstrated how this might be used to identify subglacial features beneath contemporary ice sheets. In conclusion, alternative roughness parameters were found to be less restrictive and arguably more informative than spectral analysis, because they have the advantage of allowing differing characteristics of the topography to be measured.

Conversely, this meant that no single parameter could provide a complete summary. Thus, a key conclusion of this work is that the most suitable approach to quantifying roughness is to use a suite of roughness parameters, designed to summarise a range of variables that are most relevant to the specific investigation.

Quantifying subglacial roughness and its link to glacial geomorphology and ice speed

Philip William Prescott

A thesis submitted for the Degree of Doctor of Philosophy

Department of Geography, Durham University

2013

Acknowledgements

The foremost people to thank are my family. My mum and dad equipped me with many of the skills needed to complete this project. Without their support, I would not be writing this acknowledgement page. It makes me very happy that the submission of this project coincides with the wedding of my sister Lois, and new brother-in-law Ian.

I must thank my supervisors, Chris Stokes and Nick Cox. While writing this thesis, Chris and Nick have often reminded me of the importance of brevity. However, when it comes to showing my appreciation it is difficult to remain succinct. Chris was a constant source of inspiration, and a fantastic sounding board to bounce ideas off. This allowed me to develop the more novel aspects of this thesis, and I am grateful for his patience in allowing me to explore these various pathways. Imagination alone would have been insufficient without the help of Nick. He grounded the thesis, for example, working as lead programmer to guide me through the complexities of writing scripts to analyse roughness. It has been a privilege to learn from Nick and Chris.

I would like to thank Rob Bingham for his insights into the use of spectral analysis for quantifying subglacial bed roughness. When evaluating spectral analysis, this added detail was essential in allowing me to adjust user options such as window length. I am also grateful for his feedback on this evaluation, and for the provision of several hundred kilometres of radio-echo sounding data, that underpinned much of the analysis.

My thanks also go to Dave Rippin for his feedback on methods of quantifying roughness, and on Chapter 4. His thoughts helped guide my search in identifying alternative methods of measuring roughness that might be useful to glaciologists.

My deepest thanks go to those people who helped me, not through their technical expertise, but through their constant encouragement. There are too many of these friends to thank here, so may I instead pledge to show my appreciation and hopefully return reciprocate the support they showed.

Lastly, I thank Kathryn for her steadfast support. Thank you so much. Kathryn, any sentiments I write here cannot begin to describe my appreciation for all you have done.

Table of contents

List of figures

Chapter 2: The roughness problem

Chapter 3: An assessment of the use of spectral analysis for quantifying subglacial bed roughness

Chapter 4: A review of roughness parameters

Chapter 5: Evaluating the suitability of roughness parameters for use in analysis of subglacial beds

Chapter 7: Exploring the potential of quantifying subglacial bed roughness in 3D

Chapter 8: Discussion & Conclusions

List of tables

Chapter 5: Evaluating the suitability of roughness parameters for analysing subglacial beds

Chapter 6: Investigating the relationship between roughness and ice speed, Siple Coast, Antarctica

Chapter 7: Exploring the potential of quantifying subglacial bed roughness in 3D

CHAPTER 1

Introduction

1.1 Introduction and rationale

Mass loss from ice sheets will have implications for global climate and sea-level change (Whillans, 1976; Oppenheimer, 1998; Alley *et al.*, 2005; Vaughan, 2005). Despite the need to understand processes that control ice-sheet dynamics (Bennett, 2003), knowledge of these factors remains deficient. Ice-sheets flow through a combination of the internal deformation of ice, sliding at the boundary between ice and the substrate, and deformation of the substrate itself (Benn & Evans, 1998; Knight, 1999). Basal motion has been shown to have a strong influence on ice-sheet velocity (Schoof, 2005) and so is of "fundamental concern" for modelling ice behaviour (Cohen *et al.*, 2000: 599). At the ice-bed interface, motion is controlled by the basal shear stress, water pressure, and the characteristics of the bed (Paterson, 1994). One such characteristic is *roughness* (Rippin *et al.*, 2004), and gaining insight into this may help us understand the controls on basal ice flow, allowing scientists to predict future ice sheet behaviour. The main aims of this project were to evaluate how to measure roughness, and then, to test the relationship between subglacial bed roughness and the rates of basal ice flow.

As discussed in Chapter 2, there are several definitions of roughness but, broadly speaking, it refers to variations in the topography of a surface. In this project, this *surface* is the subglacial bed. As Section 2.3 describes, a number of theories and numerical models show how the form of topography may influence ice-sheet dynamics, such as the speed of flow (Paterson, 1994). These theories are supported by measurements of roughness in Antarctica, where a relationship between ice speed and roughness has been observed (Siegert *et al*., 2004, 2005b). However, the majority of these findings are based on a single method of quantifying roughness, and the horizontal scales of topography analysed have also been limited (Bingham & Siegert, 2009). As a result, the extent to which roughness controls basal ice flow is uncertain. Furthermore, the mechanism by which the roughness of the bed affects ice speed is also unclear, because it has not been possible to link findings with theories on controls of ice-sheet dynamics.

This project analyses roughness at different scales and tests how these measurements relate to spatial patterns in basal ice speed. The agreement in results using different measurements is investigated. The effect of sampling interval and analysis options on

roughness values are tested to determine the comparability of results between studies that used data with different resolutions. Alternative sources of data and methods of quantifying roughness are extensively reviewed and evaluated. These findings are used to provide an assessment of the most suitable techniques for investigating how roughness and ice speed are related.

One of the reasons that the scales of roughness studied have been limited is the lack of available data. Difficulties in accessing the bed of contemporary ice sheets has meant that most studies (e.g. Taylor *et al*., 2004; Bingham & Siegert, 2009) have quantified roughness using radio-echo sounding data that had a sampling interval of kilometres. On the other extreme, some glaciologists have used ground surveys of roughness, with data at the millimetre resolution (e.g. Hubbard & Hubbard, 1998). However, the coverage of data measured in this manner is insufficient to permit regional studies of roughness. In this thesis, the potential of improving the resolution of radio-echo sounding measurements is explored. Other forms of data are also reviewed, in particular, the use of DEM measurements on palaeo ice-sheet beds. As shall be seen, subglacial bed roughness has traditionally been measured along profiles (Siegert *et al*., 2004, 2005a; Taylor *et al*., 2004; Bingham & Siegert, 2007a, 2009). The advantages of using measurements of both contemporary ice-sheet beds and those from formerly glaciated terrains are tested.

In addition to the choice of data being restricted, the majority of studies of subglacial bed roughness at the scale of tens of kilometres have quantified spatial variations in the topography using *spectral analysis* (Taylor *et al*., 2004). These measurements have underpinned many of the findings on relationships between ice speed and roughness (Bingham & Siegert, 2009), but the information these statistics give is limited. Potentially, other techniques for quantifying roughness could be used. However, despite the widespread use of such methods in other sciences, relatively few roughness parameters have been reviewed by glaciologists (Li *et al*., 2010). This project identifies alternative methods of quantifying roughness from a range of sciences. These methods are then evaluated to test their suitability for analysing subglacial beds.

1.2 Aims and objectives

The overarching aims of this project were *to explore how best to measure bed roughness*, then use this knowledge *to investigate how subglacial bed roughness is correlated to the rate of basal ice flow*. To achieve these aims, the project was separated into a number of smaller objectives, which are summarised below. Chapter 2 provides a history of investigating subglacial bed roughness and demonstrates why these objectives are a research priority.

- Objective 1: To evaluate existing and new methods of quantifying roughness

- Objective 2: To compare the spatial patterns in roughness with those of ice flow speed
- Objective 3: To evaluate the role of roughness in influencing ice speed using data from palaeo landscapes

1.3 Overview

This project was essentially sub-divided into a series of smaller investigations, which are now described. The completion of these objectives essentially formed the structure of this thesis, so the outline of chapters is also now provided. Given that the completion of these different stages required varying techniques, the specific detail is provided in the *methods* section of the relevant chapters. In this section, the broad approach is explained, which demonstrates how the various stages interlink to achieve the main research goal.

1.3.1 Evaluating methods of quantifying roughness

The project began with a review of the history of quantifying subglacial bed roughness. Chapter 2 summarises a number of theories describing how the shape of the subglacial bed topography interacts with basal ice flow, and how this varies with scale. These theories and findings are placed into a wider context of controls on ice dynamics. The relative importance of roughness for controlling ice speed, relative to other variables, is discussed. Furthermore, processes by which ice flow may influence the roughness are described.

Subglacial roughness was also reviewed from a practical perspective, outlining how these changes in shape have traditionally been measured and analysed. A review is given of the types of data used as sources of bed elevation measurements, and the potential of using other sources such as palaeo ice-sheet records is discussed. This chapter ends with a summary of themes where more research is required: these topics generate the research objectives of the thesis.

By reviewing the history of measuring subglacial bed roughness, it was clear that one method in particular, spectral analysis, had dominated research. Due to its importance legacy, Chapter 3 was devoted to evaluating this approach in depth. The sensitivity of the results to variations in data resolution was tested by comparing roughness results of the same area sampled at 2000 m sampling interval, (the same resolution as earlier studies), and 250 m sampling intervals. To test whether the window size affected spectral analysis, results were calculated using four different window lengths ranging from 8 km to 64 km. In both cases, the method of quantifying roughness was followed from Taylor *et al*. (2004), with further detail of the practical workings given by Rob Bingham (personal communication, 11 February 2009).

To compare the roughness results at different data resolutions and window lengths, bed elevation measurements gathered at different sampling intervals were required. A

challenge here was that no study had outlined how radio-echo sounding records could be sampled at different resolutions. Therefore, a secondary objective of Chapter 3 was to determine the feasibility of re-digitising radio-echo sounding measurements to improve their resolution. Specifically, it tested whether a resolution of tens to hundreds of metres between adjacent points could be achieved because, as Chapter 2 will demonstrate, bed roughness at these scales has been relatively understudied. Developing a technique to improve the resolution of radio-echo sounding measurements was done by manually re-digitising a photographic film record for a c.500 km long profile.

Without detailing the results here, the findings of Chapter 3 supported conclusions from other studies (e.g. Bingham & Siegert, 2009) that other methods of quantifying roughness might be considered. The next stage, therefore, was to identify alternative roughness parameters that would be applicable to glaciologists.

Identifying alternative methods of quantifying roughness was first done by a literature review. The techniques identified, along with examples of their use, are described in Chapter 4. Note that, the techniques were taken from a range of sciences, and included methods for summarising roughness in 2D analysis along profiles and, in 3D analysis across surfaces. Many of these roughness parameters had never been used with glacial data, so their suitability was unknown. As such, the next step was to test these parameters.

In all, over fifty such methods were identified, and to evaluate each of these would have been beyond the scope of this study. Therefore, a selection of parameters were chosen for further testing. This shortlisting was achieved by identifying the methods most frequently used in other sciences. The feasibility of applying the methods to glacial data was another criterion' some methods lacked versatility, e.g. being limited to a certain format of data, so these were rejected. Some parameters required specific methods of data collection that could not be readily adapted to ice-sheet beds. The aim was to identify methods that could be applied to any data of changing bed elevation over distance. Following this initial review, 18 2D and 18 3D parameters were selected for further evaluation.

In Chapter 5, the shortlisted parameters of interest were assessed. The ability of the parameters to capture different types of variation in the topography was identified, and the feasibility of using these techniques with subglacial bed measurements was investigated. The first stage of this was to generate roughness results and, to do this efficiently, each of the methods was programmed into the statistics software Stata. Due to the differences between 2D and 3D parameters, two Stata programs were developed. The methods of quantifying roughness in 2D were first evaluated using synthetic profiles. The purpose of

these was to adjust or more variables in a controlled manner, and test how this affected the results. This gave an indication of the sensitivity of each parameter to different types of topographic variation. Similar testing was not required with the 3D methods because most of these had a 2D counterpart and, thus, provided similar information on changes in topography.

Qualitative analysis was used to investigate the versatility of each parameter testing, for example, how artefacts in the data affect the results. For 3D parameters, uniform spacing of the data was a requirement but, for the 2D methods, irregular spacing was permitted. Nevertheless, with 3D parameters it was still necessary to determine how artefacts common in glacial data, such as anomalous values or tilt, affect the roughness values. Testing was done using bed elevation measurements from radio-echo sounding profiles in the Institute Ice Stream region and DEMs of Britain. The findings of Chapter 5 were subsequently used to inform the choice of parameters for subsequent analysis of contemporary and palaeo ice-sheet beds.

1.3.2 Testing the relationship between roughness and ice speed

In Chapter 6, the parameters evaluated in Chapter 5 that quantify roughness 2D were used to investigate the relationship between roughness and ice speed. Analysis of SPRI radio-echo sounding profiles for the Siple Coast region of Antarctica was used to test how the roughness varies across an ice stream margin, and along an ice stream parallel to flow.

Statistical comparison was done to compare the agreement between spatial patterns in roughness and those of ice speed. Initially, the record of ice speed was compared with the results of each parameter individually. This allowed identification of which topographic variables show the strongest relationship with variations in ice speed. Next, a generalised linear model was produced for each profile to test the strength of the relationship between ice speed and roughness. Here, the roughness parameters were used as independent variables in an attempt to predict ice speed.

1.3.3 Comparing the roughness of bedforms in a palaeo ice-sheet environment

The focus of this project was clearly to evaluate the roughness parameters and use these to assess the link between roughness and ice speed. However, in using palaeo terrains as a source of topographic measurements for evaluating 3D methods of quantifying roughness, there was also an opportunity to compare the roughness of different environments and groups of subglacial bedforms. The accessibility of the bed meant that the roughness of such features could, in theory, be measured, allowing their resistance to basal ice flow in terms of this variable to be evaluated.

Four regions of Britain were chosen for comparison. These areas had differences in their topography that could be clearly distinguished on DEM images. All four areas exhibited evidence of a glacial history, but reconstructions of the four sites had inferred different conditions: for example, one area had been interpreted as being the site of an ice, but a former ice dome had been inferred in another. Note that other variations between the four regions, such as their geology, played no role in the selection of these sites.

Based on a number of parameters, the relative roughness of these sites was calculated. From this, the former relative ice speeds of the four areas were then inferred. Note that, this interpretation was based solely on the roughness values, with the basic assumption that ice speed increases as roughness increases. At this elementary stage, although it was acknowledged that the roughness is just one possible control on ice dynamics, other variables such as the geology were not taken into account when inferring former ice speeds. The purpose was to measure and compare the roughness of the four sites.

To add context, the interpretations of ice speed were then compared to those inferred by glaciologists using alternative evidence. Through this it was possible to test whether the results of the roughness parameters showed agreement with other proxies, thus giving further insight into the role of roughness as a control on basal ice flow. Note that, because both these sets of interpretations were made independently, it avoided the problem that both are essentially based on the same information of bed topography. In other words, other proxies for ice speed were not used in inferring ice speed from roughness measurements, and vice-versa.

Chapter 9 provides a discussion of the key themes, returning to the research questions raised in Chapter 2. It evaluates the methods used for quantifying roughness, providing recommendations for future studies. Chapter 9 also reviews the importance of subglacial bed roughness in controlling ice flow, and explores how ice dynamics may influence roughness.

CHAPTER 2

The roughness problem

2.1 Introduction

This chapter first discusses the wide range of variables that influence ice sheet dynamics (Section 2.2). Focus is then given to how the roughness of the topography may be important for controlling basal ice flow, particularly in terms of flow speeds. The various theories by which the roughness of topography may influence ice flow are described. Given that these processes are scale dependent, this description is separated into a number of spatial and temporal scale. Evidence for this relationship between roughness and ice speed is then presented by summarising the findings of other studies. A review of these investigations shows that there has been a focus on areas where streaming ice flow occurs. Therefore, Section 2.3.5 then describes the controls on ice stream behaviour, again with an emphasis on the role of roughness.

The second part of this review summarises the techniques traditionally used in measuring the roughness of subglacial topography. This exploration of the methods of quantifying roughness demonstrates how some of the results shown in Section 2.3 were acquired. The section includes an introduction to the different techniques that have been used, and shows how the approach taken has often been driven by advances in technology. It will be shown that several techniques have been used to measure roughness but, in recent years, studies of subglacial bed roughness have been dominated by the use of spectral analysis to analyse radio-echo sounding data.

Having reviewed the theories and findings, Section 2.4 discusses how much scientists know about the relationship between roughness and ice dynamics. These linkages are also placed in a wider context by evaluating the relative importance of roughness versus other controls on ice flow. Furthermore, it is also shown how the roughness of topography, or methods of measuring roughness, may interlink with other controls on ice flow. From this discussion, several areas of uncertainty are identified and these are summarised thematically. It will be shown that much of the lack of information is due to the techniques for measuring roughness: for example, the link between roughness and ice speed has not been tested at some scales. Section 2.5 gives a summary of research questions raised through this review, and these form the main aim and objectives of this project.

2.1.1 Defining roughness

Before discussing the role of roughness in ice dynamics, let us first define this term. *Roughness* is a term widely used in many sciences, including glaciology, but its meaning often varies. Therefore, before going further, it is useful to define precisely what we mean by this term. Providing a definition is complicated because there are many methods of measuring this phenomenon (McCarroll & Nesje, 1996) and, while many scientists describe roughness (Gadelmawla *et al*., 2002; Feng *et al*., 2003), there is no universally accepted definition. Van der Veen *et al.* (2009: 2) acknowledge that "the literature is somewhat confusing when it comes to defining surface roughness". In the broadest sense of its use in this project, roughness (or *surface texture* as it is also termed) pertains to the variability in topography of a surface (Cuthbert & Huynh, 1992; Kalpakjian, 1997; Lou *et al.*, 1998; Raja *et al.*, 2002; Avdelidis *et al.*, 2004; Siska & Hung, 2004; Lane, 2005). Some glaciological studies have referred to roughness in general terms, such as describing an ice-sheet bed as exhibiting *rough* or *smooth* characteristics (Stokes & Clark, 2001, 2003a; Taylor *et al.*, 2004), but these descriptions lack quantification. Earlier glaciological studies define *roughness* in specific ways (Kamb, 1970), for example, modelling ice flow over a *washboard* distribution of bed perturbations (Paterson, 1994). In this review, a broad description is used, where roughness describes deviations in surface topography with distance (Kalpakjian, 1997; Taylor *et al.*, 2004; Lane, 2005). Note that other sciences use this term with specific physical interpretations, such as a frictional coefficient, or measure a specific characteristic such as in-channel roughness as with *Manning's roughness* (Chiu & Rubio, 1970; Ding *et al*., 2004; Lane, 2005). In this project, roughness is a measurement of geometry: it describes deviations in surface topography with distance (Kalpakjian, 1997; Taylor *et al.*, 2004). Variations in roughness arise because the beds of ice sheets have different topographies (Schoof, 2003; Le Brocq *et al*., 2008).

In glaciology, the study of roughness had origins in models of ice dynamics at the ice-bed interface. Here, roughness was often used as a constant value, such as the Hallet (1979) model predicting rates of bed abrasion. Indeed, the use of roughness in this manner can still be seen in more recent studies (Cuffey et al., 2009). However, as with Lane's (2005) suggestion, and supported by the comments of Li *et al*. (2010), improvements in technology allowed the topography to be measured directly. Over time, this meant that studies of roughness using various statistics to measure the shape of the subglacial topography became more common. As presented in Section 2.2, direct observations of subglacial bed roughness have shown that, rather than a constant value, there are spatial patterns. Recognition that these patterns correspond with spatial trends in ice speed suggests that the roughness of the subglacial topography is an important control on basal ice-flow.

2.2 Controls on ice sheet dynamics

Although this project focuses on the relationship between roughness and basal ice flow, this linkage cannot be studied in isolation. For example, roughness is just one of several variables that control regional patterns in ice speed (Bennett, 2003; Winsborrow *et al*., 2010). This section examines the range of factors that influence the rate, and type, of ice flow. An assessment of the relative importance of these controls in dictating the speed of flow is made, thus placing roughness in this wider framework. Given that roughness is the central theme of this project it was important to review the various ways that this may relate to ice speed, and to draw upon evidence of past studies. It will be shown that roughness is a broad topic, and that the way that the shape of topography may interact with ice flow varies with scale. As such, although Section 2.2 gives an overview of various controls on ice dynamics, Section 2.3 examines the role of roughness more closely.

The rate of ice flow is a product of the balances between the *driving forces* that act to move ice in a downstream direction, and the *resistive forces* that counteract this forward motion (Paterson, 1994). The roughness of the subglacial bed is one type of resistive control on ice speed. As described in Section 2.2.1, the primary controls on the speed of flow are the driving forces because these dictate the amount of energy available to move the ice mass forwards. In contrast, as will be detailed in Section 2.2.2, the resistive forces appear to be secondary controls on ice flow. Nevertheless, whereas the driving forces are often somewhat constant over large areas, the resistive forces may produce spatial variations in ice speed on smaller scales. As such, although not the primary control on ice speed, resistive forces may be crucial in determining localised variations in ice speed.

2.2.1 Driving forces

The energy driving the forward, downhill motion of ice sheets is gravity (Paterson, 1994). This force exerts a stress on the ice body, and the subglacial bed. When the amount of stress reaches a critical threshold, where it is greater than the forces of resistance (Section 2.2.2) strain occurs producing a forward movement. Assuming that the forces of resistance remain constant, the amount of strain increases as the shear stress increases. Therefore, to understand the driving forces of an ice sheet, it is necessary to identify the mechanisms that control the amount of shear stress.

Newton's law of motion states that the size of a force is a product of its mass and acceleration. At the scale of ice sheets, the acceleration due to gravity is taken as being constant, so differences in the amount of force result from variations in mass. The mass of an ice sheet can be assumed to be equivalent to its weight, which is a function of its density and size. In an ice sheet setting, this density relates to the composition of the ice (Zwally & Li., 2002): for example, ice that has undergone compaction has fewer air spaces and, therefore, a higher density. The thickness of an ice-sheet is a control on this process,

with the amount of compaction at a given point increasing as the thickness of the overbearing ice increases. As such, the density of ice generally increases with depth. However, for any point of an ice sheet, the ice thickness also dictates its overall size.

The driving force of gravity operates at all points of an ice sheet. However, different areas of an ice sheet have varying resistances to shear stress, which means that the type of motion also varies. The flow of ice can occur as internal deformation of the ice body, through deformation of the subglacial bed, by sliding at the interface between the bed and overriding ice, or through a combination of these. The type of movement that occurs is largely dependent on temperature (Knight, 1999), because this directly affects the resistance of the ice to strain. Therefore, many of the controls on ice dynamics relate to the climatic setting of an ice sheet (Benn & Evans, 1998). As a secondary effect, described in more detail under Section 2.2.2, the temperature may also affect subglacial beds' resistance to shear stress.

Another important factor determining the effect of gravity on ice flow is the angle at which the force exerted by the weight of the ice is exerted relative to the subglacial bed. If shear stress is directed at right angles to the bed then the amount of ice flow is minimal (Paterson, 1994; van der Veen, 1999). However, due to the gradient of the ice-sheet surface, the application of stress may not be normal to the bed. In these circumstances, the direction of force can lead to shearing, their within layers of ice, or between the ice and the bed (Hooke, 2005).

Strain as a result of *shear stress*, τ_b, is thought to be the dominant mechanism in driving the forward motion of ice sheets (Knight, 1999). As described above, the amount of force per unit area is influenced by the density, ρ, and thickness, *h*, of the overriding ice (Bennett & Glasser, 1996). The angle of the ice surface slope is important in determining the direction that this force is applied, i.e. the proportion of stress that acts in a direction that causes shear versus normal to the bed. Measurements of these factors, combined with the amount of acceleration due to gravity, *g*, which, on the scales of ice sheets can be considered constant, can be used to calculate the amount of shear stress at a given point at the base of an ice sheet (Bennett & Glasser, 1996; Benn & Evans, 1998):

$$\tau_b = \rho g h \sin \alpha$$

Although shear stress is the main driver of ice flow, this is just one type of stress induced by gravity. Another is the longitudinal stress that results from various parts of an ice sheet having differences in acceleration. Movement in one area of an ice sheet can produce compression to ice in the downstream area, and this acts as a push. Upstream of the area of movement, an extensional force is exerted on the ice mass which acts to draw down ice from this area (Paterson, 1994). The amount of movement is related to the strength of the

material, which highlights the importance of resistive forces in determining the speed of flow. The factors resisting the movement of an ice sheet are now described.

2.2.2 Resistive forces

Section 2.2.1 examined the factors that influence the amount of force driving the forward motion of ice sheets. However, for flow to occur, these forces must overcome those of resistance. If all conditions are constant then ice speed increases as the driving stress increases. However, if the resistance increases proportionally with the amount of shear stress, then the net speed will be the same.

The principle force counteracting that of gravity is friction. Several variables affect the amount of friction, with the thickness of the ice, the rheology of the ice and bed, and the shape of the subglacial topography being considered particularly important in this regard (Paterson, 1994; Hooke, 2005). This section details the first two but, given that this project includes any variations in the shape of topography under the heading roughness, this third control is described in Section 2.3.

The energy required for strain to occur is used to describe the strength of a material, with more resistant materials being said to be stronger. The strength of both the ice and the subglacial bed is important in determining the amount of stress required for ice flow to occur, and the speeds that will be produced as a result of a given input of driving force. The strength of the ice is, in itself, controlled by a number of variables, such as its composition and the presence of impurities such as debris (Marshall, 2005). Another important control is the ice temperature. As temperature increases, the strength of ice decreases (Huybrechts, 1996; Zwally *et al.*, 2002) and, therefore, the rate of ice flow through deformation also increases in a process termed *creep instability* (Payne, 1999). This demonstrates that any sources of heat are important for controlling ice speeds. Over large scales the ice temperature will be largely determined by the setting of an ice sheet (Benn & Evans, 1998), but there are several ways in which temperatures may vary locally. Tectonic processes are one such source of heat (Siegert & Dowdeswell, 1996): in Antarctica, for example, Bennett & Glasser (1996) noted that several of the fastest flowing regions of ice are situated in regions characterised by high geothermal activity. As the ice undergoes motion, frictional heating (Paterson, 1994) at the interface between ice and bed will increase temperatures further (Kalpakjian, 1997), producing more meltwater and increasing ice speeds (Rignot *et al*., 2002).

Temperature also plays a role in controlling the speed of flow in situations where ice at the bed remains below its melting point, so becomes frozen to the bed (Christoffersen & Tulaczyk, 2003a). The slowest ice speeds are observed where ice is frozen to the bed because, in these situations, flow via sliding cannot occur (Alley & Bindschadler, 2001).

However, because the melting point of ice is affected by pressure, ice at the subglacial bed may remain liquid at temperatures below 0°C (Paterson, 1994; Siegert & Dowdeswell, 1996). One of the factors controlling the amount of pressure at a given point on the bed is the thickness of the overlying ice, with a positive relationship between pressure and thickness. Furthermore, thermo-mechanical models (Payne, 1998) show that, due to the insulating effect of ice, as the thickness of an ice sheet increases, so too does the temperature (Bennett & Glasser, 1996; Payne, 1999; Huybrechts *et al*., 2000). Therefore, while Section 2.2.1 showed that the thickness of an ice sheet is important in influencing the shear stress that drives the system, it also has an indirect effect on the rate of flow by reducing the resistance.

In addition to the temperature affecting the resistance of an ice sheet to flow by influencing the strength of ice, if warming is sufficient to cause melting, heating may further lower the resistance through the production of meltwater (Boulton *et al*., 1995). The presence of meltwater at the subglacial bed acts as a lubricating layer, reducing the friction between the bed and the ice sheet (Zwally *et al.*, 2002, 2005; Bell *et al.*, 2007; Bingham & Siegert, 2007a). In contrast, provided that other variables influencing the amount of friction are constant, areas of the bed that have a lower concentration of water will have a greater resistance to flow.

The rheology of the subglacial bed, referring to the composition of the subglacial bed, is another control on the amount of resistance. Just as the resistance of the ice to flow is influenced by several variables, so too is that of the bed (Joughin *et al.,* 2004) and, therefore, not all these factors are described in bed. Nevertheless, to demonstrate the possible importance of rheology, it can be seen that the composition of the bed may affect the type of ice flow: if an ice sheet overlies soft sediments, these may have a low resistance to shear stress, and deform causing ice flow (Paterson, 1994). In contrast, sediment deformation cannot occur if the composition of the bed is more resistant to stress (Hooke, 2005). Over shorter spatial scales, differences in composition may cause localised areas, termed sticky spots, which are more resistant to flow.

As described above, the presence of subglacial meltwater reduces the resistance to ice flow yet, the way in which this mechanism operates is related to the rheology of the bed (Benn & Evans, 1998; Bell, 2008). Where the bed of an ice sheet is underlain by impermeable material, such as bedrock, meltwater can form a lubricating layer between the ice sheet and its bed. This reduction in friction favours basal ice flow through sliding of ice over the bed. Instead, if the bed comprises unconsolidated sediments, meltwater may percolate between the grains, reducing sediment strength and, here, the force of shear stress may lead to ice flow via the deformation of the bed (Nitsche *et al*., 2013).

2.3 The relationship between roughness and ice dynamics

There are several mechanisms by which the topography of the subglacial bed may influence the speed of ice flow. The theories describing these controls are now described, and field evidence for these processes is also presented. As Section 2.5.1 shall further discuss, these controls may not be termed *roughness* in other studies but, given that many of these controls are related to the shape of topography, they fall under the definition used in this project. A number of studies have modelled the effect of differences in roughness, such as the size and frequency of obstacles on the bed, on the speed of ice flow. These have been supported by analysis of contemporary ice sheet data, in particular, measurements of speed and topography gathered in Antarctica. This section now summarises both the theories and findings of how roughness and ice speed are related.

Given that the roughness of the bed relates to the shape of the topography, it operates at a range of spatial scales from millimetres (Hubbard & Hubbard, 1998) to tens of kilometres (Taylor *et al*., 2004). It is important to note that, like other processes operating the subglacial bed, there is a scale dependency (Nye, 1969; Paterson, 1994) where the way that roughness and ice flow interact varies at different spatial scales. For example, the size of obstacles may control the mechanism of ice deformation (Paterson, 1994; Schoof, 2003a). In addition to the scale of roughness influencing the processes that operate (Whitehouse, 2009), the scale at which topography is measured is important because it affects what structures are captured. For example, a surface that appears flat at one scale might produce higher roughness values if it is measured at a finer resolution.

This effect of scale does not prevent subglacial beds from being measured, but it does mean that definitions of different scales are useful (Popov & Dudko, 2004), even if these choices are arbitrary. Such an approach is often adopted in other sciences (Kalpakjian, 1997) yet, compared with these, the range in possible scales in roughness of subglacial topography is broader. This is because patterns in roughness are an expression of the nature of bedrock and sediments (Taylor *et al*., 2004), creating bumps and depressions on the landscape (Budd, 1970; Rae *et al*., 2000), but also the distribution of formations such as mountains and valleys. Studies of subglacial bed roughness have ranged from measurements of precipitates on bedrock features (Hubbard & Hubbard, 1998), to studies over mountain ranges (Bingham & Siegert, 2009).

In this project, three scales are used, based on the horizontal size of topographic features measured. Section 2.3.1 summarises theories and findings at a *macro-scale* level, where studies have investigated roughness over horizontal distances exceeding 10 km. The *meso-scale* (Section 2.3.2) describes models and studies of the effect of topography on basal ice flow within a horizontal size range of 1 m to 10 km. Section 2.3.3 presents

theories and findings on roughness at the *micro-scale*, referring to roughness over a horizontal or vertical size below 1 m. This choice of scales might appear unusual because the range differs between each of them. One reason for the choice was the legacy of research by other glaciologists. As this section will show, the logistics of collecting data have meant that studies have tended to be at a local level of less than 1 m or, have measured roughness over profiles tens of kilometres long. However, it will be seen that between these extremes, i.e. the *meso-scale*, there are theories on the role of roughness in ice dynamics, but little field research.

For each of these scales, theories on how roughness is expected to affect ice dynamics are presented. Note that some of these studies have not directly referred to the term *roughness* but have measured the form of topography, thus making them relevant. For example, a large body of research has looked at the relationship between ice-sheet behaviour and the morphology of subglacial bedforms, such as Stokes & Clark's (2002) review of the relationship between ice speed and bedform length. The shape of such features constitutes part of the topography of the bed's surface and, thus, they contribute to the roughness. Other studies have used an alternative term, but explore similar concepts as those specifically mentioning roughness. For instance, one of the components of the *Weertman Sliding Law* is *slipperiness*, referring to *small-scale basal topography* (Gudmundsson, 2011: 263); Hindmarsh's (2000) model of sliding uses a *smoothness* constant. Many theories relate to the way the bed topography influences ice flow, albeit indirectly. As such, it is not possible to cover all of these conceptual and numerical models. Instead, this chapter highlights the range in ways that roughness may control ice sheet dynamics.

In addition to modelling the role of roughness on ice dynamics, field research has also been completed over different spatial scales. Therefore, for each of the three spatial scales the major findings are also described. It will be seen that, although the theories and findings are grouped by scale, they may not be directly related because field observations have not been linked to conceptual or numerical models. As such, theories and findings are presented separately for each scale.

Finally, both the roughness of the subglacial bed and ice dynamics may change through time, making it important to consider a *temporal scale*. Theories and findings on how roughness may change through time are presented later.

2.3.1 Relationships between macro-scale roughness and ice dynamics

2.3.1.1 Theories: On scales of 10 km or greater, variations in roughness caused by mountain and valley formations may be important for controlling the speed of ice flow due to the effect of these features on the thickness of an ice sheet. If the elevation of the ice

surface is somewhat constant, then the thickest ice will be in valley bottoms. Given that the shear stress increases with thickness (Paterson, 1994; Hindmarsh, 1998; Piotrowski & Tulaczyk, 1999; Benn *et al*., 2007), the fastest speeds would also be expected to correspond with these areas. This process is referred to as *topographic forcing* (Joughin *et al*., 2004; Ottesen *et al*., 2005). As described further in Section 2.3.5, variations in roughness over horizontal distances of kilometres are thought to be one of the factors influencing the location of large-scale features such as ice streams (Bennett & Glasser, 1996; Thorsteinsson *et al.*, 2003).

The example of topographic forcing demonstrates that roughness may be indirectly related to ice speed, because the shape of topography influences other variables that control ice dynamics. Yet, the shape of the topography may have a direct influence on basal ice speeds by controlling the amount of frictional resistance to sliding. Drag is induced at the point where the ice contacts the bed (Alley, 1993), and this force counteracts the forward motion of an ice sheet (Thorsteinsson *et al.*, 2003; Stokes *et* al., 2007). The amount of drag is influenced by the shape of the bed, for example, increasing as the size and/or frequency of bumps on the bed increases, (i.e. as roughness increases). As a result, there are likely to be patterns on the subglacial bed, with some areas inducing a high basal drag but others offering less resistance (Siegert *et al.*, 2004; Schoof, 2004a, 2004b; Stokes *et al.*, 2007).

2.3.1.2 Findings: Radio-echo sounding measurements have been used to quantify roughness at the macro scale, with Bingham & Siegert (2009) providing a summary of many of these. Calculations based on radio-echo sounding (RES) data show spatial variations in subglacial surface texture across Antarctica, with an example given in Figure 2.1. (The methods used to produce these results are described in Section 2.4.) Spatial variations in roughness appear to correspond to differences in ice-sheet velocity (Siegert *et al.*, 2004, 2005b; Bingham & Siegert, 2009). There is correlation between ice-sheet basal speeds and roughness, with areas of rapid ice flow appearing to correspond to beds of low roughness (Rippin *et al.*, 2004; Siegert *et al.*, 2004; Taylor *et al.*, 2004; Bingham et al., 2007). This can be illustrated through comparison of areas of *ice streams* and *ice divides*. Ice streams are regions where ice speeds are much faster than surrounding areas (Clark & Stokes, 2003; Schoof, 2004b, 2006), while divides are characterised by speeds that approach zero. Analysis shows that ice streams are situated in areas of low roughness, with Siegert *et al.* (2004), for example, reporting that the beds of these areas have the lowest roughness values. Conversely, under ice divides, roughness values are higher (Bingham & Siegert, 2007a). Spatial variations are also seen on smaller, regional scales, with roughness decreasing in a downstream direction (Bingham & Siegert, 2009).

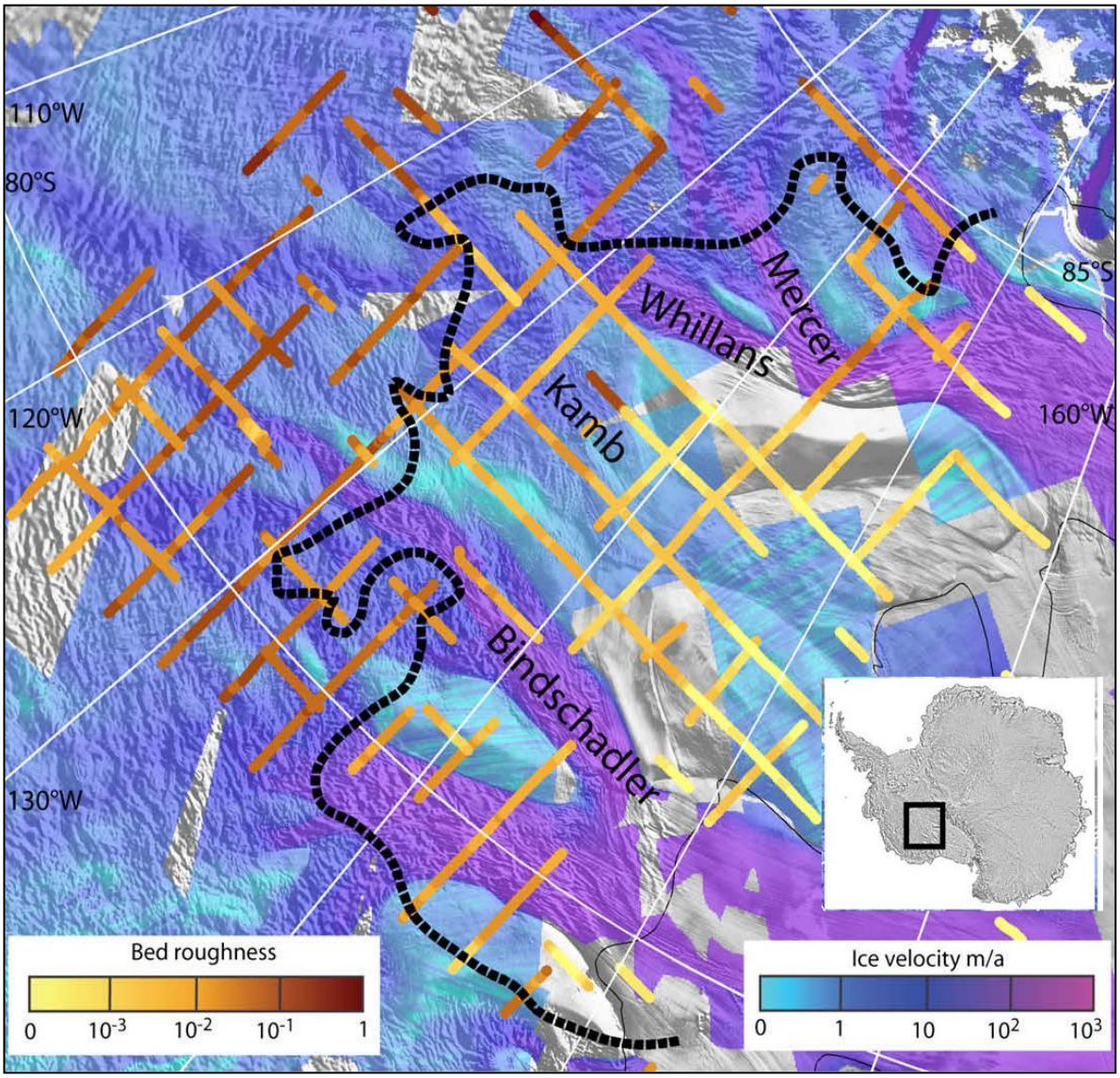

Figure 2.1: Roughness values, calculated via spectral analysis of SPRI RES data along flightlines. Values approaching zero represent a smooth bed, with roughness increasing towards a value of 1. Data suggest that ice velocities are highest where bed roughness is lowest (modified from Bingham & Siegert, 2009)

On a more localised level, analysis of profiles orientated parallel to flow, over windows approximately 50 to 70 km long, show that the roughness of the bed progressively decreases downstream (Bingham & Siegert, 2009). When results of these profiles are compared with those orientated orthogonally to ice flow, the latter produce higher roughness results (Rippin *et al.*, 2007), suggesting that there is a directional pattern to the topography. Such patterns are also observed in other sciences, such as in materials science where the movement of one surface over another can produce patterns of wear (Cuthbert & Huynh, 1992; Xiao *et al.*, 2004). The directional pattern in a surface is termed the *lay* (Kalpakjian, 1997; Lou *et al.*, 1998; Smith, 1999; Thomas *et al.*, 1999). In glaciology, the speed of ice flow may also show directional patterns that correspond with the shape of topography. For example, because of the role of topographic forcing, more

rapid speeds might be associated with large troughs (Paterson, 1994), and follow the direction of these features.

2.3.2 Relationships between meso-scale roughness and ice dynamics

2.3.2.1 Theories: Compared with studies of macro-scale and micro-scale topography, relatively few studies have modelled the roughness of subglacial topography on scales of tens to hundreds of metres. Nevertheless, although the term *roughness* has not been used explicitly, many investigations of ice sheet dynamics have been concerned with basal topography at this scale. For example, many subglacial bedforms lie within this size range including drumlins, megaflutes, and Rogen moraines (Clark, 1993; Hindmarsh, 1999; Taylor *et al.*, 2004; Schoof & Clarke, 2008). The fact that many of these features have been identified beneath contemporary ice sheets shows that they form an important part of the topography (King *et al*., 2007), so theories on their formation or effect on basal ice flow are relevant to studying roughness.

Some scientists have modelled how ice interacts with meso-scale sized perturbations on the bed. *Enhanced basal creep* is the primary means by which obstacles greater than 1 m in length are overcome (Paterson, 1994). On the upstream side of obstacles, as ice comes into contact with these faces, pressure within the basal ice increases (Bennett & Glasser, 1996). Higher pressures produce faster rates of deformation and, therefore, the larger the obstacle, the more effective this process (Hubbard *et al.*, 2000). The wavelength of roughness is a means of recording obstacle size; the higher the wavelength, the larger the obstacles. Roughness also varies with the frequency of topographic peaks and troughs; the greater the number of perturbations, the higher the resistance to flow and, therefore, the higher amount of enhanced basal sliding that will be required. Rémy *et al.* (1999) suggest that beds with low roughness, i.e. few obstacles, offer little resistance to ice flow, which in turn gives rise to high speeds. This is supported by Alley (1993), who shows that drag on the ice increases as the fraction of bed covered by bumps increases.

Some of processes by which the roughness of the subglacial bed may interact with ice dynamics occur over a wide range of scales. For example, in Section 2.3.1.1, it was described how bumps act to reduce ice speed. This effect is also identified at the meso scale. Given the importance of such areas as points of resistance to ice flow, a number of studies have referred to them as *sticky spots* (Alley, 1993; Knight, 2002; Stokes *et al*., 2004). One way that such bumps may be formed is if there are patterns in topography with a perpendicular alignment to ice speed forming *topographic steps* (Stokes *et al*., 2007). As roughness increases, there is a greater surface area of ice in contact with the bed, so drag is greater. Furthermore, when ice encounters an obstacle on the size order of 10^2 m wavelength, ice is forced to accelerate. Therefore, these bumps become areas of

localised strain heating and these increases in temperature, in turn, allow ice to deform more rapidly (McIntyre, 1985).

Modelling the effect of bumps on ice speed is complicated because the shape of topography may influence ice dynamics in other ways. For example, under certain conditions, cavities may develop where ice loses contact with the bed in the lee-side of obstacles, therefore reducing the frictional resistance. Indeed, roughness has been shown to influence cavitation, because the size and spacing of bed asperities affects the likelihood of their development (Clarke, 2005). A further complexity in assessing the role of *sticky spots* on ice flow is that roughness of the bed is just one cause of these localised increases in resistance. Other controls on ice dynamics, such as geology, also apply at this scale: for example, areas of resistant bedrock may form bumps (Stokes *et al*., 2007).

2.3.2.2 Findings: As with the lack of numerical models on meso-scale roughness, little research has expressly measured roughness at scales of tens to hundreds of metres. Despite many subglacial bedforms falling within this size range, few studies have measured their roughness directly. Furthermore, at this scale many of the subglacial features appear to have a directional pattern as a result of preferential erosion or deformation in the direction of ice flow (Hubbard *et al.*, 2000; Clark *et al.*, 2009). For example, Figure 2.2 shows examples of a drumlin field and a group of mega-scale lineations. Despite this, little research has been done to quantify how the roughness values yielded differ when these features are measured at different angles. One exception is the research by Hubbard *et al.* (2000) who found that the roughness was a magnitude less in the direction of ice flow than perpendicular to it, supporting similar observations at the macro-scale.

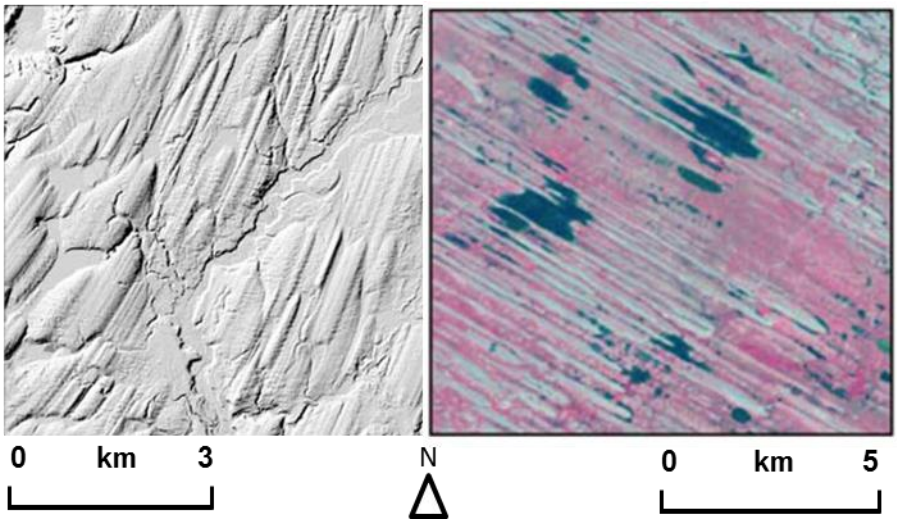

Figure 2.2: As with manufactured surfaces, subglacial topography exhibits surface texture with directional patterns. These patterns can occur over a range of scales. The left image shows a 6×6 km DEM of the Puget Sound drumlin field, Washington, USA (Schoof, 2007: 228). Image on the right depicts 10×10 km area of mega-scale glacial lineations, Dubawnt Lake, Canada (Stokes & Clark, 2003b: 349)

Much glacial research has focused on meso-scale bedforms. Just taking palaeo ice-sheet reconstructions as an example, numerous studies have used these features to infer former ice behaviour (Evans et al., 2005). Many studies have looked to link particular bedform morphometry to ice dynamics (Rose, 1987) and found that they are spatially arranged in a way that corresponds with ice speed: for example, the length (Stokes & Clark, 2002) and elongation ratio (O'Cofaigh *et al.*, 2002) of bedforms is thought to increase as ice speed increases. Given that the morphometry of these features is a component of the bed's topography, it follows that with changing bedform size the roughness also changes. However, no studies have compared the roughness of different features: for instance, is a drumlin field rougher than a group of mega-scale glacial lineations?

2.3.3 Relationships between micro-scale roughness and ice dynamics

2.3.3.1 Theories: At the micro-scale, i.e. below 1 m, the dominant mechanism resisting the flow of ice-sheets is friction between ice and bed. Friction is *the resistance to relative sliding between two bodies in contact under normal load* (Kalpakjian, 1997: 195). For movement to occur, the frictional resistance must be overcome (Benn & Evans, 1998; Cohen *et al.*, 2000). The higher the surface area in contact with the bed, the higher is the frictional resistance (Bennett & Glasser, 1996).

The roughness wavelength (i.e. horizontal size of obstacles) influences which process of ice flow will dominate in a given situation (Fowler, 2010). When obstacles are less than 1 m long, *regelation* is the primary mechanism (Nye, 1969; Paterson, 1994). Regelation involves pressure-induced melting, followed by re-freezing (Hubbard *et al.*, 2000), and requires ice at the base of an ice-sheet to be at its pressure melting point (Bennett &

Glasser, 1996). The process is shown schematically in Figure 2.3. When ice encounters a bed perturbation, high stresses develop on the up-flow side (Knight, 1999), creating a pressure gradient across the obstacle. The increase in pressure produces melting of the ice, and water flows to the down-ice side of the obstacle. Lower pressure on the lee-side causes re-freezing, releasing latent heat. A temperature gradient between stoss and lee develops, resulting in heat flow to the colder up-ice side (Paterson, 1994) that eases further melting. If a bed has many obstacles at the wavelength of less than 1 m, the bed requires more energy to overcome them (Hubbard *et al*., 2000) than a bed with fewer asperities.

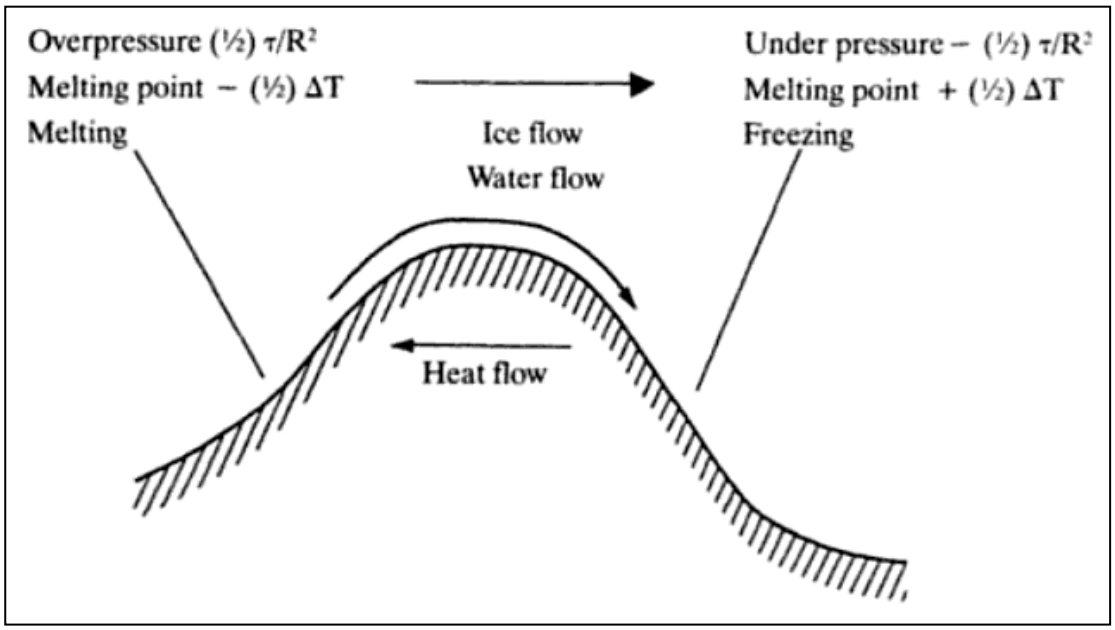

Figure 2.3: Regelation mechanism of ice flow around an obstacle (from Paterson, 1994: 137), where: τ is the average shear stress, T is temperature, and R roughness defined as the length of the obstacle divided by the distance between obstacles

2.3.3.2 Findings: A small number of studies have investigated roughness at the micro-scale. These focused on testing the interaction between ice and bed obstacles (e.g. Nye, 1969; Kamb, 1970). Hubbard & Hubbard (1998) measured micro-scale bed roughness using ground-based survey in the foreground of Glacier de Tsanfleuron, Switzerland. Roughness was found to alter depending on the amount of regelation, because this caused the precipitation of carbonate deposits (see Figure 2.4), which subsequently altered topography over millimetre scales. As with the macro-scale investigations, this study demonstrates that roughness may be a product of ice flow as well as a control.

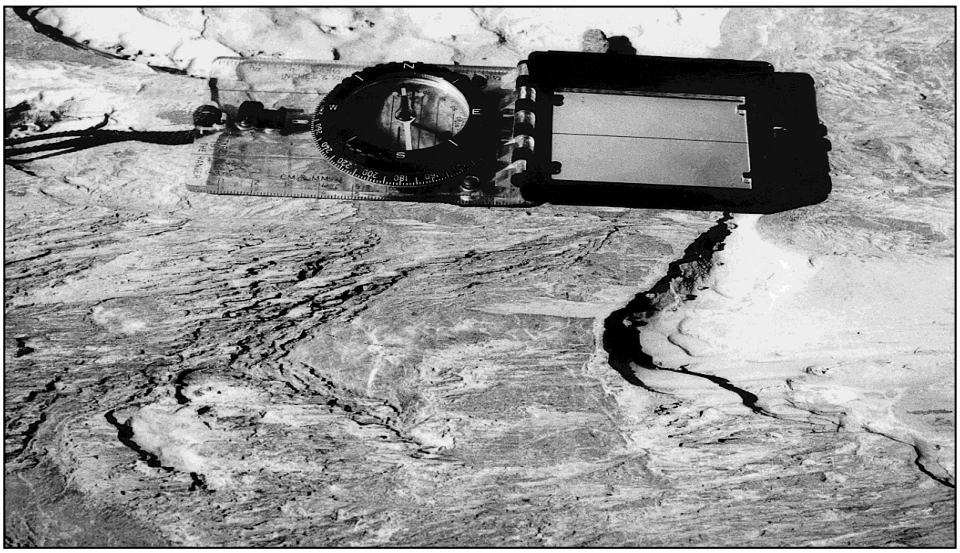

Figure 2.4: Roughness produced by precipitation of carbonates on the lee-side of an obstacle (from Hubbard & Hubbard, 1998: 262)

2.3.4 Temporal scale

In materials science, *wear* is known to reduce roughness (Lui & Li, 1999; Suh *et al.*, 2003) and, similarly, glacial processes may result in erosion and deformation of the bed (Glasser, 1995; Benn & Evans, 1998), with these processes acting to reduce the roughness (Altuhafi *et al.*, 2009). These theories highlight a reverse situation where it is the ice dynamics that control the roughness, as opposed to the form of topography influencing ice flow.

Here, the amount of modification depends on the amount of energy that is available to do work. Given that shear stresses are higher under faster ice speeds, it is in fast flow regions where the rates of deformation and/or erosion of the bed are likely to be greatest (Paterson, 1994). However, no studies have quantified the rates at which the roughness of the subglacial bed might change, and how this might affect ice dynamics.

Both the roughness of the bed and speed of flow can change through time (Haldorsen, 1981; Benn, 1994), with decreasing roughness driving faster speeds (Siegert *et al.*, 2004) that, in turn, cause more modification of the bed (Schoof, 2004a; Siegert *et al.*, 2005b). In theory this could lead to a feedback mechanism causing instability to ice sheets through, for example, the expansion of ice streams. However, such predictions are speculative because no threshold values of roughness on the onset of ice streaming have been established. Modelling is especially difficult because the spatial scales interact with the temporal variability.

As with the spatial scales, many studies have modelled temporal variations in topography without naming roughness specifically. For example, a large body of work has addressed how subglacial features might develop through time, either in their formation or through subsequent modification as a result of ice flow (Knight, 1999). These demonstrate that

there is a possible reverse interpretation where the ice flow controls the roughness over larger timescales, rather than roughness controlling ice dynamics. For example, although the roughness of a surface may be decreased through time due to wear, the susceptibility to erosion depends on the size of the features being removed (Whitehouse, 2009). In glaciology this is exhibited in the preferential removal of smaller bed obstacles (Kamb, 1970; Paterson, 1994; Hu & Dean, 2000; Hubbard *et al*., 2000).

2.3.5 Roughness as a control on ice stream location

As will be shown in Section 2.4.4, one area of ice sheets that have received much attention in roughness studies are the locations of ice streams. Due to their dominance in the roughness literature, and them underpinning much of the research in this project, it is worthwhile discussing how the controls on ice dynamics described above influence the location of these areas of rapid ice flow. This section provides an elementary background to ice streams to show their links with the various ice sheet controls described above, again with an emphasis on the role roughness. A more detailed examination of their characteristics and controls is given in Chapter 7, where the roughness of the Siple Coast region of Antarctica is investigated.

In the broadest sense, an ice stream is defined as an area of an ice sheet where ice flows more rapidly than the surrounding ice (Swithinbank, 1954): the speed of streaming ice is commonly cited as being an order of magnitude greater (Bennett, 2003). Due to this rapid ice flow, ice streams are major sources of ice sheet drainage, which makes them important controls on ice sheet stability (Bennnett, 2003). Despite ice streams being clearly discerned as large scale features, smaller scale variations within these areas of fast flow can also be observed. For example, a spatial arrangement in ice stream speed is commonly observed, with the fastest flow in the centre and decreasing towards the margins (Bindschadler *et al*., 1996). This pattern is produced because of drag at the margins between the ice that is streaming and that of the slower-flowing adjacent ice (Stokes *et al*., 2007). Analysis of the Whillans Ice Sheet in the Siple Coast region found that 50% of the resistive force came from this side drag (Echelmeyer *et al*., 1994). Furthermore, ice streams may exhibit temporal variation, on scales as short as one year (Whillans *et al*., 2001).

Winsborrow *et al*. (2010) provide an in depth review of the controls on ice stream location, and suggest a hierarchy of importance for their role in controlling ice speed. The controls are: topographic forcing, topographic steps, topographic roughness, geothermal heat flux, subglacial meltwater routing, and calving margins. Each of these mechanisms has effectively been described already, because ice streams are driven by the same variables governing ice dynamics in general. Yet, one thing that is noteworthy is that many of the main controls in ice stream behaviour are related to forces that resist ice flow.

Furthermore, many of these are also related to the shape of topography, which suggests that roughness is linked with the occurrence of these fast flowing areas.

Ice streams can be classified based on whether or not they are topographically constrained. With ice streams that are topographically controlled, the lateral boundaries of these regions of fast flow are commonly bounded by topography (Bennett, 2007). In these examples, rapid ice flow appears to be driven by differences in ice thickness: where ice is channelled into topographic lows, the increased shear stress and strain heating is thought to produce relatively faster ice speeds (Hindmarsh, 2001). As Section 2.2 described, the amount of shear stress increases as ice thickness increases, so that the location of ice streams have been found to be situated in large-scale valley formations.

In contrast, *pure* ice streams are areas of rapid ice speeds that are characterised by their lack of topographic constraint (Stokes & Clark, 1999). With these ice streams, the shape of the subglacial bed appears less influential in controlling ice stream location. Instead, evidence suggests that the locations of these ice streams are primarily influenced by the rheology of the bed, such as its ability to deform (Bindschadler *et al*., 1996). With these ice streams the roughness of the subglacial bed appears less important for supporting fast flow.

Although several controls on ice stream behaviour are linked to the shape of topography, as with ice dynamics in general there are a wider set of controls. One example of this are the rheological conditions of the subglacial bed. As described in Section 2.2, the availability of water and the compositions of sediment are important in determining the resistance to ice flow (Alley, 2000). In areas of ice streaming ice flow as a result of sediment deformation appears to be the primary form of forward motion (Paterson, 1994). As such, it is the resistive forces that appear to be relatively important in determining the location of streaming flow.

Another control on ice stream location that is not related to the shape of topography is the location of calving margins. At the zone of calving the rapid loss of ice acts to draw down ice from upstream (Hughes, 1992), thus driving rapid ice speeds. As a result, the position of the calving margin determines the location of streaming (Stokes *et al*., 2007) because this determines the upstream area that ice is drawn down from. A similar control on ice stream location is the position of ice shelves (Thomas, 1979). Unlike calving margins, these areas are thought to produce a buttressing effect that reduces the draw-down of ice, thus limiting ice speeds.

2.4 Techniques to measure and quantify roughness

Having demonstrated how roughness, and other ice sheet controls, may influence the spatial pattern of flow speeds across an ice sheet, let us now examine how scientists have

traditionally investigated the role of roughness in controlling ice dynamics, both in terms of the statistics used to quantify changes in the shape of the bed, and the choices of data.

2.4.1 Parameters used for quantifying bed roughness

The form of a surface can be described in general using terms like *rough* and *smooth* (Bennett & Glasser, 1996). However, roughness can also be measured quantitatively (Adolph's, 1999; Herzfeld *et al.*, 2000a; Shepard *et al.*, 2001; Gadelmawla *et al.*, 2002; Taylor *et al.*, 2004) using a *roughness parameter*. This latter approach is preferable for statistical analysis. In glaciology, quantifying the roughness of subglacial beds involves measuring changes in bed elevation (Rippin *et al.*, 2004; Taylor *et al.*, 2004). Such studies are similar to analysis of spatial data more generally (Mat heron, 1963; Fox & Hayes, 1985; Austin & England, 1993), where one or more statistics are used to summarise variations in topography over distance. Yet, despite the wide range of available methods for quantifying roughness (see Gadelmawla *et al.*, 2002 for over fifty examples), *spectral analysis* and *variogram analysis* have dominated glacial roughness studies.

The most common method used in recent studies to quantify ice-sheet bed roughness is spectral analysis (Taylor *et al.*, 2004; Siegert *et al.*, 2004, 2006b; Bingham *et al*., 2007). In principle, this measures roughness by decomposing a continuous profile into an infinitely large number of sinusoid (sine or cosine) curves with varying amplitudes and frequencies (or equally, wavelengths). The resulting *spectral density function* (spectrum) quantifies how much variability there is at each scale. In glacial settings, calculations have been based on some version of a discrete Fourier transform. For example, spectra were calculated in this way by Siegert *et al.* (2005) and Rippin et al. (2007), who analysed wavelengths of up to 35 km, over windows of approximately 50 to 70 km.

Despite its dominance, the use of spectral analysis is potentially limited in various ways, three of which are mentioned here. First, workers such as Bingham *et al*. (2007) have collapsed the spectrum into single measures of roughness, which although simple, discards much of the information that would otherwise allow roughness to be summarised at different scales. Second, glaciologists have used similar assumptions to those in time series analysis (Chatfield, 2003) that the data are equally spaced (Taylor et al., 2004). With many data, however, such as radio-echo sounding (RES) measurements, there are at least small irregularities in spacing and also bigger gaps in which echoes were lost (Bingham & Siegert, 2009). This problem has usually been addressed in glaciology by linear interpolation to produce an equally-spaced dataset (Taylor *et al.*, 2004). However, the effect of this procedure on the results has remained largely ignored. Third, the spectral density function is usually assumed to be estimated for a stationary process, one with constant statistical characteristics throughout. With spatial problems, substantial trends and heterogeneity are typical rather than exceptional, so this assumption may not be met.

For example, profiles along ice sheet beds may show an overall slope. In glacial science, this problem has been addressed by estimating the spectrum within a small window and/or detrending, usually by subtracting a linear trend and thus ignoring the overall slope (Taylor *et al*., 2004). The problem here, however, is that using fewer data points reduces the quality of the corresponding estimate, and removing trends raises questions over how far this is both physically and statistically the most appropriate procedure.

The second most common method of calculating roughness of glacial surfaces is variography or variogram analysis (e.g. Herzfeld *et al.*, 2000a, 2000c), which measures the pattern of spatial dependence. Roughness is measured by summarising total variability in terms of the change in the variability (measured as mean difference squared) of bed elevation values between pairs of points at varying distances apart (Herzfeld *et al.*, 2000b). With increasing roughness there is more variance in values over a given distance. As with spectral analysis, the result is a function, the variogram, but a function of distance or separation rather than frequency or wavelength. Where there is little change in elevation with distance, the variogram will remain low, while if there is much change, the variogram will be higher. Variograms, like spectra, may be summarised in terms of selected parameters. Variogram analysis is probably now used more widely than spectral analysis for spatial analysis in the Earth and environmental sciences (Webster & Oliver, 2007).

More recently, glaciologists have begun to review other methods of quantifying roughness although, as yet, these have not been fully applied to investigating ice sheet dynamics. Li *et al*. (2010) recognise the contribution of spectral analysis, but highlight the importance of considering other parameters. In their study two alternative methods are reviewed, with one designed to summarise vertical variations in topography, and the other, horizontal changes.

2.4.2 Roughness in other disciplines

Investigating subglacial beds is just one use of roughness parameters. Glaciologists have also used these methods to analyse other topography, such as the surface of ice sheets (Arya, 1975; Andreas *et al*., 1993; Adolph's, 1999; Van der Veen *et al*., 2009). Even considering these methods, relatively few parameters have been used in glacial research, but it is also recognised that other disciplines are interested in roughness. For example, Davidson *et al*., (2000, 2003) showed how roughness can be used to investigate soils, and Frankel & Dolan (2007) measured the roughness of alluvial fans. Ling & Untersteiner (1974) quantified the roughness of sea ice, and Biegel *et al*. (1992) measured the roughness of rock surfaces. Like ice sheets, the roughness of surfaces such as sand dunes (Byrne, 1968; Maurer *et al*., 2010) and river beds (Buffington & Montgomery, 1999) has been found to influence the flow of other materials and fluids (Chiu & Rubio, 1970;

Canovaro *et al*., 2007; Smoth *et al*., 2007). For example, the topography of river banks may control overland flow (Smith *et al*., 2007). Roughness has also been used to investigate slope processes and landforms, such as debris flows (Austin & England, 1993), because the ability of one material to slide over another is influenced by roughness (Biegel *et al.*, 1992). In meteorology, roughness is used to investigate surfaces that produce drag resistance to air flow (Adolph's, 1999). For example, the interaction of the sea surface and wind can be studied through measuring roughness (Csanady, 1974; Brown, 1979; Agnon & Stiassnie, 1991). Roughness is also commonly measured in remote sensing to classify surfaces, such as fresh snow (Manes *et al.*, 2008). As in subglacial bed research, roughness has been quantified using remotely sensed data allowing study of otherwise inaccessible areas. For example, roughness has been used to study lunar (Simpson, 1976) and planetary surfaces (Sakimoto *et al.*, 1999; Shepard *et al.*, 2001).

Geography has a long history of analysing topography under the names of *geomorphology* or *geomorphometry* (Mark, 1975; Cox, 2007). Studies in geomorphology may not term their methods *roughness parameters*, but many measure spatial patterns in topography. For instance, in glaciology, curvature has been used to classify cirques (Evans & Cox, 1995). Similarly, Evans (1972) has explained how surfaces can be analysed in terms of local altitude, slope, curvature, etc. and their means, standard deviations, skewness and kurtosis. As Chapter 5 will show, other sciences would consider such statistics roughness parameters. Just as glaciologists have investigated how the roughness of the subglacial bed controls ice speed, some studies in geomorphology have looked at how the topography of a surface influences flow. For example, in fluvial sciences slope is important because of its effect on drainage (Montgomery & Buffington, 1997). However, these examples from Earth and Environmental sciences compose a small percentage of the methods for quantifying roughness.

Many sciences study the roughness of topography and, as a result, there are a myriad roughness parameters that could be used (Gadelmawla *et al*., 2002; Menzes *et al*., 2009). For example, on similar scales to ice-sheet beds, Sakimoto *et al*., (1999) have quantified the roughness of planetary surfaces, and Fox & Hayes (1985) have investigated sea floor roughness. At smaller scales, numerous medical studies have evaluated roughness of surfaces (BSI, 1997b; El Fininat *et al*., 2001; Sul *et al*., 2004, 2005): for example, Kumar *et al*. (2007) measured roughness of cells, while Hall *et al*. (1997), Elfick *et al*. (1999) and Daugaard *et al*. (2007) studied roughness of synthetic bone-joint replacements. Many roughness investigations have been undertaken at a microscopic (Hudspeth *et al*., 2002; Patrikar, 2004; Fubel *et al*., 2007) and atomic level (Kumar *et al*., 2007). Because of the scale-free nature of the parameters, however, a technique commonly used on the

microscopic level can be used to analyse surfaces on the scale of ice-sheet beds. Of all sciences it is perhaps engineering, in particular, manufacturing engineering and tribology, that has the largest number of parameters in use. Tribology, the study of lubricants, is concerned with the behaviour of materials at the interface layer, and roughness is an important component of this (Bhushan, 1992, 2002; Liu & Li, 1999; Smith *et al*., 1999; Pettersson & Jacobson, 2003; Williams, 2005). Manufacturing has a long history of measuring roughness as a means of quality control (Kalpakjian, 1997; Ramalu, 1999; Moutinho *et al*., 2007; Davim *et al*., 2009). The fact that roughness influences the surface area in contact between two materials means that it controls friction (Menezes *et al*., 2008, 2009a, 2009b) and wear (Chilamakuri & Bhushan, 1998), thus affecting the longevity (Whitehouse, 1994) and functionality of parts (Cuthbert & Huynh, 1992; Najjar *et al*., 2003; Xiao *et al*., 2004). Manufacturing has led to the development of numerous technical guides, such as the International Standards Organisation (ISO) and US Military Standards (e.g. MIL-STD-10A), that define methods of quantifying roughness. In this thesis, the majority of standards cited are those published by the British Standards Institution (BSI). The methods described in such technical documentation usually refer to analysing topography from a manufacturing context, but, as with other parameters, these methods can be used in other sciences, including glaciology. Indeed, these standards appear to have guided the approaches used in other sciences (Bohm *et al*., 2009).

As with many forms of spatial analysis, roughness can be quantified in two or three dimensions (Dong *et al.*, 1994, 1995; BSI, 1997a, 2009a, 2009b; Gadelmawla *et al.*, 2002; Bingham & Siegert, 2009). As the presentation of the findings of glacial roughness studies (Section 2.3.1) showed, the approach traditionally taken has been to analyse bed elevation measurements gathered along profiles. Nevertheless, Winsborrow (2007) demonstrated that the roughness of ice-sheet beds can be measured in 3D. A possible reason why 2D analysis has remained dominant is the lack of available bed elevation measurements in the form of DEMs. For example, with the SPRI records, the relatively large distances between flightlines (Lythe *et al*., 2001; Siegert *et al*., 2005) meant that the resolution was too poor to interpolate between them, thus restricting analysis to measuring along each profile. This shows the important role that data acquisition plays in shaping the methods used to analyse topography.

2.4.3 Data acquisition

Before roughness can be quantified, raw data must be processed and digitised (Dowdeswell & Siegert, 2002), giving a record of changing subglacial bed elevation with distance (Lythe & Vaughan, 2001). Due to difficulties in accessibility, information from contemporary ice-sheet-beds is relatively limited (Bartek *et al.*, 1991; Hart & Rose, 2001; Rignot & Thomas, 2002; King *et al*., 2007). Early methods of gathering data largely

comprised borehole studies (Fischer & Hubbard, 2006; Iverson *et al.*, 2007), accessing the bed via tunnels (Paterson, 1994; Cohen *et al.*, 2000), or investigation of nunatak outcrops. However, such techniques are not suitable for roughness studies, because data are too sparse spatially.

In recent decades, remote sensing systems have allowed bed data to be gathered indirectly (Drewry, 1975). Much of the data on ice-sheet beds comes from geophysical surveys, such as seismic (Anandakrishman *et al.*, 1998; Murray *et al.* 2008), gravimetric (Bell *et al.*, 1998), magnetic (Shepherd *et al.*, 2006) and radar surveys (Robin *et al.* 1969a, 1969b; Weber & Andrieux, 1970; Small *et al.*, 1997). Since its first glacial use in 1948 (Kovacs *et al.*, 1995), radar has been used in many settings (Massonnet & Fiegl, 1998; Annan, 2002), including gathering data from contemporary ice-sheet beds in Antarctica (Swithinbank, 1969) and Greenland (Gudmandsen, 1969). A number of different formats of radar exist (see Figure 2.5), including ground-based surveys (Jacobel *et al.*, 1996), airborne campaigns (Hagen & Sætrang, 1991; Adolph's, 1999), and submarine-mounted sonar systems (Bourke & McLaren, 1992).

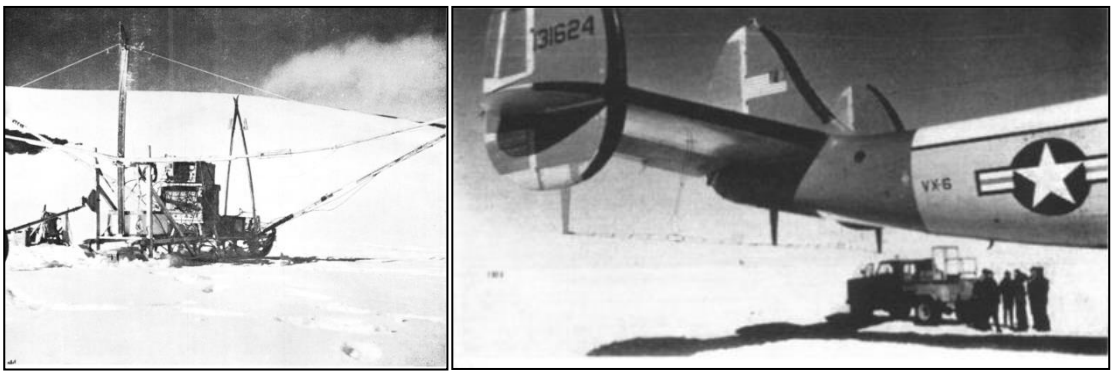

Figure 2.5: Radio-echo sounding systems:
(Left) Ground-based system propelled by snow tractor (source: Wager, 1982: 115);
(Right) Airborne scanner mounted to aircraft (source: Evans & Smith, 1969: 134)

To date, radio-echo sounding (RES) has been the most commonly-used method. These systems provide data on the subglacial bed by measuring radio-wave signal returns (Walford & Harper, 1981; Dowdeswell & Evans, 2004). As electromagnetic waves are transmitted through the ice-sheet towards the bed, they encounter changes in dielectric constant (Kovac *et al*., 1995; Siegert *et al*., 1996), which often correspond with internal layers and the ice-bed interface (Rippin *et al.*, 2003). These boundaries cause scattering of the electromagnetic energy (Berry, 1972, 1973), causing some of these radio waves to be reflected (Doake, 1981; Fujita *et al.*, 1999; Urbini *et al.*, 2001). The speed of electromagnetic waves varies between different media (Walford & Harper, 1981). The time taken for a signal to be transmitted, reflected, and received is measured (Siegert *et al.*, 1996) and can be converted into distance (Hempel & Thyssen, 1992; Tillard & Dubois, 1995) because the speed of radio waves in air and ice can be estimated (Kovacs *et al.*,

1995; Milana & Maturano, 1999; Siegert, 1999; Pattyn *et al.*, 2003). The reflected signal returns are processed to produce profiles (Hagen & Sætrang, 1991; Bingham *et al*., 2007), as illustrated in Figure 2.6.

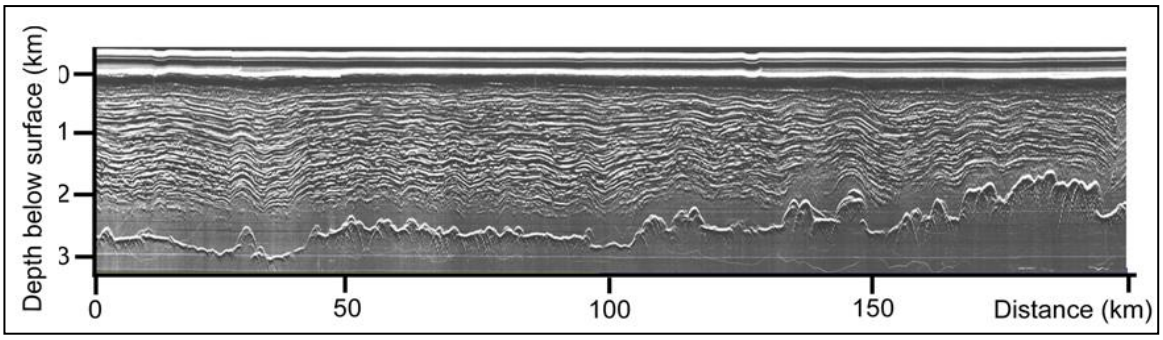

Figure 2.6: Processed Z-scope image of SPRI data, showing subglacial bed and internal layering. The subglacial bed is the bottom trace (modified from Bingham et al., 2007)

Compared with other forms of active remote sensing such as seismic surveys (Smith, 2007), airborne radar has a similar resolution (Evans, 1969; Allen *et al*., 1997; Arcone, 2008), but the added advantage is that large areas can be covered relatively quickly (Robin, 1969; Siegert, 2008). As such, RES gives the most complete coverage of Antarctic subglacial topography, including areas where there are no other data (Goldstein *et al.*, 1993; Rignot & Thomas, 2002; Bingham & Siegert, 2009). Long-range airborne surveys became practical in the 1960s (Robin, 1969; Gogineni, 1998; Vaughan, 2006) and, since then, remote sensing has been used increasingly, as it facilitates large-scale studies (Johnson & Smith, 1997; van der Veen *et al.*, 2009).

Radar has many glacial applications (Plewes & Hubbard, 2001; Eisen *et al.*, 2003; Murray *et al*., 2007; Woodward & Burke, 2007), and has been used to study three components of ice sheets: the ice surface, internal layers, and the bed. Because the ice sheet surface reflects radar energy, radio-echo sounding can be used for mapping surface topography (van der Veen *et al.*, 1998; Nolin *et al*., 2001; Gudmundsson *et al*., 2003; Young *et al.*, 2005; Conner *et al*., 2009) and measuring ice sheet velocity (Shabtaie & Bentley, 1987; Joughin, 2006). Much of the usefulness of radar, however, is due to the ability of radio waves to penetrate ice (Hattersley-Smith, 1966; Fuchs et al., 1969; Harrison, 1970; Holmund, 1986; Steinhage, 2001; Bianchi *et al*., 2003; Welch & Jacobel, 2003). Ice sheets often exhibit *internal layering* on radio-echo sounding images (Rose, 1979; Frolov & Macheret, 1999; Mayer & Siegert, 2000; Nereson *et al.*, 2000; Doake *et al*., 2003; Hindmarsh *et al*., 2003; Drews *et al*., 2009; Karlsson *et al*., 2009), arising from variations in ice density (Whillans, 1976) and acidity (Hammer, 1977; Siegert, 1999). Internal layers have been used to reconstruct accumulation rates (Vaughan *et al.*, 1999; Nereson *et al.*, 2000; Baldwin *et al.*, 2003; Leysinger-Vieli *et al.*, 2007) and deformation history (Kanagaratnam, 2002; Bingham *et al.*, 2007). Through combining data on each of these

parts, additional morphological characteristics can be calculated (Steinhage *et al.*, 1999). For example, ice thickness is calculated by measuring the vertical distance between the bed and surface of the ice sheet (Sandhäger & Blindow, 2000; Lythe & Vaughan, 2001; Parrenin *et al.*, 2004; Lythe *et al.*, 2008; Oswald & Gogineni, 2008). However, in this thesis, the information of most interest are measurements of the subglacial topography.

In the past, some RES systems were unable to detect the ice sheet bed: for example, the ground-based system used by Paterson & Koerner (1974) was unable to penetrate ice above 800 m thick. However, as subglacial studies became a priority, systems were adapted accordingly and many are now capable of penetrating ice over 4 km thick (Siegert *et al.*, 1996; Siegert, 1999; Steinhage *et al.*, 1999; Tobacco *et al.*, 1999). Many studies have used radio-echo data of *ice-sheet beds*, for example mapping subglacial topography (Björnsson, 1981). Other scientists have used RES to identify subglacial water (Copland & Sharp. 2001; Siegert *et al.*, 2006; Oswald & Gogineni, 2008) including subglacial lakes (Siegert *et al.*, 1996, 2001).

With its many applications, radio-echo technology continues to develop (Bailey *et al.*, 1964; Young *et al.*, 2008) and, through this, the detection and resolution of subglacial bed topography have continued to improve. RES datasets and radar systems are now being increasingly exploited to measure subglacial roughness and even detect subglacial bedforms (e.g. Rippin *et al.*, 2004; Shepherd *et al.*, 2006; King *et al.*, 2007, 2009; Bingham & Siegert, 2009). The improvements in technology are such that systems are now being used to investigate topography beneath ice on other planets (Thompson & Spyres, 1990). Similarly, as Shum *et al*. (1995) describe, the navigational accuracy in remote sensing technology continues to improve. From a comparison of studies it can be seen how determining aircraft position was once less accurate but, particularly since the advent of Global Position System (GPS) satellites, location data have improved significantly (cf. Fish, 1966; Kayton & Fried, 1997; Matejka & Lewis, 1997).

2.4.4 Case study: Investigating roughness of the Antarctic ice-sheet

Between 1971 and 1979, a series of RES campaigns were flown over Antarctica. The most extensive survey to date (Siegert *et al*., 2005a), with measurements gathered over 400,000 km of flightlines (Taylor *et al*., 2004; Bingham & Siegert, 2009), was gathered by a consortium consisting of the Scott Polar Research Institute (SPRI), the U.S. National Science Foundation (NSF), and the Technical University of Denmark (TUD) (Siegert *et al.*, 2005a). Hereafter both consortium and data yielded are termed *SPRI*, as is common style (Siegert, 2000). The main advantage of using SPRI data is their good coverage of both East and West Antarctica (Bingham & Siegert, 2009), as shown in Figure 2.7.

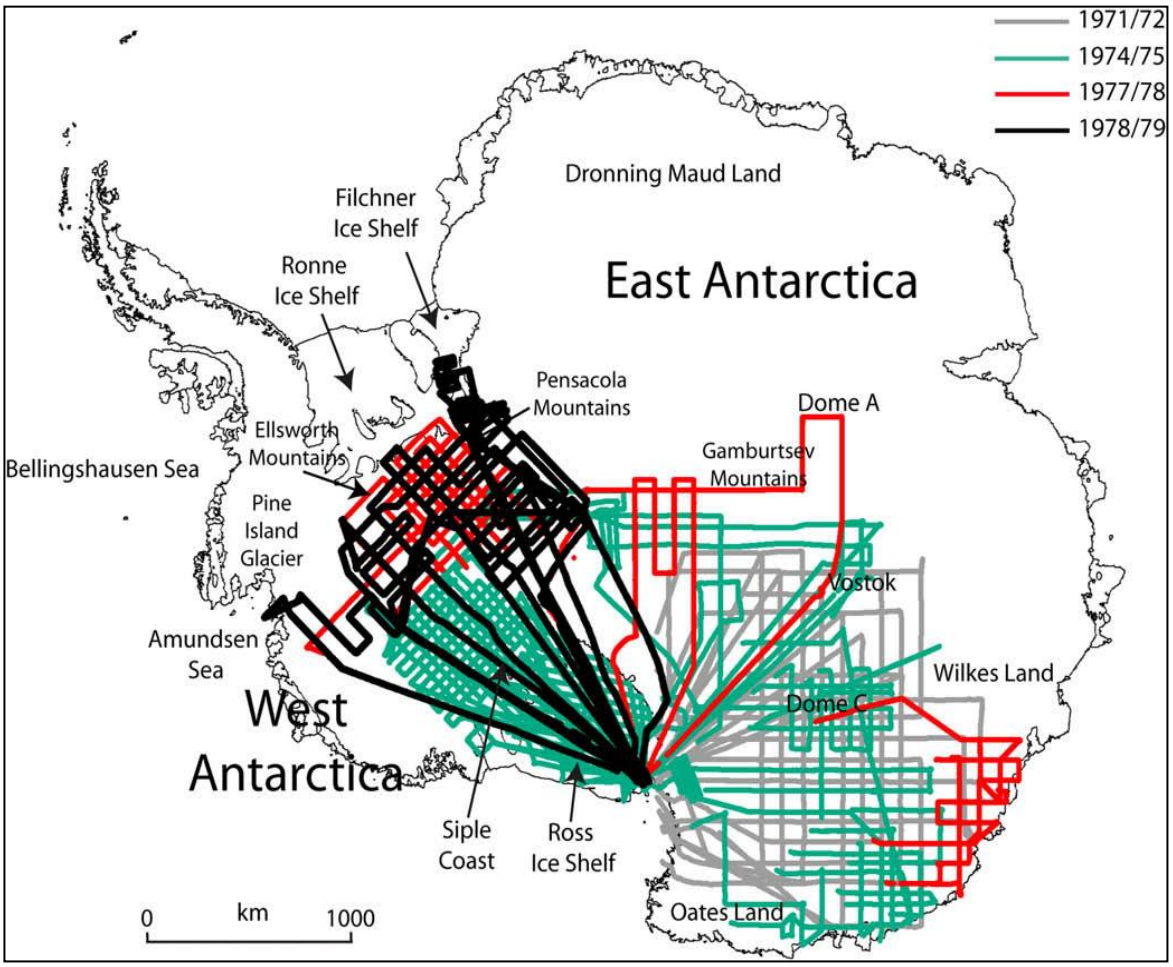

Figure 2.7: Coverage of SPRI radio-echo sounding data, showing flightlines colour-coded by year of campaign (from Bingham & Siegert, 2009)

Furthermore, because of the significance of these regions for ice sheet stability, much of the data were obtained from locations of ice streaming (Siegert & Ridley, 1998; Taylor *et al.*, 2004), typified by rapid ice speeds with slow-flowing lateral boundaries (Paterson, 1994). This made the flightlines useful for investigating relationships between ice-speed and roughness (e.g. Rippin *et al.*, 2004; Siegert *et al.*, 2004; Taylor *et al.*, 2004; Bingham *et al.*, 2007; Bingham & Siegert, 2009). As SPRI data have been commonly used to investigate ice-sheet-bed roughness and form an important part of the present study, the method of gathering and processing these data is now described in detail.

SPRI data were compiled in two formats termed *A-scopes* and *Z-scopes* (Siegert & Kwok, 2002; Bingham & Siegert, 2007b). For a single pulse of electromagnetic energy, an A-scope graphically displays the two-way travel time versus signal strength (Siegert *et al.*, 2005a). In SPRI data, A-scopes were recorded every 15 seconds (Siegert, 1999), which corresponds to approximately every 1.8 to 3 km (Bingham & Siegert, 2009). By stacking many electromagnetic pulses alongside one another, Z-scopes produce a pseudo cross-section, where time is represented along the *x* axis, and the *y* axis shows the two-way travel time of electromagnetic energy (converted into depth). The strength of the signal return is represented by the brightness of the image. Z-scopes provide a more continuous

record, as they are sampled several times per second (Siegert *et al.*, 2004). The resultant Z-scope radargrams resemble those of seismic profiles, and the bed of the ice sheet can be picked out as a discrete reflecting surface (Hargreaves, 1997), like that shown earlier in Figure 2.6. It is this ability to distinguish the subglacial bed (Siegert, 1999; Siegert *et al.*, 2003) as a near-continuous trace (Bailey *et al.*, 1964) that has made Z-scopes the primary format of RES data. Such records have been digitised (Young *et al.*, 2007), producing a dataset of bed elevation and *x-y* coordinates of position at 15 s intervals (Siegert *et al.*, 1996). These were used to calculate roughness (Rippin *et al.*, 2004).

SPRI data produce a good record of the bed, which is visible on 86% of flightlines (Taylor *et al.*, 2004). In some regions, as Figure 2.8 shows, no bed signal is visible (Bingham & Siegert, 2009). This is due to a lack of signal strength, a common limitation in radar systems (Swithinbank, 1969). There are several factors that account for loss of signal. Weaker signal returns are received from irregular surfaces (Rose, 1979), such as areas of crevassing (Raymond *et al.*, 2006), which are common where ice speeds are high (Shabataie & Bentley, 1987). Rough surfaces produce higher scatter (Peters *et al.*, 2007), so that the bed may be undetectable, or the resolution will be reduced (Hélière *et al.*, 2008).

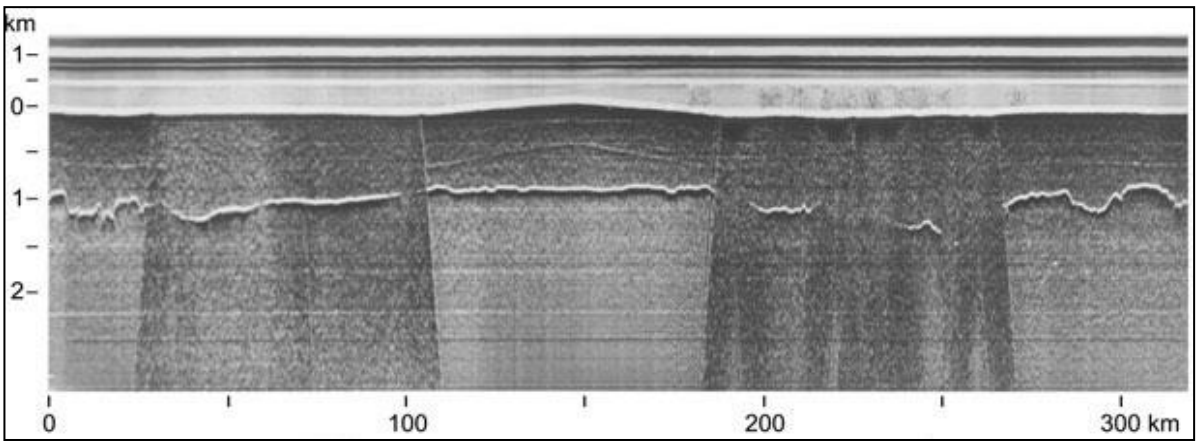

Figure 2.8: Radio-echo sounding profile showing an incomplete record of the bed (Modified from Dowdeswell & Evans, 2004)

The second major cause of a lack of bed detection is ice thickness. As radio-waves are transmitted through a medium, energy becomes absorbed and scattered (Derr & Little, 1970). For example, signal scatter results from radio-wave encounters with supraglacial (Gades *et al.*, 2000a) and englacial debris (Dowdeswell & Siegert, 2004). The further radio-waves must propagate through a medium, the higher the absorption and, therefore, the lower the signal power return. Under thick ice, signal returns may be too weak to be detected so that the bed is not captured (Gades *et al.*, 2000b).

In their current format, SPRI data do not capture most of the lower end of meso-scale (i.e. variation on the order of tens of metres) variations in roughness because the resolution is

too coarse. The along-track sampling interval of ~2.2 km (Young *et al.*, 2007; Bingham & Siegert, 2009) limits study of roughness to the macro-scale. Nevertheless, this increment arises from sub-sampling of the SPRI data (Taylor *et al.*, 2004), and it remains possible to re-digitise flightlines at higher resolution (Bingham & Siegert, 2009; Siegert *et al.*, 2004).

The SPRI measurements have a number of problems, such as poor resolution relative to modern datasets, and the fact that many of the records are incomplete due to missing observations. Nevertheless, as Turchetii *et al*. (2008) discuss, the fact that SPRI data are still much in use after several decades is a testament to their importance. Nearly all studies on bed roughness at the macro-scale have used these measurements (see Bingham & Siegert, 2009 for a summary). As a result, these data underpin many of the findings presented in Section 2.3.

2.5 Discussion

2.5.1 How much do we know about roughness and ice dynamics?

This chapter has presented a summary of the controls on ice dynamics, in particular, those that are responsible for spatial variations in ice speed. The focus of the review has been on the roughness of the subglacial bed. Theories suggest that ice dynamics (particularly basal ice speeds) are related to the roughness of the subglacial bed (Paterson, 1994; Joughin *et al*., 1998; Schoof, 2002) at a range of spatial scales. As Section 2.3 described, roughness was once used as a constant in numerical models, and some examples of this still exist (e.g. Hindmarsh, 2000). Increasingly, however, roughness parameters have been used to measure the topography of subglacial beds. In particular, research has investigated how spatial patterns in roughness are related to variations in ice speed (Rippin *et al*., 2004; Siegert *et al*., 2005b). Findings show that decreasing roughness values correspond with increasing ice speeds (Bingham *et al*., 2007; Bingham & Siegert, 2009).

Previous studies have identified an association between roughness and ice speed, but a number of uncertainties remain, and these are discussed in more detail below. First, although a pattern has been detected, the strength of this relationship has never been measured. Second, Section 2.2 demonstrated how roughness is just one of many controls that affect ice flow. Although some scientist have postulated a hierarchy of controls (Winsborrow *et al*., 2004), at present there are still uncertainties as to how important roughness is as a control versus other factors. A further complication is that the dominance of a single roughness parameter has limited understanding of the spatial patterns in roughness. Spectral analysis measures many variables, so it has not been possible to describe how particular variations in topography, such as the size or frequency of perturbations, relate to patterns in ice speed. The third challenge in understanding the

relationship between roughness and ice speed is the potential feedback between rates of ice flow and the form of topography because patterns in roughness may result from preferential modification caused by spatial variations in ice speed.

2.5.1.1 The strength of relationship between roughness and ice speed

As presented in Section 2.4.4, several studies have investigated the association between variations in roughness with spatial patterns of ice speed (Taylor *et al*., 2004). Yet, although these investigations have identified a link, the strength of relationship between corresponding patterns of roughness and ice speed has not been measured. With this lack of quantification, it is more difficult to conclude, for example, how important roughness is as a control on ice speed relative to other factors. A demonstration of this can be seen in studies of roughness in ice stream settings.

Given the importance of ice streams for ice sheet discharge and stability (Bennett, 2003), many investigations have sought to identify what drives rapid ice speeds (Stokes & Clark, 2001). Scientists have shown that the topography in ice streaming areas is less rough than the bed at the ice stream margins (Bingham & Siegert, 2009), thus suggesting it is one such control. However, there have been no reports of how distinct the roughness values within ice streams are to those in non-streaming areas. As a result, it is difficult to judge how important roughness is in influencing ice speed. As depicted in Figure 2.9, a potential test would be to determine how distinct the roughness values within ice streams are to the roughness of the surrounding margins. Areas of fast flow may overlap with those of slower flow, but it is also possible that the roughness of these two contrasting ice speeds would fit into discrete populations. If the latter situation were realised, it would imply roughness is a strong control on ice speed, and also suggest that a threshold value of roughness might exist below which fast flow is expected. The identification of thresholds is important for predicting future ice flow behaviour because, modification of the bed that reduces roughness below a critical value, could initiate rapid ice flow. At present, however, the strength of relationship has not been determined, nor have thresholds in roughness associated with rapid ice speed been investigated or found.

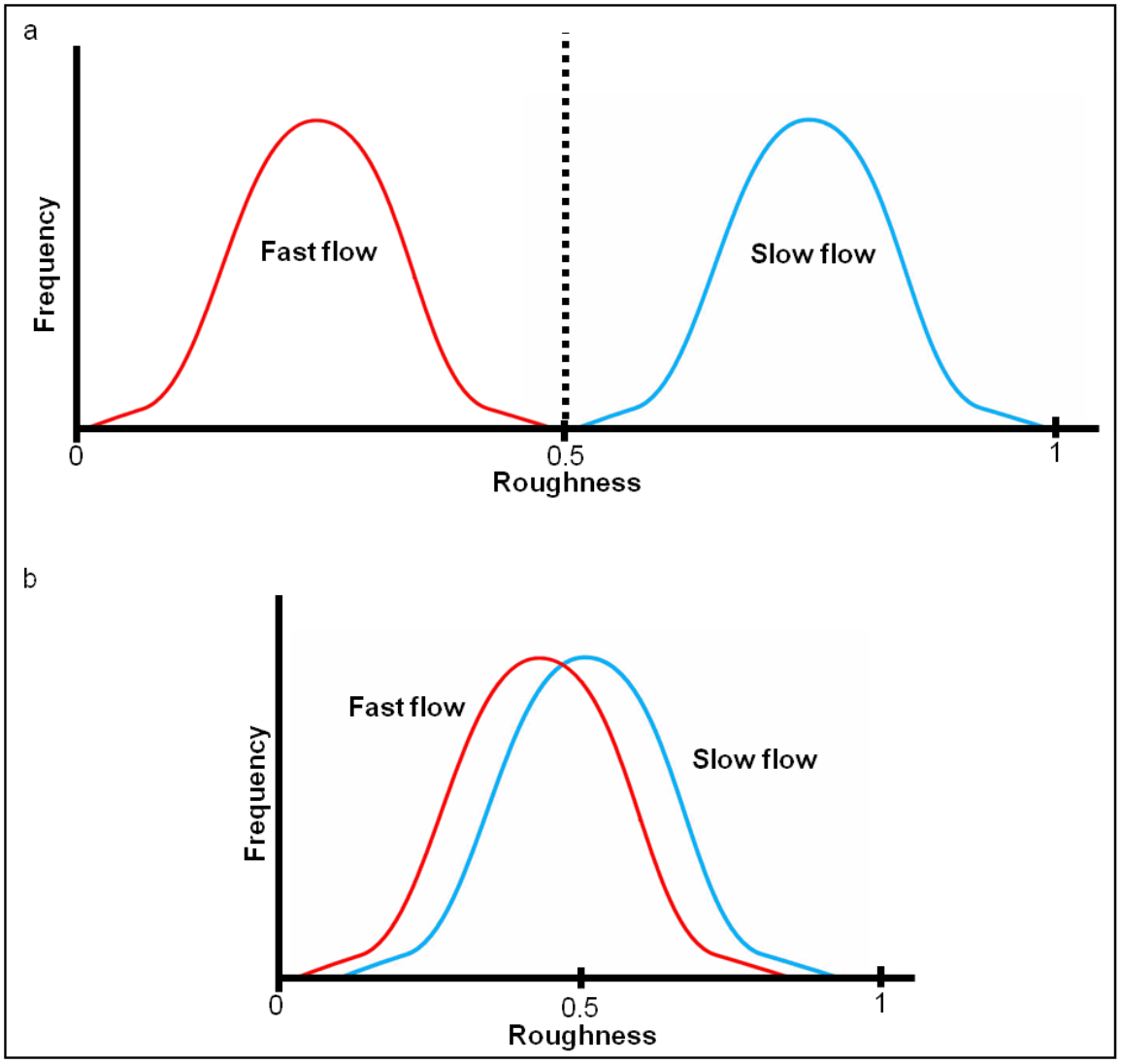

Figure 2.9: Hypothetical association between roughness and ice flow
Red curve shows roughness values from fast-flowing regions; blue curve shows values from slow-flow regions. Roughness values are purely notional.

(a) Two distinct groups: areas of low roughness are always associated with fast flow, and areas of high roughness with slow flow. Dashed line marks a roughness threshold above which flow is always slow. This distribution would support Bingham & Siegert's (2009) hypothesis that ice flow and roughness are associated.

(b) Fast flowing areas are seen to exhibit similar roughness values as slow flowing. This distribution would allow one to reject the Bingham & Siegert (2009) hypothesis that ice flow and roughness are associated.

Another uncertainty over the strength of relationship between roughness and ice speed is what scales of topographic variation are most associated with spatial variations in ice speed. In glaciology, the scales over which roughness has been measured range from millimetres (Hubbard & Hubbard, 1998) to tens of kilometres (Taylor *et al*., 2004). However, it can be seen that the majority of studies have quantified subglacial bed roughness over scales of kilometres. In particular, research done using the SPRI RES measurements has meant analysis has typically been performed over windows of 50 to 70 km (Siegert *et al*., 2005; Rippin *et al*., 2007; Bingham & Siegert, 2009). An obvious lack of information falls within the size range of tens to hundreds of metres. Given that the roughness has rarely been quantified at this scale, there is uncertainty over whether

results would show similar patterns between ice speed and roughness as observed at the macro-scale. The meso-scale is important because it accounts for the size range of many of the subglacial landforms observed on ice-sheet beds. It is interesting to note that, despite the fact that a wide range of measurements have been used to analyse subglacial bedforms and their association with ice dynamics (Clark, 1993; Mitchell, 1994; Stokes & Clark, 2002; Clark & Stokes, 2003; Clark *et al*., 2003; Evans *et al*., 2005), the roughness of these features has never been quantified specifically. This raises questions such as how do changes in the dimensions of elongated bedforms affect the roughness of these features?

In evaluating the present understanding of the strength of relationship between roughness and ice speed, a third factor to consider is that roughness and ice speed is that roughness is an umbrella term, not a single variable. The shape of subglacial topography is made up of many factors such as the vertical height of the surface, and the number and size of asperities. To analyse the link between roughness and ice speed it is necessary to determine the individual and combined effects of each of these variables. Given the dominance of spectral analysis, much of the present understanding of roughness has measured a combined effect of several variables. However, as will be discussed in Section 2.5.2.2, because this technique captures several types of topographic variation it is not possible to determine which variables are most associated with patterns in ice dynamics. Therefore, although patterns between ice speed and roughness have been identified, explaining these spatial distributions remains uncertain. This lack of information is somewhat surprising because, in modelling, several studies have considered the roles of these individual variables: for example, as described in Section 2.3.1, the horizontal size of asperities is thought to control the mechanism of basal ice flow (Paterson, 1994). To unify field observations with theories on ice dynamics, measuring different roughness variables might be useful.

2.5.1.2 The relative importance of roughness as a control on ice dynamics

Given that the roughness of subglacial beds can vary over a range of spatial scales, it follows that some scales of topographic variation may be more strongly related to variations in ice speed than others. Models suggest that the scale of roughness most important for controlling is speed is at the horizontal scale of approximately 1 m, because this affects the mechanism by which ice overcomes obstacles (Paterson, 1994). Nevertheless, under the broad definition of roughness used in this project, it also includes variations in the shape of topography at the scale of kilometres. Section 2.3.5 showed that topographic forcing plays an important role for the location of some types of ice stream. Furthermore, other studies that have not referred to the term roughness but nevertheless investigated how the shape of topography and ice speed are linked, has identified spatial

patterns: for example, the fact that the elongation ratio and length of subglacial bedforms has been found to increase with ice speed, suggests that there is a relationship at the scale of tens to hundreds of metres. Therefore, although the 1 m size range of roughness appears important in some respects, other scales of roughness may also be important. Given that the role of roughness appears to vary with scale suggests that more work is required to explain the linkages between the shape of topography and ice speed at these different scales. In particular, Section 2.3.2 demonstrated a lack of analysis at the scale of tens to hundreds of metres.

Another aspect of the *relative* importance of roughness is its influence on ice dynamics relative to other controls. This chapter has demonstrated that roughness is just one of several variables that affect the amount of resistance to flow. Other factors, such as the rheology of the bed and the temperature of the ice, also influence the amount of shear stress required for motion to occur. Furthermore, another set of variables control the input of energy into the system, and it is these that are the primary drivers of ice flow. As a result, roughness is unlikely to be a first order control on ice speed (Winsborrow *et al.*, 2010). This theory is supported by the fact that the roughness of the subglacial bed primarily appears to influence the resistance to sliding, yet this is just one mechanism of ice flow (Leysinger-Vieli & Gudmundsson, 2010): for example, flow may occur as a result of ice deformation. Evidence from observations of contemporary ice streams also implies that roughness is not a primary control: analysis of the Siple Coast region has found that at least one ice stream has stagnated despite having a smooth bed (Retzlaff & Bentley, 1993; Bingham & Siegert, 2009).

Current theories and findings indicate that roughness is not a primary control on the speed of ice flow yet, it is important to note that the strength of this relationship has never been quantified. For example, although studies using spectral analysis have identified spatial trends between ice speed and roughness, these investigations did not publish a statistical measure of the strength of this relationship. As Section 2.2 showed, although the driving forces appear to be the main control on the rates of ice flow through dictating the amount of shear stress available to do work, it is the resistive forces that are important for localised variations in ice speed. Similarly, the dominance of controls on ice speed can vary between locations. For example, at the Breiðamerkurjökull glacier, Boulton & Hindmarsh (1987) reported that 80 to 95% of the glacier's movement was due to sediment deformation, not sliding (Boulton & Hindmarsh, 1987). Here, although the size of perturbations might affect the way ice deforms (Leysinger-Vieli & Gudmundsson, 2010) roughness is unlikely to be a key factor. In contrast, in their study on ice streams, Gudmundsson (2003) found that basal sliding was responsible for the majority of forward

motion; under sliding, the roughness of the topography would be more crucial in controlling speed.

Another complication in determining the relative importance of controls on ice dynamics, is that many of these are related to the topography. For example, topographic forcing and topographic steps both arise from differences in the shape of the bed, albeit at different spatial scales. If a general definition of roughness is used, where it refers to variations in the shape of the bed topography then, technically, roughness encompasses several area of glacial research. Furthermore, many investigations of ice sheet dynamics have not referred to roughness, but have analysed the relationship between topography and ice speed. For example, although Schoof (2003) did not refer to the term *roughness*, in investigating the *effect of basal topography on ice sheet dynamics*, they effectively used methods that others might consider to be parameters for quantifying roughness. Similarly, Gudmundsson (2011) studied controls on ice dynamics, but instead referred to the term *slipperiness*. In an even broader set of examples, it can be seen how numerous studies on the relationship between bedforms and ice dynamics, and these measurements of bedform dimensions are again examples of roughness parameters. As such, the observed pattern between increasing bedform length and elongation ratios associated with fast ice speeds (Stokes & Clark, 2002), might be considered to be further evidence of a link between roughness and ice dynamics. Given that many controls on ice dynamics are associated with differences in topography, it creates a challenge in determining how important roughness is relative to these other controls. Therefore, before we continue, let us clarify our standing on this point.

One solution to the problem of separating roughness from other controls on ice behaviour would be to define roughness as a change in the shape of topography at a particular scale. Materials science uses such an approach, with variations in the shape of a surface being categorised into three bands. Here, r*oughness* refers to the relatively shortest scale of topographic variation, larger scales are termed *waviness*, and *form* refers to the largest (Kalpakjian, 1997). A similar scheme could be applied to glacial research, but such a framework might not be suitable. As Section 2.3 showed, scientists have measured subglacial bed roughness on horizontal scales ranging from tens of kilometres to millimetres. If a new scheme were devised this would be incompatible with these past publications. Moreover, glaciologists have been free to choose whether to adopt the term roughness. For example, some studies have analysed topography over scales of tens of kilometres and termed this roughness (e.g. Taylor *et al*., 2004; Siegert *et al*., 2004). Yet, in reviewing the hierarchy of controls on ice stream, WInsborrow *et al*. (2010) chose to distinguish *topographic forcing* from *macro-scale roughness*, even though both controls on ice dynamics arise because of changes in the shape of the subglacial bed at the scale of

tens of kilometres. Therefore, simply using different labels does not solve the problem of whether these other controls on ice dynamics should be included.

An alternative method of distinguishing roughness from other controls on ice dynamics such would be to determine how directly the shape of topography is considered to control ice speed. For example, differences in friction arising from variations in the shape of topography are an example where the bed roughness is directly linked to ice speed. With topographic forcing the relationship is less direct: the shape of topography influences the ice thickness that, in turn, influences the shear stress (Paterson, 1994). Using this approach, it is possible to meet the accepted view that processes such as topographic forcing are distinct from roughness. This then allows the importance of roughness in controlling ice speed, relative to these other controls, to be tested.

2.5.1.3 Roughness: a control, a product, or a proxy

Although a relationship between ice speed and roughness has been observed, there is something of a chicken-and-egg scenario, because the cause of this relationship is unclear. On the one hand, the form of topography may control ice speed, but evidence also shows how ice flow modifies the bed so spatial patterns in roughness may be the result of variations in ice speed. This point is complicated further because both the roughness and ice speed vary temporally, both responding to each other (Schoof, 2002). Theoretically, if faster ice speeds produce a lower roughness, a feedback loop might be created where ice flow becomes progressively faster. Such a scenario might lead to ice sheet instability. However, other theories suggest a moderating influence. For example, Schoof (2007) suggests that faster flow might lead to the development of bumps, which would increase the roughness.

It can be seen that the majority of the temporal variability in the roughness of the subglacial bed involve processes that occur over long timescales. In contrast, in theories where the form of the bed controls rates of ice flow, the subglacial bed roughness has an almost instant influence on the rate of basal ice flow, for example, through the presence of bumps that resist ice flow. It is possible to study the latter using observations of bed elevation and ice speed. However, it is less possible to study how roughness changes through time, because the necessary bed elevation records are not available. Therefore, although this project considers the possibility of ice speed influencing roughness, the focus is on how the roughness of the bed controls rates of ice flow.

In Section 2.5.1.2 it was discussed how some of the alterative controls on ice dynamics, relate to the shape of the subglacial bed. Even if roughness is considered to be distinct from, say, topographic forcing, when quantifying roughness it is not possible to separate the role of roughness from other controls. The reason for this is that any of the methods of

measuring roughness may indirectly capture other variables that are controls on ice dynamics. For example, statistics that summarise roughness in terms of changes in height of the ice-sheet bed may indirectly measure ice thickness, because this value is the vertical distance from the ice surface to the subglacial bed. As seen from Section 2.2, the thickness of the ice plays a key role in ice dynamics because this influences the amount of shear stress that drives motion. As a result, any parameter designed to measure roughness may also be a proxy for other ice sheet controls. If measures of roughness are proxies for other variables linked to ice dynamics, this creates a challenge of determining the extent of the direct relationship between roughness and ice speed.

Whether roughness is directly or indirectly linked to ice dynamics may be influenced by a number of factors. One of these is the scale of analysis. If roughness of subglacial topography were measured over scales of kilometres, some parameters would detect spatial variations associated with the presence of mountain ranges. As Section 2.3.1 discussed, on these scales mountains and valleys play a key role in dictating ice speeds by topographic forcing. Thus, if analysis found a relationship between roughness and ice speed this may be due to the parameters indirectly measuring changes in ice thickness for example. In contrast, Section 2.3.3 showed how roughness has also been measured at a resolution of millimetres (Hubbard & Hubbard, 1998). At these scales it is unlikely that measurements of roughness would be associated with changes in ice thickness. Therefore, analysis of the relationship between roughness and ice speed is more likely to measure the direct effects. Nevertheless, even at the millimetre scale there may still be indirect linkages, with roughness acting as a proxy for a different set of variables. For example, measurements of topography at this scale may be sensitive to differences in rheology. Another factor that may influence the likelihood of roughness variables being proxies is the type of topographic variation they are designed to measure. For example, returning to the above example of ice thickness, it is more likely that a measure of roughness that calculates the vertical change in height of a surface is more likely to be a proxy for ice thickness than one that summarises the horizontal wavelength of asperities.

Measurements of roughness appear inescapably linked to other controls on ice dynamics because many are measured from, influence, or are themselves controlled by the shape of subglacial bed topography. This creates a further challenge in assessing the importance of roughness in controlling rates of basal ice flow. Without the use of ice sheet models, it is unlikely that such proxy effects could be separated from the direct role roughness plays on ice speed. Nevertheless, this challenge has always been present in investigations of roughness that have used field measurements. Indeed, Siegert *et al*. (2004) discuss that roughness may control ice dynamics both through directly through its effect on frictional resistance, but also by influencing the hydrology, thus including any

proxy effects in their summation of the relationship. The fact remains that more research is required to determine what roughness variables are most related to ice dynamics. This is the focus of this project. The next step would then be to determine whether these variables are directly related to variations in ice dynamics, or are instead proxies.

Even if some statistical summarises of roughness are proxy measures for other variables, this may still make measurements of roughness valuable to scientists wishing to understand ice flow at the subglacial bed. In Section 2.2 the influence of rheology on ice speed was described. With the inaccessibility of the bed determining the rheological conditions of an area may be relatively more difficult than gathering information on its roughness. Thus, if roughness were found to be a proxy for these effects, it would provide useful data for locations where measurements of rheology cannot be made. To achieve this, however, it is first necessary to determine which roughness variables are most related to patterns in ice speed.

2.5.2 Quantifying roughness

2.5.2.1 Choices of data

With the use of SPRI data to quantify the roughness of contemporary ice sheet beds, previous workers have effectively been limited to investigating scales of tens of kilometres. For example, despite the use of 25 km windows by Rippin *et al*., (2011), which were relatively short compared with most studies of RES data (Bingham & Siegert, 2009), this scale was still too coarse to capture variations on the order of tens of metres. The problem does not lie with the roughness parameters because, as discussed in Section 2.4.2, spectral analysis or the other methods can theoretically analyse surfaces at a finer resolution. The limitation that prevents studies of meso-scale roughness is the lack of data.

As recognised in other areas of glacial research (e.g. Arrell & Carver, 2009), the challenges of studying processes at a finer scale can be overcome through access to better data. To achieve a finer scale analysis, one solution would be to improve the resolution of SPRI measurements through re-digitising. Although the 1.8 to 3 km sampling interval between observations (Siegert, 1999; Siegert *et al.*, 1996; Siegert *et al.* 2004, 2005b; Taylor *et al.*, 2004; Siegert *et al.*, 2005b; Bingham & Siegert, 2009) is relatedly large, it is partly due to the fact that the data were sub-sampled before being used (Siegert *et al.*, 2004; Taylor *et al.*, 2004; Young *et al.*, 2007; Bingham & Siegert, 2009). Several authors have highlighted that resolution can, theoretically, be improved by re-digitising the photographic films (Siegert *et al.*, 2004; Bingham & Siegert, 2007b; Bingham & Siegert, 2009). Siegert *et al.* (2004) and Taylor *et al.* (2004) reported that this has been achieved, re-digitising an approximately 250 km long section of z-scope at 200 m interval.

Nevertheless, a review of this procedure was not published, so the accuracy of this technique and ability to apply it to longer flightlines has not been determined.

There is no indication on the degree of improvement that could be achieved in re-digitising SPRI records but, given the reported accuracy of the system (See Section 2.4.3) it is unlikely that it would cover the full meso-scale range. Therefore, there is a need to identify alternative datasets that have superior resolution. As technology continues to advance, the resolution and navigational accuracy of bed elevation measurements has improved (Gogineni *et al.*, 1998, 2001; Steinhage *et al.*, 1999; Rippin *et al.*, 2006; Shepherd *et al.*, 2006; Bingham, 2007; Carter *et al.*, 2007; Hélière *et al.*, 2007; Peters *et al.*, 2007), but there are still some sources of inaccuracy with radar measurements. For example, the speed of wave propagation through an ice sheet is not fully understood (Barrett *et al.*, 2007), thus affecting certainty over the position of the bed. Furthermore, although some higher resolution measurements of contemporary ice-sheets settings are becoming available (e.g. Theakstone & Jacobsen, 1997; King *et al.*, 2009), the spatial coverage of these data is poor. This fact would make it challenging, for example, to compare the roughness of ice stream beds with that of the surrounding ice sheet. What is required are data that have both high resolution and large coverage.

As discussed in Section 2.5.1.1, much of our understanding on subglacial bed roughness is at the macro-scale, but to understand the relationship between ice dynamics and topography, bed elevation measurements are required from a range of areas. Here, the large spatial coverage of many remotely sensed data would be an advantage. In glaciology the SPRI data are an obvious choice. The limitation of these RES records, however, is that despite covering a large area, their resolution in terms of the distance between measurements is relatively poor. In effect, therefore, previous workers have been limited to quantifying roughness over tens of kilometres.

2.5.2.2 Roughness parameters

Spectral analysis remains the most used method in glaciology, with Bingham & Siegert (2009) summarising the many studies that have used this method to quantify roughness at the kilometre scale. Quite why is a little unclear, except that, as often happens, scientists have mostly employed similar techniques as earlier authors. For example, Paterson's (1994) classic textbook details spectral analysis in his chapter on glacier sliding, and he gives yet earlier references. However, although being useful, a number of limitations are apparent (Section 2.4.3). Furthermore, because the use of spectral analysis for quantifying subglacial bed roughness has been developed alongside the use of SPRI radio-echo sounding measurements of bed elevation, there is uncertainty how choices such as the sampling interval of data or window length would affect the results. This has implications for whether different studies are comparable because, in the future, it is likely

that different datasets will be used. From recognition of these weaknesses, there is growing acknowledgement that the methods currently used to measure roughness require evaluation (Feng *et al.*, 2003; Bingham & Siegert, 2009).

In the future, alternative parameters could be used to investigate subglacial topography. As discussed in Section 2.4.1 other research offers such roughness parameters. One advantage of adopting methods from other sciences is that many have been evaluated within particular disciplines (e.g. Gadelmawla *et al.*, 2002). Moreover, many of these techniques are dimensionless, so the scales of roughness that could be studied are limited only by the resolution of the data.

2.5.2.3 Quantifying roughness in 2D and 3D

Another factor related to data resolution is ability to quantify roughness in three dimensions. Despite the common use of 3D spatial analysis in geography and other sciences, glaciologists have rarely applied these methods to quantifying roughness, with the work by Winsborrow (2007) being one of the few exceptions. The near-exclusive use of 2D parameters may have been due to choice of data, because the large distances between flightlines (Lythe *et al*., 2001) prevent 3D methods being used. By using records such as DEMs, spatial patterns could be better understood. This may improve glaciologists' understanding of how the roughness varies with direction testing, for example, whether roughness is always lower in the direction of ice flow (Rippin *et al*., 2007). One source of 3D data is formerly glaciated terrains.

2.5.3 The potential of palaeo ice-sheet beds as high-resolution data sources

Both palaeo and contemporary ice sheets can be used to investigate ice sheet dynamics (Bamber, 2003). Formerly glaciated terrains have been used in many areas of glacial research, such as reconstructions of past ice dynamics (e.g. Kleman & Borgström, 1996; Ballantyne *et al.*, 1998; Clark & Meehan, 2001;Smith *et al.*, 2006a, 2006b; De Angelis & Kleman, 2008; O'Cofaigh & Stokes, 2008). Analysis of these landscapes have been used to determine former flow speeds (Clark, 1997; Stokes & Clark, 1999, 2001) and flow directions (Näslund *et al.*, 2003) of former ice sheets by analysing the topography and sediments of areas that were once glaciated (Evans *et al.*, 2005). Yet, despite the range of research, few investigations have analysed the roughness of these landscapes, let alone used such measurements to infer former ice sheet conditions.

The reason why palaeo landscapes have rarely been used in roughness studies is unclear, especially given that such studies appear theoretically possible. With palaeo beds being accessible in many countries, data are widely available (Knight & McCabe, 1997; Christofferson & Tulaczyk, 2003b; De Angelis, 2007; Dyke, 2008). Such DEMs have been used in a number of ways to analyse spatial patterns in topography (Etzelmüller, 2000),

but for some reason, these data have been under-used in studying roughness. One of the few exceptions is Winsborrow (2007), who used summary statistics to compare the roughness of different areas in Britain. The reason for their lack of use is unclear, especially considering that they might have some advantages over contemporary records. Bamber (2003) discusses how studies of ice dynamics, such as the controls on ice streaming, can be investigated in both palaeo and contemporary environments. With studies of roughness however, research has been focused only on the

Like contemporary ice sheet datasets, those of palaeo-beds produce a record of elevation change (Stokes & Clark, 2003a) which could be used to calculate roughness. However, an advantage of formerly glaciated terrains over contemporary ice-sheet settings is that the better accessibility of the former means that their coverage and their resolution is often higher. This potential has been recognised (Taylor *et al.*, 2004; Bingham & Siegert, 2009), but, thus far, not exploited. Through ease of access, the resolution of palaeo-bed datasets such as Digital Elevation Models (DEMs) is superior to RES data (Clark, 1997; Smith & Clark, 2005; Smith *et al.*, 2006b; Racoviteanu *et al.*, 2007). Examples of this are given in Table 2.1, which summarises the horizontal resolution of some palaeo-bed DEMs. All of these have sampling intervals superior to that of the SPRI radio-echo measurements. Some, such as the 5 m resolution of NextMap data (Clark *et al*., 2009), are considerably finer. Palaeo data are available for numerous terrestrial locations, from the 30 m resolution terrestrial records of the Canadian Digital Elevation Data (CDED) of Canada, to bathymetric measurements (Johnson & Smith, 1997; Ottesen *et al.*, 2008). The use of bathymetry in studying roughness has been demonstrated by Fox & Hayes (1985), who used various statistical techniques to investigate roughness of the sea floor. The availability of these data might allow roughness to be quantified in 3D.

Resolution (m)	Source
1000	Stokes & Clark (2004)
500	Clark & Stokes (2001); Stokes & Clark (2003)
235-930	Alexanderson *et al.* (2001)
200	Glasser & Jansson (2005)
50	Clark *et al.* (2004); Jansson & Glasser (2005)
30	Hubbard (1999)
25	Clark & Meehan (2001)
10	Gupta *et al.* (2007)
5	Clark *et al.* (2009)

Table 2.1: Horizontal resolution of a selection of Digital Elevation Models used to investigate palaeo-ice sheet beds. Note: in comparison, SPRI data have a horizontal sampling of ~2.2 km.

2.5.3.1 Uses of palaeo-roughness measurements

To an extent, it might not be possible to reproduce the studies done in contemporary environments. For example, comparing the relationship between roughness and ice speed would be challenging because formerly glaciated terrains can only be estimated through the use of proxies. Among the most common techniques for reconstructing ice speeds in palaeo environments is analysis of bedform morphometry, such as the length and elongation ratio of features (Clark, 1993; Mitchell, 1994; Iverson *et al*., 1995; Hart & Smith, 1997; Hindmarsh, 1997; Hart, 1999; Maltman *et al*., 2000; Stokes & Clark, 2002; Clark & Stokes, 2003; Clark *et al*., 2003; Moreau *et al*., 2005; Roberts & Long, 2005). However, one potential problem is that these only give relative differences in ice speed, not specific measurements.

Another limitation is that the features used to infer former ice-sheet behaviour are also those measured when quantifying roughness. For example, the morphology of subglacial bedforms such as drumlins is a common proxy for ice speed and direction (Dyke & Morris, 1988; Mitchell, 1994), but these features would be captured in records of bed elevation. Even other proxies for ice flow such as sedimentology (Evans *et al.*, 2005), erratic dispersal trains (Clark *et al.*, 2000; Kjær *et al.*, 2003), surface weathering of rocks (McCarroll & Nesje, 1993), or striae (Kleman, 1990; Rae *et al*., 2000) form part of the subglacial topography, so technically affect the roughness at some scale. The only way to avoid this problem might be to use numerical ice sheet models (e.g. Tarasov & Peltier, 2004), but even these may have been calibrated using topographic variables.

Although the techniques used to analyse roughness and ice speed in contemporary settings may not be applicable to palaeo ice-sheet beds, there are other methods that allow formerly glaciated terrains to be analysed. For example, these locations would lend

themselves to the study of meso-scale subglacial bedforms because, here, different landform assemblages can be readily identified (Clark *et al*., 2004). This would allow the roughness of different types of features to be measured and compared. A search of the scientific literature found no such studies where the roughness of bedforms had been compared.

An interesting possibility is that, if groups of bedforms show a pattern of roughness, this could mean that certain roughness values would act as *signatures* allowing particular assemblages to be identified beneath current ice sheets or in formerly glaciated areas. In other sciences, roughness has been used to identify landforms (e.g. Grohmann *et al*., 2009). Many glacial features are defined by their dimensions, such as the length of their long axis and elongation ratios (Rose, 1987; Evans *et al.,* 2005). Other types of statistics have been used to measure these variables (Evans, 1987; Hattestrand *et al*., 1999; Spagnolo *et al*., 2012), allowing spatial patterns to be detected, and roughness parameters could be used in a similar way. Here, the intrinsic link between morphometry and roughness is an advantage because, if roughness parameters capture these bedform dimensions, it would allow them to be used to classify topography. For example, areas with similar topography (such as two drumlin fields) should produce similar results allowing landscapes to be classified.

Another way to use data from formerly glaciated terrains would be to reconstruct former ice speeds based on how roughness is expected to control basal ice flow. For example, the hypothesis that ice speeds decrease as roughness increases could be used to infer relative patterns in ice speed. These reconstructions based on roughness could then be compared with ice speeds inferred from other evidence. This would test, for example, whether areas of fast flow inferred using bedform morphometry have a lower roughness.

2.5.3.2 Sources of information on other variables

Formerly glaciated terrains also offer additional information that is frequently unavailable from contemporary settings. Ice speeds do not depend solely on bed topography; other controls such as sediment rheology (Rattas & Piotrowski, 2003) and geology (Bell *et al.*, 1998; Bingham & Siegert, 2007a, 2009) influence ice speeds (Stephenson & Bindschadler, 1998; Raymond *et al.*, 2006; Stokes *et al.*, 2007; Anderson & Fretwell, 2008). Furthermore, geology also influences the susceptibility of the bed to erosion (Paterson, 1994; Bennett & Glasser, 1996; Siegert *et al.*, 2005a; Iverson *et al.*, 2007), and so might control the rate at which roughness might change through time (Siegert *et al.*, 2005b; Rippin *et al.*, 2006). Although rheology and geology vary spatially across ice sheets (Gordon, 1981; Alley, 1993; Harbor *et al.* 1997; Rippin *et al.*, 2006), recent studies using RES data have not taken account of this. In formerly glaciated terrains, readily available information on sediments and geology would allow testing of how these play a

role in the roughness. For example, are particular roughness values associated with a certain structure or type of rock?

2.6 Conclusions

A review of the methods currently used for quantifying roughness is required. Section 2.4.2 identified that relatively few techniques have been used, and demonstrates the potential benefits of applying other methods of measuring roughness. Therefore, there is a need to identify other parameters that might be relevant to glacial research and evaluate their suitability. In support of this, testing is needed on the potential of using other types of bed elevation data, such as that from formerly glaciated terrains.

The second major theme is the need to further our understanding of how the roughness of subglacial topography relates to variations in ice dynamics. In particular, studies at the scale of tens to hundreds of metres are required because there is currently a lack of measurements on roughness at this scale. Studies might investigate the roughness of the subglacial bedforms lying within this size range.

2.6.1 Research themes

This chapter on the history of studying subglacial bed roughness has identified a number of areas where more research is required, and these formed the main objectives of this project. Below it can be seen that these objectives were subdivided into a number of smaller research goals:

Objective 1: Evaluate new and existing methods of quantifying roughness

- 1.1: Improve the resolution of RES bed elevation measurements
- 1.2: Test the effect of sampling and window length on spectral analysis
- 1.3: Test how the orientation and location of profiles affects results
- 1.4: Examine the feasibility of quantifying subglacial bed roughness in 3D
- 1.5: Identify alternative methods of analysing roughness
- 1.6: Evaluate the compatibility of various roughness parameters for use with subglacial bed data
- 1.7: Determine the sensitivity of roughness parameters to different topographic variables

Objective 2: Investigate whether there is a relationship between ice speed and roughness

- 2.1: Analyse changes in roughness along an ice stream
- 2.2: Compare the roughness inside and outside of an ice stream at the lateral margin
- 2.3: Evaluate the strength of relationship between subglacial bed roughness and ice speed

Objective 3: Evaluate the role of roughness in influencing ice speeds using data from palaeo landscapes

3.1: Compare the roughness results of different bedform assemblages

3.2: Measure the roughness of area that has remained unmodified by ice flow

3.3: Determine whether roughness parameters can be used to identify and classify subglacial bedforms

CHAPTER 3

An assessment of the use of spectral analysis for quantifying subglacial bed roughness: the effects of data resolution and window size

3.1 Introduction

Spectral analysis has been used to quantify roughness by measuring changes to the power spectral density along a profile (Taylor *et al*., 2004). As described in Chapter 2, this method has been widely used for investigating ice-sheet beds (e.g. Siegert, 1999; Siegert *et al.*, 2004; Taylor *et al.*, 2004; Bingham *et al.*, 2007; Bingham & Siegert, 2009; Rippin *et al*., 2011). Several options can be used to adjust its functionality but, traditionally, the same values for user-defined variables have been used. In response to changing technology, which has seen a constant increase in data resolution, it is likely that future analyses will require modification to the method. Two such variables are the sampling interval of the bed elevation measurements and the window size used to calculate roughness. Because glacial studies have never changed these criteria, it is unclear how they may influence the results: for example, one uncertainty is whether results produced using data with different resolutions are comparable.

The method of spectral analysis traditionally used to quantify the roughness of subglacial beds required the users to choose the number of points analysed by selecting a power of 2 (Taylor *et al*., 2004). In all cases, this chosen *N*-value was 5, giving analysis windows of 32 points (Siegert *et al*., 2004; Bingham & Siegert, 2009). However, with no published review of this method, the motivation for this choice is unclear. The driving factor may have been the need to compromise resolution with statistical reliability. Taylor *et al.* (2004) highlights that assessing local changes in roughness was a priority in their study, but such ability is lost as window length increases: had an *N*-value of 6 or greater been chosen, windows would have been over 100 km long, giving a poor resolution to the results. Had a lower *N*-value was used (i.e. 4 or below), calculating roughness over 16 points or fewer might have jeopardised the reliability of results. It is notable that Siegert *et al.* (2004) suggest that larger window sizes than 32 points could be used, but they do not suggest the use of smaller. In effect, the continued use of SPRI data maintained the status quo, and demonstrates that the choice of window length is partly determined by the sampling interval of the raw data. With the growing availability of other measurements, it has

become possible to assess roughness over different scales and, with the emergence of these data, the window size may be changed in response.

3.2 Objectives

The primary aim of this chapter is to assess how resolution affects spectral analysis values, and whether the interpretations made about the roughness of the topography would differ as a result. The two aspects of resolution considered were the sampling interval of bed elevation measurements, and the length of analysis window.

Determining the effect of data resolution on results required a record of bed elevation measure at different sampling intervals. As described in Section 2.5.2, scientists have postulated that radio-echo sounding measurements gathered during the SPRI campaigns could be re-digitised. By using these profiles it allowed their theory to be tested, and also provided the measurements needed for testing.

3.3 Methods

3.3.1 Finding a suitable flightline for re-digitising

The first objective of this study was to develop a method capable of manually re-digitising z-scope images at different resolutions. In practice, there are some difficulties in re-digitising: for example, it is not possible to re-sample the bed automatically. Re-digitising the SPRI dataset was done using scanned images of z-scope photographic films, which had been provided by Rob Bingham (personal communication, 11/02/09). To digitise bed elevation, a number of conditions had to be met. First, the bed had to be visible as a near-continuous trace. Although over seventy images were provided, many were unsuitable because the bed trace could not be distinguished for much of the profiles' length. Such problems are commonly reported in the literature (e.g. Taylor *et al.*, 2004): the bed may not be resolvable under thick ice (Gades *et al.*, 2000b; Bingham & Siegert, 2009), or where the aircraft changed direction (Siegert *et al.*, 2004). Other flightlines had a high number of artefacts, such as parabolas, on the image. It must be remembered that many of the measurements were gathered on missions where radio-echo sounding technologies were being developed and tested (Turchetti *et al*., 2008) and, as such, suffer from problems such as noise. This noise may have been produced by scatter of radio-waves (Rose, 1979; Siegert *et al.*, 2005b), such as in areas where the ice exhibits crevassing (Raymond *et al.*, 2006). If only flightlines with a complete record of the bed had been used, few, if any, of the SPRI profiles would have been suitable. Previous studies had overcome the problem of missing data by using interpolation over short sections (Siegert *et al*., 2004; Taylor *et al*., 2004) and, as discussed in Section 3.3.3, a similar approach was used in this project.

Spectral analysis also requires the data to be normally distributed about the mean. Taylor *et al*. (2004) report that, once detrended, the SPRI measurements meet this criterion, so this method was adopted. A third condition of the data was the need for navigational information, so that the position of bed elevation observations could be georeferenced. Additional files listed the coordinates for each of the shotpoints, but these were missing for some profiles and meant these could not be used. Where included, the location of each shotpoint was listed in Decimal Degrees. These coordinates were converted to South Pole Stereographic Projection, so that the distance between points in metres could be calculated.

A fourth necessity was a means of comparing the re-digitised data with those gathered by the semi-automatic trace reader so that agreement could be tested. All z-scopes have tick marks (also termed *shotpoints*) along their horizontal axes (see Figure 3.1). These points are marked at a regular interval equivalent to 20 s flight time (Taylor *et al*., 2004) and it is at these points that a subsample of the data were taken and used in investigations of roughness (e.g. Rippin *et al.*, 2004; Siegert *et al.*, 2005b; Bingham & Siegert, 2009). Each shotpoint has a unique numerical ID (Bingham, personal communication 11 February 2009), making it possible to co-reference positions along the z-scope to both navigational coordinates and measurements used in earlier studies. However, on some profiles the shotpoints were absent and, on others, the shotpoints were recorded as tick marks but were not labelled with their ID number, making it impossible to link them with the navigational coordinates.

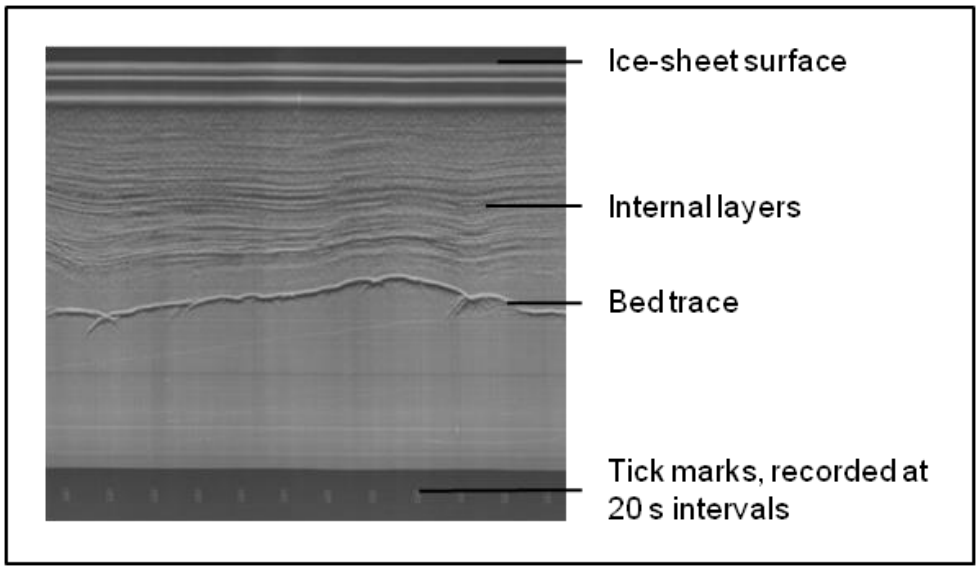

Figure 3.1: A SPRI z-scope image. Shotpoints, marked as tick marks along the horizontal axis, were a requirement for manual re-digitising. On this profile, the ice-sheet bed appears as a near-continuous trace, thus fulfilling one of the other conditions needed for re-digitising.

Of the z-scope images provided, *Flightline 122 part 2* (known hereafter as *Flightline-122*) was found to meet all of the above criteria. In addition, this profile appeared to exhibit a

range of topography in terms of variable amplitude, wavelength, and shape of peaks and troughs. This variation was advantageous because a range of roughness results would be produced. Located in central Antarctica (see Figure 3.2 for map), Flightline-122 was captured during the 1974/75 SPRI-NSF-TUD campaign. At approximately 572 km long, the image had 286 bed tick marks giving navigational data. Having identified a profile, the next step was to construct a method of manually re-digitising the profile.

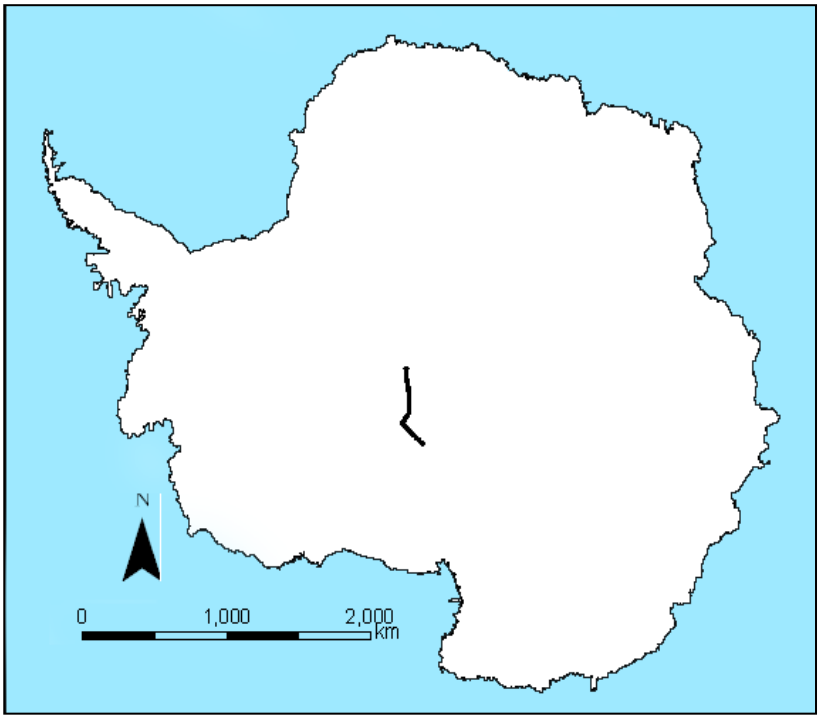

Figure 3.2: Location map for Flightline-122

3.3.2 Steps taken to improve sampling resolution

The z-scope photographic film of Flightline-122 was uploaded into Adobe Photoshop. On the initial image the tick marks were labelled at intervals so, to ease their identification, ID numbers were written onto each unlabelled tick mark. The labelled z-scope image was then uploaded into ESRI ArcMap to be re-digitised. Shapefile points were manually added, marking the horizontal position of shotpoints along the profile. As illustrated in Figure 3.3, vertical lines were then drawn from each tick mark. At the position where each of these lines intersected with the ice-sheet bed, its height was recorded using another set of shapefile points. This gave a record of changing bed elevation at the same interval as the semi-automatic trace-reader measurements used in other studies (such as Taylor *et al.*, 2004).

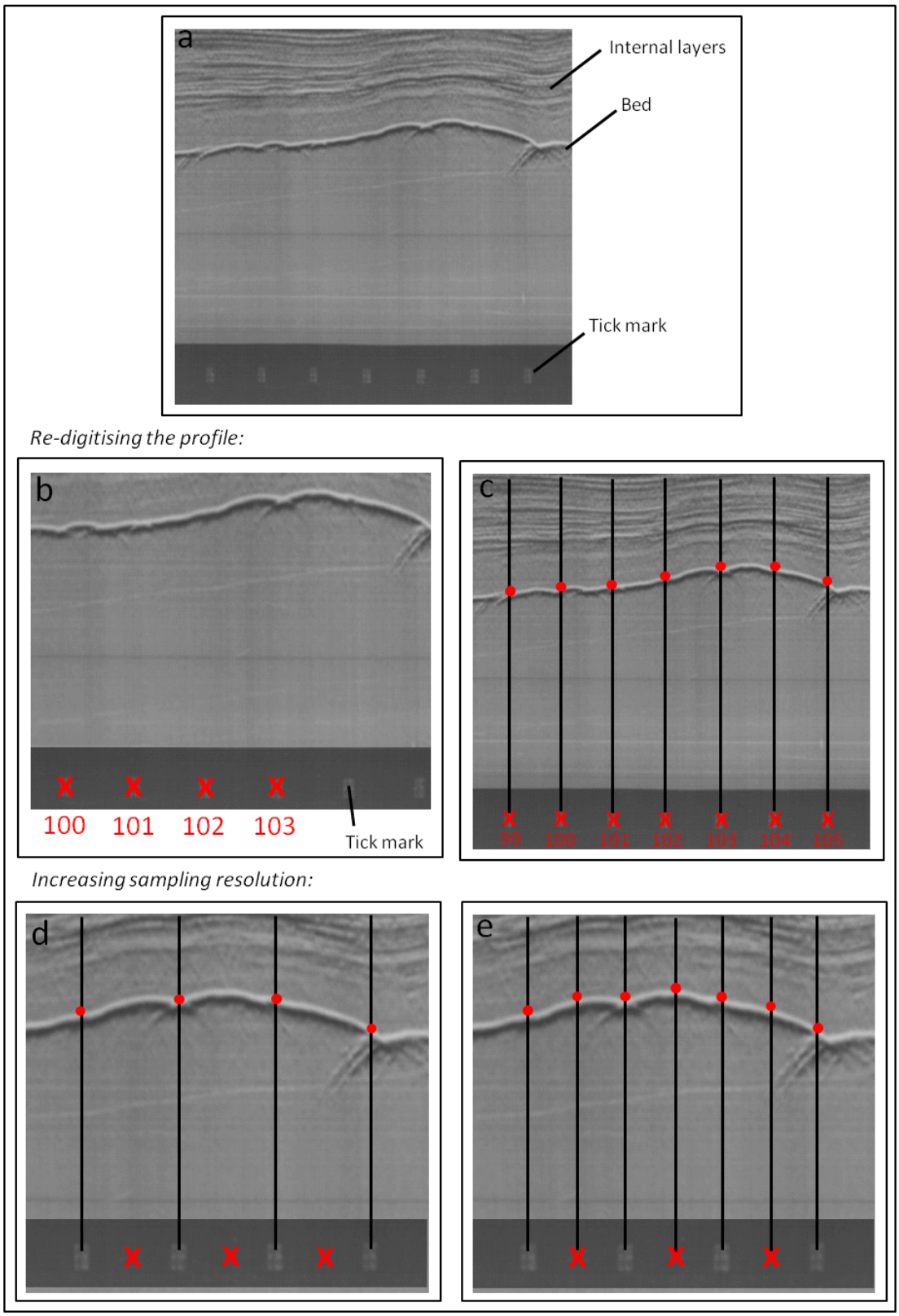

Figure 3.3: Digitising of Flightline-122 in ArcMap. (a) Profile in its raw format. (b) Each tick mark was labelled, and its position recorded. (c) Vertical lines were extended from each tick mark, and where each crossed the bed trace, the position was marked. (d) Sampling resolution was increased by adding additional points between each tick mark. (e) Vertical lines were drawn from new tick mark positions, and the bed marked. This process was repeated, each time doubling resolution.

To reduce the sampling interval, additional points along the bed were digitised (Figure 3.3d & e). The number of points was first doubled by linearly interpolating the horizontal mid-point between each tick mark. From these points, vertical lines were again added and the position of the bed marked. To determine where each re-digitised point was located, coordinates were calculated by linearly interpolating the latitudes and longitudes of tick marks. The process of halving the sampling interval, marking the bed elevations, and determining the coordinates was repeated twice more, each time doubling the number of points.

Rather than doubling the number of points in a series of repeated steps, interpolation could have been used to simultaneously create six points between each pair of shotpoints. However, the approach of repeatedly doubling the number of points was taken because, it was not known at that stage, how long it would take to record the bed elevations: linear interpolation was a simple and rapid step, but this only determined the positions of where new bed elevation data were to be gathered. Marking the position of the bed was a manual process.

Ultimately, 2189 bed elevation measurements were gathered, resulting in an eight-times higher resolution than earlier studies. As Table 3.1 demonstrates, this reduced the sampling interval to c.294 m compared with approximately 2355 m spacing of the trace-reader data used by earlier workers (e.g. Taylor *et al.*, 2004).

	Trace-reader	**Re-digitised**
Mean	2354.89	294.36
SD	327.14	40.83
Minimum	1253.37	156.67
Maximum	3081.41	385.18

Table 3.1: Summary statistics (in metres) for the sampling interval between adjacent shotpoints. A comparison of trace-read and re-digitised data

In some areas, the bed could not be digitised as the trace appeared indistinct or was absent, appearing similar to the z-scope image, see for example, Figure 3.4. For data manually re-digitised at 20 s intervals, bed elevation could not be determined in 8 observations (2.8% of the total); 100 observations (4.4% of the total) could not be digitised for the data re-digitised at eight-times-higher resolution, although many of these were grouped at specific locations rather than distributed throughout the profile's length.

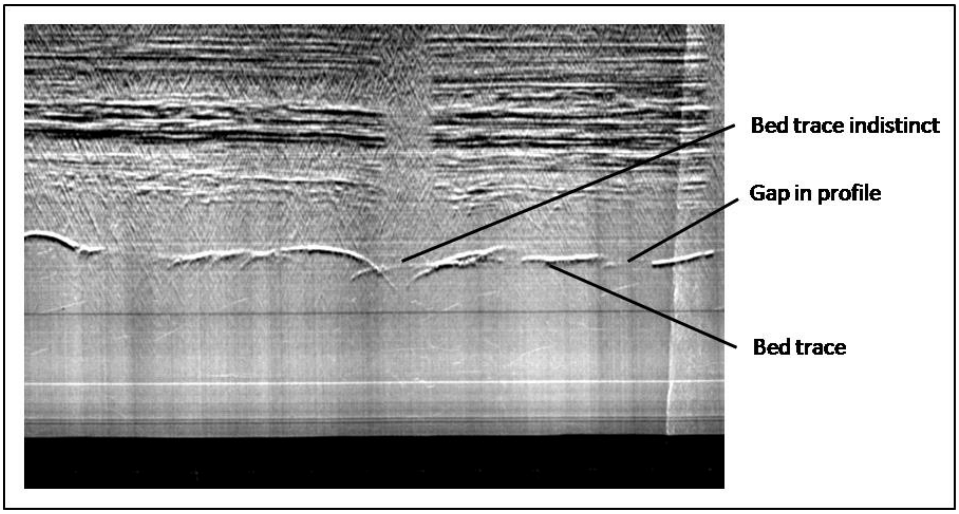

Figure 3.4: Z-scope image exhibiting gaps in the profile and areas where the bed trace is indistinct

It is important to note that, although there were tick marks giving horizontal distance, the z-scope images had no vertical markers. Therefore, although re-digitising allowed the position of the bed to be measured, the bed elevation values were not in metres. This was not a problem because trace-read measurements could be used to calibrate the re-digitised data. In effect, each point in the re-digitised record measured at a shotpoint had a corresponding trace-read measurement for which bed elevation was known. Using these points it was possible to determine the vertical scale of the image, thus allowing the remaining points to be converted.

The need for manual re-digitising meant that inferring the height of the bed in z-scopes was partly subjective. To determine the reliability of manual re-digitising, the agreement between results sampled using different methods was evaluated. Roughness statistics for both sets of data were then produced using spectral analysis. These values were then compared to determine how the sampling interval of the data had affected the results.

3.3.3 Calculating roughness using spectral analysis

To calculate roughness using spectral analysis, earlier workers have followed a set method (Rippin *et al.*, 2004; Taylor *et al.*, 2004), producing macro-equipped spreadsheets to expedite the process. To maximise the comparability between this study and those of earlier workers, the same Microsoft Excel spreadsheets were used to process the re-digitised coordinates and bed elevations, detrending the profile and removing large wavelengths. The macros grouped the data into windows, then detrended the data using least squares best-fit (Siegert *et al.*, 2004), and calculated midpoint values for each window. The midpoint values were later used to plot roughness values for each window (as with Bingham & Siegert, 2009; shown in Figure 3.5).

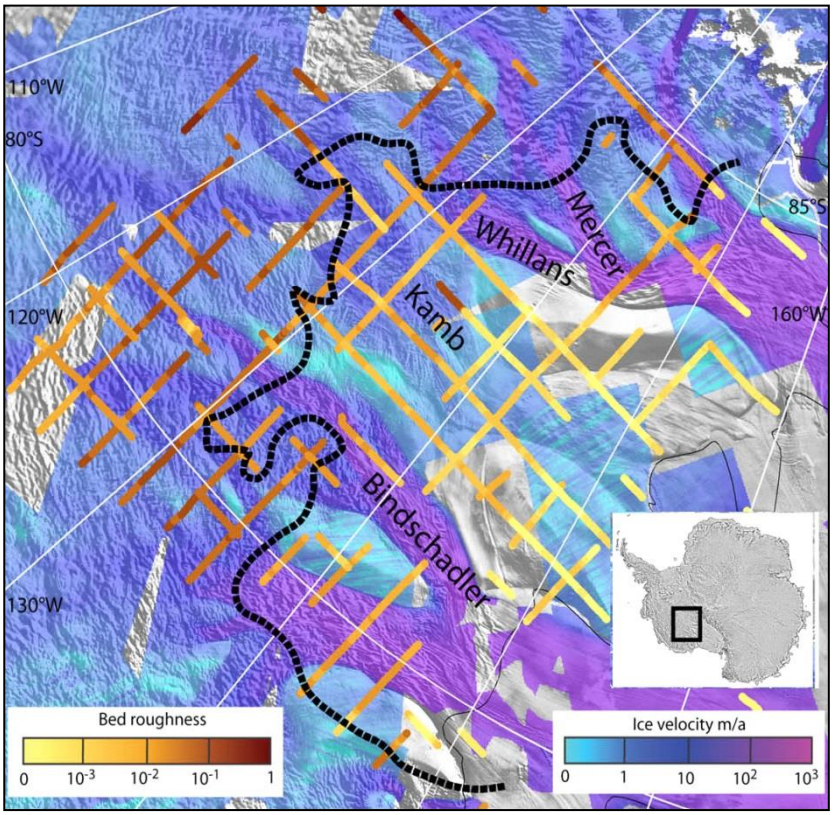

Figure 3.5: An example results map plotted using midpoint coordinates and roughness values for each window (modified from Bingham & Siegert, 2009: 228)

The version of spectral analysis applied required the observations to be uniformly spaced (Taylor *et al*, 2004). For data re-digitised at a similar resolution to earlier studies, the distance between points was taken to be 2000 m. It naturally followed that the assumed distance for measurements gathered at an eight-times shorter sampling interval would be 250 m. In past studies, scientists removed gaps using linear interpolation over short distances (Siegert *et al.*, 2004; Taylor *et al.* 2004), and this technique was adopted in this project. It is noted that linear interpolation may not be the best method for filling these gaps, and future studies may wish to test alternatives. Thirty-three gaps needed interpolation, and this was carried out over distances no longer than 3055 m. As Table 3.2 shows, 60.6% of the points interpolated were done so over distances less than 1000 m, and 81.8% over distances less than 1500 m.

Size of gap, m	Observations
$x < 1000$	20
$1000 \leq x < 1500$	7
$1500 \leq x < 2000$	2
$2000 \leq x < 2500$	2
$2500 \leq x < 3000$	1
$3000 \leq x$	1

Table 3.2: Summary statistics for the distances over which points were interpolated to remove gaps

Having checked data spacing was uniform, the next processing phase was to remove long wavelengths. Traditionally this had been done by detrending over the same number of points as the window length used to analyse the measurements (Siegert *et al*., 2005b; Bingham & Siegert, 2007a). This meant that studies like Siegert *et al*. (2004) and Bingham *et al*. (2007) detrended over 32 points, giving study lengths of 60 to 70 km long. In this project, detrending followed a similar method in that the analysis length was the same as the detrending distance. For investigating the role of sampling interval on results, the two datasets were detrended over a distance of 64 km. For data with a 2000 m sampling this was equivalent to detrending over 32 points but, with the higher resolution data, this same 64 km length was equivalent to 256 points. For investigating the effect of window size on roughness, each of the four datasets required a different detrending distance, ranging from 32 points (8 km) to 256 points (64 km).

To quantify roughness by spectral analysis two types of results can be produced, depending on the wavelengths over which the power spectral density values are summarised. In glacial roughness studies these different types have been referred to as *integrated* and *decomposed* values (e.g. Siegert *et al.*, 2004; Taylor *et al.*, 2004). The total roughness, described hereafter as *integrated* roughness, is the integral of the FFT power spectral density plot, so combines all wavelengths within the theoretical range to give a single value per sample length (Siegert *et al.*, 2004; Bingham *et al.*, 2007). The maximum possible wavelength is half the window size, and the minimum wavelength is equivalent to the sampling interval.

Decomposed results assess roughness over a series of scales, termed *wavelength classes*, by integrating the FFT power spectral density plot over specific frequencies (and therefore wavelengths). Apart from the maximum and minimum limits, which are the same as those of integrated results, the number of bands and their range of wavelength are arbitrary. Traditionally, four wavelength classes have been used and Table 3.3 shows those chosen by Taylor *et al*. (2004). Due to the minimum wavelength being controlled by the data resolution, analysis of re-digitised bed elevation measurements allowed a larger overall range. This meant extending the Taylor *et al*. (2004) approach to include an

additional three classes, and this new scheme and naming convention is summarised in Table 3.4. Here it can be seen that the classes for the four largest wavelength bands are the same as those used by Taylor *et al*. (2004). This table also shows whether each class was applicable depending on data resolution and analysis window size. The number of classes that could be used increased with window length because longer window sizes capture longer wavelengths.

Name of class	Wavelength, km
Very long	>35
Long	17.5 – 35
Medium	8.75 – 17.5
Short	4.38 – 8.75

Table 3.3: Wavelength classes for decomposed roughness results used by Taylor et al. (2004)

		Applicable to data with the following sampling intervals?		Applicable to results analysed with the following window sizes?			
Name of class	**Wavelength (km)**	**250 m**	**2000 m**	**8 km**	**16 km**	**32 km**	**64 km**
Longest	>35						
Very long	17.5 – 35						
Long	8.75 – 17.5						
Medium	4.38 – 8.75						
Short	2.19 – 4.38						
Very short	1.09 – 2.19						
Shortest	0.55 – 1.09						

Table 3 4: Wavelength classes for decomposed roughness results. Applicable classes shown in green, with those that do not apply are marked in grey

Roughness was calculated by spectral analysis in the graphs package *OriginPro 8*, a later version of the same software used in earlier studies (Bingham, personal communication 11 February 2009). Spectral analysis was used to calculate power spectral density for each of the sampling windows. To yield roughness values, the results for each window were integrated using a second worksheet with in-built macros: this produces one roughness measurement per window, and it is these results that were ultimately published by earlier workers (Bingham & Siegert, 2007).

An artefact of using different window sizes (number of observations) is that the magnitude of the integrated and decomposed results varies. Traditionally, a higher spectral analysis value was used to infer higher roughness (Taylor *et al*., 2004) but, when the window size varies, one set of results might have consistently higher values. To allow a comparison of the results, the spectral analysis values were standardised. This linear transformation

ensures that all results are within a constant range, independent of window size (Guh *et al*., 1999). In statistics a common method of doing this is to create z-values, z (e.g. Fischer *et al*., 2012; Kozak *et al*., 2008). For each observation a z-value is defined as the number of standard deviations, σ, the raw value, x, was above or below the population's mean, μ:

$$z = \frac{x - \mu}{\sigma}$$

The new sets of values are hereby termed *standard roughness* to distinguish them from results published in past studies. As will be seen in Section 3.4.4, this conversion of results to z-scores was successful in allowing the different datasets to be compared. However, a proviso of interpreting these standard results is that, although results are summarised on the same scale, it must be noted that the range in wavelengths measured varies with window size. This means that, even if two areas show the same value, the scales of roughness being measured differ. To avoid any difficulty this might cause in the results, the effect of window size was assessed by determining whether the four sets of results showed similar spatial patterns in terms of their general shape when plotted: this meant testing, for example, whether all profiles showed an increase at the same distance along profile, rather than comparing the actual values.

3.3.4 Testing the effect of sampling interval on results

To test the accuracy of the re-digitising process, bed elevations gathered by semi-automatic trace-reader were compared with those manually re-digitised at the same resolution. Integrated and decomposed results were produced via spectral analysis of both these datasets. Examination of the results allowed an assessment of how different interpretations of bed elevation would affect roughness.

Having determined the reliability of the re-digitising method, the focus then shifted to examine whether sampling interval influences the results of the parameter. This was done via a statistical comparison of roughness values derived from data digitised at two different resolutions.

3.3.5 Assessing the influence of window length on results

In a similar approach to testing how sampling interval controls the results, the influence of window length was investigated by comparing different datasets. Spectral analysis was run over a 180 km section profile (Figure 3.6), digitised at 250 m intervals, using four different window sizes (see Table 3.5 for detail). The minimum value chosen was 5, (equivalent to 32 points), as this *N*-value has commonly been used in earlier studies (e.g. Taylor *et al.*, 2004). To produce roughness values with a similar resolution to earlier investigations (c.64 km long), an *N*-value of 8 was chosen. *N*-values of 6 and 7 were also used to produce windows 16 km and 32 km long, respectively.

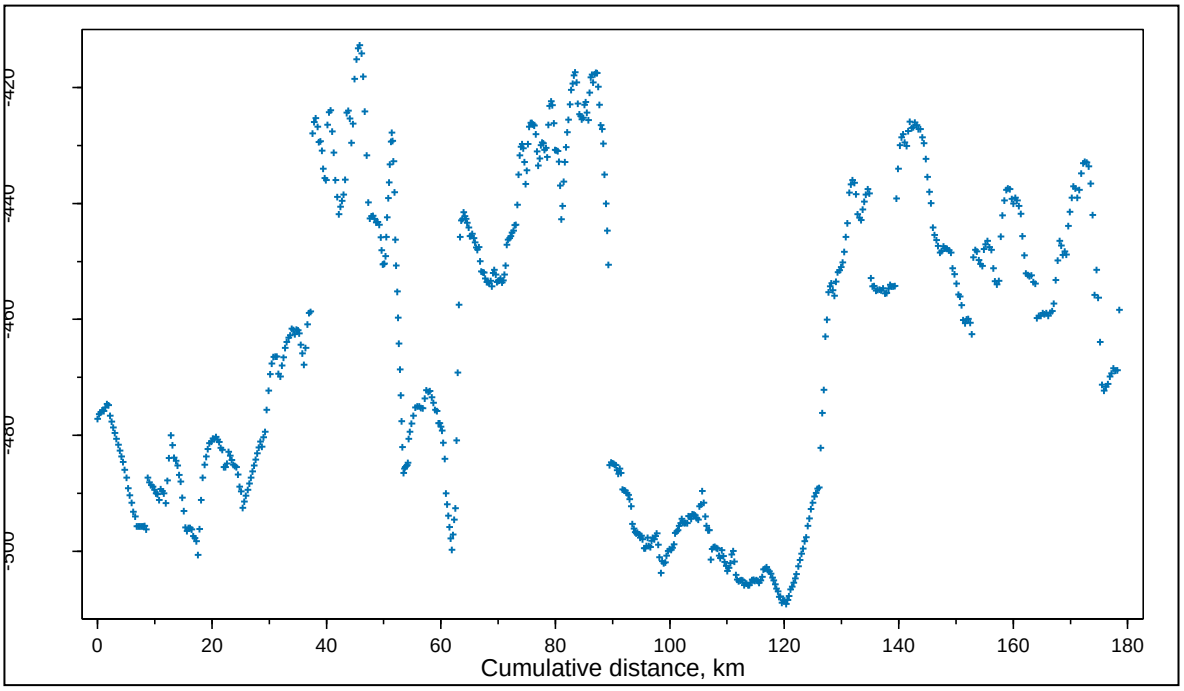

Figure 3.6: Bed elevation measurements for the 180 km section of RES profile used in this investigation

***N*-value**	**Number of points**	**Length, km**
5	32	8
6	64	16
7	128	32
8	256	64

Table 3.5: Influence of N-value on the length of window, assuming that the sampling interval between points is 250 m

3.4 Results and analysis

3.4.1 The agreement between trace-read and re-digitised data

To test the accuracy of the re-digitising process, bed elevations gathered by semi-automatic trace-reader were compared with those manually re-digitised at the same resolution. Figure 3.7 shows a plot of both sets of bed elevation measurements along the profile. Note, in this figure the re-digitised points are plotted because these are in their purest form, before being converted into metres. To better depict the agreement between both sets of measurements, a scatter plot of the results is shown in Figure 3.8. Here, the converted bed elevation measurements are used, so both datasets have a metre scale. It can be seen that there is not perfect correlation between the two datasets; the sources of these discrepancies are discussed in Section 3.5.1.

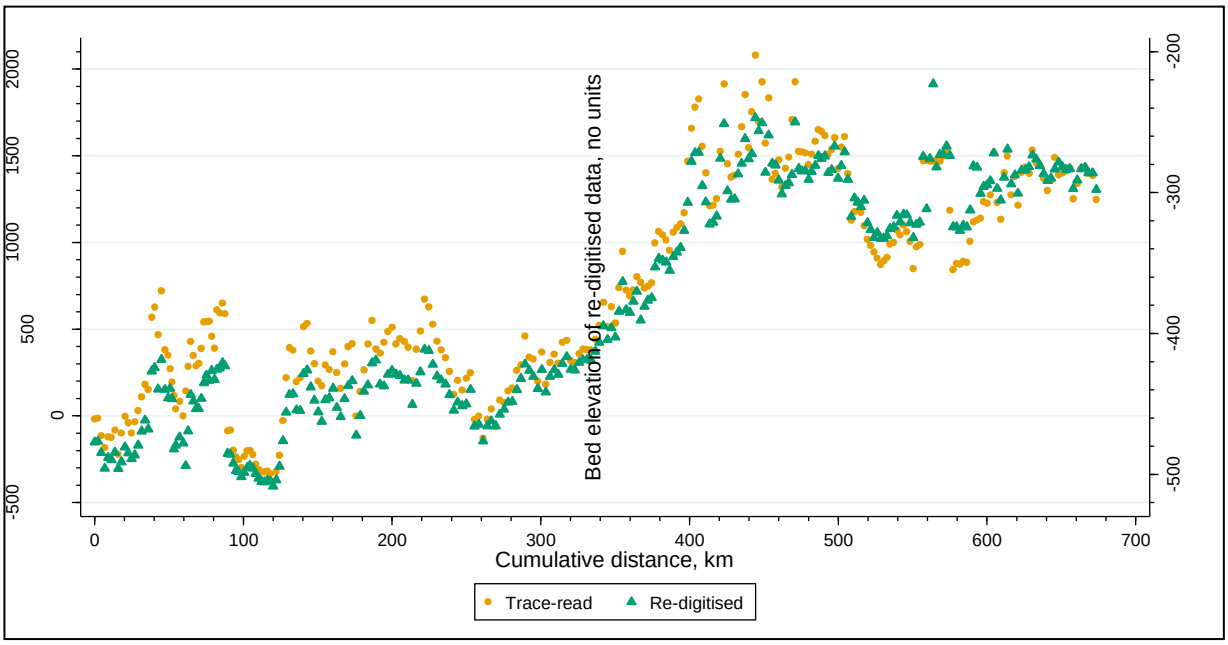

Figure 3.7: Plot of trace-read versus manually re-digitised bed elevation measurements

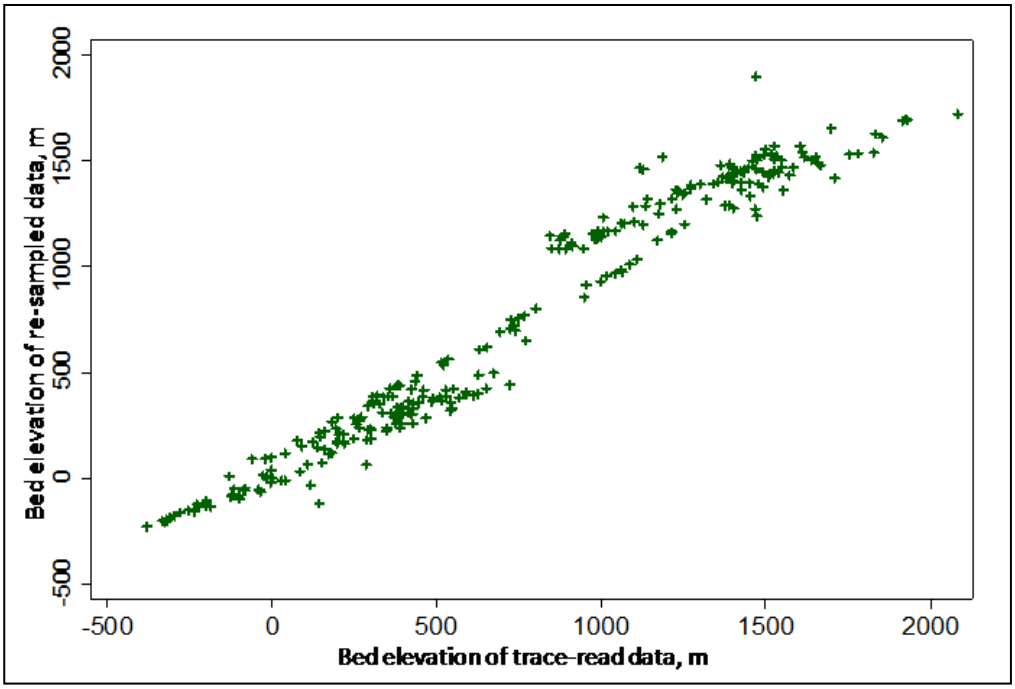

Figure 3.8: Scatterplot of converted trace-read bed elevation measurements, and data derived from manual re-digitising

The agreement between both datasets is better illustrated by plotting their differences (Cox, 2006; Bland & Altman, 2010). Figure 3.9 shows that there is a clustered pattern to the data where the re-digitised measurements flip between over-estimating and under-estimating bed elevation every 20 to 50 shotpoints. For example, from shotpoints 475 to 500, the manually re-digitised results record lower elevations than those of the trace reader, yet in shotpoints 500 to 520, the re-digitised data recorded systematically higher bed elevations.

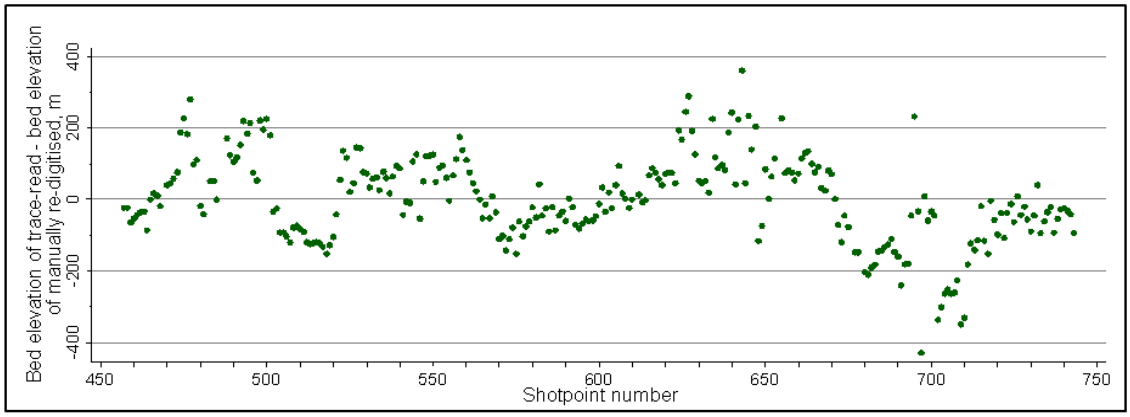

Figure 3.9: Plot of differences between trace-read and re-digitised bed elevation data

Summary statistics (Table 3.6) show there is reasonably-good agreement between both datasets. Across the entire study area, the average height and standard deviation of both datasets is similar. However, in some areas of the profile Figure 3.9 shows that the data exhibit differences of over 400 m. Therefore, although the overall results for the profiles are similar, more locally there are differences in the bed elevation measurements.

	Trace-read	**Re-digitised**
Mean	738.84	741.99
SD	612.14	601.06
Minimum	-379	-226.75
Maximum	2081	1900.23
Obs.	287	279

Table 3.6: Summary statistics for bed elevation measurements (in metres) between trace-read data, and converted re-digitised data, sampled at the same resolution

Figure 3.10 shows a plot of differences versus means, and it is apparent that 94.6% (264/279) of the differences lie within ±1.96 standard deviations (±237 m). A high concordance correlation coefficient (ρ_c) of 0.98 shows there is strong agreement (Steichen & Cox, 1998, 2002), while a bias correction factor (c_b) of 1.00 and Pearson correlation coefficient (ρ) of 0.00 shows there is high accuracy and precision, respectively (Lin, 2000). However, a more pessimistic view might highlight that fifteen results are outliers exhibiting disagreement greater than 1.96 standard deviations.

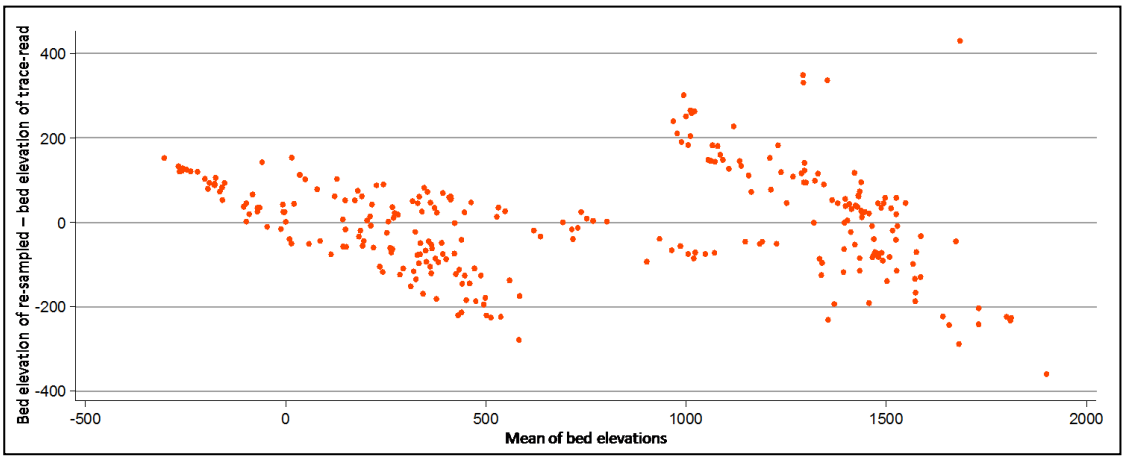

Figure 3.10: Differences versus means for re-digitised and trace-read bed elevation measurements

Rather than these large differences occurring randomly along the profile, further analysis shows that the greatest differences occur when the SPRI image exhibits one of two characteristics: first, many of the large differences are found in areas where the bed trace is very faint (e.g. shotpoint 640); second, large differences (e.g. shotpoints 643, 691, and 697) are in areas of parabolas where the bed appears as multiple traces rather than a single line. Arguably, the largest differences may be attributed to the quality of the SPRI images, rather than being due to the method of sampling. As a result of indistinct bed traces, re-digitising is subjective and the user must determine which trace is the bed.

Errors are problematic when calculating roughness, particularly because the effect of artefacts on results is unpredictable: for example, variations in bed elevation due to noise might manifest as over-estimates of bed roughness, because radio-wave diffractions on the image might be digitised as undulations. Alternatively, Siegert *et al.* (2005b) show how diffractions smooth out relief producing under-estimates of roughness. Nevertheless, the agreement between methods is assurance that the method of re-digitising presented in this experiment can be used to gather bed elevation measurements at a similar or higher accuracy as the trace-reader technique.

3.4.2 Comparison of bed elevation measurements at different resolutions

Having investigated the agreement between trace-read and manually re-digitised bed elevation measurement at the same 2000 m sampling, the next step was to compare the re-digitised measurements gathered at different resolutions. Figure 3.11 shows a plot of bed elevation values digitised at 2000 m and 250 m intervals. There are no apparent anomalies in the results, suggesting that the re-digitising has been accurate. Overall, there is good agreement between the bed elevations recorded at different resolutions. Comparing bed elevation data at different resolutions also gave insight into the sensitivity to measuring asperities. Data with an eight-times-shorter sampling interval appear to exhibit more peaks and troughs, suggesting the data have captured a smaller scale of bed topography.

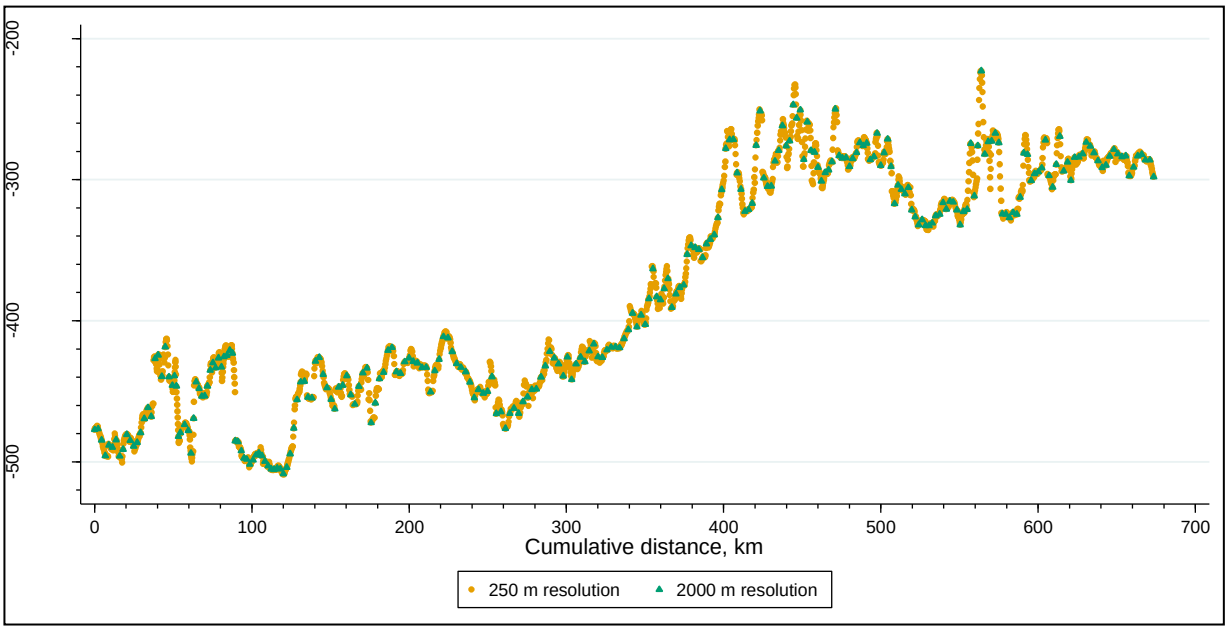

Figure 3.11: Comparison of bed elevation measurements manually re-digitised at different resolutions.

3.4.3 Effect of sampling interval on spectral analysis roughness results

Summary statistics for integrated results calculated from trace-read and manually re-digitised data re-digitised at the same resolution are shown in Table 3.7. In some studies, (e.g. Bingham & Siegert, 2009), the values range from 0 to 1 for low-roughness to high-roughness, respectively. However, the range in values produced is influenced by the format of the data. In the case of integrated results calculated from the trace-read measurements, roughness ranged from 0.1206 to 2.208, while results of manually re-digitised data ranged from 0.0009 to 0.0176. The two causes for this difference in magnitude are the units of bed elevation measurements, and the version of OriginPro used for analysis. Because the trace-reader measured bed elevation on the metres scale, while the re-digitised data were unit-less, the results vary. A further difficulty is that, because of changes in the OriginPro software, the roughness results produced in this study cannot be compared with those of earlier workers (e.g. Taylor *et al.*, 2004). In previous investigations, data were normalised so that values ranged between 0 and 1 (Bingham *et al.*, 2007). Version 8 of OriginPro differs from earlier software (c.f. version 5.0 used by Siegert *et al.*, 2005b), because the option to *normalize amplitude* while running FFT analysis is omitted (Bingham, personal communication 28/09/09). To ease comparison between the data, regression was used to convert the trace-read results: the summary statistics for the converted results are listed in Table 3.7 under the *trace-read (converted*) column. Hereafter, further reference to *trace-read* results refers to these converted measurements.

	Trace-read	Trace-read (converted)	Manually re-digitised
Mean	0.6356	0.0056	0.0056
SD	0.3874	0.0034	0.0036
Maximum	0.208	0.0196	0.0176
Minimum	0.1206	0.0010	0.0009
Observations	256	256	256

Table 3.7: Summary statistics of integrated roughness results derived from trace-read data, and measurements manually re-digitised at the same c.2000 m resolution. The converted trace-read results were calculated using regression to ease comparison between the two sampling methods

The integrated roughness results for trace-read, and manually re-digitised bed elevations at the same resolution, are plotted in Figure 3.12, where the mid-point coordinates for each window are used to plot the position for each window along profile. Here, it can be seen that, overall, there is good agreement between the data, and this is supported statistically with a ρ_c of 0.959. Along almost all of the assessment length, the general shapes of both profiles closely mimic one another. Therefore, although the specific roughness values at each point may vary, the overall pattern is the same. One exception to this is between 425 and 475 km, where the results are mirrored so that the trace-read results show a rise-and-fall, while the manually re-digitised show a fall-then-rise. The greatest differences in the results occur between 510 and 560 km. The reason for this may relate to the quality of the bed trace on the z-scope image because, in this region, the image is characterised by greater scatter.

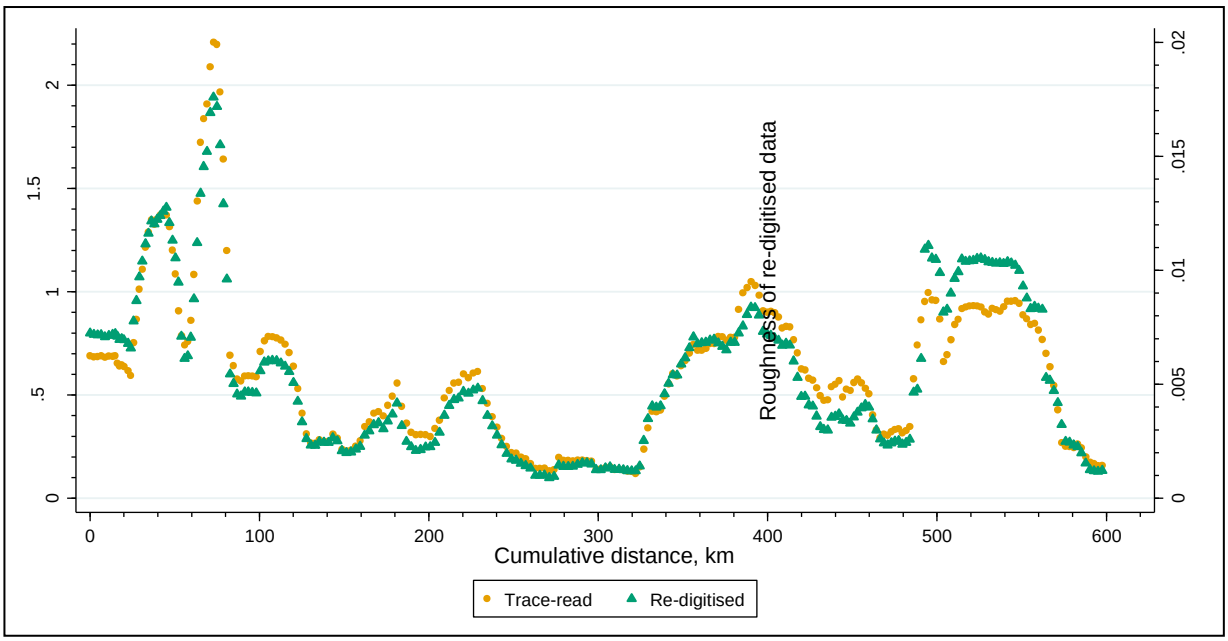

Figure 3.12: Comparison of roughness results yielded from re-digitised and converted trace-read bed elevation measurements

While areas of high roughness produced the least consistent results, areas of low roughness correspond with some of the smallest differences. For example, in the low-roughness region between c.275 and 325 km, there is little disagreement between the

manually re-digitised and trace-read data. It is possible that this smooth area of the bed strongly reflected radio waves, making a distinct trace on the image. This implies that there may be a relationship between roughness and differences in the results, with disagreement increasing as roughness increases. To test this idea Figure 3.13 shows a plot of differences in results versus the trace-read results. The plot confirms that as roughness increases the disagreement between the data increases.

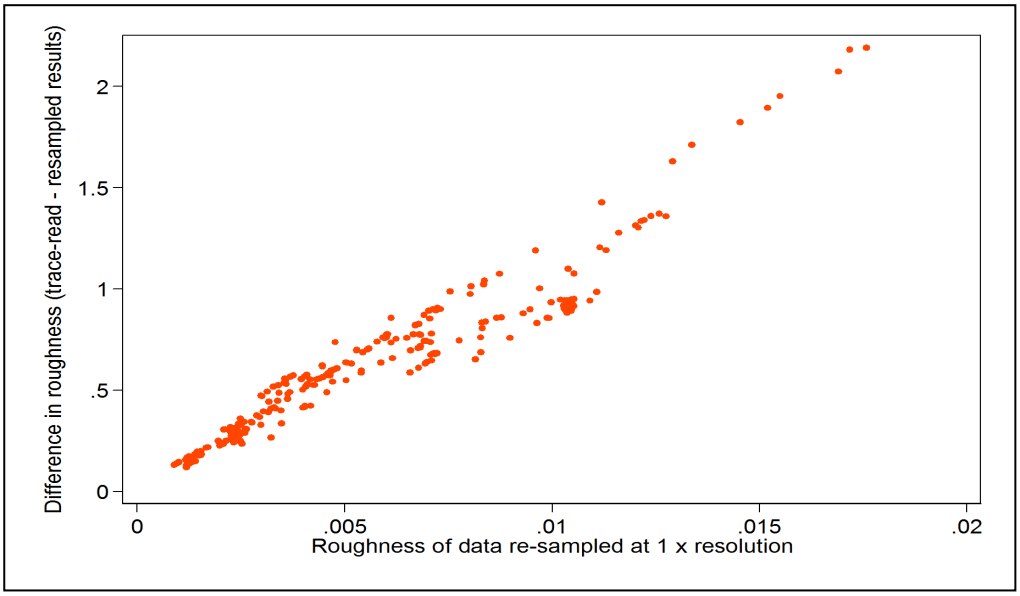

Figure 3.13: Differences between roughness results at different resolutions, versus roughness results for data sampled at 1 × resolution (2000 m interval)

Overall, *integrated* roughness measurements derived from spectral analysis of re-digitised data are nearly identical to results calculated from trace-read data, with the exceptions seemingly being areas where the z-scope image exhibited noise. The most agreement occurs in areas of low roughness, with agreement increasing as roughness increases. However, results may differ in magnitude. For example, despite the same general trend, relative to trace-read results, the re-digitised data are higher in some areas but lower in others. The general agreement suggests re-digitising of z-scopes can produce results consistent with those of earlier studies, and is therefore a suitable method of digitising the bed.

Having tested the influence of sampling interval on results, the next stage was to determine whether the roughness results were affected by data resolution. One option here was to compare the results of the data re-digitised at 250 m, with the lower-resolution trace-read measurements. However, because of the possible discrepancies in inferring the bed elevation between two different methods of sampling, this was avoided. Instead, the re-digitised bed elevation measurements sampled at different resolutions were compared. The results for data with 250 m and 2000 m sampling are shown in Table 3.8.

	Manually re-digitised (2000 m intervals)	Manually re-digitised (250 m intervals)
Mean	0.0056	0.0057
SD	0.0036	0.0036
Maximum	0.0176	0.0179
Minimum	0.0009	0.0010
Observations	256	2034

Table 3.8: Summary of integrated roughness results for data manually re-digitised at different resolutions

Earlier studies of subglacial bed roughness presented their measurements as maps (e.g. Bingham & Siegert, 2009), which plot the mid-point coordinates and integrated power spectral density (roughness) values for each window. Figure 3.14 shows roughness results for Flightline-122 displayed in a similar format. The left-hand map shows integrated values for data gathered at the same resolution as the semi-automatic trace reader, and the right profile shows roughness results for measurements sampled at eight-times higher resolution. Immediate comparison suggests that the results for both profiles are very similar, for example, both show high roughness in the central area of the profile, with low roughness values on both either side.

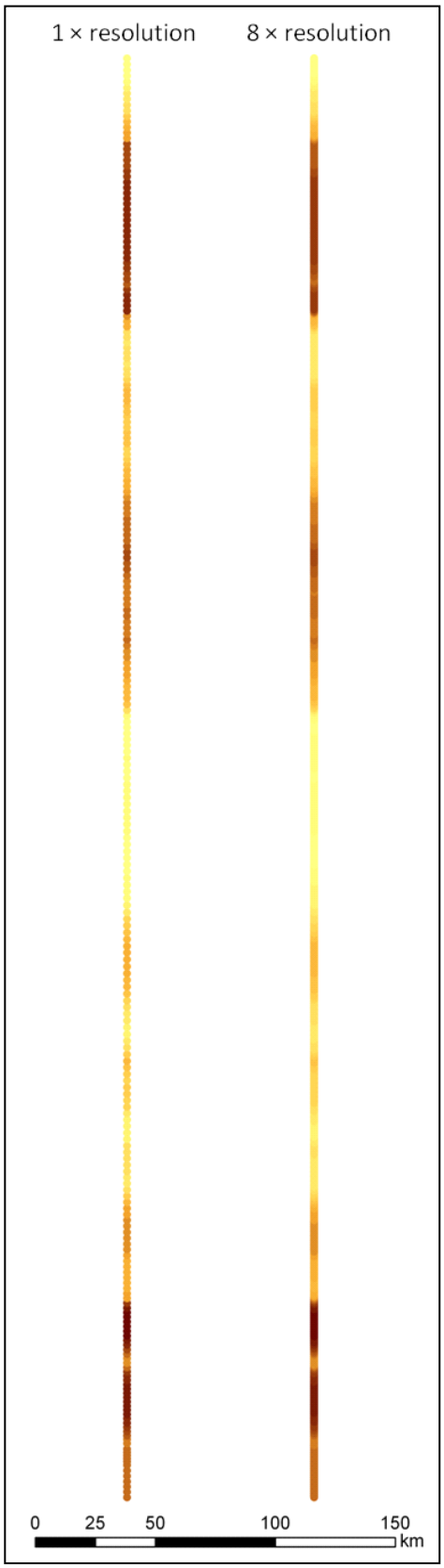

Figure 3.14: (a) Map of roughness results from data manually re-digitised at different resolutions. Lightly-coloured areas depict areas of low roughness, while dark areas correspond to high roughness

One difficulty of comparing data using roughness maps (e.g. Figure 3.14) is that detail is diminished because, to display the map, smaller spatial variations along the profile are

lost. For more detailed analysis of data on these re-digitised scales, it is useful to display the results as scatter-plots. Figure 3.15 shows plots of integrated roughness results manually re-digitised at the two resolutions. Visually, there is strong agreement along the complete profile length. These results appear more similar than those comparing trace-read and re-digitised measurements.

Nevertheless, there is not perfect agreement between the two sets of power spectral density values. Rather than the disagreement being randomly distributed there is some structure in the disagreement when viewing the profile left-to-right. Initially, the results produced by data with a 2000 m interval are lower. Towards the centre of the graph there is strong agreement between both datasets with almost complete overlap to the point where they are difficult to distinguish. Finally, on the right-hand section of the assessment length the results gathered at 2000 m intervals are higher.

A second apparent trend is that the amount of agreement appears to change depending on the roughness of the topography. Where roughness is low, such as around 300 km distance, the results are more similar. In the areas of peaks, which imply rough topography, there is less similarity in the measurements. Yet, despite some differences in terms of absolute values, both datasets show the same changes in roughness in terms of the relative change in the plot shape. Therefore, it is likely that the same conclusions would be drawn in terms of inferring which areas of the bed are rough and which are smooth.

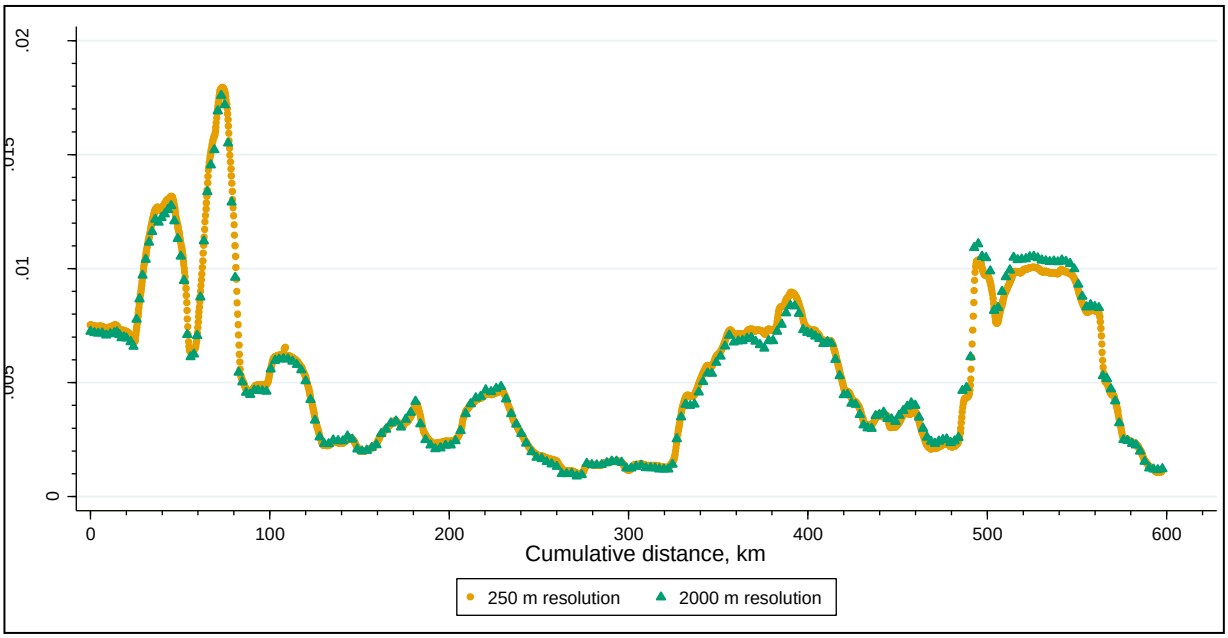

Figure 3.15: Comparison of integrated roughness results for data manually re-digitised at 2000 m and 250 m sampling intervals

Figure 3.16 shows the decomposed roughness results for data digitised at 250 m resolution. Unlike the integrated values these were not compared with results generated

from data at a different resolution, but were instead used to test whether results are consistent at different wavelength classes. The advantage of using the high-resolution dataset was that it allowed a large number of wavelength classes to be used. Recall from Table 3.4 that some of these classes are analogous with those of other studies, but others measure smaller-scale changes.

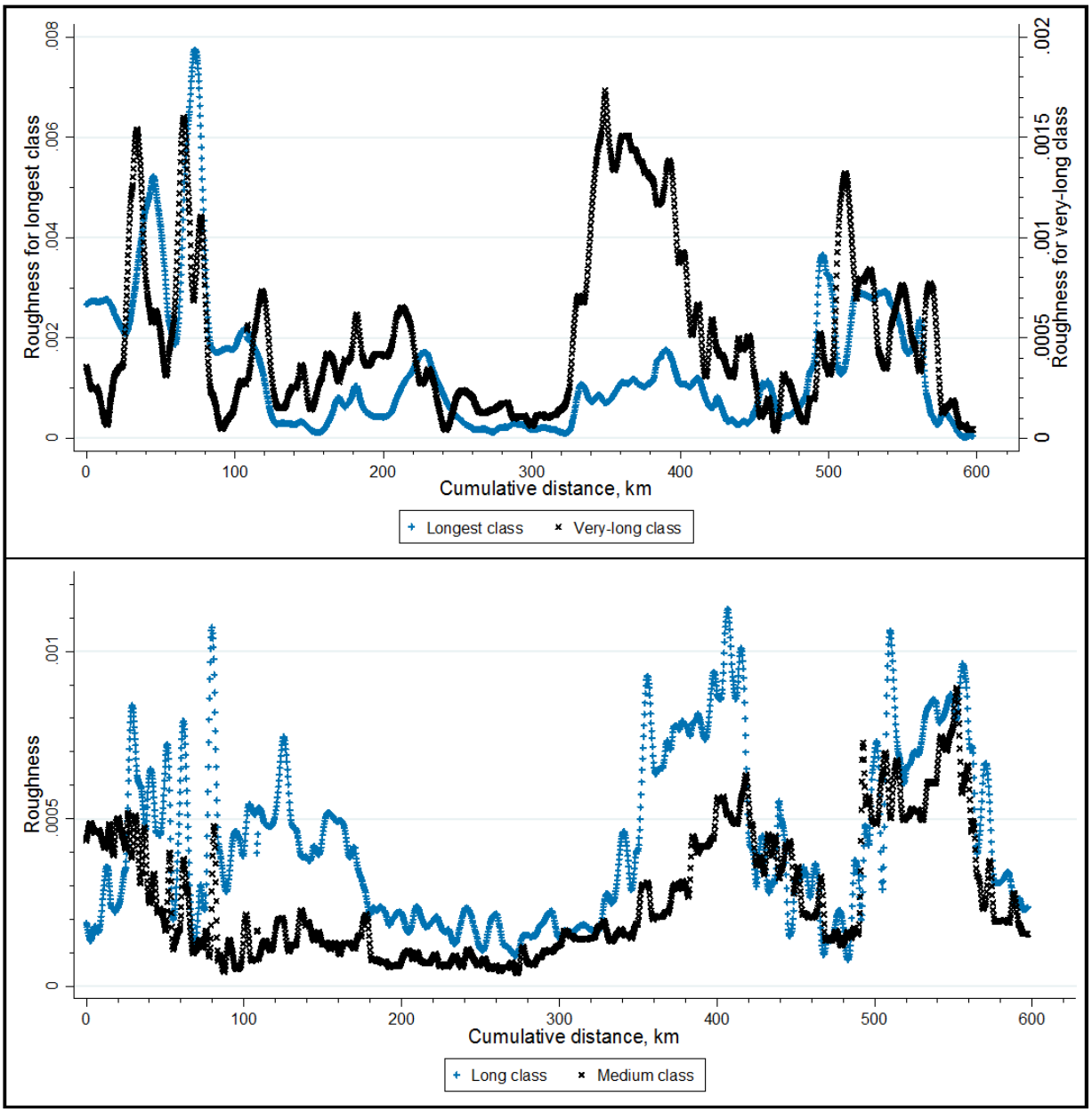

Figure 3.16 (part 1 of 2): Decomposed roughness results for data manually re-digitised at a sampling interval of 250 m

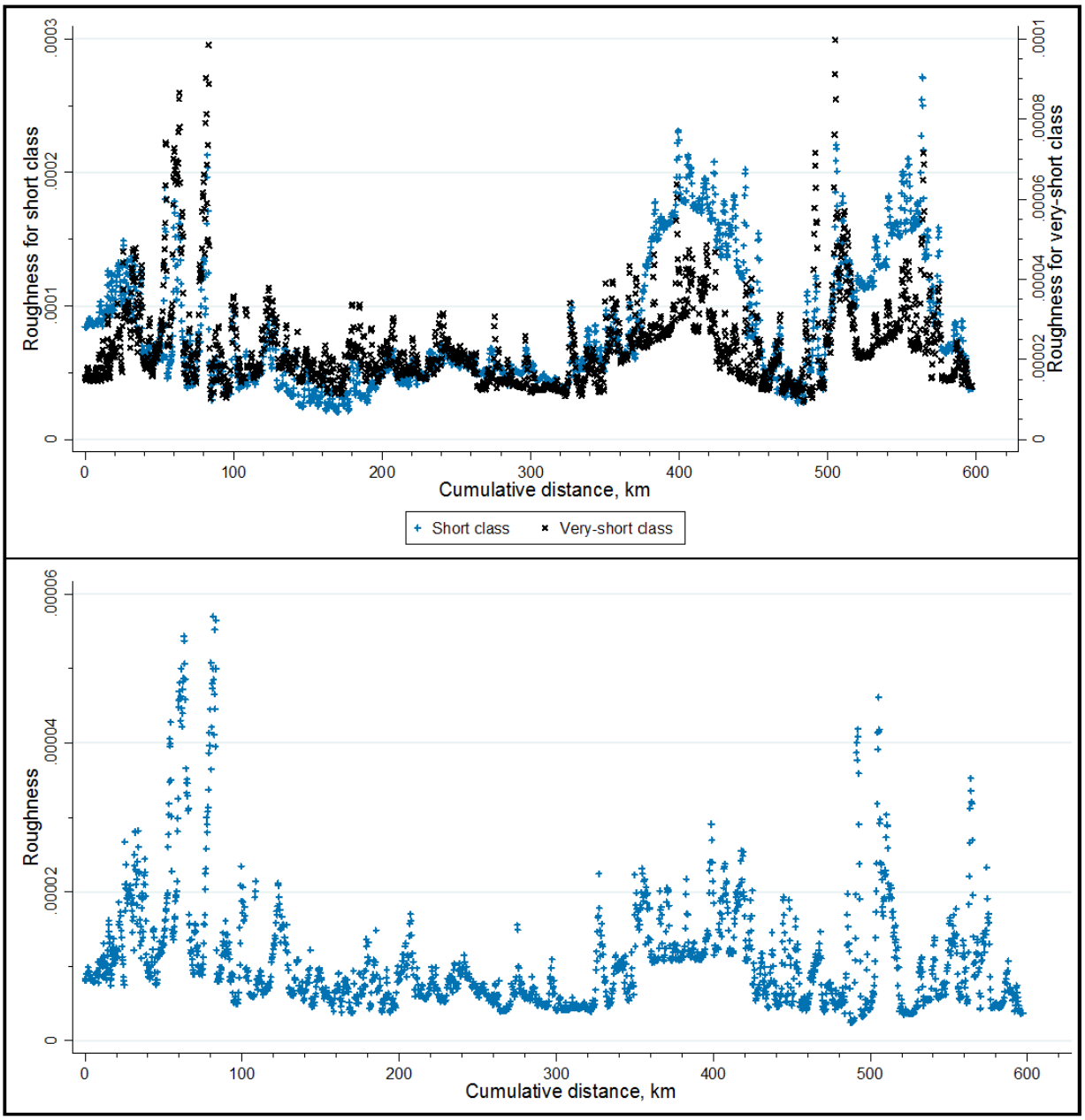

Figure 3.16 (part 2 of 2): Decomposed roughness results for data manually re-digitised at a sampling interval of 250 m

On the whole, the broad pattern of roughness is the same for each of the wavelength classes. However, over shorter scales there is more localised variation. As wavelength decreases the amount of variability increases, and the amount of detail captured appears to increase. An example of this can be seen by focusing on the section of profile between 500 and 600 km. For most wavelength classes this area appears as a zone of high roughness values but, from the short class and below, the same region appears as two areas of high roughness with an intervening area of lower values. Another factor that may explain some of the lack of variability with the longest class is the role of detrending, which would have smoothed the data at this scale.

3.4.4 Influence of window size on spectral analysis results

The integrated roughness results for each window length are shown in Figure 3.17. There is some agreement in terms of general shape, but this breaks down in places. Unlike the results that tested the role of sampling interval on power spectral density, window length produces less consistent results. In some sections along the assessment length, the plots show differing interpretations, e.g. with some plots suggesting rough topography but others smooth topography.

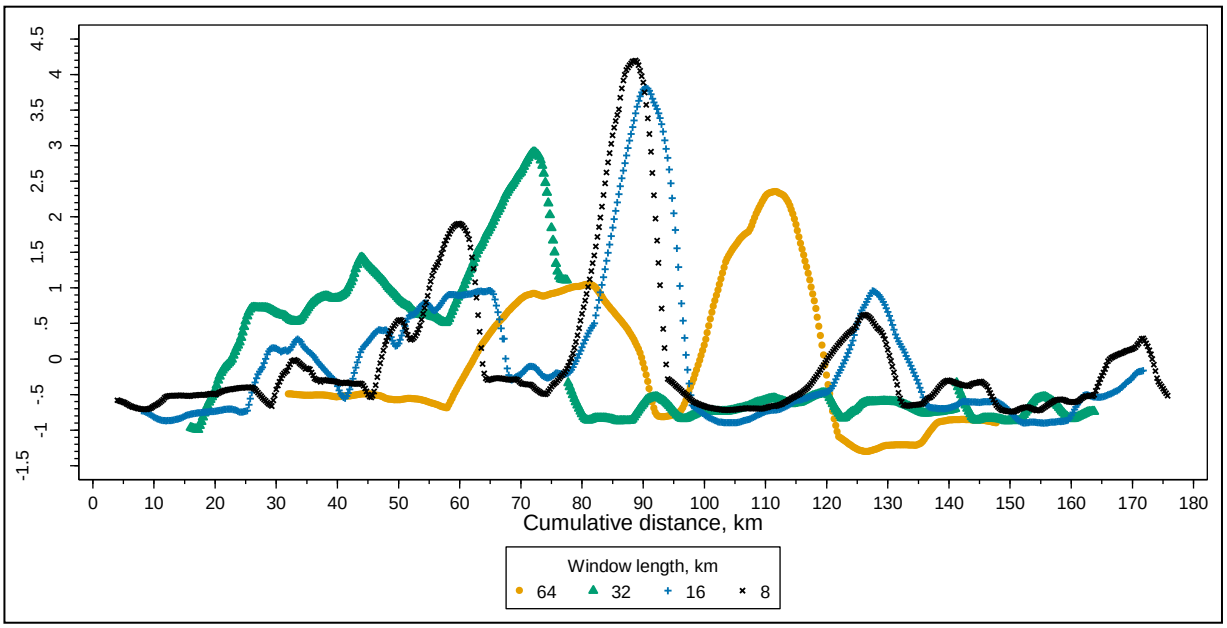

Figure 3.17: Integrated roughness results calculated using different window lengths

Spectral analysis results were plotted using the midpoints for each window, which means that an artefact is produced whereby increasing window length makes the first result plotted shift to the right (shown diagrammatically in Figure 3.18). The first result is always half the distance of the window length from the first observation: e.g. the first observation for data with 9 km windows is 4 km along profile, but the first result plotted when using 64 km windows is 32 km from the first bed elevation measurement. Analysis windows do not extrapolate beyond known observations so, because the assessment length was a fixed distance of 180 km, the last result plotted also varies for each of the different window lengths.

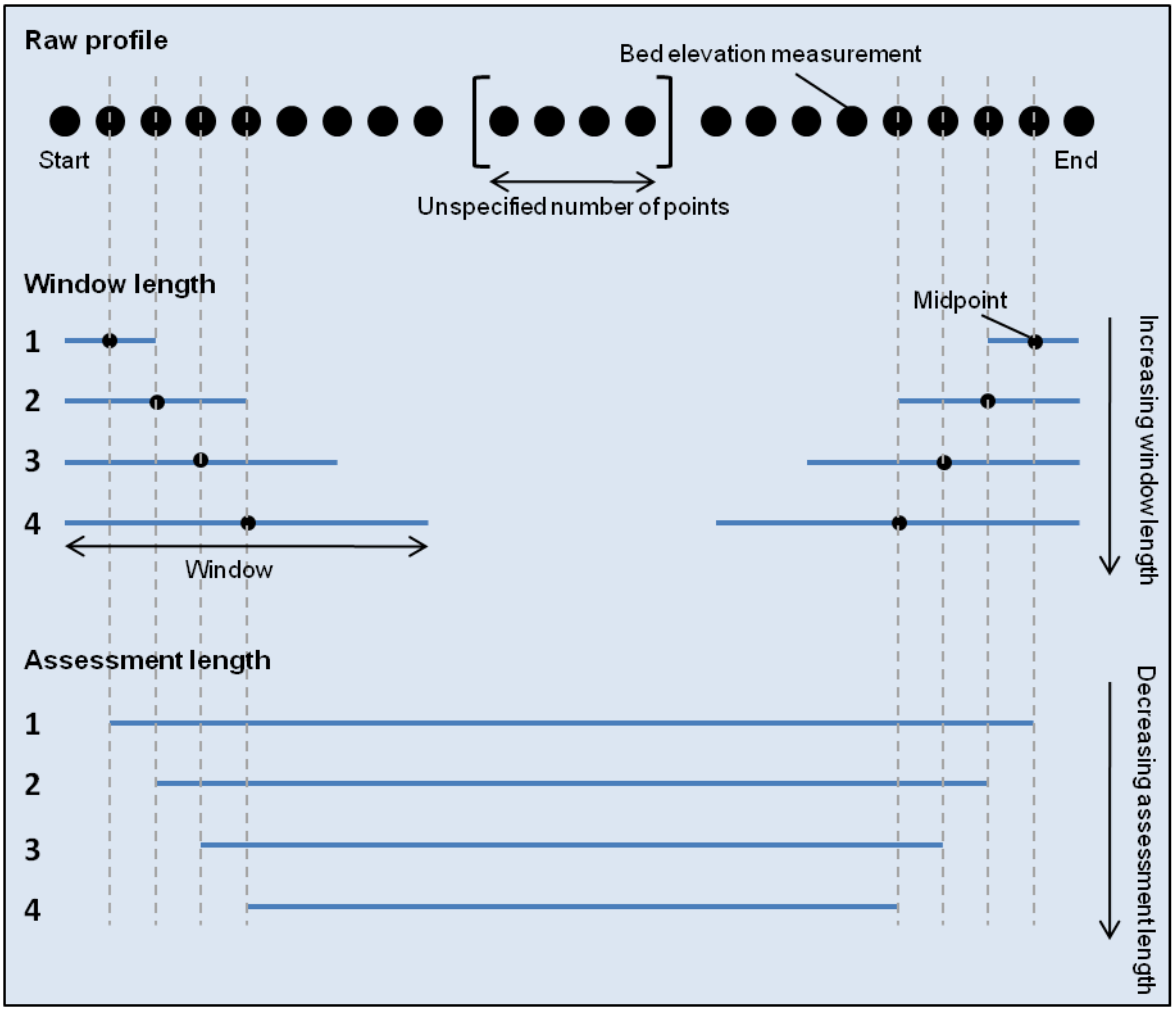

Figure 3.18: Role of window length on the total length of results profiles. Numbers 1 to 4 depict scenarios with differing window lengths. Because a fixed number of points for a window is used (i.e. the length of window does not diminish towards the edges of the profile), with assessment length decreasing as window length increases. Adjusting the window length by 2^N points has a more pronounced effect than shown here

As with integrated results, window length influences the range in power spectral density values for decomposed results to the extent that displaying them for comparison is difficult. An example of this is shown in Figure 3.19a, a plot of decomposed values for the *shortest* wavelength class. The results for windows evaluated over 32 points are consistently higher at all classes than the other window lengths necessitating two axes. Despite this, the spatial changes in roughness are still difficult to see, with the plots for 8 km and 16 km windows being bunched together. This prompted the need to find a method of standardising the results and, as described in Section 3.3.3, this was achieved by producing z-values.

Figure 3.19b shows the standardised results for the *long* class, and it is apparent that they can be compared more easily. One issue, however, is that relative changes in shape is the only means of comparing agreement. Another problem is that standardising appears to modify the results, thus influencing the shape of the results plots. This can be seen in Figure 3.20 that shows the raw and standardised plots for the *long* wavelength class; the

results produced using 32 km window show more distinct switches in roughness with the standard measurements, but those calculated using 64 km windows are largely unchanged. Nevertheless, as visual comparison is the primary method of assessing agreement, some modification to produce a clearer plot was preferable.

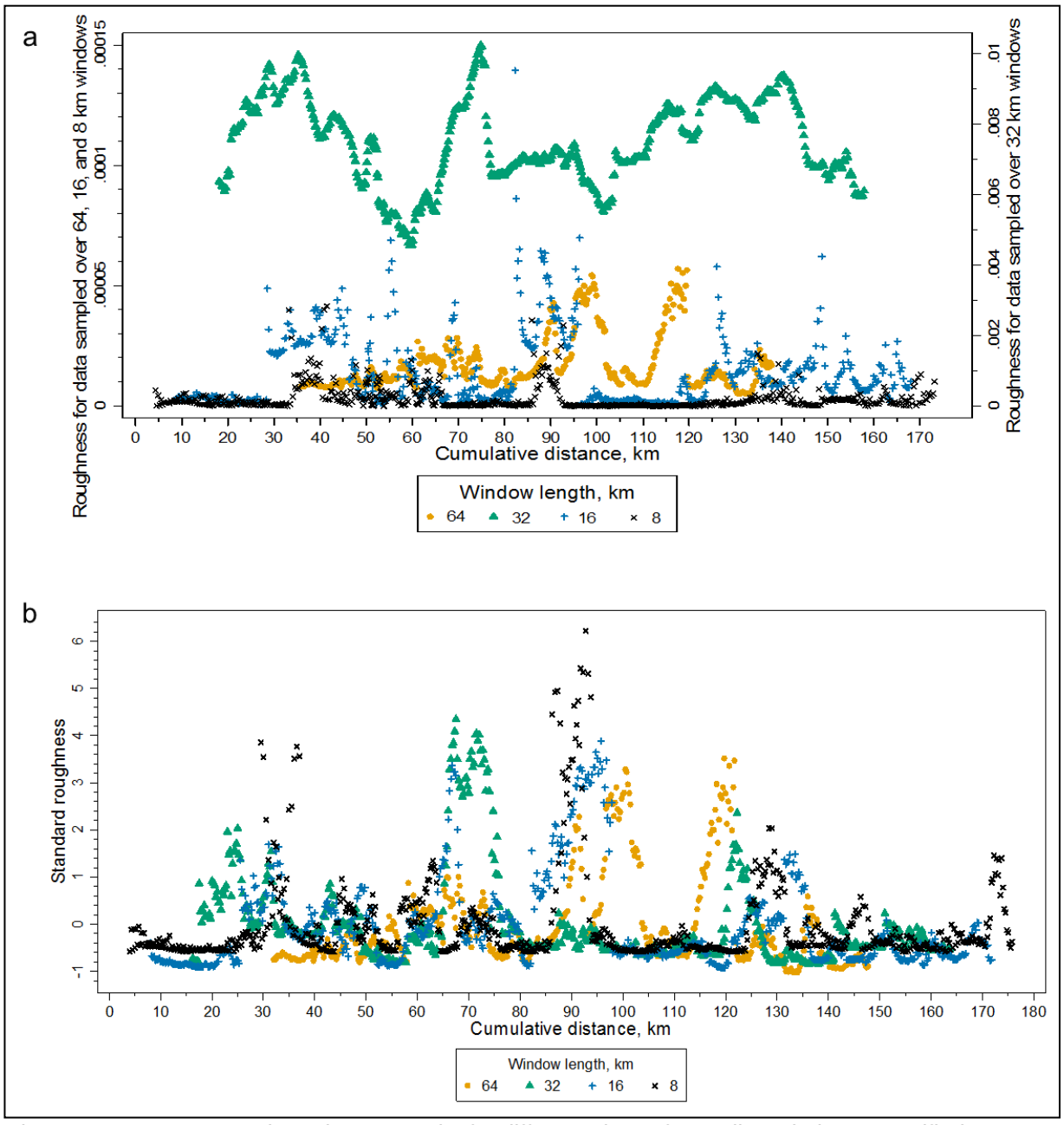

Figure 3.19: Decomposed roughness results for different sizes of sampling window, quantified over the shortest wavelength class. (a) Results in their raw output. (b) Results standardised using z-values.

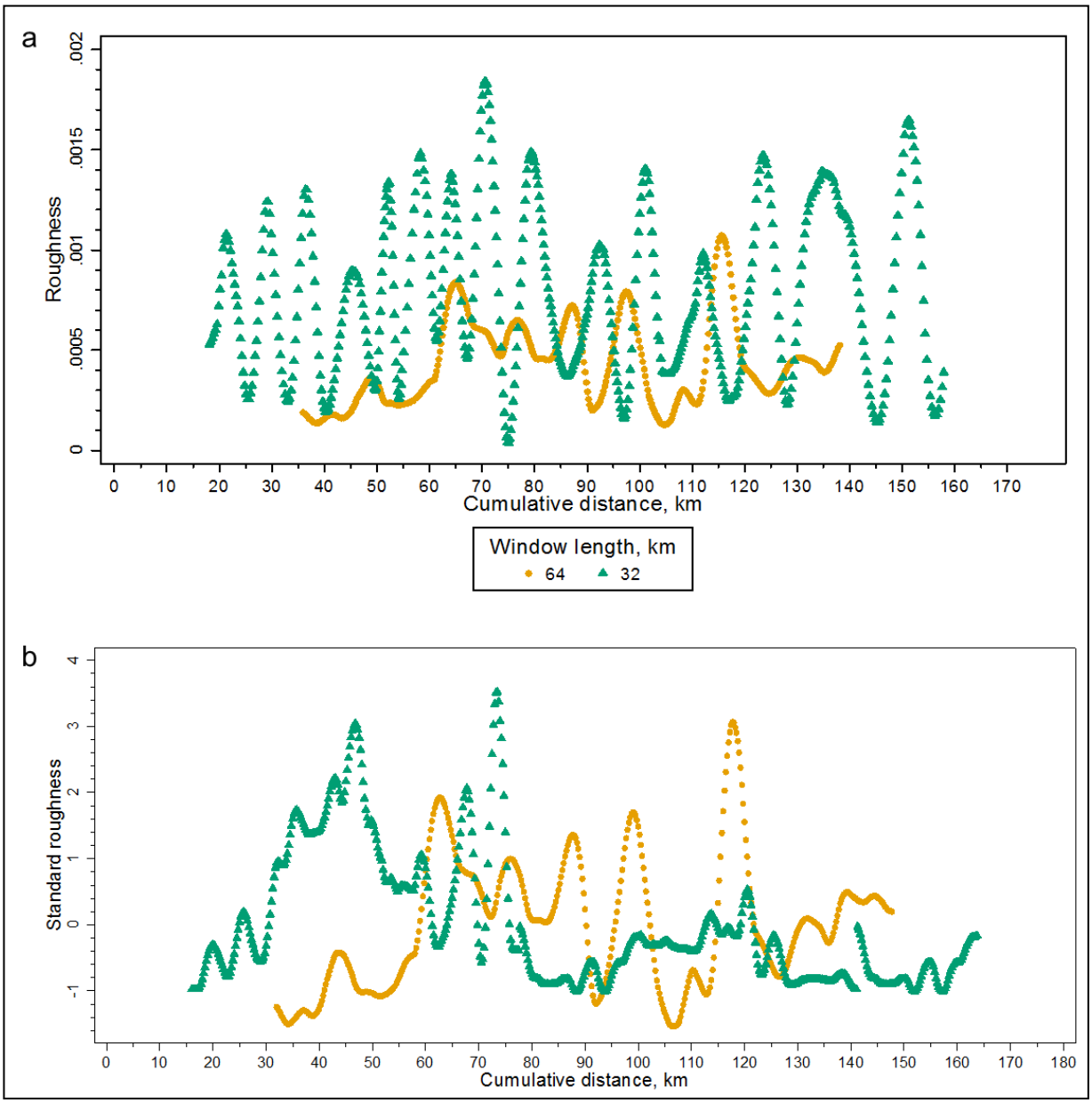

Figure 3.20: Decomposed roughness results for different sizes of sampling window, quantified over the long wavelength class. (a) Results in their raw output. (b) Results standardised using z-values.

Figure 3.21 presents the decomposed roughness values calculated using each of the four window lengths. Although some choices of window permitted wavelengths of over 17 km to be employed (refer to Table 3.4 earlier), these were only applicable to data analysed over 64 km windows, so the *very-long* and *longest* classes are not presented. Compared with the integrated data, these generally show more variation in terms of the number of transitions from *rough* to *smooth*. For example, with the integrated data, there were two peaks of higher roughness; the *shortest* class suggests that roughness changes more frequently along the assessment length, with four or five areas where roughness values are distinctly higher than adjacent topography. A similar situation occurs with results calculated using different lengths of window: aside from the frequency of rough and smooth areas, their locations also vary with wavelength class, and also to those identifiable in the integrated data.

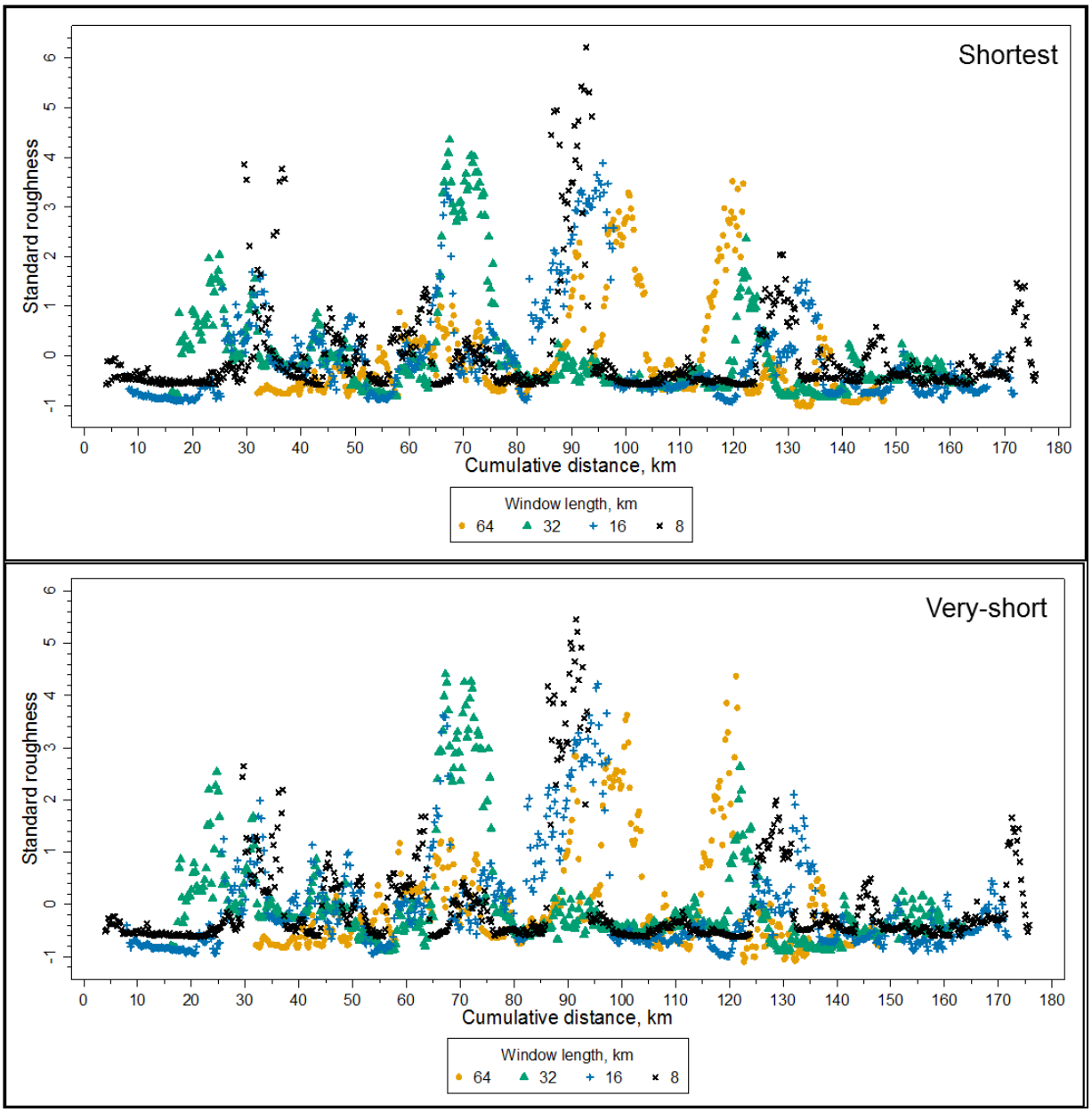

Figure 3.21 (part 1): Decomposed roughness results showing the influence of window length

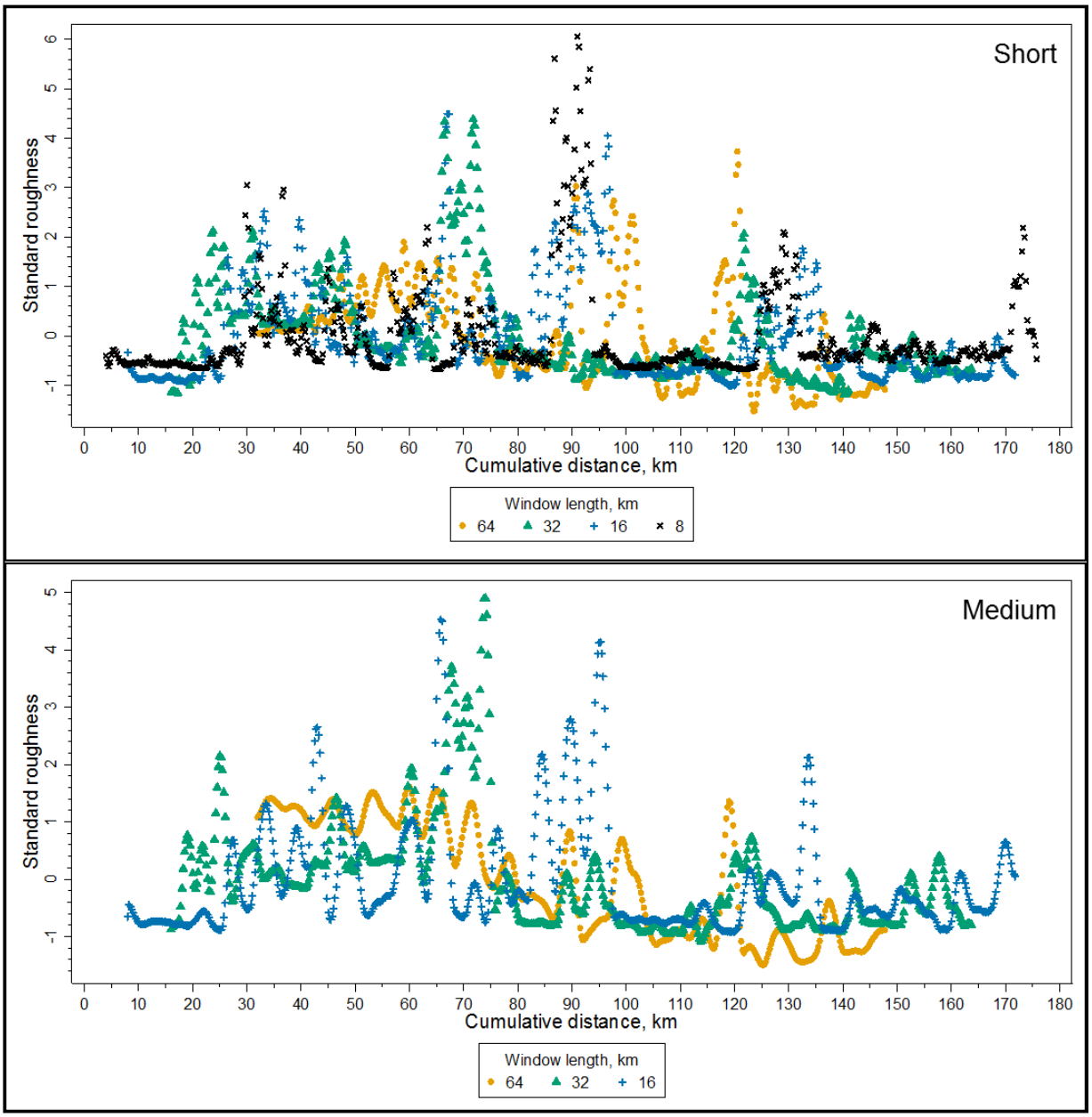

Figure 4.21 (part 2): Decomposed roughness results showing the influence of window length

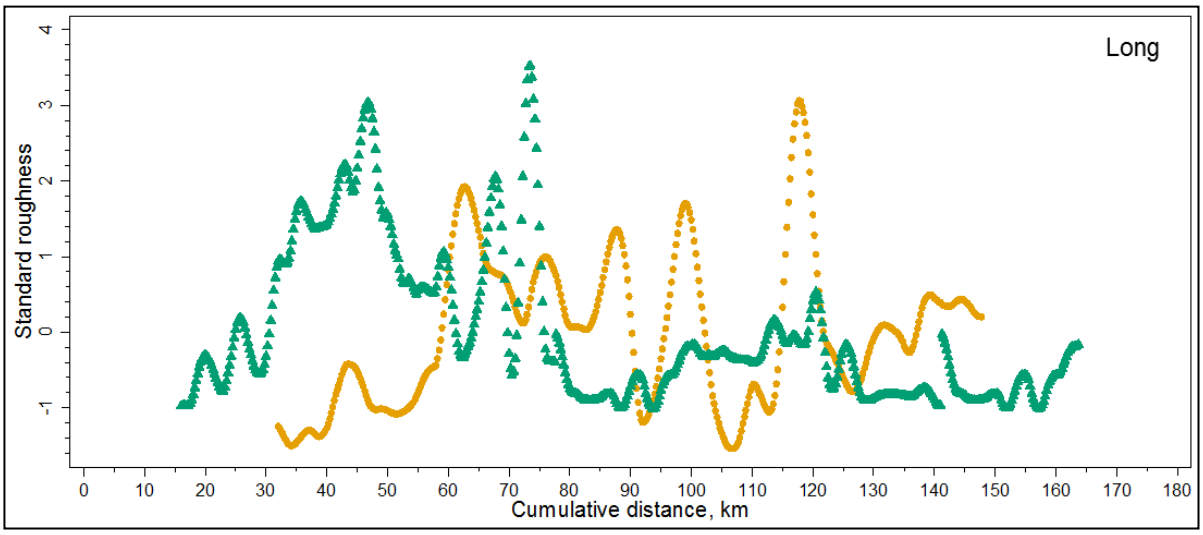

Figure 4.21 (part 3): Decomposed roughness results showing the influence of window length. Window lengths: 64 km (orange), 32 km (green)

In terms of the agreement between data measured using different window sizes, some regions show that roughness values are consistent. Nevertheless, there are few regions, at any wavelength class, where results for all four windows show the same pattern. Areas of agreement tend to occur over relatively short distances. On the contrary, the results commonly differ with window size. In some cases, this disagreement is only for one window length yet, in other instances all four windows show a different pattern of roughness. The long wavelength class is an extreme example of this, where results show an inverse relationship for much of the profile. It appears that, moving towards longer wavelength classes, the amount of disagreement increases, which is the converse to the results where sampling interval was the variable.

Even where results calculated using different windows are consistent in terms of the general position of peaks (high roughness) and troughs (low roughness), the magnitude of change in terms of the steepness of the changes in roughness may vary. For example, at approximately 73 km for the *shortest* class (Figure 3.21 part 1), all results show a general increase in roughness but the size of the increase differs.

Upon first inspection, areas of high roughness appear to have close agreement: for example, at the *very-short* class the three central rough zones were produced for several of the window lengths (Figure 3.21 part 1). Nevertheless, this apparent agreement may be caused by the areas being relatively eye-catching to the viewer due to their markedly higher roughness values compared with the rest of the assessment length. Closer inspection shows that within these rough zones there is much fluctuation in the values over relatively short distances. In contrast, in areas of lower roughness values the spread of results is tighter.

A second factor affecting the amount of similarity between results appears to be the difference in window length. Where the difference in window length is large (e.g. comparing results calculated using 8 km windows with those analysed over 64 km lengths), the agreement appears to be lower. Conversely, with a shorter difference in window length (such as 8 km vs. 16 km windows), the agreement is higher.

3.5 Discussion

3.5.1 Is re-digitising SPRI flightlines possible?

This project developed a technique to manually sample the height of the bed using z-scope imagery, demonstrating that SPRI flightlines can be re-digitised. The method was successful in decreasing the horizontal interval between points to a distance of approximately 250 m, which represents an eight-fold increase in resolution compared with data recorded by semi-automatic trace-reader (Young *et al.*, 2007). Therefore, it is possible to re-digitise SPRI flightlines. Nevertheless, as discussed below, this chapter has shown that this method may not be the most suitable technique of sampling the z-scopes. Furthermore, findings suggest that these radio-echo sounding measurements are incompatible with spectral analysis.

3.5.1.1 The reliability of re-digitising

Despite good overall agreement between trace-read and manually re-digitised points, there were some localised differences in the inferred position of the bed. These may arise from scatter on the z-scope image: for example, in some areas the subglacial bed appears as multiple traces, rather than a single line, making the process of identifying the bed subjective. The issue of having to infer which signal return is the bed is illustrated in the cartoon in Figure 3.22, with an actual example of the complexity being seen between shotpoints 475 and 500 for Flightline-122 (Figure 3.23). The implications are that the semi-automatic trace reader measured different traces from those recorded in this study. A visual comparison between the differences in bed elevation and the z-scope implies an association, with higher disagreement in areas of scatter: the most inconsistency corresponds to sections of profile where the bed trace is faint, or appears parabolic with multiple traces. Nevertheless, the vertical accuracy of the trace-read measurements is reported to be ±25 m (Taylor *et al*., 2004), and the differences in mean and standard deviation between trace-read and re-digitised measurements falls within this range.

Figure 3.22: Depiction of scatter on a z-scope image, where parabolas cause subjectivity in inferring the bed trace

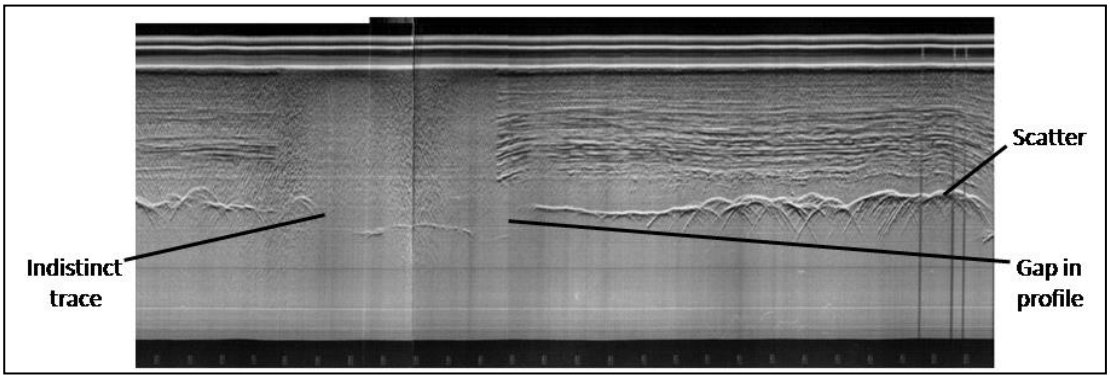

Figure 3.23: Section of z-scope between shotpoint numbers 475 (left) and 500 (right)

Although the measurements sampled at a shorter interval appear to resolve more detail, there is no assurance that the actual bed topography has been captured at a higher resolution. Rather than variations in bed elevation, the data at higher resolution may have recorded artefacts such as scatter on the z-scope. An example of this is illustrated in Figure 3.24, which depicts how digitising a parabola would produce measurements that appear to show change in bed elevation. However, any re-digitising method is likely to encounter this problem, which is more an issue of data quality.

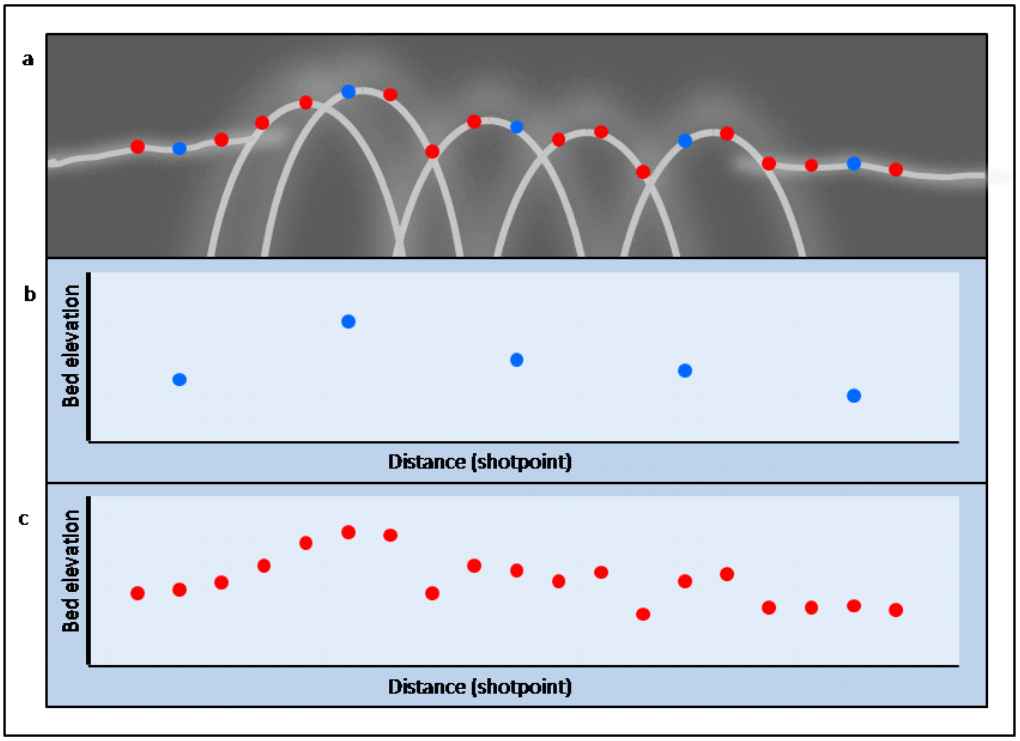

Figure 3.24: The role of scatter in inferring bed traces on a z-scope (a) Depiction of a z-scope image exhibiting scatter in the form of parabolas. (b & c) Bed elevation measurements sampled at different resolutions. Re-digitising may capture noise (e.g. parabolas) rather than actual changes in topography

3.5.1.2 What resolution could be achieved through re-digitising?

Re-digitising went some way to improving resolution, achieving a sampling interval of 250 m between points, which fell within the upper range of the meso-scale defined in Section 2.3. Nevertheless, the data would not be able to capture many of the subglacial bedforms of the order of tens to hundreds of metres in length (Clark, 1993; Hindmarsh, 1999). It remains possible to further increase the number of observations, by reducing the sampling interval between points. However, given that Siegert *et al*. (2004) cite 400 m as being the RES footprint, it could be argued that re-digitising has already exceeded the recorded accuracy of the SPRI dataset. Furthermore the fact that spectral analysis uses windows of multiple points meant that results were still calculated over macro-scale lengths. This makes it unlikely that these SPRI flightlines would allow meso-scale analysis, but the potential remains to study this scale by quantifying roughness via spectral analysis with other datasets.

Another important consideration is that, the resolution of the data is not the same as the scale of roughness that can be quantified using these measurements. With spectral analysis for example, a minimum of 32 points has always been a requirement. Therefore, although the sampling interval of re-digitised data was around 250 m, the minimum window size was 8 km. Other methods of quantifying might have less strict requirements, but as Chapter 5 will show, the majority of techniques for quantifying roughness do so

using groups of points. Therefore, it is unlikely that SPRI data could be used to analyse meso-scale (tens to hundreds of metres) variations in topography.

3.5.1.3 The accuracy of SPRI measurements

Much of this chapter has assessed the accuracy of re-digitised measurements based on their agreement with trace-read data. However, another aspect of the data's accuracy is that of the system when the raw z-scope images were produced. One example of this is the navigational accuracy of the system, which is reported to be ±5 km (Siegert *et al.*, 2004). Table 3.1 showed that, because tick marks were recorded at a regular time interval, the distance between them is not constant. It is clear that, although re-digitising allows points to be sampled over distances of hundreds of metres, the position of these measurements is less certain.

Another cause of inaccuracy related to navigation is the flight path taken during the collection of RES data. If the aircraft changed direction while gathering RES data, this would influence the transmission and reception angle of radio-waves, thus affecting signal returns (Taylor *et al.*, 2004). In this experiment, the results showed an increase in roughness at the bottom of the map (Figure 3.15), but these could be explained by change in aircraft direction. When first selecting a flightline it was clear that the start and end points of many profiles correspond to where the aircraft changed direction. This is perhaps to be expected because profiles were collected in sorties, rather than each one individually. This meant that at the end of one run, the aircraft would have to change direction to setup for its next sweep. The amount of data collected was much higher than that actually used; for example, Bingham & Siegert (2009) shows numerous maps with results profiles plotted, but the interconnecting measurements that join these profiles are not plotted (Bingham, personal communication 11/02/09). The flight path taken for the acquirement of data for Flightline-122 is shown in Figure 3.25: at one end of the profile used in this study, there is a dramatic loop where the aircraft appears to have circled. Furthermore, it can be seen that, along the profile, there are two large changes in direction, and other small kinks. However, although these direction changes may have affected the functionality of the radio-echo sounding equipment, there was no noticeable difference in the roughness values yielded.

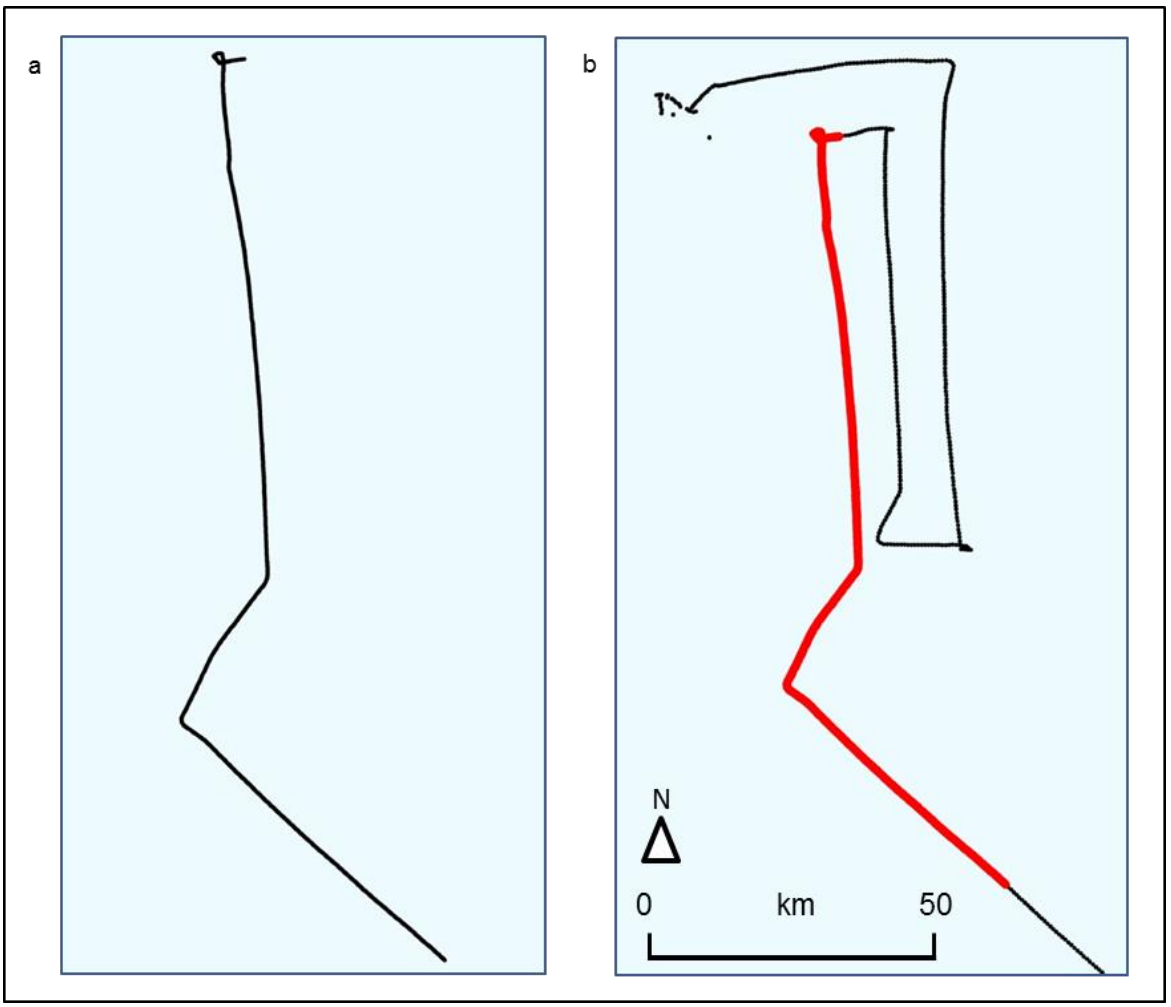

Figure 3.25: Map showing the change in direction along fligthline-122. (a) Flightline-122, the source of bed elevation measurements. It can be seen that rather than a straight line, the profile is characterised by kinks and bends. (b) The complete flight path that the aircraft took during capture of flightline-122. Image is orientated to north

Processing techniques such as re-digitising permit the usefulness of SPRI data to be extended, in this case allowing roughness to be quantified over shorter spatial and wavelength scales. Nevertheless, there is a limit to what can be achieved with these measurements. The problem, however, is that no other records of contemporary ice-sheets match the spatial coverage of these data. To investigate meso-scale patterns in roughness the challenge, therefore, is to identify suitable data that have both a high resolution and cover a large extent. Radio-echo sounding measurements may not be the best choice.

3.5.1.4 The suitability of RES measurements for quantifying roughness

In their raw format, the bed elevation measurements derived from z-scope images are incompatible with many of the requirements of spectral analysis, such as the method's need for a uniform distance between observations (Bingham & Siegert, 2009). Statistics presented in Table 3.1 (Section 3.3.2) showed that the mean sampling intervals of both the trace-read (2354.89 m) and re-digitised (294.36 m) are 17.7% longer than expected (i.e. 2000 m and 250 m respectively). Furthermore, it can be seen that there is a large

range in values for both datasets showing that, in reality, the data are far from equally spaced. To quantify roughness using spectral analysis, the data must be adjusted.

Earlier studies have used linear interpolation to fill gaps of <7 km (e.g. Siegert *et al.*, 2004; Taylor *et al.*, 2004); a similar method was used for manually re-digitised data in this study, interpolating over gaps of <4 km. However, in past studies the 7 km distance equated to less than 4 points yet, with the higher-resolution data used in this project, 4 points equates to just 2 km which is why distance was used to define the acceptable gap. Nevertheless, it is clear that gaps of 3000 m equate to the absence of 12 data points, which draws into question the reliability of linear interpolation over this number of observations. Another issue with linear interpolation is that it effectively smooths out bed perturbations, leading to under-estimates of surface roughness. Further work is required to evaluate methods of interpolating gaps in SPRI profiles.

The gaps in SPRI measurements suggest that these data are not the most suitable records for quantifying roughness. However, given the relative inaccessibility of contemporary ice-sheet beds, the problem of missing data affects other RES data. For example, as Chapter 2 highlighted, missing values are common in areas of crevassing. Moreover, even if the records were complete, they may still have overall slopes that would require detrending. This suggests that, rather than modifying data to fit the method, alternative techniques of quantifying roughness could be used. As the next chapter will demonstrate, some methods make fewer assumptions about the data, making processing such as detrending and linear interpolation unnecessary. Spectral analysis is one approach to quantifying roughness, but others may be more suitable.

3.5.2 A critique of spectral analysis:

Spectral analysis is a versatile method of quantifying roughness. In this chapter for example, the use of this technique allowed different scales of roughness to be investigated. However, there are a number of limitations with spectral analysis that make investigating subglacial bed roughness more difficult. In particular, this investigation has shown how user choices, such as the size of window, influence the spectral analysis values produced. This creates difficulty in comparing the results of different studies.

3.5.2.1 The importance of the sampling interval of data on spectral analysis results

A comparison of roughness results for data gathered at different sampling intervals showed good agreement. This suggests that the resolution of the bed elevation measurements is not an important variable. Ultimately, however, the scale of roughness that can be captured depends on the sampling interval between points: as the sampling interval decreases, the scale of roughness that can be measured also decreases. This

means that if, for example, scientists are to investigate meso-scale patterns in the roughness of subglacial topography, then higher resolution data are required.

Aside from the direct effect of sampling interval on spectral analysis results, the sampling interval of the data also has an indirect influence through influencing analysis decisions. For example, a user's choice over the size of window to be used is based on the resolution of the data. Similarly, the resolution of the data controls the minimum wavelength that can be captured, thus affecting the choice of wavelength classes when decomposed results are produced. Compared with variations in sampling interval, differences in these user choices were found to have a more substantial effect on the results.

3.5.2.2 The effect of user choices on results

By modifying the *N*-values used, spectral analysis can be adjusted to measure roughness over different lengths of window. This technique is useful because it means that, as the resolution of data improves, shorter windows and wavelength classes can be used, allowing finer scales of roughness to be measured. However, a significant finding of this project is that both integrated and decomposed roughness results are influenced by window length.

Comparing the trends of the results showed that window length affects the results. For most classes it is rare for the spectral analysis results of different windows to exhibit the same trend. On the contrary, it was frequently seen that the results show inconsistent interpretations: for example, in some zones the roughness measured at one window length may increase as roughness values for another window decrease. The magnitude of change also varied. In some cases, interpretation of the data may lead to different conclusions being drawn, which may question the relationships inferred between ice dynamics and roughness.

The precise cause of these differing values is unknown. With integrated data, one explanation is that the window length influences the wavelengths of roughness that are measured so, in effect, different scales are being summarised. Another reason for the inconsistency in results is that the observations being used to summarise topography are different depending on the window size. As window size doubles, so too does the number of observations, and this means that intervals being analysed are not the same. As an example, take a situation where two high-roughness areas are separated by an interval of low roughness. A long wavelength might capture two or more of these intervals, producing a value that is moderated by the different environments. With a short window that only captures one of these intervals the values would be high or low, but if all these intervals fell within a larger window the results produced would be moderated. This means the most

agreement between different window lengths is likely to occur where topography remains consistent over a long distance. This may explain why areas with low roughness show the most agreement because many of these intervals appear to be characterised by long sections of profile with few asperities.

Processing may be another cause of the disagreement between results. Detrending followed the method used by Taylor *et al*. (2004) and subsequent studies, where detrending is completed over the same number of points as the window size. Therefore, for testing the influence of window size on roughness, four sets of detrending were required: before running spectral analysis over 64 km windows, processing was completed over a moving band of 256 points, while 32 km windows first required detrending of the profile over 128 points. As Figure 3.26 and Table 3.9 show, there is an issue with this technique because the detrending distance affects the profile shape, which will subsequently alter the roughness values. Therefore, there is an inherent problem with the method of calculating roughness results because processing will influence the results.

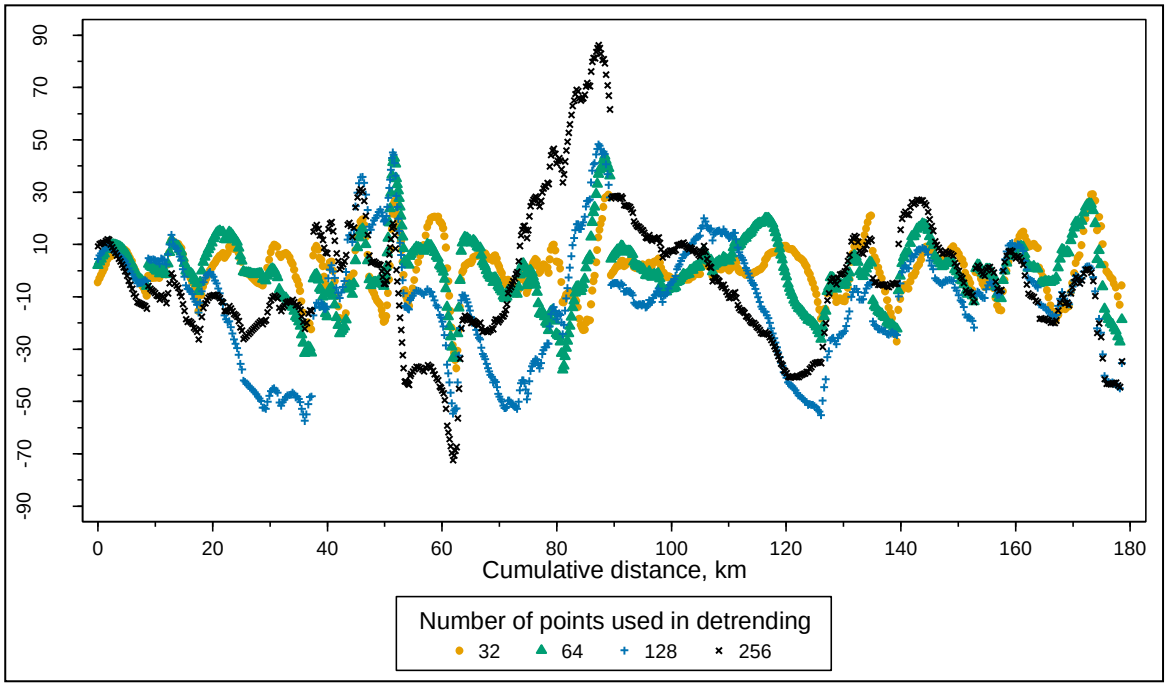

Figure 3.26: Comparison of spectral analysis results produced from bed elevation measurements detrended over different numbers of points. (For length, multiply number of points by 0.25 km, e.g. 32 points is equivalent to 8 km)

Number of points used for detrending	Bed elevation, m (1dp)			
	Min	Max	Mean	SD
32	-37.2	29.6	0.2	9.9
64	-37.9	43.7	0.3	13.4
128	-57.4	48.3	-11.2	23.1
256	-72.5	86.2	-2.1	26.7

Table 3.9: Summary statistics for the 180 km section of Profile shown in Figure 3.27, showing the influence of detrending distance on bed elevation values

To remove this sensitivity to window size, data could be processed independently of window choice by detrending over an arbitrary distance (as used by Rippin *et al*., 2011). The disadvantage of this approach, however, is that smoothing the data in this manner may result in loss of detail, negating the benefits of quantifying over short windows, because the largest window length still dictates the minimum detrending distance that can be used. In this project, adopting this method would have meant detrending would be done over at least 256 points long, a distance eight-times longer than the shortest window size. One might postulate that the method adopted is a more realistic reflection on how scientists are likely to operate with future high-resolution data: it may be expected that, when analysing high resolution data, short window lengths would be chosen, thus requiring the need for short processing lengths. As an extension to this project, a second set of results were produced by varying window length but using a consistent detrending distance of 64 km. These data are not presented, but analysis showed that the values still showed disagreement with window length, thus indicating that detrending was not the main cause of this inconsistency. Furthermore, an issue of using a larger detrending distance than the window size is that it might fail to remove slope as intended. This is illustrated in Figure 3.27 where, although detrending has moved a large overall tilt, on shorter scales a series of slopes still exist so that, when short windows are used, these would produce an overall trend. Such discrepancies could potentially be removed by using roughness parameters that does not require as much processing of the bed elevation measurements.

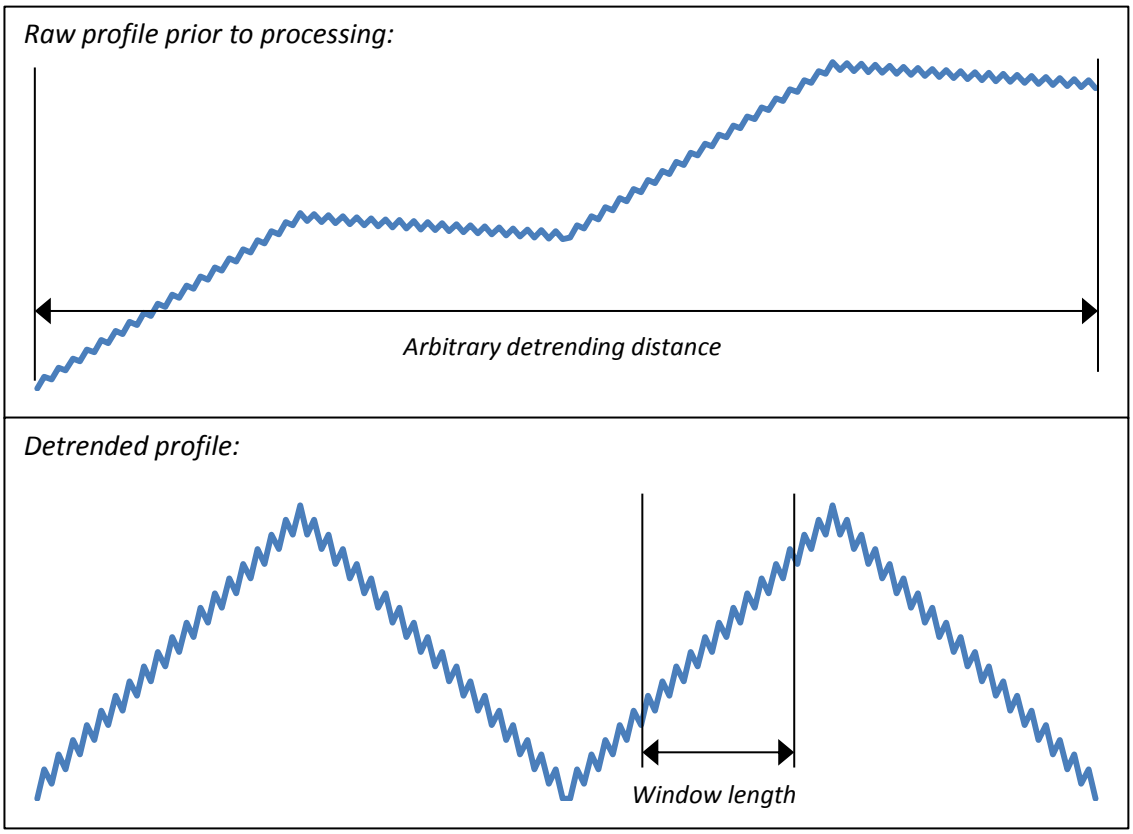

Figure 3.27: Detrending of the profile is designed to remove wavelengths that exceed the window length. Here, it can be seen that processing has removed the overall slope of the profile, yet wavelengths longer than the sample length remain

In addition to the window length being an important choice, another variable that must be considered with decomposed results is the number and size of wavelength classes. Decomposed results are integrations of power spectral density values over fixed wavelength bands, rather than the total roughness of the complete spectrum captured. Unlike integrated results, these are less affected by window length because the choice of wavelength is somewhat independent. This would allow roughness to be compared even when the window size differs, for example, if different resolutions of data had been used. Nevertheless, although decomposed results work over discrete wavelength classes, the results were similar to those of the integrated in that disagreement was still produced. Another problem is that the arbitrary nature of these wavelength classes makes choosing an optimum length difficult. For example, if only short wavelengths were used, they might capture some types of bedforms (say, drumlins), but not larger features (such as mega-scale glacial lineations). A wide selection of wavelength classes might be required to capture the diversity of subglacial bedform sizes possibly present in an area. To give this breadth of classes, large window sizes would be required because this controls the minimum size of roughness that can be measured. Therefore, while much of this chapter has focused on going smaller to improve resolution, achieving a more detailed picture of roughness may require using large windows but short wavelength classes.

With integrated data, results are summarised over a group of wavelengths, but this overall wavelength is restricted by sampling interval and window size: the resolution of the raw data determines the minimum wavelength that can be captured, and the window length the maximum wavelength. In the past, this has not been a problem because the same data have been used (Bingham & Siegert, 2009), but in the future the combined effects of sampling interval and window size mean that, if different data are used, so too will the overall wavelength of integrated data. Without standardisation, this makes comparison of the results between studies difficult, because a given integrated value must be placed in context of the scale that has been summarised.

3.5.2.3 Interpreting the results

The final consideration in evaluating the use of spectral analysis for quantifying subglacial bed roughness is the ability to relate the results to mechanisms that control ice dynamics. Chapter 2 showed how many of the theories on basal ice flow involve the way that asperities on the bed act as obstacles. Although spectral analysis may capture these features, the values yielded give no information on the size or frequency of the asperities. As a result, it is not possible to relate the spectral analysis results with theories on basal ice flow.

Another aspect of spectral analysis is that it captures many types of variation in the topography, for example, from differences in the height of peaks, to the spacing of valleys. Due to the fact that many variables are measured, it is difficult to understand why a given roughness value has been produced. Ideally, a method of quantifying roughness would measure a single variable, so the effect on ice speed of changing that variable could be measured.

3.5.2.4 Specific and wider-reaching advantages and disadvantages

Testing the influence of window size and sampling interval on spectral analysis identified a number of limitations with the method. However, it is important to acknowledge that some of these limitations would apply to other methods of quantifying roughness. One example of this is the effect of window length on the results. In this chapter it was shown that the size of window influenced the roughness values, with the likely explanation for this being due to the fact that this variable influences the population analysed: following the theory of collinearity, longer window lengths are expected to show more dissimilarity in bed elevation values. Therefore, a comparison of values calculated with different window lengths may capture this spatial variation. Arguably, for any parameter that summarises roughness over a series of bins, the roughness yielded will depend on the choice of window length.

Some limitations with spectral analysis apply to other methods of quantifying roughness, yet, this is not the case with all of the difficulties encountered with this method. Again, using window length as an example, it is clear that the sampling length chosen in this project was constrained by the need to use 2^N datapoints. In fact, as discussed in Section 3.5.2.2, a compromise between statistical reliability and resolution somewhat leads studies to choose 32 points. Although any statistical analysis must make similar compromises, it will be shown in the next chapter that alternative methods of quantifying roughness allow more choices in the size of window to be used.

3.6 Conclusions

In this chapter it was shown how the SPRI z-scope images of the subglacial bed can be manually re-digitised to achieve a higher resolution record of bed elevation. Here, an eight-times-improvement was achieved. Nevertheless, although feasible, re-digitising is time-consuming and not the best choice for sourcing higher-resolution measurements. Furthermore, despite the merits of SPRI radio-echo sounding records as an extensive dataset on topography beneath a contemporary ice sheet, there are problems such as navigational accuracy and artefacts on the images. These weaknesses limit the potential of using these data to analyse smaller scales of roughness.

Spectral analysis is a versatile parameter in that the user can define several variables, allowing roughness to be quantified on a range of scales. However, the types of data compatible with this method are limited, and the methods used to adjust the data to fit are not ideal. If analysis options such as the size of window or choice of wavelength classes are changed, it is difficult to compare measurements of roughness between different studies. More importantly, adjusting such variables can significantly affect the results produce.

Sampling interval does not appear to have a major effect on roughness results, but with the use of higher-resolution data, it is also likely that the window size and/or wavelength classes will vary. Both criteria were shown to influence spectral analysis values to the extent that the interpretations drawn from these measurements differed. As such, it may become difficult to compare the results of different studies. This draws into question the suitability of using spectral analysis, and provides impetus for identifying other parameters to quantify roughness, which are reviewed in the next chapter.

At the macro-scale of tens of kilometres, the spectral analysis method followed here has gained much prominence, with relatively little variation in the approach used. Yet, there is no standard approach to analysing roughness at different scales. The fact that this chapter has found the choice of scale to be important in controlling results, illustrates the

importance of analysing the relationship between roughness and ice speed at different scales.

CHAPTER 4
A review of roughness parameters

4.1 Introduction

The purpose of this chapter is to review the most common methods of quantifying surface roughness in a range of sciences. From Chapter 3, it was seen that there are some limitations with measuring subglacial bed roughness using spectral analysis. This prompted a search to find alternative methods that might better allow roughness to be compared between different datasets. There are, however, many methods of quantifying roughness so an initial review was required to achieve some shortlisting.

Other sciences provide a useful source of methods for quantifying roughness (see Section 2.4). One advantage of using these parameters is that they have often undergone some evaluation (e.g. Rudzit, 1975). Questions remain, however, over the usefulness of these methods to glaciologists. For example, many parameters have been designed for a specific purpose, and measure variables not relevant to subglacial beds. The aim of this study was to evaluate a selection of such techniques. Because of the large number of parameters, it would be beyond the scope of this chapter to report them all. Indeed, some technical papers are dedicated to this (e.g. BSI, 2010a), and other scientific papers are solely aimed at reviewing the variety of methods (Gorlenko, 1981; Czichos *et al*., 2006). An example of this is Gadelmawla *et al*. (2002), who not only present 59 of the most common methods of quantifying roughness, but also provide an evaluation on how they might be used.

4.2 Definitions

For clarity, a series of terms are used throughout this chapter to define characteristics of topography. In particular, several definitions are used to describe the form of bumps and depressions along a profile. *Peaks* or *bumps* are used to refer to convex-upwards sections of profile. Concave-downward shapes are termed *valleys* or *depressions*. Collectively, peaks and valleys are referred to as *asperities* or *perturbations*, the two terms being used interchangeably throughout this chapter. Note that these definitions of asperities give no sense of size, e.g. peaks may range in height from less than a metre, to hundreds of metres. Other terms are used to describe the parts of asperities, such as high

or low points. The highest value of a peak is termed the *crest*, more precisely defined as a local maximum that has a higher value than the observations immediately before and after it. For analysis of 3D data, a crest is a pixel whose neighbours are lower. Except for edges and corners a crest is a point that has eight neighbouring lower values. The lowest amplitude observation of a valley is termed a *trough*; troughs have two immediately adjacent higher values. With surface data, a pixel that has a height lower than its neighbours is termed a *pit*.

Several terms describe variations in topography along the profile. These names also apply to the roughness parameters, being used to describe what they are designed to measure. *Amplitude* refers to the vertical height of perturbations. Note, however, that amplitude can be compared between individual points as well as perturbations. In contrast, the *wavelength* is used solely for the description of asperities, describing their horizontal magnitude. More technically, the wavelength is the horizontal period of a valley or peak, measured from crest-to-crest, trough-to-trough, or node-to-node. *Frequency* describes the number of perturbations within a given sample length, and is inversely related to wavelength, decreasing as wavelength increases. For some parameters, this definition may be more precise, for example, the frequency of peaks would measure only convex-upwards topography. With the parameters discussed in this chapter, the frequency of peaks and troughs is calculated by counting the number of crests and/or troughs, respectively. Because of the relationship between frequency and wavelength, some parameters that are designed to measure one characteristic may permit information on another type of variation in asperities to be inferred.

When describing the spatial variations in topography, it is natural to use the terms *rough* and *smooth*. As was discussed in Chapter 2, these words have vague meanings, but are nevertheless useful for drawing contrast between topographies. Therefore, these names are used through this chapter. As shall be seen however, depending on the parameter, the definitions of rough and smooth may vary.

Section 2.4.1 showed how roughness can be quantified two-dimensionally (e.g. Whitehouse, 1994) along profiles, and three-dimensionally (e.g. Fox & Hayes, 1985; Farshad *et al*., 2001; Gadelmawla *et al*., 2001) across surfaces. By convention (see Dong *et al*., 2004), 2D parameters are prefixed with *R*, followed by lowercase letters that denote the method used: for example, R_a describes the *arithmetic average* (Gadelmawla, 2004). 3D parameters adopt a similar format, but are prefixed with *S*. However, there are some exceptions, such as *w* that describes the *interface width*, because the naming convention has failed to receive universal acceptance. Due to the inconsistency in abbreviating parameters, this chapter avoids their use where possible.

Two-dimensional parameters are used to analyse variations in topography along a profile. Aside from glaciology, 2D methods dominate much of the scientific literature, appearing particularly common in engineering (e.g. Gadelmawla *et al*., 2002). As much of the available glacial bed data beneath contemporary ice sheets, such as radio-echo sounding, comprises 2D profiles, the majority of this chapter is given to the presentation of methods for quantifying roughness in 2D. Future datasets may increasingly be gathered across surfaces, so some methods of quantifying roughness in three-dimensions are also described. Many of these 3D parameters are derived from 2D techniques, while others are more *ad hoc* in nature.

Many roughness measures only give information on a certain characteristic of the bed, such as the vertical variation in topography. As such, in manufacturing and similar disciplines, 2D roughness parameters are sub-divided into three categories, namely: *amplitude*, *spacing*, and *hybrid* parameters. In this chapter, a similar nomenclature is used, along with a fourth class termed *shape* parameters. Amplitude parameters measure the vertical characteristic of a surface; spacing parameters are used to take account of the horizontal component of a profile, such as wavelength or frequency of asperities; shape parameters describe the general form of topography, e.g. slope, rather than peaks or troughs specifically; and hybrid parameters combine amplitude and spacing measurements to describe the shape of the profile, such as its sinuosity (Hall *et al*., 1997). Methods for quantifying roughness in 3D methods can also be categorised (Arvidsson *et al*., 2006). British Standards Institution (2008a, 2008b) describes five such categories: *height*, *spatial*, *hybrid*, *function*, and *segmentation* parameters.

Section 4.5.5 provides a summary list of the 2D and 3D parameters ultimately used in this project. A mathematical description of these is presented in Appendix 1.

4.3 Review of 2D roughness parameters

4.3.1 Amplitude parameters

Most roughness methods are used to assess the amplitude of a profile. These techniques rely on classifying a surface based on the height of peaks (Kupko *et al*., 2007), the depth of depressions (Mendeleev, 1997), or both (Lowe & Splindoe, 2007). Many of these methods use measurements made relative to a base line, typically, the mean amplitude of a profile (Gadelmawla *et al*., 2002) as shown in Figure 4.1:

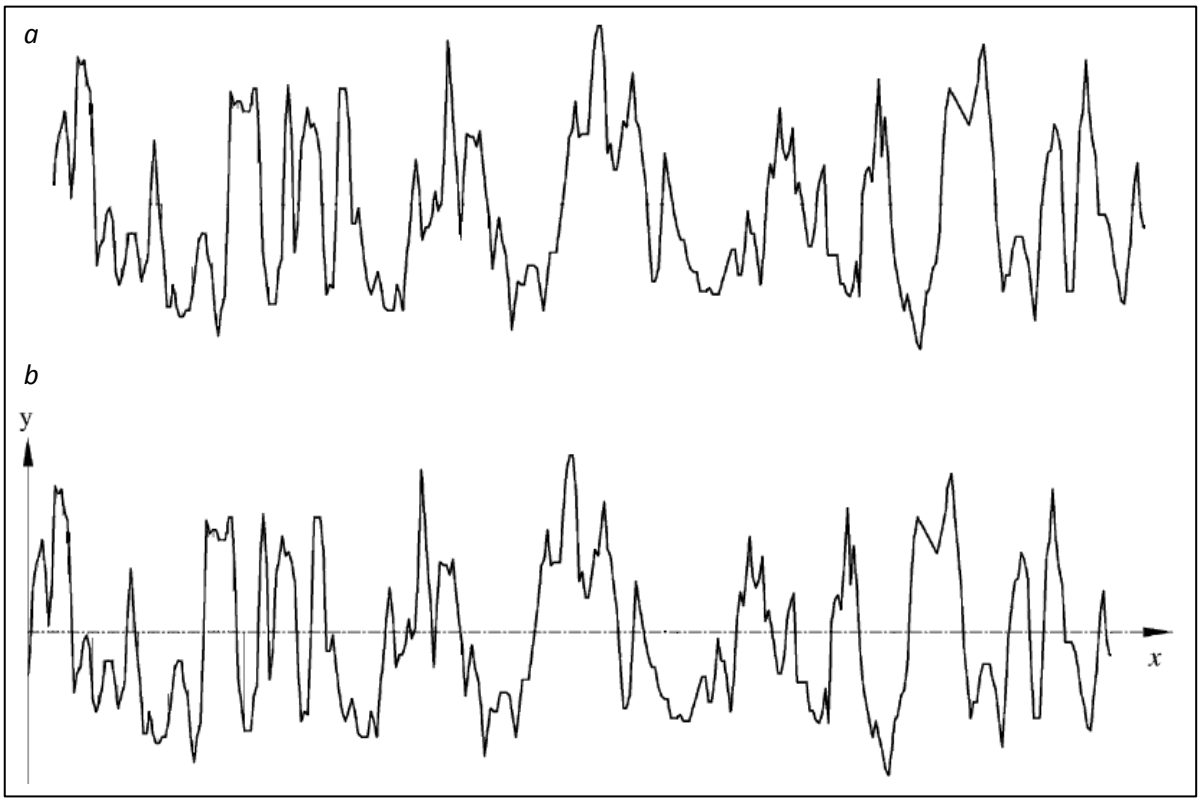

Figure 4.1: In calculating roughness using amplitude parameters for a given profile (a), the first step is often to determine a base line, such as the mean amplitude of a profile, as shown in (b) (modified from Gadelmawla et al., 2002: 135)

4.3.1.1 Mean height

An overall summary of amplitude variation can be produced by calculating the *mean height* (Gadelmawla, 2004; Gadelmawla *et al*., 2002). The parameter measures the average vertical distance of observations, which effectively gives a centreline value (Elfick *et al*., 1999; Kupko *et al*., 2007; Shaw, 2007; Bohm *et al*., 2009), as illustrated in Figure 4.2 below.

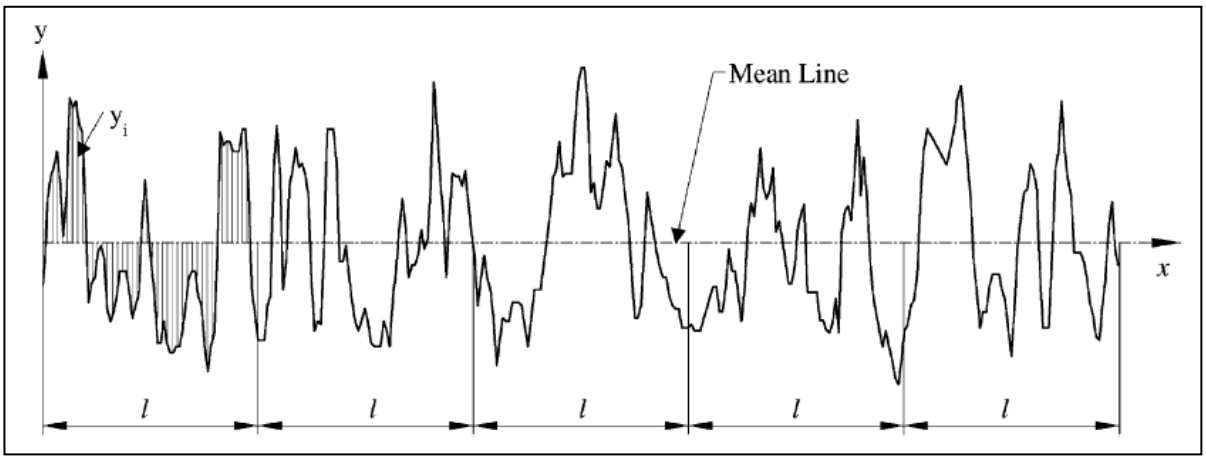

Figure 4.2: Calculation of the mean height (from Gadelmawla et al., 2002: 135)

This method is arguably the most-used parameter across many sciences (Mendeleev, 1997; Kupko *et al*., 2007), from medicine (Koh *et al*., 2002) to physical sciences (Menzes *et al*., 2008). This parameter commonly appears in manufacturing and engineering, where

it is used to monitor quality of parts (Spragg & Whitehouse, 1970; Bigerelle *et al*., 2003), and functionality of tools (Yang & Jeangm 1994). The wide application of this parameter perhaps gives some assurances as to its reliability and suitability.

Although widely used, this parameter it is also one of the most criticised. One weakness is that it does not distinguish between profiles of different shapes (Ripa *et al*., 2003) so different topographies may produce the same value (Feng *et al*., 2003). For example, a surface dominated by many peaks may have the same roughness as one with numerous valleys. As a result, surfaces with different functional characteristics (e.g. frictional behaviour) may have the same value. Nevertheless, as Section 4.5.2 discusses, this is an unavoidable fact that applies to all roughness parameters. Scientists have also identified that the parameter is insensitive to small-scale changes in height (Sedlaček *et al*., 2009), which may limit the scales of roughness that can be summarised.

In many sciences, the mean height would be calculated over a single assessment length. In glaciology, the use of long profile lengths is common, which means that such an approach would likely give results with an unacceptably low resolution. Only producing one result per profile would inhibit the comparison of different regions, and produce values that are over-general. Nevertheless, it is possible to calculate this parameter over a series of sampling windows, which could be discrete or moving in design. In practice, many parameters aside from the mean height are usually measured over assessment lengths.

Changes in roughness due to differences in amplitude can be further explored by looking at variations in amplitude in more detail, using the mean height to produce further results. For example, the *mean above height* gives the average amplitude of observations that are above the mean line. Similarly, the *mean below depth* is defined as the average amplitude of values that lie below the window's mean amplitude. These parameters give an average height measurement that is more specific than *the mean height* as, in effect, a different zone is measured by each of the methods. Further information could be gained by comparing both results, making it possible to assess whether results of some sections of bed exhibit skewness. Nevertheless, these parameters cannot determine whether a zone is dominated by crests or troughs: both peaks and valleys may lie above or below the mean line, and neither the mean above height nor the mean below depth are able to distinguish between the two types of asperities.

4.3.1.2 Measuring deviation

The dispersion in heights about the mean can be measured using the *mean deviation* parameter. This method quantifies roughness by summarising the mean distances between each observation and the mean line, with higher values indicative of a rougher surface. However, a problem with this parameter is that observations above the mean line

might cancel-out those below, giving a low value even if the surface is relatively rough (Suh & Polycarpou, 2003).

Another method of dispersion is the *interface width* or *vertical correlation length* (Jiang *et al*., 1997), and is defined as the root mean square of the surface height function. When measured from the mean line, this parameter is termed the *root mean square roughness* (BSI, 2009c), or, as in the case of this thesis, the *RMS height*. The RMS height is equal to the standard deviation of the surface height (Boon & Bhushan, 1995; Aguilara *et al*., 1999; Kumar *et al*., 2007; Bohm *et al*., 2009). This parameter is one of the most widely used across a range of sciences, but has a particular prominence in manufacturing (e.g. Gadelmawla *et al*., 2002). This method is often used to complement the mean height, and, because of their wide usage many studies have attempted to establish the correlation between these two methods for the respective surfaces being measured (Mironchenko, 2005, 2009).

One advantage of these techniques is that they are less sensitive to tilting of the profile (McCarroll & Nesje, 1996), which means that fewer processing steps (e.g. detrending) would be needed to prepare the data for analysis. There are several limitations with the interface width, for example, although it takes all amplitudes of perturbations into account, they are sensitive to the largest amplitude irregularities (Sedlaček *et al*., 2009). Furthermore, like the *mean* deviation, the RMS height suffers from the problem that different shapes can yield the same value (Li *et al*., 2009).

4.3.1.3 Identifying extreme values

Thus far, the parameters described have been designed to give general summaries in amplitude. The majority of such methods use every observation, or at least consider them, to give a roughness value. A more specialised group of parameters take a subset of the population to give information on the height of asperities (peaks and/or valleys). Usually, these parameters identify peaks and valleys by determining which observations are crests or troughs, and do nothing with those observations that are neither of those identities. A crest is the pinnacle of a peak and is defined as an observation with two adjacent lower values; a trough is the reverse situation, i.e. a low-point that has two adjacent higher values.

Just as methods to quantify the height of peaks are a subset of amplitude parameters, a further sub-category can be used to distinguish parameters that measure extreme asperities, and those designed to give a more general summary of asperity sizes. Those in the former category include the *highest peak* and *deepest valley* parameters (ISO/DIS 23519; Mendeleev, 1997; Kupko *et al*., 2007; Shaw, 2007).

To determine the highest value it is necessary to use a datum. The highest peak is often measured relative to the mean line (Boon & Bhushan, 1995) and, as a result, it is not uncommon for this parameter to be termed the *peak-to-mean distance*. Interestingly, a corresponding term the *valley-to-mean distance* does not occur, and is perhaps a quirk of manufacturing engineering: peaks appear to be of more importance to engineers for various reasons. Nevertheless, measurement of the deepest valley is possible and can take the mean line as a datum (as depicted by Gadelmawla *et al*., 2002 in Figure 4.3). The use of the mean line as a datum might be an appropriate choice for glaciology, where the datum may not otherwise be constant between sets of data.

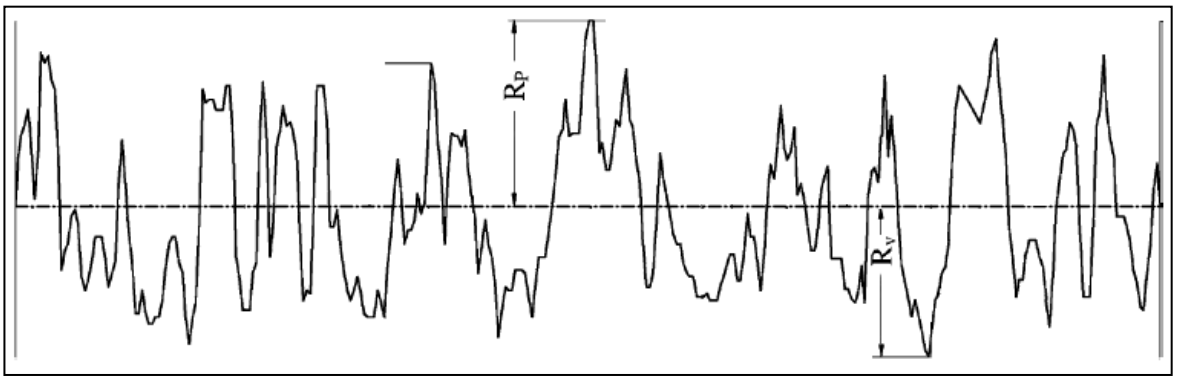

Figure 4.3: Definition of the highest peak (R_p) and deepest valley (R_v) (modified from Gadelmawla et al., 2002: 135)

Upon first impressions, these methods may appear basic to the point of being almost crude, especially when compared with the complex techniques for calculating roughness via a method such as spectral analysis (Chapter 4). Yet, in terms of investigating ice-sheet roughness, it is obvious how such parameters could be useful: glacial theory suggests that obstacles on the bed inhibit ice flow (Section 2.3), so identification of the largest obstacle gives an estimate of the maximum theoretical resistance.

Strictly speaking the highest crest may not be equivalent to the highest amplitude for a profile. Similarly, the lowest trough may not equal the lowest height. This is because, when calculating roughness over a series of bins, it is possible for asperities to occupy two or more windows. Figure 4.4 below illustrates how the large peak extends from the first window and into the second. As a result, the highest value for the first window is actually the rising limb of this asperity. Although, statistically, such a situation is unlikely, strictly speaking, determining the most extreme values requires the whole profile to be inspected, and not just crests and troughs. In this manner, it is possible to define the *maximum above height*, which calculates the highest amplitude for a sampling window, and the *maximum below depth* that is defined as the lowest amplitude.

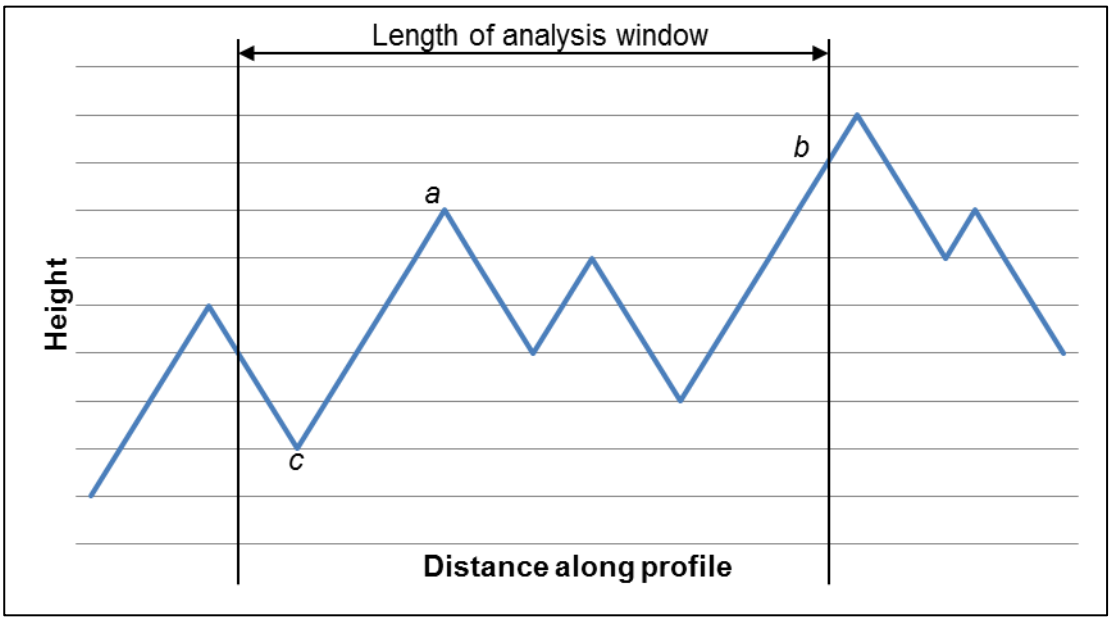

Figure 4.4: Distinction between the highest peak parameter, and the maximum above height. The marker (a) shows the highest peak, which is a crest with two immediately lower values. Label (b) shows the maximum above height, which is the highest observation within the window. The position (c) is both the deepest trough, and the maximum height below.

The main issue with these parameters is that, summarising only one observation, the results may be unrepresentative of the sampling window. In many sciences these parameters that identify extreme values are designed to find anomalies, such as those caused by flaws (Thomas, 1981). Giving no detail on the standard deviations of heights, so it is not possible to identify whether the value is representative of the typical perturbation size or whether, instead, it is anomalous.

4.3.1.4 Range

With many roughness parameters the values used to calculate them are measures of roughness in their own right. In this manner some parameters are especially useful because they can be used to derive other information. Despite the limitations of *highest peak* and *deepest valley* they are among the most widely used parameters and this is, in part, through their use for quantifying roughness using other techniques (Hall *et al*., 1997; Gadelmawla *et al*., 2002; Kupko *et al*., 2007; Shaw, 2007). A clear example of this is the use of extreme values to determine the overall *range* in height for a sample length.

There are various methods of calculating range, one of these being the peak-to-valley height. This parameter is derived by adding the amplitudes of the highest peak and the deepest valley (see Figure 4.5). An alternative method is to subtract the height of the lowest valley from that of the highest peak, and is sensibly called the *peak-minus-valley* (P-V) parameter (Boon & Bhushan, 1995; Kumar *et al*., 2007). In both cases, the height of the peaks and depth of valley are measured using the mean line as a datum (Gadelmawla *et al*., 2002).

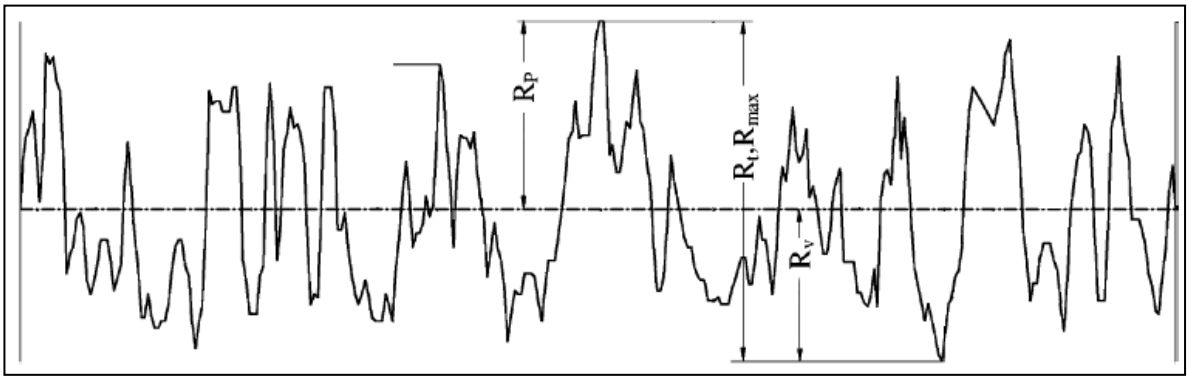

Figure 4.5: Definition of the peak-to-valley height (R_t or R_z) (from Gadelmawla et al., 2002: 135)

Like the mean, the range is a familiar statistic, although not generally thought of as a method for measuring roughness. From a glaciological perspective, however, it can be seen how the range may be a proxy for roughness, e.g. determining the resistance to ice flow: measuring the overall amplitude of a profile this parameter could be used by glaciologists to estimate the maximum theoretical obstacle size. However, as with other parameters that use a subset of the data, methods that calculate range have been identified as being prone to be unrepresentative (Hall *et al*., 1997; Kupko *et al*., 2007) and sensitive to anomalous values (Smith *et al*., 1999; Gadelmawla *et al*., 2002). Another issue is that the range is unlikely to measure obstacle size. The highest and lowest value may not be spatially adjacent along the profile and, if sampling window length is relatively large, they may be some distance apart. As a result, the range is only an upper estimate of the obstacle size that ice may encounter. Furthermore, a high range could be produced by deep valleys as well as high peaks, which is important because the role of these features in controlling ice dynamics might vary.

Some roughness parameters are measured at two or more scales with the results sometimes being compared. In engineering, the *peaks-minus-valleys* may be calculated over a window, R_t, or for the entire assessment length, R_z (Lowe & Splindow, 2007). By comparing the range at different intervals along profile with the range for the profile overall it is possible to determine whether there are local extremes. In engineering these may point to flaws in the surface, but with glacial data such information might be used to identify anomalously high or deep relief.

Using range values calculated for each sampling length, R_z, it is possible to calculate the *mean maximum peak-to-valley height* for the complete profile (El Feninat *et al*., 2001; Davim *et al*., 2009), as illustrated in Figure 4.6. Again, this demonstrates how results from one parameter are often used to derive another. Summary statistics for the complete assessment length might be useful, but with the long profile lengths typical of glacial data (e.g. recall the SPRI flightline in Chapter 4), such statistics might be over-simplifications.

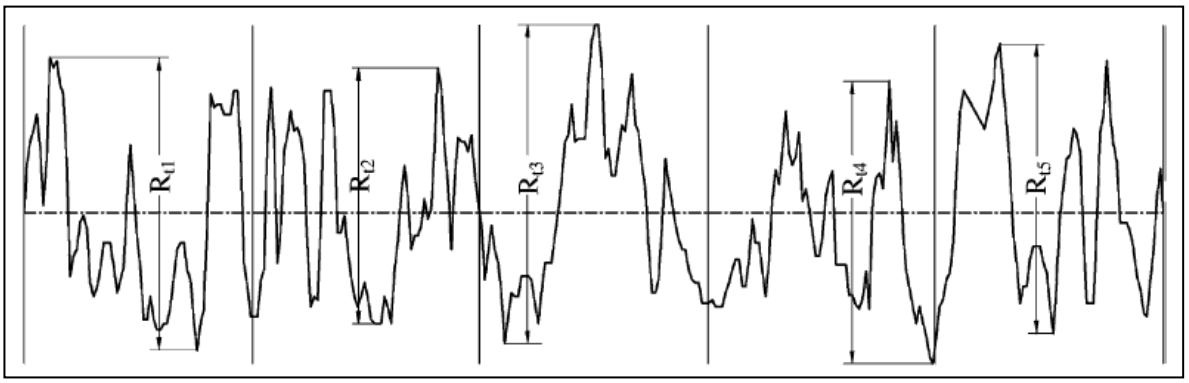

Figure 4.6: Definition of the mean peak-to-valley height parameter, averaging R_t over several sample lengths ((from Gadelmawla et al., 2002: 136)

Some methods of quantifying roughness, such as the *peak-to-valley* height*,* may be inaccurate because they are based on a limited number of data points. To overcome this, some methods calculate the average amplitude for a series of perturbations. One example is the *ten-point height,* R_{z10} (Whitehouse, 1974; Thomas, 1981), which is defined as the mean of the absolute values for the five highest peaks and five deepest valleys (Daugaard *et al*., 2007; Kupko *et al*., 2007), as illustrated in Figure 4.7:

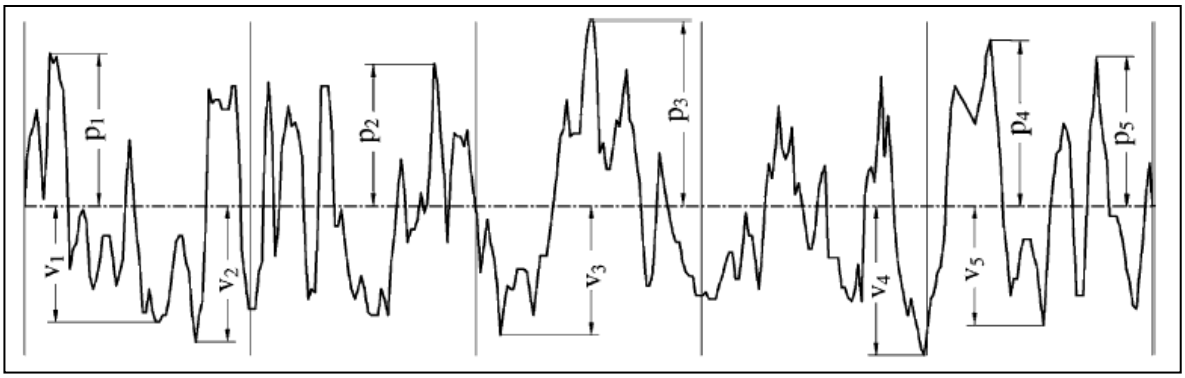

Figure 4.7: Definition of the ten-point height (R_{z10})

An advantage of calculating the range in amplitude over ten measurements is that it may be more representative of the profile: Gadelmawla *et al*. (2002) comment that, compared with R_a, this parameter is more sensitive to occasional high peaks or low valleys. However, the inability to not distinguish between peaks and valleys (Shaw, 2007) would be a disadvantage to glaciologists because peaks are likely to influence ice-sheet behaviour differently than valleys. Furthermore, the choice of 10 asperities is only arbitrary, and it is not known how representative this would be of glacial perturbations. More testing would be needed to test the suitability of this parameter, perhaps calibrating the number of asperities averaged depending on the size of window; as a result, this method is not included in the evaluation.

4.3.1.5 Asperity size

In many sciences identifying the size of perturbations, especially peaks, is a priority because it is these that determine much of the surface finish: for example, peaks affect the quality of finish, frictional resistance, and can play a role in how a surface will wear (Najjar *et al*., 2003). Unsurprisingly, this means that there are many parameters designed to measure the size of perturbations.

Measuring the highest peak in a sampling window has some uses but, as discussed, it may be unrepresentative of the population. An alternative approach is to quantify the average peak size (Militky & Bajzik, 2003), and there are several variations on methods for doing this. One example calculates the *mean peak height* for several sampling windows (Gadelmawla *et al*., 2002), as illustrated in Figure 4.8. For example, five sample lengths appears a common choice (e.g. Hall *et al*., 1997), but the decision is arbitrary. Although this makes the result more representative for the entire assessment length, it lowers the resolution of the results, so the number of bins the result is calculated over will be a compromise between spatial resolution and gathering enough observations to represent the population. Due to the coarseness of this parameter, it may be poorly suited to glacial data. In Chapter 4 it was shown how RES data gathered from the SPRI campaigns have been the main choice for investigating roughness. Hypothetically, calculating the mean height over five 64 km windows (i.e. the size used in studies such as Bingham & Siegert, 2009), a single value would be produced for each 300 km length.

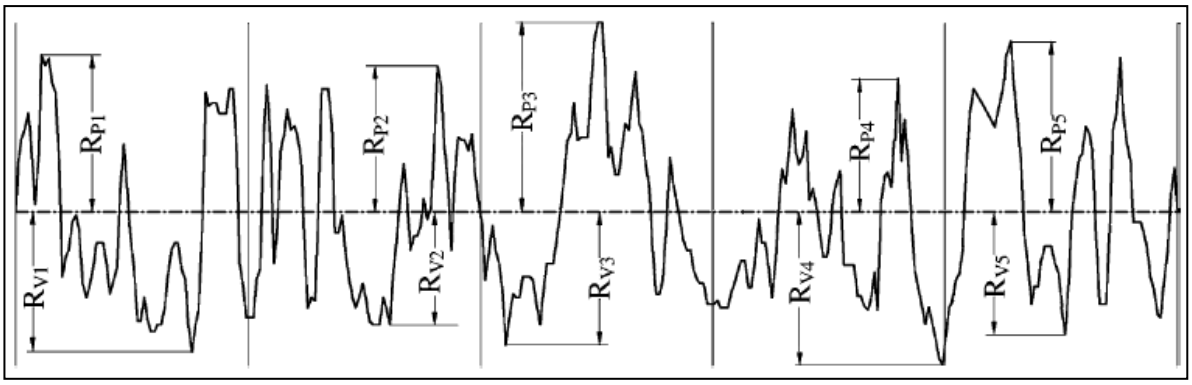

Figure 4.8: Definition of the mean peak height. In this example, results are averaged over five sample lengths (modified from Gadelmawla et al., 2002: 135)

In some studies, the mean height of peaks defined as the average amplitude measured between the reference line and the highest peak (Gadelmawla *et al*., 2002). When the reference datum is the mean height, then the mean peak height is effectively the average peak-to-mean distance.

Rather than restricting the summary of peak size to the largest asperities in each window, it is possible to measure the height of every crest in a given window, and calculate the mean value. This approach is arguably more representative of the population because all

peaks are considered. Furthermore, compared with results that summarise over several windows, the resolution of results produced within a single window will be finer.

To get information on the amplitude variation of a profile, it is insufficient to look solely at the peaks. Just as some parameters are specifically designed for measuring positive topography, there are methods designed to measure the *mean depth of valleys*. Such methods are essentially the same as the *mean peak height* parameters, except that they are designed to measure the amplitude of troughs rather than crests. As the counterparts to the methods of calculating the average peaks, the mean valley depth parameters have similar benefits and limitations (Menzes *et al*., 2009).

4.3.2 Spacing parameters

Amplitude parameters only measure roughness in terms of the height of the profile surface. Another form of topographic variation is in the horizontal plane, and these variables can be measured using *spacing parameters*. Roughness in the x-axis is only detected when there is a change in the magnitude or frequency of asperities; where height is constant along-profile the horizontal component of roughness is constant. Therefore, unlike amplitude parameters that can use any part of the profile (i.e. all observations) within a sample length, spacing parameters only measure the frequency and/or wavelength of asperities.

4.3.2.1 Number of asperities

A simple measure of asperity frequency is to count their total number for each a sample length (Najjar *et al*., 2003; Shaw, 2007). The *number of peaks* parameter, also termed *peaks per unit length* (Gadelmawla *et al*., 2002), counts the number of crests, and the *number of valleys* measures the number of observations that are troughs. These results allow the density of asperities to be compared between windows. Such information may be useful to glaciologists in allowing them to identify areas with a higher number of peaks, which are expected to be more resistant to ice flow.

It is possible to tune peak and valley counts to quantify roughness at different scales. This can be done by defining thresholds and cut-offs (BS EN 10049:2005(E)), which are illustrated in Figures 4.9 and 4.10. When these are in place, a peak is only counted if its height is equal to or greater than the threshold value; depths must be below the threshold. Cut-offs control the maximum size of asperity counted: e.g. using a peak cut-off of 1000 m means that only crests with heights below this value are counted. Therefore, it can be seen how a relatively simple parameter can be adjusted to give detailed information.

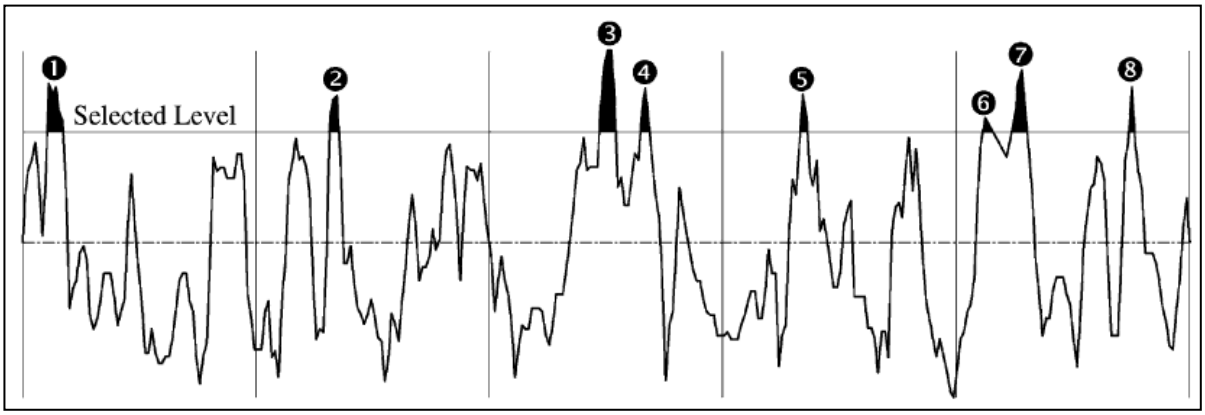

Figure 4.9: The use of a threshold to measure the frequency of peaks that are above a certain height (from Gadelmawla et al., 2002)

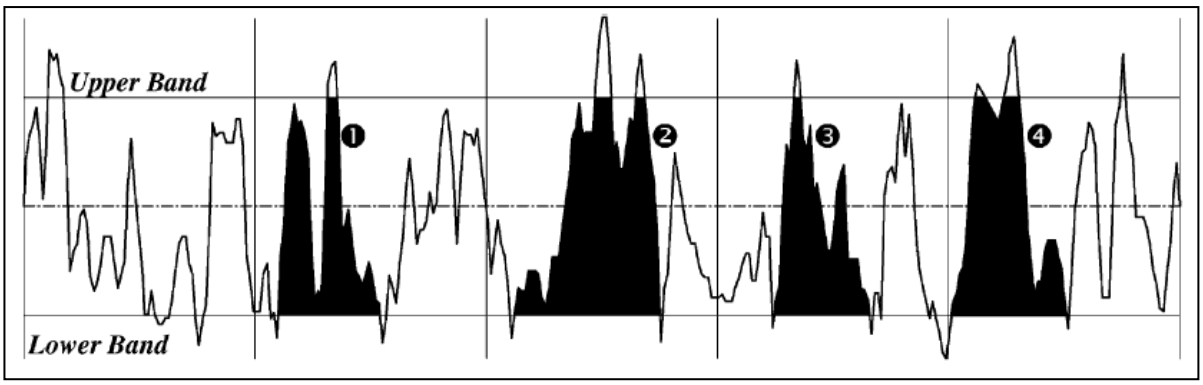

Figure 4.10: The use of a cut-off to constrain the maximum height of peaks counted (from Gadelmawla et al., 2002)

Combined counts of the number of peaks with the number of valleys can be used to give the total number of perturbations. Further information can be gained by comparing peak and valley counts, as the ratio between these two parameters acts as a measure of *skewness*. This approach might work well in glaciology, especially when coupled with thresholds, to test whether subglacial beds are dominated by asperities of a particular type and size.

A difficulty with the number of peaks and number of trough parameters is that comparing data with different window sizes is problematic. As the window length increases it is probable that so too will the number of asperities, particularly when no thresholds are used. To take account of the length of window and the resolution of the data, the results can be standardised using the number of observations. The *percentage of peaks* is defined as the percentage number of observations that are classified as crests. Similarly, the *percentage of troughs* summarises the percentage of the population that are troughs.

4.3.2.2 Horizontal size of asperities

Using frequency it is possible to infer wavelength. For example, a higher frequency of perturbations would imply shorter wavelengths, but unlike the science of waves (where

wavelength is the reciprocal of frequency), surfaces may exhibit complex shapes. Furthermore, one of the main limitations of spacing parameters is that they do not allow the shape of the profile to be deduced. For example, if a section of profile returns a low peak count, there are several profile shapes that could yield such a result, such as flat topography versus an area with large-wavelength peaks. One approach to overcome the lack of information on horizontal size would be to count the number of asperities over a series of bands. This could be done using thresholds (either vertically or horizontally), allowing the frequency of asperities to be tallied by size. However, a number of parameters specialise in quantifying the wavelength of asperities.

The *average wavelength* (Aguilara *et al*., 1999) can be calculated via a number of methods, and these are useful for giving a general summary of asperity size. The average wavelength gives the mean distance between peaks or valleys, and these lengths can be measured peak-to-peak or valley-to-valley (Shaw, 2007). Measurement of wavelength using peaks is much more common in the literature, but this may be due to peaks seemingly being of more interest in many sciences. One such example that uses the peak-to-peak distance is the *mean spacing of adjacent local peaks* (Mendeleev, 1997, 2003; Robbe-Valloire, 2001).

For a given sampling length it is possible to calculate the mean wavelength using the distance between every peak. However, like with amplitude parameters, thresholds can be used so that only peaks above a certain size are counted. Sometimes in engineering for example, the mean wavelength is used to summarise peaks that have a ≥10% difference in crest height from that of their neighbours (Gadelmawla *et al*., 2002).

An alternative method of measuring wavelength is to record the horizontal distance between peaks (or valleys) where they intersect the mean line (Shaw, 2007). Here, a peak is defined as the highest point of a profile between an upwards and downwards crossing of the mean line (Mendeleev, 1997).

Methods that summarise the average wavelength are subject to many of the same difficulties as the *mean height* amplitude parameter. For example, these parameters give no information on the range of wavelengths, or the standard deviation, so it is not possible to determine the distribution of values about the mean.

Given the vast number of roughness parameters, it is likely that some of these are designed to assess the frequency of depressions. No examples were found in the literature, but it is clear that these could be easily developed by adapting parameters for calculating peak frequency. One approach would be to use or adapt a method to evaluate both peaks and valleys in one step. This would give information on the total number or size of perturbations. However, the difficulty with such a parameter is that it draws no

distinction between peaks and valleys. It is advantageous to know whether a surface is rough due to the presence of peaks, as the processes by which the bed interacts with ice flow will differ in both scenarios. This could be achieved by calculating both the frequency of peaks and the frequency of valleys individually, then analyse use both sets of results to analyse the profile.

4.3.3 Shape parameters

Shape parameters are a relatively broad category of methods. The types of topographic variation these techniques are designed to measure varies widely. A number of parameters are designed to summarise the shape and size of perturbations by taking account of their horizontal wavelength and/or frequency. Other shape parameters are not designed to measure frequency or magnitude of asperities but, instead, give information on their shape, such as the sharpness of peaks. Other methods are used to quantify the shape of the profile more generally, and are not limited to measuring perturbations: for example, a parameter may describe how observations are distributed about the mean.

4.3.3.1 Number of points

One measure of shape is the distribution of observations along profile. As this is not a measure of topography it is not strictly considered to be a measure of roughness. However, information on the number of points per sample window may be useful for putting other parameters in context. For example, with methods that use the complete population, such as the mean height, the number of points parameter can be used to calculate the population size the roughness is based on. Furthermore, the parameter may be useful for judging the quality of glacial data: for example, when window size is consistent, a lower number of points relative to other areas along the assessment length would indicate gaps.

4.3.3.2 Symmetry

With spacing parameters, it was shown how the distribution of peaks and valleys could be used to give an indication of profile symmetry. However, the flaw with this analysis is that it assumes peaks lie above the local (or global) mean, and all valleys lie below this reference. In reality, such organisation is unlikely: Figure 4.11 that shows a profile where the fluctuations in heights produce valleys above the mean line, and peaks below. A more accurate method of characterising the distribution of points about the mean line is *skewness* (Aguilara *et al*., 1999; Smith *et al*., 1999; Gadelmawla *et al*., 2002; Pohl & Stella, 2002. As illustrated in Figure 4.11, a negative value implies a surface with deep valleys and shallow peaks, while a positive value implies that a surface has high peaks and shallow valleys (Lowe & Splindoe, 2007; Sedlaček *et al*., 2009). Where the height distribution of peaks and valleys is the same, the profile is said to be symmetrical (Hall *et al*., 1997) and, statistically, such profiles return skewness of zero. Such a parameter might

be suited to studying glacial bedforms. For example, some glacial studies have investigated the mechanisms of flute formation (e.g. Hubbard & Reid, 2006). Skewness might be useful in determining whether a field of flutes comprises positive relief features, or whether the topography is formed by grooves.

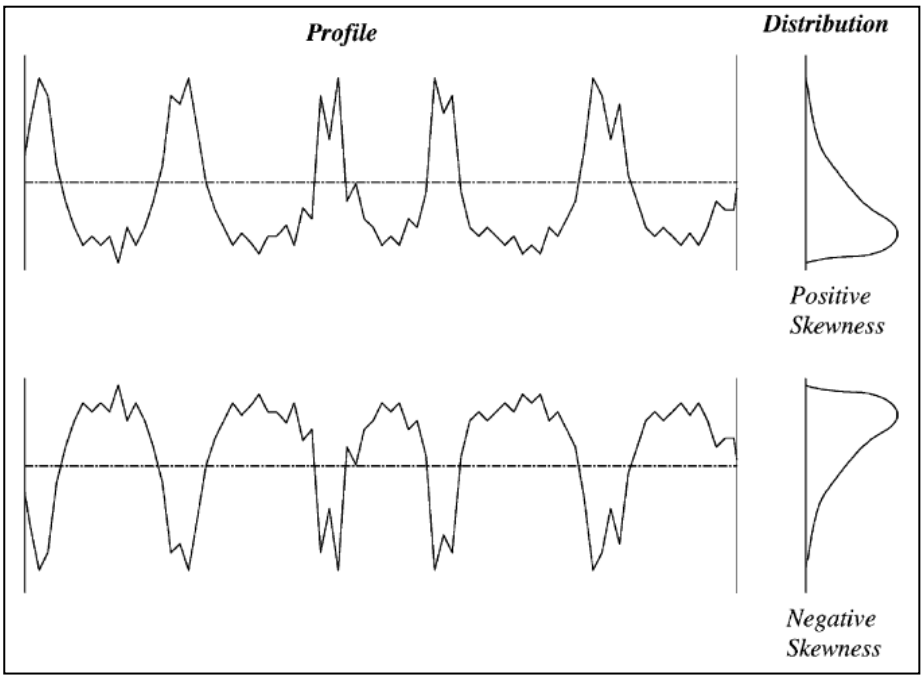

Figure 4.11: Examples of surfaces exhibiting positive and negative skewness (modified from Gadelmawla et al., 2002: 137)

Although skewness can be used to measure the symmetry of the profile, it does not provide measurements on the size of perturbations. In addition, this parameter does not measure the horizontal components of variation, such as the density of peaks and valleys, or their wavelength.

Other methods of measuring profile symmetry/skewness use subsamples of the population. For example, *solidarity factor* is defined as the ratio between the deepest valley and the highest peak (Gadelmawla *et al*., 2002; Davim *et al*., 2009) so just two observations are used.

4.3.3.3 Kurtosis

Skewness illustrates the usefulness of measuring the amplitude distribution of peaks and valleys. Further information on the shape of asperities can be gained by calculating *kurtosis*, which measures the *sharpness* or *peakedness* of peaks or valleys (Hall *et al*., 1997; Gadelmawla *et al*., 2002).

Typically, a surface characterised by many high peaks and deep valleys, as illustrated in Figure 4.12a, will return a kurtosis value below 3 (Gadelmawla *et al*., 2002). A profile with fewer high peaks and deep valleys (Figure 4.12b) will typically have a kurtosis above 3

(Sedlaček *et al*., 2009). This parameter therefore reflects both the amplitude of peaks and their distribution (Elfick *et al*., 1999).

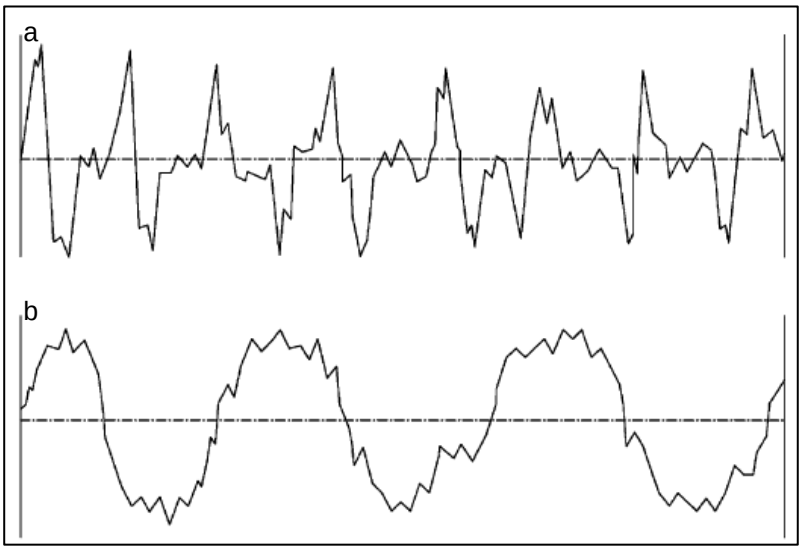

Figure 4.12: Examples of profiles with varying sharpness of asperities , which can be measured using the kurtosis parameter a) kurtosis > 3, b) kurtosis <3

4.3.3.4 Slope

The slope parameter summarises roughness by measuring the gradient of a surface. This method can capture limbs of asperities, so is another proxy of obstacle size. For example, over the same horizontal distance, a steeper slope angle indicates a higher peak. Slope can be positive or negative so, potentially, it is possible to detect both rising and falling limbs of asperities. Over larger spatial scales, the parameter might be used to detect an overall gradient along a section of subglacial bed.

4.3.3.5 Sinuosity and curvature

Rather than measuring the length of a profile as a straight line distance between two points, it is possible to trace the pattern of rises and falls in height. This measure of total line length is termed the *sinusoidal wavelength* (Stover, 1995), and increases as the number and/or size of asperities increases. This makes the total line length a measure of roughness. Using sinusoidal wavelength alone is problematic because the choice of window size will dictate the results. Therefore, it is necessary to remove the effect of sampling window so that only spatial variation due to changing profile shape is measured. This can be done by calculating *sinuosity*, which is the ratio between the sinusoidal wavelength and the straight-line distance.

An advantage of the sinuosity parameter is that it takes into account both the amplitude and wavelength of asperities, and captures perturbations on a range of scales. However, many studies have published limitations with this method. McCarroll & Nesje (1996) reported that the results are inconsistent with those calculated by other techniques. One

issue is that, as resolution of the data increases, there will be more asperities captured, making the sinusoidal wavelength longer. A further problem is that the method does not distinguish between the amplitude, wavelength, and frequency of perturbations. This makes it difficult to determine why a particular area has a certain sinuosity value. Furthermore, many different profile shapes can produce a similar value: for example, a profile comprising numerous short amplitude perturbations may return the same value as one containing fewer but higher amplitude or wavelength peaks.

Sinuosity is often used in fieldwork (McCarroll & Nesje, 1996) and this is partly reflected in the design. For example, the parameter requires a complete record of the bed and, when gathering data, especially over small, exposed surfaces, this requirement can be met. However, as Section 2.4.3 showed, glacial datasets often have gaps of missing data. The parameter would still produce a value, but the sinusoidal wavelength would be an underestimate.

Measuring multiple variables, sinuosity does not give a direct value on the frequency of perturbations. An alternative measure, *changes in curvature* (or *number of turning points*), measures the frequency of asperities by counting how often adjacent sections of the profile switch from convex to concave or *vice versa* (McCarroll & Nesje, 1996). In a sense, this method could be considered a spacing parameter, but is placed under the shape category because it uses the changing direction of the profile, rather than crests or troughs, to identify asperities.

Although in relatively wide use, McCarroll & Nesje (1996) found that the number of turning points shows no correlation with other parameters, suggesting that results yielded are inconsistent with those of other methods. In Chapter 4 it was also shown that areas of flat topography are relatively uncommon; instead, the subglacial bed is characterised by asperities on a large range of scales. As a result, it is perhaps likely that any section of profile measured would have a relatively high number of changes in curvature.

A problem shared by both the sinuosity and changes in curvature parameters is that they are sensitive to the number of observations per unit area: if the same profile is sampled at a higher resolution, it allows smaller perturbations to be captured, resulting in a greater number of changes in curvature or sinusoidal wavelength. Potentially, this could be overcome by the use of thresholds. This need for filtering perhaps explains why engineers use a variation on this parameter termed the *number of inflection points*. Here, changes from concave to convex, or *vice versa*, are measured where the profile crosses the mean line which, as illustrated by Figure 4.13 means that some asperities are not counted as inflections.

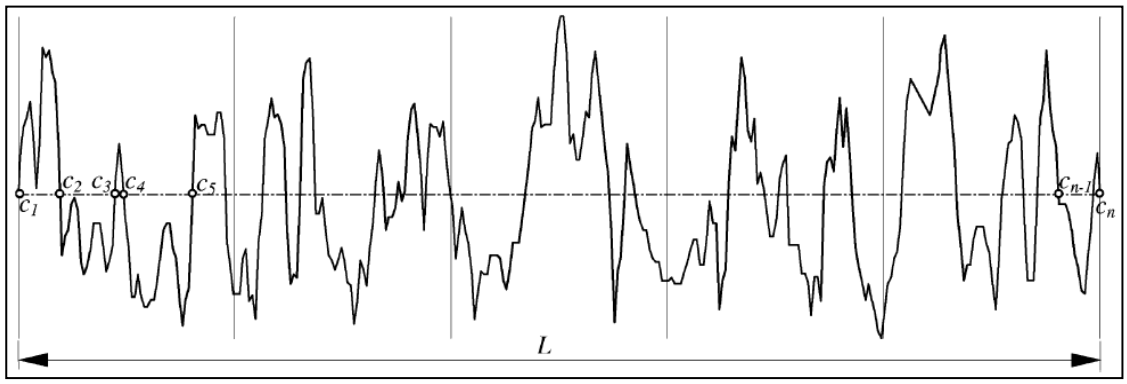

Figure 4.13: Definition of number of inflection points. Change in curvature is recorded where the profile crosses the mean line (from Gadelmawla et al., 2002: 141)

4.3.4 Hybrid parameters

While some roughness parameters are designed to quantify a singular characteristic of topography, such as amplitude, hybrid parameters measure two or more variables. Commonly, hybrids account for the amplitude of perturbations, as well as their spatial distribution (Suh & Polycarpou, 2003). These parameters are a mixed bag making their methods of calculation varied.

4.3.4.1 Spectral analysis

Spectral analysis would probably fall under the category of hybrid parameters because it summarises a range of variables. As shown in Chapter 2 most glacial studies on the scale of kilometres have used this method. The use of spectral analysis for measuring surface roughness appears in other sciences, e.g. manufacturing (Cuthbert & Huynh, 1992), so is far from unique to glaciology.

One of the benefits of this technique is that it allows contributions to surface relief from different spatial frequencies to be separated out (Kumar *et al*., 2007). This makes the technique capable of assessing subglacial roughness at a range of scales. This was demonstrated in Chapter 4, where results were broken down into a series of wavelength classes. However, the previous chapter also highlighted a number of issues with this method.

4.3.4.2 Variography

In spatial analysis *semi-variance* is used to measure dissimilarity in a variable as a function of distance. As a roughness parameter, this method measures the variance in the height of a surface against lag distances at different scales (Mat heron, 1963; McCarroll & Nesje, 1996; Herzfeld & Schneider, 2000). As roughness increases, there is less similarity over a given distance along profile. Recall from Section 2.3.3 that studies of micro-scale bed roughness (e.g. Herzfeld *et al.*, 2000a, 2000c) have used this technique. One of the main limitations of this method is that it is sensitive to the slope of the profile (McCarroll & Nesje, 1996) and, therefore, the data may have to be detrended.

4.3.4.3 Autocorrelation

The principle of autocorrelation is that it is used to measure the general dependence of the data at one position to their values at another (Fox & Hayes, 1985; Patrikar, 2004), and so, in the case of roughness, measures the relation between wavelength or amplitude properties (Gadelmawla *et al*., 2002). In studies of roughness, especially those in engineering, autocorrelation allows the spatial variations in topography to be analysed. In rough areas of a profile, where topography varies over relatively short distances, the autocorrelation value will be low, whereas more-smooth areas yield higher values (Gadelmawla *et al*., 2002; Militky & Majzik, 2003).

There are two common uses for roughness analysis in engineering (Mattia *et al*., 2003). More generally, the *autocorrelation function* (ACF) is used to assess *the correlation of a source with itself* (Stoud & Hubbard, 2009: 2411). Having calculated the ACF, some studies then apply a second parameter termed *correlation length* (ß), which provides information about the distribution and density of asperities. The correlation length is the shortest distance in which the value of ACF drops to a certain value (Gadelmawla *et al*., 2002), which could be adjusted according to the data.

4.4 A review of 3D roughness parameters

The scientific literature lists many methods of quantifying roughness in three dimensions and, as with 2D methods, engineering and manufacturing dominate the literature (e.g. Vermeulen *et al*., 1995; Ebdon & Blunt, 1996; Kubiac *et al*., 2009; Zeng *et al*., 2009), demonstrating their wide use in this field. Nevertheless, 3D techniques are also relatively common in other sciences, for example, Elfick *et al*. (2009) used 3D methods to quantify joint replacements. It is interesting to note that, relative to 2D parameters, the scientific literature has few critiques of methods for quantifying roughness in 3D.

Whereas 2D parameters are calculated using a series of sampling windows along an assessment length, 3D methods usually sub-divide a large surface into a series of grid squares using a mesh. Many 3D parameters are modifications of the methods used for quantifying roughness in 2D; it is common for many 3D parameters to have a 2D counterpart (Jonasson *et al*., 1998), where the same characteristic is measured, but the equation is modified to work with areal data. This means that many of the 3D parameters are simply adaptations, and so share the same advantages and disadvantages as their corresponding 2D version. Nevertheless, there are occasionally some differences between the methods. One example is that 2D methods are often summarised observations over several sample lengths, but most 3D techniques are calculated using a single window (Dong *et al*., 2004).

4.4.1 Amplitude parameters

Amplitude or *height parameters* quantify the vertical characteristics of surface roughness (Suh & Polycarpou, 2003). Many of these methods are equivalent to the 2D versions, and some examples of this are described below.

4.4.1.1 Mean height and range

The *arithmetic mean surface height* is used to summarise the average height of observations within a grid cell. Like its 2D equivalent (Section 4.3.1.1) it is one of the most used parameters (Suh *et al*., 2003), especially in manufacturing sciences. The mean height is used in other sciences. A clutch of papers in the medical literature describing the use of the mean height parameter (e.g. Wennerby *et al*., 1998; Elfick *et al*., 1999) show the prominence of the method in this field of research. Although this parameter is generally used to measure roughness on the scale of nanometres (Suh & Polycarpou, 2003), the scale-free nature of the parameter means it could be used to quantify roughness at the scale of ice-sheet beds.

The *maximum height of surface* parameter is used to summarise the range of amplitudes and is defined as the difference between the highest and lowest pixel (Peltonen *et al*., 2004). Although this gives an overall summary of the surface, it gives no information on other characteristics of the profile, such as the horizontal size of asperities, or their spatial distribution.

4.4.1.2 Root Mean Square surface height

The *root mean square height* measures the RMS value of surface asperity departure from the reference datum (Dong et al., 2004). Therefore, the method measures the same characteristics as the 2D RMS height (Section 4.3.1.2) except summarising observations within a grid rather than along a profile.

RMS height is among the most common areal parameters in use in materials science (Suh *et al*., 2003; Peltonen *et al*., 2004). However, this method is prone to similar weaknesses as its 2D equivalent. For example, both methods are sensitive to extreme values (Suh *et al*., 2003). The sample size also affects results (Dong *et al*., 2003) demonstrating that, like many 2D methods, three-dimensional techniques have variables (in this case grid size) that must be optimised.

4.4.1.3 Measures of dispersion

As demonstrated in Section 4.3.1.2, some roughness parameters are designed to measure the dispersion in height values. The use of standard deviation as a roughness parameter is worth highlighting because, to date, this appears to be the only example of 3D analysis of roughness in glaciology. In her study of the topographic controls on ice

streaming, Winsborrow (2007) identified that the standard deviation of bed elevation measurements was a proxy for the roughness of the bed over scales of tens of kilometres.

4.4.1.4 Asperity size

Some 3D parameters identify the highest peak and valley heights relative to a datum. One example is the *highest peak* parameter (ISO 25178), which is defined as the height from the mean plane to the highest peak within a sample area (Elfick *et al*., 2009). To measure the largest negative asperities, the *largest valley* parameter is used (ISO 25178), and in this project the name used is deepest pit. Both the *highest peak* and *largest valley* parameters are limited by the fact they are unrepresentative of the surface, again showing how 3D counterparts to 2D parameters may have similar limitations.

To determine the size of peaks that is more representative of the grid cell, the *ten-point height* can be calculated (ISO 25178 and Kubiac *et al*., 2009). Like its 2D equivalent, this method quantifies roughness using the five highest summits and five deepest valleys (Suh & Polycarpou, 2003; Suh *et al*., 2003). A further alternative of summarising asperity size that is more representative of the grid cell is to measure their average amplitude. Two separate parameters can be used to separately peak height and valley height. The *mean height of* peaks is defined as the average of the vertical distance of pixels that are peaks; the mean height is used as a datum to reference the height of each crest. The literature does not describe a *mean depth of valleys*, but this information could be produced by modifying average height of peaks to measure pixels that are troughs.

4.4.2 Shape parameters

Shape parameters characterise roughness in planar directions, such as the horizontal size or frequency of bumps. In some sciences this group of methods are referred to as *spatial parameters* (Suh *et al*., 2003; ISO 25178). These techniques are typically used to describe the anisotropy and directionality of surface patterns (Suh & Polycarpou, 2030). Therefore, although these methods give little or no information on the vertical size of asperities, they can be used to evaluate the spatial variation in roughness. As with other types of parameter, many of these statistics are equivalent to those used to summarise roughness in 2D. However, some of the methods in this section have no counterparts.

4.4.2.1 Skewness and Kurtosis

Skewness (Suh *et al*., 2003; Peltonen *et al*., 2004) measures the asymmetry of the surface about the mean plane (Suh *et al*., 2003; Dong *et al*., 2004; ISO 25178). It is similar in functionality to the 2D version (Section 4.3.3.2). K*urtosis* summarises the peakedness of the surface (Suh *et al*., 2003; Dong *et al*., 2004; Peltonen *et al*., 2004), and is also similar to its 2D counterpart (Section 4.3.3.3).

4.4.2.2 Surface aspect ratio

The *surface aspect ratio* is used to measure the anisotropy/isotropy of a surface (Blunt & Ebdon, 1996; Potsiadlo & Stachowiak, 1998; Suh *et al*., 2003). The parameter uses measurements of autocorrelation, and determines the rate at correlation decays to a given percentage. This method is commonly used in engineering to identify the presence of surface patterns (Whitehouse, 1994).

In glaciology, it is well documented that movement of ice across the surface may produce patterns of wear, such as bedforms orientated to ice-flow direction. The texture aspect ratio could be used to detect such patterns, which may allow groups of bedforms to be identified. Comparison of glaciated and non-glaciated surfaces using this parameter could also be used to determine whether certain environments create a particular signature in terms of roughness values.

Although this parameter is useful for identifying anisotropy, it gives no information on the orientation of roughness elements across the surface. Also, the method does not measure the dimensions of the pattern, so it may not be possible to determine the type of bedform. In terms of glacial features, it is uncertain whether different assemblages (e.g. drumlins vs flutes) would produce distinct surface aspect ratios.

4.4.2.3 Number of asperities

As with 2D methods it is possible to quantify the number of peaks or valleys within a grid. For example, a peak count is given by the *density of summits* parameter (Peltonen *et al*., 2004). Unlike 2D parameters where the crest is identified as a highpoint with two neighbouring lower values, the density of summits identifies pixel values that are higher than their eight nearest neighbours (Suh *et al*., 2003). The density of summits can be further tuned using a threshold, so that only crests projecting above a particular value are counted (Sacerbotti *et al*., 2000). The frequency of valleys could be calculated by modifying the parameter, perhaps terming it the *density of valleys*, so that it identifies the presence of troughs within each grid.

4.4.3 Function, segmentation, and hybrid parameters

There are several other types of method designed to quantify roughness in three dimensions, and these can be categorised as *function*, *segmentation*, and *hybrid* parameters. Many of these methods are highly specialised in nature, so are less applicable to glacial data. Function parameters measure properties of a surface that have been found to relate well with a functional property of a surface (Sacerbotti *et al*., 2000). For example, these are used in manufacturing engineering to characterise the bearing or oil retention properties of a surface (Blunt & Ebdon, 1996). Methods such as the *core fluid*

retention index (Dong *et al*., 2004) are used to measure the amount of surface that can hold lubricant.

Given that function and segmentation parameters are not analogous with subglacial data, they are not evaluated in this project. Some hybrid parameters are relevant, and include those presented in Section 4.3.4, such as autocorrelation, that are adapted for use with 3D data. Another hybrid parameter is the *slope of surface topography* parameter (Pawlus & Śmieszek, 2005) that determines the root mean square of the surface slope (Ramasawmy & Blunt, 2002; Wiklund *et al*., 206). The parameter commonly appears in manufacturing engineering literature (e.g. Lavernhe *et al*., 2003; Aris & Cheng, 2008).

4.5 Discussion

4.5.1 The diversity of roughness parameters

This chapter demonstrates that there are many methods of quantifying roughness, and these are available from numerous sources. Many of these methods are specifically designed to analyse surfaces. In addition, a large proportion of statistics in everyday use, such as the mean or range, can be considered measures of roughness when used to summarise changes in the amplitude or wavelength of topography. Therefore, despite glacial studies of roughness having focused on a narrow set of methods, with particular emphasis on spectral analysis (Bingham & Siegert, 2009), there are numerous alternatives.

The sources of potential methods are widespread. It has been shown that many areas of research already use techniques for quantifying roughness, and it is possible that some of these could be used in glaciology. In particular, the measurement of roughness is crucial in manufacturing engineering. The breadth of sciences that could provide a useful guide to glaciologists is further increased by the fact that many of the methods can be used at any scale. As identified in Chapter 2 (Section 2.5.2), an advantage of adopting parameters from other sciences is that they often have undergone some form of evaluation. For example, in literature that describes the calculation of these methods, their strengths and weaknesses are commonly cited (as shown extensively in Gadelmawla *et al*., 2002).

4.5.2 Measuring a single variable

In sciences such as engineering, roughness appears to be given stricter definitions. Rather than being viewed as a broad term, the form of a surface is viewed as a number of variables. As a result, roughness parameters are designed with a specific purpose: some might measure amplitude; others summarise the frequency of asperities. As this chapter showed, the parameters can even be grouped into categories based on their design. Using these parameters, it would be possible to make a systematic analysis of subglacial bed topography into a number of variables.

Given that the parameters are designed to measure a single variable, it follows that no parameter can capture everything. For example, a method designed to summarise amplitude may give no information on variations in wavelength or frequency. This is not a problem and, may in fact be useful. Measuring specific variables might allow the role of roughness in controlling rates of basal ice flow to be better understood. For example, comparing the results of different parameters it would be possible to determine whether the frequency of asperities, or the size of these perturbations, is most related to patterns in ice speed. In contrast, as shown in Chapter 4, spectral analysis captures several variables and, as such, it is difficult to determine why a particular value has been produced.

The difficulty in interpreting results is compounded by the fact that, using a single parameter, surfaces do not produce unique values. Instead, the same results can be yielded from different topographies. This point is illustrated in Figure 4.14, which shows eight profiles that all have the same roughness when measured using the *mean height* or *mean deviation*. The difficulty here is that variations in the shape or frequency of asperiteis are likely to influence the functional characteristics of the bed surface, such as its friction (Gadelmawla *et al*. 2002). Therefore, to fully understand how ice speed is related to roughness it may be necessary to use several parameters.

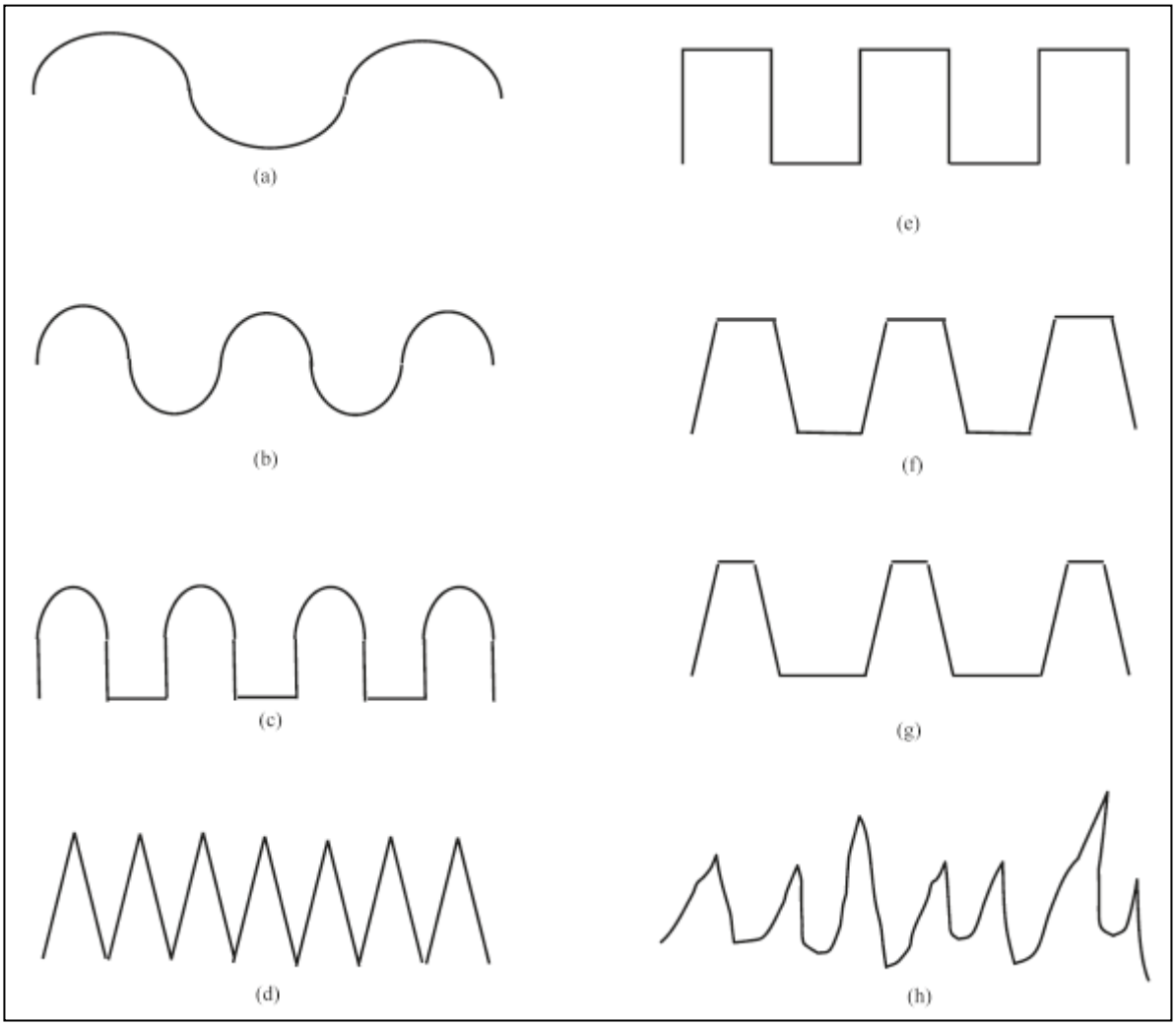

Figure 4.14: Different surfaces may produce the same roughness value. Profiles a – h have the same mean height and mean deviation (from Li et al., 2009)

4.5.3 The ability to measure scales of roughness

Chapter 4 demonstrated how the use of spectral analysis required certain window lengths to be used because 2^N datapoints were required (Taylor *et al*., 2004). The parameters reviewed in this chapter have fewer restrictions, meaning that the user has more choice over the scales of roughness quantified. Compared with spectral analysis, these alternative roughness parameters would allow the same data to be analysed over shorter window lengths, thus allowing a finer resolution of results.

A number of other user-controlled options can be used to further refine the scales of roughness quantified. For example, Section 4.3.2.1 described how thresholds or cut-offs allow asperities of a certain size to be measured. This would allow glaciologists to investigate how certain sizes of obstacle relate to spatial variations in ice speed.

4.5.4 Why roughness parameters need to be reviewed

The parameters identified in this chapter offer much potential for investigating subglacial bed roughness. However, given that the majority of these have never been used for this purpose, there are uncertainties over which of the methods are most suitable. Section 4.2

showed how some methods are designed with a specific purpose in mind, but these characteristics are not relevant to glaciology. For example, some parameters are used to categorise the functional properties of machine parts are not appropriate for ice-sheet beds. Even with parameters that are less specialised, not all of the methods may be useful to glaciologists. For example, some parameters within the same category of methods may be redundant because they give similar information. Therefore, there is a need to identify which methods are most relevant to glaciologists. What is important to one science may not be the most important in controlling ice-sheet behaviour: for example, in engineering the identification of extreme values is often a priority because of their control on the functionality of parts (Najjar *et al*., 2003), but these asperities may not be the most influential on ice flow.

Another reason why the methods need evaluation before they can be used is that their response to different changes in topography is unknown. Although the methods are designed with a specific purpose, it is possible that they would be affected by other variables. For example, an amplitude parameter measuring the average size of peaks might be influenced by the number of asperities within the given window length. Therefore, testing is required to determine how each parameter responds to various types of topographic variation.

Finally, there is uncertainty over how well these parameters can be applied to glacial data. As Chapters 2 and 4 showed, records of bed elevation are often incomplete and this was a problem for using spectral analysis. Although the methods reviewed in this chapter do not require processing to fill gaps or remove large slopes, it is not known how such characteristics along a profile would affect the results. Therefore, the feasibility of using these methods with subglacial bed data requires testing.

4.5.5 Shortlisting the roughness parameters

To address the need for reviewing parameters to determine their usefulness in glacial research, the next chapter quantitatively and qualitatively assesses each of the methods. It would be beyond the scope of this project to test every roughness parameter. Indeed, even to evaluate all those methods described in this chapter would be ambitious. A number of criteria were used as a framework to make an initial selection. The first motivation when selecting parameters to be tested was to identify those that are simple yet effective. For example, measurements such as the arithmetic mean, standard deviation, and range are commonly reported statistics, but could also be used to quantify roughness. Where possible, parameters that measured a single characteristic were chosen because, in future, these methods could be used by modellers to investigate what characteristics of topography are most associated with ice flow (i.e. speed, direction, or some other behaviour)

Another criterion for identifying which methods to test was determining those that would give *meaningful* results. For instance, some methods, especially those that measure obstacle dimensions, could be linked to current theories on how asperities impede ice flow. The intention here was also to identify those methods that would be applicable to both 2D and 3D analysis, so that results from different areas could be covered. This meant that the majority of 3D parameters chosen had 2D counterparts.

The third motivation for selecting which parameters to test was identifying those methods that would not require extensive processing of the data before results could be calculated. As described in Section 5.2.3, the methods were programmed into the statistical software Stata to allow automated analysis: a single program was to calculate all of the 2D results, and a second for all the 3D methods. Alternative programs could have been used but, for efficiency in testing, those parameters that could readily be programmed in were selected. As a result, hybrid parameters were not used. Using these criteria, 18 2D parameters and 18 3D methods were selected for evaluation, as summarised in Table 4.1.

Amplitude parameters	
Tested	*Not tested*
Mean height	Highest peak
Mean deviation	Deepest valley
Mean above height	Peak-minus-valley range
Mean below depth	Mean max peak-to-valley height
RMS height	Ten-point height
Range	
Maximum above height	
Maximum below depth	
Mean peak height (crest height)	
Mean valley depth (pit depth)	
Standard deviation (3D)	
Spacing parameters	
Tested	*Not tested*
Number of peaks	Average wavelength
Number of valleys	
Percentage of peaks	
Percentage of valleys	
Shape parameters	
Tested	*Not tested*
Number of points	Solidarity factor (2D)
Skewness	Changes in curvature (2D)
Kurtosis	Surface aspect ratio (3D)
Slope (2D)	
Sinuosity (2D)	

Table 4.1: List of parameters that will and will not be evaluated in the following chapter. Unless otherwise specified, these names refer to both 2D and 3D methods

CHAPTER 5

Evaluating the suitability of roughness parameters for use in the analysis of subglacial beds

5.1 Introduction

In this chapter, a quantitative review of 2D roughness parameters is performed using artificially generated profiles and real subglacial bed measurements. Due to the similarity of the 2D and 3D roughness parameters, these findings determined the sensitivity of the methods to different variables. To test the feasibility of applying the methods to glacial data, the parameters are used to analyse RES and DEM measurements for 2D and 3D methods, respectively, reviewing the results qualitatively to assess the utility of each parameter.

5.2 Methods

As discussed in Section 2.5, the roughness of topography is linked with ice dynamics in different ways, both directly and indirectly. Furthermore, it was shown that shown that measurements of roughness may by proxies capturing other variables that are themselves controls on ice flow. In this chapter these linkages between the methods of quantifying roughness and ice dynamics are not explored. Instead, the focus was on determining which methods are compatible with glacial data, and to determine what characteristics of the topography these statistics measure. In Chapter 6 and 7 a discussion is made on how these different variables in the shape of topography can be directly and indirectly associated with ice flow. This elementary stage of testing functionality was performed through a quantitative and qualitative review of each method, supported by the use of artificially-generated data and real-world measurements of ice-sheet beds.

The parameters for quantifying roughness in 2D were evaluated using a set of synthetic profiles, and a RES dataset. The choices of profile are described in Section 5.2.1. As the last chapter showed, the methods of quantifying roughness in 3D often have 2D counterparts and, as a result, the type of information they provide is similar. This meant that evaluating the 3D methods using synthetic profiles was not required because the findings of the 2D parameters on sensitivity would apply. Yet, it was necessary to apply the methods to real-world data to ensure that they functioned correctly and to identify

whether the data produced any artefacts in the results. The DEM data used for this testing are described in Section 5.2.2. Roughness results were calculated in the statistical software Stata, and this procedure is outlined in Section 5.2.3.

5.2.1 Choice of profiles for evaluating 2D roughness methods

5.2.1.1 Synthetic profiles

There are many ways in which the topography of a surface may lead to spatial differences in roughness. Generally speaking, the roles of three variations in topography were considered, namely: differences in roughness due to the vertical and horizontal size of perturbations, the frequency of perturbations and how the profile varies in terms of its shape (e.g. slope or skewness). Each parameter was evaluated by testing its ability to capture each of these topographic variations.

The parameters were assessed using five profiles that had been artificially produced. Each profile was designed by adjusting one or more variables in a controlled manner, such as the height or width of asperities. Roughness results were then compared with these known results to assess whether the pattern of changing topography was captured. For the majority of the profiles, a single variable, such as the amplitude of asperities, was changed; but note that adjusting a single value altered other characteristics of the topography, such as the shape in terms of slope angles. The asperities in all of the profiles were designed to be of the order of bedforms found in glacial environments, ranging from the tens-of-metres scale in height and width, to 200 m high kilometre-long features (e.g. see Clark *et al*., 2009). Each profile was 20 km long, and had a sampling interval of 5 m between points. Such a resolution mimics that of high resolution topographic data, such as NextMap measurements of the UK (Clark *et al*., 2009).

Profile A, shown in Figure 5.1, was designed to simulate two extreme situations between a flat surface that represents the lowest roughness, and one with peaks and valleys. In addition, the ability for the parameters to detect sharp changes in topography was tested at the points where the profile transitioned from the flat outer zones to the central area of perturbations.

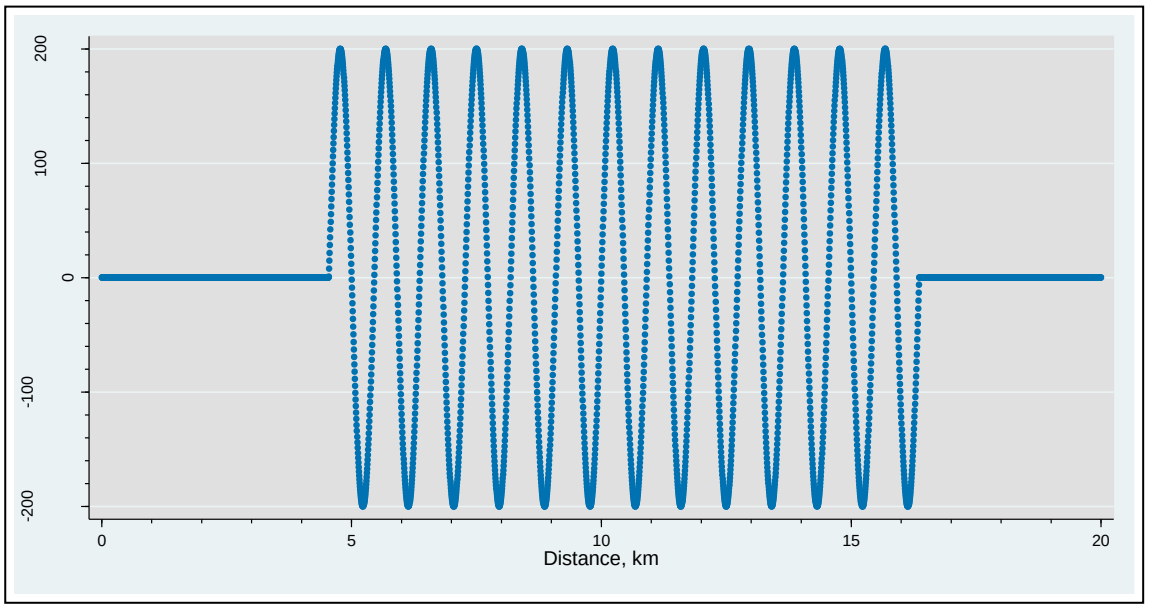

Figure 5.1: Cross-section of Profile A

In Profile B, see Figure 5.2, the entire profile comprised an area of sinusoidal peaks and valleys with a constant frequency/wavelength. However, the amplitude of these asperities decreased from over 200 m to below 50 m. Therefore, this parameter was designed to test whether roughness parameters were sensitive to changing height.

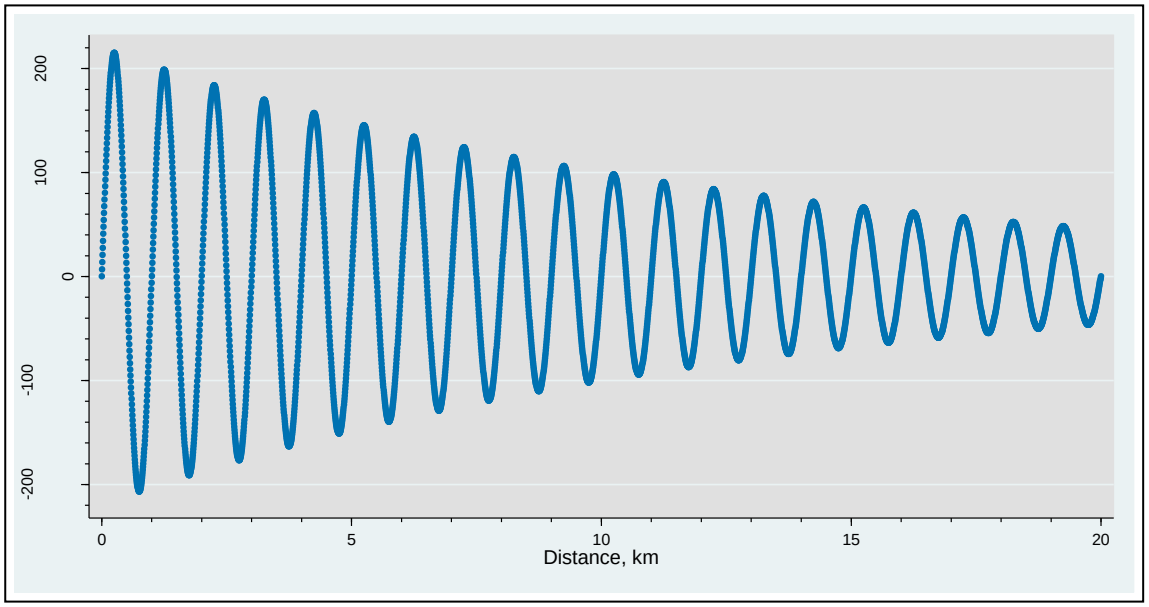

Figure 5.2: Cross-section of Profile B

Profile C, see Figure 5.3, was the reverse of Profile B in that the amplitude of asperities is constant for the entire profile length, but the wavelength gradually increases. This produces an effect of decreasing asperity frequency moving from left to right. The purpose of this profile was to determine whether parameters could capture changes in frequency and/or wavelength of perturbations.

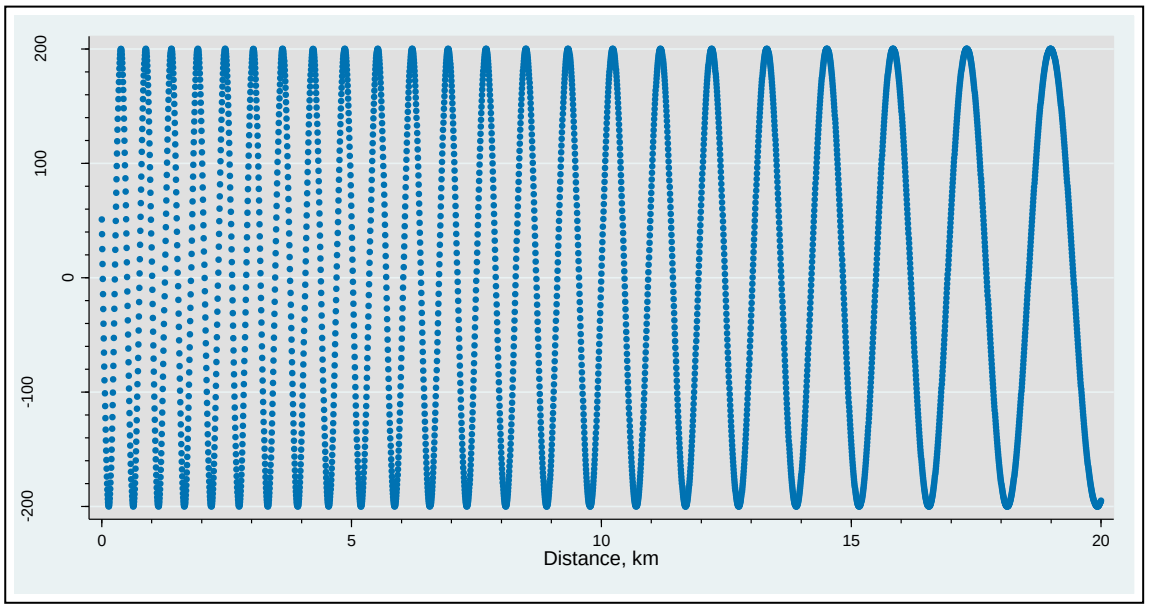

Figure 5.3: Cross-section of Profile C

In Profile D, changes in amplitude and frequency/wavelength were combined to produce an overall increase in asperity size; see Figure 5.4. Moving from left to right the height and width of asperities progressively increases. This design was used to test how vertical and horizontal variations might interact to affect the roughness results.

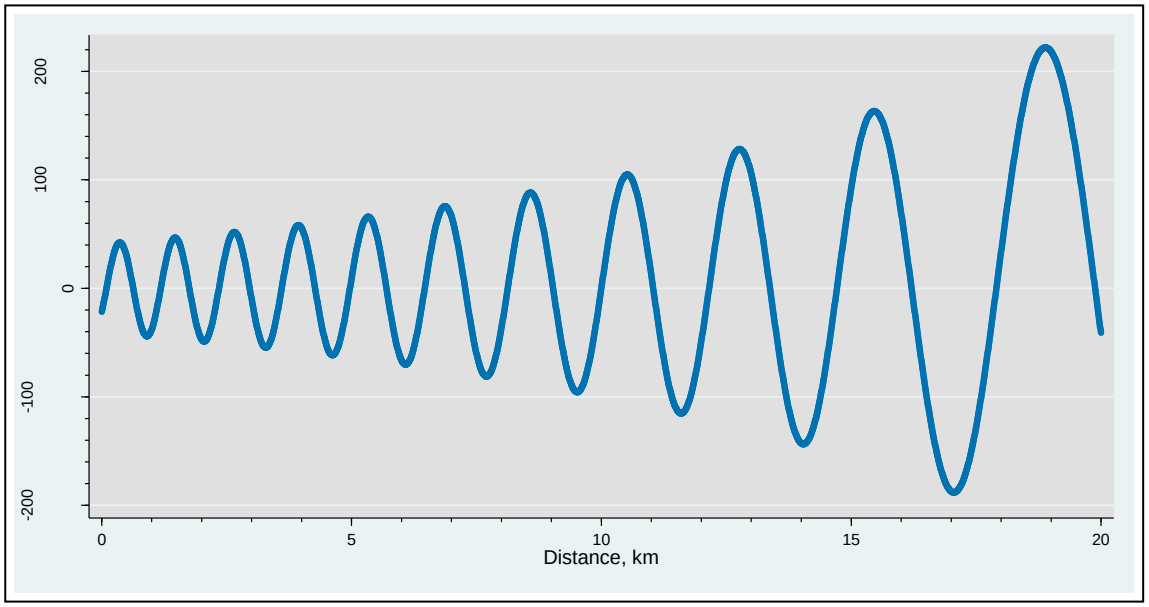

Figure 5.4: Cross-section of Profile D

Profile E was more specific in design in that it modelled two hypothetical situations; see Figure 5.5. In the first section of the profile the topography represented a subglacial bed that has deep grooves. The central area comprised a 2 km section of flat topography. It can be seen that the right-hand section of the Profile comprises a group of features that appear to sit on the landscape. These might simulate subglacial bedforms that have been formed on the surface of the subglacial bed, as opposed to *grooved out* topography. Note that between the troughs in the left-hand environment and peaks on the right the

topography is relatively flat rather than the sinusoidal shape of the other profiles. The purpose of this profile was to see whether the different types of environment could be distinguished using the roughness parameters, and to specifically evaluate the shape parameters.

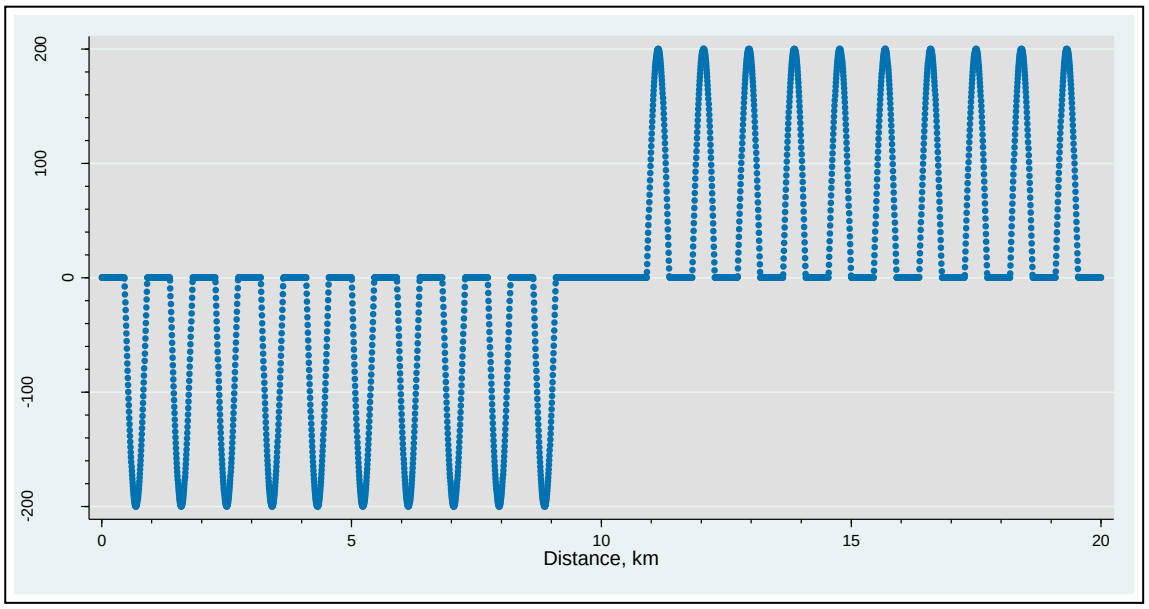

Figure 5.5: Cross-section of Profile E

5.2.1.2 Subglacial bed data

The synthetic profiles all had a complete record of bed elevation with a constant sampling interval of 5 m. As Chapter 4 has shown, however, complete records are rare in subglacial bed data, and this irregular spacing might affect the results. To test the feasibility of applying parameters to glacial data they were evaluated using a RES profile. The same profile used for testing spectral analysis in Chapter 4 was chosen, thus allowing the results for the other parameters to be placed in context. Figure 5.6 shows the approximately 540 km section of profile used. These data had been sampled by other workers using a trace-reader (Siegert *et al.*, 1996; Rippin *et al.*, 2004) and, where there were no gaps, had a distance between observations of approximately 2 km (Bingham & Siegert, 2009). Unlike spectral analysis, the measurements did not require adjustment (i.e. interpolation or detrending) to produce equal spacing or to remove slope. Indeed, sections of missing observations were deliberately included to test if the parameters would still operate, and whether these areas had a noticeable effect on the parameter results.

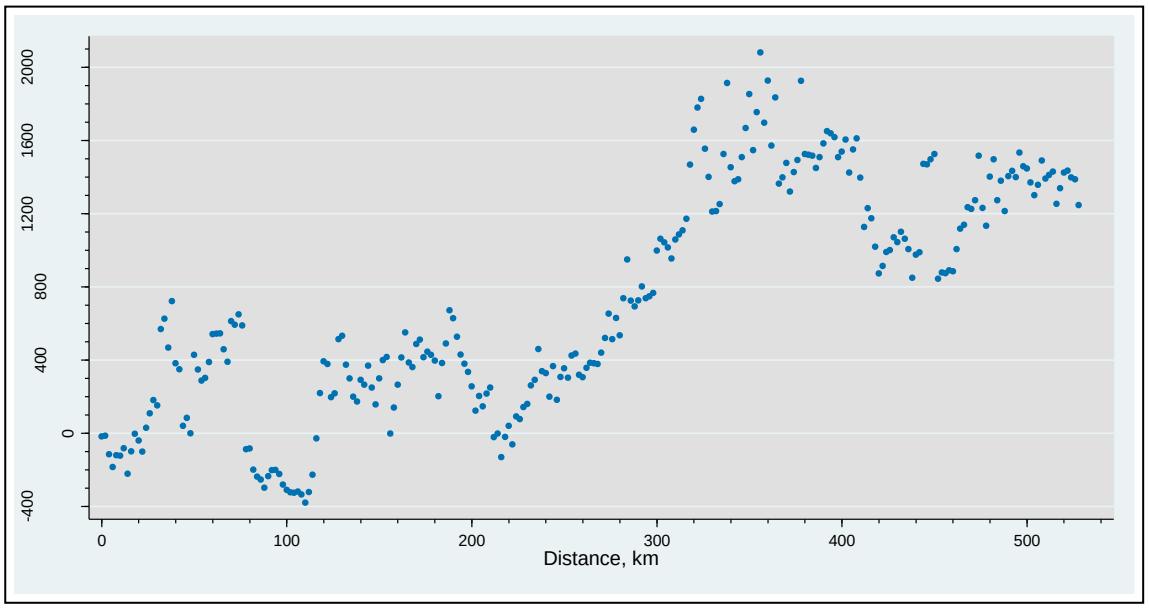

Figure 5.6: Cross-section of radio-echo sounding profile used to evaluate roughness parameters

5.2.2 Choice of data for evaluating 3D roughness parameters

As described in Section 5.2.3, quantifying roughness in 3D required the bed elevation data to have a regular pixel size, which meant that there could be no missing values. The chosen source of measurements was NextMap imagery from Britain because, although having an extensive coverage, there were few gaps. The specific study location was the valley of the River Tweed in NE England and SE Scotland. Figure 5.7 below shows the 5 x 5 km area selected for analysis. Several studies had identified that glacial features are preserved in this area on a range of scales (Everest & Lawrence, 2006). The image below shows the presence of elongated features with roughly a SW-NE alignment, situated within a broad valley feature. Therefore, although some post-glacial modification may have occurred, much of the glacial patterns appear to have been preserved. Indeed, the presence of these features has been used in several palaeo-environmental reconstructions of former ice flow and extent, and the area has been hypothesised as a palaeo-ice stream with large numbers of elongate subglacial bedforms (Evans *et al*., 2005; Everest *et al*., 2005; Staines, 2009).

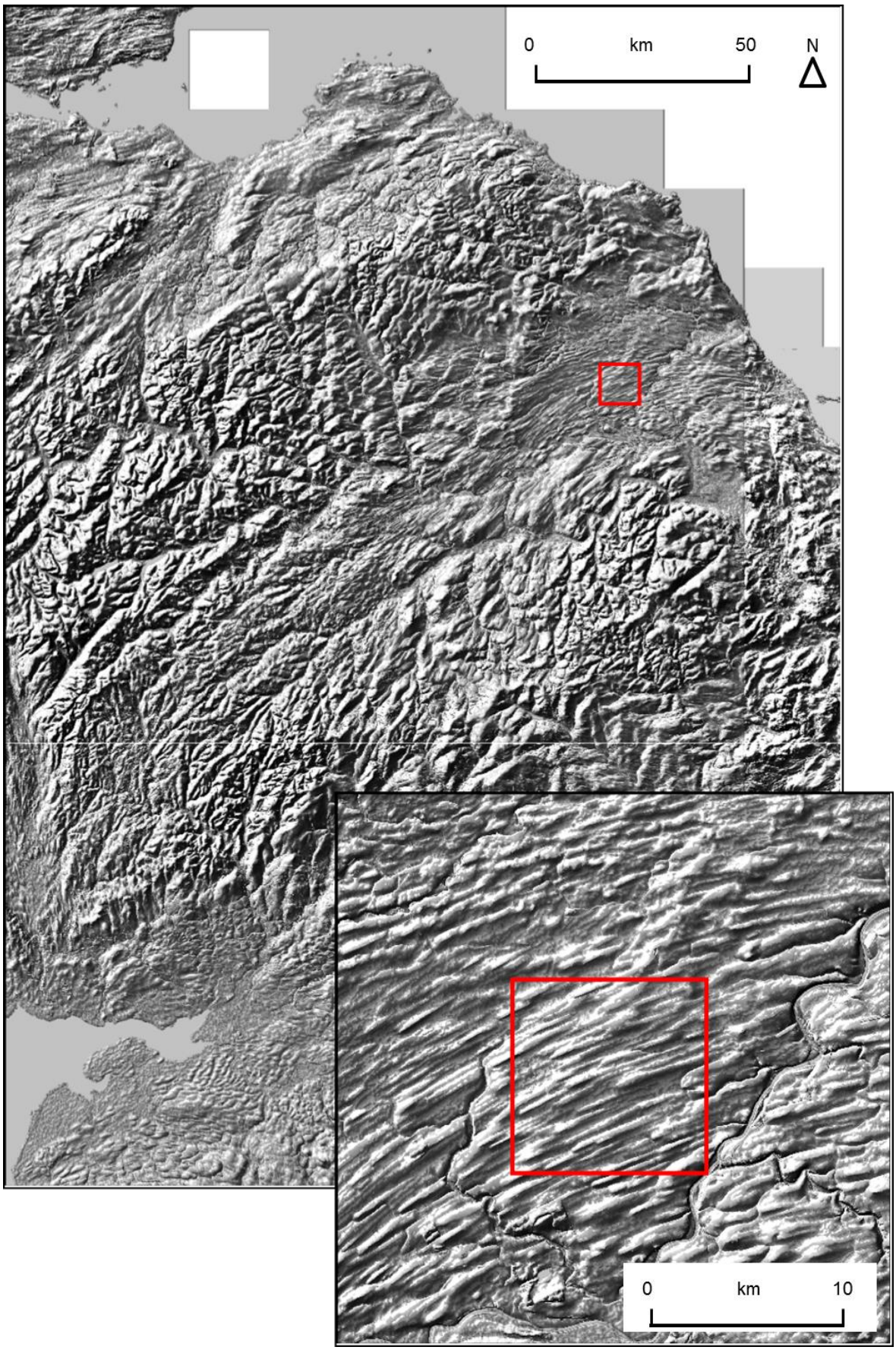

Figure 5.7: NextMap DEM data used for evaluating the 3D roughness parameters. The red box marks the 5×5 km study area within the valley of the River Tweed. The image is aligned north-south, with north at the top. Elongate features in the study site can be seen to trend in a SW-NE alignment

5.2.3 Calculating results for each parameter

With the large number of parameters to evaluate, a procedure was needed to efficiently calculate the results with little user input. Furthermore, because the methods would ultimately be used to assess many types of data, there was a need to have control on options such as the window size. To achieve this, the parameters were programmed into Stata. The methods of quantifying roughness varied between 2D and 3D parameters, so two separate programs were developed.

The 2D program (given in Appendix 2.1) calculated roughness for all 19 of the parameters using a single command. All of these statistics could be calculated using inbuilt commands for other statistics. For example, the software already had code for the calculation of average values, while other measures such as the skewness and kurtosis could simply be called from inbuilt scripts (Cox, 2010). Please refer to Appendix 2 for the code that this command executed. The user fed in height observations and the horizontal distance of these points from the start of the profile. Inbuilt options allowed adjustment of the functionality of the program, one of these being the size of moving window. For the synthetic profiles, the 2 km windows were a magnitude shorter in length than that of the total profile. For many of the profiles this choice of window allowed the full wavelength of the largest features to be measured, because most peaks and valleys were no longer than 2 km. Given that the resolution of the data was 5 m, each of the 2 km windows contained 400 points. For analysing the radio-echo sounding measurements, the sampling length was similar to that of the previous chapter, and was consistent with the size traditionally used for quantifying roughness using spectral analysis (e.g. Taylor *et al*., 2004) as in the previous chapter. Assuming the distance between points was approximately 2 km, the 62 km choice gave windows of around 31 points.

To quantify roughness in three dimensions a second program was used (see Appendix 2.2). This was similar to the first in that, by issuing a single line of code, the results of all parameters were generated. With this program roughness values can be summarised in two formats. With the first, one value is produced per parameter for a given study area. The second method is to define a mesh, allowing results to be produced over a grid. In a similar way to the use of windows, this latter approach permits spatial patterns of roughness to be measured.

There were some differences between the program for 2D analysis and that used for quantifying roughness in 3D. With the latter it was necessary to input the geographic coordinates of each observation, which were taken to be the coordinates for the centres of each pixel. Like the 2D program, it was possible to adjust the number of points measured by adjusting the grid size. The program used a square mesh, with the user defining the width of grid. This width had to be an odd number because the program summarised

results by determining the coordinates for the central pixel in each grid, and attaching the parameter values to this coordinate so that their spatial variations can be plotted.

Another requirement of the 3D analysis was uniform spacing between observations. The NextMap DEM met this requirement with a regular pixel size of 5×5 m, with no missing values within the study area. To analyse the 5×5 km area of interest, a mesh size of 400×400 m was used. This choice of mesh was based on the size of features in the area, many of which having reported lengths of hundreds of metres (Everest & Lawrence, 2006).

5.3 Results and analysis of 2D parameters

5.3.1 Synthetic profiles

Figures 5.8 to 5.13 present the roughness parameter results for each of the five synthetic profiles. For each profile, the results are grouped into four sets of graphs labelled *a* to *d*. Those with the suffix *a* are amplitude parameters that quantify roughness using all observations within a window. In contrast, parameters in the graphs suffixed with *b* use a subset of the data within each window, for example, measuring extreme values. Spacing parameters are presented in graphs suffixed *c*, and spacing parameters in graphs suffixed *d*.

For all of the parameters there is a limitation at the ends of the profile caused by the way results were generated. Roughness results were calculated for each of the bed elevation observations, with the window extending in equal directions either side. With the size of moving window being fixed, this meant that the window extended beyond the assessment length. For example, for the first point of a profile at 0 m distance, a 2 km window extends 1 km to the right of this point, but also in an equal distance to the left where there are no observations. As a result, the number of observations used to quantify roughness is fewer. This drop off is apparent from the results from the *number of points* parameter (see, for example, Figure 5.8c2).

5.3.1.1 Profile A

Figure 5.8 shows the results of Profile A, grouped by type of roughness parameter.

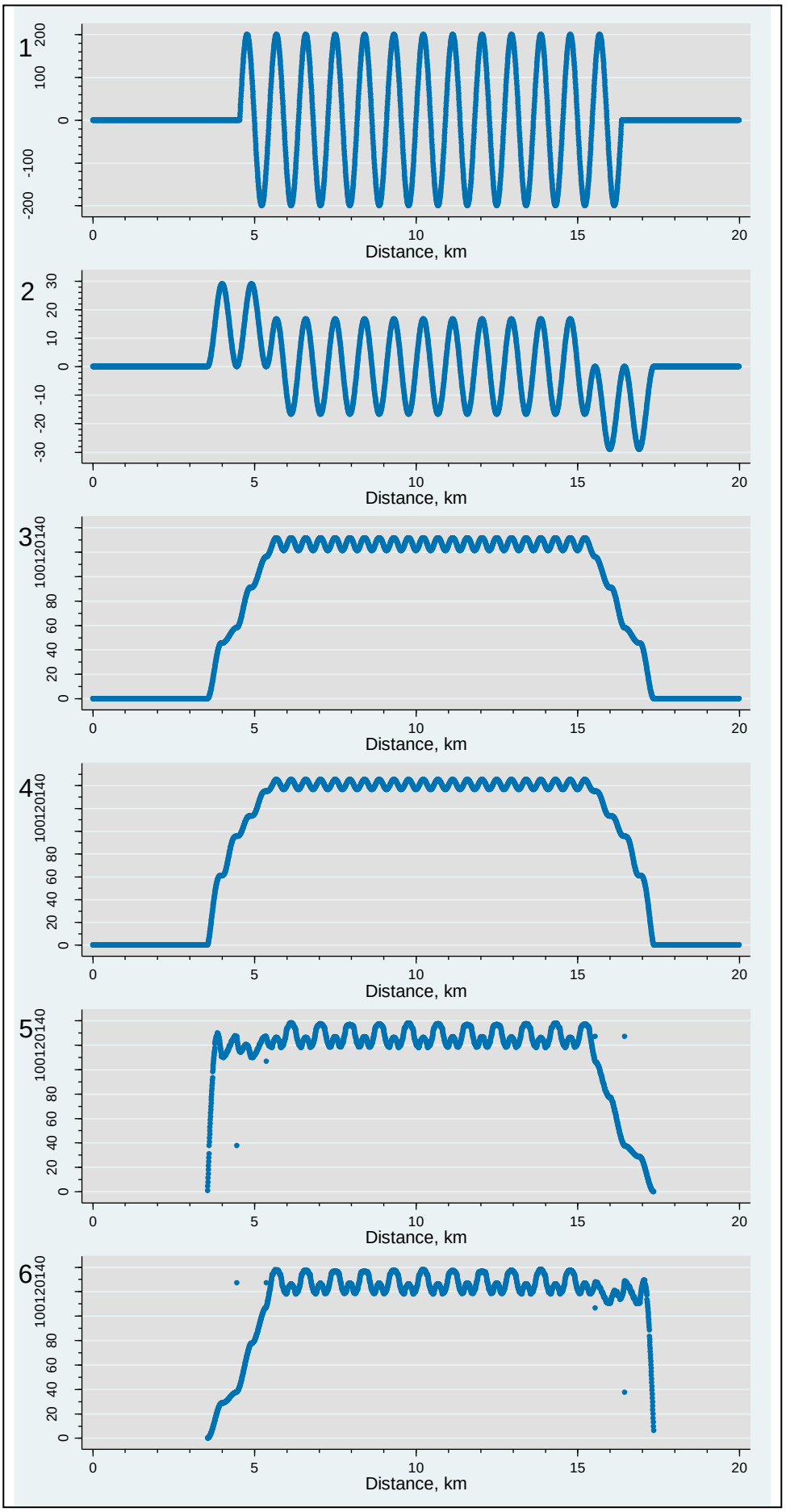

Figure 5.8a: Amplitude parameter results for Profile A

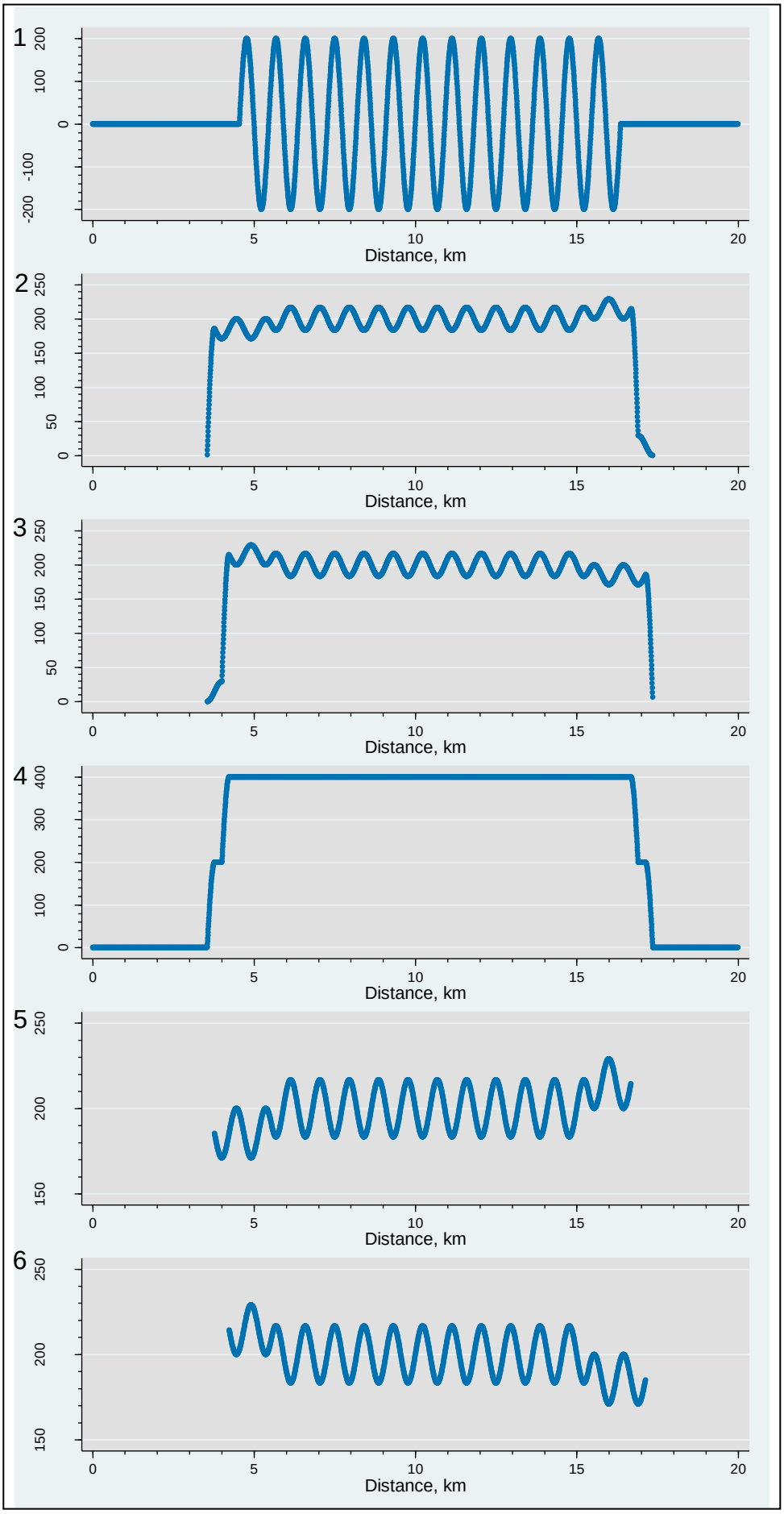

Figure 5.8b: Results for Profile A of parameters that measure specific amplitude characteristics

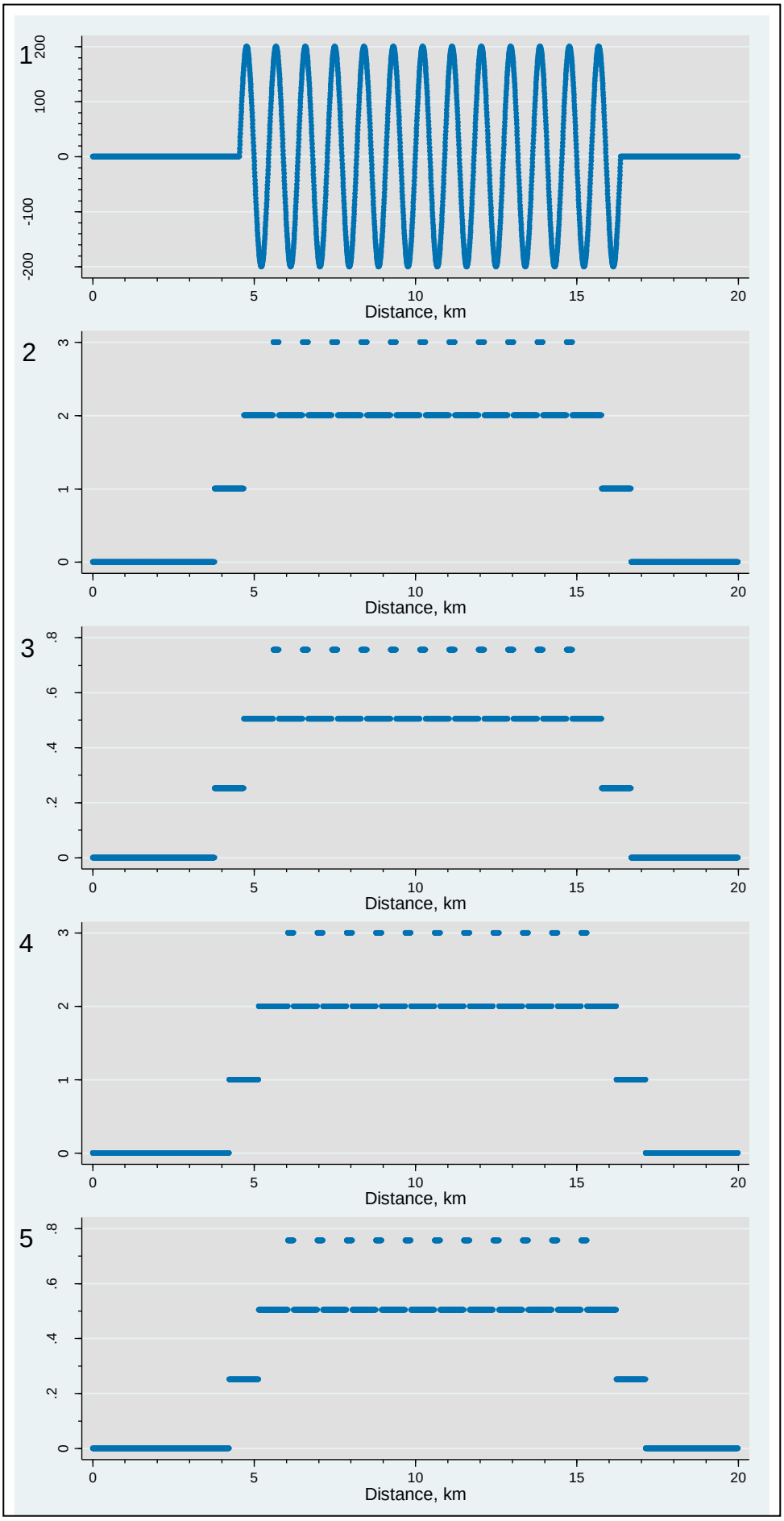

Figure 5.8c: Spacing parameter results for Profile A

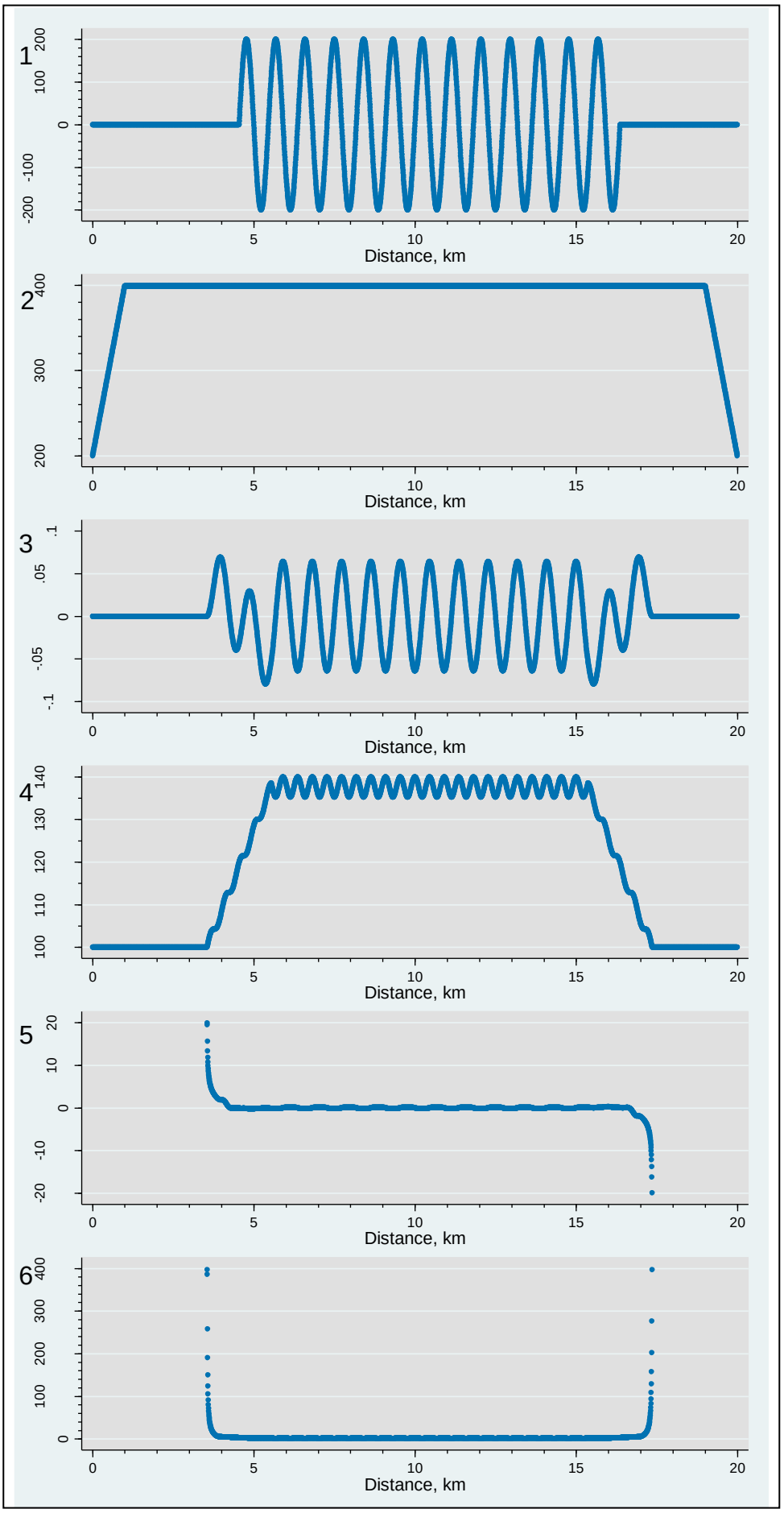

Figure 5.8d: Shape parameter results for Profile A

At a broad scale, the results of the **mean height** parameter distinguish between the zones of different topography. In general, the central area of asperiteis has a larger (positive or negative) mean height than the adjacent flat regions. Nevertheless, within the central area there is some variability. Some of the values in this area have the same mean height values (c.0 m) as the sections of flat topography. This pattern appears to be due to two causes. First, the size of the window and the wavelength of asperities (e.g. measuring the horizontal distance peak-to-peak) is the same.

The second factor that appears to have influenced the results is the fact that the size of peaks in terms of their amplitude and wavelength is the same as the valley size. It is this combination of asperity size and window choice that have influenced the results: in some windows, where a peak and a valley are captured, the distribution of points cancel out, so that the mean value is 0 m. As the window moves, some sample lengths have a higher distribution of values that form the peak, and other windows have more values that are valleys. In these windows the mean is shifted higher or lower respectively.

The fact that peaks and valleys in Profile A cancel out is, perhaps, something of an extreme case. The design of this profile, combined with the choice of window length, has resulted in a symmetry about 0 m. However, throughout the profile there has been something of a moderating effect: at no point does the mean height exceed ± 30 m, despite the fact that the height of asperities far exceeds this.

Although, in some sections of profile flat areas of topography have the same mean height values as the central area, the different regions could still be distinguished. Furthermore, two zones that have produced a more pronounced change in the values are the boundaries between the different topographies. At the boundary around 4 km along profile, as the window has shifted right it has encountered the first peak of the central area if asperities. As a result, the distribution of values is positively skewed, producing a higher mean height. The reverse has occurred at the right-hand boundary, where windows captured a valley and the flat zone, with this distribution producing a negative mean value.

The third plot of Figure 5.8a shows the results of the **mean deviation**. Whereas the distribution of peaks and valleys caused a cancelling-out effect in the results of the mean height, this is not the case for the mean deviation results, which show a clear distinction between the different zones of topography. The central area of asperities produced higher mean deviation values. The main reason that the mean deviation shows this definite contrast between the zones is that, unlike the mean height, it uses absolute values, so there is no moderating effect between peaks and valleys.

As with the mean height, the size of the mean deviation is lower than the maximum absolute amplitude of the asperities. However, this effect is expected because the

parameter measures the average amplitude based on observations in the window, and the majority of these points are lower than the maximum perturbation height.

With the mean deviation the boundary between the different zones of topography can be identified. Here, moving into the area of peaks and troughs the mean deviation increases. However, as with the mean height, the point at which the transition in topography occurs appears less sharp. This is apparent in the results for all parameters, but can be more clearly discerned with the mean deviation results: moving left to right, the first change in bed elevation occurs at c.4.5 km. However, the first change in the mean deviation occurs approximately 1 km before this. The likely cause of this pattern is the use of the moving windows. Given that results are plotted using the central point of each window, the topography they are summarising leads this point by half a window length.

The results of the **RMS height** are very similar to those of the mean deviation. The likely reason for this is that the RM height also uses absolute values. Also, both these parameters summarise similar information (refer to Appendix 1.1 for more detail), measuring the dispersion of bed elevation values. Therefore, some redundancy between these two parameters is identifiable.

The **mean height above** parameter somewhat resembles the results of the RMS height and the mean deviation parameters, despite the fact that the former does not use absolute values. The explanation for this similarity is that only observations that are above the mean for a sample window are included. Given the shape of Profile A, this parameter has been weighted towards measuring the amplitude of peaks, thus producing positive mean above height values. Nevertheless, it is important to note that on other profiles this may not be the case as both peaks and troughs may lie above the mean.

A second striking observation with the mean height above results is that no values were generated for the two sections of flat topography. The reason for this pattern is that, where topography is flat, none of the observations are above the windows' mean which is a criterion of this parameter.

Once again the boundaries between different regions of topography have been detected by the parameter. The results of the mean height above increase at the transition from flat topography to the area of perturbations. As with the other parameters, using windows to analyse the data has resulted in the sharpness of this boundary being less distinct than on the bed elevation plot. However, unlike other parameters the results of the mean height above also show additional artefacts at the transition points in topography. Viewing the fifth plot of Figure 5.8a, it can be seen there are a several outliers, which appear to correspond to the highest and lowest points in the topography within the transition area. The cause of these anomalies again appears to choice of window length being similar to

the wavelength of asperities, so that the distribution of points in each sampling length is affected.

With the mean height above, the boundaries between zones of different topography exhibit another pattern. The transition from flat to smooth topography at approximately 3.5 km along profile is sharper than the change from perturbations to flat topography on the right. This is in contrast to the other amplitude parameters so far described where the patterns at the boundaries are mirrored on either side of the central zone. The reason for this effect again appears to be the fact that the parameter only includes observations that are above the mean value for each window. At the left-most section of the central zone of asperities there is a peak. At the right hand side of this region, the final perturbation is a trough. As such, the distribution of points in the analysis varies: on the left the amplitude of a peak is summarised, whereas on the right it is a trough.

The results of the **mean depth below** parameter are similar to those of the mean height above. In fact, because of the design of Profile A, the results of the mean depth below appear identical to those of the mean height above when flipped horizontally. The most noticeable difference between these two parameters is at the boundaries, and this appears due to whether the windows at these points included any valleys. With the similarity in the way topography is analysed by these two parameters, the mean depth below results exhibit similar characteristics, such as outliers, and can be explained by the same causes.

The **maximum height above** and **maximum depth below** parameters operate in a similar manner to those that quantify roughness in terms of mean above and mean below, in that only observations that are above or below a given datum are included. As a result of this similarity, these parameter exhibit similar features such a as lack of measurements for sections of profile where the bed elevation is constant. Note that, despite the perturbations having a vertical size of ±200 m, the results of the maximum height above and maximum depth below are lower. This demonstrates the way in which the amplitude is measured relative to a datum for each window, and not 0 m.

The fact that the maximum and minimum parameters summarise roughness based on a single observation within each window, means that they are more sensitive to extreme changes along the profile. In this case of Profile A this has meant that shorter-wavelength variations in height caused by switches from peaks to valleys have been detected, resulting in a sawtooth pattern. For example, taking analysis of the central zone using the maximum above height, some windows have included values that are the crests of peaks, whereas others did not contain these high points giving a lower maximum height above value. Note that, if the frequency of peaks had been higher, or the window length was

sufficiently large then each window may have contained a crest, which would have resulted in the results for the central area having more constant values, so that the effects of individual peaks and valleys would be less discernible.

Another parameter that measured the overall dispersion in height along Profile A is the **range**. From the forth plot of Figure 5.8b it can be seen that, unlike the maximum height above and maximum depth below parameters, the range has produced results for the complete assessment length. The area of peaks and valleys in the centre is clearly distinguishable from the two flat areas. With this profile, the frequency of perturbations and the choice of window length are such that the results of the central area are constant. Thus, unlike other amplitude parameters, shorter horizontal scales of roughness cannot be identified.

Other examples of parameters that summarise roughness using a subset of the data are those that specifically measure the amplitude of parameters by using only those observations that are crests and/or troughs. Analysis of Profile A using the **mean peak height** shows that only observations considered crests have been summarised by this parameter. As such, there are no results for the flat regions of topography. The fact that results have been produced for the entire central zone suggests that every window in this section had at least one crest.

Another important observation of the mean peak height is the range in values that have been produced. Although none of the peaks in Profile A exceed 200 m in height, the parameter, the results of the parameter are greater. As with other methods of summarising amplitude, the results are calculated relative to a datum. The mean peak height is the average height of crests measured from the datum for each window. Although the design of Profile A is centred around 0 m, this is not the datum for some windows, thus producing higher results.

The three sections of topography along Profile A can be distinguished from the mean peak height results. The most striking pattern is the lack of results in the flat regions, but there are more subtle variations that allow the boundaries to be detected. At the transitions between the flat topography and central area, the mean peak height results vary from those of the central section. Given that the crest value is constant, the only explanation for this pattern is that the datum from which height is measured has varied between windows. As seen with the results of the other amplitude parameters earlier, the boundaries along Profile A are areas that produce marked differences in the distribution of points because, here, skewness in results is introduced. As earlier explained, towards the centre of the area of perturbations, the distribution of peaks and valleys is such that they cancel out. At the boundary on the left side, the presence of the first peak has resulted in

the datum being relatively higher. Therefore, when crests are measured from this higher datum, they appear lower.

Although not designed to specifically measure the frequency of peaks, like other amplitude parameters (excluding the range), finer-scale horizontal variations in roughness have been detected. In the central region of Profile A, the mean peak height fluctuates with a periodicity on the order of the wavelength of peaks and valleys. The ability to detect this pattern appears due to the size of windows and the wavelength/frequency of asperities. Had the wavelength of peaks been larger, or the windows smaller, then the central area may not have expressed this pattern.

With the amplitude parameters, many of the patterns appear to be the result of the distribution of peaks and troughs within each window. For example, where windows contain both types of asperity the results are somewhat moderated; windows containing more of one type of asperity produced higher or lower values. In the case of Profile A, therefore, the number of asperities in each window has had an important effect on results. Using spacing parameters it has been possible to detect this change in the number of asperities per window.

From the **number of crests** it can be seen that most windows in the central zone of Profile A contained two crests. However, in some of the sample lengths, the window captures three crests. The fact that the wavelength between asperities is constant in this zone demonstrates the importance of the moving window because it is this that has led to variations in the results. These measurements appear to confirm the interpretations made for the amplitude parameters.

As with the methods that summarise roughness in terms of amplitude variations, the number of crests shows clear distinctions between the different zones of topography along Profile A. Moving left to right across the first boundary there is a gradual increase in the number of crests. This is another demonstration of the effect of the moving window, as it progressively moves into the zone of asperities.

The percentage of crest results show an identical pattern as the number of crests. Given that the way in which these two parameters measure the number of asperities, this was expected. Similarly, given the design of the profile having the same frequency/wavelength as crests, the number of troughs and percentage of troughs parameters have also produced similar results to their counterparts.

Although different types of parameter are designed to summarise different information, many of the spatial variations in the amplitude and spacing statistics are similar, suggesting that they are controlled in similar ways. Several examples have already shown

that the horizontal window length appears to be important in explaining many of the patterns. One parameter that gives further insight into this role of window length is the **number of points**. For Profile A it can be seen that most windows contained 400 points, suggesting that the profile had a regular sampling interval with no gaps. However, towards both ends of the assessment length the number of points decreases. Knowing that the profile was designed to have uniform spacing, these results are an artefact of using a moving window. Each of the bed elevation measurements acts as the centre location for the window. Therefore, for observations that are close to the ends of the profile, the window, despite its fixed size, extends beyond the section being analysed. As a result, fewer observations fall within the window, thus explaining the decrease seen with the number of points parameter.

Figure 5.8d presents results that quantify roughness in terms of the shape of the profile. The plot of **slope** somewhat resembles that of the mean height: in the two flat regions of topography the results are lower, with an increase at the boundaries towards the area of asperities. Within the inner zone of perturbations there is a shorter-scale variation in the slope measurements. This repeating sawtooth pattern has the same periodicity as the wavelength of the asperities. However, it is important to note that the slope is a fitted value based on all observations within a window, and not simply a measure of the angles of each individual asperity. The fact that this level of spatial variation is evident in the results of Profile A is again due to a combination of the combination of the wavelength of perturbations and the choice of window.

As described in Section 4.3.3.5, the **sinuosity** parameter quantifies roughness by measuring the ratio between the total line length for a section of profile (i.e. within each window) and the straight line length (equal to the window length). In the two outer zones of Profile A, the total line length and sinusoidal length are equal, thus giving a value of 100. It can be expected, therefore, that this is the lowest possible value for this parameter. Moving through the transition zones from the flat regions to the inner zone of asperities, the sinuosity increases. This trend occurs because the presence of perturbations produces a larger total line length.

The fact that the sinuosity is measured as a ratio means that, regardless of the choice of window length the results are always standardised. However, the choice of window length remains an important factor with this parameter. Analysis of the boundary areas between different topographies along Profile A demonstrates that the results of this measure of roughness have also been affected by the window length: the boundary between areas of different topography is broader on the roughness results than the bed elevation plot.

Focusing on the central section of Profile A there is some fluctuation in the sinuosity. This has a higher frequency than that visible in, say, the horizontal distance between crests. The explanation for this pattern appears to be that the sinuosity parameter has captured both peaks and valleys. Thus, this is another example of how window lengths that exceed the wavelength of asperities may capture more than one perturbation that, in turn, affects the distribution. In this example, those windows that contain more crests and/or troughs have longer total line lengths thus resulting in a higher sinuosity.

Earlier, the inability to distinguish different zones of topography from the mean height parameter results was attributed to the peaks and valleys in some windows cancelling out. As such, this symmetrical distribution of observations produced similar values as the flat topography. One shape parameter specifically designed to measure the vertical distribution of points is the **skewness**. For the central area of Profile A, the results of this parameter (plot five of Figure 5.8d) confirm that the distribution of points in this central zone is essentially symmetrical. Nevertheless, small fluctuations in the results are discernible, and these suggest that some windows had a higher distribution of points above or below the windows' mean values.

With this parameter, the sections of different topography can be identified from the fact that only the central area yielded parameter results. Although, technically, the regions of flat topography have no skewness, an artefact of the program meant that the flat areas of topography did not yield any skewness measurements. This lack of results is only expected if all observations within a window have the same value. In the area of transition between the three main patterns in topography, the boundaries correspond to highest and lowest skewness values. The change in values also appears relatively sharp at the boundary, especially compared to the gradual change evident in the results of other parameters such as sinuosity. Taking the boundary at approximately 3.5 km along profile, windows have captured the flat topography and the first peak. Due to the presence of this high amplitude feature, the distribution of points is positively skewed. The reverse is the case on the right-hand transition zone, where the presence of a valley has produced a negative skewness. Moving towards the centre of the profile, windows have captured an equal distribution of peaks and valleys.

The **kurtosis** parameter is essentially similar to the skewness in that it is a measure of the distribution. For example, in the middle section of the profile the symmetry of peaks and valleys means that the kurtosis is close to 0 because the data are normally distributed. However, at the transition zones in topography, the distribution of points within these windows are skewed: for example, on the left-hand boundary between flat topography and asperiteis, the presence of the first peak would produce a positive skewness in the distribution, leading to a higher kurtosis. Nevertheless, another striking pattern is the fact

that on the right-hand boundary, the distribution is also skewed, but here windows contain a valley. Despite one set of windows containing a peak, and the other a valley, the kurtosis of both areas is identical. Therefore, the parameter has not distinguished the type of asperity.

Profile A has been used to demonstrate the way in which the parameters operate. In particular, it has explained how some of the patterns and artefacts have been produced. In particular, it is apparent that many of the trends are the result of a combined role of the moving window and the size of this sample length relative to the asperity wavelength. We now turn to examine the results of the other profiles. It will be apparent from the plots that many of the same artefacts are also apparent in these results. Therefore, rather than giving a written summary of every parameter, the following sections focus on describing and explaining any new patterns.

5.3.1.2 Profile B

Figures 5.9a to 5.9d present the parameter results for Profile B. Recall that the window size used was 2 km.

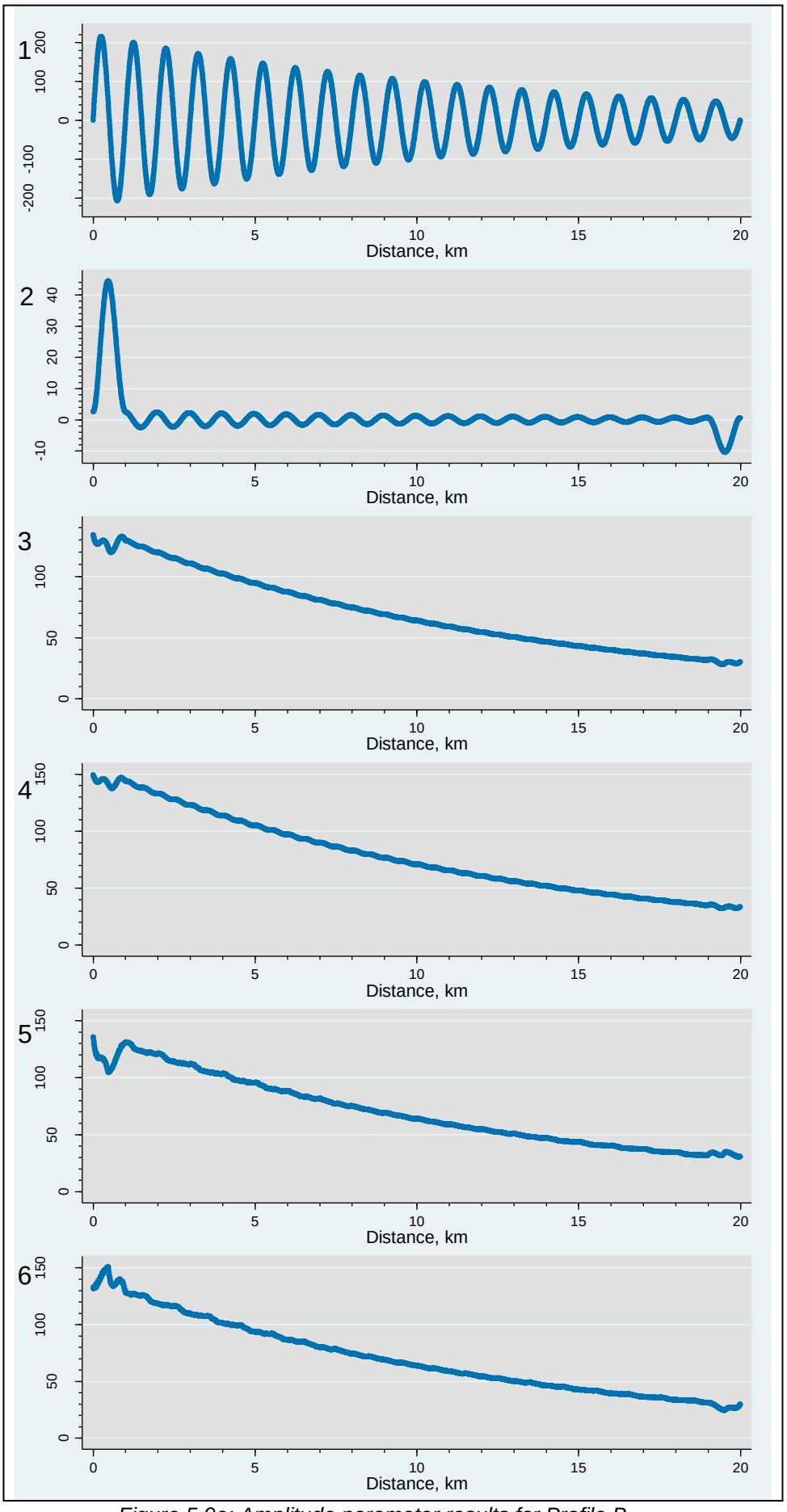

Figure 5.9a: Amplitude parameter results for Profile B

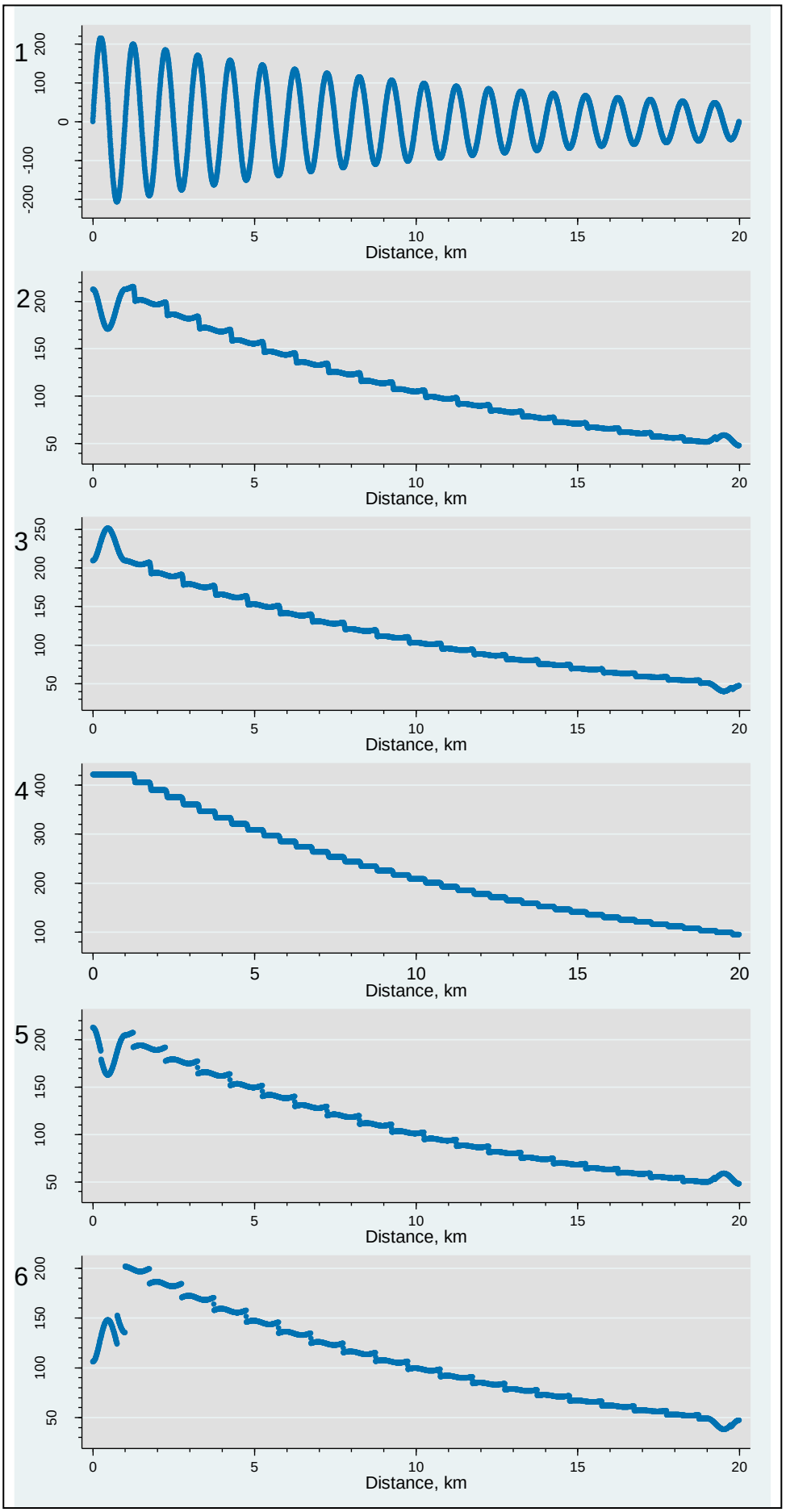

Figure 5.9b: Results for Profile B of parameters that measure specific amplitude characteristics

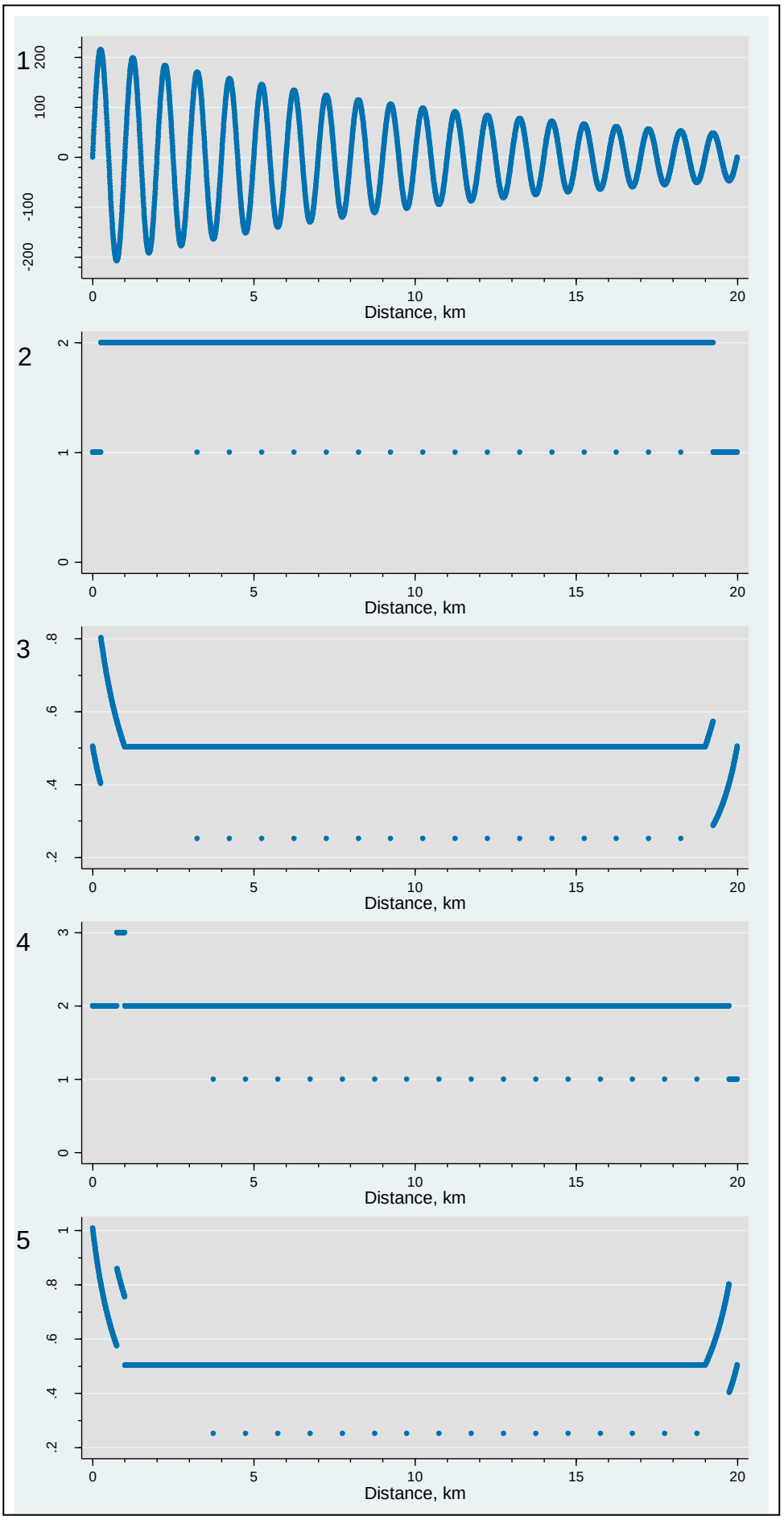

Figure 5.9c: Spacing parameter results for Profile B

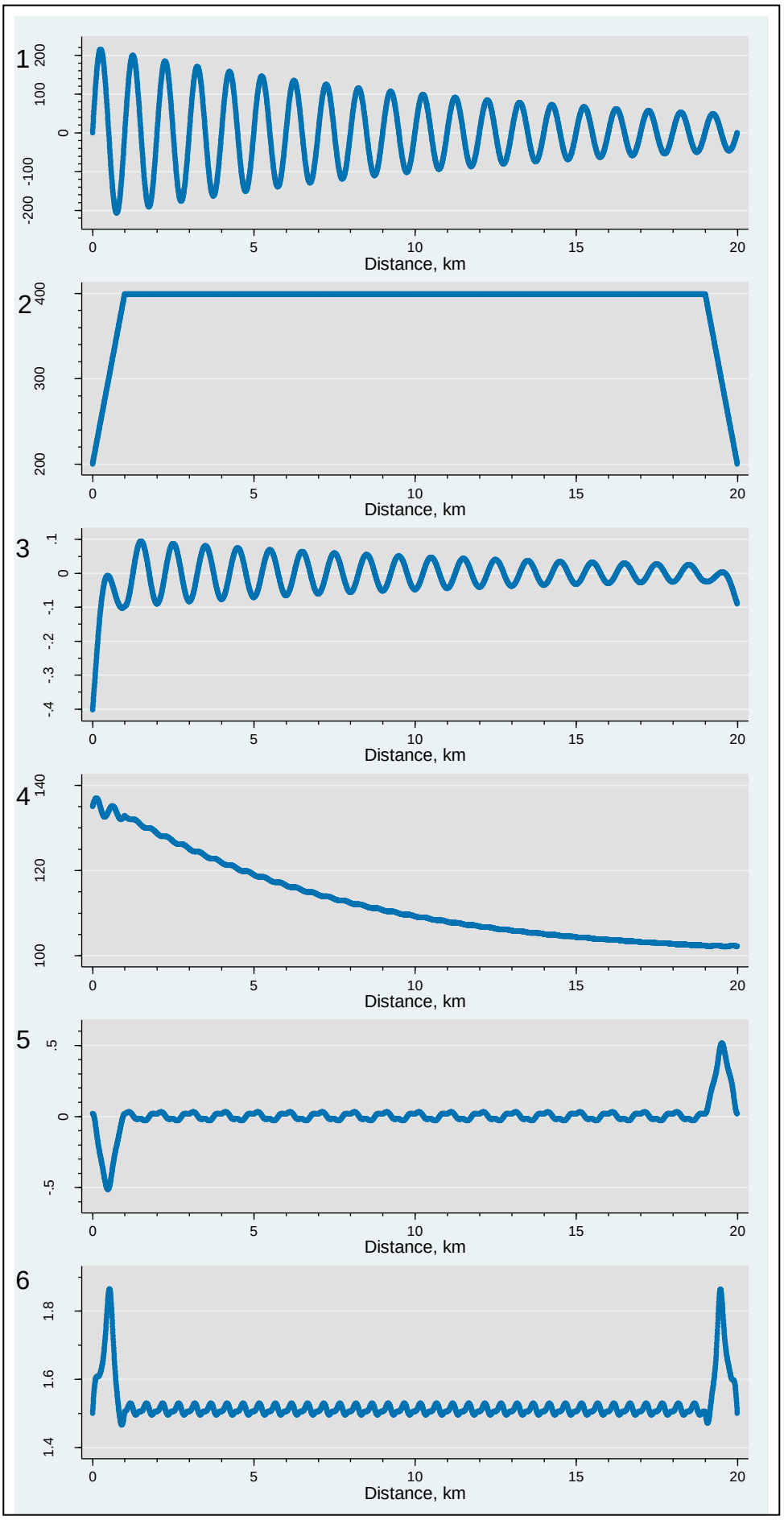

Figure 5.9d: Shape parameter results for Profile B

From Figure 5.9a it can be seen that many of the amplitude parameters, such as the *mean deviation* (Figure 5.9a3), show a decrease in value. This pattern corresponds with the decreasing vertical size of peaks and troughs. However, although these methods show a general trend, there are no localised fluctuations, say, at the scale of 1 km kilometres. Therefore, the variations in height between individual peaks and valleys are less distinct. The *mean height* is an exception among the amplitude parameters in that its pattern of results does not correspond with the decreasing size of asperities. Figure 5.9a2 shows that the values of this parameter are more constant around 0 m. However, on a shorter scale some variation in visible. As the size of peaks and troughs decreases, the range in mean height decreases, with values becoming closer to 0 m.

From Figure 5.9c it is apparent that the spacing parameter results are constant along Profile B. These results do not show any correspondence to variations in the vertical size of asperities. With shape parameters (summarised in Figure 5.9d), some of the methods show a pattern of changing values along profile, but others, such as *skewness* and *kurtosis* summarised in Figures 5.9d5 & 6, do not. Both these parameters are measures of the distribution of values. Therefore, within these windows, the heights appear to have something of a normal distribution, with the kurtosis indicating a slight skew to the right. These results suggest that there is a symmetry in the height values of each window, suggesting that they have typically captured an equal number of peaks and troughs. As the spacing parameters confirmed, this is the case.

The profile with the most visible trend is that of *sinuosity*, which shows a decrease along profile. This pattern appears to have been produced by the fact that, as the height of asperiteis decreases, so too does the total line distance. Therefore the ratio between the this sinusoidal length and the horizontal straight line length also decreases. The sinuosity remains above the 100 m minimum value of the flat topography in Profile A. Another parameter showing a trend along profile is *slope*, which again decreases. With both the *sinuosity* and *slope* parameters, the pattern of results appears to correspond with changes in the decreasing amplitude of asperities.

As with the previous profile, it can be seen how some filtering has occurred, where the broad decrease in amplitude has been detected, but the localised fluctuations between individual peaks and valleys are not shown. This is the case for all categories of parameter, e.g. the *sinuosity*, but is most apparent with methods that summarise height.

For all parameters, the most dramatic change in the roughness values occurs at the edges of the profile. These patterns appear to be due to the fact that the window extends beyond the assessment length. On the left-hand side of the profile, this means that the first set of windows only contain the peak. This affects the shape parameters because it

produces a positive skewness. The spacing parameters detect this area because there are a higher proportion of crests than valleys. Due to the skewed distribution, these areas lack the moderating effect between peaks and valleys, so the results are higher.

5.3.1.3 Profile C

Figure 5.10a to 5.10d show the parameter results for Profile C analysed over windows of 2km.

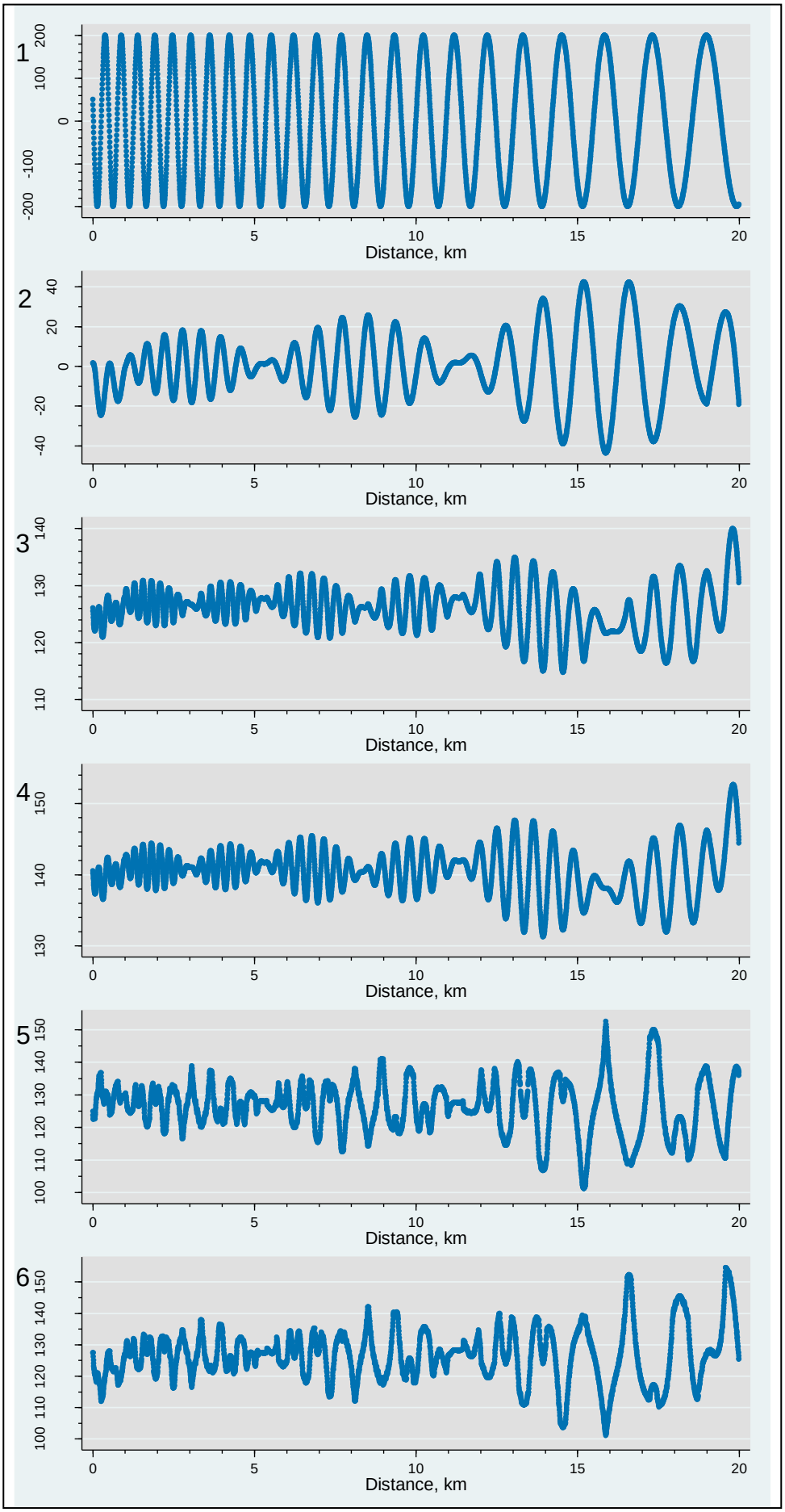

Figure 5.10a: Amplitude parameter results for Profile C

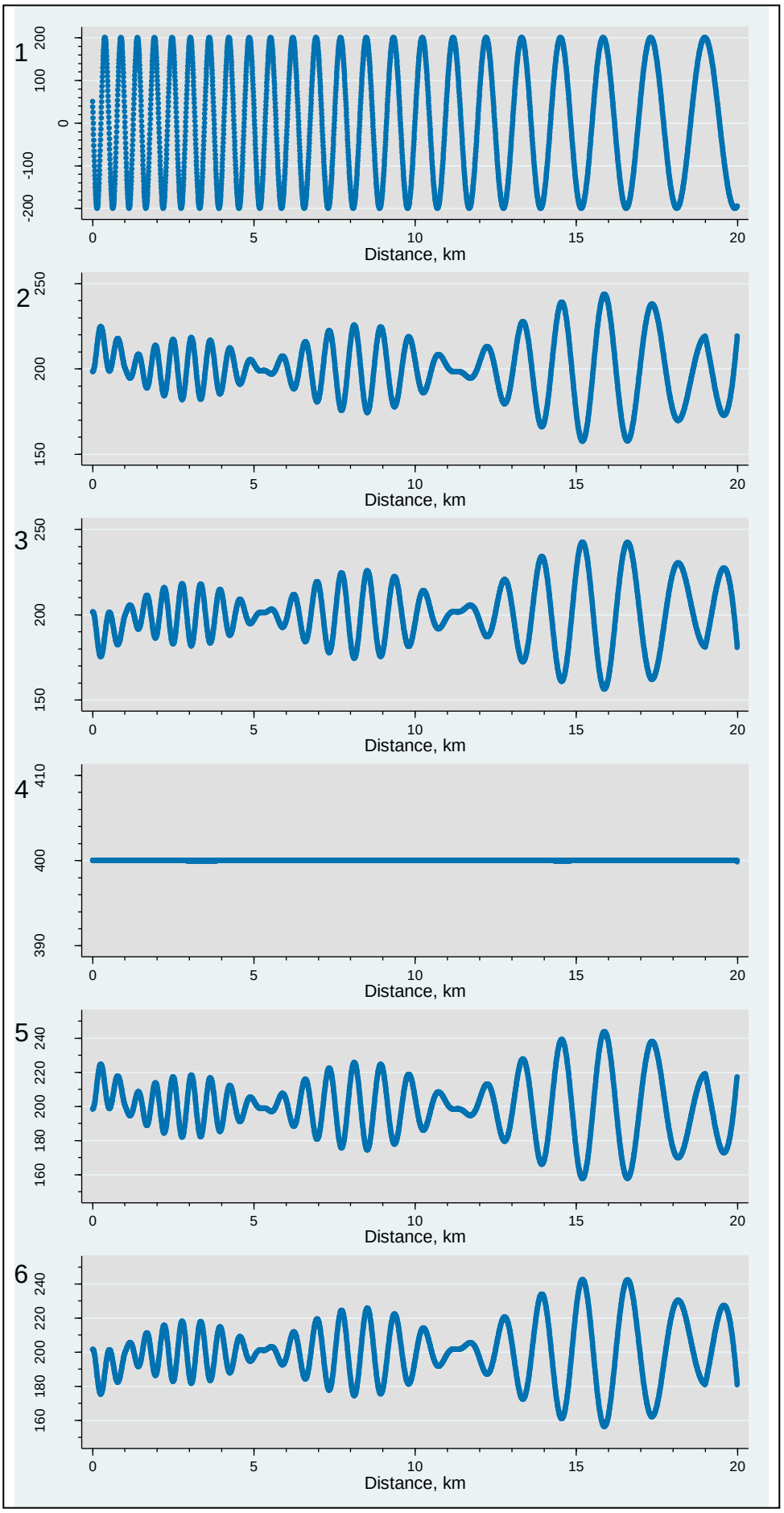

Figure 5.10b: Results for Profile C of parameters that measure specific amplitude characteristics

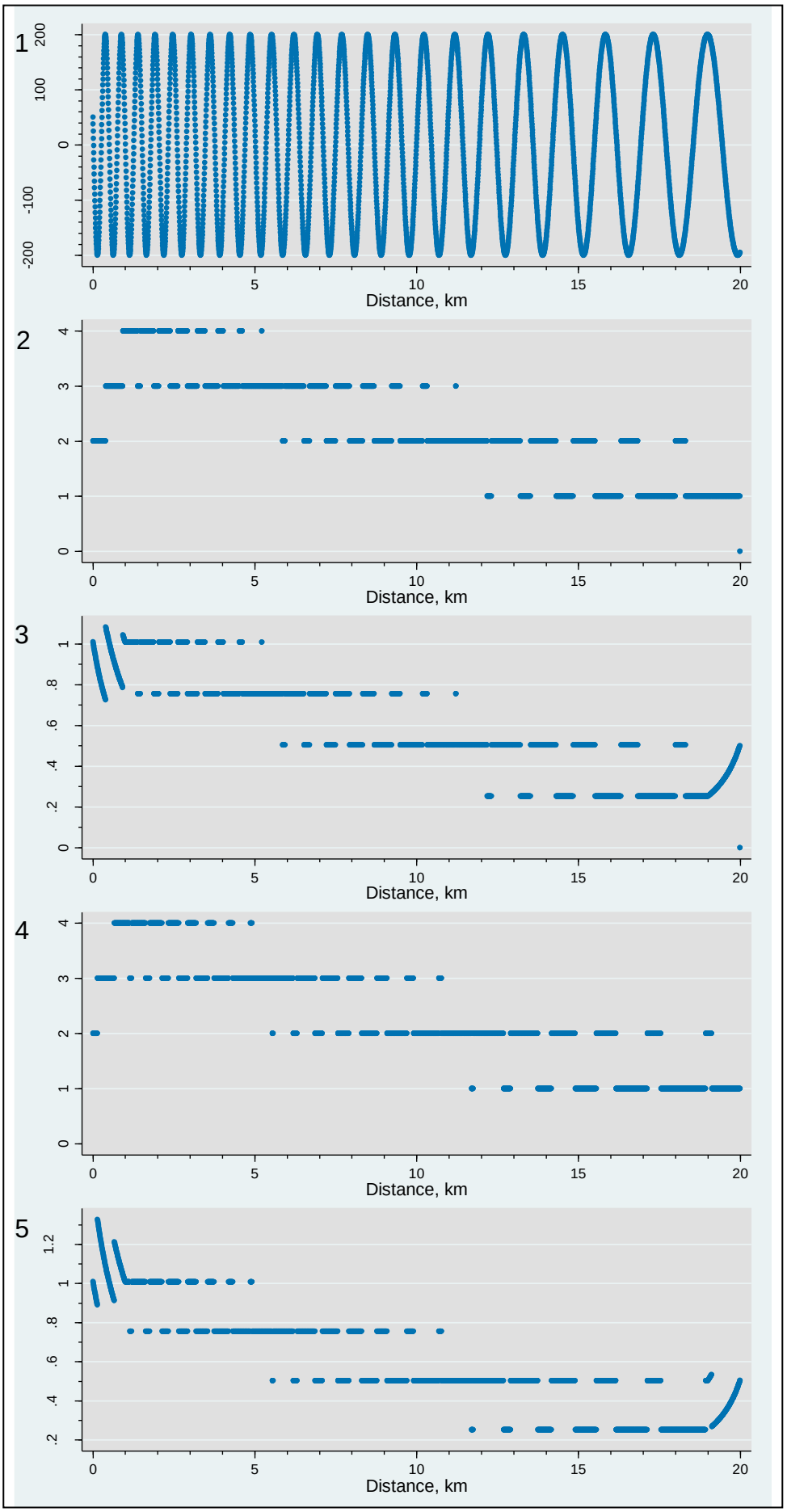

Figure 5.10c: Spacing parameter results for Profile C

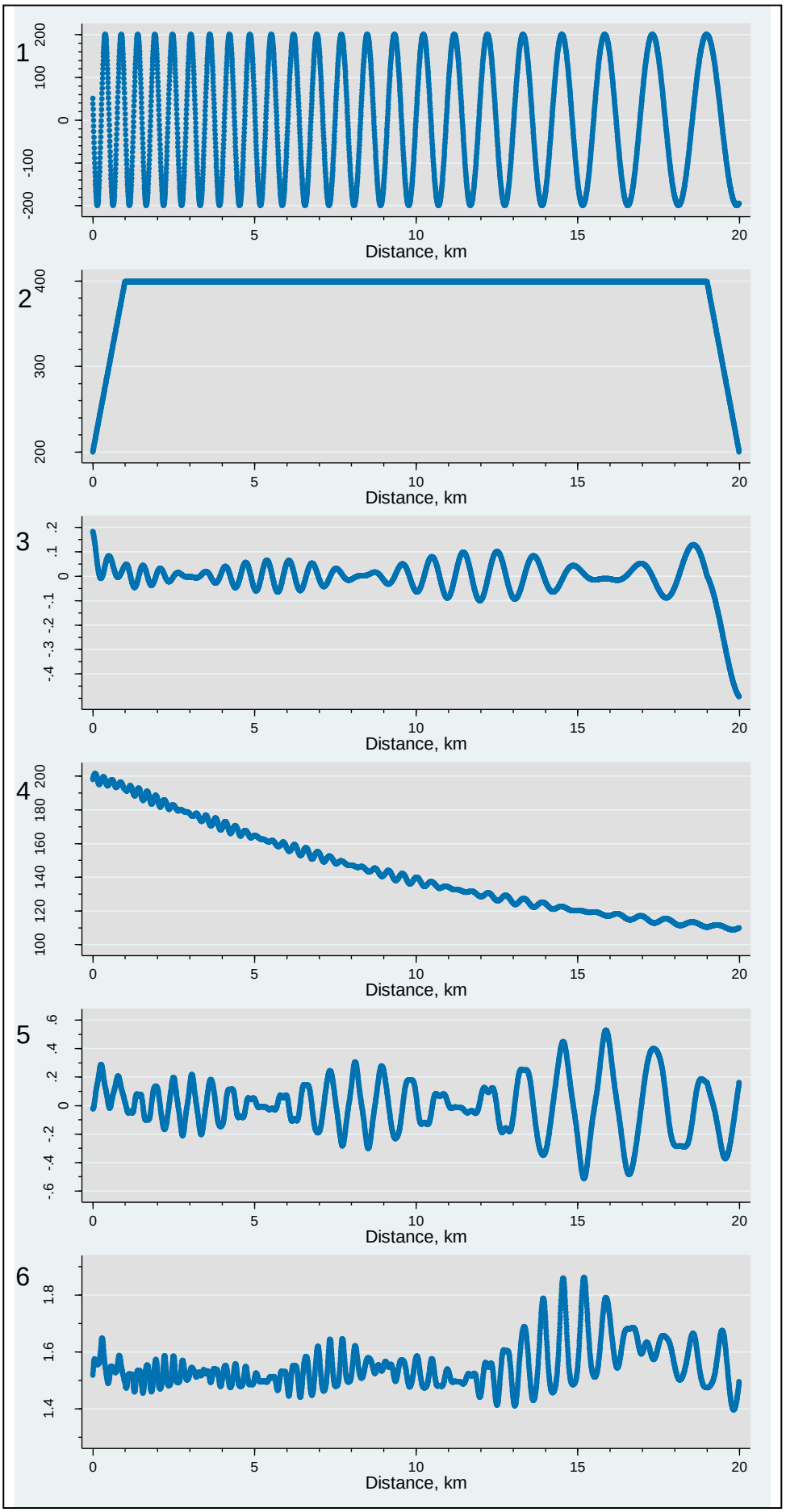

Figure 5.10d: Shape parameter results for Profile C

In Profile C, the overall height and depth of asperities is constant, with only the wavelength/frequency varying along profile. However, this horizontal variation appears to have influenced the amplitude parameters. For example, results of the *mean height* (Figure 5.10a2) show an overall increase in amplitude along profile. The likely cause of this is that changes in the wavelength of asperiteis influences the shape of the height distribution between windows. As already demonstrated, the similar height of peaks and valleys results in something of a symmetrical distribution, producing a moderating effect on the results of amplitude parameters. However, as the window length changes, some windows have proportionally more higher or lower observations, and this skewed distribution causes the results of the amplitude parameters to be larger or smaller depending on whether windows have a positive or negative skewness. As the window size increases, the distribution of points becomes increasingly skewed because windows no longer contain an equal number of peaks and valleys. Therefore, although the overall size of asperiteis in terms of their crest and trough heights remains the same, the amplitude changes.

Despite an overall trend of an increasing range in the results of amplitude parameters as wavelength increases, there are several areas that do not fit this pattern. Here, the amplitudes. For example, at two points the mean height results are closer to zero. This signal appears to be produced through a combination of the wavelength and the choice of window. In some places the distribution of points within a window falls into phase, with a symmetry between the number of peaks and the number of valleys. As a result, the moderating effect of these features is stronger. In other areas, the window length and the wavelength are out of phase so that windows contain a disproportionately larger number of high-amplitude or low-amplitude values. These regions produce the most dramatic spatial variations in roughness results.

The number of observations used to calculate the results also appears to have affected whether changes in wavelength influence the results. For example, the results of the *range* parameter (Figure 5.10b4) are constant along the assessment length. This shows that, despite the increasing wavelength, all windows contain at least one crest and one trough. Given that these points represent the highest and lowest values along Profile C, the range is always 400 m.

The results of the spacing parameters confirm that the increasing wavelength affects the distribution of peaks and valleys within each window. These type of statistics are designed to capture changes in the frequency of asperities, and the results of Profile B confirm that all have done so, with a decrease across these parameters moving left to right. However, it must be pointed out that although these methods show a decrease in the number of

crests and troughs, they do not show that this is attributed to changes in the wavelength of these features.

As with Profile B, all of the shape parameters show some variation along profile, but the agreement between these patterns and that of the changing wavelength of asperities differs. Parameters such as *sinuosity* show a trend of decreasing values (Figure 5.10d4), which appear to correspond with the changing amplitude along profile. However, although there is an overall increase in *skewness* (Figure 5.10d5) that fits the broad pattern of increasing wavelength, there is more variability in the results, similar to that of the *mean height* of Profile B (see Figure 5.9a2).

5.3.1.4 Profile D

The results for Profile D are presented in Figures 5.11a to 5.11d analysed over windows of 2 km.

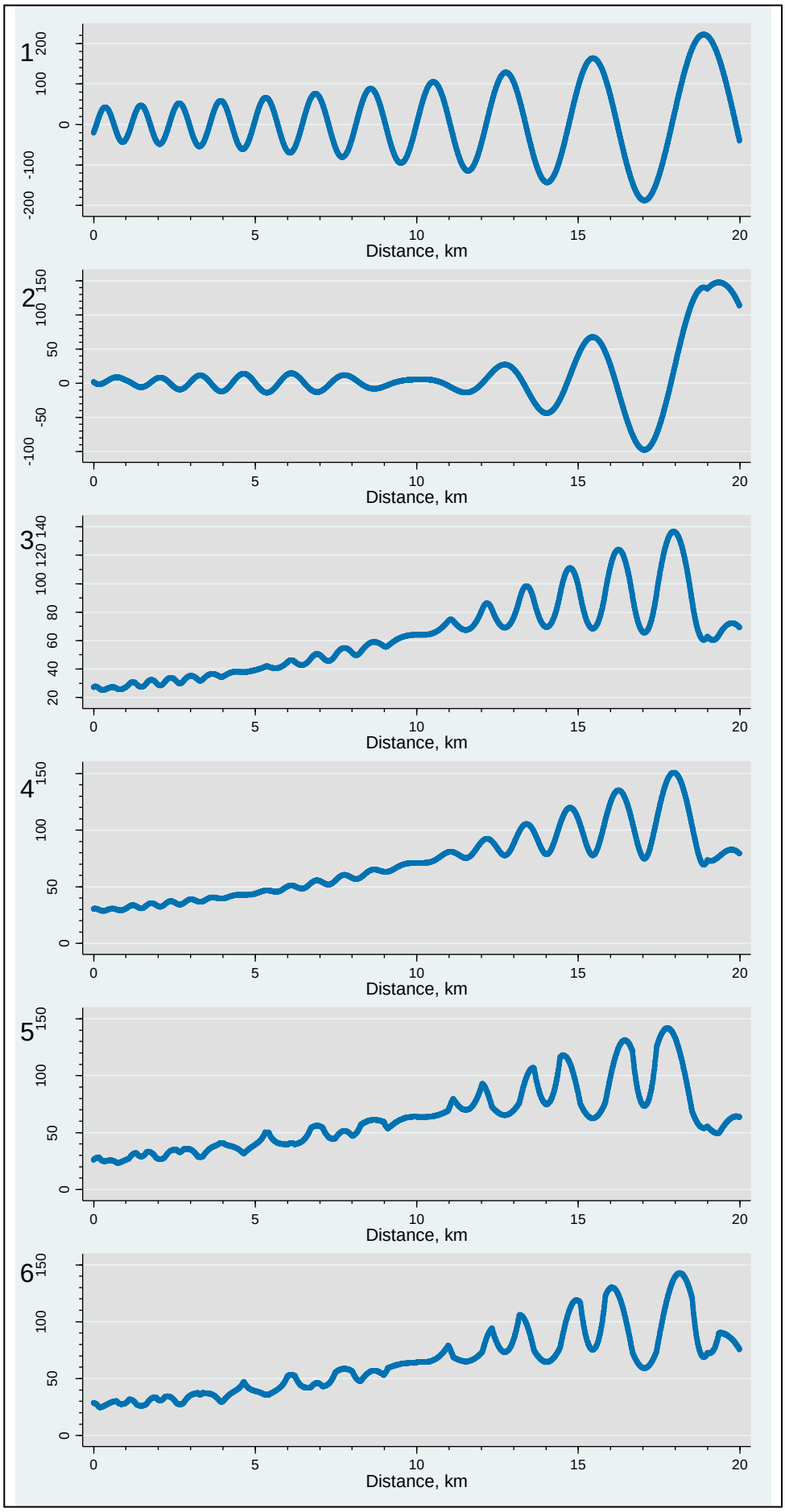

Figure 5.11a: Amplitude parameter results for Profile D

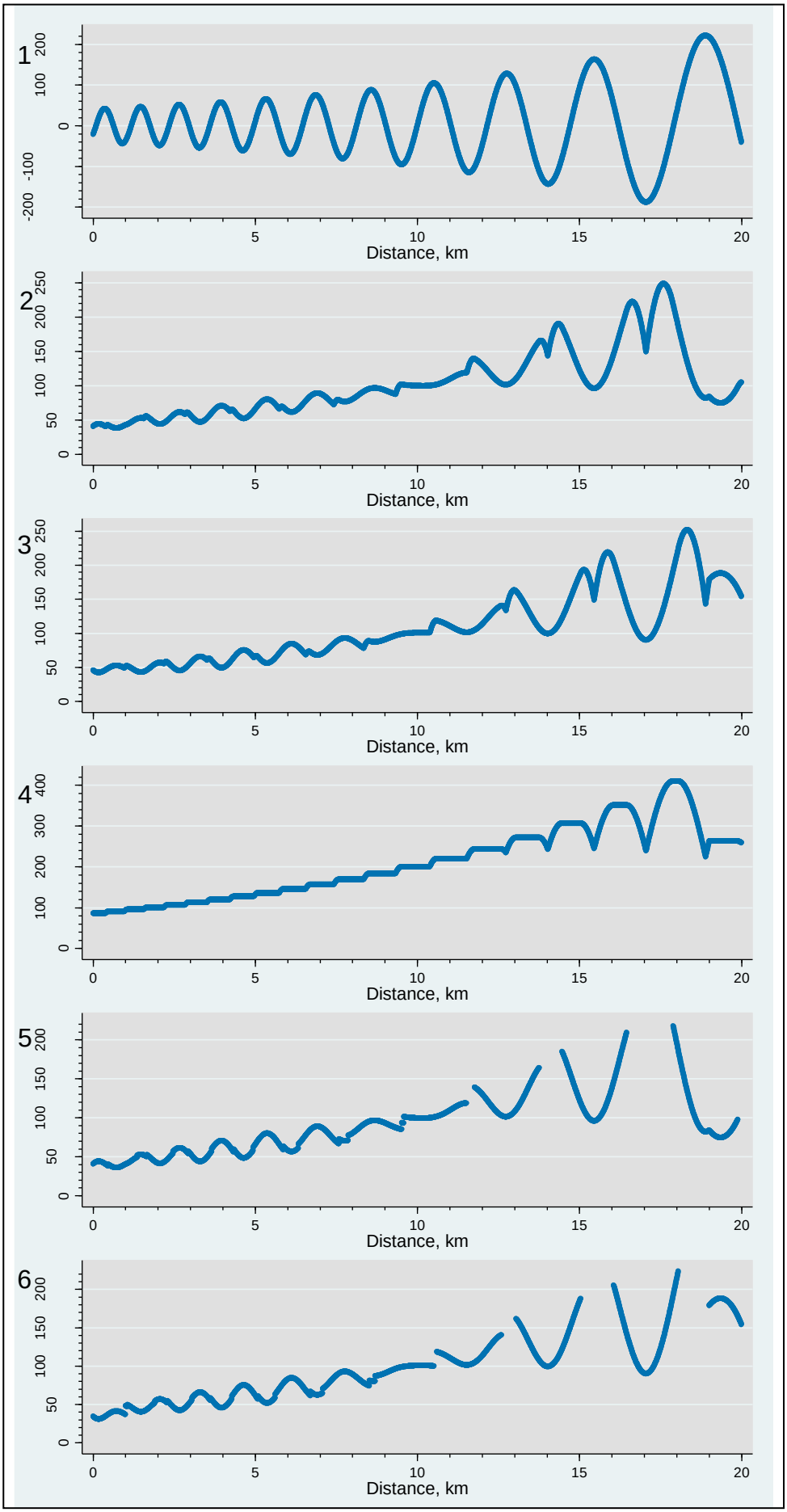

Figure 5.11b: Results for Profile D of parameters that measure specific amplitude characteristics

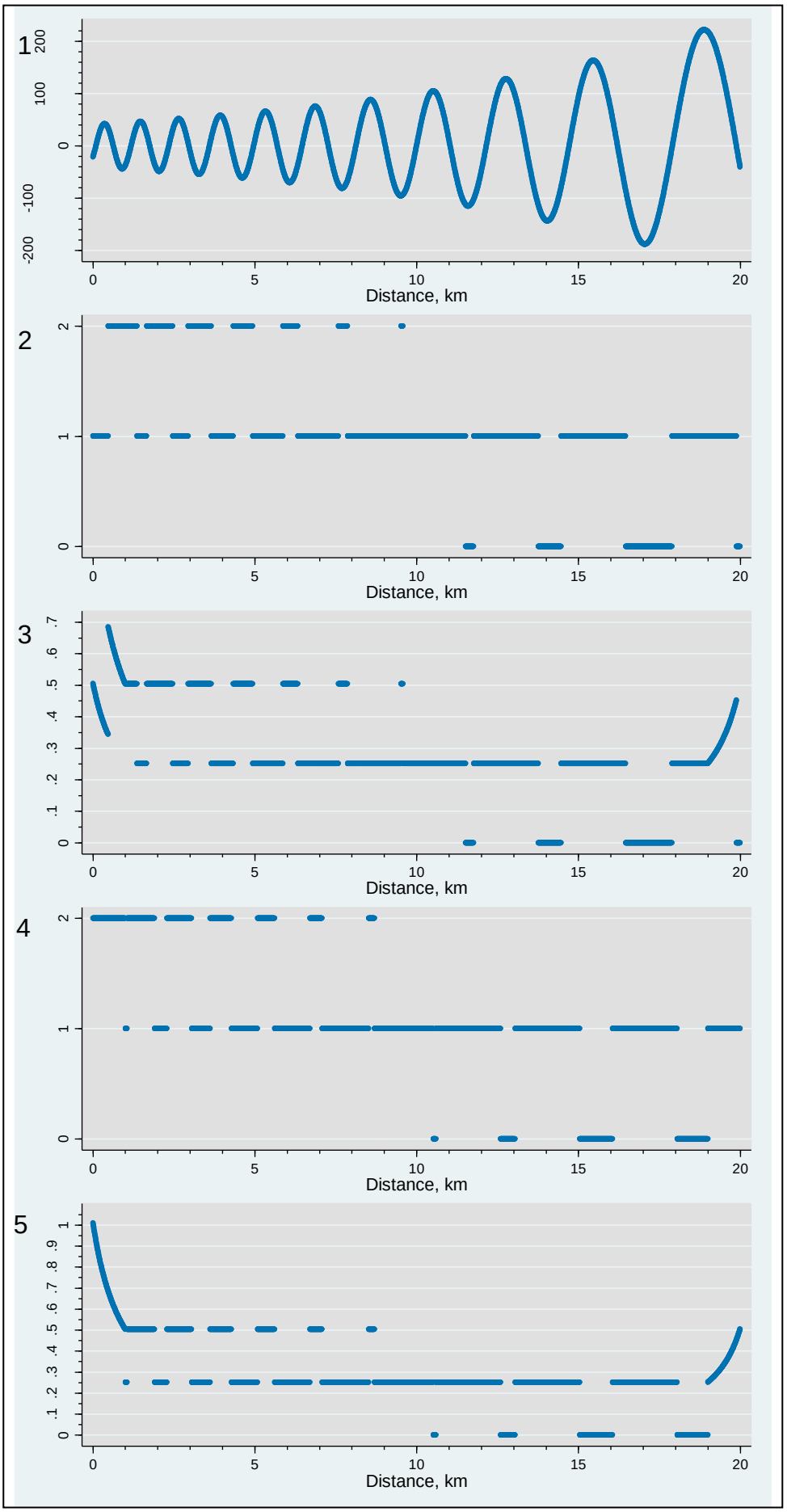

Figure 5.11c: Spacing parameter results for Profile D

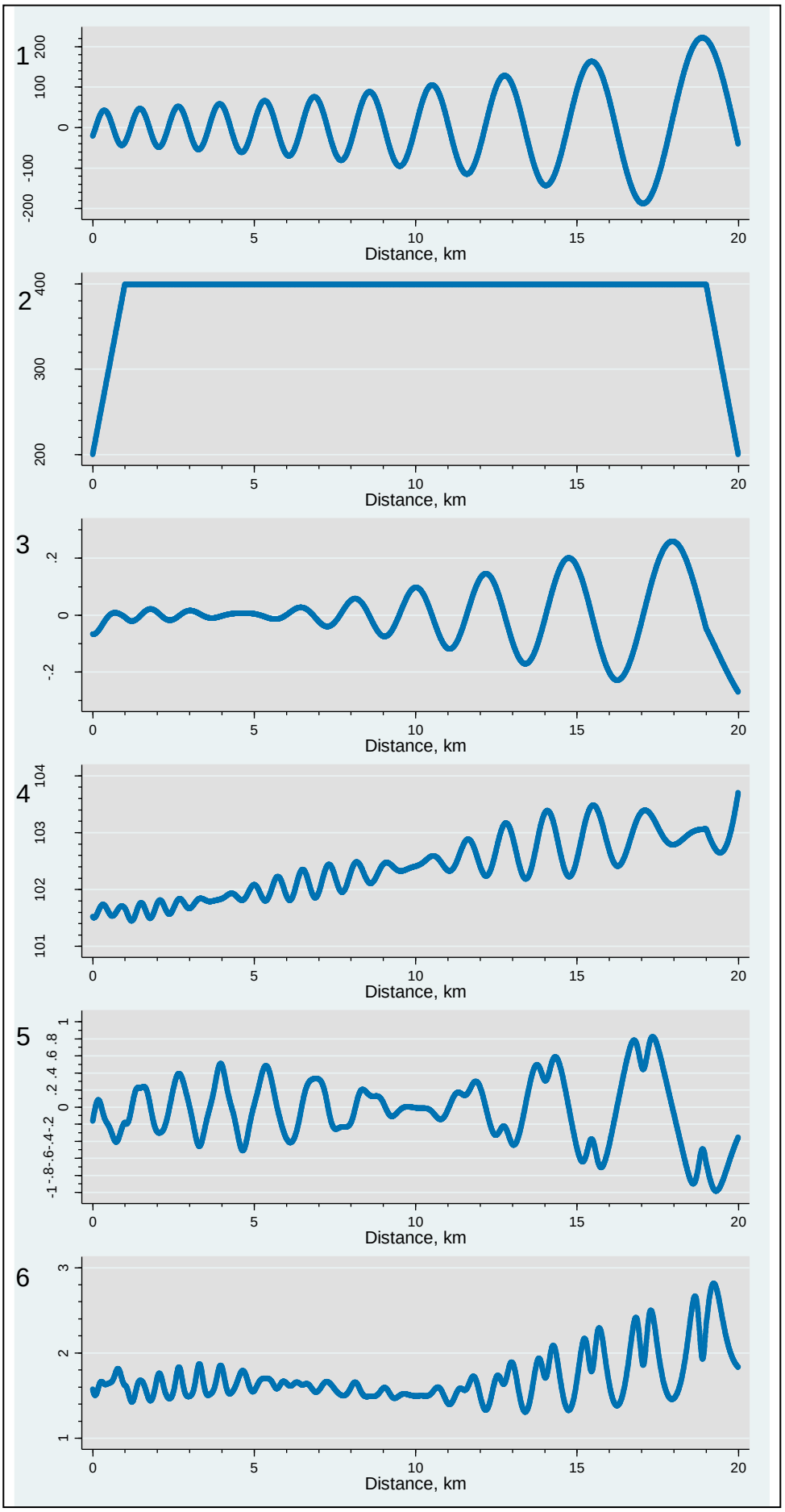

Figure 5.11d: Shape parameter results for Profile D

Recall that the increasing asperity size along Profile D was a product of increasing amplitude and increasing wavelength (decreasing frequency). From Figure 5.11a it can be seen that the amplitude parameter results increase along profile. However, compared with Profile B where only asperity height was adjusted, there is more variation in the results. With Profile D, although the overall pattern of increasing parameter values indicates increasing amplitude of the asperities, there is more fluctuation in the results. Furthermore, moving to the right, the results have a sinusoidal pattern, with the range in values between nearby areas (below 1 km apart) increasing.

The shape parameters (Figure 5.11c) all show a decrease in the frequency of peaks or valleys along profile. Towards the right-hand side the wavelengths of asperities relative to the window length are such that some windows have only crests or troughs, whereas, on the left-hand side of the profile, windows contained both peaks and valleys. This effect is also seen with amplitude parameters that use crest and trough observations. For example, at 17 km, the *mean peak height* (Figure 5.11b5) produced no values because there were no crests in this area.

The shape parameters (Figure 5.11d) have produced similar results to the amplitude parameters, which appear to have captured variations in both height and frequency/wavelength. However, the cause for the changing values with these methods is less clear. For example, variations in skewness may be the result of both amplitude and wavelength.

The results of Profile D appear to show many of the same patterns as those of the other profiles. For example, at some points along the profile the results of the mean height decrease. It is likely that these characteristics are produced by similar factors: for example, there are likely to be phase effects between the window length and size of features that affect the distribution of points within each window, thus producing a moderating influence. However, in Profile D, more variables are affecting the changes in topography. Therefore, with a combined effect of differences in amplitude, wavelength, and frequency, it is more challenging to determine the cause of any patterns. More insight into this is given when several variables are compared together. For example, analysis of spacing parameters shows that that areas where the mean height amplitude parameter is closer to 0 m correspond to windows that have a similar distribution of peaks and valleys; the skewness and kurtosis spacing parameters show that the distribution of points in such windows is more symmetrical.

5.3.1.5 Profile E

The results of analysis over 2 km windows for Profile E are shown in Figures 5.12a to 5.12d.

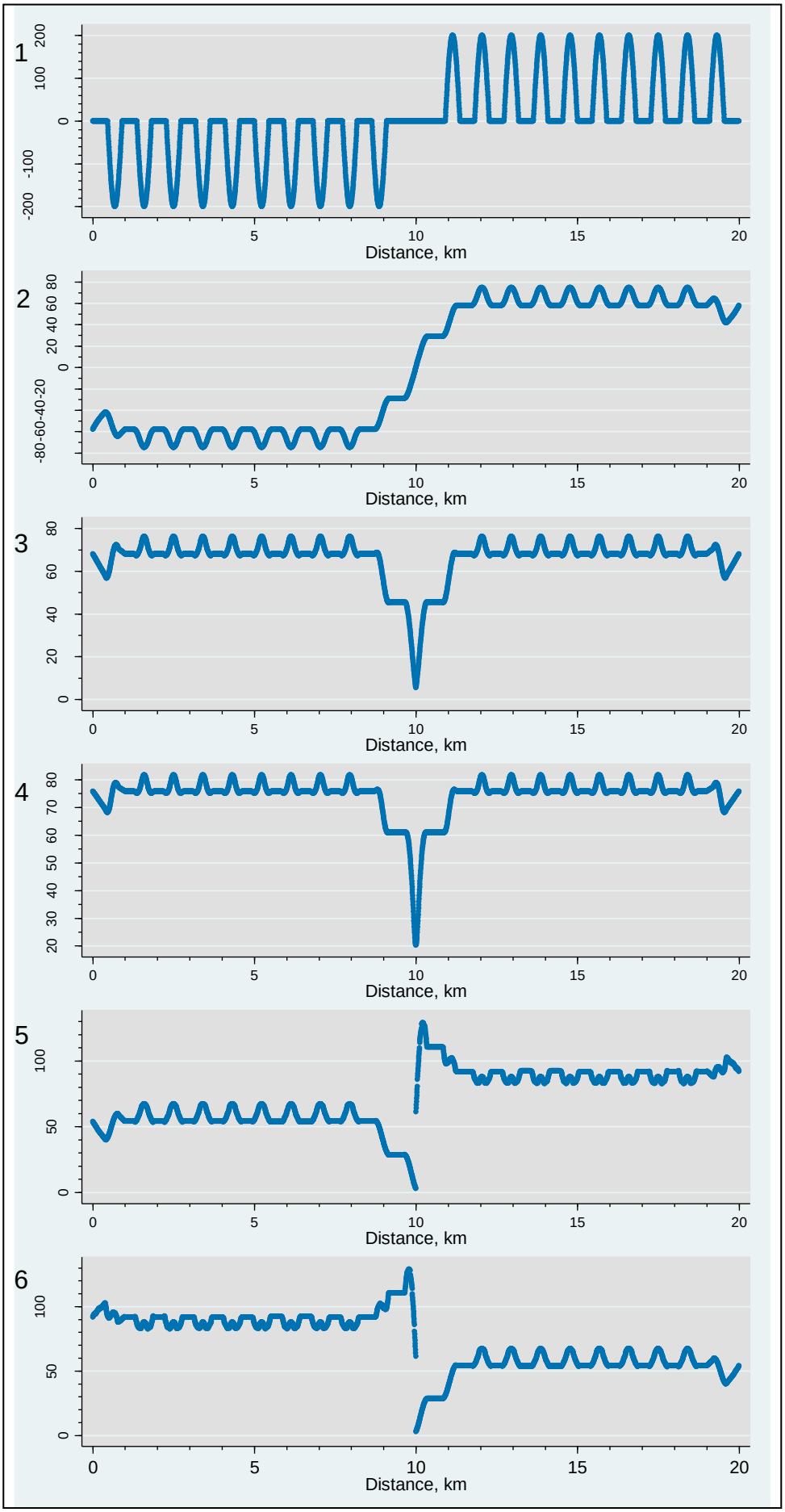

Figure 5.12a: Amplitude parameter results for Profile E

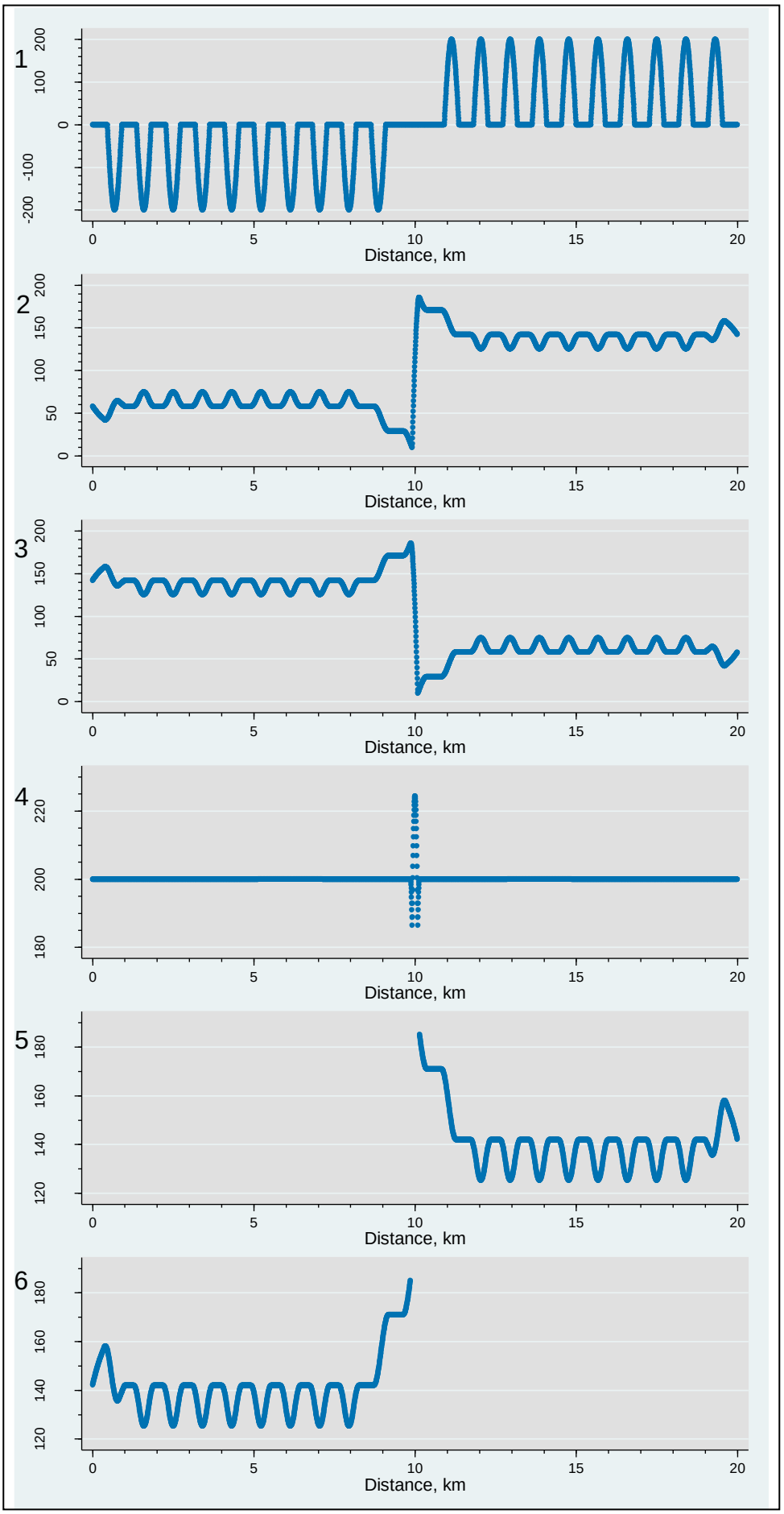

Figure 5.12b: Results for Profile E of parameters that measure specific amplitude characteristics

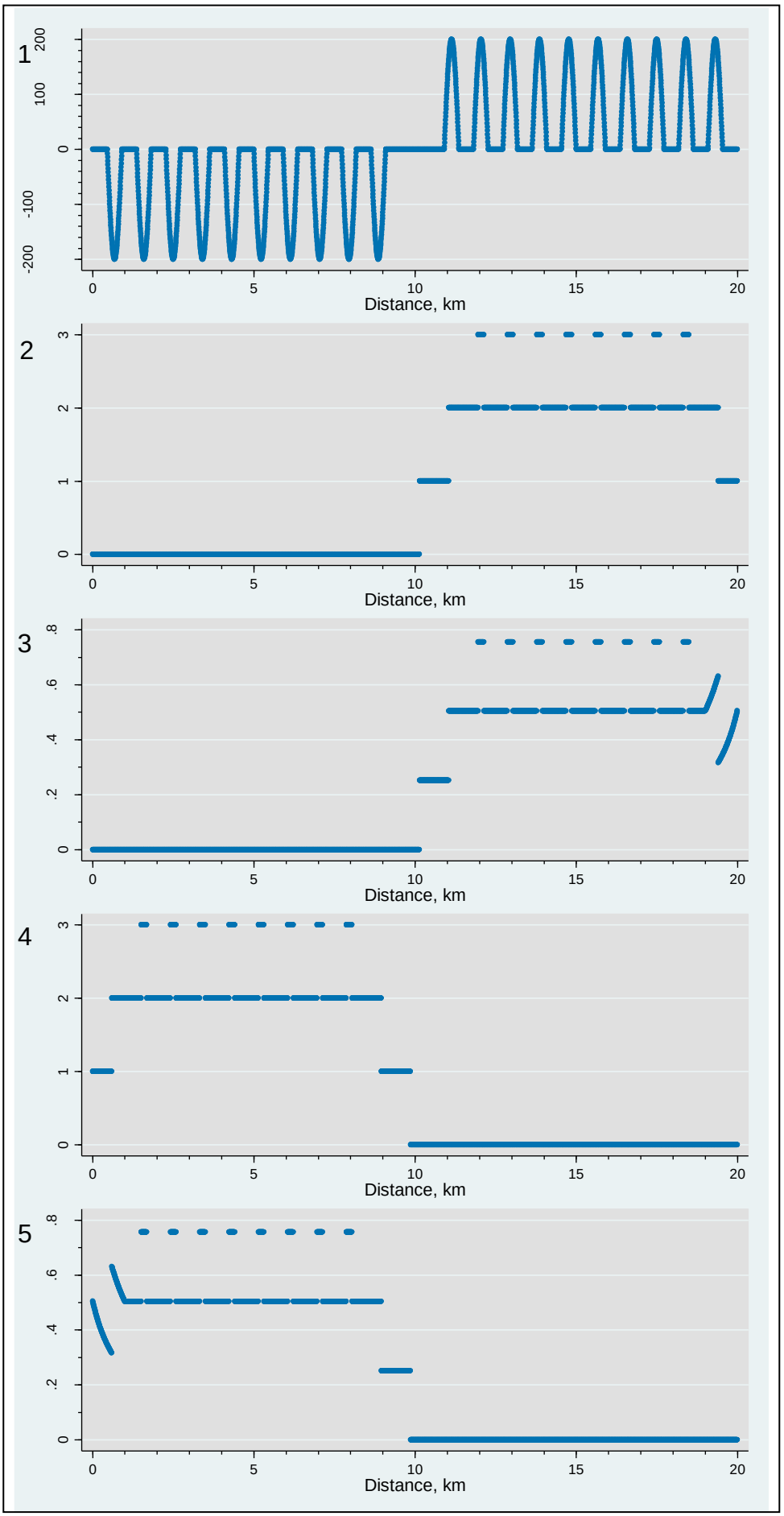

Figure 5.12c: Spacing parameter results for Profile E

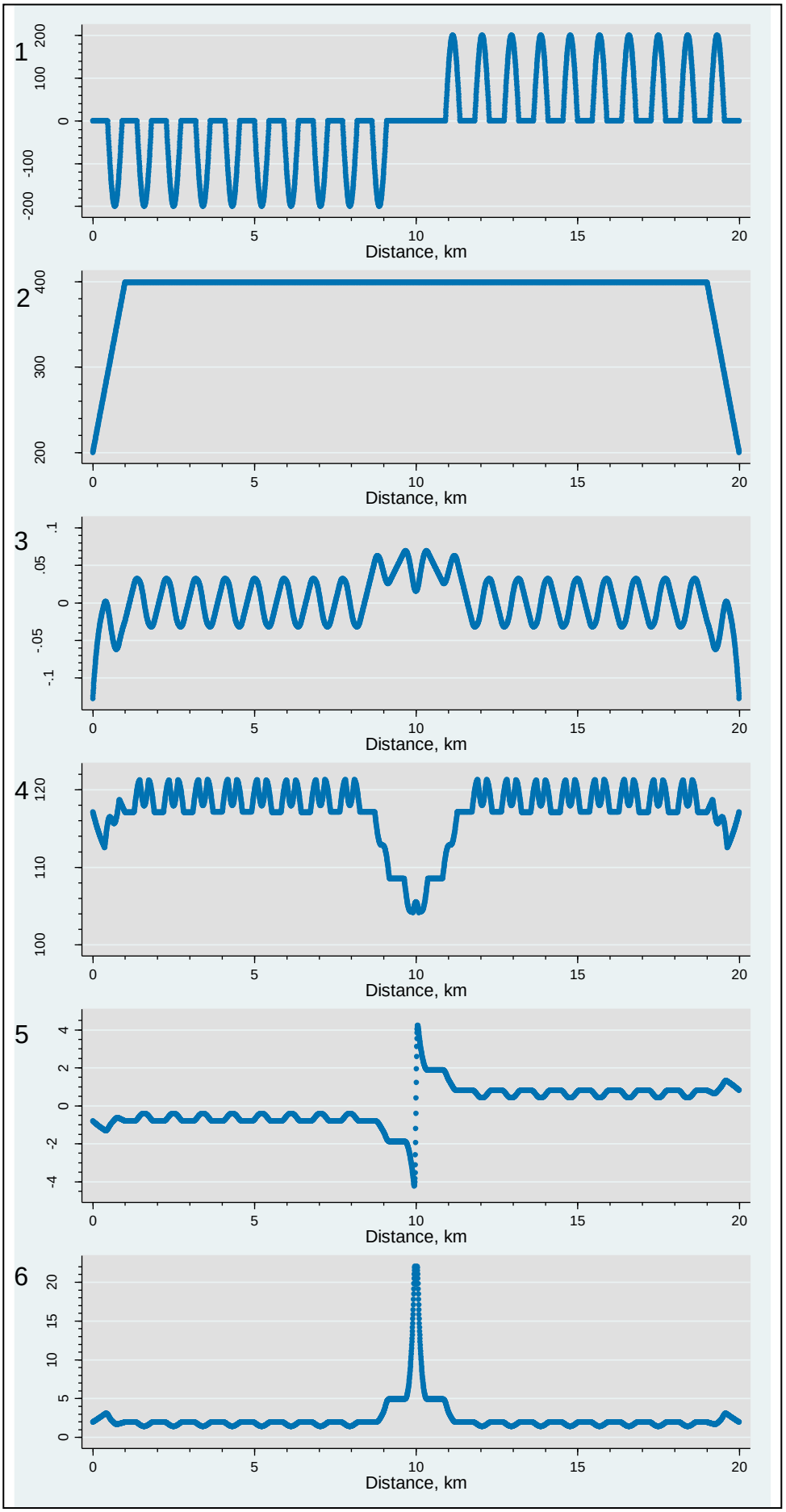

Figure 5.12d: Shape parameter results for Profile E

Despite differences in height between the two zones, many of the amplitude parameters do not distinguish between the two areas. For example, with the *mean deviation* the only variation in results occurs at the flat transition zone between the area of valleys and area of peaks. Nevertheless, parameters that do not use absolute values (such as the *mean height*) have detected the change in topography, as have parameters that use a subset of the observations.

Using parameters that measure the number or size of asperities it is possible to identify the differences in topography between the two areas. However, this is because some areas produce no results. For example, because *crests* are defined as a high point with two immediately lower values, the plateaued tops of the left-hand side of the profile are not considered peaks. Similarly, the flat-bottomed areas on the right are not identified as *troughs*.

With the exception of the *skewness* parameter, the methods of quantifying roughness by variations in profile shape have failed to detect the differences between the two zones. For example, in Figure 5.12d4 it can be seen that the only variation in *sinuosity* occurs at the central transition area between the two topographies. With the *skewness* parameter, the left-hand profile has produced a negative skewness, and the right-hand side a positive skewness.

5.3.2 RES data

As with the synthetic profiles, the roughness parameter results of the radio-echo sounding data are summarised in four sets of graphs. Figure 5.13a presents those methods that use all observations within a window to summarise variations in amplitude, with Figure 6.13b showing those that use a subset. Figures 5.13c and 5.13d, respectively, show the results of spacing and shape parameters. Recall that a larger window length of 62 km was used.

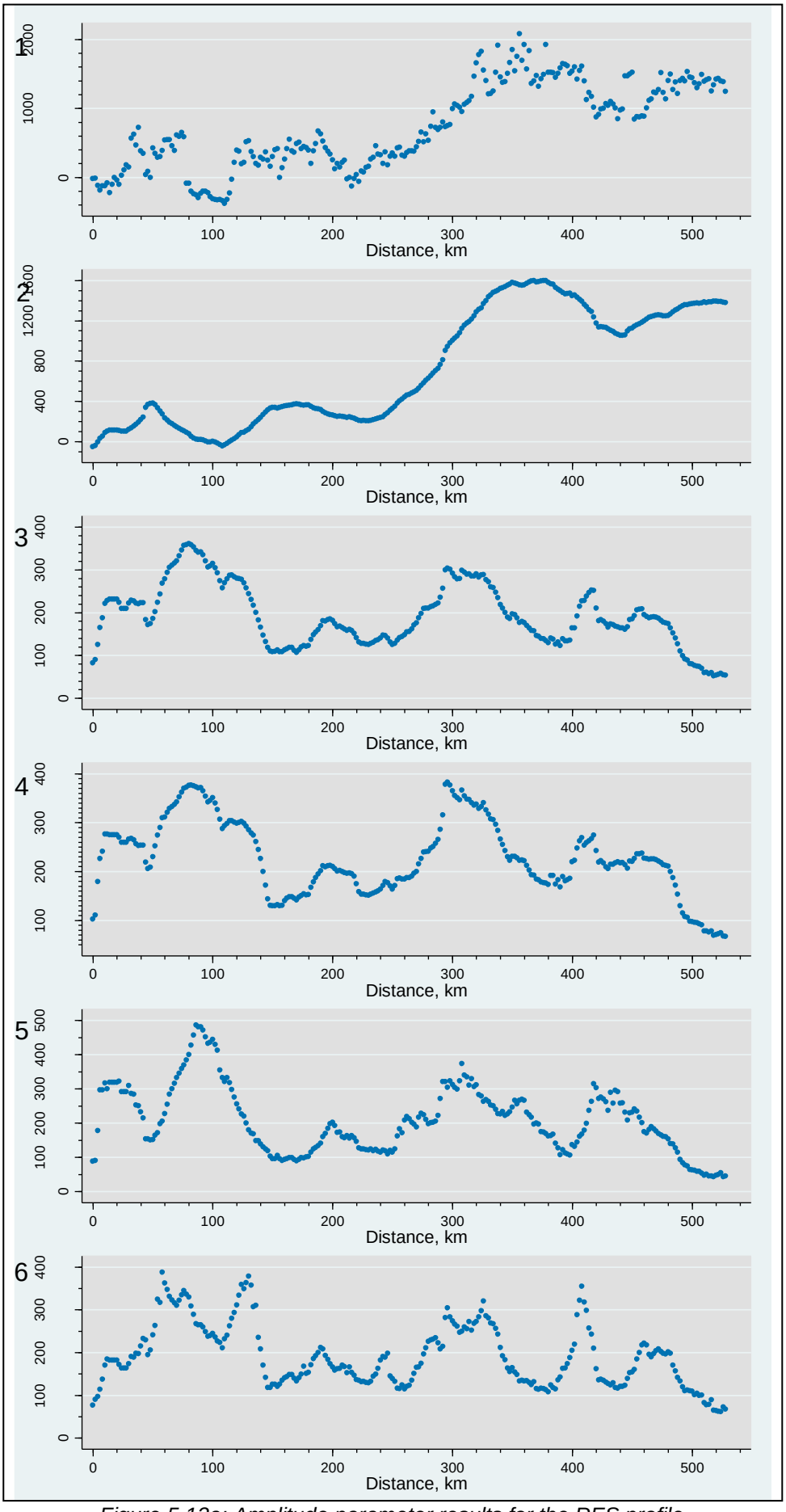

Figure 5.13a: Amplitude parameter results for the RES profile

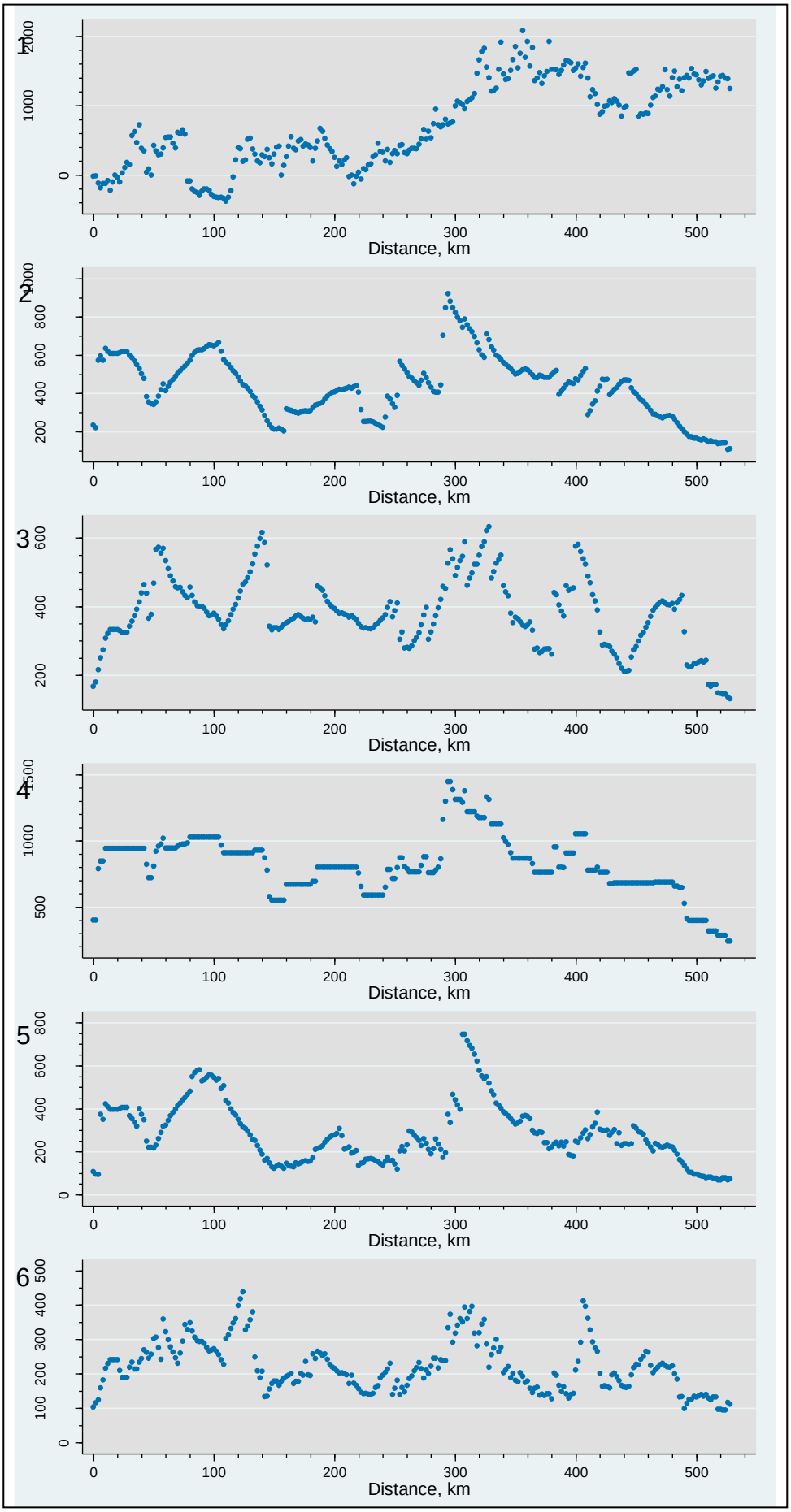

Figure 5.13b: RES profile results or parameters that measure specific amplitude characteristics

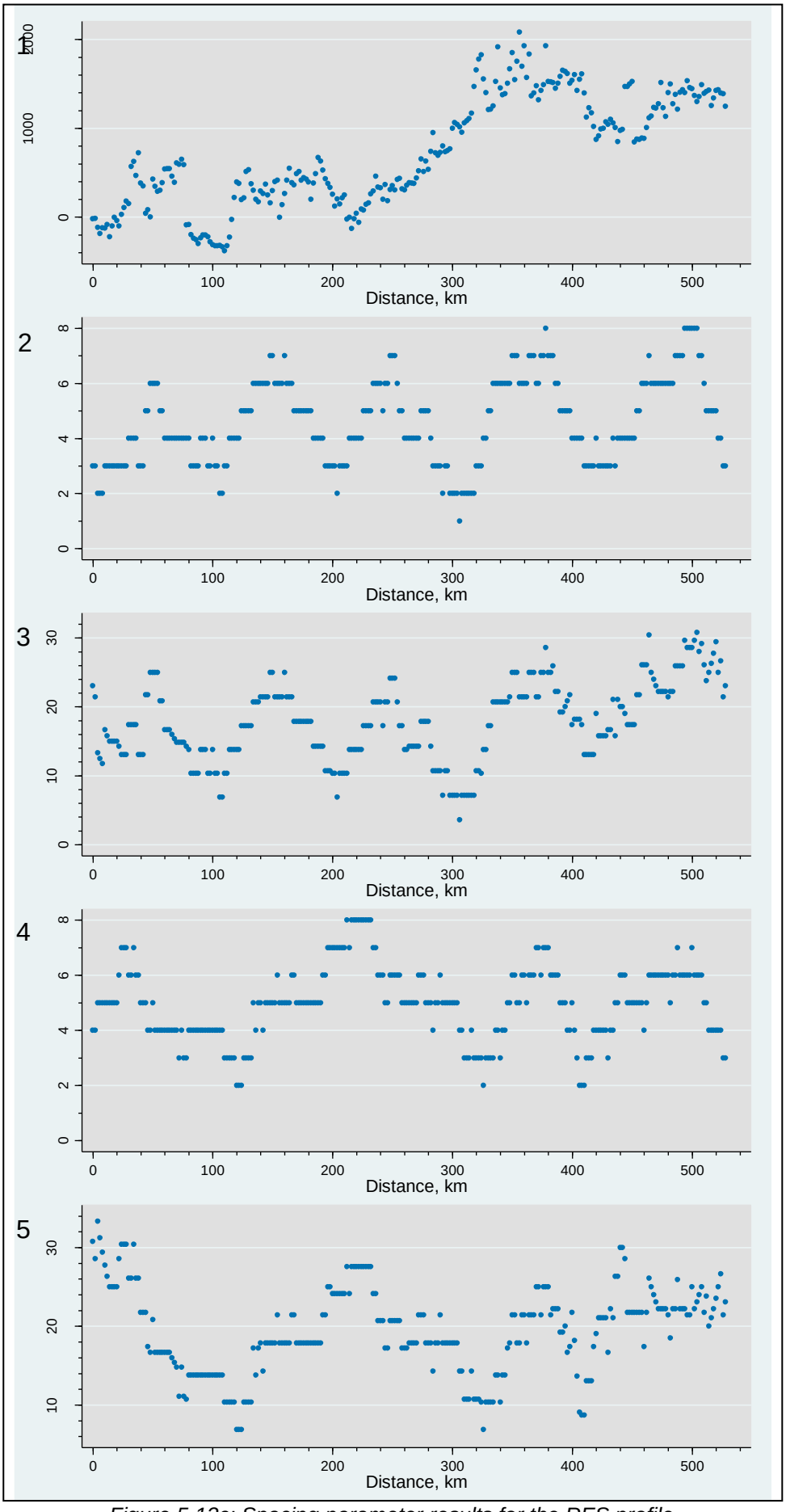

Figure 5.13c: Spacing parameter results for the RES profile

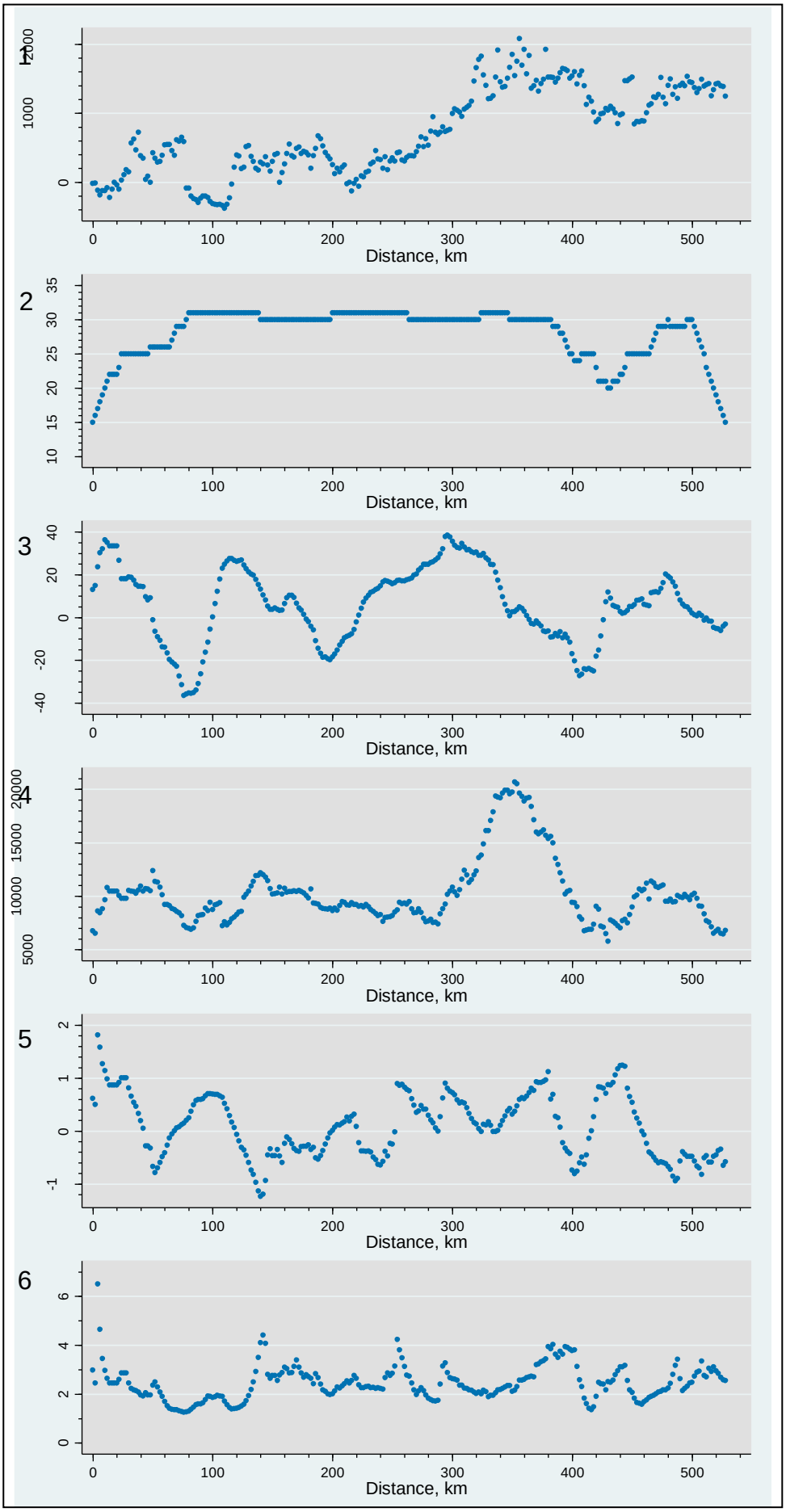

Figure 5.13d: Shape parameter results for RES profile

The first thing to note are the results for the *number of points* parameter shown in Figure 5.13d2. Some of the 62 km windows had fewer than 31 points, indicating that there was irregular spacing between points or missing observations. At approximately 410 km along profile, the number of points decreases to 20, indicating that the average sampling interval of points in this area was over 3 km.

The *mean height* parameter (Figure 5.13a2) has smoothed some of the local variation removing the noisy appearance of the data. It can be seen that the bed shows an overall increase in height moving to the right, and three large-scale bumps are clearly visible. Other roughness parameters, such as the *mean deviation* shown in Figure 5.13a3, have removed some of the overall trend of increasing bed elevation. These results show that the bed has more localised variations. Again three large bumps are identifiable, but their position differs from those seen with the *mean height* parameter. Furthermore, smaller scale peaks and valleys are more apparent.

The amplitude parameters that identify extreme values and specifically measure asperity size show a similar pattern to the other methods of quantifying roughness using amplitude. These results are complemented by the spacing parameters that show the spatial variations in asperity frequency. It can be seen that there is an overall increase in the number of asperities along profile, but there are marked fluctuations. The *number of crests* (Figure 5.13c2) shows a structure where, despite an overall increase, the values oscillate over lengths of approximately 100 km. This feature is not apparent with the amplitude parameters.

Shape parameters show similar patterns to the amplitude and spacing methods. For example, the *slope* results (Figure 5.13d3) have some correspondence with *RMS height* (Figure 5.13a4) measurements. The *number of points* shape shows that some windows had fewer than the 31 points selected. Therefore, there are some missing values in the RES dataset, but the software has produced results for all of the 19 methods used. Therefore, irregular spacing or gaps has not prevented roughness values to be generated, yet results in these areas are based on fewer observations.

5.4 3D roughness parameters

As discussed in Section 5.2.3, the program for quantifying roughness in 3D can produce results in two formats. Table 5.1 shows summary statistics for the River Tweed study area. These measurements give a single, overall value for each parameter measured over the entire 5 × 5 km study area. Such information could be used to compare different regions, and this is aided by the fact that the results use a local datum so, even if the topography of one area was considerably higher than that of another, the results would be comparable. For example, height or number of peaks in this Tweed valley study site could

be compared with those in another region to measure how the frequency or size of subglacial bed obstacles varies.

Parameter	Results	Units
Mean height	57.1	m
RMS height	10.8	m
Mean deviation	8.6	m
Standard deviation	10.8	m
Maximum height above	41.1	m
Maximum depth below	51.1	m
Range	92.1	m
Mean height above	7.4	m
Mean depth below	10.3	m
Mean crest height	7.8	m
Mean pit depth	9.9	m
Number of crests	23980	Count
Percentage of crests	2.4	Percentage
Number of pits	17731	Count
Percentage of pits	1.8	Percentage
Number of points	1000000	Count
Skewness	-0.6	Unit free
Kurtosis	2.8	Unit free

Table 5.1: Summary roughness results of the 3D roughness parameters for the whole 5×5 km study region of the River Tweed

One limitation with these results is that they do not summarise the range or standard deviation of the parameters, so it is not possible to determine how representative these results are of the overall distribution. Furthermore, the summary results give little spatial information. For instance, the results identify that the highest point had an elevation of 41.1 m above the local datum, but the location of this value within the 25 km^2 study area is uncertain.

More spatial information is given when roughness is analysed over a grid. This ability to detect directional patterns of roughness is shown in Figures 5.14a to 5.14e that plot the 3D results for a selection of parameters. Recall from Section 5.2.3, that the grid size used to analyse topography in this manner was 400 × 400 m. As with the approach to presenting the results of the 2D parameters (Section 5.3.1), the patterns in the results of the 3D methods are now described. The likely factors that have produced the spatial patterns are explored, again focusing on how the operational aspects of the methods, such as the use of grids, have influenced the results. The variations in roughness values

are not attributed to any glacio-dynamic cause; emphasis was given to explaining patterns produced by the functionality of the parameters, because this affects their feasibility of use with glacial data.

The results of the *mean height* parameter are shown in Figure 5.14a. Across the entire site there is a pattern of increasing values for this parameter from the SE to the NE. The elongate bedforms of the Tweed can be clearly seen on the DEM imagery, and some of these have widths that are smaller in size than the grid (<400 m). Therefore, it might be expected that these would be visible on the mean height results. In fact, the locations of the subglacial bedforms cannot be readily discerned from the parameter results. It appears that, for any grid containing bedforms, the higher elevation of these features has been moderated out by the surrounding lower-amplitude topography.

The bedforms in this Tweed area exhibit a strong parallel alignment, with their long axe orientated approximately West-East. In this orientation the length of these features are all over 400 m, so it would be expected that the bedforms would cross several grids. Despite this, the general trend of the bedforms cannot be clearly seen in the mean height results. Instead, the results of this parameter show a pattern that does not match the orientation of the bedforms. Here, it appears that the mean height of the topography increases towards the north west of the study area. This change in height produces a band trending SW-NE where the mean height of the topography is over 70 m. This pattern appears to have been produced by the general trend in the changing elevation of the topography on a scale larger than that of the subglacial bedforms, despite the fact that the choice of window was below the size of these elongate landforms.

Another amplitude parameter that was analysed using these 3D plots was the range, and the results of this are shown in Figure.14b.

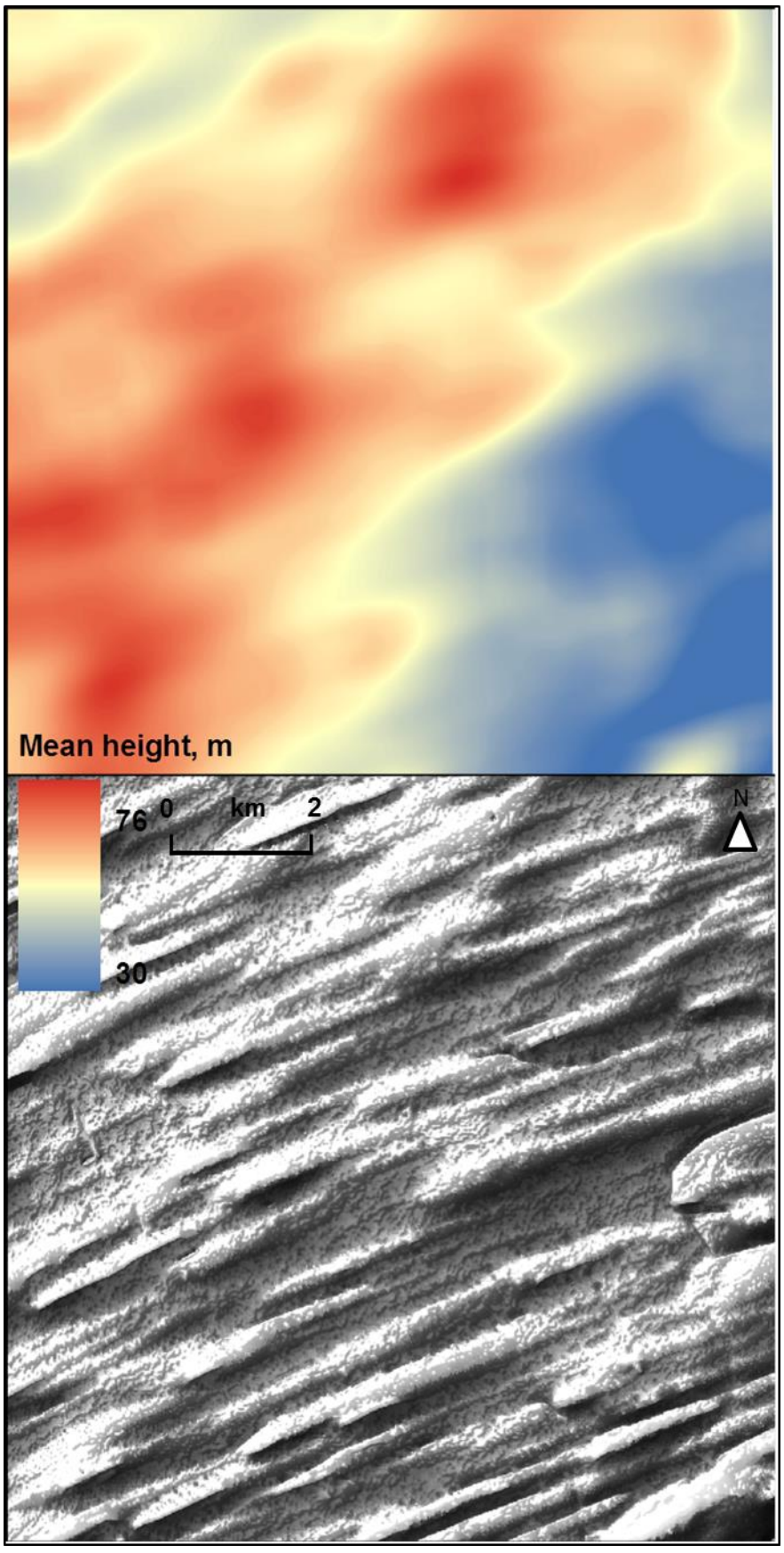

Figure 5.14a: 3D mean height roughness parameter results for the River Tweed study area, analysed using 400 × 400 m windows. The image below shows shaded relief of the topography based on the NextMap bed elevation measurements

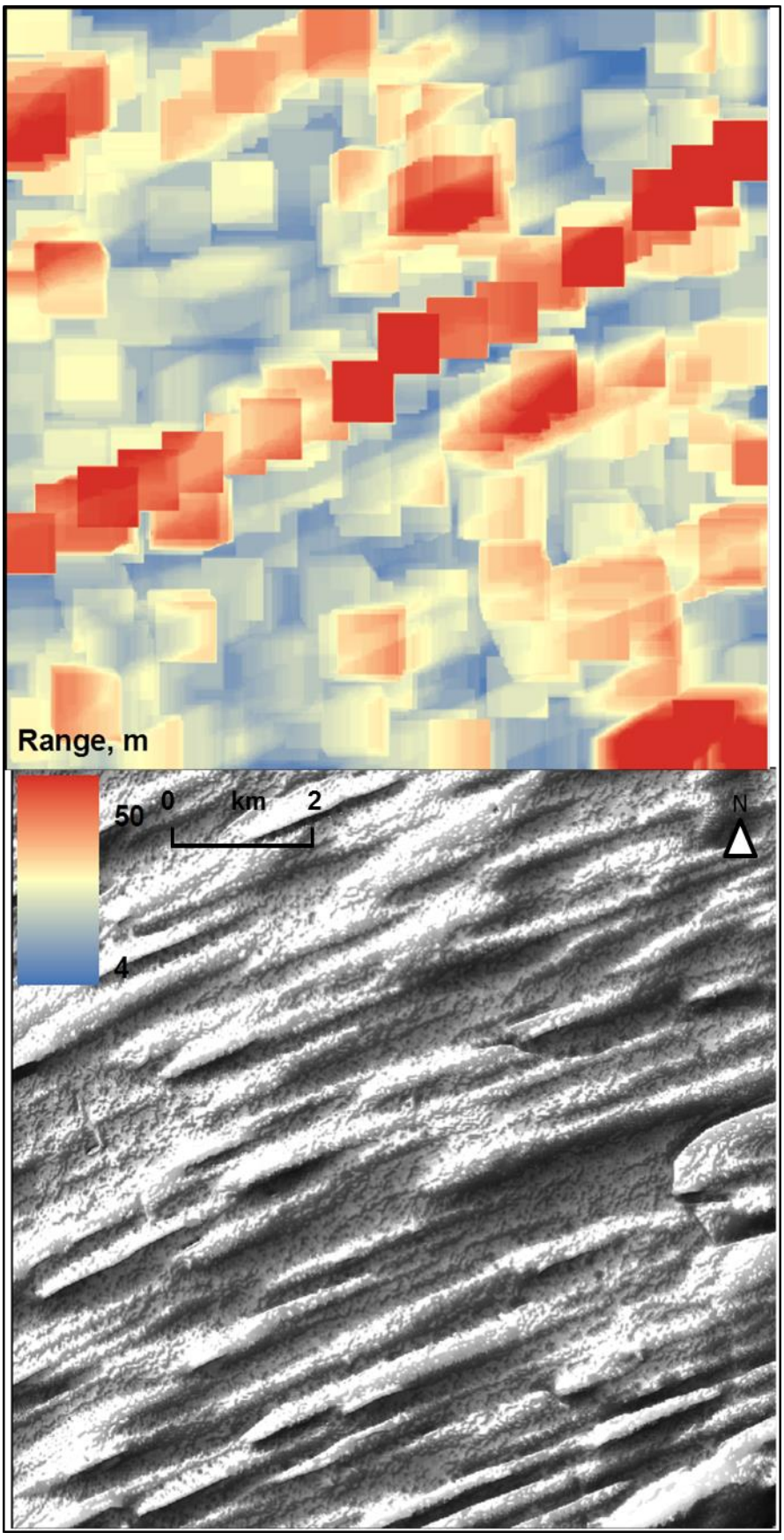

Figure 5.14b: Roughness results of the 3D Range parameter

The range results show a different pattern to those of the mean height. Rather than a transition of decreasing values from the NW to the SE, there is a central band of higher

values spanning from the SW to the NE. Viewing the actual bed topography, this strip of high values does not directly correspond to certain subglacial features, despite the fact that the orientation of the pattern in results is similar to that of the bedforms. Nevertheless, in some parts of this region the results do match features that are visible on the DEM image: for example, in the bottom-right corner of the study site, high range results of over 50 m correspond with a large feature.

A dramatic difference in the results of the mean height and the range parameters is that those of the former appear as large pixels with the same dimensions as the chosen grid, while those of the mean height have a smooth appearance. Across the Tweed study area, a strip of high range values can be seen trending from left to right across the centre of the image.

The reason for the pixelated patterns of the range parameter is that these results are based on just two observations, namely, the highest amplitude and the lowest amplitude. Therefore, while the results of the mean height were based on thousands of points for each grid, those of the range only use two, making them highly sensitive to changes in these extreme values. Consider this scenario: if a grid is situated over an area where there is a large difference in height, such as an area characterised with a deep valley and a high peak, then this will produce a high range. However, over a relatively short distance, a grid may move over an area where only the deep valley or the high peak is captured. Here, the range will abruptly decrease. In this case, although the choice of a 400 m grid is relatively small in terms of traditional studies on roughness, it has been sufficiently large to capture these dramatic changes. In theory, in a region of subglacial bedforms, that are often marked with sharp breaks of slope and steep surrounding topography (Mitchell, 1994), such sudden transitions might be expected. For example, as a grid encounters a bedform the elevation of the bed will rise rapidly over relatively short distances.

Note that this pixilation is not limited to the use of the range results. For example, as shall be seen next in a plot of the *RMS height* (Figure 5.14c), this parameter also exhibits similar artefacts. However, the likelihood of producing such a pattern is controlled by the number of observations used by a parameter to summarise the topography: the fewer the number of points used, the more sensitive the parameter to abrupt changes. For parameters that use a sub-set of the data, another factor that will affect the likelihood of generating these pixelated artefacts is the choice of grid size. As the size of grid increases, there is a higher likelihood that there will be extremes in values within a given sample area.

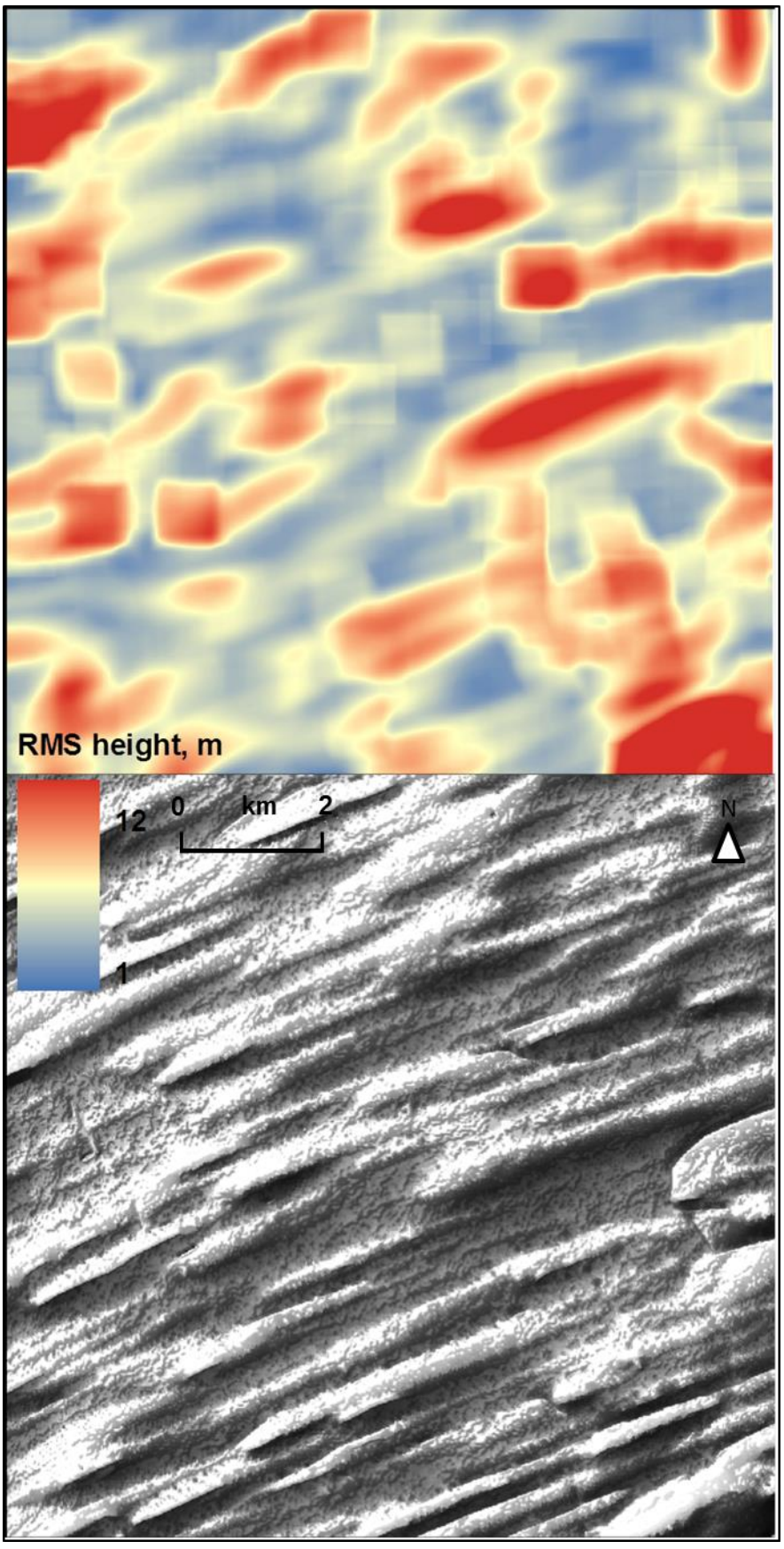

Figure 5.14c: 3D RMS height roughness results for the Tweed study site

With the *RMS height* parameter, as can be seen from Figure 5.14c, there is a more apparent association between the roughness values and the form of the topography. Here, values over 10 m correspond with the distribution of elongate bedforms. Therefore,

relative to the mean height, this parameter appears more sensitive to smaller scale changes in roughness: whereas the mean height appeared to capture the general trend in bed elevation across the area, the results of the RMS height have more sensitivity to smaller-scale variations. One explanation for this is that the results of the RMS height are measured from a datum for each grid. Given that this datum is the average height of topography within the grid it effectively filters out larger scale variations.

Although the patterns in the RMS height clearly match the locations of some bedforms, producing higher parameter results in these areas, there is not a perfect correspondence between the roughness and these features. Comparing the plots visually, the areas where the parameter results most correspond with the spatial pattern of bedforms are where these features are largest. Smaller subglacial bedforms, such as those in the SW of the image appear to have been less influential on results. With the mean height the reason that bedforms appeared due to a moderating effect in the distribution of points within each grid. However, given that the RMS height uses absolute values, no such moderating effect can occur, so this does not explain why some subglacial bedforms cannot be identified in the roughness results. Therefore, the more likely cause is that some bedforms can be detected but not others can be attributed to the effects of scale: over a given distance, the topography of the larger features varies more rapidly, so these produce a stronger signal. This suggests that the choice of grid may be important in determining the scale of roughness detected. Again, despite the choice of grid being smaller than the majority of the bedforms, particularly in terms of their long-axes lengths, not all strongly appear on the results.

Another explanation as to why the results of the RMS height have a stronger agreement with the patterns of the landforms is the use of absolute values. The parallel alignment of bedforms in this region of the Tweed means that, not only do the ridges of these features produce a pattern, but so too do the intervening valleys. Given that the parameter does not distinguish between peaks and valleys, it is sensitive to the directional trends of both of these.

Thus far we have analysed spatial patterns in amplitude parameters. The same approach was used to assess the *skewness* shape parameter, with the results for the Tweed study site being shown in Figure 5.14d.

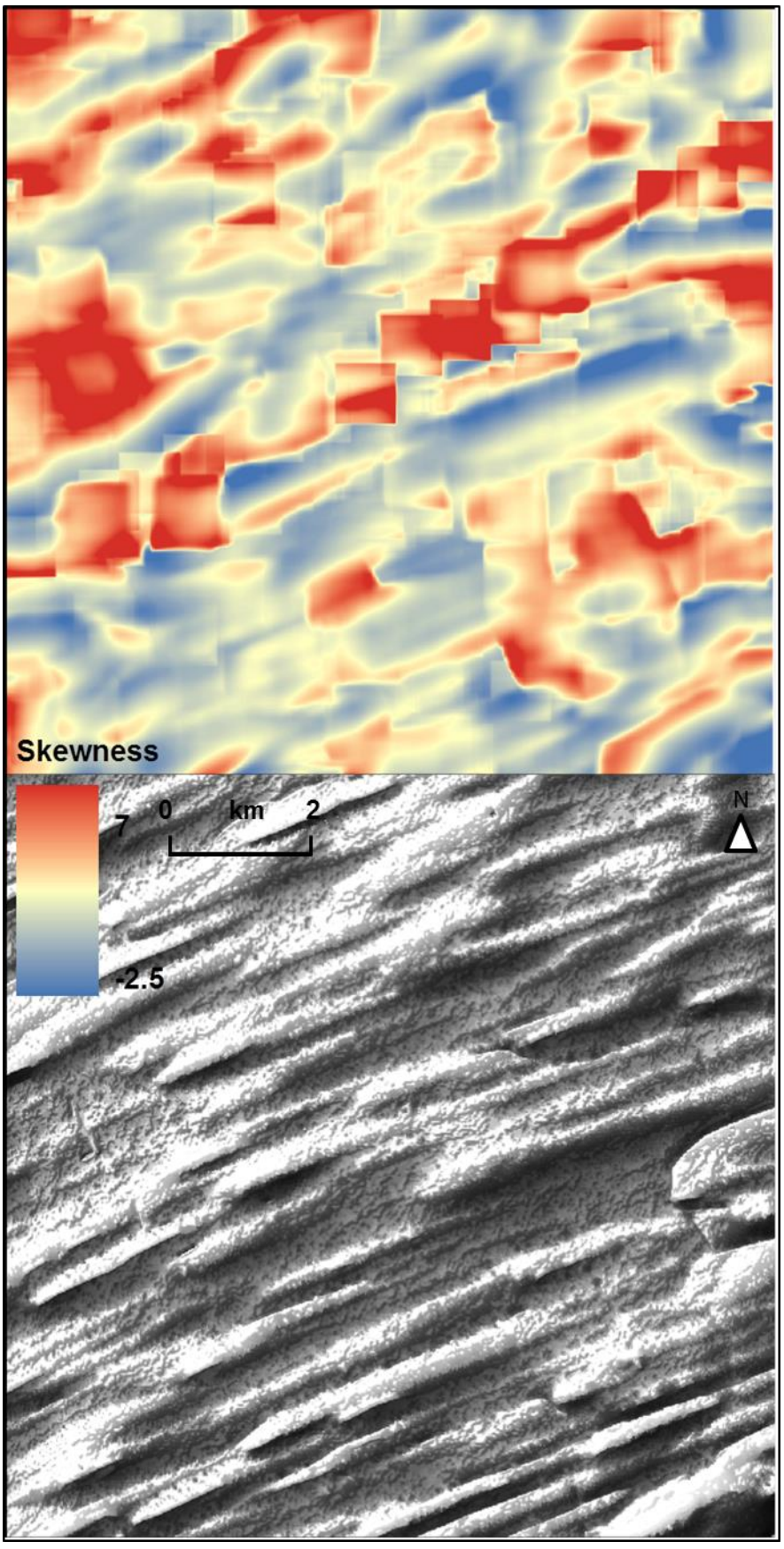

Figure 5.14d: Results of the 3D skewness parameter

Whereas the RMS height amplitude parameter does not distinguish between peaks and valleys, these formations are detected by the skewness parameter because they influence the distribution of points within each grid. From the plot of results it can be seen that there

is a pattern in the skewness results that corresponds with the alignment of the subglacial bedforms. Comparison of the bed image with the skewness results suggests that positive skewness corresponds with the location of elongate features. It appears that grids containing bedforms have a larger distribution of high-amplitude values, causing this weighting. The intervening areas between these ridges have a lower or negative skewness.

As with the other parameters, the pattern in roughness results does not show complete agreement with the bedform distribution. Interestingly, however, whereas the amplitude parameters showed the strongest correspondence with large features, with the skewness results it can be seen that the smaller features show the closest match with the results. The explanation for this is that, if a grid contains a large features, the height of the topography is relatively similar within that grid. As such, the distribution is more symmetrical, so the skewness is closer to zero. However, if a grid contains a smaller bedform, there will be more variation in the distribution of bed elevation values, thus producing a greater (positive or negative) skewness. Importantly, this shows that even at the same choice of grid, the sensitivity of different parameters varies. In terms of their ability to detect changes in roughness caused by small-scale bedforms, in this instance the skewness parameter appears to be the most sensitive.

Given that the parameter measures the distribution of points, it is sensitive to sudden changes in topography. Therefore, like the range parameter, a pixelated appearance may be produced. In fact, the results of the skewness parameter show some agreement with those of the range parameter, with one example being around the NW area of the study site. In this top left area of the image, many of the grids appear to contain both high-amplitude and low-amplitude elevations. (This is confirmed by the high range values in this region, and demonstrates the usefulness of using different types of parameters.) Yet, it the proportion of the high-amplitude values in these grids is greater than that of the low-amplitude, thus producing a positively skewed distribution.

Although the skewness parameter uses all values within a window, because it is a measure of the distribution of points it may be more sensitive to anomalous values. Potentially, a single anomalous value within a grid would produce a sharp increase in the absolute skewness. Something of this effect may explain the pattern in results across the central area of the study site, where it can be seen that there is a strip of high skewness values that do not directly correspond to the subglacial features. In this band, the typical elevation of the bed appears to be relatively high but, the grids must also contain at least one observation with substantially lower amplitude. As a result, this has produced a distribution that is highly skewed.

Another shape parameter that summarises the distribution of points is the kurtosis parameter. The 3D results for this measure of roughness are shown in Figure 5.14e.

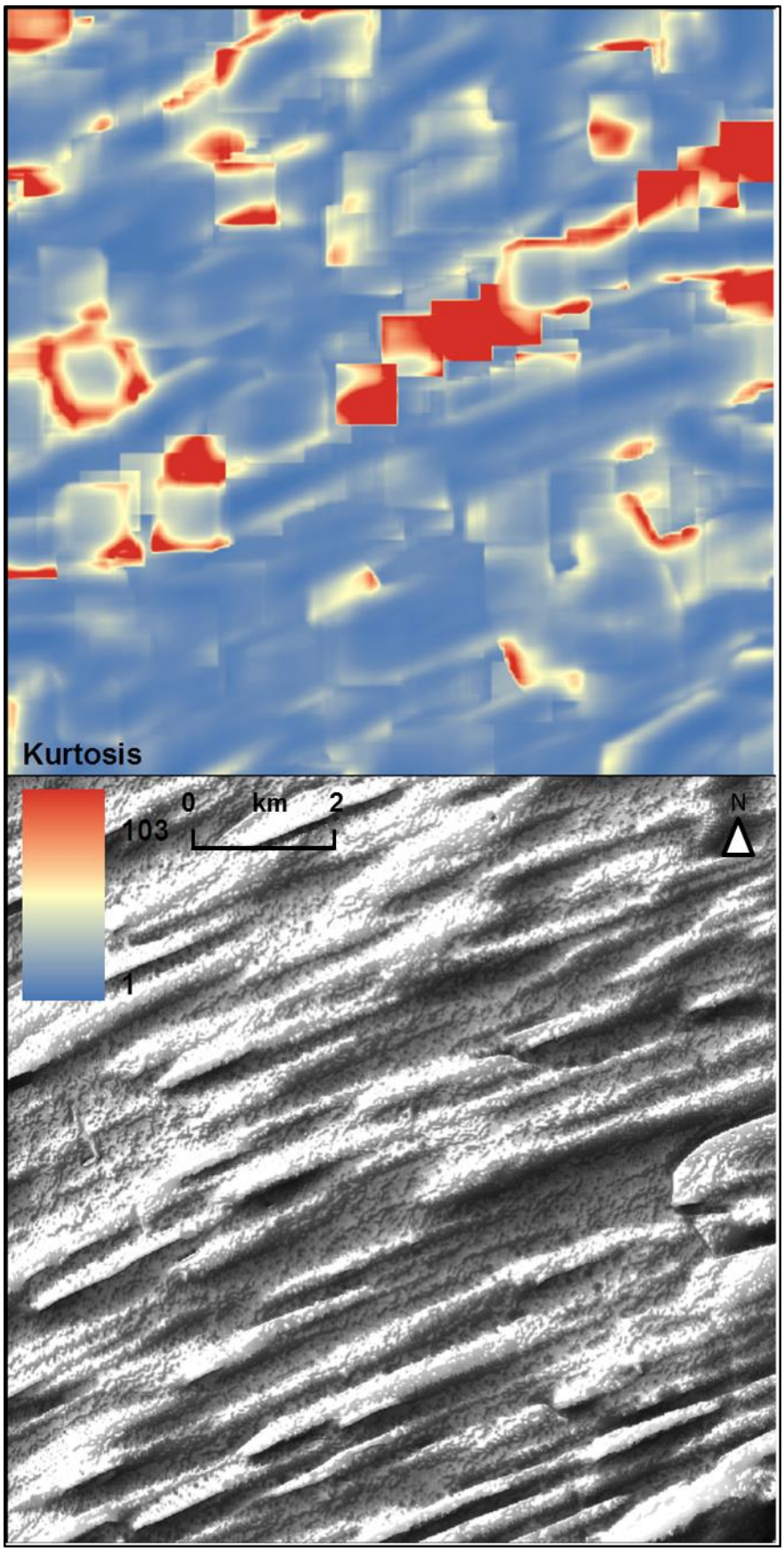

Figure 5.14e: Analysis of the River Tweed subglacial bed using the kurtosis roughness parameter

K*urtosis* another method of measuring the distribution of observations but the results of this parameter for the Tweed site vary dramatically from those of the skewness parameter. The majority of the study site has a kurtosis value around 1, indicating that there is something of a positive skewness across the entire site. The possible reason for this is the dominance of subglacial bedforms in this region analysed. As such, it is likely that many of the grids would contain at least one bedform, which may have resulted in the there being a slightly higher distribution of high-amplitude values.

For a number of grids the kurtosis results are considerably higher, showing that the distribution of points is strongly skewed to the right. The locations of these grids correspond to areas where the range and skewness parameters also produced higher results. Therefore, it is likely that all the influence on all three parameters is the same. As explained above, one possibility attributed to the higher values is that grids in this area contain mostly high-amplitude values, with the large subglacial bedforms being a potential source of these heights, but also a smaller number of low-amplitude values, possibly from the grid being situated over a valley. As a result, there is a strong range in height within the grid, but the distribution of these is skewed towards the higher elevations.

The kurtosis results also show a smaller-scale pattern, with higher values being associated with the SW sides of the subglacial bedforms. Given that an easterly flow direction of ice has been inferred in this region (Evans *et al*., 2005; Everest *et al*., 2005; Staines, 2009), and that bedforms are generally steeper on higher on the stoss side to ice flow (Stokes & Clark, 2002), it follows that the SW sides of these bedforms will have sharper breaks of slope. Therefore, over a given distance, the bed elevation at these stoss sides will change more rapidly, and this may result in a skewed distribution, thus explaining the higher kurtosis values.

As with the 2D parameters, there were a number of artefacts that were present in all of the results, irrespective of the choice of parameter. One such example is the number of observations within each grid. With profile data it was seen how the *number of points* in each window diminishes towards the ends of the profiles (Section 5.3.1). Similarly, with 3D analysis, fewer points are included when roughness is measured at the edges of the study area. This is illustrated by Figure 5.15 which shows how, at the edges of the study area the mesh extends beyond the region of bed elevation measurements. In analysis of the NextMap data, grids in the centre of the study area each had 6241 points because there were no pixels with missing values. At the edges and corners the number of points decreases to a minimum of 1600.

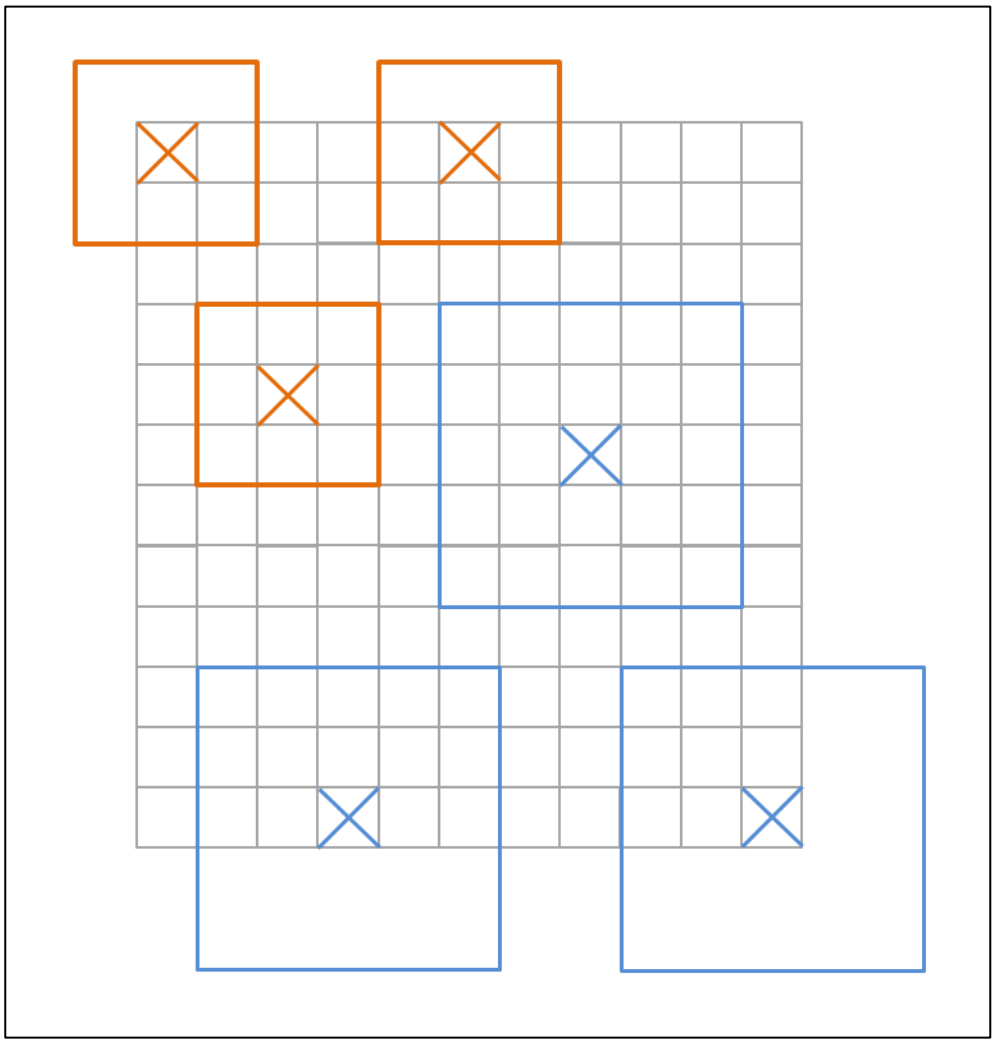

Figure 5.15: Illustration of how the use of a mesh, centred on each pixel value, causes missing values at the edges and corners of the study area. As with the use of windows in 2D analysis, as the size of grid increases, the number of points omitted increases. For example, with the 3×3 grid (shown in orange) analysis at the edges results in 3 missing observations; with a 5×5 grid, there are 10 missing observations when edges are measured. The fewest number of points used occurs at the corners

Finally, as a general note on the feasibility of using quantifying roughness in 3D, all of the parameters programmed into the software worked successfully with the DEM data. Therefore, it can be confirmed that palaeo records of bed elevation are compatible. However, it must be highlighted that if the measurements had not been uniformly spaced, the program would not have run to completion. Therefore, in the format used, all of the parameters have the same disadvantage as the 2D method of using spectral analysis reviewed in Chapter 3. Nevertheless, the need for uniform spacing was a requirement of the programming, and is not tied directly to the parameters; considerably more processing power would have been required to quantify roughness in 3D using data that was not uniformly spaced. Therefore, with further development of the program, this challenge could be overcome.

5.5 Discussion

5.5.1 A critique of alternative methods for quantifying roughness

5.5.1.1 Efficiency

In Chapter 4 it was shown how one of the problems with spectral analysis was the user-intensive steps needed to process the data and produce roughness results. In contrast, the alternative methods presented in this chapter allowed results to be calculated more efficiently. The two programs developed allow reliable results to be produced between datasets by ensuring the steps used to calculate roughness are consistent.

5.5.1.2 User-controlled variables

As with spectral analysis, user options can be used to adjust the way results are calculated such as the scale of roughness studied. Here, the high degree of automation in the software allowed variables such as window size to be readily adjusted. For example, analysis of RES data used windows tens of kilometres long, but those of the synthetic profile were just 2 km. To modify the window lengths in this way using the traditional method of Excel and OriginPro for spectral analysis (see Section 3.3.3), extensive modification would have been required. Furthermore, this chapter has demonstrated that many roughness parameters have fewer restrictions on the choice of window length compared to those imposed by the spectral analysis requirement of 2^N data points (Section 3.1). However, like spectral analysis, user decisions are important because they influence results. This point can be illustrated by discussing the role of window length in allowing spatial patterns to be detected.

For several synthetic profiles, the results showed a smoothing where the broad trend was detected but localised fluctuations, especially in height, were less apparent. Window size also affects the ability to detect areas where there are distinct changes in topography, such as the different zones in Profiles A or E. With these profiles, many of the parameters detected the boundaries, but the roughness results transitioned more gradually than the sharp boundaries observable in the bed elevation measurements. As window length increases, the transitions are detected earlier along profile, so the change in topography appears more gradual. More research is required to determine what lengths of window would be the optimum choice.

5.5.1.3 Interpretation of the results

The simplicity of many of the methods in summarising a single variable is a strength because variations in topography can be more clearly understood: a rising number of peaks clearly shows that the number of perturbations has increased. Contrast this with spectral analysis results where it is difficult to explain what has produced the difference in results for this parameter.

Analysis of the synthetic profiles highlighted a difficulty in interpreting results that other factors can influence a parameter, even when it is not necessarily designed to summarise these variations. An example of this was seen in Profile C where the variation in asperity frequency affected the amplitude parameter results, despite the overall vertical size of asperities being constant. The reason for this appears to be that the wavelength influenced the distribution of measurements within each window. With all the parameters based on local datums, larger wavelength features meant that some windows had local highs, and others local lows so there was more fluctuation. At shorter wavelengths, the distribution of results meant that higher absolute bed elevations were cancelled out by lower values.

The influence of other variables on parameter results has both advantages and disadvantages. For example, the role of wavelength on amplitude parameters means that they might be used to estimate the size of asperities. However, the fact that the same values can be produced by different topographies makes interpretations based on a single parameter more uncertain. For instance, if only amplitude parameters were used, it would not be possible to determine whether differences in results were produced by variations in profile height, the wavelength of asperities, or a combination of both. Furthermore, the relative dominance of different types of topographic variation on the results appears to differ, as can be demonstrated by comparing the amplitude parameter values for Profiles B, C, and D. With Profile B the parameter results increased as amplitude increased, but in Profile C amplitude also increased with wavelength. In Profile D, the increasing amplitude parameter results along profile are likely to be a combined effect of both higher asperity heights but also their longer wavelengths.

5.5.1.4 The feasibility of using alternative parameters to quantify subglacial bed roughness

The fact that 2D parameters functioned with radio-echo sounding measurements demonstrates that the roughness parameters evaluated in this chapter can be used with subglacial bed data. Moreover, unlike spectral analysis it was not necessary to process the data to detrend the profile or remove gaps, which might increase the number of suitable datasets that could be used. The inclusion of the *number of points* parameter provided a means of identifying gaps because these cause a decrease in the number of observations per window. Therefore, it is possible to identify areas where the results may be less reliable.

With 3D parameters, a uniform spacing is required, and if a single pixel had a missing value analysis of an area would not be completed by the program. As described in Section 2.5.2.3, there are relatively few DEMs available in contemporary ice sheet settings that have both a high resolution and large spatial coverage. Combining this with the fact that

uniform observations are required means that there are few suitable datasets. Nevertheless, this chapter has demonstrated how formerly glaciated areas can be used as sources of data. The Tweed valley study site covered an area of 25 km^2 at a resolution of 5 m. Despite the size of the area, and its high resolution, there were no missing observations. Although measurements of bed elevation may be incomplete in other areas of the UK, this chapter demonstrates the potential of using NextMap data. This suggests similar, high resolution datasets of formerly glaciated areas (see Section 2.5.3) may also be suitable.

5.5.1.5 A comparison with spectral analysis

In Chapter 3, given the dominance of spectral analysis, a detailed critique of this method was necessary. That chapter also investigated the importance of quantifying roughness at different scales, addressing the fact that the majority of conclusions on the relationship between roughness and ice speed have been based on analysis over scales of tens of kilometres. As such, the role of window and sampling length were compared. In contrast, the purpose of this chapter was not to investigate issues of scale and data choice, but to specifically evaluate the feasibility of using other methods of quantifying roughness. Given that these parameters have never been used to analyse subglacial bed topography, the focus here was to determine the types of information that each parameter might provide.

The result of the differing objectives between Chapters 3 and 5 means that it is not possible to directly compare spectral analysis with the alternative methods. Nevertheless, when focusing on the practical aspects of employing the different techniques for quantifying roughness, some similarities and differences between spectral analysis and these alternative parameters can be drawn.

It is apparent that there are some similarities between the roughness parameters and spectral analysis, with one example being the effect of window length. A use of Profile A was to test the parameters' ability to detect zones of transition between areas with distinct differences in topography. Although most of these measures showed distinct values between the flat topography and central area of asperities, the results consistently showed that the boundaries between these different zones appeared less distinct on the plots of roughness than on those of bed elevation. Therefore, as with spectral analysis, the other parameters were affected by the choice of window. In testing it was also shown that the ability to detect smaller-scale spatial patterns in the topography depended on the relative size of the window compared to that of the features.

Despite some similarities between the operation of spectral analysis and the alternative methods of quantifying roughness, this project also identified some distinguishing features. One practical aspect is the relative flexibility in user-controlled options of the

other parameters versus those strictly imposed by the version of spectral analysis traditionally used. In this project, the choice of window length could be readily adjusted, so that the parameters could be used to analyse data with a range of resolutions, and measure roughness at a range of spatial scales. Had the data exhibited gaps, no processing of the data would have been required before it could be analysed. In contrast, as shown in Chapter 3, spectral analysis has typically been limited to analysis over 32 point windows (Taylor *et al*., 2004), and sometimes considerable processing of the data is first required before roughness can be quantified.

5.5.2 The most suitable parameters for analysing subglacial bed roughness

When used for their intended purpose, all of the parameters functioned as expected. The parameters that best described a particular variable (such as height, or number of asperities) were those were designed to capture that characteristic. For example, in Profile B where the height of peaks and valleys was the variable, the spatial pattern in the size of asperities was best detected by the amplitude parameters. From analysis of synthetic profiles, however, it was shown how some parameters were better able to capture variations in topography than others. For example, compared with other amplitude parameters, the changes in height along Profile B were less apparent from the *mean height* values. Nevertheless, none of the parameters had no usefulness that would suggest they needed to be eliminated. In the case of the *mean height*, this was one of the few amplitude methods that detected the different zones in Profile E.

Interestingly (as described in Chapter 5), the *mean height* appears as one of the most commonly used measures of roughness in other sciences but, for analysis of the synthetic profiles, this parameter did not stand out as being better than the other methods. This suggests that the methods most dominant in other sciences might not be the best for glaciologists.

The choice of roughness parameters is likely to be controlled by the nature of the investigation, rather than an elimination of certain methods. For example, analysis of Profile E demonstrated the potential for the *skewness* parameter to detect features. For investigating fluted topography, this method might indicate whether flutes are developed on the landscape as bumps, or whether they are higher ridges where intervening sediment has been removed. Alternatively, if scientists were interested in measuring variations in roughness due to differences in bedform size, then amplitude parameters might be needed to give vertical height, and spacing parameters to capture the horizontal size of asperities.

Certain parameters may hold advantages for certain types of investigation because the variables that they measure may be of more interest or relevance. At this stage it is not

possible to conclude which parameters will be the most useful for these different types of study. However, one might argue that it is not necessary to attempt to place these various methods in a table of *best* to *worst*, especially since this is likely to be highly situational and potentially subjective. For example, some scientists may favour the use of the methods of quantifying roughness tested in this chapter over the use of spectral analysis, because the former require less processing of the bed elevation data. Yet, the fact that spectral analysis has become the dominant method of summarising subglacial bed roughness demonstrates its usefulness in this field. This project makes no claim that one parameter is superior to another. Instead, the *alternative* methods of quantifying roughness might be thought of as *additional* techniques. For example, if the results of amplitude and/or spacing parameters were studied alongside those of spectral analysis, they might help explain why certain integrated roughness values have been produced. As the next chapter will show, measuring roughness using several types of parameter may have numerous advantages over the use of a single method.

5.5.2.1 Redundancies between the roughness parameters

Despite all the parameters having some utility, there are redundancies, particularly within categories of parameters. For example, the *mean deviation* and *RMS height* showed the same patterns for each of the five profiles suggesting that only one would be required. The spacing parameters also produced similar results, although here the similarity between the *number of crests* and *number of troughs* for many of the profiles is a result of the profiles having a symmetrical design. In profiles such as E, where the topography switches from an area of deep valleys to one of high peaks, the two parameters were useful in distinguishing the different areas. With the *percentage of crests* and *percentage of valleys*, the information they provided was essentially the same as that of the *number* of asperity parameters. The choice of parameter here is one of taste. The *number of crests/troughs* parameters give values that can be more easily visualised: e.g. *there are three crests in this window* might be preferable as a description to *0.8% of the observations are crests*. However, the percentage values would be a useful means of standardising results when different window lengths are used.

5.5.2.2 Reviewing more methods of quantifying roughness

Rather than decreasing the number of parameters used, more methods should perhaps be included. For example, the spacing parameters are only proxies for wavelength, which is assumed to decrease as frequency increases but is not always the case. Other measures of roughness could be added that measure the horizontal size of these features, e.g. from crest-to-crest, or at a given point such as the distance between the point where the rising limb of an asperity passes through a local datum and where the falling limb transects the datum. Some parameters could be used to generate other

results. For example, comparing the amplitude parameters that measure *above* the local mean with those that measure *below* would be an alternative measure of skewness. The ability to use software to quantify roughness through a series of commands means that results can be generated efficiently. The challenge would then be to identify which of the methods are most relevant. As the next chapter will show, one way to do this would be to model ice speed using roughness parameters as predictor variables and identify which account for the most variation in ice speed.

5.5.2.3 Combining many roughness parameters

For glacial surfaces, quantifying the roughness using a single parameter appears an unsuitable approach because the many variables influencing the results create difficulties in interpreting the values (Section 5.5.1.3). These findings suggest that, instead, a suite of techniques are required. Many of the roughness parameters are complementary and, together, allow variations in roughness to be more easily explained. For example, using spacing parameters it would be possible to ascertain whether variations in amplitude parameter results were produced by changes in the height of the profile, or whether the frequency of horizontal size of asperities had played some role. This would aid interpretation of data, such as in Profile D, where both the amplitude and wavelength of asperities increased along profile. With analysis of the RES data, amplitude and spacing parameters showed that roughness increased in terms of not only the number of asperities, but also their size.

Another motivation for using multiple parameters is that interpretations may be unreliable if only a single parameter is used. For example, with Profile A it was shown how flat areas produce no results for many of the roughness parameters. Had spacing parameters been used to quantify the roughness of Profile E, it might be assumed that the topography was similar to that of the flat zones of A because, in the left-hand side, the plateaued sections of topography were not counted as peaks. In nature, flat topography is produced on scales ranging from mountain plateaus to rock surfaces fractured along bedding planes. If these features were measured using parameters that use only crests and troughs, it is possible that some parameters might over-estimate or under-estimate the size or number of asperities, or even produce no results if the area remained flat for the entire window length. By applying other roughness parameters, which are not affected by missing observations, some checks can be made.

5.6 Conclusions

All of the 2D and 3D parameters can be used to quantify the roughness of subglacial beds. The use of two Stata programs facilitates efficient analysis of bed elevation measurements. The advantage of this group of roughness parameters is that each measures a specific variable in the topography, which can be related to theories on basal

ice flow: for example, some methods summarise the vertical size of peaks, while others measure the frequency of perturbation. However, the use of parameters individually makes interpretation of the results difficult because, although only summarising one variable, the statistics are affected by other types of topographic variation. A more suitable approach appears to be using a set of parameters that measure a range of different variables.

CHAPTER 6

Investigating the relationship between roughness and ice speed, Siple Coast, Antarctica

6.1 Introduction

This chapter demonstrates the potential of using 2D roughness parameters, reviewed in Chapter 6, for investigating relationships between ice dynamics and bed topography. Specifically, it investigates how roughness varies along and across ice streams on the Siple Coast, West Antarctica, and tests whether spatial patterns in ice speed correspond with those of roughness.

On a theoretical level, models indicate that the form of the ice-sheet bed will affect friction and, therefore, the speed and direction of ice flow (see Joughin *et al*. 1998; Schoof, 2002). These hypotheses are gaining acceptance through field research findings, with a growing body of literature to support the relationship between speed and roughness. In particular, results from analysis of SPRI RES profiles show a link between decreasing roughness and faster ice speeds (e.g. Rippin *et al*., 2004; Bingham & Siegert, 2009). However, these findings are all based on spectral analysis of bed elevation data. As Chapter 4 showed, this method captures several variables, so it is difficult to identify what changes in topography are most responsible for the spatial pattern in roughness, i.e. are variations in topography due to the size or frequency of asperities?

The previous two chapters have demonstrated how other methods of quantifying roughness are often designed to measure a single variable. Testing whether these methods show a change that corresponds with variations in ice speed would allow the effects of different types of topography to be established. For example, the relative importance of asperity height versus the number of perturbations could be tested. The objective of this chapter was to determine which roughness variables were most associated with ice speed, and measure the strength of this relationship.

Due to their importance for ice sheet dynamics (Bamber *et* al., 2000; Bennett, 2003), regions of ice streaming were of particular interest. Another motivation for this choice is that ice streams have significantly faster ice speeds than surrounding ice, thus producing clear spatial patterns. As described in Section 6.2, the first stage was to compare spatial patterns between roughness and ice speed using two profiles. This chapter also used Generalised Linear Models (GLMs) to assess the relationship between ice speed and roughness. The previous chapter had suggested that groups of parameters could be used

to measure the roughness of topography, and GLMs allowed such an approach to be taken. Furthermore, through modelling it was possible to quantify the relationship between roughness and ice speed, for the first time also measuring the strength of the relationship.

6.2 Background and methods

Before investigating the relationship between roughness and ice speed in the Siple Coast region, it was important to consider the setting of these ice streams in terms of their thermal regime and composition of the bed because, as Section 2.2 showed, these affect driving and resistive forces to ice flow.

In the Siple Coast region the ice streams have typical lengths of 300 to 500 kilometres, and widths of approximately 40 km. A common feature is the presence of crevasses along the lateral margins of these ice streams, which are formed due to extensional shear of the ice. From these crevasses it is possible to identify the approximate dimensions of these fast flowing regions, and this facilitates the study of determining controls on their location.

An interesting feature of the ice streams in this region is that they have relatively low ice surface slopes (Bennett, 2007). As Section 2.2.1 described, the gradient of slope is an important driver of ice flow because it affects the amount of shear stress. Therefore, in this region, the occurrence of fast speeds appears due to some locations having less resistance to flow than others. The two controls that appear most dominant in providing areas of streaming with this low resistance are the warm-based thermal regime and, the rheological composition of the subglacial bed (Bindschadler *et al*., 1996). Several studies have identified that the location of ice streams corresponds to areas of saturated subglacial sediments (Alley, 1998), which support sediment deformation (Blankenship *et al*., 1987; 2001). Sergienko & Hulbe (2011) present evidence for subglacial lakes beneath some areas of fast flow. As a result, it is thought that much of ice flow at the subglacial bed occurs as a result of deformation of the substrate rather than sliding (Alley, 1998). In Chapter 2 it was also discussed how ice flow generates heat through friction, which in turn lowers the resistance to flow. Given their ice thicknesses of over 1 km, coupled with the role of frictional heating, the beds of the Siple Coast ice streams are at pressure melting point (Bentley *et al*., 1998). Yet, an additional source of heating is through geothermal activity that further increases the amount of basal meltwater (Blankenship *et al*., 1993). In contrast, Harrison *et al*. (1998) reports that non-streaming areas of ice in this region are cold-based, with the ice sheet frozen to its bed. Thus, a strong link between the thermal regime and the speed of flow can be observed.

The importance of rheology and the thermal regime suggest that roughness is unlikely to be a direct control on roughness in these areas. This theory is supported by the fact that Ice Stream C has shown evidence of switching off around 150 years ago (Retzlaff &

Bentley, 1993; also recall Section 2.5.1.2). Analysis by Siegert *et al*. (2004) showed that the bed of this ice stream had low spectral analysis values; if roughness were the sole control, relatively fast flow would be predicted. The ice streams of the Siple Coast region are viewed as the only contemporary examples of *pure* ice streams rather than topographically controlled (Bennett, 2003). Thus, by definition these areas of fast flow are not confined to large-scale depressions (Stokes, 2001). As a result the shape of the subglacial bed, at least at the scale of tens of kilometres, does not appear to be the primary influence on ice speed.

Although roughness is likely to be only a secondary control on the speed of the Siple Coast ice streams, there are still uncertainties as to how important it is. Even the strength of the relationship between roughness and ice speed has not been fully explored: for example, given the dominance of spectral analysis, it has not been determined how different variables such as the amplitude of the bed or the frequency of asperities relate to ice speed.

A further contradiction to the suggestion that speed is somewhat independent of topography is the fact that other studies have identified spatial patterns between roughness and ice speed. For example, Siegert *et al*. (2004) identified that roughness in the downstream direction along ice streams corresponded with increasing ice speed. These results show that, although not a first order control, roughness is still linked to the behaviour and location of these areas. Another specific area where roughness may be important is the onset zone that marks the inland position where streaming speeds begin. Some ice stream onsets have been found to be associated with topographic steps (Bindschadler *et al*., 1996) and topographic lows (Shabtaie *et al*., 1997). Although the ice streams of the Siple Coast do not show evidence of such transitions in topography (Retzlaff & Bentley, 1993), they demonstrate how roughness may be important in determining ice stream locations.

There is also anecdotal evidence to support that the roughness of topography is associated with the location of ice streams. For example, the subglacial lakes described above were found to correspond with troughs on the bed (Sergienko & Hulbe, 2011). This again highlights that measurements of roughness may show a relationship with ice speed by acting as proxies in capturing other controls. Furthermore, as explored in Section 2.5.1.3, roughness may be related to ice speed but be a product of variations in ice flow that have formed a spatially variable topography. In the soft marine sediments of the Siple Coast, where deformation is favourable, there is a likely feedback between basal ice flow and the sculpting of topography.

6.2.1 Methods

6.2.1.1 Examining the association between roughness and ice speed

Two specific ice stream locations were used to test the relationship between ice speed and roughness. The first area was across the lateral margin of an ice stream, where a distinct change in roughness was expected to correspond to the abrupt increase in speed. In addition, the changing speed and roughness along an ice stream were compared.

Data on ice-speed were sourced from the *MEaSUREs InSAR-based Antarctic Velocity Map* (Rignot *et al*., 2011a, 2011b), which consisted of a DEM with a resolution of 900 m. A point to note with these measurements of ice speed is that they refer to the rate of flow at the ice surface, and some of this motion may be due to internal deformation. Nevertheless, studies suggest that basal ice flow constitutes the major component of motion (Cohen *et al*., 2000) and, from a practical standpoint, this dataset was the only one available with the necessary coverage and resolution.

Other studies had used these velocity measurements by plotting them in a DEM layer, allowing spatial patterns in ice speed to be viewed (Joughin *et al*., 1999, 2002; Joughin, 2006; Rignot & Kanagaratnam, 2006). A similar approach was taken in this project and, as can be seen from the bright portions of Figure 6.1, the ice streams in this region of the Siple Coast can clearly be distinguished from the slower-flowing surrounding ice. In this chapter, it was these areas of fast flow that were of interest in investigating patterns of roughness.

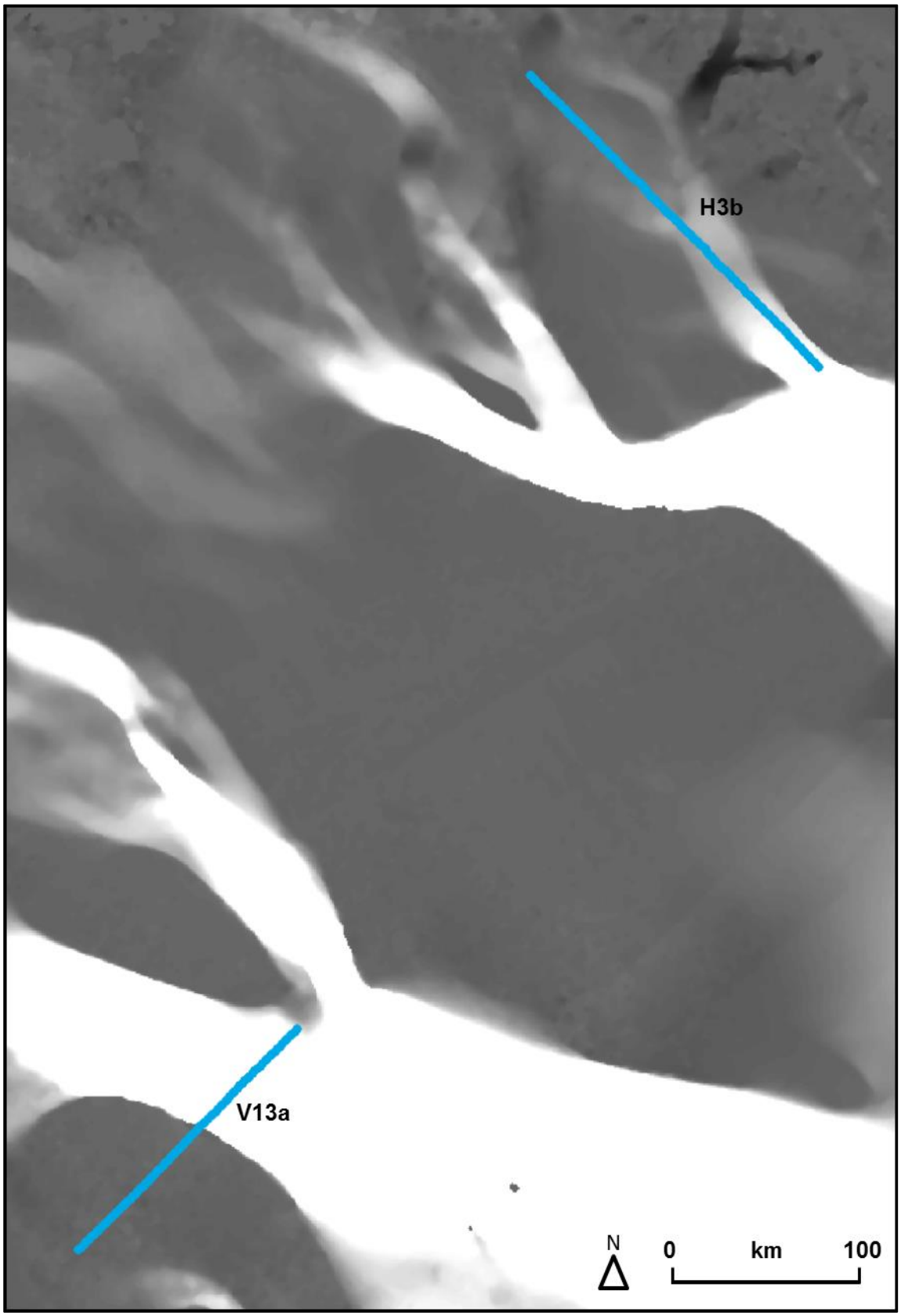

Figure 6.1: Location map of the two profiles analysed. The image is orientated N-S vertically, with north to the top. The locations of ice streaming are shown by the shaded basemap of MEaSURE inSAR speed measurements. Ice speed increases with brightness, with the white areas represent ice speeds of over 200 m/a.

The SPRI radio-echo sounding records of the Siple Coast were used as a source of information on ice-sheet bed topography. The resolution of this dataset was consistent with that used in previous roughness studies (such as Taylor *et al*., 2004), with a sampling interval of approximately 2 km between points. Data were plotted into ArcMap in their raw format, so that profiles of interest could be selected. Most of the profiles had a north-south or west-east orientation and, given that the current direction of ice flow in this region is approximately to the south, the alignment of profiles was therefore, either parallel or perpendicular to ice flow.

For testing the effect of profile orientation on results, two profiles were used with their locations shown in Figure 6.1. The 228 km long Profile H3b was located in an upstream area of Whillans Ice Stream (Ice Stream B), and had an alignment parallel to ice flow. Profile V13a was a 173 km section oriented approximately at right angles to flow across the SW lateral margin of MacAyeal Ice Stream (Ice Stream E). To link these observations with bed elevation measurements, ice speeds were extracted from the DEM via the Hawth's Tools extension of ESRI ArcGIS. Using the Stata program for quantifying roughness in 2D, roughness results were generated for each profile. A 50 km long moving window of uniform weighting was chosen because this increased the likelihood that each sample length would have at least 20 observations, and gave similar sampling lengths as earlier studies (Rippin *et al*., 2004; Taylor *et al*., 2004).

As Section 2.3 described, the possible relationship between roughness and ice speed depending on whether the shape of topography varies orthogonally or parallel to ice flow. For example, topographic bumps aligned transverse to ice flow may behave as resistant steps (Stokes *et al*., 2007), whereas differences in topography aligned parallel to flow could potentially have a channelling effect (Hindmarsh, 2001). Therefore, by assessing the relationship between roughness and ice speed using profiles with different orientations, it was possible to account for some of these different linkages.

6.2.1 Modelling ice-speed

In many sciences, models are used as a method of determining the strength of relationship between variables. In some cases, a model may be used to identify what variables control a certain response (McKenzie & Austin, 1993): for example, Donoghue *et al*. (2004) investigated the strength of agreement between remotely sensed imagery and the height of trees, to test whether satellite imagery could be used to detect forestry change. In the literature the terms *independent*/*predictor* and *dependent*/*response* are typically used to describe the different variables (Cox *et al*., 2008). These descriptions may imply that one set of variables, the predictors, control a response variable. Often this is the case, but it must be acknowledged that although the nomenclature alludes to this relationship, in reality models are less restrictive than this. Many approaches simply

measure the strength of the relationship between different variables, and do not determine the direction of this control. This point is important in justifying the use of models to investigate the between roughness and ice speed because, as Chapter 2 discussed, roughness may be both a response and a control of ice speed.

Using models to measure the strength of agreement between ice speed and roughness showed potential, but the first challenge was to find the most suitable method given the nature of the data. In statistics, a common method of investigating the relationship between different variables is to use multiple linear regression (Aiken & West, 1991; Weisberg, 2005). These models fit a linear prediction to a response variables based on two or more predictor variables. The goodness of fit between the values predicted by the model and those observed is used to determine the strength of the model. The *best* models are those that have the closest agreement, (smallest residual values), between the predicted and observed values. Thus, statistically summarising this strength of relationship can be used to determine what set of variables are most related to another response variable. However, one limitation of multiple linear regression is that it requires all of the response variables to have a normal distribution (Nelder & Wedderburn, 1972). With ice speed data, it can be seen that this requirement is often not met: for example, moving across the lateral margin of an ice stream rapid transitions in ice speed are a characteristic feature. A second limitation of multiple linear regression is that, by fitting a linear trend it is possible for the predicted response variable to have negative values (Lane, 2002; Cox *et al*., 2008), but such values are not theoretically plausible when considering the speed of ice flow.

The solution to the two above problems was to use a Generalised Linear Model (GLM). The distinction between this and multiple linear regression is that the former fits the response on a logarithmic scale (Cox *et al*., 2008). In the case of ice speed, this ensures that predicted values are never below 0 m a^{-1}. A second important advantage of GLMs is that, through a link function, they can transform variables (both dependent and independent) on the log scale, but then return predictions on the original scale without the need for back-transform*at*ion (Zheng & Agresti, 2000).

In this project, the relationship between roughness and ice speed was quantified using GLMs. The roughness parameters were used as the predictor variables, with ice speed being the response variable. Analysis was completed using the same RES profile, V13a, described in Section 6.2.1.1 that measures bed elevation and ice speed across the lateral margin of the MacAyeal Ice Stream. As Section 6.3 will show, ice speeds across this margin are somewhat bimodal, with the rate of flow inside the ice stream being at least 200 m a^{-1} faster than the surrounding ice.

Testing all of the possible combinations of roughness parameters would have resulted in over 260,000 possible models. Therefore, some judgement was required to shortlist those for testing. First, given the relatively short length of the profile and coarse resolution, parameters that used all of the observations were chosen, thus excluding parameters that measure just crests or troughs. In addition, summary statistics and scatterplots were used to identify any redundant parameters. For example, the correlation between the *RMS height* and *mean deviation* suggested that they captured similar information. Therefore, six predictor variables were chosen, giving 63 possible model combinations. Further shortlisting was not required because, as explained below, part of building the model was identifying which of the parameters were most relevant by testing their correlation with ice speed.

For the six predictor variables Stata was used to analyse all possible model combinations from those that only used a single predictor variable, to models that included all six roughness parameters. Summary statistics were interrogated to judge the improvements in accuracy of ice speed predictions by adding more variables. This included the calculation of the coefficient of determination, R^2 that is the square of the correlation between response and fitted values (Zheng & Agresti, 2000). As Cox *et al*. (2008) describes, there are several factors to consider when building models. The aim of this project was to produce a model that accurately predicted ice speed, but was also simple in terms of the number of predictors used.

When constructing a model the ideal predictor variables are those that measure a single characteristic. One advantage of this is that it avoids possible redundancies between variables. Many of the roughness parameters are designed to measure a particular type of topographic variation and, as Chapter 4 described, they can be classified based on their purpose. This makes these measures of roughness good candidates for model construction. In contrast, Chapter 3 showed how the spectral analysis parameter summarised several topographic variables, so would likely to have been less suitable. However, the alternative methods of quantifying roughness may still have some redundancies. For example, a group of methods are designed to summarise the amplitude of topography. Furthermore, some parameters are based on the results of others. The fact that the range is based on the highest and lowest values is a demonstration of this.

A second important factor to note is that although the model tests the relationship between the roughness parameters and ice speed, the strength of the relationship between some variables may be due to indirect effects. As discussed in Section 2.5.1.3, although roughness may directly control ice speed, it may also be a proxy for other controls on ice dynamics. As a result, any relationship between the parameters and ice speed may be due to the parameters included in the model capturing these other effects.

One solution would have been to remove any roughness parameters that are associated with other controls: for example, the mean height could be omitted because it is linked to ice thickness. Nevertheless, this project defines roughness as deviations in topography and, as discussed in Section 2.3, the topography of ice sheet beds plays an integral role in many controls on ice dynamics at a range of scales. The only way to ensure that none of these secondary effects were included in the model would be to exclude all of the roughness parameters. A second issue of excluding parameters is the unscientific nature of this approach. Using judgement to identify what parameters are linked to other controls on ice speed draws premature conclusions over the nature of the relationship.

Given the possible nature of roughness parameters as proxies for other controls on ice sheet dynamics, it is important to justify the use of these parameters in modelling. First, given the inescapability between roughness and other controls, omitting parameters was not a practical option. Furthermore, past investigations based on spectral analysis would also have captured these secondary effects, yet these techniques were still used: for example, Siegert *et al*. (2004) recognise that the roughness is indirectly related to ice speed because of its influence on hydrology. The fact that this parameter is included despite these secondary linkages suggests that other methods could also be used. Similarly, some theories on the role of roughness in controlling ice speed do not distinguish these direct and indirect controls: for example, in their description of how the shape of topography, namely the presence of bumps, controls the rate of basal ice flow, Winsborrow *et al*. (2010) also acknowledged that the occurrence of these obstacles may due to them comprising sediments that are more resistant deformation, a variable that is itself a control on ice speed.

Second, the fact that roughness parameters may capture the effects of other controls on ice dynamics is not necessarily a problem. Even if roughness parameters were proxies for other controls on ice speed, modelling still provides useful insight. For example, if a given parameter appeared strongly related to ice speed, it may indicate that this type of topographic variation was important for ice sheet dynamics, whether through a direct control or by influencing other, external variables.

The third justification is that, by analysing roughness using a GLM, is that it offers a quantitative measure of the association between roughness and ice speed. As reviewed in Chapter 2, many studies have identified spatial patterns between roughness and ice speed, but none have reported the statistical strength of these trends. Even if the model has captured the effects of other variables, the statistics of merit give an indication of upper limit in the strength of relationship between roughness and ice speed for a given location and scale of analysis. For example, if a model showed a low correlation between the parameters and ice speed, it would indicate that the two are relatively independent.

6.3 Analysis

6.3.1 Subglacial bed roughness across an ice-stream margin

Figure 6.2a shows the bed elevation measurements and ice speed data for Profile V13a. For the first 90 km the ice speeds are below 20 m per year but, beyond this point, there is a sharp transition to higher ice speeds. From Figure 6.3 it can be seen that this change in ice speed corresponds with the point where the profile crosses into the area of ice streaming. The *number of points* parameter (Figure 6.2c) also shows that there are fewer observations at this point of transition. For the reminder of the profile, ignoring the edge effects, the number of points increases with distance from the transition zone to a maximum of 25 observations within each 50 km window.

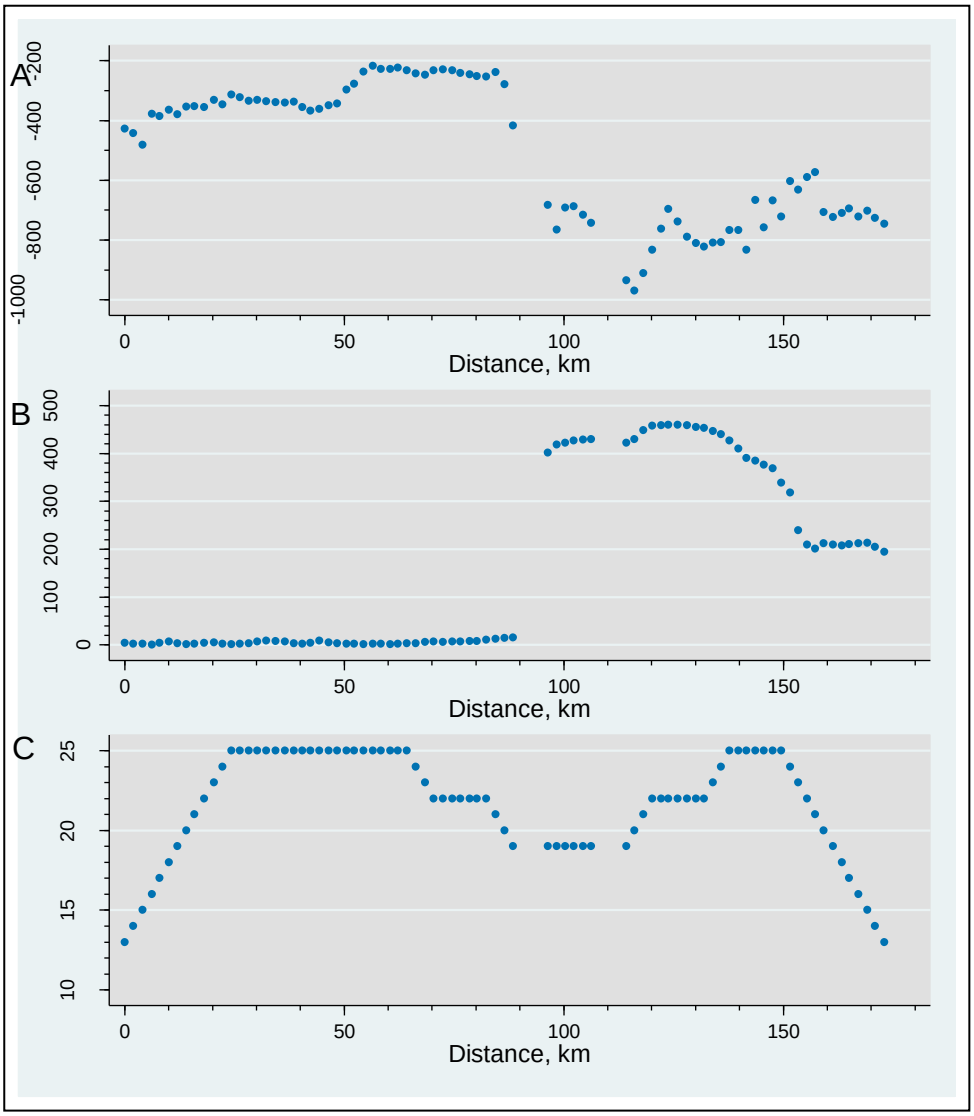

Figure 6.2: Summary of bed elevation and ice speed along Profile V13a. Number of observations summarised in each window when quantifying roughness is also shown

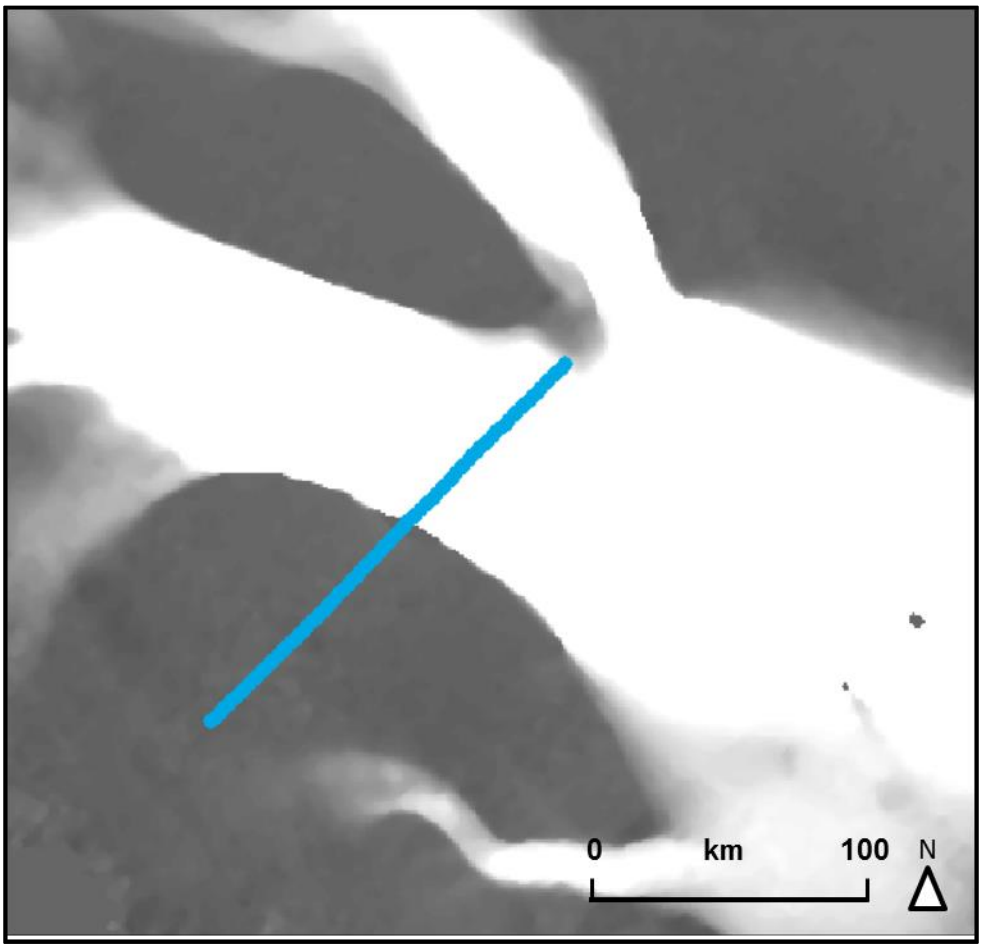

Figure 6.3: Location map of Profile V13a crossing the MacAyeal Ice Stream. Increasing brightness of greyscale image indicates faster ice speeds. A clear boundary is visible where ice speeds vary from <20 m/a on the outside of the margin, to >200 m/a within the ice stream.

Figures 6.4a to 6.4e present the changing roughness parameter values along Profile V13a. Figure 6.4a shows the amplitude parameters that use all observations within the window, whereas those in Figure 6.4b measured extreme amplitudes. Similarly, the amplitude parameters shown in Figure 6.4c only use a limited number of observations within each window to summarise the height of crests or troughs, such as only measuring those values that are crests or troughs. The shape parameter results are shown in Figure 6.4d, and the spacing parameters in Figure 6.4e.

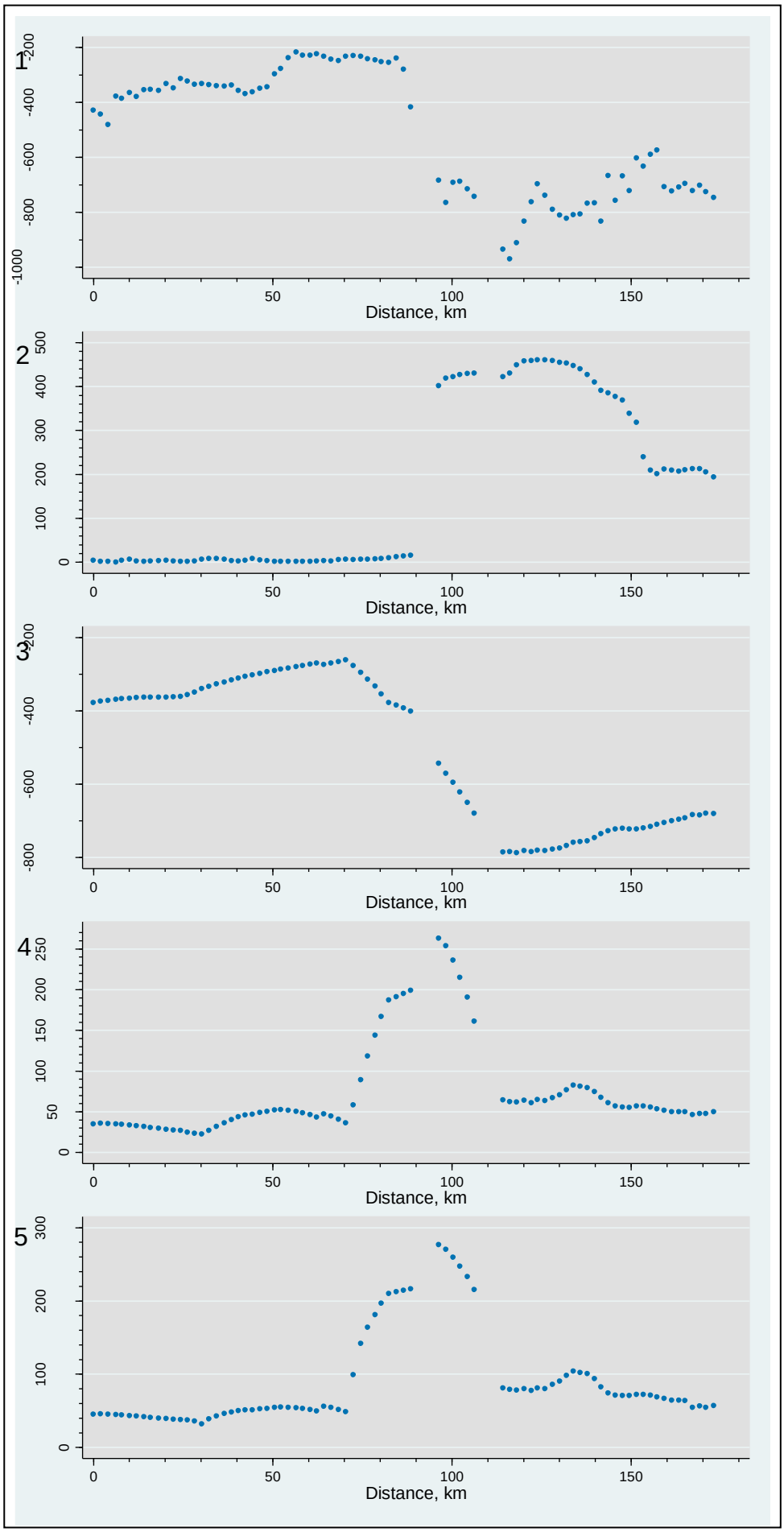

Figure 6.4a: Amplitude parameter results for the Profile V13a

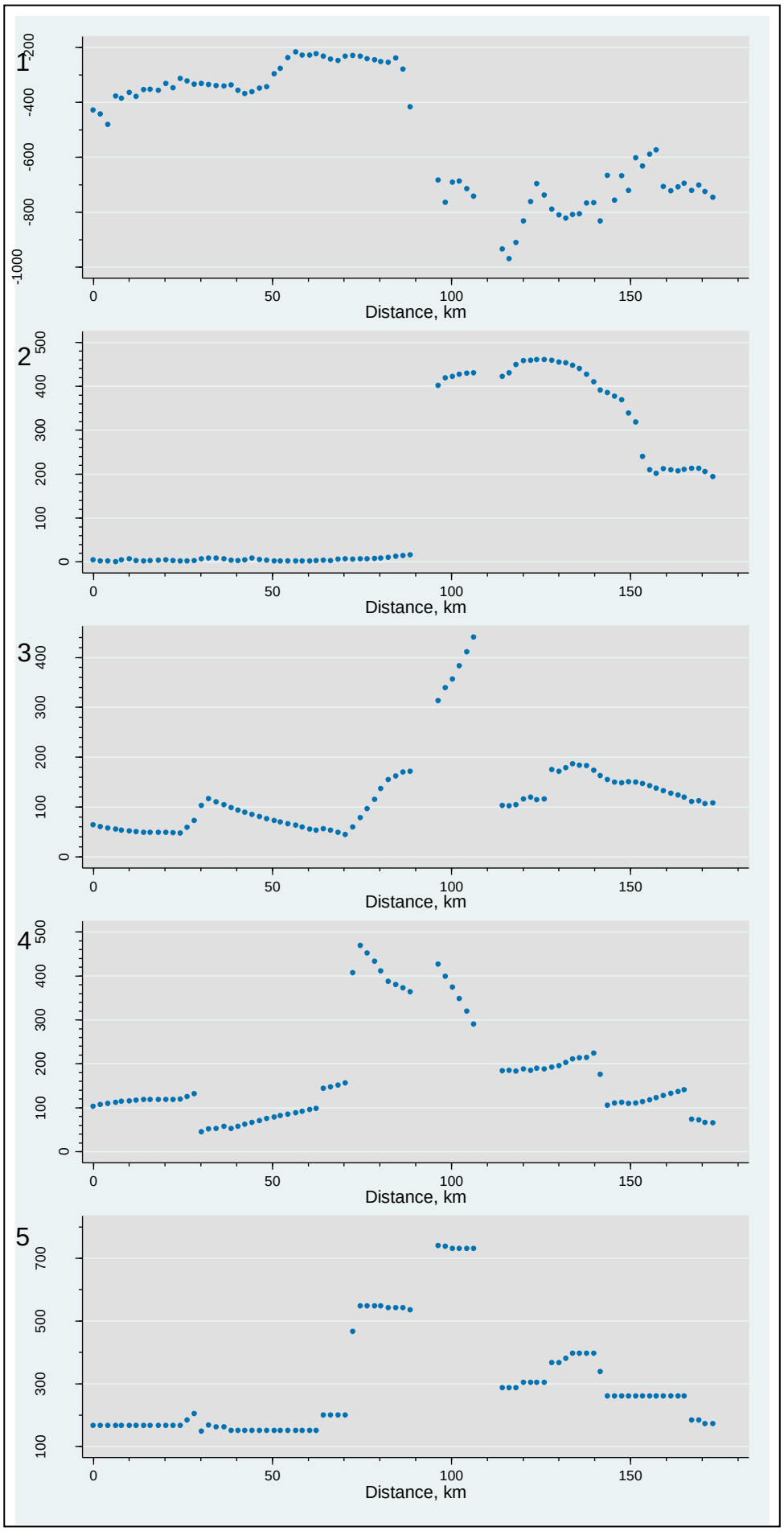

Figure 6.4b: Results for Profile V13a for parameters that measure extremes in amplitude

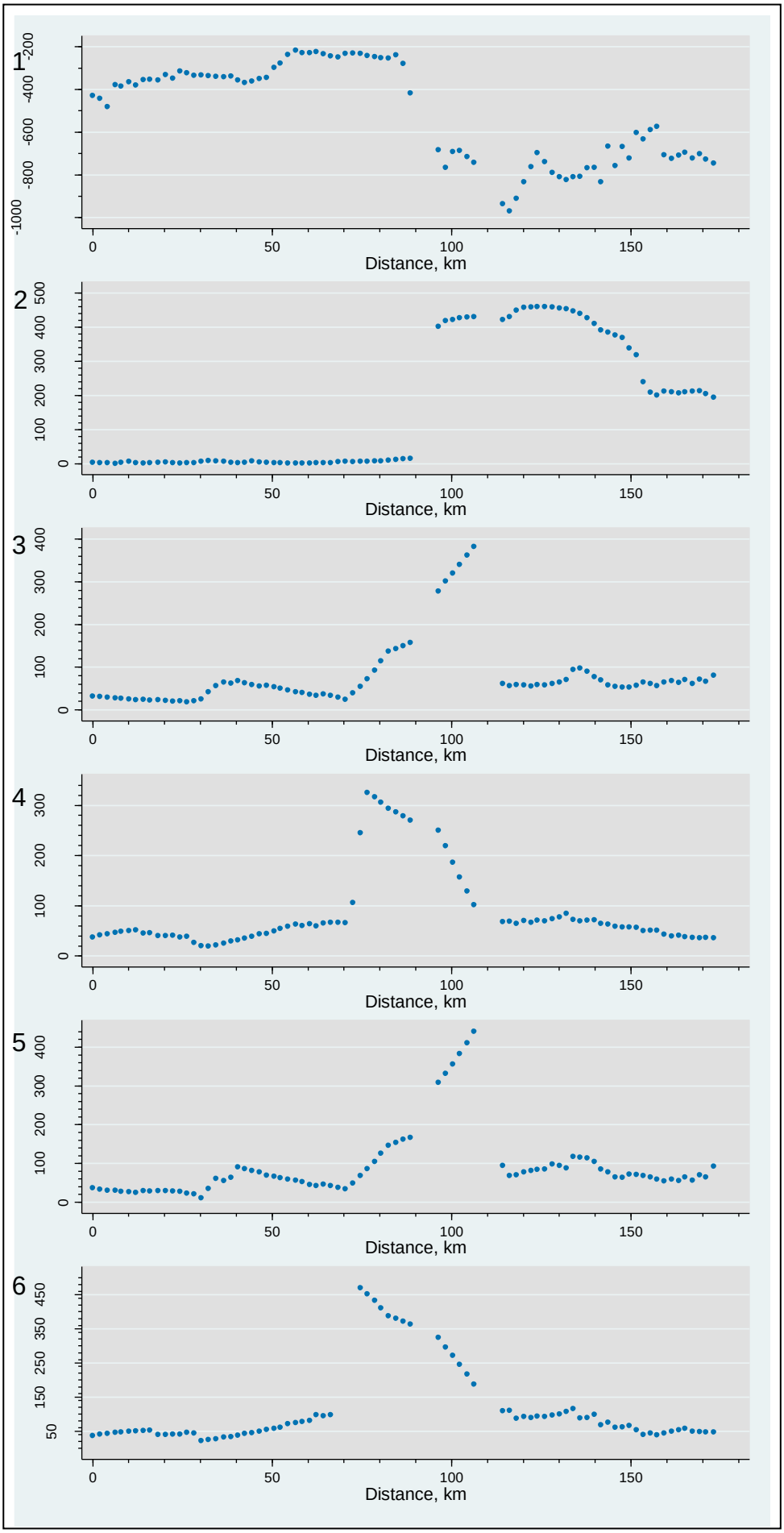

Figure 6.4c: Results of Amplitude parameters measuring a sub-set of the data for Profile V13a

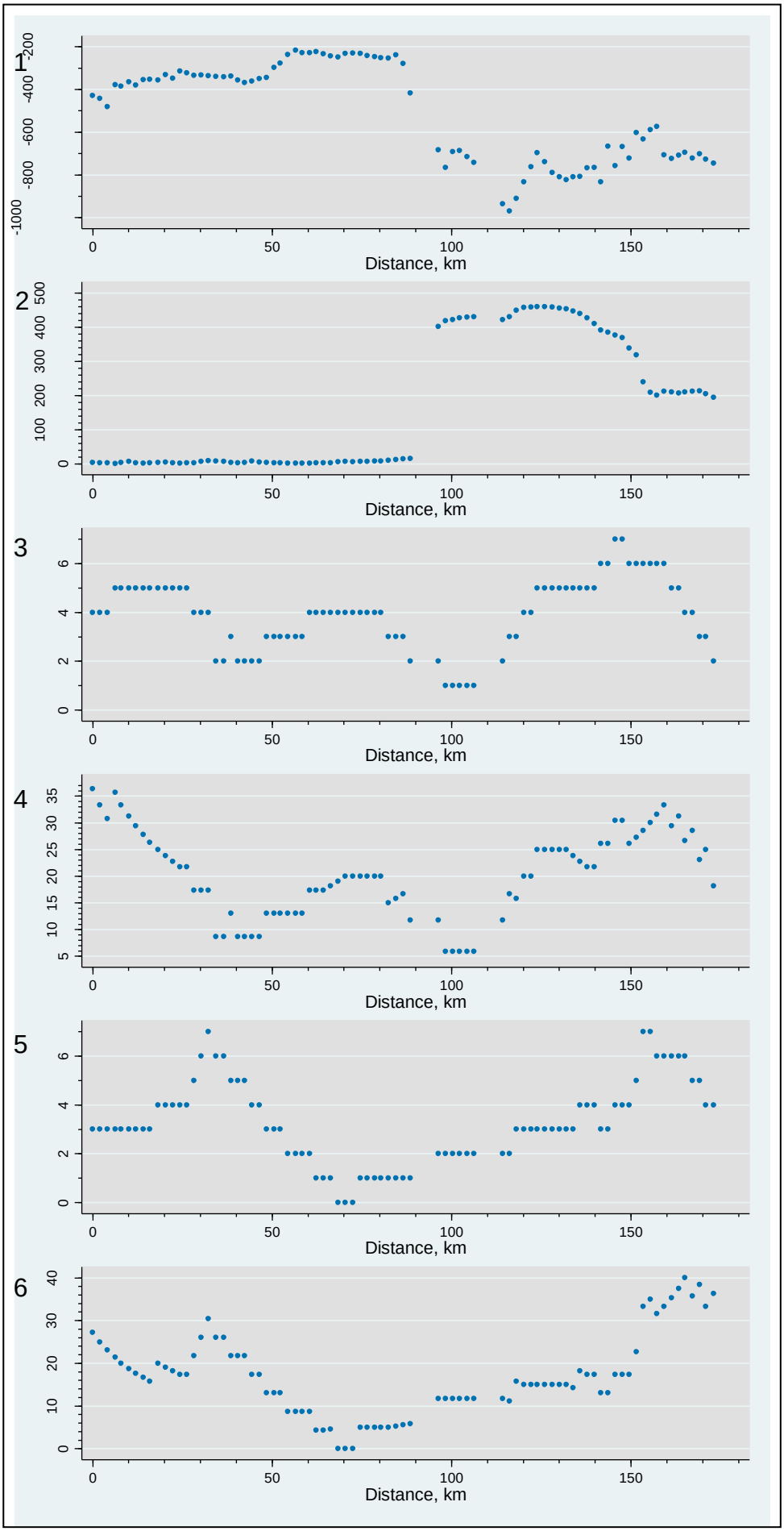

Figure 6.4d: Spacing parameter results for Profile V13a

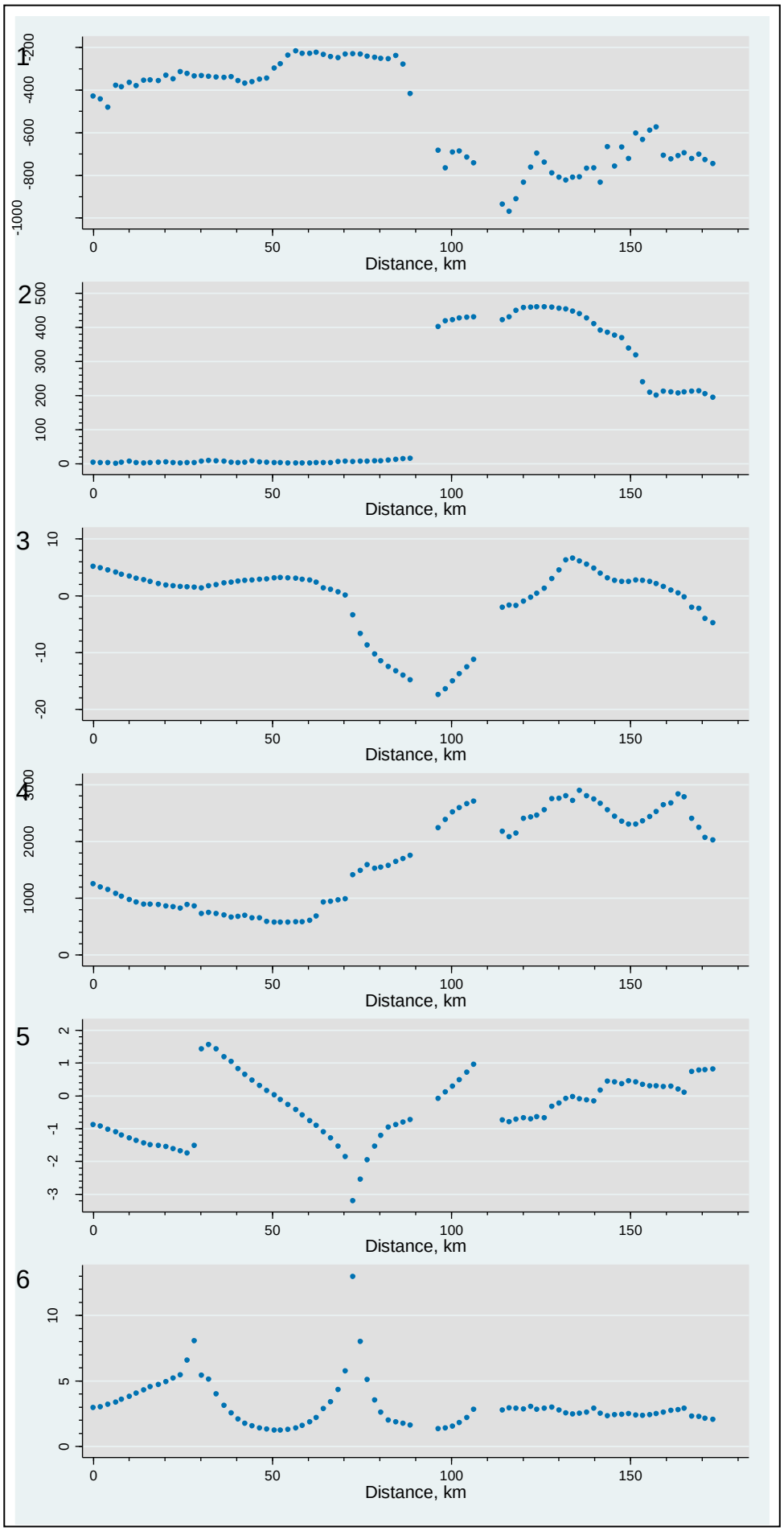

Figure 6.4e: Shape parameter results for the Profile V13a

Several of the parameters show a change in roughness that has a similar pattern to the variations in ice speed. For example, with the *mean height* (Figure 6.4a3) the rapid increase in ice speed corresponds with a decrease in the average height of the profile, although variations in roughness are less abrupt than changes in speed. The correlation between ice speed and this parameter is 0.97.

Other amplitude parameters do not show an agreement between roughness and ice speed for all sections of the profile. For example, the *mean deviation* (Figure 6.4a4) values are similar in the first and last 80 km of profile, despite a distinct difference in ice speed. However, this parameter does show a 200 m increase in the mean deviation to a maximum at c.95 km along profile. This zone of increasing values broadly corresponds with the transition zone between slow and fast flow, but it can be seen that the roughness of the bed increases approximately 20 km before the rise in ice speed. The methods that summarise extreme height values show a similar pattern. The *maximum height above* (Figure 6.4b3) shows that the highest bed elevations in each window are consistent to within 100 m for the majority of the profile. However, from 70 km along profile the values increase to a maximum of over 400 m.

Many of the roughness parameter values increase sharply at 70 km. In several examples, such as the *mean depth below* (Figure 6.4c4), these values then decrease to a similar size as the first 70 km. As a result, the roughness values inside and outside of the ice stream are similar, but the area corresponding with this transition in speed had a higher roughness.

Results of the spacing parameters (Figure 6.2d) show that the number of asperities is lower in the central area of the profile. This decrease in the number of crests and troughs corresponds with the increase in ice flow. The area of fewest asperities corresponds more closely between the boundary of fast and slow flow than results of the amplitude parameters, with the change in frequency occurring over a shorter distance. However, the spacing parameters show much variation along the entire profile length. The similarity of results in the left and right sides of the profile, especially with the *number of troughs* (Figure 6.4d5), shows there is not complete agreement. With the *number of* crests, the right-hand side appears to have a higher frequency of asperities than the left.

Unlike the amplitude or spacing parameters that have similar results between different methods, those designed to measure shape are more variable. Figure 6.4e3 shows that the *slope* parameter has produced a similar pattern to that of the amplitude parameters. Here, the left and right sides of the profile have a similar slope, but the central section between 70 and 130 km has lower values. The lowest slope is at 95 km. In terms of

agreement with variations in ice speed, the lowest slope values correspond with the large increase in speed, but variations in slope occur over a larger area than the transitions in speed.

The *Sinuosity* results in Figure 6.4e4 show an overall increase across the entire assessment length, with more localised fluctuations. The sinuosity increases more steeply from 60 km, then fluctuates from 105 km onwards. The general pattern of decreasing values is the reverse situation to the overall increase in ice speed but, locally, the results do not correlate strongly.

6.3.2 Along-flow changes in roughness

The second profile analysed was H3b, with Figure 6.5 showing the change in bed elevation and ice speed along the direction of ice flow. Like Profile V13a there is a trend of increasing ice speed along profile, but in Profile H3b the rate of change is more gradual. The steepest increase in ice speed occurs between 100 and 120 km distance. Compared with Profile V13a, the maximum speeds reached along Profile H3b are lower, but there is still a range of 150 m a^{-1} between the fastest and slowest areas.

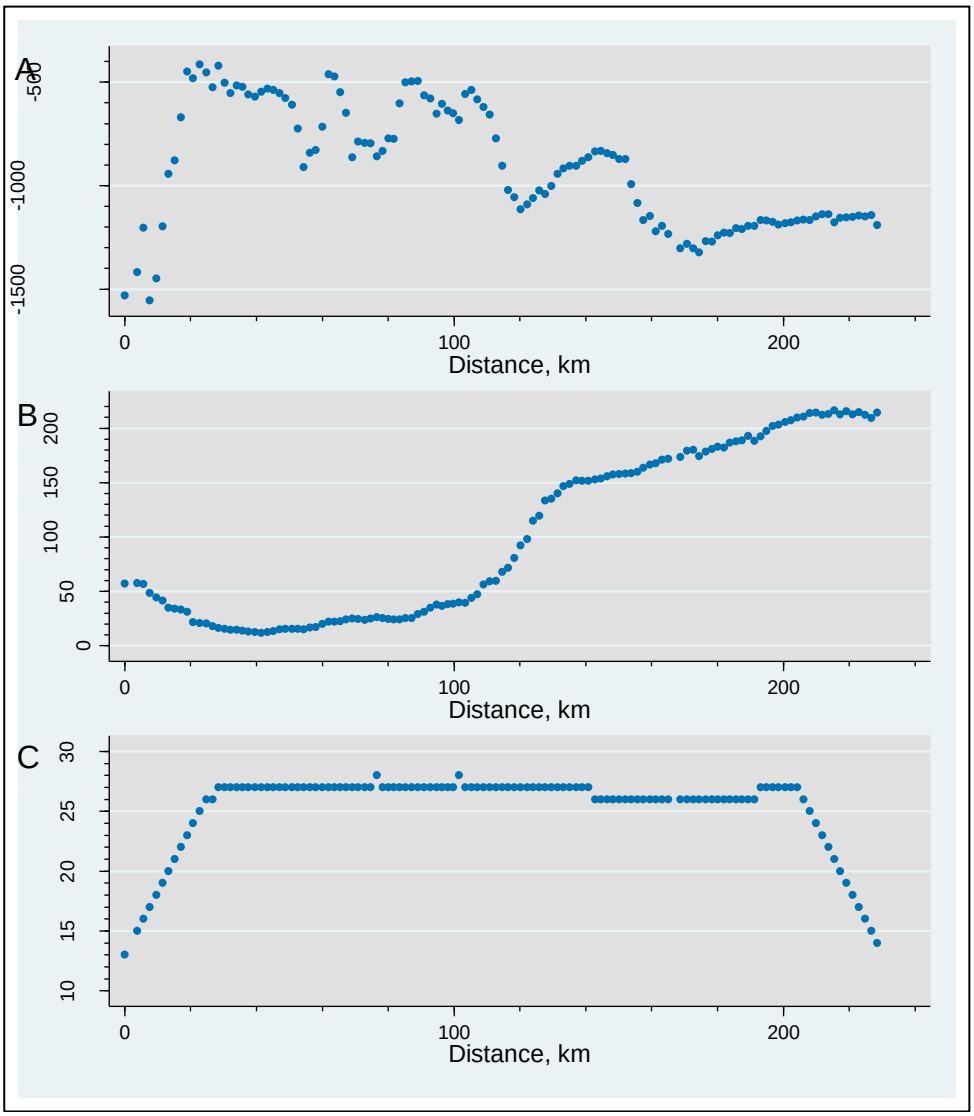

Figure 6.5: Summary of bed elevation and ice speed along Profile H3b. Number of observations summarised in each window when quantifying roughness is also shown

Figure 6.5c also shows the number of points in each 50 km window used to quantify roughness. Like Profile V13a, there is at least one gap but the number of missing observations in these areas is fewer. Two sections of profile have 28 observations per window, showing that the sampling interval between bed elevation measurements in these sections is shorter.

As with the analysis of Profile H3b, the parameters presented in Figure 6.6 are grouped by the type of parameter. Therefore, Figure 6.6a to Figure 6.6c present the amplitude parameters, Figure 6.6d the results of the spacing parameters, and Figure 6.6e the shape parameters.

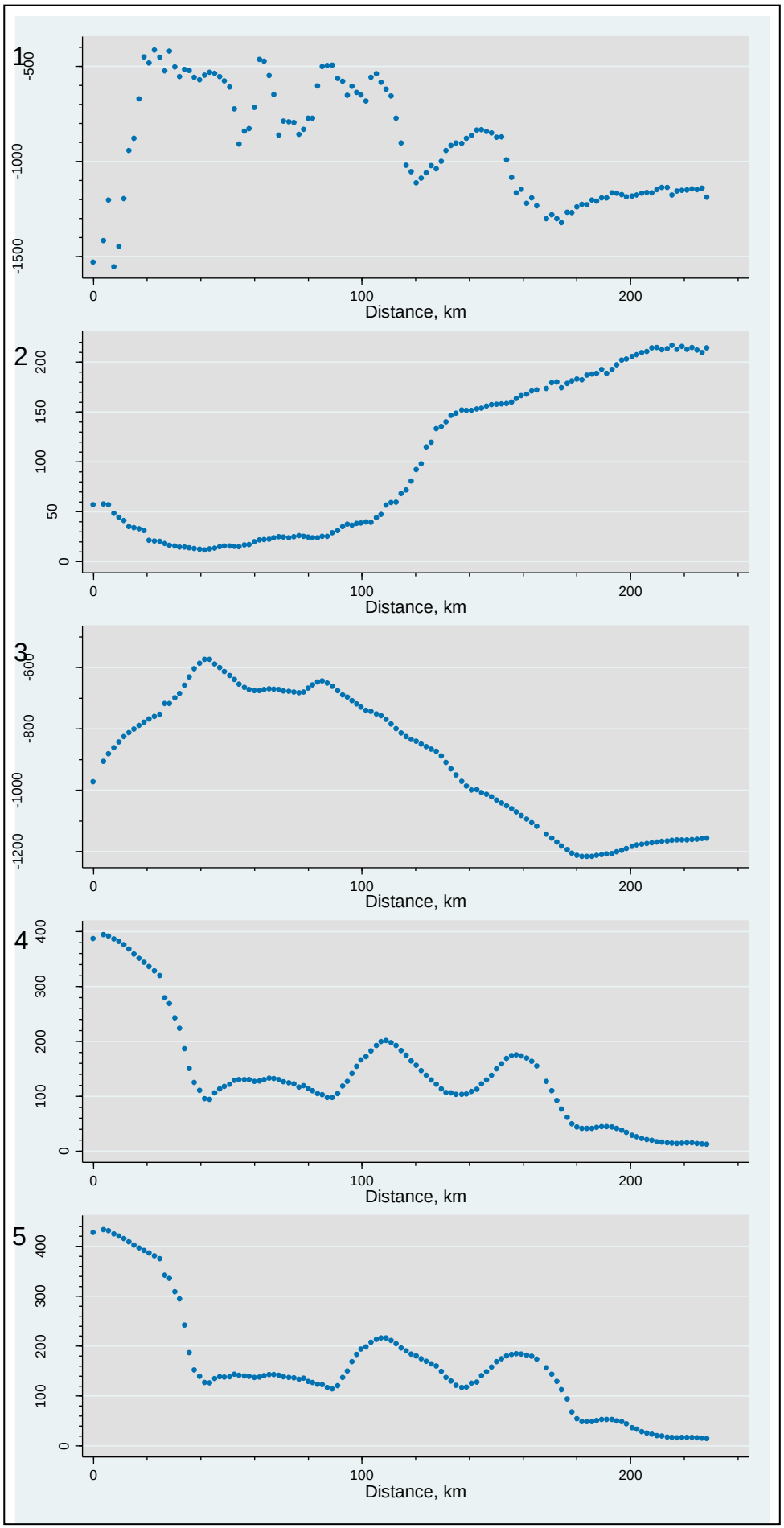

Figure 6.6a: Amplitude parameter results for the Profile H3b

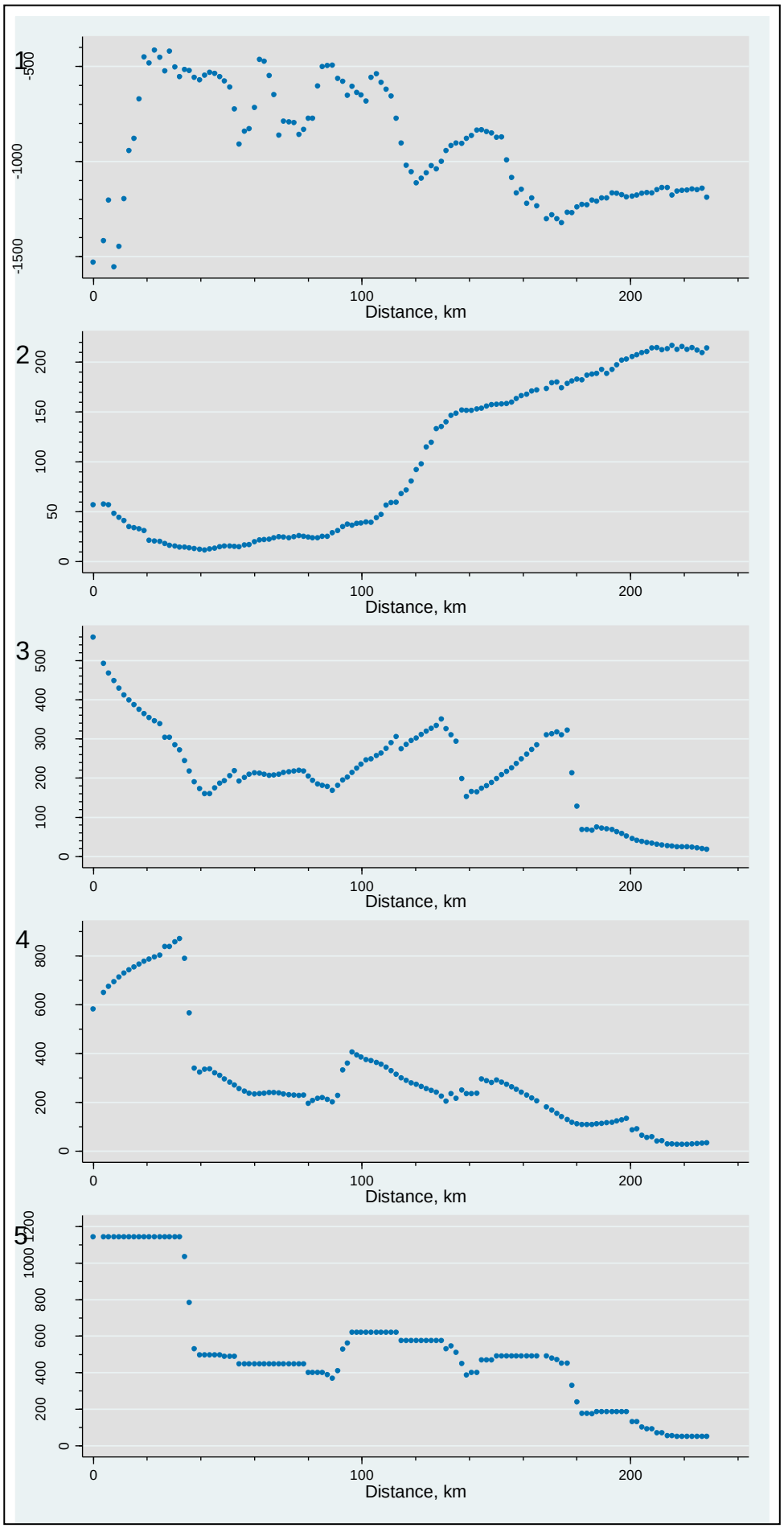

Figure 6.6b: Results for Profile H3b for parameters that measure extremes in amplitude

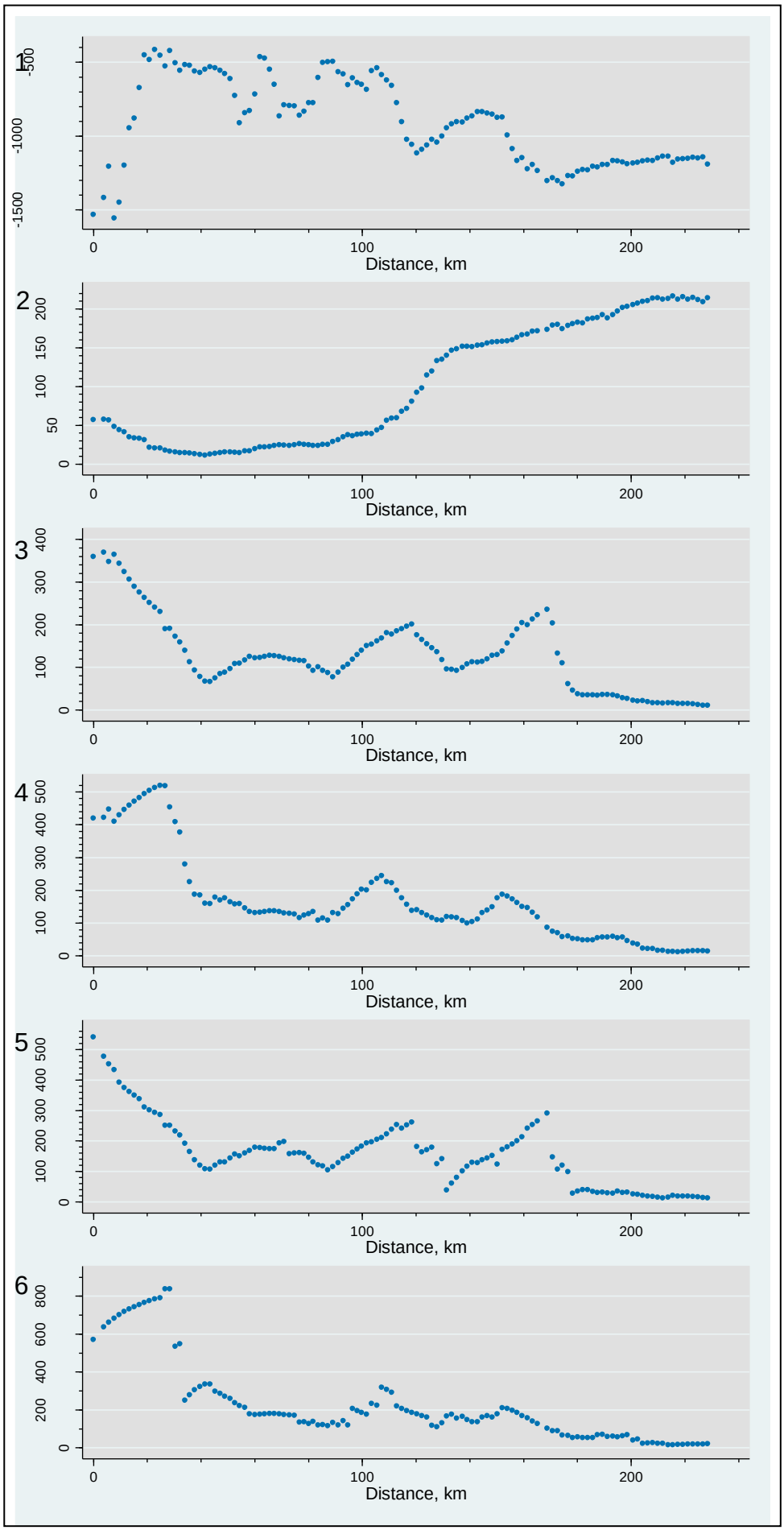

Figure 6.6c: Results of Amplitude parameters measuring a sub-set of the data for Profile H3b

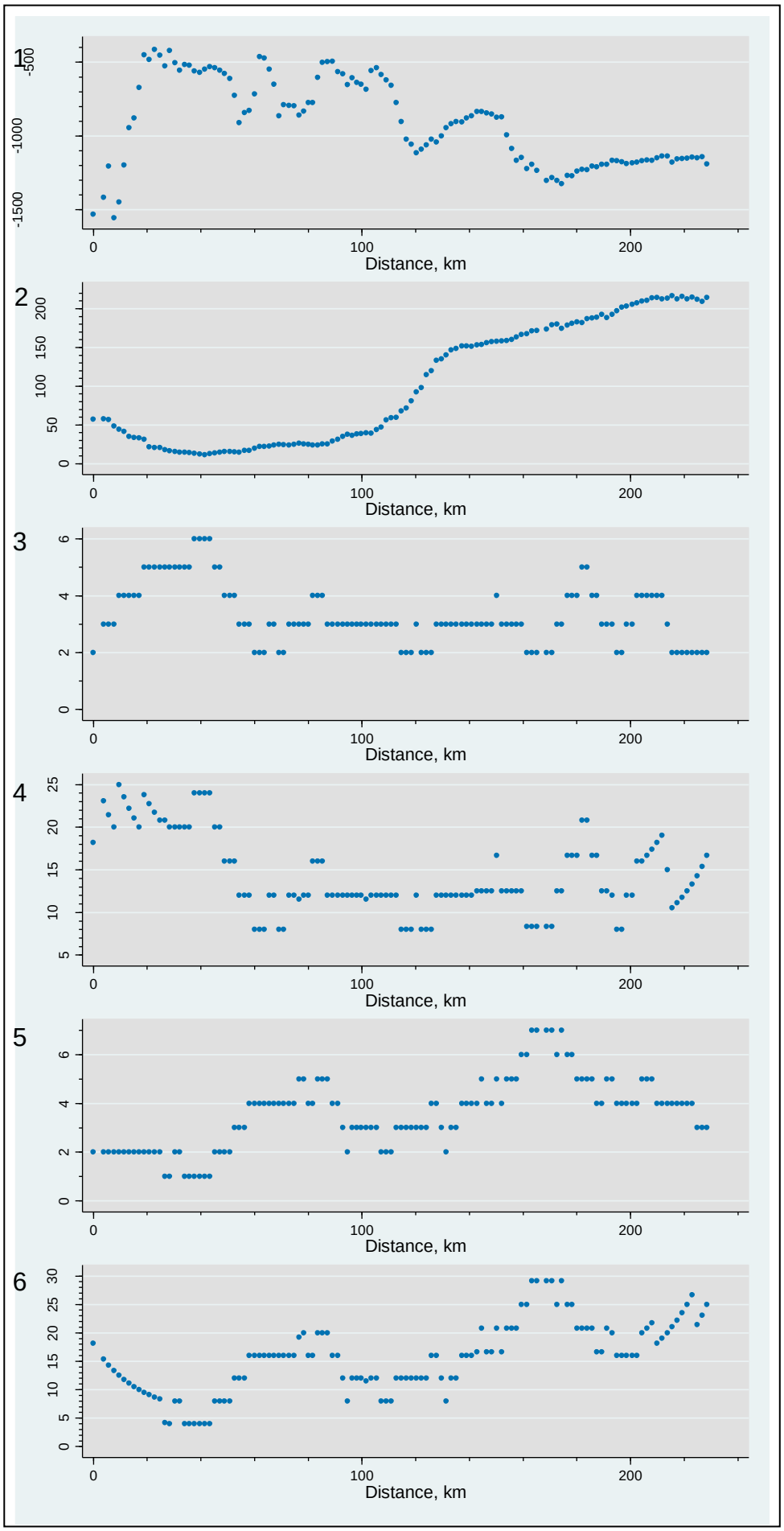

Figure 6.6d: Spacing parameter results for Profile H3b

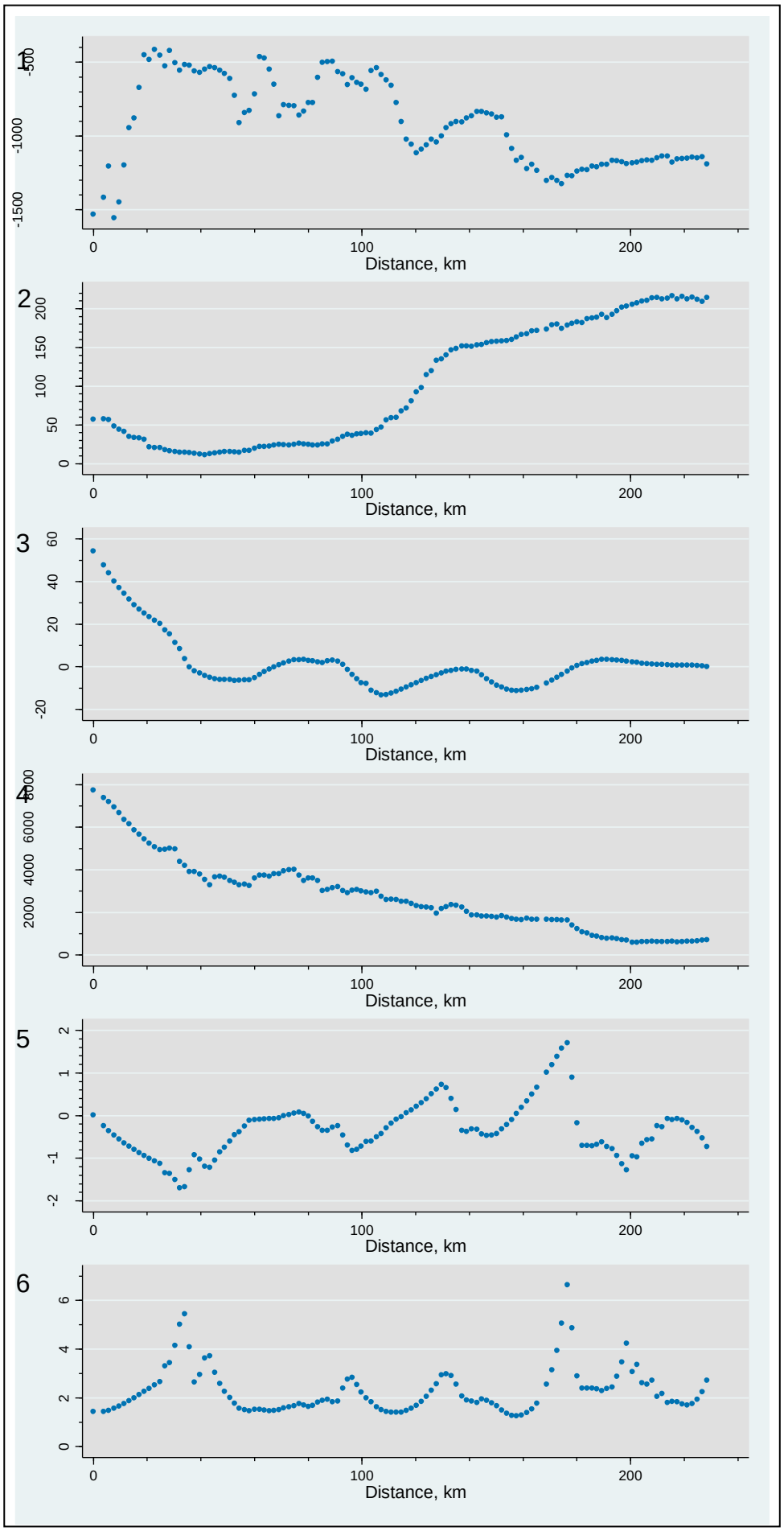

Figure 6.6e: Shape parameter results for the Profile H3b

In Figure 6.6a3 the *mean height* values show that the average amplitude increases for the first 25 km of profile before becoming more consistent until c.95 km. From this point, the mean height decreases more steeply, reaching its lowest value at 190 km distance. The trend in mean height along profile has an inverse relationship to that of ice speed. As well as a pattern for the assessment length as a whole, there are similarities at a shorter scale. For example, in the first 30 km, the flattening off of the mean height corresponds with the switch to consistent ice speeds. However, there is not complete agreement. For example, at c.115 km the rate of change in ice speed decreases, but the rate in mean height decrease is constant at approximately 75 m height loss per 10 km horizontal distance.

Other amplitude parameters, such as the *mean deviation* (Figure 6.6a4), show a general trend of decreasing amplitude along profile. However, with this parameter smaller scale changes in height (on the order of 10 km for instance) are more apparent. The rapid increase in ice speed at c.110 km corresponds with a peak in mean deviation, from which the height decreases to c.135 km along profile. At this 135 km distance, the rate in ice speed change is slower. The amplitude parameters measuring asperity size (e.g. Figure 6.6c5) show that the average size of peaks and valleys decreases along profile. This pattern fits the pattern of increasing ice speeds. Some of the results show agreement with ice speed more locally. For example, the increasing mean depth of valleys (Figure 6.6c6) corresponds with the decreasing ice speed.

The spacing parameters show that the frequency of crests varies between 2 and 6 per window (Figure 6.6d3). The *number of troughs* (Figure 6.6d5) is more variable, ranging between 1 and 7. The highest trough count equates to approximately 30% of the observations within the window being troughs. The *number of crests* shows a spatial pattern where the central section has fewer asperities than upstream or downstream. This zone, although broader, corresponds with a steeper rate of ice speed increase. The *number of troughs* also shows lower values for this central area, but there is less agreement with speed in other locations. Despite the right-hand side having a higher number of peaks overall, there is much fluctuation and this variation does not correlate with changes in ice speed.

Compared with the results measured across flow, there was more agreement in the parameters measured along the ice stream. The majority of parameters show a decreasing roughness in the downstream direction.

6.3.3 Modelling ice speed

6.3.3.1 One predictor variable

The first set of models predicted ice speeds using one roughness parameters. From the figures of merit in Table 6.1 it was found that the parameter capturing the most variation in

ice speed was the *mean height*. The Root MSE for this model was 78 m a^{-1}. A plot of the fit between the values predicted by the model, and those observed along the profile are shown in Figure 6.7.

Predictor variables	R^2	Root MSE, ma^{-1}
1	0.837	87.3
2	0.013	189.5
3	0.094	181.6
4	0.081	183.4
5	0.073	184.1
6	0.763	95.1

Table 6.1: Figures of merit for GLMs that used a single roughness parameter as the independent variable. Predictor variables are abbreviated as follows:
1 Mean height, 2 Slope, 3 RMS height, 4 Skewness, 5 Kurtosis, 6 Sinuosity

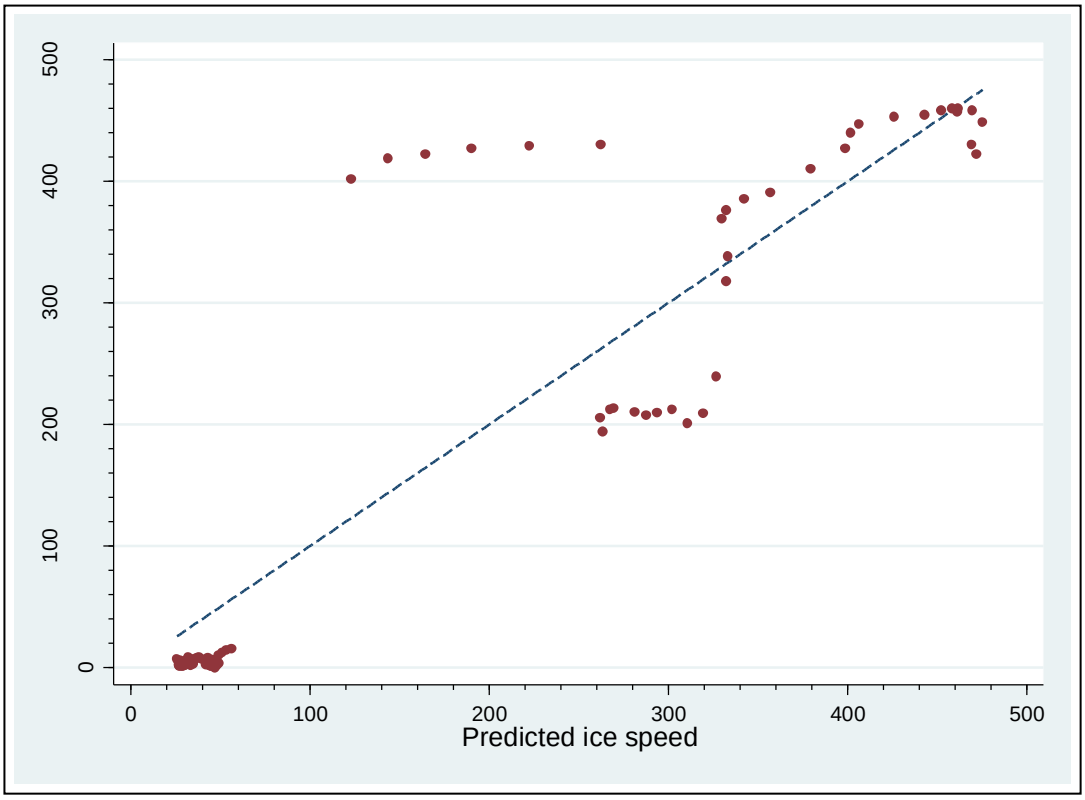

Figure 6.7: The fit between observed ice speeds, and those predicted by a GLM that used the mean height as the only independent variable. The units of ice speed are metres per year.

The next best predictor of ice speed was found to be *sinuosity*. Using only this shape parameter produced a model with an R^2 of 0.76, allowing ice speeds to be predicted with a typical error (Root MSE) of 95 m a^{-1}. Although capturing less variation than the mean height, sinuosity was considerably better than the other predictor variables. Statistics of merit for the remaining models showed that other measures of roughness were only

capable of predicting ice speed with an error of around 180 m a^{-1}. For reference, the highest possible Root MSE, when no predictor variables are used, was 189.6 m a^{-1}.

6.3.3.2 Two predictor variables

The next set of models used two predictor variables. Table 6.2 shows the figures of merit for the 15 possible combinations. Using the *mean height* along with any of the five other roughness parameters gave an R^2 of at least 0.85. A possible combination was the *mean height* and *sinuosity*. For models using a single predictor variable, these parameters had produced the best figures of merit. However, when combined, although giving an R^2 of nearly 0.86, this was not the best model.

Predictor variables	R^2	Root MSE, ma^{-1}
1 2	0.892	64.9
1 3	0.969	34.9
1 4	0.839	77.7
1 5	0.876	68.0
1 6	0.856	73.9
2 3	0.350	154.8
2 4	0.109	181.3
2 5	0.079	184.4
2 6	0.770	93.9
3 4	0.204	171.5
3 5	0.134	178.9
3 6	0.775	92.7
4 5	0.113	181.1
4 6	0.764	95.3
5 6	0.776	92.4

Table 6.2: Figures of merit for GLMs that used two roughness parameters as independent variables. Predictor variables are abbreviated as follows:
1 Mean height, 2 Slope, 3 RMS height, 4 Skewness, 5 Kurtosis, 6 Sinuosity

The use of the *RMS height* with the mean height produced the best model, improving the R^2 to 0.969, equivalent to a prediction error of c.35 m a^{-1}. Therefore, the use of two variables improved prediction by 43 m a^{-1}. The improvement in predicting ice speed when adding a second variable is illustrated by Figure 6.8, an observed versus fitted or calibration plot below (see Cox, 2004 for more information on this type of graph). Here, it can be seen that the predicted ice speeds have a stronger fit with the observed speeds, indicating that the addition of a second variable has improved the model.

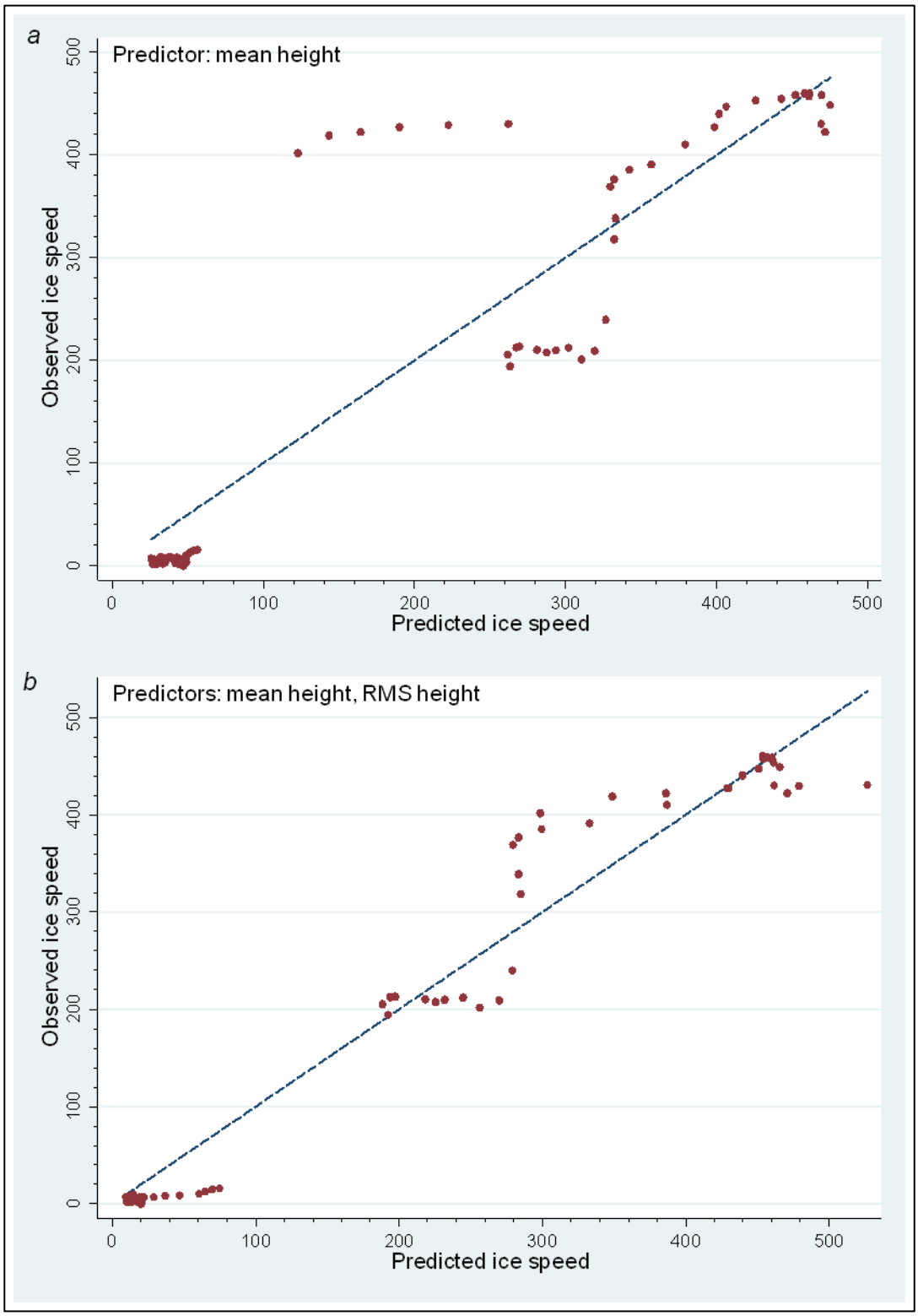

Figure 6.8: The fit between ice speeds predicted by two GLMs, with those observed along Profile V13a. Ice speeds are displayed as metres per year. In a, the mean height was the predictor value. In b, the mean height and RMS height were used as independent variables. The closer fit (shorter distance from the line of equality) in the second model show that there is less residual variation. Therefore, model b is an improvement on a.

When building models that used a single roughness parameter, sinuosity had been a good predictor of ice speed, with an R^2 of around 0.76. However, apart from the above exception of using the mean height, GLMs of sinuosity and any other variable showed

minimal improvement to model accuracy, with the R^2 of these models ranging from approximately 0.76 to 0.78.

6.3.3.3 Three predictor variables

Table 6.3 summarises the figures of merit for models that included three independent variables. It can be seen that the combination of the *mean height*, *RMS height*, and *kurtosis* produced the most accurate prediction, with an R^2 of 0.979. This represents an improvement of 0.01 over the best model using two predictors. The improvement in prediction is visible by plotting the predicted and actual ice speed values for the best models using one, two, and three independent variables (see Figure 6.9).

Predictor variables	R^2	Root MSE, ma^{-1}
1 2 3	0.970	34.9
1 2 4	0.894	64.2
1 2 5	0.919	55.4
1 2 6	0.928	52.3
1 3 4	0.969	35.0
1 3 5	0.979	28.2
1 3 6	0.969	35.1
1 4 5	0.891	64.1
1 4 6	0.856	74.4
1 5 6	0.891	64.0
2 3 4	0.417	147.5
2 3 5	0.358	154.8
2 3 6	0.776	93.2
2 4 5	0.132	180.1
2 4 6	0.774	93.3
2 5 6	0.778	92.6
3 4 5	0.209	171.9
3 4 6	0.778	92.5
3 5 6	0.781	92.0
4 5 6	0.791	89.6

Table 6.3: Statistics of merit for GLMs that used three roughness parameters as independent variables. Predictor variables are abbreviated as follows:
1 Mean height, 2 Slope, 3 RMS height, 4 Skewness, 5 Kurtosis, 6 Sinuosity

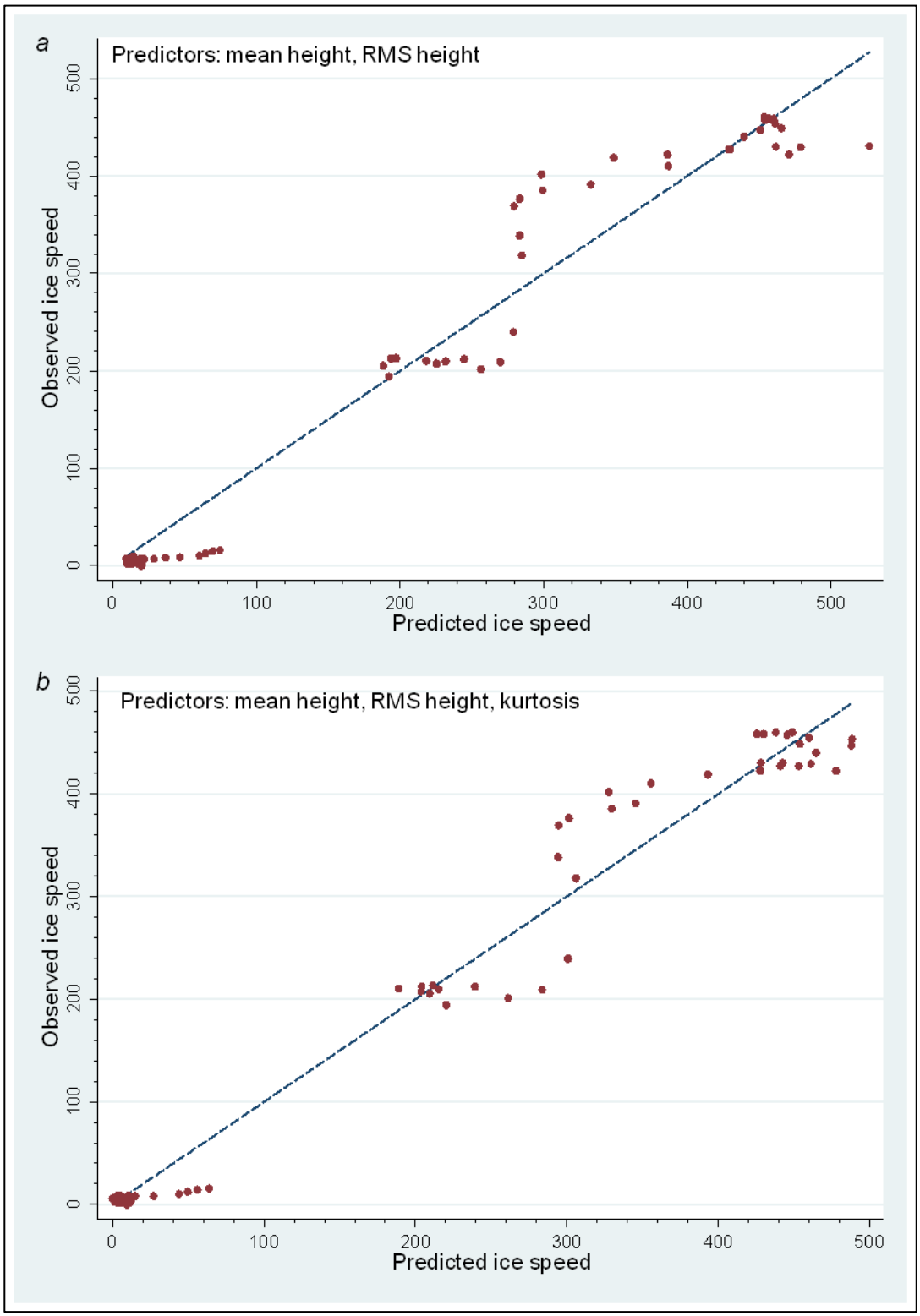

Figure 6.9: The fit between observed ice speeds and those predicted from GLM. a shows the best model achieved by using two independent variables. b shows the best model for three predictor variables, namely the mean height, RMS height, and kurtosis. Although the summary statistics showed an improvement in adding a third predictor to the model, the improvement in fit is more negligible than that in Figure 6.8.

The other possible combinations of three predictors were found to be less accurate at predicting ice speed than the best combination of two independent variables (i.e. mean height and RMS height). The exception to this was the use of the mean height, RMS height, and sinuosity. Here, adding sinuosity improved the R^2 by 0.001. For other

combinations, although the R2 was improved, the Root MSE decreased, with the use of mean height, RMS height and slope being one such example of this.

6.3.3.4 Four or more predictor variables

Table 6.4 presents the figures of merit for models of ice speed that used 4, 5, or 6 independent variables. It is clear that none of the possible 22 combinations showed a substantial improvement in prediction error over the use of mean height, RMS height, and sinuosity.

Predictor variables	R^2	Root MSE, ma^{-1}
1 2 3 4	0.970	35.1
1 2 3 5	0.979	28.4
1 2 3 6	0.970	35.1
1 2 4 5	0.920	55.4
1 2 4 6	0.929	52.2
1 2 5 6	0.963	37.5
1 3 4 5	0.979	28.4
1 3 4 6	0.969	35.2
1 3 5 6	0.979	28.4
1 4 5 6	0.914	57.5
2 3 4 5	0.417	148.5
2 3 4 6	0.778	93.1
2 3 5 6	0.782	92.4
2 4 5 6	0.794	89.6
3 4 5 6	0.793	89.8
1 2 3 4 5	0.979	28.5
1 2 3 4 6	0.970	35.1
1 2 3 5 6	0.979	28.4
1 2 4 5 6	0.965	36.6
1 3 4 5 6	0.979	28.6
2 3 4 5 6	0.794	90.2
1 2 3 4 5 6	0.979	28.6

Table 6.4: Figures of merit for GLMs that used four or more roughness parameters as independent variables. Predictor variables are abbreviated as follows:
1 Mean height, 2 Slope, 3 RMS height, 4 Skewness, 5 Kurtosis, 6 Sinuosity

6.4 Discussion

6.4.1 The relationship between roughness and ice speed

Comparison of 18 roughness parameters with changes in ice speed suggested that there is a relationship between ice speed and roughness. Along the Whillans Ice Stream, there was a trend of decreasing roughness as ice speed increases. Similarly, across the MacAyeal Ice Stream, the results for the majority of parameters indicated that the bed of the ice stream has lower roughness than that of the surrounding topography. These findings support those of earlier studies that measured spatial patterns in ice speed and roughness using spectral analysis (Rippin *et al.*, 2004; Siegert *et al.*, 2004; Taylor *et al.*, 2004; Bingham & Siegert, 2009).

Visually comparing the agreement between parameter results and ice speed has been a common method of evaluating this relationship. For example, Section 2.3.1.2 showed how other studies have used maps to compare the spatial patterns between these variables. In this project, a similar technique was used by plotting the roughness results for each parameter. However, for the first time, the strength of the relationship between roughness and ice speed has been quantified. Figures of merit for the GLMs showed a strong correlation, thus measuring the extent of the relationship between subglacial topography and rates of ice flow in this region.

The use of GLMs for a profile measured across the MacAyeal Ice Stream, supported the visual comparison of agreement between ice speed and roughness. Again, a relationship was apparent with faster ice speeds predicted as the roughness of the subglacial bed decreased. When used individually, several of the variables showed a high R^2 indicating that there is a correlation between spatial changes in ice speed and that of topography. Results indicated that the *mean height* and *sinuosity* were the best predictors of ice speed.

In GLMs with a single independent variable, the roughness parameter that explained the most variation in ice speed was the *mean height*. With a visual comparison of the plots, the mean height results showed that the roughness inside of the ice stream was distinct from that outside. In the model, the coefficient for the mean height showed that ice speeds are expected to increase as the mean height of the bed decreases. Given that this parameter summarises the vertical amplitude of the profile, it supports theories that obstacle size controls the rate of basal ice flow (Cohen *et al.*, 2002; Schoof, 2002; Thorsteinsson *et al*., 2003) by influencing the amount of drag on the base of the ice sheet (Alley, 1993). However, it is again reiterated that, although these models quantify the strength of agreement between the roughness parameters and ice speed, it is not possible to determine what the control is. An alternative explanation is differences in

topography have produced spatial patterns in the topography: for example, given that the energy to erode and deform ice increases with ice speed, in areas of rapid ice flow the bed may have been preferentially modified reducing its roughness.

Another difficulty in interpreting the cause of the association between ice speed and the parameters is that, as explained in Section 2.5.1.3, these methods of quantifying roughness may act as proxies to other variables. In the case of the mean height, given that it measures vertical change in the height of the profile, this parameter may be related to thickness of the ice. Section 2.2.1 described how ice thickness influences the amount of basal shear stress and temperature, making it one of the controls on ice flow (Bennett & Glasser, 2006), with faster ice speeds expected beneath thicker ice (Paterson, 1994; Hindmarsh, 1998; Piotrowski & Tulaczyk, 1999). If the ice surface remains somewhat constant, then ice thickness would increase as the mean height decreased. In this case, the correlation between the mean height and ice speed may be due to the roughness parameter capturing the effect of ice thickness. Given the fact that the SPRI data captured the surface elevation of the ice-sheet, it was possible to calculate the ice thickness, thus testing this theory. Figure 6.10 shows that, despite the mean height being lower inside the area of ice streaming, the surface elevation of the ice-sheet is also lower, so that the ice thickness is somewhat constant for the entire profile length. Therefore, the relationship between the mean height and ice speed appears due to the shape of topography, rather than the influence of ice thickness. Nevertheless, the mean height shows some agreement with the surface elevation with both displaying an overall decrease from left to right, which might suggest there is some linkage.

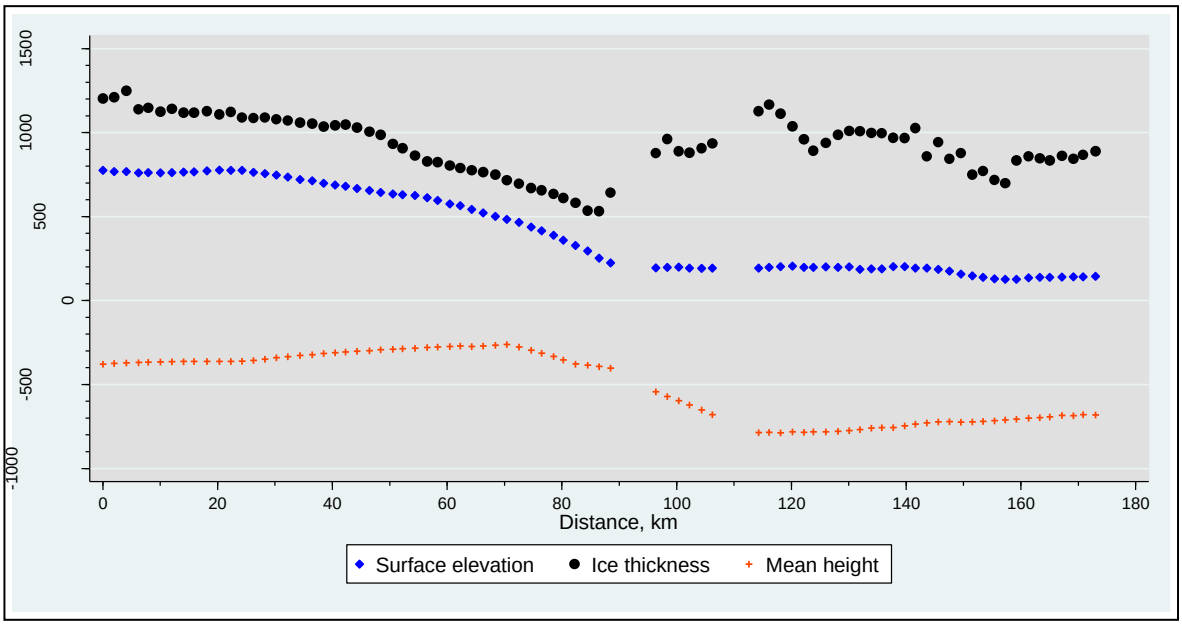

Figure 6.10: Changes in the mean height of the bed, surface elevation of the of the ice-sheet, and ice thickness along Profile V13a. Moving left to right, the profile extends across the lateral margin of the MacAyeal Ice Stream, into the area of faster ice speeds

Whereas the mean height may have captured secondary effects, some of the other variables used are less likely to be influenced by effects such as ice thickness. One such example is sinuosity. A GLM of this parameter showed a strong correlation with ice speed. The trend of decreasing sinuosity as ice speed increases was also witnessed in plots of ice speed and sinuosity both along flow and across flow. A possible reason for the inverse relationship between sinuosity and ice speed is that the parameter gives information on the surface area of the bed in contact with the ice. As this surface area increases, so too does the friction (Bennett & Glasser, 1996) and, because friction is a resistive force to sliding (Kalpakjian, 1997; Cohen *et al*., 2000) this results in slower ice speeds.

Sections 6.3.1 and 6.3.2 showed that that the spatial patterns in roughness values have similar patterns to variations in ice speed. Furthermore, these trends were apparent from a number of roughness parameters. Using modelling, it was possible to quantify the extent of this agreement. Results indicated that, if used individually, some roughness parameters were able to capture over 70% of the spatial variation in ice speed. However, building GLMs by adding more variables demonstrated that a substantial improvement to prediction could be achieved by combining two or more parameters. Although the explanation for this relationship is unclear, this research has not only quantified the strength of the relationship between roughness and ice speed, but also shown which roughness variables are most linked to spatial patterns in ice flow at this particular scale. Similar tests could be completed on smaller scales of roughness. Ultimately, these results might guide scientists in understanding the controls on ice dynamics, such as determining the types of topographic variation that are most important for controlling ice speeds.

In this project, studying the possible combinations of six methods of quantifying roughness showed that the use of *mean height*, *RMS height*, and *kurtosis* was the best choice for predicting ice speed. It is clear that this model included different types of parameter, in this case amplitude and shape parameters. This was not unexpected because model building in this manner relies on adding independent variables that measure different characteristics, thus capturing the variation not captured by other predictors. In fact, parameters of the same type are more likely to capture similar variations, adding redundancy that can be detected by increasing P-values in the models. The fact that the best models in this project had P-values reported as essential zero showed the values were statistically significant at conventional levels. Furthermore, measurements of correlations between the independent variables showed they lacked multicollinearity.

6.4.2 The influence of roughness on ice stream location

Analysis of the lateral margin of the MacAyeal Ice Stream (Profile V13a) showed a pattern where the position of the margin corresponded with an abrupt decrease in roughness moving into the zone of fast flow. This pattern of higher roughness values within an ice

stream than for the beds of the surrounding ice sheet have also been reported in results using spectral analysis (Bingham & Siegert, 2009). However, analysis using the group of roughness parameters suggested that the area of higher-roughness forms a relatively narrow band of approximately 40 km where, beyond this, the roughness of topography decreases, although values remain higher than within the area of streaming.

If certain roughness parameters show a stronger relationship with ice speed than others, and this relationship is assumed to be due to roughness controlling ice dynamics, it also follows that certain roughness variables are more important in controlling ice stream position than others. In this case, parameters measuring the roughness in terms of the vertical height of topography showed the strongest link with variations in ice speed. The higher roughness results at the margin suggest it is characterised by one or more high-amplitude asperities, such as a mountain range, whereas the zone within the ice stream has lower-amplitude perturbations. It is possible, therefore, that the higher roughness at the lateral margin of the ice stream has constrained its position, in a similar way topographic forcing channels flow (Joughin *et al*., 2004; Winsborrow *et al*., 2010). Interestingly, however, as Section 6.2, the areas of rapid ice flow in the Siple Coast region have traditionally been classed as *pure* ice streams (Stokes, 2001), and suggested that their lateral extent is not constrained by topography.

Given that some models showed that the strength of this relationship was almost 98%, it implies that roughness is strongly linked to the speed of flow. As Section 2.3.5 described, studies such as Winsborrow *et al*. (2010) have proposed a hierarchy of controls on ice streaming. If patterns in roughness are responsible for these spatial patterns of ice speed, then the results of this chapter suggest that roughness may be more important in controlling ice stream location than previously thought. Again, however, the difficulty in drawing such inferences is that roughness may be a response to variations in ice speed, not just a control. Furthermore, alternative evidence suggests that roughness is not the primary control on ice stream behaviour in the Siple Coast region. As highlighted in Section 2.5.1.2 for instance, the Kamb Ice Stream shows evidence of stagnation, despite the bed of this area having relatively low roughness values (Retzlaff & Bentley, 1993; Bingham & Siegert, 2009). As a result, the strong association between roughness and ice speed may again demonstrate that these parameters have captured the effects of other variables.

Although it is not possible to determine whether roughness is a control or a response to ice speed, the results of the model can be used to predict what values for various roughness variables would be expected beneath a region of streaming. Even if the parameters are merely proxies for other controls on ice dynamics, this usefulness still applies. For example, the model for the McAyeal Ice Stream predicts that in regions where

ice speeds exceed 200 m a^{-1}, the mean height of the topography is expected to be below -540 m.

Ice streams are susceptible to changes of direction or width through time (Conway *et al*., 2002), and understanding changes to the size and position of ice streams is crucial for predicting future ice sheet discharge (Paterson, 1994; Joughin & Tulaczyk, 2002; Stokes & Clark, 2003b, 2006; Schoof, 2006a; Bamber *et al*., 2010). If more knowledge on the nature of the relationship between roughness and ice speed became available, then models such as GLMs could be used to predict the future evolution of contemporary ice sheets. To demonstrate this, let us assume for the moment that roughness is a direct control on ice speed and other variables that influence ice speeds are constant. Given that the mean height of the McAyeal Ice Stream margin is currently as high as -270 m (refer back to Figure 6.4a), and the model suggests a threshold value of -540 m is required to support rapid ice speeds, lateral expansion of the ice stream would need the average height of the topography to decrease by a further 270 m. In theory, this decrease in roughness could be achieved by erosion, decomposition, or deformation for the topography (Siegert *et al*., 2005b), but the next challenge will be to identify the rate at which this change may occur. With an understanding of the temporal variability of roughness, and its role in ice dynamics, it would be possible to determine the likelihood of ice stream migration or expansion within a given time frame.

6.4.3 A further evaluation of roughness parameters

Chapter 6 presented an evaluation of roughness parameters and provided some shortlisting. However, it was also suggested that the choice of parameter may depend on the nature of the investigation. This chapter has acted as a further assessment of the parameters, identifying those most useful for studying the spatial relationships between roughness and ice speed.

Comparison of 18 roughness parameters showed that some are more related to spatial patterns in ice speed than others. One conclusion that can be drawn this is that the parameters with the strongest relationship are more useful in studying spatial patterns in ice speed. Analysis of Profile V13a aligned orthogonally to flow (Profile V13a) showed that the slope was similar inside and outside of the ice stream, suggesting it is less useful. In contrast, the sinuosity showed distinct results between areas inside and outside the MacAyeal Ice Stream. Therefore, for measuring roughness using a single parameter this method appears to be one of the most useful.

For six of the parameters, a modelling approach allowed a more detailed examination of these methods of quantifying roughness. The fact that the best model contained two types of amplitude parameters (namely, the mean height and RMS height), generally suggests

that measurements of the vertical changes in topography are the most useful. Yet, it is important to note that some amplitude parameters, such as the RMS height when used individually, were less correlated with ice speed. Furthermore, other types of roughness parameters were also useful, For example, the best model contained the shape parameter *kurtosis* and, as discussed above, sinuosity was a good stand-alone predictor of ice speed.

Modelling ice speed using roughness parameters has given an initial assessment on the methods most useful to glaciologists. Future studies might include other methods of quantifying roughness to test the relationship of these with ice speed and, thus, the usefulness in explaining spatial patterns in rates of ice flow. In particular, an evaluation of spacing parameters using this technique would help determine whether knowledge of asperity frequency would provide insight into variations in ice speed.

Aside from an evaluation of individual methods of measuring roughness, this study has also demonstrated the value of using groups of parameters. By adding more predictor variables to the model, Section 3.3.3 demonstrated that more of the variance in ice speed was accounted for, improving the fit: e.g. moving from a single independent variable to two predictors resulted in a decrease in Root MSE of 43 m a^{-1}. Therefore, whereas some sciences may use a single parameter to quantify roughness (see Chapter 5), for subglacial beds a more appropriate technique is to measure several characteristics.

As Chapter 4 described, spectral analysis measures several variables and, therefore, supports the idea of measuring different characteristics of the topography. However, the advantage of modelling over a single technique is that the various contributions of different characteristics can be assessed. For example, although the best model included kurtosis, the majority of the variation in ice speed was accounted for by the mean height, suggesting that the vertical variation is more important. For the first time, therefore, it has been possible to determine how certain variations in the shape of topography influence roughness, and which of these are most linked to patterns in ice speed.

6.5 Conclusions

Analysis of two locations in the Siple Coast ice stream area of Antarctica has shown a link between decreasing roughness and increasing ice speeds. These findings confirm the observed patterns presented in other glacial roughness studies (e.g. Bingham & Siegert, 2009). Further to previous investigations, it was possible to give a quantitative estimate of the extent of this relationship. Modelling showed that roughness parameters could be used to predict annual ice speeds to with Root MSE of 28 m a^{-1}. However, these findings are insufficient to determine whether variations in ice speed are a control or a response to ice flow.

For the first time, rather than subglacial bed roughness being related to ice speed using a single parameter, a range of topographic variables were measured. The roughness of the subglacial bed was found to vary in a number of ways, but some of these variations were more related to ice speed than others. Using GLMs it was possible to assess which variables are most related to patterns in ice speed, giving a further evaluation of the methods. Using a single parameter, the mean height and sinuosity showed the strongest relationship with ice speed suggesting that, at the scale of kilometres, vertical variations in bed height and the surface area in contact with the bed are the most linked to changes in the rate of flow.

Some roughness parameters, such as the mean height, had a strong correlation with ice speed. However, it was found that no single parameter captured all of the spatial variation in the rates of ice flow. In a change from the traditional approach of quantifying roughness using a single parameter, this study combined several parameters through the use of GLMs. A stronger fit between roughness and ice speed was produced. Therefore, the use of several parameters, each measuring different variables, appears to be a more suitable approach. The advantage of this technique, rather than using a single parameter that captures many roughness variables, is that the link between each of these and ice speed can still be identified, whereas, with a single measure it is more difficult to determine what patterns in topography have produced those values.

CHAPTER 7

Exploring the potential of quantifying subglacial bed roughness using 3D data and roughness parameters

7.1 Introduction

This chapter discusses the potential of quantifying roughness of subglacial beds in 3D. In earlier chapters, profiles have been exclusively used to analyse spatial variations in bed elevation, but these chapters also identified a number of limitations with using 2D records. Section 2.5.3 described some of the advantages quantifying roughness through the use of DEM measurements. However, the current problem with such analysis is that there are relatively few high-resolution 3D data available, at least, in contemporary ice sheet settings. Although bed elevation is increasingly being measured in 3D (e.g. Rignot, 2001; King *et al*., 2009), the logistical challenges involved in acquiring such measurements (Bartek *et al*., 1991; Hart & Rose, 2001) mean that there is still a low coverage in contemporary ice sheet environments. For example, many studies are ground-based (e.g. Jacobel *et al*., 1996) so do not measure a sufficient area to allow variations in roughness to be measured over regions as extensive as ice streams.

An alternative source of bed elevation data are DEMs from formerly glaciated terrains. Examples such as the NextMap LiDAR measurements of the UK demonstrate how some of these datasets have an extensive spatial coverage, which would permit the roughness of different regions to be compared. Another advantage of data from palaeo environments is that the resolution is often higher (see Table 2.1) than those of contemporary ice sheet beds, possibly because better access means that there are fewer logistical problems to overcome in collection. This superior resolution allows meso-scale roughness on the scale of tens to hundreds of metres to be resolved, thus making it possible to quantify the roughness of subglacial bedforms. As Section 2.5.1 demonstrated, knowledge at this scale is limited, and Chapter 4 showed how, even with re-digitising, measurements such as the SPRI radio-echo sounding record are unable to achieve this resolution.

Given that relatively little research has been done to quantify the roughness of subglacial beds using 3D records of bed elevation, there are many unanswered questions over how patterns of roughness vary with direction. For example, an issue encountered with profile data is that the orientation in which roughness is quantified along the bed affects the

results. Evidence for this comes from analysis of SPRI data (Section 2.4.3) where measurements of the bed in a parallel orientation to ice flow direction have lower values than those measured orthogonally to flow. However, it is unclear whether parallel and orthogonal aligned profiles are end members, i.e. lowest and highest roughness values respectively. With SPRI data, scientists have been limited to quantifying roughness in two orientations, with this being apparent in the summary maps of Bingham & Siegert (2009), As a result, influence of the measurement angle has never been tested. By extracting a series of profiles from DEMs, however, it is possible to measure this effect.

Another potential use of formerly glaciated terrains is to investigate the association between ice-sheet behaviour and the roughness of topography. The ability to quantify the meso-scale is an advantage as it permits roughness on the order of subglacial bedforms to be measured and related to theories on ice flow. As stated in Section 2.5.3.1, it is not necessarily easy to test the relationship between bed roughness and ice speed in formerly glaciated terrains, because both the proxies for former ice speeds and the roughness measured are based on topography. Nevertheless, it is still possible to investigate the link between roughness and ice dynamics by comparing the agreement between roughness results and reconstructions of ice speed based on other methods. For example, analysis in Chapters 4 and 7 showed that the roughness results in contemporary ice sheets show a pattern of decreasing speed as roughness decreases so, following uniformitarian principles, formerly glaciated terrains are expected to exhibit the same relationship.

7.2 Methods

7.2.1 Testing the effect of measurement direction on 2D roughness results

To investigate the directionality of roughness results it was necessary to use bed measurements taken from within a small spatial area, and gathered along profiles with a range of alignments. In contemporary landscapes, such data appear rare; no SPRI records were found to have more than two orientations for the same locality. Therefore, this project turned to generating profiles from DEM records where measurements of height are more complete.

A NextMap DEM of the UK, with a pixel size of 5 m, was used as a source of height measurements. The study site chosen was the Tweed valley, the same as that used for evaluating 3D parameters (Section 6.2.2). However, the size of the area covered was 10 × 10 km, equating to twice the size of that used in Chapter 6.

From Figure 7.1 it can be seen that this area is dominated by a broad valley formation, within which are groups of high, drumlinised features. The topography of the Tweed is characterised by elongate features, which occur in a 20 km wide belt that is over 65 km long, extending out to sea (Evans *et al*., 2005). Analysis suggests that these bedforms are

formed of till that has been smoothed and streamlined by glacial activity (Everest & Lawrence, 2006). The types of bedform in this area range from flutings to megadrumlins (Clark *et al*., 2004) with scales of these features ranging from approximately 1 m to hundreds of metres. Therefore, given the resolution of the DEMs, it is likely that the bed elevation data would capture many of these landforms. In Figure 7.1 it can be seen that features that are over fifty metres long can be clearly seen, with the orientation of their long axes appearing to form patterns aligned in west-east and NE-SW directions.

The orientation of the landforms of the Tweed, have been used to reconstruct former ice flow directions: the region is thought to have been a major pathway for the easterly drainage of the last ice sheet (Evans *et al*., 2005; Everest *et al*., 2005; Staines, 2009). Scientists have determined that the morphometry of the features in this region is analogous to those beneath areas of the West Antarctic Ice Sheet (Everest & Lawrence, 2006) and, following uniformitarian principles, this similarity has been used to reconstruct the former ice speeds of the Tweed. The relatively large size of the landforms, particularly in terms of their length and elongation, are consistent with topographic characteristics typical of fast flow environments (Stokes, 2001; Stokes & Clark, 1999). This evidence suggests that the area was once a palaeo ice-stream track, with Everest *et al*. (2005) describing the Tweed as the best British example of such flow.

In addition to the elongate bedforms, the topography of the Tweed varies at larger scales. In particular, the region sits between the Cheviot and Lammermuir hills. Given that the setting is within a large-scale valley formation, the Tweed may be analogues with topographically controlled ice streams (Staines, 2009) where, as Section 2.2.1 described, ice flow is channelled into a depression causing rapid flow by increasing shear stress (Hindmarsh, 2001; Bennett, 2007).

The high degree of parallelism between the features has been used as evidence that the features were formed during the same glacial cycle during the Devensian glacial period, rather than the cross-cutting topography typical of palimpsest landscapes produced by multiple glacial events (Clark, 1999). Yet, during this period there is evidence of changing ice behaviour: for example, evidence suggests that the Tweed Ice Stream changed direction in response to the development of the North Sea Lobe of the last ice sheet (Staines, 2009; Livingstone et al., 2012).

If the inferred ice dynamics are correct, the area might be analogous to that beneath current ice streams, such as those studied in Chapter 6. Having identified the research site, the next stage was to digitise profiles across the study site.

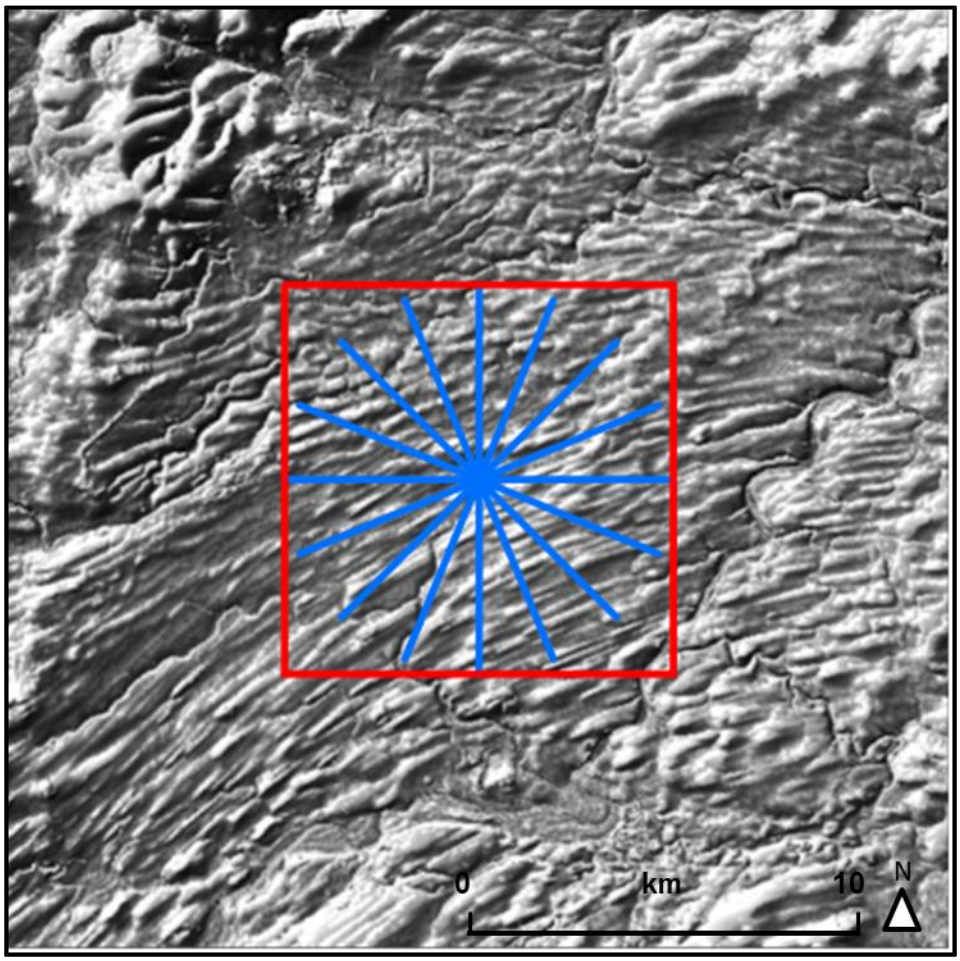

Figure 7.1a: Study site for comparing the effect of measurement direction on roughness. Blue lines depict the eight profiles used. The red area shows the extent of the study area, and is 10 × 10 km in size. The NextMap DEM in the background shows the position of the study area within the Tweed. It can be seen that the location is situated within a large valley, with higher topography to the NW and SE. Reconstructions of ice-sheet history of this area suggest that the direction of flow was from SW to E (Everest et al., 2005)

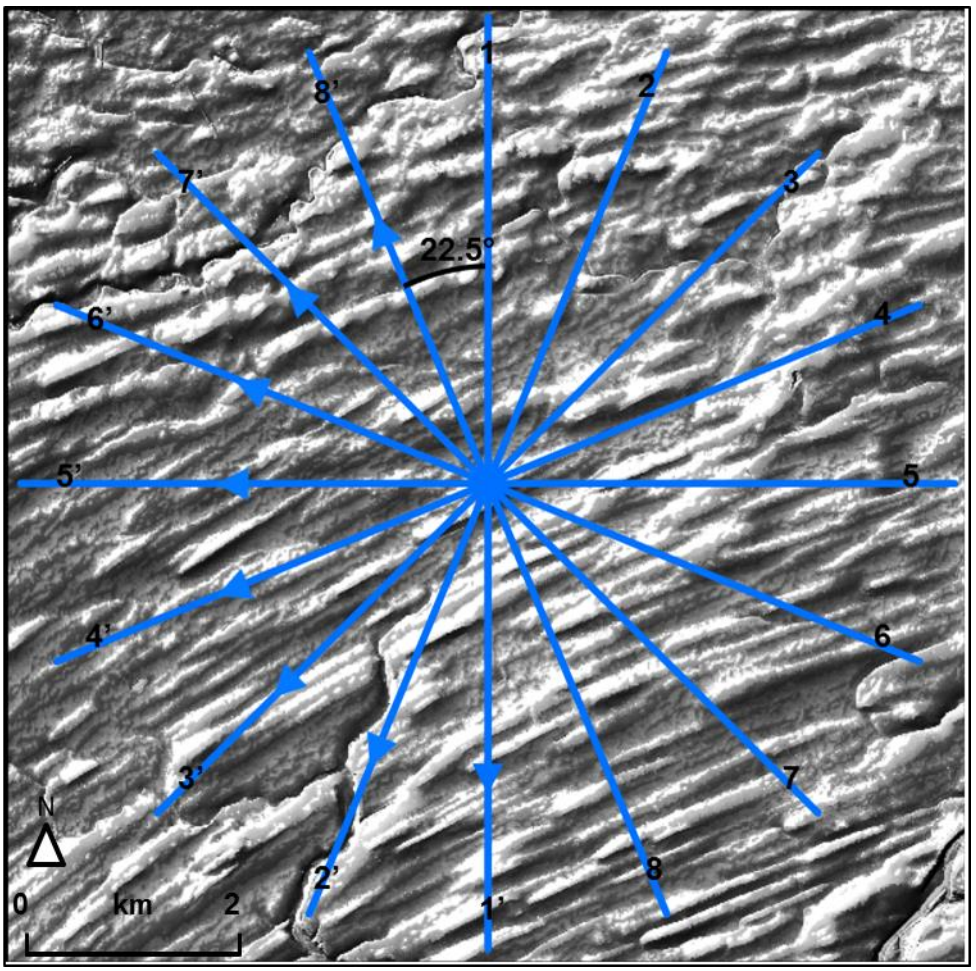

Figure 7.1b: The eight profiles used for testing the effect of measurement direction on roughness. Note the running direction of each profile shown by the arrowheads. It can be seen that the underlying topography has a pattern, with the long-axis of the features approximately parallel to Profile 4

The effect of profile orientation was tested using eight profiles. The first step was to digitise these profiles and overlay them onto the bed elevation data (see Figure 7.1a above). To ensure the total line length of each profile would be 10 km, and the angle between profiles was exactly 22.5°, the locations for the ends of the profiles were determined using trigonometry. These sixteen *x*,*y* coordinates, plus the origin node, were then imported into ArcGIS. Using these shapefile points, profiles were then drawn to connect these points as straight lines through the origin. Measurements of elevation were then needed for positions along each profile. Initially, each profile consisted of a vector feature, based on the start point and end point of the line. To extract measurements, it was necessary to break each profile down into a series of points. This was achieved using the Hawth's Tools extension to ArcMap that determined the *x,y* coordinates at 5 m intervals along each profile. The same extension was then used to extract height values from the DEM for each of the newly created points. These data could then be used to quantify roughness.

For each profile, the coordinates and heights of each point measurement were imported into Stata. Note, when calculating the roughness the analysis the results had to be inputted in order, which meant that there is a direction to the moving windows. As shown in the last chapter, it is important to consider these directions when interpreting results. The arrowheads on Figure 7.1b above show the analysis directions used. Reconstructions of this area suggest that former ice flow was towards the NE direction across the image, which means that some profiles were analysed in an opposite direction to ice flow. However, this is not a problem and, with analysis of the SPRI datasets for example, is actually common (Bingham, personal communication 11/02/09). The data were gathered without making prior assumptions about the former ice behaviour. Importantly, the roughness values produced at each point along the profile are the same regardless of the direction measurements are fed into the program; a plot of the results only shows the position of the values from an arbitrary datum.

Using the program for 2D roughness analysis (the same as that in Chapter 7), results were calculated using a 400 m window. Deciding the size of analysis window was a difficult choice because, on the one hand, the resolution permitted very short windows to be used, but other glacial studies had reported that many of the elongated ridges in this region had sizes over 1000 m (Staines, 2009). To fully capture a single feature of this size it would have been necessary to have sampling lengths of at least 200 points. Choosing a window size of 400 m meant that each set of results, (provided the parameter used all observations), was based on 80 points. Although these windows might not capture the total length or width of many features, they did maintain a good spatial resolution.

7.2.2 A regional comparison of roughness in formerly glaciated terrains

In the UK, many studies have used the morphology and distribution of bedforms to reconstruct the last British Ice Sheet (see Evans *et al*., 2005 for a review). In this chapter, the roughness of four regions was measured using the 3D parameters. Using these results, a reconstruction of the former ice speed in the area was made using the hypothesis that speeds increase as roughness decreases. From a review of the literature the reconstructions of these areas based on other evidence were established. This evidence included numerical modelling (e.g. Hubbard *et al*., 2009), as well as bedform morphometry, erratic dispersal mapping, and geology. These reconstructions were then compared to test the agreement.

The four regions chosen for study are shown in Figure 7.2. The characteristics of these regions in terms of their geology are now described, and the reconstructions made by other studies based on paleo-environmental indicators are also presented. It is notable that, none of these reconstructions suggest that the roughness of the topography was the primary control on ice dynamics. Nevertheless, it is also clear that the shapes of

topography, i.e. their roughness, differ between the different regions, and these patterns are thought to, at least in part, arise from differences in ice behaviour. These areas were selected because they all showed evidence of glacial activity, with three of them exhibiting drumlinoid topography (Evans *et al*., 2005) at the meso-scale. This indicates that, although there may have been some post-glacial modification to the landscape, much of the glacial signal is preserved. Other evidence for these areas having being formerly glaciated included the use of British Geological Survey data that showed the distribution of glacial sediments and glacially-eroded bedrock. The choice of study site was based primarily on the differences in the shape of their topography, particularly the presence and size of bedforms, and the interpretations on ice dynamics that scientists had drawn from these variations.

The first site studied was the Tweed valley, and the precise grid from which measurements were taken is depicted in Figure 7.3. Note that this location was the same as that used to test the effect of profile direction on results, allowing the parameter results of 2D and 3D parameters to be compared. Recall from Section 7.2.1 that the long, elongate bedforms in this region suggest that the topography of the region facilitated the development of streaming flow, making the area a major drainage pathway (Evans *et al*., 2005; Everest *et* al., 2005; Everest & Lawrence, 2006).

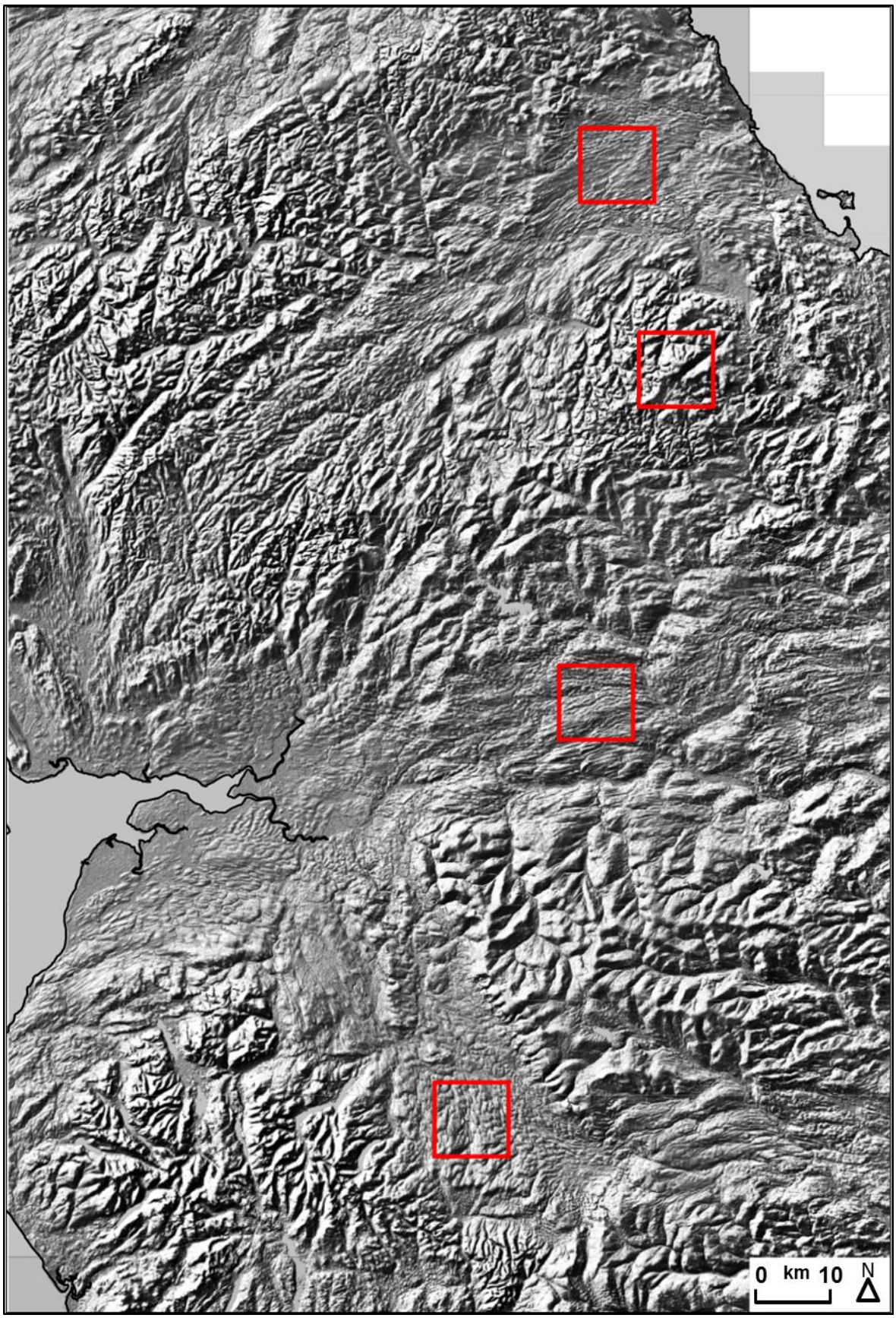

Figure 7.2: NextMap DEM of the UK used as the source of bed elevation measurements, orientated to north. The four study sites analysed are shown by the 10×10 km red boxes. The most northerly area is the River Tweed valley site, and that below to the south is the Cheviot study area. The central location is the Tyne Gap, and most southerly location is the Appleby area

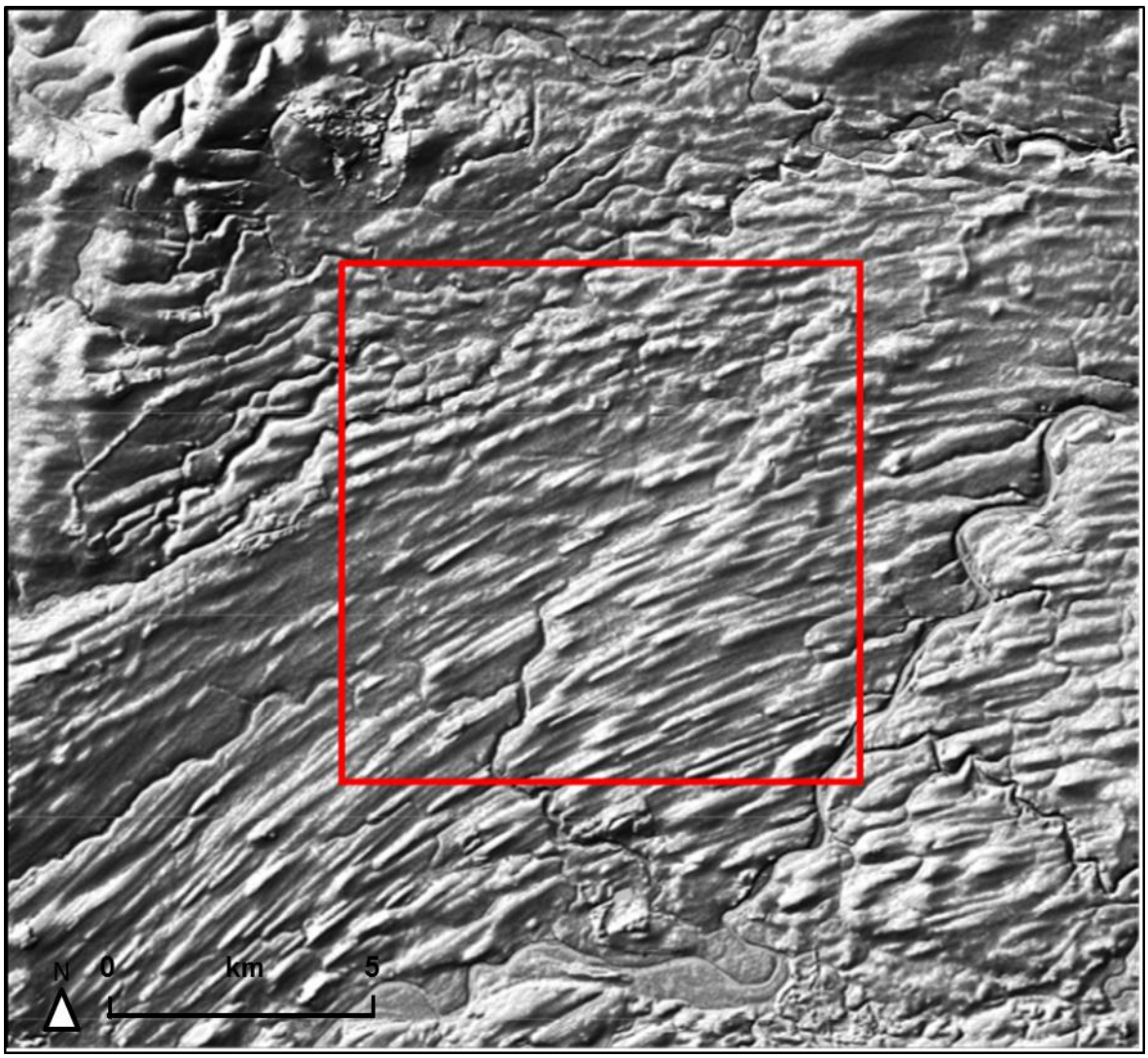

Figure 7.3: The River Tweed valley study site. The bed elevation measurements were taken from within the 10 × 10 km grid shown above. The NextMap image clearly shows a directional pattern, which has been identified as elongated subglacial bedforms (Evans & Lawrence, 2006). Nevertheless, from the presence of channels it is clear that the region has also undergone some post-glacial modification from fluvial activity

The second location investigated was the Tyne Gap (Figure 7.4). As with the Tweed this area is also characterised by elongate features. These form a belt, smaller in coverage than those of the Tweed, with a width up to 6 km wide, and approximately 20 km long (Krabbendam & Bradwell, 2011). Analysis of the drift geology shows that these landforms consist of sediments that have been modified by glacial activity (Everest & Lawrence, 2006; Livingstone *et al*., 2012). However, in addition to sedimentary features, some of the elongate bedforms are composed of bedrock, such as the doleritic Whin Sill (Krabbendam & Bradwell, 2011).

While deformation has been a possible mechanism for the formation of the Tweed bedforms, the occurrence of bedrock landforms suggests that at least some of those in the Tyne Gap have an erosional origin. Differences in rock hardness can produce

differential rates of abrasion (Roberts *et al*., 2009), so the sedimentary limestone may have been eroded more quickly, with the volcanic rocks being left as streamlined bumps.

Reconstructions based on landform morphometry have been used to reconstruct the ice dynamics of this region, and the interpretations are similar to those of the Tweed. For example, size and orientation of the landforms suggest that ice streamed rapidly in an easterly direction (Evans *et al*., 2009; Livingstone *et al*. 2010). The situation of the Tyne Gap within a large-scale trough formation also suggests that streaming in this area was topographically controlled, with convergent ice flow into this area (Mitchell, 2007). Despite the general easterly trend, evidence of overprinted bedforms suggests that there was some temporal variation in the ice dynamics of the area (Evans *et al*., 2009).

It is because of the similarities between the Tyne Gap and Tweed that both sites were chosen: it was predicted that the roughness values of both sites would be similar. Nevertheless, a number of differences must be acknowledged, and it is possible that these would cause the roughness results of both areas to vary. First, given that the geology of the two regions shows some variations, it is possible that the mechanisms of ice flow differed. For example, although the geology of both areas is predominantly sedimentary, the Tyne Gap also comprises igneous rocks. As a result, in till-covered areas of the Tweed and Tyne Gap, ice flow may have occurred via sediment deformation, impermeable volcanic topography of the Tyne Gap would also have favoured sliding (Paterson, 1994).

Like the Tweed, the stratigraphic evidence of the Tyne Gap suggests that the topography of the area has evolved through time in response to changing ice dynamics. For example, the flow patterns of the area appear to have varied as a result of the changing dominance and positions of ice divides and ice lobes (Livingstone *et al*., 2008, 2012). However, the Tyne Gap also shows topographic evidence for ice sheet retreat in the form of a series of transverse moraines, thought to have been formed by the gradual recession of ice sheet in this area (Livingstone *et al*., 2012). Therefore, although such features are of a glacial origin, the present shape of the topography is likely to have some differences from that of the bed during the time of ice flow.

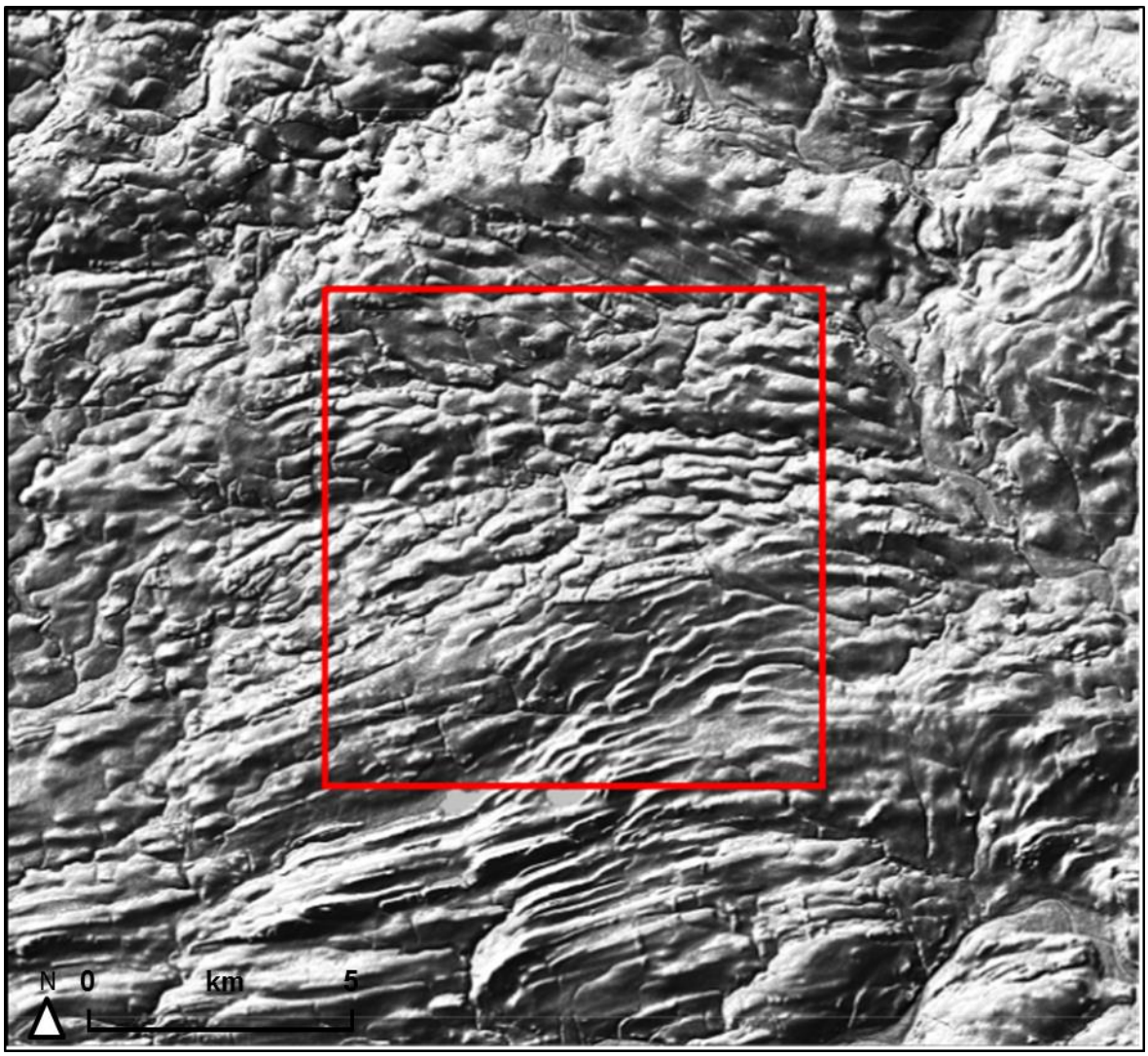

Figure 7.4: Tyne Gap study area. Like the Tweed, this area exhibits bedforms within a large valley formation

The third study region was situated near Appleby (see Figure 7.5). Like the Tweed and the Tyne Gap, the topography in this area is drumlinoid (Mitchell & Riley, 2006; Livingstone *et al*., 2012), and has been interpreted as a directional pattern with a long axis orientation parallel to former ice flow direction (Evans *et al*., 2005, 2009). The geology of the area comprises sedimentary rocks, with an overlying drift of glacial till (Hughes, 2003a, b). Compared to the Tweed however, with its till thickness of approximately 60 m, the British Geological Survey (BGS) describe that of Appleby as being a *veneer*, with a typical thickness of less than 5 m (Hughes, 2003a). As a result, many of the drumlins of this area are composed of till but have rock cores.

Relative to the size of features in the River Tweed study area, the bedforms in this region are smaller. As such, although exhibiting a directional pattern, the ice speed in this region has not been inferred as streaming. Therefore, relative to the Tweed and Tyne Gap, this Appleby area appears less important for the glacial drainage history of northern Britain. Another distinction with the bedforms in this region is that they are relatively more variable

in terms of their orientations (Evans et al., 2009). This suggests that these features were formed beneath ice that varied in direction, which can cause overprinting where the shape of the bedforms changes through time (Mitchell & Clark, 1994).

By choosing this site it was possible to determine how the size of subglacial features affects the roughness. Furthermore, this site was used to test the sensitivity of the parameters for developing roughness signatures. With a similar type of bedforms in this area to the Tweed and Tyne Gap, one might expect some of the roughness results to be similar. If the values yielded were very similar then this would suggest that roughness signatures cannot be developed, because the parameters have not captured the differences in size. However, if the roughness results are similar but with some distinctive characteristics, this would lend support to the notion that parameter values can be used as criteria for identifying assemblages of bedforms.

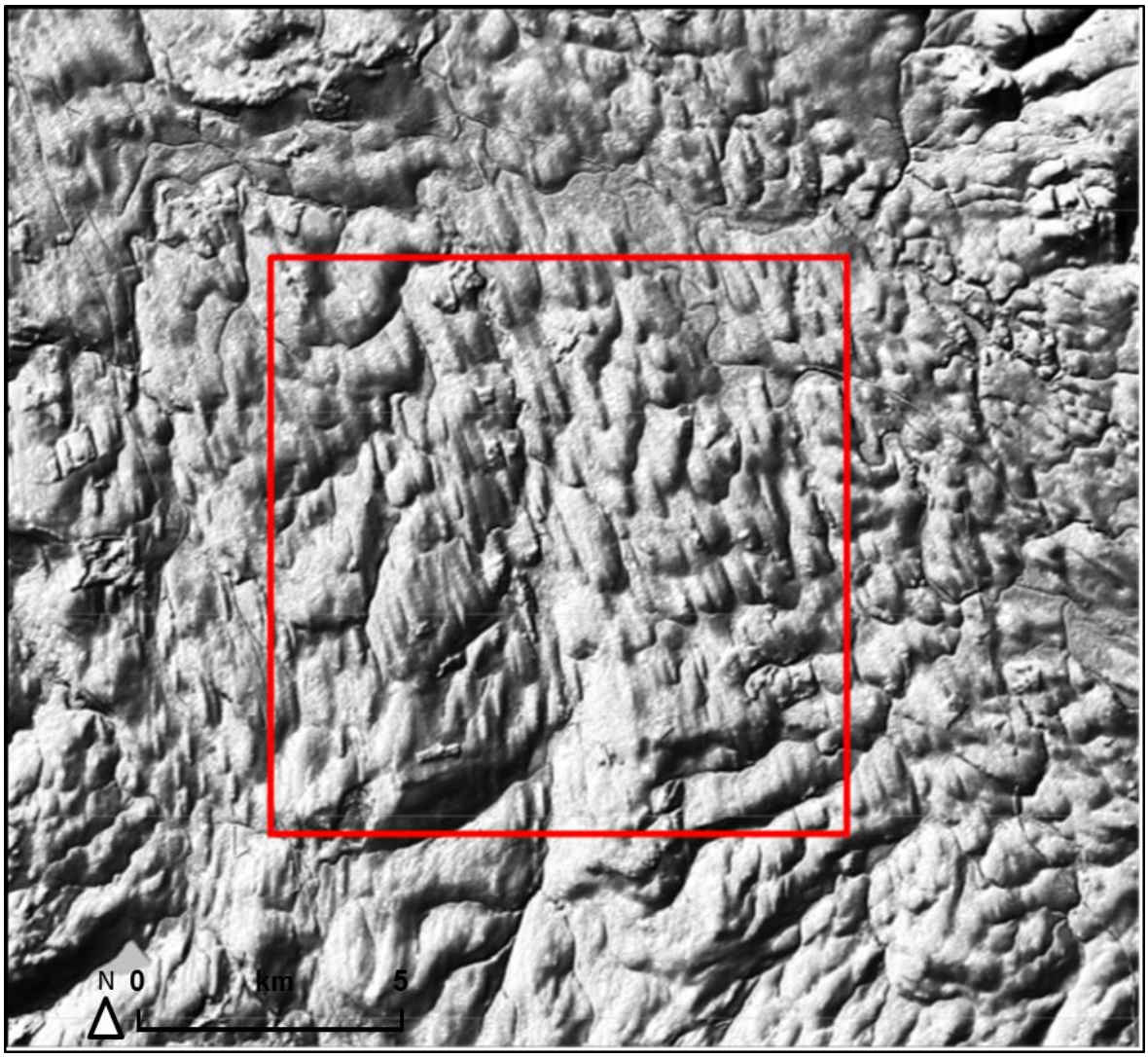

Figure 7.5: Appleby study site. This region once again exhibits drumlinised features; reported sizes are smaller than those in the Tweed and the Tyne Gap

The forth location analysed was an area of the Cheviots (see Figure 7.6) that lies between the Tweed and Tyne Gap study sites. However, whereas the geology of these two areas comprises till-covered surfaces, the Tweed has a thinner covering of till. Instead, the geology of the area has been identified as *unmodified* bedrock, suggesting the area was covered by the ice but little ice erosion occurred (Everest & Lawrence, 2006).

Given that little modification of the topography appears to have occurred, the evidence suggests that the former ice sheet was frozen to the bed in this area. This, and the fact that ice in the surrounding region appears to have diverged around the Cheviots (Everest & Lawrence, 2006; Staines, 2009) has been used infer an ice dome over this region.

This area was selected because the inferred speeds in this area are markedly different from those of the Tweed and Tyne Gap. Having selected study sites, bed elevation data had to then be collected from these regions.

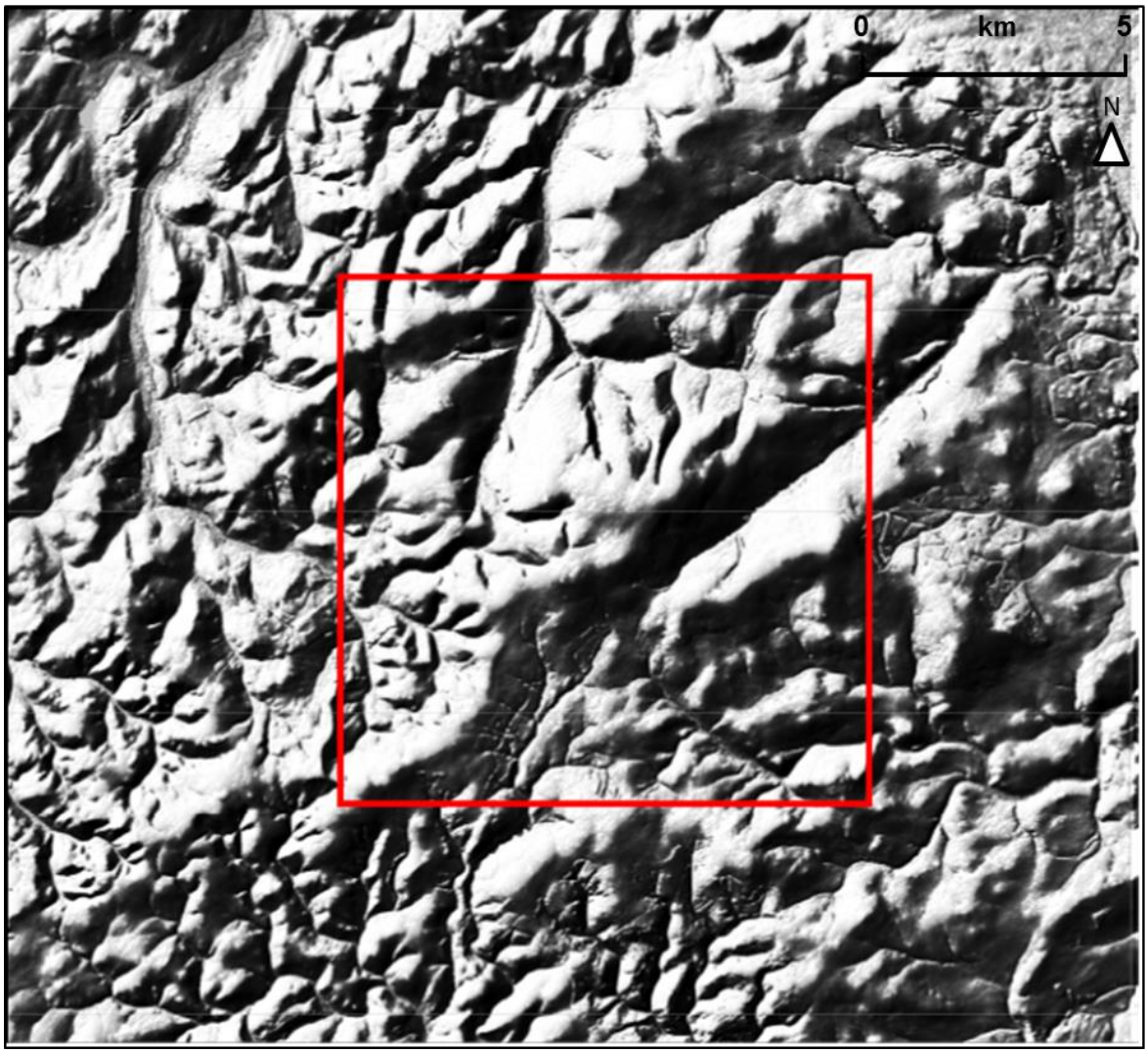

Figure 7.6: the Cheviot study site. With its high elevation, this area is reported as bedrock that has been unmodified by ice flow. As such, it does not exhibit drumlinsed features

In all four of the study sites there are a number of features, some appearing glacial in origin, and others formed by other processes. In the area between the Tweed and Cheviots sites, the occurrence of channels has been used as evidence to infer an interaction between areas with differing flow speeds (Staines, 2009). Studies of Jakobshavn Isbræ, Greenland, have shown that large amounts of strain occur along zones where there is a strong difference in the rates of flow. This extensional force can produce crevasses that allow meltwater to penetrate the bed (Mayer & Herzfeld, 2000), causing the development of subglacial drainage channels (Paterson, 1994). As a result, the topography of the bed may be a product of interactions between different flow speeds. To minimise such effects, the areas chosen in this project are beyond this inferred boundary between fast and slow flow, although it is important recognise that the topography in any of the zones may have been influenced by external factors.

With all four study sites it is also acknowledged that the shape of topography has not been entirely formed by glacial activity. For example, the landscape of the Cheviots exhibits a number of incised fluvial channels (Staines, 2009), and the Appleby region is famous for its extensive Carboniferous limestone pavements (Hughes, 2003). Nevertheless, given the scale of the features, such as the elongate bedforms in three of the study sites, it is clear that for ice sheet activity has played a key role in the development of these landscapes.

The NextMap DEM was again used as the source of height measurements. To ensure each study area was the same size, a 10 × 10 km polygon was repositioned over each location and used as a mask, with all pixels within this boundary being sampled. Calculating roughness was done following the same procedure as the 3D evaluation, with analysis over a 400 × 400 m moving grid.

To allow a true comparison of the 2D and 3D results (in the Tweed study site) it was necessary to ensure that the same scale of roughness was measured. Ideally a direct comparison would have been used by ensuring the same maximum wavelength was used. This could have been done by selecting a 400 × 400 m mesh. However, given the relatively large size of such a grid combined with a high pixel density, considerable processing power would have been needed to generate the results for a moving grid of this size. Therefore, analysis of the region was done at the regional scale by producing summary roughness statistics for the whole 10 ×10 area. Although this is imperfect, the 3D results will still capture all of the scales of roughness as measured by the 2D.

7.3 Analysis

8.3.1 Influence of measurement direction on 2D parameter results

Figures 7.7 shows summary statistics for the roughness parameter results of each profile. Some parameters show a pattern, with a progressive increase or decrease in the results with changing orientation, depending on the type of parameter used. When considering the actual values, the differences are relatively small, with many parameters having a range in the average value of less than 10 m yet, the majority of parameters show some variation based on measurement direction.

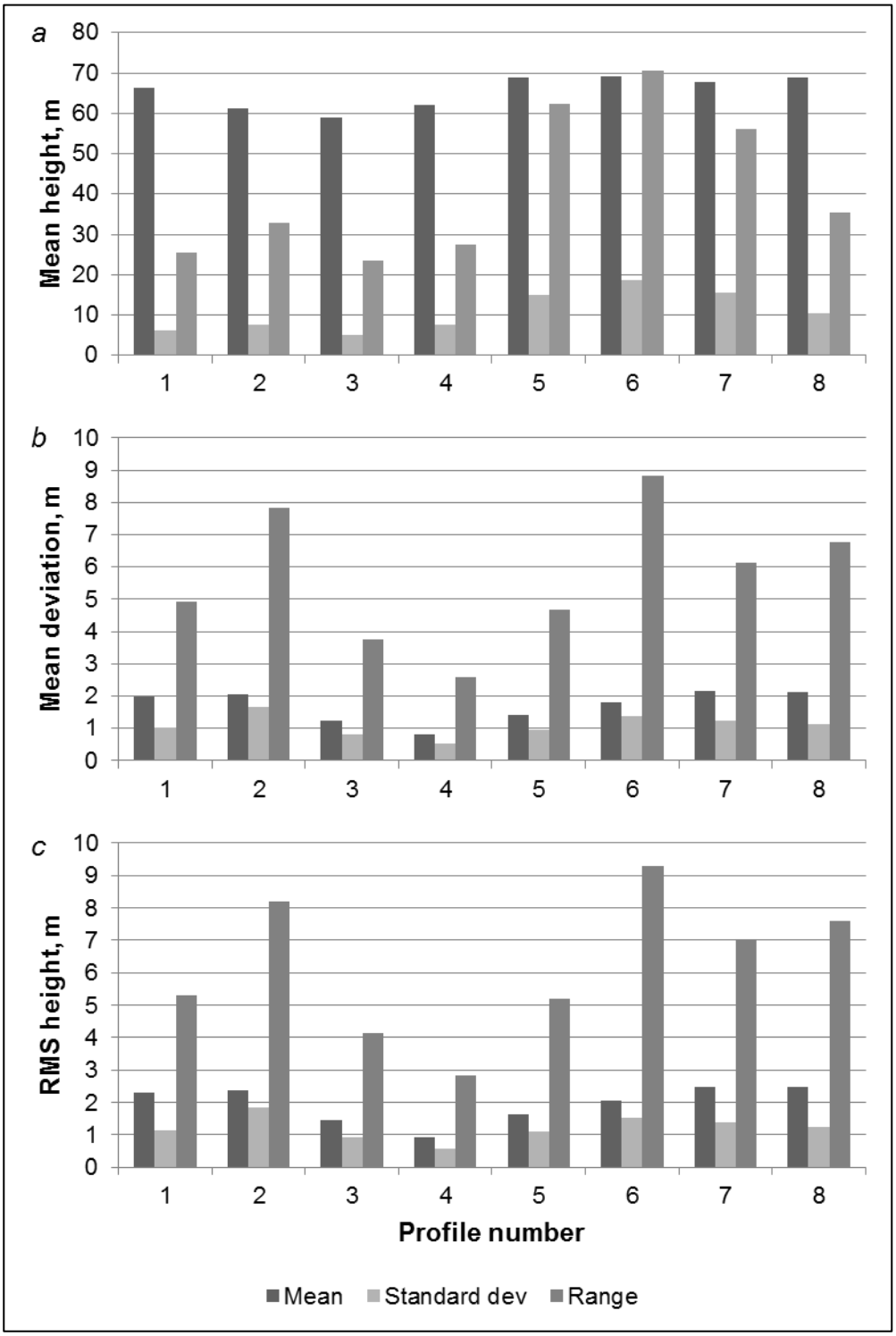

Figure 7.7 (a to c): Roughness results for the eight profiles. Graphs here show amplitude parameters that give a general summary of vertical variations in height

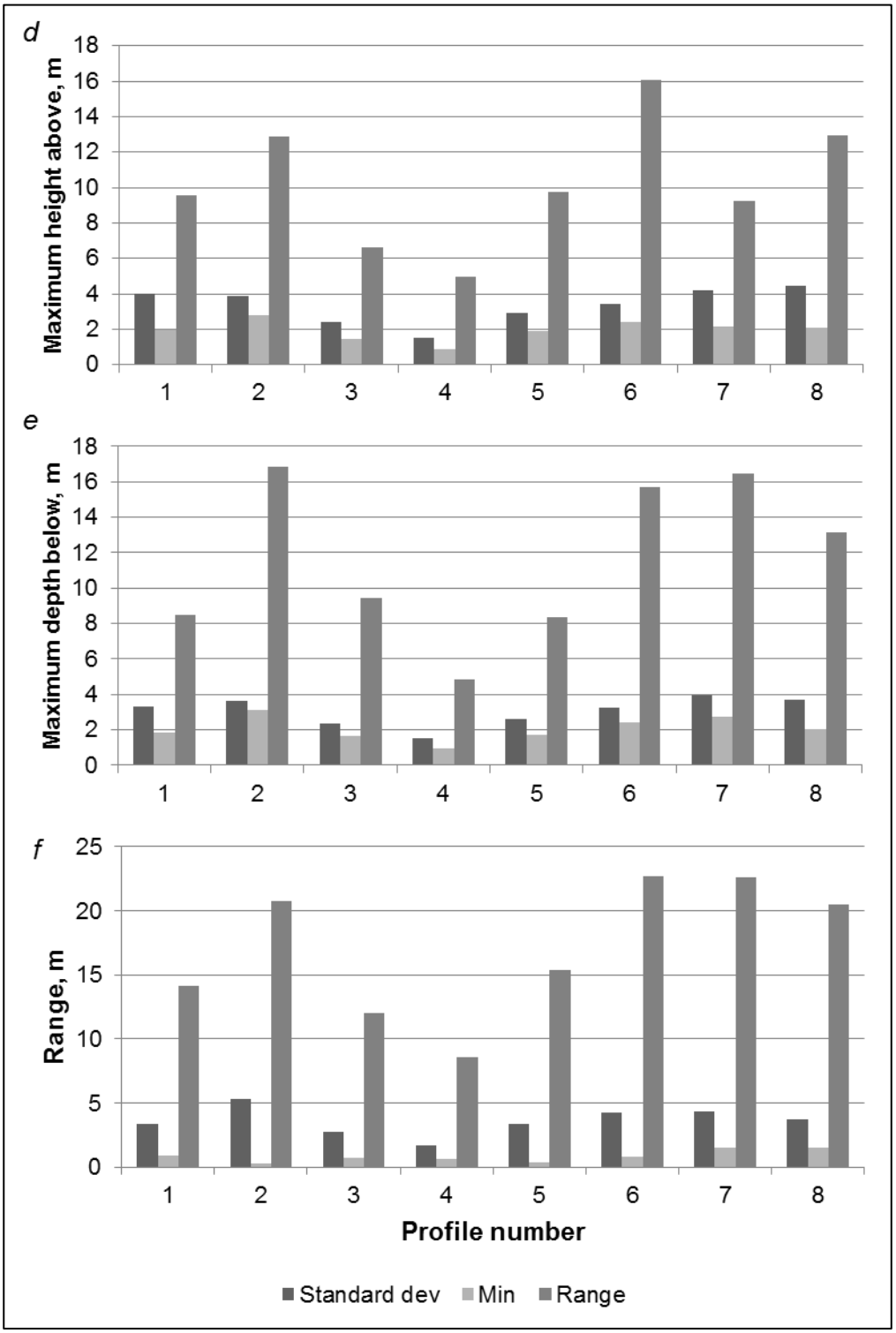

Figure 7.7 (d to f): Roughness results for the eight profiles. Graphs here show amplitude parameters that measure extreme values, and the range that uses these to summarise the overall variation in bed elevation

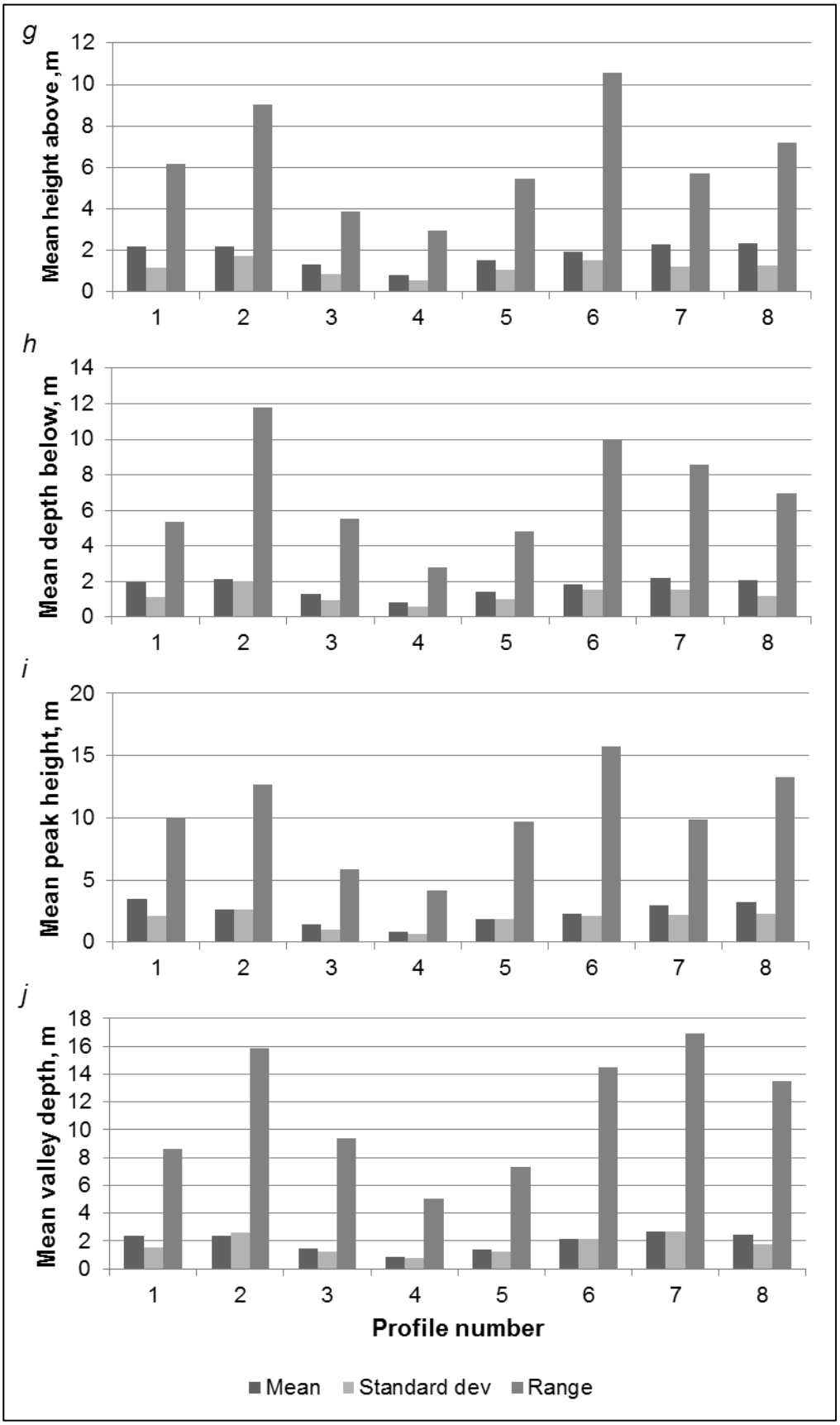

Figure 7.7 (g to j): Roughness results for the eight profiles. Graphs here show amplitude parameters that summarise bed elevations above and below the mean line, and those that measure the average height/depth of peaks or valleys

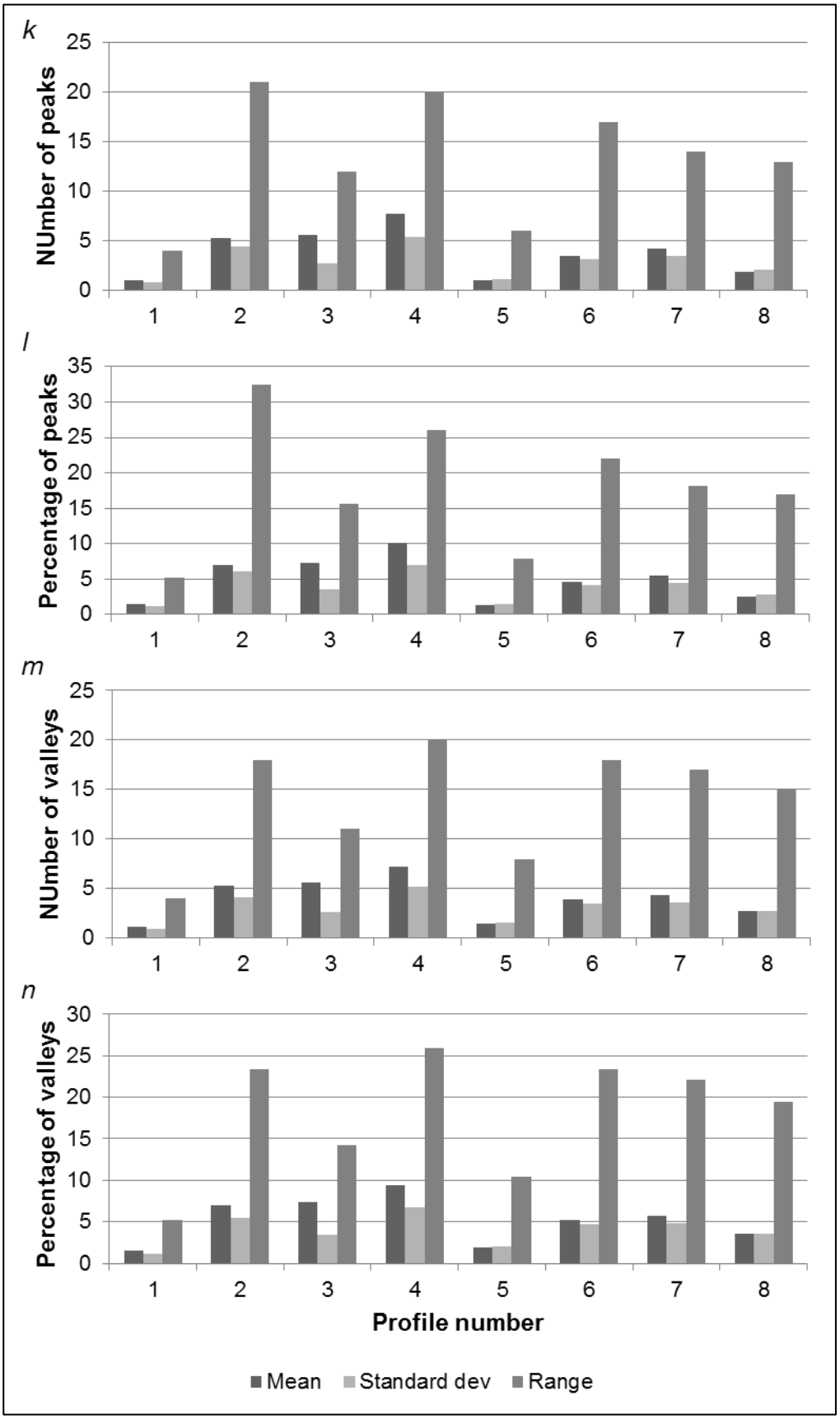

Figure 7.7 (k to n): Spacing parameter roughness results for the eight profiles, showing variations in the frequency of asperities

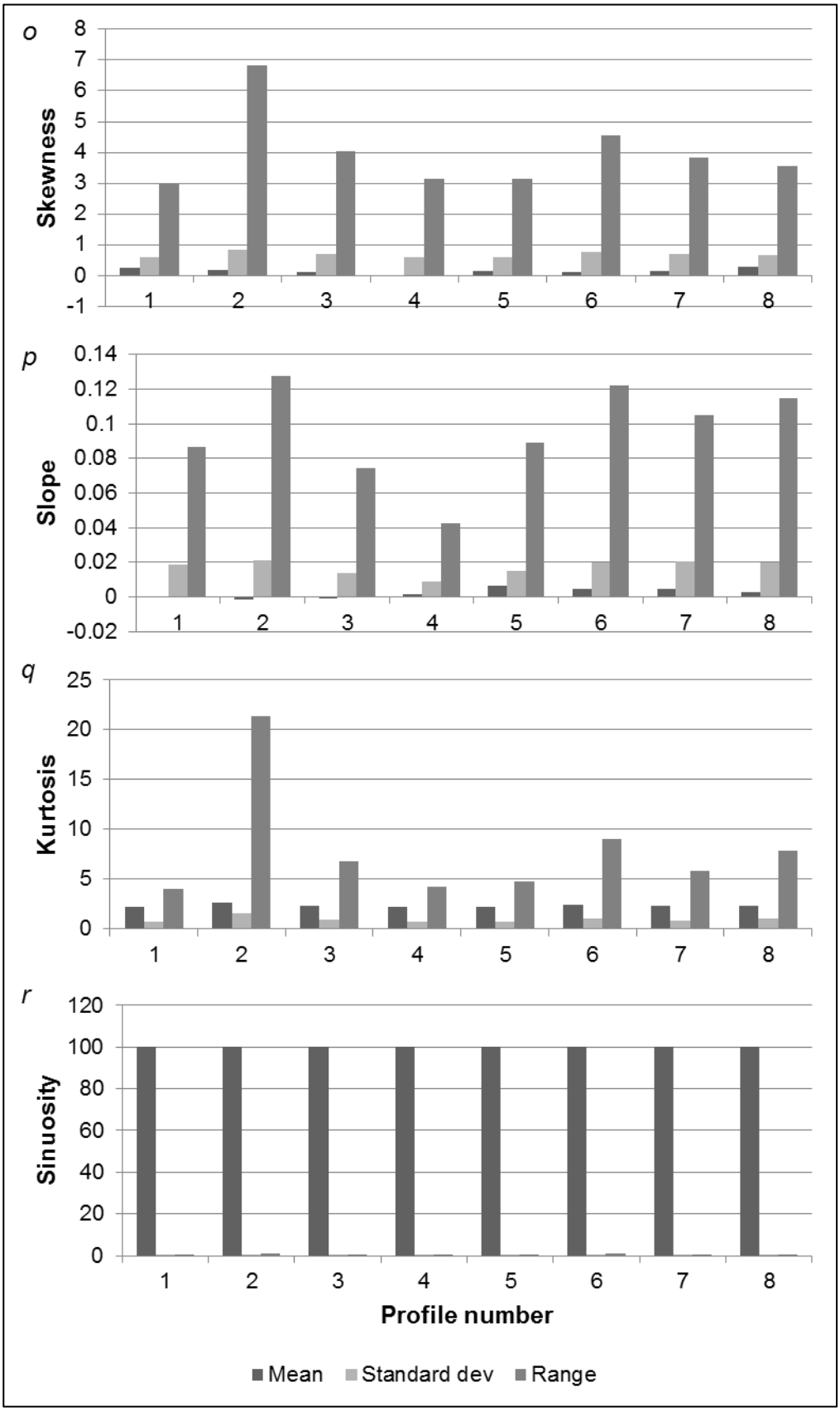

Figure 7.7 (o to r): Shape parameter roughness results for the eight profiles

For many of the amplitude parameters, such as the mean deviation, the results for Profile 4 were the lowest, and increased radially from this alignment. From Figure 7.1b it can be seen that the orientation of this profile is aligned with the former flow direction. For most of the parameters the roughness of Profiles 3, 4, and 5 are generally the lowest. Therefore, formerly glaciated terrains have a similar pattern as those seen in contemporary ice-sheet beds (Section 6.3.2), where roughness measured along the direction of ice flow is lower.

The profile with the highest values was less consistent but Profiles 2, 6, and 7 consistently produced high values. The difference in orientation between Profiles 2 and 4 is just 22.5°, while that between Profiles 4 and 7 is 67.5°. As well as the mean roughness value for Profile 4 being lower than the other profiles, the range is also lower showing that the results are more consistent along this profile length. The largest ranges correspond to the areas where mean amplitude values were highest.

Spacing parameters also show that there is a pattern of changing orientation. However, this contradicts the amplitude results. Although the amplitude parameter results for Profile 4 were the lowest on average, the number of asperities (both peaks and valleys) is highest for this profile. Therefore, using the former set of methods this profile aligned parallel to the bed would appear the least rough but, if roughness is assumed to increase as the number of asperities increases, the transect along the valley floor appears rougher than those measured across it.

7.3.2 UK regional variations in the roughness of the palaeo ice-sheet bed

Figure 7.8 shows the summary roughness results for the four summary sites (with Table 7.1 giving the specific values). Note that, because the focus of this investigation was to test compare between different regions, the overall roughness of these areas was of primary interest. The intention was not to investigate spatial patterns within each of these areas. Therefore, summary roughness values were produced for each site, rather than analysing over a grid. Although this technique does not permit smaller-scale patterns of roughness to be displayed, unlike the approach of using profiles, all directions of roughness are still taken into account. Furthermore, the number of points on which 3D results are based is considerably higher than those using 2D analysis. As a review of the 3D methods demonstrated (Section 5.4), this approach gives one summary value for each parameter, and Figure 7.8 demonstrates that they can be graphed clearly. It is clear that different localities have produced variation in the results for all parameters. For each method of quantifying roughness Table 7.2 shows the position of each study site on a spectrum of increasing values.

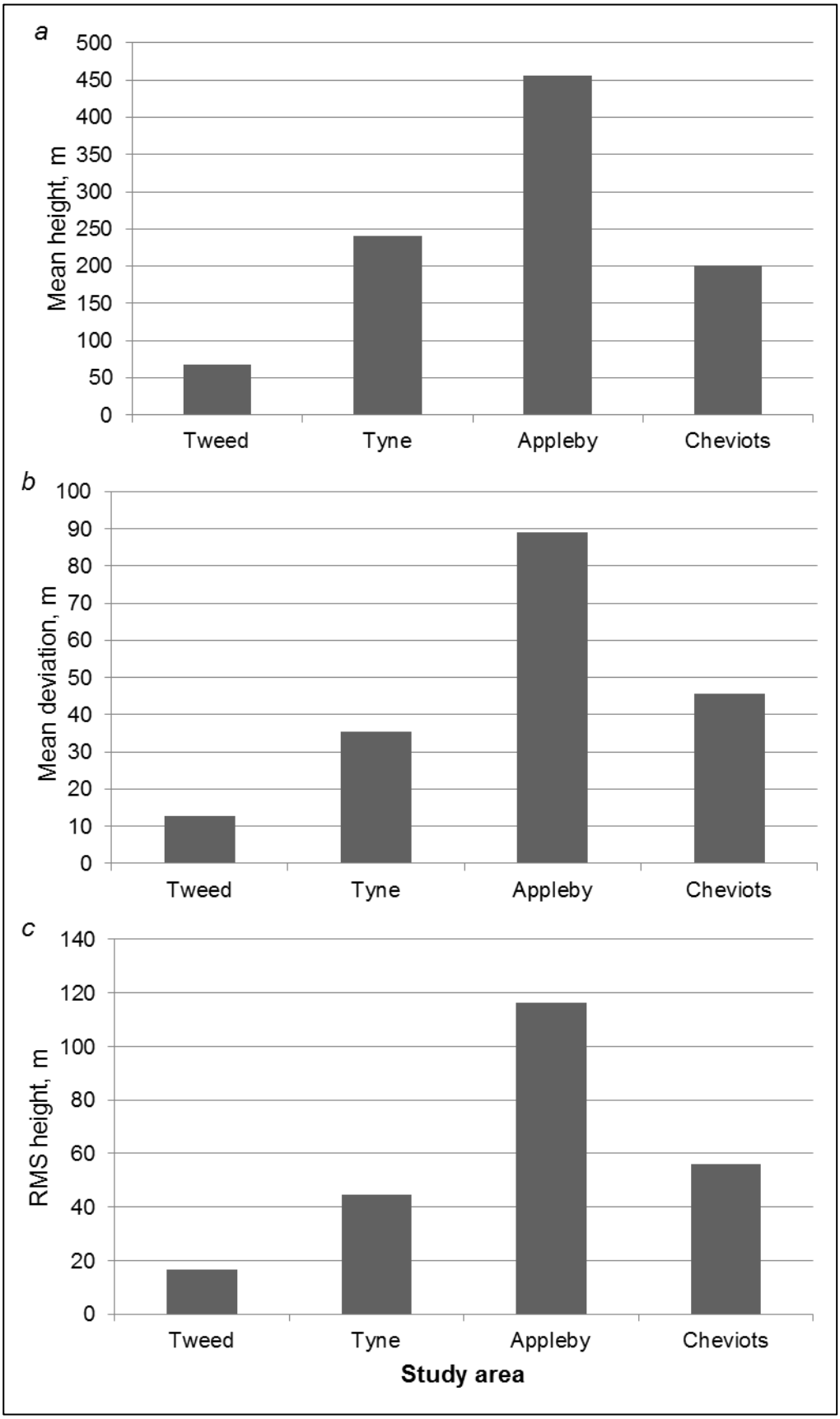

Figure 7.8 (a to c): Summary statistics between the four study sites for the amplitude parameters that quantify roughness in 3D

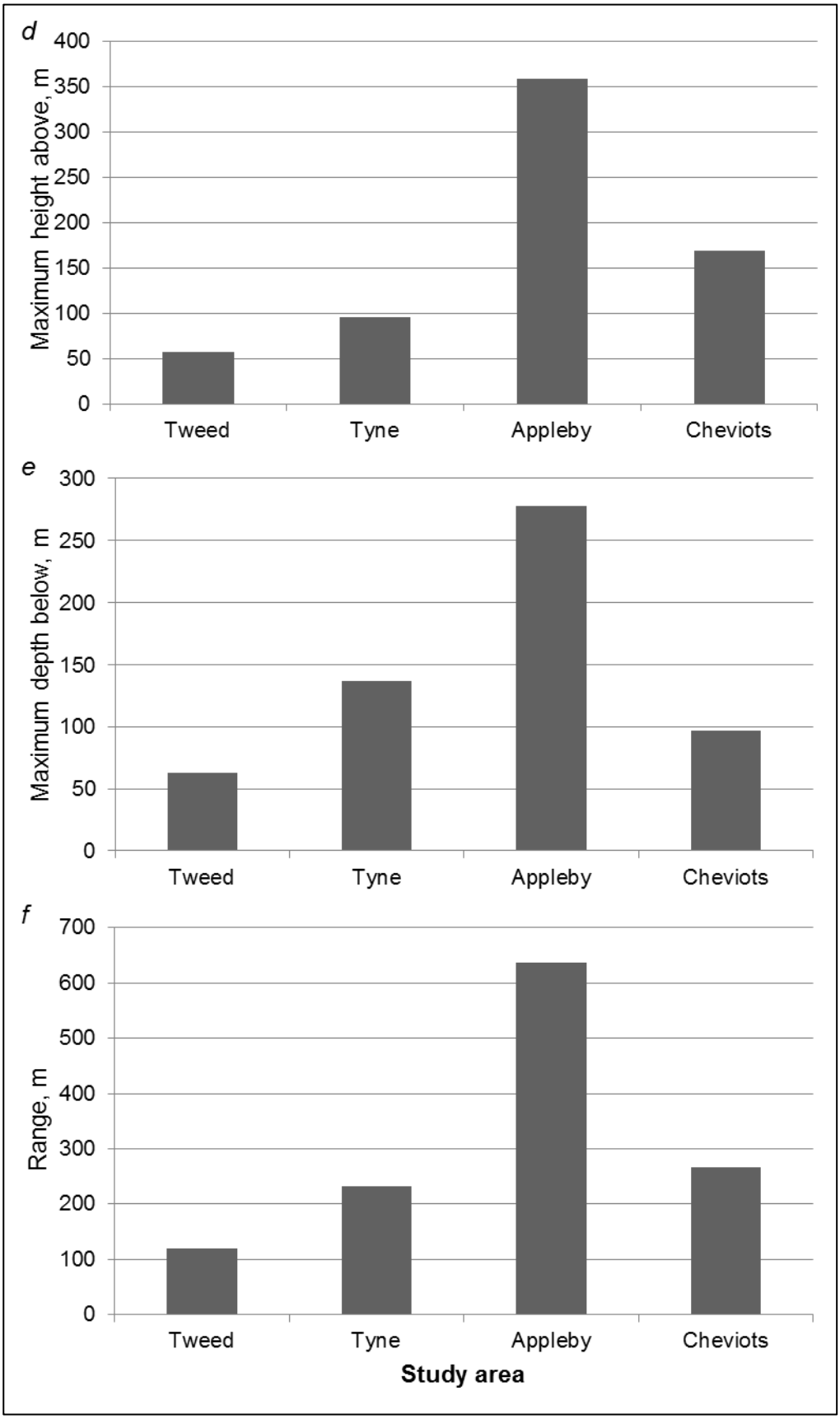

Figure 7.8 (d to f): Summary statistics between the four study sites for the amplitude parameters that measure extreme amplitude values

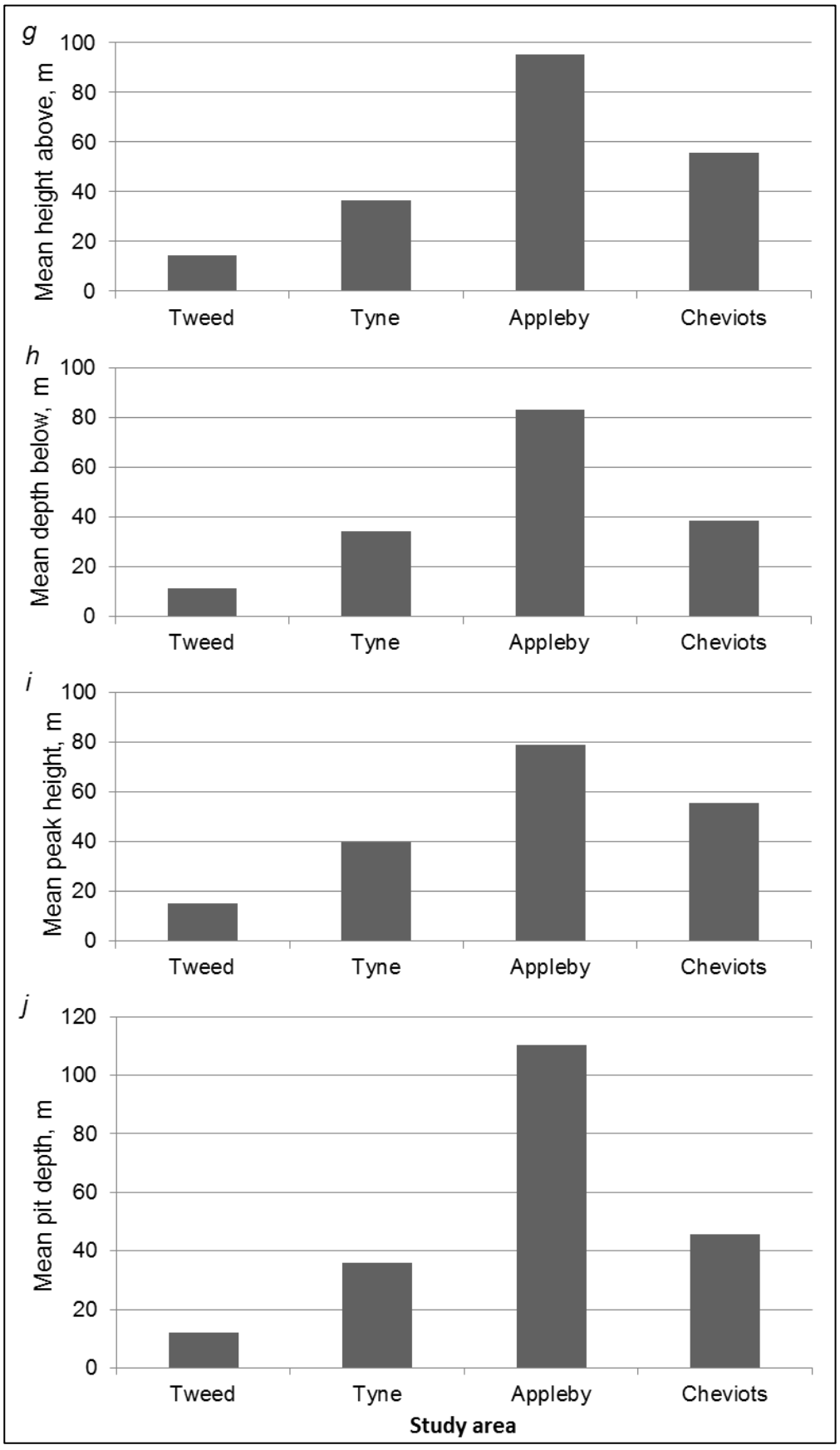

Figure 7.8 (g to j): Summary statistics for the amplitude roughness parameters between the four study sites

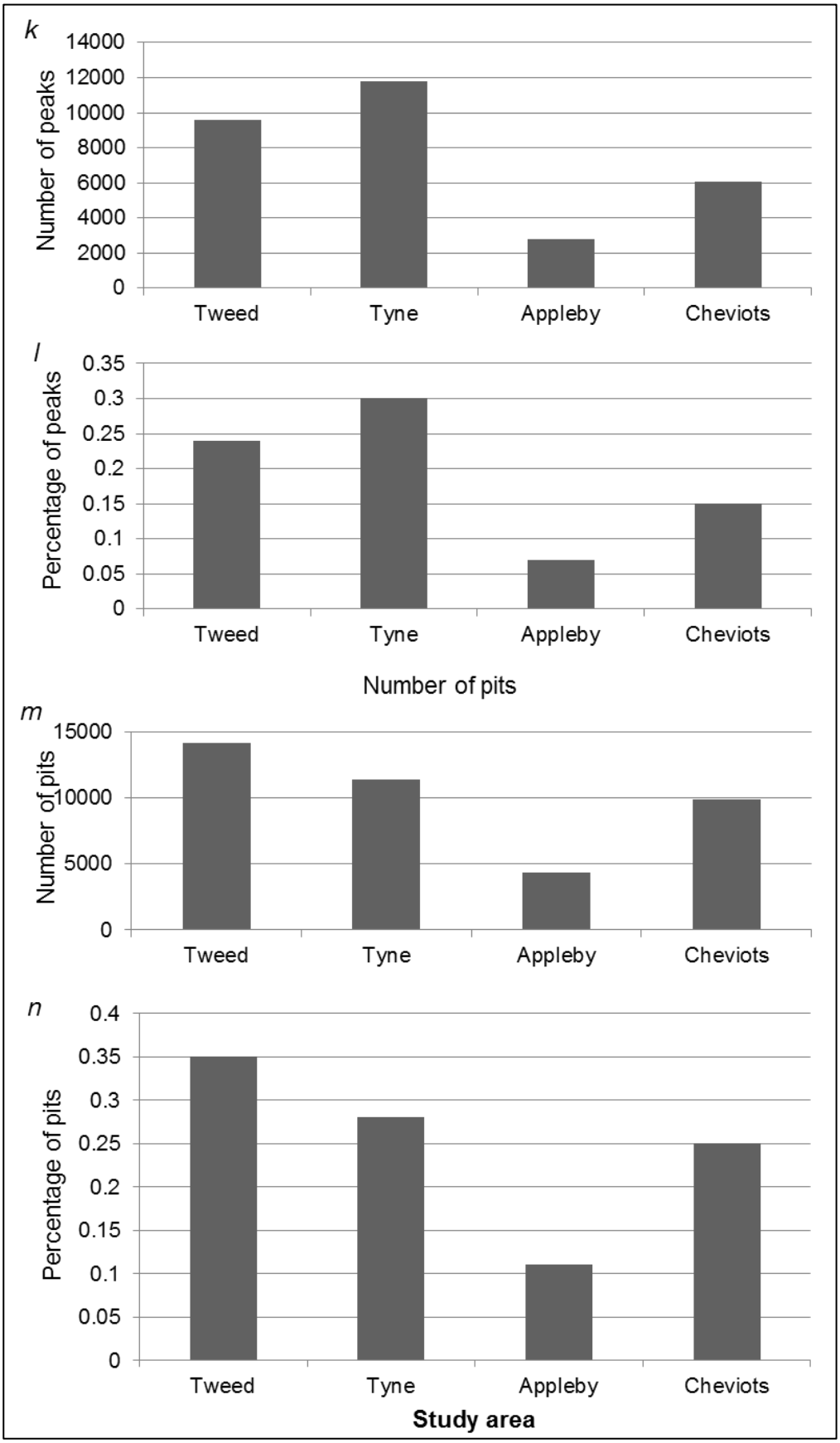

Figure 7.8 (k to n): Summary of 3D roughness results between the four study sites. These spacing parameters quantify the frequency of asperities

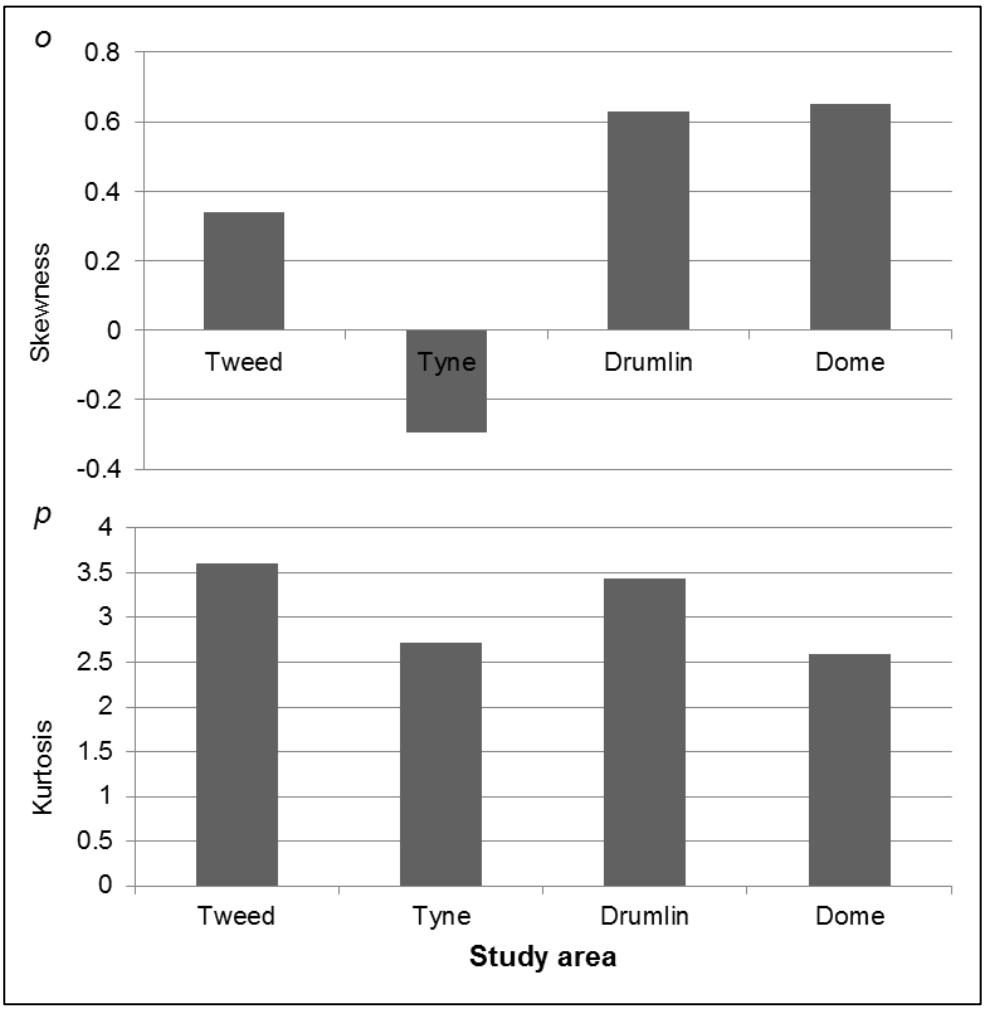

Figure 7.8 (o and p): Shape parameter summary statistics for the four study sites

	Study area			
Parameter	**Tweed**	**Tyne**	**Appleby**	**Cheviots**
Number of points	4004001	4004001	4004001	4004001
Mean height, m	68.3	240.3	456.0	200.7
Range, m	119.8	232.0	636.4	266.1
RMS height, m	16.7	44.5	116.3	56.1
Standard deviation, m	16.7	44.5	116.3	56.1
Mean deviation, m	12.8	35.3	88.9	45.6
Skewness	0.3	-0.3	0.6	0.7
Kurtosis	3.6	2.7	3.4	2.6
Maximum height above, m	57.0	95.7	358.5	169.4
Mean height above, m	14.4	36.3	95.1	55.5
Maximum depth below, m	62.8	136.4	277.9	96.7
Mean depth below, m	11.4	34.4	83.5	38.7
Mean peak height, m	15.3	39.9	79.0	55.8
Mean pit depth, m	12.1	35.9	110.4	45.7
Number of peaks	9561	11812	2770	6054
Percentage of peaks	0.2	0.3	0.1	0.2
Number of pits	14146	11384	4306	9875
Percentage of pits	0.4	0.3	0.1	0.3

Table 7.1: Mean values for the 3D roughness parameters in each of the four study areas

		Increasing values →			
Amplitude	*Mean height*	Tw	Ch	Ty	Ap
	Range	Tw	Ty	Ch	Ap
	RMS height	Tw	Ty	Ch	Ap
	Mean deviation	Tw	Ty	Ch	Ap
	Maximum height above	Tw	Ty	Ch	Ap
	Mean height above	Tw	Ty	Ch	Ap
	Maximum depth below	Tw	Ch	Ty	Ap
	Mean depth below	Tw	Ty	Ch	Ap
	Mean peak height	Tw	Ty	Ch	Ap
	Mean pit depth	Tw	Ty	Ch	Ap
Spacing	*Number of peaks*	Ap	Ch	Tw	Ty
	Percentage of peaks	Ap	Ch	Tw	Ty
	Number of pits	Ap	Ch	Ty	Tw
	Percentage of pits	Ap	Ch	Ty	Tw
Shape	*Skewness*	Ty	Tw	Ap	Ch
	Kurtosis	Ch	Ty	Ap	Tw

Table 7.2: Relative differences in the average roughness value for each region, by parameter. Moving left to right indicates increasing values. For the amplitude parameters, increasing values are taken to indicate increasing roughness; spacing values increase as the frequency of asperities increases. The River Tweed valley (Tw) is shown in green; results for the Tyne Gap (Ty) are highlighted in blue; the Cheviots (Ch) is shown in purple; results for the Appleby (Ap) site are shaded orange

From Tables 7.1 and 7.2 it can be seen that there is a trend in the amplitude parameter results. The Tweed study area consistently produced the lowest values for this group of parameters, and the Appleby area the highest. For some of the measures of roughness, the difference between these two end members is relatively large. For example, on average the mean height of the Appleby topography is 400 m higher than that of the Tweed. Recall that all of these parameters are calculated using local means (Section 5.3), so this difference is not solely due to one region having a greater elevation above sea level. Larger variations of this nature would be filtered out. For eight of the ten amplitude parameters, the results of the Cheviot site were the second highest, followed by the Tyne Gap.

A trend is also apparent with those amplitude parameters that use a subset of the data, such as those designed to measure the vertical size of asperities. These results show that

the peaks and pits in the Appleby region are larger than those of the Tweed. However, the actual differences in height between are generally smaller than for those parameters that use all observations. For example, the average height of peaks in the Tweed was 15 m, versus a mean of 79 m for the Appleby area.

Despite having the highest amplitude values, the Appleby study site produced the lowest spacing parameter results showing that the area has the fewest peaks and pits. The pattern of frequency is somewhat reversed to that of the amplitude results, indicating that the largest amplitudes correspond with the lowest frequencies. The difference between the highest (Tyne Gap) and lowest (Appleby) number of peaks is over 9,000 although, when measured as a percentage of the overall area, this increase constitutes a difference of c.0.2%. Conversely, areas such as the Tyne Gap and the Tweed are dominated by lower magnitude but higher frequency of perturbations.

7.4 Discussion

7.4.1 Quantifying the roughness of formerly glaciated terrains

This chapter has demonstrated how formerly glaciated terrains can be used to compare regional patterns in subglacial bed roughness. By extracting the bed elevation at a constant sampling interval along transects it was possible to gather profile measurements of topography. These values allowed formerly glaciated terrains to be investigated using the same 2D parameters used for quantifying the roughness of contemporary ice-sheet beds. In theory, this would allow the roughness of palaeo environments to be compared with current subglacial beds.

As with Chapter 6, the high resolution of the DEM imagery, and regular spacing of pixels without gaps, meant that the 3D parameters could also be used to analyse topography. Relative to the 5 x 5 km study area used to evaluate the parameters (Section 5.2.2), the spatial extent covered in this chapter was considerably larger. The fact that none of these locations had missing observations again demonstrates the high quality of palaeo datasets, especially when compared to radio-echo sounding measurements such as the SPRI data of Antarctica (Taylor *et al*., 2004). Nevertheless, despite their superiority over records from contemporary ice-sheet beds, in some aspects, there are disadvantages of using measurements of palaeo landscapes.

One limitation of analysing palaeo terrains is that they may have been modified post-glacially (Ballantyne, 2002), which means that the topography being measured is not that of the subglacial bed at the time of ice flow. Nevertheless, in the areas tested in this chapter, the topography exhibited subglacial features in the order of tens of metres or greater in size and, in some locations, even micro-scale features such as striae are reported (Section 7.2.2). The presence of these bedforms indicates that, even though

some modification of the topography may have occurred, much of the original signal is preserved. The survival of subglacial bedforms is notable because many fall within the size range of tens to hundreds of metres and, as Section 2.3.2 discussed, this meso-scale range is poorly understood.

7.4.2 The influence of measurement direction on 2D parameters

This chapter compared the roughness results of eight profiles to determine the influence of profile direction on roughness values. For the majority of parameters, Profiles 3 and 4, which have a NE-SW alignment along the valley, yielded the lowest values. Inferred ice flow direction in this area is along the valley to the NE (Everest *et al*., 2005). Assuming this interpretation is correct, the results of this project support the findings of other studies that roughness is lower when measured parallel to flow (Bingham & Siegert, 2009). These findings suggest palaeo roughness is analogous with that of current ice sheets such as those in Antarctica, and lends more support to using the former for studying roughness.

Past studies of subglacial bed roughness had also identified that results perpendicular to flow were rougher (Bingham & Siegert, 2009). This study again supported these findings, indicating that the measurements across flow were rougher than those aligned parallel to the former flow direction. However, what is striking is that the measurements 90° to flow were not the most rough. This indicates that parallel and orthogonal azimuths are not end members, and so, cannot be used to identify the highest and lowest roughness values.

7.4.2.1 The relative sensitivity of roughness parameters to profile orientation

Differences in results with profile alignment were not consistent for all parameters. The amplitude and spacing parameters appeared to have been more influenced than the shape methods. With the sinuosity parameter (Figure 7.7r), for example, the values were unusual in being consistent irrespective of measurement orientations.

One possibility is that some characteristics of the topography did not vary with direction, so any results designed to measure these variables showed consistent results. Another explanation is that certain parameter values are more sensitive than others. For example, with some of the amplitude parameters, such as the range, a profile capturing an anomalously high peak would have had a dramatic effect on these results. For other amplitude parameters that average out results, a single high point has less effect.

An interesting question raised by these findings is how important is measurement direction for the results of spectral analysis? The fact that roughness parameter varies with profile orientation has implications for their use in predicting the resistance of the bed to basal ice flow.

7.4.2.2 Implications of profile orientation for inferring roughness

The effect of measurement direction on roughness results is important because it may affect the interpretation of topography. In some cases, the profiles with the highest and lowest roughness values, for a given parameter, were separated by 22.5°. The implications are that the inferred resistance to ice speed may be under- or over-estimated.

If spectral analysis is influenced by profile direction in a similar way, this is problematic for using SPRI measurements to quantify roughness in Antarctica. As Section 3.5.1.3 described, these measurements were gathered by aircraft in a series of sweeps. Although the overall coverage of these data is extensive, an area such as an ice stream may be captured by just one or two profiles. Another problem with these measurements is that, although the data are assumed to be measured parallel or orthogonal to ice flow, in reality this is not always the case (see, for example, the alignment of profiles in Figure 2.1).

7.4.3 Regional variations in bed roughness

Analysis of four sites using 3D roughness parameters showed that different assemblages of subglacial features produce different roughness results. Between the study areas, there was a consistent pattern in the results, and this allows the regions to be ranked in terms of their relative differences in roughness. The Tweed valley and Appleby localities appeared as end members, representing a progressive increase in roughness from the former to the latter. For example, using amplitude parameters, the average height of asperities in the Tweed valley area was c.15 m, compared with approximately 79 m in Appleby.

One challenge to this notion of ranking topography by their roughness is that the order is determined by the roughness parameters used. If amplitude parameters are used, then the Cheviots study area had higher values relative to the Tyne Gap, implying the former is rougher. However, with spacing parameters, the Tyne Gap had a higher frequency of asperities than the Cheviots, which would suggest that the Tyne Gap is rougher. Overall, the order in roughness based on the amplitude parameters is the reverse of that produced by the spacing parameters. This again demonstrates that there is a need to identify which parameters are most closely associated with ice flow: are high-magnitude low-frequency bedforms more resistant to ice flow than low-magnitude high-frequency perturbations?

Although inferences of roughness depend on the parameters used, it is clear that the parameters were able to distinguish between different topography. This suggested that the parameters might be used to classify different assemblages of landforms.

7.4.3.1 The use of roughness parameters to classify bedform assemblages

In this chapter, the Tyne Gap and Tweed study areas were chosen because both exhibit long, elongate bedforms (Section 7.2.2). Compared with the other regions, the amplitude parameter results for these areas were lower than those of the Cheviots and Appleby (see

Table 7.2). The results of the spacing parameters showed that the Tyne Gap and Tweed study sites had more asperities than Appleby and the Cheviots. Therefore, there is a similarity between the results of the Tyne Gap and Tweed. These findings suggest that roughness parameters could be used to identify areas with similar topography.

The Appleby area also exhibited drumlinised topography, but the length and elongation of these features was smaller (Livingstone *et al*., 2012). In terms of the roughness results, however, the parameters do not appear to have measured these characteristics. For example, one might have expected the frequency of spacing parameter values to be higher, and the amplitude values lower, relative to the other regions. However, the results indicate a reverse pattern, with the average size of peaks and valleys being larger in the Appleby region. Again, as discussed in Section 5.5.2.2, the spacing parameters could only be used as a proxy for horizontal size of the features, because no parameters measured the length or width of asperities. Therefore, the chosen set of methods for quantifying roughness may be incapable of detecting changes in the length or elongation of features.

Although, in the case of the Appleby study area, the parameters do not appear to have captured the size of features versus those in the Tyne Gap and Tweed, the areas did consistently produce differences in the roughness results. Appleby yielded the lowest values for the amplitude parameters, and the highest values for the spacing methods. This consistent pattern across 15 different statistics suggests that the measures of roughness are sensitive to differences in landform assemblages. The current limitation to using these methods to classify morphology is that the effect of differences in topography on the parameters is unknown.

With further testing, it may be possible to produce a training set. For example, measuring the roughness of known bedform assemblages would give an indication of how these parameters respond to differences in the size and shape of subglacial features. Ultimately, this information could be used, for example, in automated analysis of topography to identify bedforms beneath subglacial beds.

7.4.3.2 Roughness parameters in ice speed reconstruction

Roughness parameters have never been used to infer former ice speeds. However, the use of geomorphometry in such reconstructions is well practised (Evans *et al*., 2005). For example, provided other conditions such as sediment availability are constant, the length and elongation of bedforms are used as evidence of increasing flow rates (Stokes & Clark, 2002).

In contemporary settings, lower roughness has commonly found to correspond with regions where ice flow is faster (Bingham & Siegert, 2009). This pattern was observed in Chapter 7 where lower amplitude parameter values were associated with regions of ice

streaming. Following uniformitarian principles, one can reconstruct former ice speeds based on the roughness of the palaeo ice-sheet bed. It is only possible to give comparative ice speeds between regions, rather than actual rates of flow, however, this is the case for most tools of reconstructing ice dynamics in formerly glaciated areas.

Given the relatively lower amplitude parameter results in the Tweed valley, one can deduce that this area had the fastest speeds of the four regions, followed by the Tyne Gap, and then Cheviots. The amplitude parameters also show that the highest topography and highest asperities were located in the Appleby region, which would imply that this site had the slowest ice speeds.

Using different methods of quantifying roughness, an alternative interpretation is reached. From the spacing parameters it can be seen that the Appleby region had the fewest asperities, which would indicate the area had the fewest obstacles resisting ice flow, so speeds would have been the fastest. This demonstrates how the interpretation of ice speed depends on the choice of parameter used. Although the parameters can measure many variables in the topography, their importance for controlling ice speed remains unclear.

One of the challenges in using roughness parameters in ice sheet reconstruction is that the shape of topography is not solely controlled by ice flow. For example, in Section 7.2.2 it was described how the formation of some bedforms in the Tyne Gap appears to have been partially controlled by differences in geology, with the sub-parallel alignment of resistant volcanic rock and ice speed producing long groves (Krabbendam & Bradwell, 2011). With further testing it might be possible to determine how such variables affect the roughness parameters, allowing clearer interpretations to be drawn.

Another drawback in using parameters to reconstruct ice flow is that, even in contemporary settings where ice streams are still active, there is not a perfect correlation between ice speed and roughness. Some of the other controls on ice dynamics, (Section 2.2), may not have affected the shape of the topography, so roughness parameters would be unable to account for these effects. Nevertheless, this point applies to many of the methods of analysing the shape of the topography to interpret ice flow. Given that statistics such as the length and elongation of bedforms have commonly been used in ice sheet reconstructions (Evans *et al*., 2005), it suggests that other summarises of topography may also be useful.

7.4.3.3 Comparing interpretations of former ice speed: bed roughness versus other evidence

By comparing the parameter results for the different regions with the reconstructions made by other scientists it is possible to see how the roughness fits their interpretations, thus indicating how roughness might be linked to ice speed.

The amplitude parameter results suggest that the area with the lowest roughness was the Tweed valley study site. This conclusion fits with other reconstructions of the area, where evidence including the dimensions of bedforms and geology/rheology has been used to infer ice streaming (Everest *et al*., 2005; Everest & Lawrence, 2006; Staines, 2009). The agreement with amplitude parameters with this reconstruction implies that the vertical size of asperities is more important than the frequency of perturbations in controlling ice speed. However, these findings are contradicted by the results of the Cheviots.

In the Cheviot study site, the amplitude parameters suggested that this area was less rough than the Appleby area, although more rough than the Tweed or Tyne Gap. The spacing parameters showed a similar pattern, with the Appleby area having fewer asperities than the Cheviots. Based on measures of roughness, one might infer slower speeds than the Tweed valley, but faster than other locations. Palaeo-reconstructions of the Cheviots suggest that this area once supported an ice dome (Everest & Lawrence, 2006), making ice flow in this region the slowest of the four locations studied. Indeed, as described in Section 7.2.2, the geology of the area shows no evidence of being sculpted by flow (Everest & Lawrence, 2006), indicating minimal basal ice flow. Therefore, the roughness parameters contradict other methods of reconstruction.

If the Cheviots was a former ice dome, it demonstrates that it may be difficult using roughness parameters to differentiate glacially modified areas to those that have not been altered by basal ice flow. In contemporary environments, remotely sensed data have been used to measure the topography of the bed and relate these to spatial patterns in roughness. Analysis of the parameters raises questions over how reliably ice domes can be distinguished beneath contemporary ice sheets by measuring roughness.

7.5 Conclusions

This chapter showed how formerly glaciated terrains can be used to quantify the roughness of subglacial beds. With the signal of former ice-sheet behaviour being preserved in such environments, it is possible to link theories such as bedform development or palaeo-reconstructions to variations in topographic form. Compared with contemporary ice-sheet settings, many of these terrains have a superior resolution of height measurements. This study demonstrated the use of terrestrial measurements but studies have shown how bathymetric data might detect palaeo-subglacial bedforms (e.g. Stewart *et al*., 2010), which might also be a useful resource. Through this, it is possible to

investigate changes in roughness in new dimensions: using DEMs it is possible to extract measurements along profiles of any orientation, or also quantify roughness in 3D.

Quantifying roughness in 2D for eight profiles showed the importance of measurement angle on the results. Findings supported earlier workers who suggested that roughness calculated parallel to flow was the least rough but, at right-angles to flow was not found to be the roughest. A relatively small change in the measurement angle of just 22.5° produced large differences in the results. Potentially, if the roughness values had been used in reconstruction, such variations might be sufficient for glaciologists to infer different ice-sheet behaviour. These findings have implications for the way in which roughness is quantified, particularly in contemporary environments where the range of measurement directions available is small. A move to 3D analysis of surfaces may prevent these difficulties, although the lack of data in contemporary settings means that this is challenging at present. For this reason palaeo environments are a valuable resource.

This chapter demonstrated how roughness might be used to identify and classify surfaces based on the roughness of bedforms. Different assemblages produce differing sets of results and, by developing a training set, it may be possible to use roughness to reconstruct past ice flow behaviour or to identify landsystems beneath current ice sheets. The regional variations in roughness for UK sites fits with some ice speed reconstructions again supporting a linkage between ice speed and the form of topography. However, the study identified that some areas do not fit this pattern, such as the increasing roughness form an ice dome to a drumlinised environment. These findings suggest other factors must be taken account of to make regional comparisons.

The topography of an ice sheet bed might be controlled by factors other than ice speed and direction. The regional patterns shown in the analysis of UK DEM data might be explained by changes in rheology or geology, which differ between the four study sites. The importance of these other variables is further motivation to use formerly glaciated terrain where such information is available.

CHAPTER 8
Discussion & Conclusions

This chapter identifies the over-arching themes that link the chapters of this project. It returns to the research objectives outlined in Section 2.6.1. As Chapter 3 described, this project was effectively broken down into three sections. First, the way in which roughness is quantified was evaluated. Second, these findings informed the development of other methods of investigating the relationship between roughness and ice speed. Third, the project explored other uses of roughness parameters, such as identifying subglacial landforms. To summarise the findings of each of these areas, this chapter is broken down into the same three sections, beginning with a discussion on techniques for measuring roughness.

8.1 Methods of quantifying roughness

8.1.1 Sources of bed elevation data

As reviewed in Chapter 2 the majority of studies on subglacial bed roughness have analysed data over tens of kilometres (Bingham & Siegert, 2009). The reason for this choice is uncertain, but was probably dictated by the availability of data. The use of SPRI radio-echo echo sounding measurements has underpinned many of the investigations of roughness in Antarctica (Taylor *et al*., 2004; Rippin *et al*., 2007), but the limitation of these measurements is that they have a relatively coarse resolution. As a result, there is a lack of measurements of roughness on scales of tens to hundreds of metres.

Chapter 4 demonstrated that the resolution of SPRI RES measurements can be improved by re-digitising the z-scope records. Summary statistics (Table 3.1) showed that an eight-times improvement in resolution produced a sampling interval of hundreds of metres. It appeared that the z-scope could have been further digitised at a shorter horizontal interval, although such sampling falls below the reported accuracy of the system (see Section 3.5.1.3).

Although the resolution of the SPRI data was improved, other problems with the data were identified. For example, the navigational accuracy is relatively poor, thus questioning the accuracy of the measurements. Furthermore, the method of re-digitising was time consuming. Therefore, although re-digitising is feasible, it is not the best method for acquiring data of a higher resolution.

When considering data resolution, an important point is that most parameters summarise windows of points. Therefore, even though a sampling interval of approximately 250 m was achieved, the range in wavelengths measured was larger than the meso-scale. For example, with spectral analysis, the use of 32 points sampled at 250 m intervals gave window sizes approximately 8 km in length. Within these windows, the higher resolution of the data permitted shorter wavelengths of roughness to be captured, making this the first project to use SPRI data for quantifying roughness at the meso-scale. However, for analysis to fully capture the meso-scale of tens to hundreds of metres, data with considerably finer resolution than SPRI records are required.

Given that re-digitising does not appear to be the most suitable method of acquiring high-resolution measurements, and is reaching the limits in accuracy of the SPRI measurements, it is worth considering alternative sources of bed elevation data. As discussed in Section 2.5.3, such datasets are becoming increasingly available. Nevertheless, many of these records are still unsuitable for quantifying roughness because they do not meet other requirements such as spatial coverage.

As seen in Chapter 2, many of the studies of subglacial bed roughness have measured spatial patterns in roughness over large areas. Similarly, this project investigated roughness along profiles hundreds of kilometres long. To do this, it is necessary to have access to data with an extensive spatial coverage. One of the advantages of the SPRI measurements is that the profiles cover a total length of over 400,000 km (Taylor *et al*., 2004; Bingham & Siegert, 2009). Despite newer datasets having higher resolution, the area covered by these measurements is often limited. It appears that there is a trade-off between spatial extent and the sampling interval of points. The implications are that, in contemporary ice-sheet environments, there are relatively few datasets suitable for quantifying roughness.

The areas that currently have the best data, in terms of resolution and coverage, are those of formerly glaciated terrains. Arguably they offer the only means of quantifying meso-scale roughness at the scale of tens of metres over large areas. Through the use of NextMap DEMs of the UK, this project has shown how such data might be used to analyse roughness.

An argument against using formerly glaciated terrains is that they may have been modified by post-glacial activity, which would modify or even destroy the bed topography. A counter-argument is that measurements of formerly glaciated terrains may be superior to those of contemporary ice sheets. In this project, although an area of 400 km^2, with a pixel size of 5×5 m, was analysed, there were no missing height values. In contrast, with the 572 km long re-digitised SPRI profile, there was no height measurement for 100

observations. Thus, a key outcome of this study is in highlighting the potential of palaeo ice-sheet beds to offer a more comprehensive picture of spatial patterns in subglacial bed roughness.

8.1.2 The effect of sampling and window length on spectral analysis

As summarised in Chapter 2, the use of spectral analysis has dominated glacial research into bed roughness (Siegert *et al*., 2004, 2005b; Rippin *et al*., 2004 Taylor *et al*., 2004). Despite this, a critique of the method has never been published, at least in the context of glacial studies. This project tested how the sampling interval of the data, and choice of window length, affected the results.

The roughness results for a profile digitised at two different resolutions showed strong agreement (Section 3.4.3). This suggested sampling interval is not an important control on spectral analysis results. However, with the higher resolution data it was possible to select a different set of window sizes, and these had a more significant effect on the results. As a result, changes in the resolution of data might indirectly influence the results by altering the way results are summarised.

Analysis of four window sizes showed that the results of spectral analysis were inconsistent. In this example, different patterns in the roughness of the surface may have been inferred. Furthermore, varying the window size affected the magnitude of the results. In the future, this might make it difficult to compare the results of spectral analysis if studies have used different window sizes. In this project for example, it was difficult to compare the agreement between the profiles.

Spectral analysis values can be standardised but this is not the best option because, ultimately, varying the window size means that the topography being measured is different. As the sampling interval of the data increases, the minimum wavelength that can be measured decreases. In a reverse trend, as window length increases, the maximum wavelength of variation captured increases. Unless analysed in context, standardised measurements hide this information. A similar problem is identified in the use of *integrated* results (Section 3.4.3), which summarise total roughness across all wavelengths that fall within a window (Siegert *et al*., 2004). If window size or sampling interval varies, the range of wavelengths also varies, so integrated results are not directly comparable. To continue using spectral analysis, decomposed results may be more suitable because these allow arbitrary ranges in wavelength to be chosen.

8.1.3 Quantifying roughness by scale

The results of spectral analysis indicate that the roughness of the subglacial bed is not the same at all scales. A section of bed appearing to have low roughness at one resolution

may appear rough at another. This has implications not only for spectral analysis, but for any method of quantifying roughness.

One consequence of the importance of scale is that it suggests glaciologists' understanding of spatial patterns in roughness is probably quite limited and restricted to certain scales. For example, the majority of studies have assessed roughness over windows tens of kilometres in length, using data with a relatively coarse resolution (Siegert *et al*., 2004; Taylor *et al*., 2004; Bingham & Siegert, 2009). Therefore, although there is good information on *macro-scale* roughness, spatial variations on the order of tens to hundreds of metres in horizontal length are less understood.

If roughness controls ice speed, but the roughness of the topography varies with scale, it follows that certain scales of roughness may be more important than others in influencing ice dynamics. Due to the focus on macro-scale roughness, the relative importance of different scales of topographic variation is not known. Nevertheless, this project identified a strong agreement between spatial patterns in ice speed and roughness along and across ice streams in the Siple Coast (Section 6.3.2). Therefore, macro-scale roughness appears to have a strong link with ice speed. In other sciences large-scale topographic features have been suggested to be the most influential on ice speed. For example, Winsborrow *et al*. (2010) place topographic forcing at the top of their hierarchy of ice stream controls. Until more research is completed, it is not possible to deduce which scales of roughness are most important, but numerical ice-flow modelling has much potential in this regard.

To investigate the roughness of subglacial topography at different scales, it is necessary to adjust the way roughness parameters function. As described above, two ways this can be done is through the choice of data and window length. However, other options allow finer-tuning. Section 5.3.2.1 described how the use of thresholds and cut-offs can constrain the size of features measured. This might include the height of asperities, but also their width. Using these techniques allows high-resolution datasets or large window sizes to be preserved, while filtering out some of the variations. For example, the roughness of subglacial bedforms could be measured, but patterns in the underlying topography removed.

A criticism of filtering is that some information is lost. However, without such constraints on scale, it is difficult to interpret why a particular set of results has been produced. This was seen with analysis of the Tweed palaeo ice-stream bed when testing the effect of profile orientation (Section 7.2.1). Here, the scales of roughness measured ranged from the resolution of the data (5 m) to the length of window (400 m). Although the fact that parameters use local datums, and windows will have filtered out some of the larger-scale

topography, it is not possible to determine whether differences in the results are due to changes in topography at the scale of bedforms, or because of the larger-scale differences of measuring along and across a valley.

If roughness parameters are to be tuned through the use of these filters, it will be necessary to determine which scales of roughness are most important for a particular study. Sensitivity analysis could be done to measure the effect of adding cut-offs and thresholds, or varying the window length. The results could be compared with variations in ice dynamics, to determine which scales are important for a particular phenomenon, for example, measuring the size of features most related to patterns in ice speed.

In glaciology, different scales of subglacial bed roughness have been measured (Section 2.3), but this is somewhat confusing because the term *roughness* then refers to variations in topography ranging from millimetre-sized precipitates on rocks (Hubbard & Hubbard, 1998), to features tens of kilometres in length (Taylor *et al*., 2004; Siegert *et al*., 2004, 2005b). A possible solution to this would be to adopt an approach used in materials science, where *roughness* explicitly refers to a certain scale. Other terms, such as *waviness*, and *form* (Kalpakjian), are then used to describe larger scales of variation. In a glacial scenario, a possible method of adopting this system would be to use roughness to refer to variations over tens or metres, waviness to summarise topography over hundreds of metres, and form to describe the shape of topography over kilometres. An alternative scheme, perhaps based on the average size of bedforms, could be used. Although arbitrary, the advantage of this approach is that it increases the comparability of results between studies.

8.1.4 Techniques for quantifying roughness in two and three dimensions

In addition to the scale of roughness being important in controlling results, the direction along the bed that the measurements are collected is also important. This indicates that there are directional patterns of roughness in the topography. For example, findings show that the roughness in the direction of ice flow was lower than that measured at right angles to flow (Section 73.1). Such patterns had been identified in other studies (e.g. Bingham & Siegert, 2009), but the sensitivity of profile orientation on results had never been tested.

This project found that, although measuring topography in the direction of ice flow yielded the lowest roughness values, measurements at right-angles to flow were not the most rough. More strikingly, analysis showed that a relatively small change in angle of 22.5° had a strong influence on the results of spectral analysis. These findings raise questions over the use of 2D datasets for quantifying subglacial bed roughness: for example, if predicting the resistance of the bed to ice flow, profiles would have to be precisely

measured parallel to flow direction, otherwise the results might over-estimate the roughness. This is particularly a problem in contemporary ice sheet environments where, as Section 2.3.1.2 discussed, datasets such as the SPRI records are measured in one of two directions, but these orientations may not be aligned to flow.

Another problem with the use of profiles is that the results are sensitive to the location of the profiles. This is more of a problem for measuring the roughness of small-scale features such as subglacial bedforms. Weertman (1962) suggests that, if a profile across a subglacial bed starts at one obstacle, i.e. a subglacial bedform, it is unlikely to meet another. This can be demonstrated by Figure 8.1, which depicts three profiles across a hypothetical field of bedforms, but none are representative of the bedforms. The challenge of measuring a representative sample of the topography is compounded by the fact that many 2D datasets, such as the SPRI measurements, have relatively large distances between profiles (Lythe *et al*., 2001; Siegert *et al*., 2005).

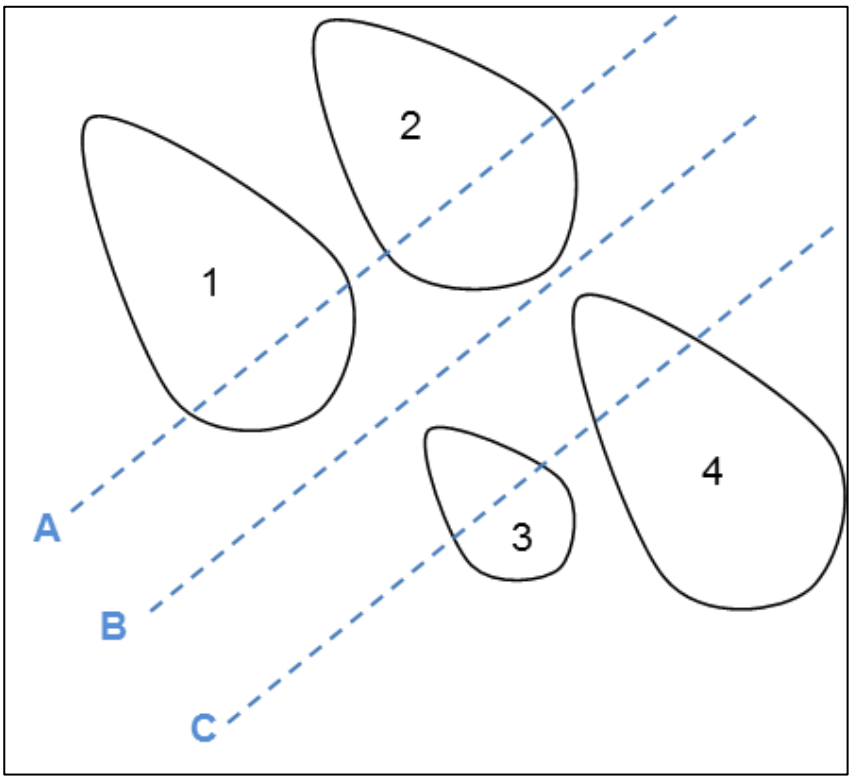

Figure 8.1: The importance of profile location. Measurement of a drumlin field using three profiles. Profile A captures two of the drumlins, but the results may over-estimate the total size. Profile B misses all the features, so the roughness of bedforms cannot be measured. Profile C under-estimates the dimensions of the features

Due to the limitations of 2D analysis, there was a motivation to analyse roughness in 3D. As Chapter 5 discussed, there is a history of using 3D analysis for investigating spatial phenomena in general, but for quantifying subglacial bed roughness, 2D analysis has remained prevalent. As a result, it was not known whether 3D parameters could feasibility be used to quantifying the roughness of subglacial topography.

Using NextMap DEM data for the UK it was found that 3D roughness parameters could be used to quantify the roughness of glacial topography. The biggest challenge that restricts their use is the availability of data. In this project, the program used for quantifying roughness in 3D required data with uniform spacing (Section 5.2.3). As described in Section 3.3.1, however, the data from formerly glaciated terrains often exhibit gaps. This problem might be overcome by adjusting the way results are generated. However, a second requirement for 3D analysis is a 3D record of bed elevation. In contemporary ice-sheet settings, there are presently few such datasets with an extensive spatial coverage. As a result, analysis is somewhat limited to formerly glaciated terrains.

A review of the methods of quantifying roughness showed that many of the 2D techniques had a 3D counterpart (Section 4.4). This is useful in allowing the results of different datasets to be compared. Yet, the main advantage of 3D parameters over 2D methods is that the former are superior in allowing directional patterns in roughness to be detected. For example, in Section 5.4 the parameters showed trends in the amplitude across the River Tweed Study area. Had only profiles been used to investigate this area, such patterns would have been more difficult to detect. When analysing the roughness of a surface using a profile, the spatial patterns in topography are only measured in one direction. With 3D analysis the only limitation on the direction in which roughness can be measured is the resolution of the data.

Another advantage of 3D methods is that, provided the data have the same sampling interval, they use more observations per given area than a profile. This means that, if data have adequate resolution, smaller-scale features such as the drumlinoid features depicted in Figure 8.1 are more likely to be captured by 3D analysis.

As reviewed in Chapter 2, many investigations have looked at the role of roughness on ice speed, but none have looked at how roughness may control the direction of ice flow. Directional patterns in topography and its relationship with ice flow have long been recognised. For example, the orientation of bedforms has been found to correspond to ice flow direction, while large-scale features appear to control the direction of ice streams (Winsborrow, 2007). Although spatial patterns in subglacial bed roughness have been identified, interestingly, the role of roughness in controlling ice flow direction has never been tested and this is an area that future work might want to address, i.e. the scales of which roughness might start to influence ice flow direction.

8.1.5 The choice of parameters for summarising subglacial bed roughness

This project is underpinned by the use of alternative methods of quantifying roughness. However, their suitability for use in analysing subglacial bed roughness is, in part, judged by comparing these methods with spectral analysis. With the dominance of spectral

analysis in glacial roughness research, it has become standard, with at least five studies using this technique (e.g. Rippin *et al*., 2004, 2007; Siegert *et al*., 2004; Taylor *et al*., 2004; Bingham & Siegert, 2009). Therefore, before critiquing the advantages and disadvantages of other roughness parameters, it is worthwhile to summarise merits and limitations of spectral analysis.

Chapter 5 demonstrated how, in other sciences, roughness parameters are often chosen to fulfil a particular purpose. In glaciology, the main purpose of these parameters has been to investigate the relationship between ice speed and roughness. Given that the results of spectral analysis show agreement with spatial patterns in roughness, it suggests that this parameter is suited to this purpose: the variables this parameter captures appear to be related to the ice dynamics. However, although a correlation between ice speed and roughness is apparent, explaining the cause of the relationship is not possible because spectral analysis is difficult. Spectral analysis captures several variables, but this makes interpretation of the results difficult because it is not possible to attribute the cause of spatial variations in roughness to one characteristic. In Section 2.3, it was shown how many of the findings between roughness and rates of ice flow have not been linked to ideas on how bed topography controls basal ice speeds. For example, the size of asperities is thought to influence rates of flow by acting as resistant obstacles (Paterson, 1994). Although spectral analysis would capture the height of peaks, this information cannot be separated out from the other variables measured by this parameter. In contrast, by using roughness parameters that measure a single variable, it is possible to determine how a particular characteristic, such as the height of peaks, relates to ice flow.

The biggest limitation of spectral analysis identified in this project was the constraints placed on the data. The need for 2^N datapoints has restricted the scales of roughness that could be quantified. However, what is more significant is that certain requirements of this parameter have resulted in data being modified to fit the method. Section 2.4.1 described how, before roughness values can be produced, it is first necessary to remove slopes and remove gaps (Taylor *et al*., 2004). The problem is that the impact of adjusting the data in such a way is not known.

From the review of spectral analysis it was concluded that alternative methods of quantifying roughness should be identified. A literature review showed that measuring roughness was common many sciences, with numerous examples listed in Section 2.4.2. An interesting finding here was that, despite the diversity of parameters reviewed in Chapter 5, few had been used in glaciology. Furthermore, when assessing the parameters used across a range of sciences, those used in glaciology were not among the most common.

A review of these methods showed that many roughness parameters are designed with a specific purpose and are, in fact, categorised based on the types of topographic variation they measure. For example, spacing parameters summarise horizontal variations in topography, and amplitude parameters measure changes in the vertical height of a surface (Section 4.2). Some of the methods are even more refined, designed to specifically measure the sizes of asperities. It was foreseeable how such information might be useful to glaciologists in determining how obstacles on the bed control rates of ice flow.

Identifying possible roughness parameters was relatively unchallenging and it is, perhaps, surprising that many of these simple parameters had not been previously applied to subglacial data. For example, Gadelmawla *et al*. (2002) summarise over 50 parameters designed to assess profile data. The difficulty was in producing an initial shortlist of methods to be tested. Some parameters were found to be highly specialised (Section 4.2), so these could be immediately excluded. However, the vast majority of methods could, in principle, be used with subglacial bed data. Ultimately, 36 parameters were chosen for testing. This allowed a selection of methods from each of the categories to be used, and included both 2D and 3D parameters (Table 4.1, Section 4.5.5).

In the future, other methods of quantifying roughness could be considered. For example, using the parameters in Chapters 7 and 8 demonstrated that, although spacing parameters were included, these methods only measured the frequency of asperities. Including spacing parameters that measure the horizontal size of perturbations might also be useful. Due to the fact that two programs were used to calculate all the results, *hybrid* parameters (Section 4.2) were not included. Therefore, these too may be included. Furthermore, other sciences also refer to terms such as *straightness* (BSI, 2007b, 2009e) and flatnesss (BSI, 2007c, 2009f). Like roughness parameters, these methods describe variations in the shape of surface topography. Perhaps future studies will consider the role of these characteristics of the bed on ice dynamics.

8.1.6 Using combinations of roughness parameters

Before the various parameters could be used to investigate the relationship between roughness and ice speed, it was necessary to measure their sensitivity to different variables. The results indicated that the best methods for measuring a certain characteristic were those belonging to that category: for example, for summarising changes in roughness due to the height of topography, amplitude parameters were most useful.

Importantly it was found that the parameters were influenced by a range of variables, but this might not be apparent in the results. For example, although amplitude parameters

give no indication on the frequency of asperities, the number of peaks or troughs might influence the vertical distribution of values. When used individually, this makes it difficult to interpret the results, especially since different topographies can produce the same values.

The sensitivity of each parameter to many variables suggests that, rather than being used in isolation, a group of methods should be used. For example, amplitude and spacing parameters might be used in combination. Through this it is possible to place the results in context determining, for example, how the frequency of asperities changes as their size changes. However, unlike spectral analysis (Section 2.4.1) the fact that each parameter measures a certain characteristic makes it possible to separate out these variables. In combining roughness parameters in this manner it can be seen that the methods can be considered as *additional*, rather than *alternative* choices. No one method, including spectral analysis, is necessarily better or worse than another. Instead, the use of GLMs showed that certain methods, or combinations of methods, are more useful in certain situations. In this project, using a group of methods was used for investigating the relationship between roughness and ice speed.

8.2 The relationship between ice speed and roughness

A fundamental challenge in reviewing the role of roughness in ice sheet dynamics is determining the causality of these patterns: it has been demonstrated that roughness may control ice speed, and differences in the rate of flow may create patterns in the shape of topography. With this chicken-and-egg scenario, the roughness of the bed might have dictated ice speeds, e.g. with protrusions resisting ice flow (Nye, 1970; Alley, 1993; Cohen *et al*., 2002; Schoof, 2002; Thorsteinsson *et al*., 2003; Remy *et al*., 2009). An alternative view might suggest that the speed of ice has caused preferential development of the topography with faster speeds creating a lower roughness (Siegert *et al*., 2005b) due to higher basal shear stresses (Pattyn, 2003; Bennett & Glasser, 2006). In Chapter 7, GLMs were used to assess the relationship between roughness and ice speed. Although roughness parameters were used as predictor variables, the topography of the bed may be the response. A correlation between speed and roughness could still be produced if variations in the speed of flow led to preferential modification of the bed.

Using data from real-world subglacial beds, where there are many variables at work rather than a modelling approach, it is arguably not possible to give a definitive answer on this point. In reality, it is likely that there will be a two-way interaction with adjustments in both roughness and ice speed towards an equilibrium (Paterson, 1994). Yet, this fact has always applied to, and been acknowledged by, studies of roughness using data from actual ice sheet beds (Siegert *et al*., 2004). However, although the direction of the relationship cannot be identified, this project has provided more insight into the strength of the link between roughness and ice speed. By treating roughness as a series of variables,

it has shown how some changes in the shape of the bed show a stronger association with patterns in ice speed. In this project, the parameters with the strongest correlation to patterns in ice speed were amplitude parameters. Given that these measure differences in the height of the profile, including the vertical size of peaks, it suggests these variables are most linked with ice flow and that roughness in terms of the wavelength or frequency of asperiteis secondary factors. Nevertheless, other methods of quantifying roughness also showed agreement, such as the sinuosity parameter, indicating that other variables are also related to patterns in ice speed.

The fact that patterns in ice speed and roughness do not show a perfect fit emphasis that other controls influence the ice dynamics. With the majority of studies on roughness, these alternative controls have rarely been taken into account. For example, most have assumed that the material forming the bed is constant (Bingham & Siegert, 2009). Yet, such variables may influence not only the roughness of the topography, but also ice sheet behaviour. For instance, these variables control the ability of the bed to be deformed or eroded (Paterson, 1994; Siegert *et al*., 2005a) and, therefore, may affect both the shape of the bed (Phillips *et al*., 2010; Krabbendam and Bradwell, 2011). This study has demonstrated that taking these other controls into account is crucial in trying to interpret roughness results, because parameters that summarise the shape of topography may be capturing the effects of these other variables. For example, the strong relationship between amplitude parameters and ice speed may be due to these parameters being proxies for ice thickness, which is thought to be one of the most important controls on ice sheet dynamics (Winsborrow *et al*., 2010).

It is not possible to determine whether roughness parameters capture the direct link between roughness and ice speed, or if instead it captures the role of other variables. Nevertheless, in either case, this project has demonstrated that roughness parameters could be a valuable tool in predicting former ice sheet behaviour. In theory, if a training set is developed, it will become possible to use roughness parameters as tools in palaeo environmental reconstruction. Analysis of four sites in Britain showed that, even in this elementary stage, interpretations of former ice speeds based on roughness values showed good agreement with those made using other proxies, thus proving the concept. For example, the Tweed and Tyne where the fastest ice speeds were predicted had the lowest roughness values. The fact that the inferences using roughness parameters did not fully correspond with other interpretations, especially for the Cheviot site, is further demonstration of the need for studies of roughness to take other variables into account.

Measurements of roughness may also be important in predicting the changing behaviour of ice sheets, particularly areas of streaming flow, through time. Take analysis of the MacAyeal Ice Stream as an example. Results showed that the position of the lateral

margin of this ice stream corresponded with an area of higher roughness. GLM models showed that the fit between roughness and ice speed in this area was as much as 98%. Assuming for a moment that roughness is a control on ice dynamics, these findings suggest that the shape of the bed may be restricting the lateral position of the ice stream. In such a case, it would be important to determine how roughness may change through time because it follows that, after a sufficient decrease in roughness, the speed of flow would become unconstrained, with a decrease in roughness producing faster flow. This project has shown how much research has focused on the spatial patterns in roughness. More research is now required into how roughness varies temporally.

Finally, this project showed that the use of 3D parameters allows directional patterns in roughness to be explored in more detail than with the use of 2D profiles. The majority of roughness studies, this one included, have focused on testing the patterns between the speed of ice flow and the shape of topography. Yet, this project has also shown how the use of 3D parameters would allow the links between the direction of ice flow and subglacial bed roughness to be assessed. Such analysis might provide further insight on the location controls of ice streaming, and provide another tool in the reconstruction of former ice sheet behaviour.

8.3 Using roughness parameters to identify and classify subglacial bedforms

In glaciology, roughness parameters have been used to investigate the linkages between bed topography and ice speed. However, this project has demonstrated that there are other potential uses for these parameters. One example of this is using roughness to classify subglacial landscapes, such as identifying specific groups of subglacial bedforms (e.g. drumlins versus mega-scale glacial lineations).

The use of statistics that summarise topography to classify subglacial landscapes is nothing new. For example, many subglacial bedforms are defined by their shape (e.g. Rose, 1987), and these dimensions are effectively measures of topography. This suggested that roughness parameters could be used in the same way although, until this project, they had not been.

Chapter 5 described how, for a single parameter, two different surfaces might produce the same roughness values. This point was demonstrated in Chapter 6 where, for some synthetic profiles, some methods yielded the same results despite visual differences in the shape of the profiles. However, this evaluation of the methods also showed that, through the addition of more parameters, it was possible to distinguish different topographies. For example, although Profiles A and B had the same frequency of asperities (Section 5.2.1.1), by adding amplitude parameters that detected the differences in height, it was

possible to differentiate the profiles. Ultimately, this means that, if a group of methods is used, the same result should only be produced if the topography is similar overall.

Assuming the Cheviots has remained unmodified by glacial activity, and then the inability to distinguish it from the glacially-sculpted topography of Appleby identifies the current weaknesses of using roughness in this manner. Yet, the results of Chapter 8 showed that different landscapes appeared to show a pattern in roughness values. Ultimately, if groups of bedforms are found to produce a characteristic range of roughness values, it might be possible to identify them solely from roughness parameter values.

To use roughness for classifying topography, it would be necessary to produce a training set by analysing known bedform assemblages. Through this, it would be possible to assess how each parameter changes given certain variations in topography. Again, it would be necessary to take account of other variables such as geology or rheology, and also consider the scale of roughness being measured.

Once patterns in the results had been identified, these findings could be used to identify bedforms beneath contemporary ice sheets, or provide an automated means of classifying features in formerly glaciated terrains.

8.4 Conclusions

This project has evaluated techniques to quantify subglacial roughness, and used these methods to investigate the relationship between roughness and ice speed in both contemporary and palaeo ice-sheet settings. This chapter summarises the key findings of this thesis.

This project reviewed the use of spectral analysis for quantifying the roughness of ice-sheet beds. Changing the sampling interval on SPRI records had little effect on the results, provided that other analysis options remained constant. However, it was shown that differences in data resolution would likely influence the choice of window length: analysis of the same profile using different lengths of window produced inconsistent results. The evaluation of spectral analysis also showed that interpreting the values yielded is difficult because it is not possible to determine what variables in bed topography have influenced the results. Furthermore, it was found that the need for 2^N, regularly spaced data points limits the choices of scale that can be measured, and also the type of data that can be used for this type of spectral analysis. This led to the conclusion that alternative sources of bed elevation measurements, and other techniques for quantifying the roughness using these data, were required.

In light of the above, 36 alternative methods of quantifying roughness were reviewed. The majority of these had never before being used to measure the roughness of subglacial

beds, so an evaluation was required. Several advantages over spectral analysis were identified: e.g. many of the parameters are designed to measure a particular facet of topographic variation, giving insight into how different variables such as the height of asperiteis have influenced results. Relative to spectral analysis the parameters had more flexibility for use with glacial data: e.g. uniform sampling intervals are not a requirement, and the option of window size is more flexible. Yet, some of the disadvantages with spectral analysis also apply to these methods. For example, all parameters are sensitive to the choice of window. Rather than alternative methods to replace spectral analysis, it is suggested that these methods should be additional techniques.

A new method of re-digitising SPRI z-scope records of bed elevation was developed. The technique achieved a sampling interval of approximately 250 m, which is equivalent to an eight-fold improvement in the resolution of SPRI data used in previous roughness studies (Taylor *et al*., 2004*;* Rippin *et al*., 2004). Yet, artefacts in the imagery and relatively coarse navigational accuracy limit the potential of these radio-echo sounding records for use in quantifying shorter scales of roughness. The traditional choices of data have resulted in a lack of roughness measurements at scales of tens to hundreds of metres.

2D roughness parameters were used to investigate the relationship between ice speed and roughness. Results concurred with those of previous studies that ice speeds increase as roughness decreases. However, the use of GLMs allowed this project to further extend such investigations by quantifying the extent of this correlation. For the MacAyeal Ice Stream, West Antarctica, and R^2 of c.0.98 indicated that subglacial bed roughness is strongly linked to spatial patterns in ice speed. These results indicate a strong fit between roughness and ice speed. Therefore, although a secondary control on ice dynamics, roughness may be more important for controlling ice flow than previously thought. Nevertheless, it was not possible to determine the causality of this relationship; patterns may be produced by variations in the speed of flow creating a spatially variable roughness.

Similarly, roughness parameters may act as proxies for other controls on ice dynamics. For example, it was demonstrated how roughness may detect changes in ice sheet thickness, or respond to differences in the composition of the bed. More testing is required to determine these relationships: for example, comparisons in areas with consistent geology would remove this particular effect. If roughness parameters are proxies, they may be useful for predicting ice behaviour in locations where other variables cannot be measured as easily.

The role of roughness in ice stream behaviour was assessed. Analysis of the MacAyeal Ice Stream also showed that the lateral margin of this fast-flowing area corresponded with

a zone of high roughness. It is concluded that the roughness of topography is linked with ice stream location. Again, it is not possible to determine causality yet, the fact that an association is observed, suggests that measurements of roughness could be used to predict ice speeds. This makes them a potential tool in palaeo-environmental reconstruction.

This project showed that, rather than using a single parameter to quantify roughness, several can be combined in a model. In analysis of the Siple Coast ice streams, a combination of amplitude parameters and kurtosis measuring the vertical distribution of heights produced the strongest fit between roughness and ice speed. This indicates these variations in topography are most linked with ice speed. In other studies, such as quantifying differences in the roughness of subglacial bedforms, a different combination may be more suitable. Through the high level of automation achieved in this project, it was demonstrated that sets of parameters can be used to analyse topography, rather than selecting a single technique.

The high-resolution of palaeo ice-sheet bed measurements permitted 2D and 3D methods of quantifying roughness to be evaluated. DEMs of Britain were used to extract profiles at a range of orientations. A difference in measurement angle of just 22.5° had a substantial effect on roughness values. The least-rough results were not found to be at right angles to the profile with the highest roughness. These findings indicate that, although profiles measured parallel and orthogonal to ice flow have traditionally been used (Bingham & Siegert, 2009), they do not represent end members in bed roughness. Analysis of DEM measurements demonstrated that 3D data better-allow directional patterns in roughness to be identified. In the future, such measurements might be used to investigate relationships between roughness and ice flow direction.

Formerly glaciated areas of Britain were used to assess the relationship between roughness and ice speed by comparing predicted speeds based on roughness parameters with those made using other evidence. In areas such as the Tweed and Tyne Gap where fast ice speeds have been reconstructed, the low roughness values of the parameter results supported these inferences. However, for the Cheviots, which have been identified as a further ice dome, the roughness results were less rough than those of Appleby. This shows that, at present, roughness cannot be used as a reliable method for reconstructing ice speed although, with more training, there is strong potential to do so.

This project looked at other uses of subglacial roughness measurements. For the first time it was shown that roughness parameters can be used to compare assemblages of bedforms. With more testing it may be possible to use roughness measurements in

identifying groups of bedforms, for example, classifying topography beneath contemporary ice sheets.

Appendices

Appendix 1: Roughness parameter equations

A1.1 Quantifying roughness in 2 dimensions

For a profile across the subglacial bed, suppose height h_i is measured at a series of distances x_i from some origin. The subscript i runs from 1 to the number of points in the profile n. There is no presumption that the positions of x_i are equal spaced, only that they are distinct.

The user is able to define the size of window. If no window length is selected, then all of the points in the profile are used and n is equivalent to the total number of observations. If windows are used, then each data point is treated as the centre of the window. The size of window is controlled by defining the horizontal distance from the central point *d*. Points falling within this selection are included in the analysis for that window. The total window length is, therefore, $2d$. In this case, n is equivalent to number of points within a window.

The equations for each 2D parameter are now summarised. To reduce the quantity of summation signs and subscripts, equations follow the form of Whittle (2000 where $A[]$ is used to indicate taking the mean or averaging, either for a profile or for selected points within a window.

A1.1.1 Mean height

The mean height over the profile is $\frac{1}{n}\sum_{i=1}^{n} h_i$.

A1.1.2 Mean deviation

The mean deviation is $A\left[|h - A[h]|\right]$

A1.1.3 RMS height

The root mean square height is $\sqrt{A[(h - A[h])^2]}$. This is the standard deviation also, but calculated with a divisor of the number of points, not minus 1. Call this s.

A1.1.4 Range

The height range is the difference between the maximum and minimum heights.

A1.1.5 Mean and maximum heights above/below

The maximum height above is the largest value of $h - A[h]$ for points with $h > A[h]$. The mean above height is the corresponding mean.

The maximum depth below is the largest value of $A[h] - h$ for points with $h < A[h]$, and the mean below depth is the corresponding mean.

A1.1.6 Measuring asperity frequency and size

A peak is a point with $h > A[h]$ that is also strictly higher than its neighbours, namely the point before and the point after in the profile. Here, strictly emphasis that being equal in height to either neighbour is not sufficient. The percentage of peaks is calculated from the number of peaks and the number of points minus 2. This subtraction takes account of the fact that there is no observation before the first point, and no measurement after the last point. The mean peak height is the mean height of those peaks, $A[h - A[h]]$.

A trough is a point with $h < A[h]$ that is also strictly lower than its neighbours, referring to the point before and after in the profile. The percentage of troughs is calculated from the number of troughs and the number of points minus 2. As with the percentage of peaks, this subtraction takes account of the fact that there is no measurement before the first point, and none after the last point. The mean trough depth is then the mean depth of those troughs, $A[A[h] - \mathrm{h}]$.

A1.1.7 Skewness

The skewness is $A[(h - A[h])^3] / s^3$. This measurement is dimensionless and has no units.

A1.1.8 Kurtosis

The kurtosis is $A[(h - A[h])^4] / s^4$. This measurement is also dimensionless and unit free.

A1.1.9 Slope

The slope is the gradient, or slope coefficient, of a linear regression of h on x.

A1.1.10 Sinuosity

Sinuosity is calculated as the ratio of the total distance when measured along the profile, to the horizontal distance between the first and last points. The former is calculated as the sum of the lengths of the hypotenuses of a series of right-angles deranges with horizontal sides (x_i, x_{i+1}) and vertical sides (x_i, x_{i+1}). The ratio is reported as a percentage.

A1.2 Quantifying roughness in three dimensions

For a surface, heights h_i are supposed known at points x_i, y_i. These points are equally spaced on a regular grid with a square mesh. There is no presumption that the dataset in map projection has any particular shape (e.g. square or even rectangular). Results may be analysed for the entire grid, or over square windows. Windows are all $k \times k$ points and centred on each data point in turn. k must be odd and, unless defined by the user, defaults to a minimum allowed value of 3. Each window is centred on a bed elevation data point.

The program calculates the number of data points, mean height, height range, RMS height, skewness and kurtosis for a surface. The equations are the same as those for profiles. The exception is the treatment of peaks and pits, which have a different definition. A peak is a point that is higher than the mean height and also higher than all its known neighbouring points. The qualification *known* is inclusive rather than exclusive. For example, at the corners of a rectangular grid, only the heights of 3 out of 8 values for a 3 × 3 grid are known, but classification is based on those known values. Conversely, a pit is defined as a point that is lower than the mean height, and also lower than all its known neighbouring points. The mean peak height and mean pit depth are the means of $h - A[h]$ and $A[h] - h$ over the peaks and pits respectively.

Appendix 2: Stata programs

A2.1 Script for quantifying roughness in 2D

2D roughness parameters were calculated using a single program written in Stata. This program required a record of bed elevation *heightvar*, and the cumulative horizontal distance of each point measured from the first observation,*distvar*. The program was called with syntax:

```
roughprofile heightvar distvar [if] [in], [uniform(#) biweight(#) width(#) saving(filename)]
```

Roughness results were calculated using moving windows. The program allowed the points within each window to be weighted depending on their position, so that the points at the edges would be treated differently for those in the centre. This could be done through the `biweight` option. The rationale for weighting is to give less weight to points that are further away from the centre but still within the window. In practice, however, the use of weighting would have meant more testing would be needed to evaluate each parameter. Therefore, the points were not weighted, which meant points in a window were treated uniformly, as specified by the `uniform()` option.

The program was designed to allow windows of different sizes to be specified, or none used at all. If no length of window was selected, roughness values were calculated for the entire profile. The roughness value for each parameter was then displayed as a list in the Stata results window.

To analyse roughness over windows it was necessary to specify the window width. This value inputted had the same units as the horizontal distance value. The program generated roughness results using the midpoint coordinates of each window, and so window size was measured from the centre to the edge. That meant that, for the window size required, the user specifies half that distance. Measuring this value from the same direction for each point, the program determined which observations fell within each window. For example, if a 10 km window was required, the option `uniform(5)` would be used. For each datapoint, the program would then determine which observations fell within 5 km in either direction from the central point. Once the observations within each window were identified, the program would then calculate results for each parameter in turn.

Having calculated the results for each parameter, the program was designed to write these results to a new file using the `saving()` option, with the user specifying the name of the file. Any of the variables in the original dataset were also copied into the new file. Given that each window used an observation from the original file, the results were paired

to the bed elevation measurements. Furthermore, the fact that the original data had geographic coordinates meant that the roughness results shared these values, allowing them to be plotted as maps (as in Figure 3.14).

For each of the parameters, a new variable was created that would hold the results. These variable names are summarised in Table A1. Once these were added, any temporary variables were then defined. For example, to calculate the size of peaks, it was necessary to identify which observations were crests. This was done by scripting a check where, for a given point, the height h of the preceding, indexed by _n-1, and the following observation, indexed by _n+1, were compared:

```
`h' > `h'[_n-1] & `h' > `h'[_n+1]
```

_n is the observation number in Stata.

Name of parameter	Variable name
Mean height	hmean
Mean deviation	meandev
Mean above height	hmeanab
Mean below depth	hmeanbe
RMS height	hrms
Range	hrange
Maximum above height	hmaxab
Maximum below depth	hmaxbe
Mean peak height	pkmean
Mean valley depth	trmean
Standard deviation	sd
Number of peaks	npeaks
Number of valleys	ntroughs
Percentage of peaks	pcpeaks
Percentage of valleys	pctroughs
Number of points	npoints
Skewness	skew
Kurtosis	kurt
Slope	slope
Sinuosity	sinu

Table A1: The variable names used for scripting each 2D and 3D parameter in Stata

Stata has its own scripting language and, therefore, rather than building a program from the ground up, users are able to invoke many of the inbuilt commands. For example, many summary statistics are coded into the software, and can be used in scripting. For each parameter reviewed in Chapter 5, the mathematical definition was broken down into the smallest components that could be calculated using the native Stata commands. For example, where an average value was required, rather than writing a line of code to calculate the mean, the command was used.

The script for quantifying roughness in 2D is shown on the following three pages. The fact that this program is made up of many in-built commands means that, should the reader require more insight into the program's functionality, but is unfamiliar with the programming language, they are recommended to consult Baum's (2009) book, or access the extensive resources of *The Stata Journal*.

```
program roughprofile, rclass
      syntax varlist(max=2 min=2 numeric) [if] [in] ///
      [, Biweight(numlist >0 max=1) uniform(numlist > 0 max=1) ///
      SAving(str asis)]

/// Checking choice of weighting:
      if "`biweight'`uniform'" != "" {
            if "`biweight'" != "" & "`uniform'" != "" {
                  di as err ///
                  "may not specify both biweight() and uniform()"
                  exit 198
            }
            else if `"`saving'"' == "" {
                  local opt = ///
                  cond("`biweight'" != "", "biweight", "uniform")
                  di as err "saving() required with `opt'()"
                  exit 198
            }
      }

      tokenize "`varlist'"
      args h x
      tempvar dev w hypo
      marksample touse
      qui count if `touse'
      if r(N) == 0 error 2000
      preserve
      qui keep if `touse'
      drop `touse'
      sort `x'

      /// no window selected, calculates summary values
      if "`biweight'`uniform'" == "" {
            qui su `h', d
            local mean = r(mean)
            di " "
            di "# data points     " %6.0f r(N)
            return scalar npoints = r(N)
            local N = r(N)
            di "mean height       " %6.1f r(mean)
            return scalar hmean = r(mean)
            di "range             " %6.1f r(max) - r(min)
            return scalar hrange = r(max) - r(min)
            di "RMS height        "  ///
            %6.1f sqrt(r(Var) * (r(N) - 1) / r(N))
            return scalar hrms = sqrt(r(Var) * (r(N) - 1) / r(N))
            di "SD                "  %6.1f r(sd)
            di "skewness          "  %6.3f r(skewness)
            return scalar skewness = r(skewness)
            di "kurtosis          "  %6.3f r(kurtosis)
            return scalar kurtosis = r(kurtosis)
            * local p90 = r(p90)
            * local p10 = r(p10)
            * qui count if `h' > `p90'
            * di "# points > 90%    " %6.0f r(N)
            * qui count if `h' < `p10'
            * di "# points < 10%    " %6.0f r(N)
            qui gen `dev'  = abs(`h' - `mean')
            qui su `dev'  if `h' > `mean', meanonly
            di "max above height  " %6.1f r(max)
            return scalar hmaxab = r(max)
            di "mean above height " %6.1f r(mean)
            return scalar hmeanab = r(mean)

            su `dev'  if `h' < `mean', meanonly
            di "max below depth   " %6.1f r(max)
            return scalar hmaxbe = r(max)
            di "mean below depth  " %6.1f r(mean)
            return scalar hmeanbe = r(mean)

            qui su `dev'  if `h' > `mean' ///
            & `h' > `h'[_n-1] & `h' > `h'[_n+1], meanonly
            di "# peaks           " %6.0f r(N)
```

```
        return scalar npeaks = r(N)
        di "% of peaks        " %6.1g 100 * r(N) / (`N' - 2)
        return scalar pcpeaks = 100 * r(N) / (`N' - 2)
        di "mean peak height  " %6.1f r(mean)
        return scalar pkmean = r(mean)

        qui su `dev'  if `h' < `mean' ///
        & `h' < `h'[_n-1] & `h' < `h'[_n+1], meanonly
        di "# troughs         " %6.0f r(N)
        return scalar ntroughs = r(N)
        di "% of troughs      " %6.1g 100 * r(N) / (`N' - 2)
        return scalar pctroughs = 100 * r(N) / (`N' - 2)
        di "mean trough depth " %6.1f r(mean)
        return scalar trmean = r(mean)

        qui su `dev', meanonly
        di "mean deviation    " %6.1f r(mean)
        return scalar meandev = r(mean)
        qui regress `h' `x'
        return scalar slope = _b[`x']
}
/// window: moving results for each data point
else {
        qui gen `w' = .
        qui gen `dev' = .
        qui gen double `hypo' = sqrt((`h' - `h'[_n+1])^2 + (`x' -
        `x'[_n+1])^2)
        local res npoints hmean hrange hrms skewness kurtosis ///
        hmaxab hmeanab hmaxbe hmeanbe npeaks pcpeaks pkmean   ///
        ntroughs pctroughs trmean meandev slope sinuosity

        qui foreach r of local res {
                gen `r' = .
        }

        qui forval i = 1/`=_N' {
                replace `w' = abs(`x' - `x'[`i'])
                if "`uniform'" != "" {
                        replace `w' = `w' < `uniform'
                }
                else replace `w' = ///
          cond(`w' <= `biweight', (1 - (`w'/`biweight')^2)^2, 0)

                su `x' [w=`w'], meanonly
                local xrange = r(max) - r(min)
                su `hypo' if `w' > 0 & `x' < r(max), meanonly
                replace sinuosity = 100 * r(sum) / `xrange' in `i'

                su `h' [w=`w'], d
                local mean = r(mean)
                replace npoints = r(N) in `i'
                local N = r(N)
                replace hmean = r(mean) in `i'
                replace hrange = r(max) - r(min) in `i'
                replace hrms = sqrt(r(Var) * (r(N) - 1) / r(N)) in `i'
                replace skewness = r(skewness) in `i'
                replace kurtosis = r(kurtosis) in `i'
                replace `dev'  = abs(`h' - r(mean))
                su `dev' if `h' > `mean' [w=`w'], meanonly
                replace hmaxab = r(max) in `i'
                replace hmeanab = r(mean) in `i'

                su `dev' if `h' < `mean' [w=`w'], meanonly
                replace hmaxbe = r(max) in `i'
                replace hmeanbe = r(mean) in `i'

                su `dev' if `h' > `mean' ///
                & `h' > `h'[_n-1] & `h' > `h'[_n+1] [w=`w'], meanonly
                replace npeaks = r(N) in `i'
                replace pcpeaks = 100 * r(N) / (`N' - 2) in `i'
                replace pkmean = r(mean) in `i'

                su `dev' if `h' < `mean' ///
```

```
                        & `h' < `h'[_n-1] & `h' < `h'[_n+1] [w=`w'], meanonly
                        replace ntroughs = r(N) in `i'
                        replace pctroughs = 100 * r(N) / (`N' - 2) in `i'
                        replace trmean = r(mean) in `i'
                        su `dev' [w=`w'], meanonly
                        replace meandev = r(mean) in `i'
                        regress `h' `x' [w=`w']
                        replace slope = _b[`x'] in `i'
                }

                drop `w' `dev' `hypo'
                save `saving'
        }
end
```

A2.2 Script for quantifying roughness in 3D

There are a number of similarities between the program for quantifying roughness in 3D and that for 2D. For example, both utilise the in-built commands to produce the roughness statistics, and the results are summarised in a similar way. For example, the `summary` option could be used to calculate a single roughness value for each parameter over the entire study area. It was these results that were used to compare regions in Chapter 8.

Another similarity between the 2D and 3D scripts was the use of the `saving()` option. This created a new file to which roughness results were written. Again, the variables from the original dataset were copied to the new file, thus pairing the results with the raw data. With the 2D results this had been a useful step to link the roughness values to the geographic coordinates. However, for the 3D parameter, the need for an *x* and *y* variable meant that these data were already required.

Whereas 2D analysis used the cumulative distance along profile, quantifying roughness in 3D required the geographic position of each coordinate to be specified, referred to as `xvar` and `yvar` in the script. This was so that neighbouring values could be identified. A third variable required was the bed elevation, `heightvar`. The command used to execute the script was:

```
roughsurface heightvar xvar yvar [if] [in], <options>
```

The fundamental difference in the methods is the way that observations are grouped. With 2D analysis, the program identified which data points were within each window. For 3D analysis, the program had to identify all the points that fell within a grid. The position of each observation was used to define the central point of a grid. Being square, the size of this grid was defined using its width, with the user specifying this length via the `width()` option. All of the observations that fell within this grid were then identified and stored by the program. The software would then move to the next observation, use it as a central point, and again identify all its neighbours.

Note that the identification of what points fall within which grid is resource-intensive. number of parameters programmed into the software was fewer than those for the 2D. With a typical desktop computer, using the below script to analyse a 10x10 km area of NextMap data took in excess of 24 hours. The high resolution of the data, along with the choice of window, meant that such a study region contained 20 million points. For each of these points, the program had to identify and store all of the neighbouring values.

To reduce the load, fewer roughness parameters were included in the 3D program. Although summary statistics were produced for all 18 methods (Section 4.14), only a selection were used with the mesh. Nevertheless, this set of methods nevertheless

included amplitude, spacing, and shape parameters. Furthermore, the approach was sufficient inasmuch as demonstrating the feasibility of 3D analysis of subglacial bed roughness. In the future, more parameters could be added.

The full script used to measure roughness in 3D is now given:

```
program roughsurface, rclass
      syntax  varlist(max=3  min=3  numeric)  [if]  [in]  [,  Saving(str)
SUmmary Width(str) ]

      /// checks and initialisations

      if "`width'" == "" local width = 3
      else {
            local width = real("`width'")
            if  missing(`width')  |  (`width'  !=  floor(`width'))  |
mod(`width', 2) == 0 | `width' < 3 {
                  di as err "width must be an odd integer >= 3"
                  exit 498
            }
      }

      if "`summary'" == "" {
            if "`saving'" == "" {
                  di as err "saving() must be specified"
                  exit 498
            }

            gettoken filename stuff : saving, parse(,)
            confirm new file "`filename'"
      }

      quietly {

      preserve
      marksample touse
      count if `touse'
      if r(N) == 0 error 2000

      tokenize "`varlist'"
      args h x y

      tempvar nw n ne w e sw s se
      tempvar xpy xmy

      /// calculate neighbouring altitudes
      gen `xpy' = `x' + `y'
      bysort `xpy' (`x') : gen `nw' = `h'[_n+1]
      by `xpy': gen `se' = `h'[_n-1]
      drop `xpy'

      gen `xmy' = `x' - `y'
      bysort `xmy' (`x') : gen `sw' = `h'[_n-1]
      by `xmy': gen `ne' = `h'[_n+1]
      drop `xmy'

      bysort `x' (`y') : gen `s' = `h'[_n-1]
      by `x' : gen `n' = `h'[_n+1]

      bysort `y' (`x') : gen `w' = `h'[_n-1]
      by `y' : gen `e' = `h'[_n+1]

      /// single summary measures for entire grid
      su `h', d
      }

      local mean = r(mean)
      di " "
      di "# data points     " %8.0f r(N)
      return scalar npoints = r(N)
      local N = r(N)
      di "mean height       " %8.1f r(mean)
      return scalar hmean = r(mean)
      di "range             " %8.1f r(max) - r(min)
      return scalar hrange = r(max) - r(min)
      di "RMS height        "  ///
      %8.1f sqrt(r(Var) * (r(N) - 1) / r(N))
      return scalar hrms = sqrt(r(Var) * (r(N) - 1) / r(N))
      di "SD                "  %8.1f r(sd)
```

```
di "skewness          "  %8.3f r(skewness)
return scalar skewness = r(skewness)
di "kurtosis          "  %8.3f r(kurtosis)
return scalar kurtosis = r(kurtosis)

quietly {
tempvar dev
gen `dev'  = abs(`h' - `mean')
su `dev'  if `h' > `mean', meanonly
}

di "max above height  " %8.1f r(max)
return scalar hmaxab = r(max)
di "mean above height " %8.1f r(mean)
return scalar hmeanab = r(mean)

su `dev'  if `h' < `mean', meanonly
di "max below depth   " %8.1f r(max)
return scalar hmaxbe = r(max)
di "mean below depth  " %8.1f r(mean)
return scalar hmeanbe = r(mean)

foreach X in w e n s nw ne sw se {
      local exp1 `exp1' & ((`h' > ``X'') | missing(``X''))
      local exp2 `exp2' & ((`h' < ``X'') | missing(``X''))
}

qui su `dev'  if `h' > `mean' `exp1', meanonly
di "# peaks           " %8.0f r(N)
return scalar npeaks = r(N)
di "% of peaks        " %8.1g 100 * r(N) / `N'
return scalar pcpeaks = 100 * r(N) / `N'
di "mean peak height  " %8.1f r(mean)
return scalar pkmean = r(mean)

qui su `dev'  if `h' < `mean' `exp2', meanonly
di "# pits            " %8.0f r(N)
return scalar npits = r(N)
di "% of pits         " %8.1g 100 * r(N) / `N'
return scalar pcpits = 100 * r(N) / `N'
di "mean pit depth    " %8.1f r(mean)
return scalar trmean = r(mean)

qui su `dev', meanonly
di "mean deviation    " %8.1f r(mean)
return scalar meandev = r(mean)

if "`summary'" == "summary" {
      exit 0
}

drop `nw' `n' `ne' `w' `e' `sw' `s' `se' `dev'

/// window: moving results for each data point
quietly {
      gen hmean = .
      gen hrange = .
      gen hn  = .
      gen hrms = .
      gen hskew = .
      gen hkurt = .

      fillin `y' `x'

      tempvar ix iy
      egen `ix' = group(`x')
      su `ix', meanonly
      local nx = r(max)
      egen `iy' = group(`y')
      su `iy', meanonly
      local ny = r(max)
      drop `ix' `iy'
```

```
            sort `y' `x'

            local wd2 = floor(`width'/2)

            mata : _grid("`h'", `wd2', `nx', `ny')

            keep if `touse'
            keep `x' `y' `h' h*
      }

      di
      save "`filename'" `stuff'
end

mata :

void _grid(string scalar hname, real scalar w, real scalar nx, real
scalar ny) {

      real matrix h
      real colvector work, dev
      real colvector hmean, hrange, hn, hrms, hskew, hkurt
      real scalar x, y, i, N, n, mean

      h = colshape(st_data(., hname), nx)
      N = st_nobs()
      hkurt = hskew = hrms = hn = hrange = hmean = J(N, 1, .)
      i = 1

      for(x = 1; x <= nx; x++) {
            for(y = 1; y <= ny; y++) {
                  xmin = x - w >= 1  ? x - w : 1
                  xmax = x + w <= nx ? x + w : nx
                  ymin = y - w >= 1  ? y - w : 1
                  ymax = y + w <= ny ? y + w : ny
                  work = vec(h[|xmin, ymin \ xmax, ymax|])

                  hmean[i] = mean = mean(work)
                  hrange[i] = max(work) - min(work)
                  hn[i] = n = nonmissing(work)
                  dev = work :- mean
                  hrms[i] = sqrt(mean(dev:^2))
                  hskew[i] = mean(dev:^3) / (mean(dev:^2))^(3/2)
                  hkurt[i] = mean(dev:^4) / (mean(dev:^2))^2
                  i++
            }
      }

      st_store(., "hmean", hmean)
      st_store(., "hrange", hrange)
      st_store(., "hn", hn)
      st_store(., "hrms", hrms)
      st_store(., "hskew", hskew)
      st_store(., "hkurt", hkurt)

}

end
```

References

Adolphs, U. (1999) Roughness variability of sea ice and snow cover thickness profiles in the Ross, Amundsen, and Bellingshausen Seas. *Journal of Geophysical Research-Oceans,* 104 (C6)**:** 13577-13591.

Agnon, Y. & Stiassnie, M. (1991) Remote-sensing of the roughness of a fractal sea-surface. *Journal of Geophysical Research: Oceans,* 96 (C7)**:** 12773-12779.

Aiken, L.S. & West, S.G. (1991) *Multiple regression: testing and interpreting interactions*. Sage Publications, London.

Alexanderson, H., Hjort, C., Moller, P., Antonov, O. & Pavlov, M. (2001) The North Taymyr ice-marginal zone, Arctic Siberia - preliminary overview and dating. *Global and Planetary Change,* 31 (1-4)**:** 427-445.

Allen, C., Gogineni, S., Wohletz, B., Jezek, K. & Chuah, T. (1997) Airborne radio echo sounding of outlet glaciers in Greenland. *International Journal of Remote Sensing,* 18 (14)**:** 3103-3107.

Alley, R.B. (1993) In search of ice-stream sticky spots. *Journal of Glaciology,* 39 (133)**:** 447-454.

Alley, R.B. (2000) Continuity comes first: recent progress in understanding subglacial deformation. IN: Maltman, A.J., Hubbard, B. & Hambrey, M.J. (Eds.) *Deformation of glacial materials*. Geological Society, special publication. London, pp. 171-179.

Alley, R. B. & Bindschadler, R.A. (2001) *The West Antarctic Ice Sheet: behaviour and environment*. American Geophysical Union, Washington.

Alley, R.B., Clark, P.U., Huybrechts, P. & Joughin, I. (2005) Ice-sheet and sea-level changes. *Science,* 310 (5747)**:** 456-460. Doi 10.1126/science.1114613.

Altuhafi, F.N., Baudet, B.A. & Sammonds, P. (2009) On the time-dependent behaviour of glacial sediments: a geotechnical approach. *Quaternary Science Reviews,* 28**:** 693-707.

Anandakrishnan, S., Blankenship, D.D., Alley, R.B. & Stoffa, P.L. (1998) Influence of subglacial geology on the position of a West Antarctic ice stream from seismic observations. *Nature,* 394 (6688)**:** 62-65.

Anderson, J.B. & Fretwell, U.O. (2008) Geomorphology of the onset area of a paleo-ice stream, Marguerite Bay, Antarctic Peninsula. *Earth Surface Processes and Landforms,* 33 (4)**:** 503-512. Doi 10.1002/Esp.1662.

Anderson, J.B., Shipp, S.S., Lowe, A.L., Wellner, J.S. & Mosola, A.B. (2002) The Antarctic Ice Sheet during the Last Glacial Maximum and its subsequent retreat history: a review. *Quaternary Science Reviews,* 21 (1-3)**:** 49-70.

Andreas, E.L., Lange, M.A., Ackley, S.F. & Wadhams, P. (1993) Roughness of Weddell Sea ice and estimates of the air-ice drag coefficient. *Journal of Geophysical Research-Oceans,* 98 (C7)**:** 12439-12452.

Annan, A.P. (2002) GPR: history, trends, and future developments. *Subsurface sensing technologies and applications,* 3 (4)**:** 253-270.

Arcone, S.A. (2008) Glaciers and ice sheets. *In:* Jol, H.M. (ed.) *Ground penetrating radar: theory and applications.* Oxford, Elsevier Science.

Aris, N.F.M. & Cheng, K. (2008) Characterization of the surface functionality on precision machined engineering surfaces. *International Journal of Advanced Manufacturing Technology,* 38**:** 402-409. Doi 10.1007/s00170-007-1340-1.

Arrell, K. & Carver, S. (2009) Surface roughness scaling trends. *Proceedings of Geomorphometry, Zurich, Switzerland, 31 August - 2 September*.

Arvidsson, A., Satar, B.A. & Wennerberg, A. (2006) The role of functional parameters for topographic characterization of bone-anchored implants. *Clinical implant dentistry and related research,* 8 (2)**:** 70-76. Doi 10.1111/j.708-8208.2006.00001.x.

Arya, S.P.S. (1975) Drag partition theory for determining large-scale roughness parameter and wind stress on Arctic pack ice. *Journal of Geophysical Research: Oceans and Atmospheres,* 80 (24)**:** 3447-3454.

Austin, R.T. & England, A.W. (1993) Multi-scale roughness spectra of Mount St. Helens debris flows. *Geophysical Research Letters,* 20 (15)**:** 1603-1606.

Avdelidis, N.P., Delegou, E.T., Almond, D.P. & Moropoulou, A. (2004) Surface roughness evaluation of marble by 3D laser profilometry and pulsed thermography. *NDT&E International,* 37**:** 571-575.

Bailey, J.T., Robin, G.D.Q. & Evans, S. (1964) Radio echo sounding of polar ice sheets. *Nature,* 204 (495)**:** 420-421.

Baldwin, D.J., Bamber, J.L., Payne, A.J. & Layberry, R.L. (2003) Using internal layers from the Greenland ice sheet, identified from radio-echo sounding data, with numerical models. *Annals of Glaciology,* 37**:** 325-330.

Ballantyne, C.K. (2002) Paraglacial geomorphology. *Quaternary Science Reviews,* 21 (18-19)**:** 1935-2017. Pii S0277-3791(02)00005-7.

Ballantyne, C.K., Mccarroll, D., Nesje, A., Dahl, S.O. & Stone, J.O. (1998) The last ice sheet in north-west Scotland: Reconstruction and implications. *Quaternary Science Reviews,* 17 (12)**:** 1149-1184.

Bamber, J.L. & Huybrechts, P. (1996) Geometric boundary conditions for modelling the velocity field of the Antarctic ice sheet. *Annals of Glaciology,* 23**:** 364-373.

Bamber, J.L., Vaughan, D.G. & Joughin, I. (2000) Widespread complex flow in the interior of the Antarctic ice sheet. *Science,* 287 (5456)**:** 1248-1250.

Barrett, B.E., Murray, T. & Clark, R. (2007) Errors in radar CMP velocity estimates due to survey geometry, and their implication for ice water content estimation. *Journal of Environmental and Engineering Geophysics* 12: 101-111. Doi 10.2113/JEEG12.1.101.

Bartek, L.R., Vail, P.R., Anderson, J.B., Emmet, P.A. & Wu, S. (1991) Effect of Cenozoic ice-sheet fluctuations in Antarctica on the stratigraphic signature of the Neogene. *Journal of Geophysical Research: Solid Earth and Planets,* 96 (B4)**:** 6753-6778.

Baum, C.F. (2009) *An introduction to Stata Programming.* Texas, Stata Press.

Bell, R.E. (2008) The role of subglacial water in ice-sheet mass balance. *Nature Geoscience* 1: 297-304. Doi 10.1038/ngeo186.

Bell, R.E., Blankenship, D.D., Finn, C.A., Morse, D.L., Scambos, T.A., Brozena, J.M. & Hodge, S.M. (1998) Influence of subglacial geology on the onset of a West Antarctic ice stream from aerogeophysical observations. *Nature,* 394 (6688)**:** 58-62.

Bentley, C.R., Lord, N. & Liu, C. (1998) Radar reflections reveal a wet bed beneath stagnant Ice Stream C and a frozen bed beneath ridge BC, West Antarctica. *Journal of Glaciology* 44: 149-156.

Bell, R.E., Studinger, M., Shuman, C.A., Fahnestock, M.A. & Joughin, I. (2007) Large subglacial lakes in East Antarctica at the onset of fast-flowing ice streams. *Nature,* 445 (7130)**:** 904-907. Doi 10.1038/Nature05554.

Bell, R.E., Ferraccioli, F., Creyts, T.T., Braaten, D., Corr, H., Das, I., Damaske, D., Frearson, N., Jordan, T., Rose, K., Studinger, M. & Wolovick, M. (2011) Widespread persistent thickening of the East Antarctic Ice Sheet by freezing from the base. *Science*, 331: 1592-1595. Doi 10.1126/science.1200109.

Benn, D.I. (1994) Fluted moraine formation and till genesis below a temperate valley glacier - Slettmarkbreen, Jotunheimen, Southern Norway. *Sedimentology,* 41 (2)**:** 279-292.

Benn, D.I. & Evans, D.J.A. (1998). *Glaciers and Glaciation,* London, Arnold.

Benn, D.I., Hulton, N.R.J. & Mottram, R.H. (2007) 'Calving laws', 'sliding laws', and the stability of tidewater glaciers. *Annals of Glaciology,* 46**:** 123-130.

Bennett, M.R. (2003) Ice streams as the arteries of an ice sheet: their mechanics, stability and significance. *Earth-Science Reviews,* 61 (3-4)**:** 309-339. Doi 10.1016/S0012-8252(02)00130-7.

Bennett, M.R. & Glasser, N.F. (1996). *Glacial geology: ice sheets and landforms,* Chichester, John Wiley.

Berry, M.V. (1972) On deducing the form of surfaces from their diffracted echoes. *Journal of Physics, Part A General,* 5 (2)**:** 272-291.

Berry, M.V. (1973) The statistical properties of echoes diffracted from rough surfaces. *Philosophical Transactions of the Royal Society of London Series A, Mathematical, Physical and Engineering Sciences,* 273 (1237)**:** 611-654.

Bhushan, B. (1999) *Principles and applications of tribology,* New York, Wiley.
Bhushan, B. (2002) *Introduction to tribology,* New York, Wiley.
Bianchi, C., Cafarella, L., De Michelis, P., Forieri, A., Frezzotti, M., Tabacco, I.E. & Zirizzotti, A. (2003) Radio Echo Sounding (RES) investigations at Talos Dome (East Antarctica): bedrock topography and ice thickness. *Annals of Geophysics,* 46 (6)**:** 1265-1270.
Biegel, R.L., Wang, W., Scholz, C.H., Boitnott, G.N. & Yoshioka, N. (1992) Micromechanics of rock friction 1. Effects of surface-roughness on initial friction and slip hardening in Westerly Granite. *Journal of Geophysical Research: Solid Earth,* 97 (B6)**:** 8951-8964.
Bigerelle, M., Najjar, D. & Iost, A. (2003) Relevance of roughness parameters for describing and modelling machined surfaces. *Journal of Materials Science,* 38 (11)**:** 2525-2536.
Bindschadler, R., Vornberger, P., Blankenship, D., Scambos, T. & Jacobel, R. (1996) Surface velocity and mass balance of Ice Streamd D and E, West Antarctica. *Journal of Glaciology*, 42: 461-475.
Bingham, R.G. & Siegert, M.J. (2007a) Radar-derived bed roughness characterization of Institute and Moller ice streams, West Antarctica, and comparison with Siple Coast ice. *Geophysical Research Letters,* 34 (21) L21504. Doi 10.1029/2007gl031483.
Bingham, R.G. & Siegert, M.J. (2007b) Radio-echo sounding over polar ice masses. *Journal of Environmental and Engineering Geophysics,* 12 (1)**:** 47-62.
Bingham, R.G. & Siegert, M.J. (2009) Quantifying subglacial bed roughness in Antarctica: implications for ice-sheet dynamics and history. *Quaternary Science Reviews,* 28**:** 223-236. Doi 10.1016/j.quascirev.2008.10.014.
Bingham, R.G., Siegert, M.J., Young, D.A. & Blankenship, D.D. (2007) Organized flow from the South Pole to the Filchner-Ronne ice shelf: An assessment of balance velocities in interior East Antarctica using radio echo sounding data. *Journal of Geophysical Research-Earth Surface,* 112 (F3). F03s26 Doi 10.1029/2006jf000556.
Björnsson, H. (1981) Radio-echo sounding maps of Storglaciären, Isfallsglaciären and Rabots glacier, Northern Sweden. *Geografiska Annaler Series A, Physical Geography,* 63 (3/4)**:** 225-231.
Bland, J.M. & Altman, D.G. (2010) Statistical methods for assessing agreement between two methods of clinical measurement. *International Journal of Nursing Studies,* 47 (8)**:** 931-936. Doi 10.1016/j.ijnurstu.2009.10.001. Reproduced from *Lancet* (1986) 1: 307-310.
Blankenship, D.D., Bentley, C.R., Rooney, S.T. & Alley, R.B. (1987) Till beneath Ice Stream B: 1. Properties derived from seismic travel times. *Journal of Geophysical Research*, 92 (B9): 8903-8912.
Blankenship, D.D., Bell, R.E., Hodge, S.M., Brozena, J.M., Behrendt, J.C. & Finn, C.A. (1993) Active volcanism beneath the West Antarctic Ice Sheet and implications for ice-sheet stability. *Nature*, 361: 526-529.
Blankenship, D.D., Morse, D.L., Finn, C.A., Bell, R.E., Peters, M.E., Kempf, S.D., Hodge, S.M., Studinger, M., Behrendt, J.C. & Brozena, J.M. (2001) Geologic controls on the initiation of rapid basal motion for West Antarctic ice streams: a geophysical perspective including new airborne radar sounding and laser altimetry results. IN: Alley, R.D. & Bindschadler, R. (Eds.) *The West Antarctic Ice Sheet: behaviour and environment*. Antarctic Research Series, 77: 105-121. American Geophysical Union, Washington.
Blunt, L. & Ebdon, S. (1996) The application of three-dimensional surface measurement techniques to characterizing grinding wheel topography. *International Journal of Machine Tools & Manufacture,* 36 (11)**:** 1207-1226.
Bohm, J., Jech, M., Vorlaufer, G. & Vellekoop, M. (2009) Comparison of parametric and profilometric surface analysis methods on machined surfaces. *Proceedings of the Institution of Mechanical Engineers Part J: Journal of Engineering Tribology,* 223 (J5)**:** 799-805. Doi 10.1243/13506501jet532.

Boulton, G.S. & Clark, C.D. (1990) A highly mobile Laurentide ice sheet revealed by satellite images of glacial lineations. *Nature*, 346: 813-817.
Boulton, G.S. & Dobbie, K.E. (1998) Slow flow of granular aggregates: the deformation of sediments beneath glaciers. *Philosophical Transactions of the Royal Society of London, A*, 356: 2713-2745.
Boulton, G.S., Caban, P.E. & Van Gijssel, K. (1995) Groundwater flow beneath ice sheets: Part 1 - Large scale patterns. *Quaternary Science Reviews,* 14**:** 545-562.
Bourke, R.H. & Mclaren, A.S. (1992) Contour mapping of Arctic Basin ice draft and roughness parameters. *Journal of Geophysical Research-Oceans,* 97 (C11)**:** 17715-17728.
British Standards Institution (1988) BS134-1:1988 *Assessment of surface texture. Part 1: methods and instrumentation.* London, BSI.
British Standards Institution (1990) BS1134-2:1990 *Assessment of surface texture. Part 2: guidance and general information*. London, BSI.
British Standards Institution (1997a) BS ISO 4287:1997 *Geometrtic product specifications (GPS) - surface texture: profile method. Terms, definitions and surface texture parameters*. London, BSI.
British Standards Institution (1997b) BS 7251-4:1997; ISO 7207-2:1996 *Orthopaedic joint prostheses. Part 4: specification for articulating surfaces made of metallic, ceramic and plastics materials of hip joint prostheses*. London, BSI.
British Standards Institution (1997c) BS EN ISO 12085:1997 *Geometric product specifications (GPS) - surface texture: profile method - Motif parameters*. London, BSI.
British Standards Institution (2004) BS EN 623-4:2004 *Advanced technical ceramics - monolithic ceramics - general and textural properties. Part 4: determination of surface roughness*. London, BSI.
British Standards Institution (2005) BS EN 10049:2005 *Measurement of roughness average Ra and peak count RPc on metallic flat products*. London, BSI.
British Standards Institution (2007a) DD CEN ISO/TS 12181-1:2007 *Geometrical product specifications (GPS) - roundness. Part 1: vocabulary and parameters of roundness*. London, BSI.
British Standards Institution (2007b) DD CEN ISO/TS 12780-1:2007 *Geometrical product specifications (GPS) - straightness. Part 1: vocabulary and parameters of straightness*. London, BSI.
British Standards Institution (2007c) DD CEN ISO/TS 12781-1:2007 *Geometrical product specifications (GPS) - flatness. Part 1: vocabulary and parameters of flatness*. London, BSI.
British Standards Institution (2008a) Draft International Standard ISO/DIS 25178-2 *Geometrical product specifications (GPS) - Surface texture - Areal. Part 2: terms, definitions and surface texture parameters.* London, BSI.
British Standards Institution (2008b) Draft BS EN ISO 25178-3 Geometrical product Specification (*GPS) - Surface texture - Areal. Part 3: specification operators*. London, BSI.
British Standards Institution (2009a) Draft BS 1134-1 *Assessment of surface texture. Part 1: methods and instrumentation (guidance)*. London, BSI.
British Standards Institution (2009b) Draft BS 1134-2 *Assessment of surface texture. Part 2: guidance and general information*. London, BSI.
British Standards Institution (2009c) BS EN 15610:2009 *Railway applications - noise emission - rail roughness measurement related to rolling noise generation*. London, BSI.
British Standards Institution (2009d) Draft BS ISO 12181-1 *Geometrical product specifications (GPS) - roundness. Part 1: vocabulary and parameters of roughness*. London, BSI.
British Standards Institution (2009e) Draft BS ISO 12780-1 *Geometrical product specifications (GPS) - straightness. Part 1: vocabulary and parameters of straightness*. London, BSI.

British Standards Institution (2009f) Draft BS ISO 12781-1 *Geometrical product specifications (GPS) - flatness. Part 1: vocabulary and parameters of flatness*. London, BSI.
British Standards Institution (2010a) BS ISO 23519:2010 *Sintered metal materials, excluding hardmetals - measurement of surface roughness*. London, BSI.
British Standards Institution (2010b) BS EN ISO 25178-6:2010 *Geometrical product specifications (GPS) - Surface texture - Areal. Part 6: classification of methods for measuring surface texture*. London, BSI.
Brown, G.S. (1979) Surface-roughness slope density estimates for low sea state conditions. *Journal of Geophysical Research,* 84 (Nb8)**:** 3987-3989.
Budd, W.F. (1970) Ice flow over bedrock perturbations. *Journal of Glaciology,* 9 (55)**:** 29-48.
Buffington, J.M. & Montgomery, D.R. (1999) Effects of hydraulic roughness on surface textures of gravel-bed rivers. *Water Resources Research,* 35 (11)**:** 3507-3521.
Burdek, M. & Sikorsi, S, (2008) The influence of surface topography on physical and technological properties of low carbon steel sheets. *Steel Research International*, 79, *Special edition metal forming conference 2008, Volume 2.*
Byrne, R.J. (1968) Aerodynamic roughness criteria in aeolian sand transport. *Journal of Geophysical Research,* 73 (2)**:** 541-547.
Canabarro, A., Figueiredo, F., Paciornik, S. & De-Deus, G. (2009) Two- and three-dimensional profilometer assessments to determine titanium roughness. *Scanning,* 31**:** 174-179. Doi 10.1002/sca.20156.
Canovaro, F., Paris, E. & Solari, L. (2007) Effects of macro-scale bed roughness geometry on flow resistance. *Water Resources Research,* 43 (10). W10414 Doi 10.1029/2006wr005727.
Carter, S.P., Blankenship, D.D., Peters, M.E., Young, D.A., Holt, J.W. & Morse, D.L. (2007) Radar-based subglacial lake classification in Antarctica. *Geochemistry Geophysics Geosystems,* 8. Q03016 Doi 10.1029/2006gc001408.
Chatfield, C. (2003). *The analysis of time series: an introduction,* Boca Raton, Chapman and Hall.
Chen, Y.H. & Huang, W.H. (2004) Numerical simulation of the geometrical factors affecting surface roughness measurements by AFM. *Measurement Science & Technology,* 15 (10)**:** 2005-2010. Doi 10.1088/0957-0233/15/10/010 Pii S0957-0233(04)76954-4.
Chilamakuri, S.K. & Bhushan, B. (1998) Contact analysis of non-Gaussian random surfaces. *Proceedings of the Institution of Mechanical Engineers Part J-Journal of Engineering Tribology,* 212 (J1)**:** 19-32.
Chiu, C.L. & Rubio, G.A. (1970) Statistical roughness parameter as indicator of channel flow resistance. *Water Resources Research,* 6 (2)**:** 622-628.
Christoffersen, P. & Tulaczyk, S. (2003a) Response of subglacial sediments to basal freeze-on. 1: theory and comparison to observations from beneath the West Antarctic Ice Sheet. *Journal of Geophysical Research*, 108 (B4), 2222. Doi 10.1029/2002JB001935.
Christoffersen, P. & Tulaczyk, S. (2003b) Signature of palaeo-ice-stream stagnation: till consolidation induced by basal freeze-on. *Boreas,* 32 (1)**:** 114-129. Doi 10.1080/03009480310001065.
Clark, C.D. (1993) Mega-scale glacial lineations and cross-cutting ice-flow landforms. *Earth Surface Processes and Landforms,* 18 (1)**:** 1-29.
Clark, C.D. (1997) Reconstructing the evolutionary dynamics of former ice sheets using multi-temporal evidence, remote sensing and GIS. *Quaternary Science Reviews,* 16 (9)**:** 1067-1092.
Clark, C.D., Evans, D.J.A., Khatwa, A., Bradwell, T., Jordan, C.J., Marsh, S.H., Mitchell, W.A. & Bateman, M.D. (2004) Map and GIS database of glacial landforms and features related to the last British Ice Sheet. *Boreas,* 33 (4)**:** 359-375. Doi 10.1080/03009480410001983.

Clark, C.D., Hughes, A.L.C., Greenwood, S.L., Spagnolo, M. & Ng, F.S.L. (2009) Size and shape characteristics of drumlins, derived from a large sample, and associated scaling laws. *Quaternary Science Reviews,* 28**:** 677-692.

Clark, C.D., Knight, J.K. & Gray, J.T. (2000) Geomorphological reconstruction of the Labrador Sector of the Laurentide Ice Sheet. *Quaternary Science Reviews,* 19 (13)**:** 1343-1366.

Clark, C.D. & Meehan, R.T. (2001) Subglacial bedform geomorphology of the Irish Ice Sheet reveals major configuration changes during growth and decay. *Journal of Quaternary Science,* 16 (5)**:** 483-496.

Clark, C.D. & Stokes, C.R. (2003) Palaeo-ice stream landsystem. *In:* Evans, D.J.A. (ed.) *Glacial landsystems.* London: Arnold.

Clark, C.D., Tulaczyk, S.M., Stokes, C.R. & Canals, M. (2003) A groove-ploughing theory for the production of mega-scale glacial lineations, and implications for ice-stream mechanics. *Journal of Glaciology,* 49 (165)**:** 240-256.

Clarke, G.K.C. (2005) Subglacial processes. *Annual Review of Earth and Planetary Sciences,* 33**:** 247-276. Doi 10.1146/annurev.earth.33.092203.122621.

Cohen, D., Hooke, R.L., Iverson, N.R. & Kohler, J. (2000) Sliding of ice past an obstacle at Engabreen, Norway. *Journal of Glaciology,* 46 (155)**:** 599-610.

Connor, L.N., Laxon, S.W., Ridout, A.L., Krabill, W.B. & Mcadoo, D.C. (2009) Comparison of Envisat radar and airborne laser altimeter measurements over Arctic sea ice. *Remote Sensing of Environment,* 113 (3)**:** 563-570. Doi 10.1016/j.rse.2008.10.015.

Conway, H., Catania, G., Raymond, C.F., Gades, A.M., Scambos, T.A. & Engelhardt, H. (2002) Switch of flow direction in an Antarctic ice stream. *Nature,* 419 (6906)**:** 465-467. Doi 10.1038/Nature01081.

Copland, L. & Sharp, M. (2001) Mapping thermal and hydrological conditions beneath a polythermal glacier with radio-echo sounding. *Journal of Glaciology,* 47 (157)**:** 232-242.

Cox, N.J. (2004) Speaking Stata: Graphing model diagnostics. *The Stata Journal*, 4(4): 449-475.

Cox, N.J. (2006) Assessing agreement of measurements and predictions in geomorphology. *Geomorphology,* 76 (3-4)**:** 332-346. Doi 10.1016/j.geomorph.2005.12.001.

Cox, N.J. (2007) Kernel estimation as a basic tool for geomorphological data analysis. *Earth Surface Processes and Landforms*, 32: 1902-1912. Doi 10.1002/esp.1518

Cox. N.J. (2010) Speaking Stata: the limits of sample skewness and kurtosis. *The Stata Journal*, 10(3): 482-495.

Cox, N.J., Warburton, J., Armstrong, A. & Holiday, V.J. (2008) Fitting concentration and load rating curves with generalized linear models. *Earth Surface Processes and Landforms*, 33(1): 25-39. Doi 10.1002/esp.1523.

Cressie, N. & Hawkins, D.M. (1980) Robust Estimation of the Variogram .1. *Journal of the International Association for Mathematical Geology,* 12 (2)**:** 115-125.

Csanady, G.T. (1974) Roughness of sea-surface in light winds. *Journal of Geophysical Research,* 79 (18)**:** 2747-2751.

Cuffey, K.M., Conway, H., Hallet, B., Gades, A.M. & Raymond, C.F. (1999) Interglacial water in polar glaciers and glacier sliding at -17°C. *Geophysical Research Letters*, 26(6):751-754.

Cuthbert, L. & Huynh, V.M. (1992) Statistical-analysis of optical Fourier-transform patterns for surface texture assessment. *Measurement Science & Technology,* 3 (8)**:** 740-745.

Czichos, H., Saito, T. & Smith, L.R. (2006) *Springer handbook of materials measurement methods,* New York, Springer.

Daugaard, H., Elmengaard, B., Bechtold, J.E. & Soballe, K. (2007) Bone growth enhancement in vivo on press-fit titanium alloy implants with acid etched microtexture. *Journal of Biomedical Materials Research, Part A,* 87 (2)**:** 434-40. Doi 10.1002/jbm.a.31748.

Davidson, M.W.J., Le Toan, T., Mattia, F., Satalino, G., Manninen, T. & Borgeaud, M. (2000) On the characterization of agricultural soil roughness for radar remote

sensing studies. *IEEE Transactions on Geoscience and Remote Sensing,* 38 (2)**:** 630-640.
Davidson, M.W.J., Mattia, F., Satalino, G., Verhoest, N.E.C., Le Toan, T., Borgeaud, M., Louis, M.M.B. & Attema, E. (2003) Joint statistical properties of RMS height and correlation length derived from multisite 1-m roughness measurements. *IEEE Transactions on Geoscience and Remote Sensing,* 41 (7)**:** 1651-1658. Doi 10.1109/Tgrs.2003.813361.
Davim, J.P., Clemente, V.C. & Silva, S. (2009) Surface roughness aspects in milling MDF (medium density fibreboard). *International Journal of Advanced Manufacturing Technology,* 40 (1-2)**:** 49-55. Doi 10.1007/s00170-007-1318-z.
De Angelis, H. (2007) Glacial geomorphology of the east-central Canadian Arctic. *Journal Of Maps***:** 323-341.
De Angelis, H. & Kleman, J. (2008) Palaeo-ice-stream onsets: examples from the north-eastern Laurentide Ice Sheet. *Earth Surface Processes and Landforms,* 33 (4)**:** 560-572.
Derr, V.E. & Little, C.G. (1970) A comparison of remote sensing of the clear atmosphere by optical, radio, and acoustic radar techniques. *Applied Optics,* 9 (9)**:** 1976-1992.
Ding, Y., Jia, Y. & Wang, S.S.Y. (2004) Identification of Manning's roughness coefficients in shallow water flows. *Journal of Hydraulic Engineering,* 130 (6)**:** 501-510. Doi 10.1061/(Asce)0733-9429(2004)130:6(501).
Doake, C.S.M. (1981) Polarization of radio waves in ice sheets. *Geophysical Journal of the Royal Astronomical Society,* 64**:** 539-558.
Doake, C.S.M., Corr, H.F.K., Jenkins, A., Nicholls, K.W. & Stewart, C. (2003) Interpretation of polarimetric ice penetrating radar data over Antarctic ice shelves. *Forum For Research into Ice Shelf Processes (FRISP) Report*, 14: 135-148.
Dong, W.P., Mainsah, E. & Stout, K.J. (1995) Reference planes for the assessment of surface roughness in three-dimensions. *International Journal of Machine Tools and Manufacture,* 35 (2)**:** 263-271.
Dong, W.P., Sullivan, P.J. & Stout, K.J. (1994) Comprehensive study of parameters for characterizing three-dimensional surface topography. III: parameters for characterising amplitude and some functional properties *Wear,* 178**:** 29-43.
Donoghue, D.N.M, Watt, P.J., Cox, N.J., Dunford, R.W., Wilson, J., Stables, S. & Smith, S. (2004) An evaluation of the use of satellite data for monitoring early development of young Sitka spruce plantation forest growth. *Forestry,* 77 (5): 383-396.
Dowdeswell, J.A. & Evans, S. (2004) Investigations of the form and flow of ice sheets and glaciers using radio-echo sounding. *Reports on Progress in Physics,* 67 (10)**:** 1821-1861. Doi 10.1088/0034-4885/67/10/R03.
Dowdeswell, J.A. & Siegert, M.J. (2002) The physiography of modern Antarctic subglacial lakes. *Global and Planetary Change,* 25**:** 221-236.
Drews, R., Eisen, O., Weikusat, I., Kipfsuhl, S., Lambrecht, A., Steinhage, D., Wilhelms, F. & Miller, H. (2009) Layer disturbances and the radio-echo free zone in ice sheets. *The Cryosphere*, 3: 195-203.
Drewry, D.J. (1975) Comparison of electromagnetic and seismic-gravity ice thickness measurements in East Antarctica. *Journal of Glaciology,* 15 (73)**:** 137-150.
Dyke, A.S. (1993) Landscapes of cold-centred Late Wisconsinan Ice Caps, Arctic Canada. *Progress in Physical Geography,* 17 (2)**:** 223-247.
Dyke, A.S. (2008) The Steensby Inlet Ice Stream in the context of the deglaciation of Northern Baffin Island, Eastern Arctic Canada. *Earth Surface Processes and Landforms,* 33 (4)**:** 573-592. Doi 10.1002/Esp.1664.
Dyke, A.S. & Morris, T.F. (1988) Drumlin fields, dispersal trains, and ice streams in Arctic Canada. *The Canadian Geographer / Le Géographe Canadien*, 32 (1): 86-90.
Echelmeyer, K.A., Harrison, W.D., Larsen, C. & Mitchell, J.E. (1994) The role of the margins in the dynamics of an active ice stream. *Journal of Glaciology* 40 (136): 527-538.

Eisen, O., Wilhelms, F., Nixdorf, U. & Miller, H. (2003) Revealing the nature of radar reflections in ice: DEP-based FDTD forward modelling. *Geophysical Research Letters,* 30 (5). 1218 Doi 10.1029/2002gl016403.

El Feninat, F., Elouatik, S., Ellis, T.H., Sacher, E. & Stangel, I. (2001) Quantitative assessment of surface roughness as measured by AFM: application to polished human dentin. *Applied Surface Science,* 183 (3-4)**:** 205-215.

Elfick, A.P.D., Hall, R.M., Pinder, I.M. & Unsworth, A. (1999) The influence of femoral head surface roughness on the wear of ultrahigh molecular weight polyethylene sockets in cementless total hip replacement. *Journal of Biomedical Materials Research,* 48 (5)**:** 712-718.

Etzelmüller, B. (2000) On the quantification of surface changes using grid-based digital elevation models (DEMs). *Transactions in GIS,* 4 (2)**:** 129-143.

Evans, D.J.A., Clark, C.D. & Mitchell, W.A. (2005) The last British Ice Sheet: A review of the evidence utilised in the compilation of the Glacial Map of Britain. *Earth-Science Reviews,* 70 (3-4)**:** 253-312. Doi 10.1016/j.earscirev.2005.01.001.

Evans, D.J.A., Linvingstone, S.J., Vieli, A. & Ó Cofaigh, C. (2009) The palaeoglaciology of the central sector of the British and Irish Ice Sheet: reconciling glacial geomorphology and preliminary ice sheet modelling. *Quaternary Science Reviews*, 28: 739-757. Doi 10.1016/j.quascirev.2008.05.011.

Evans, I.S. (1972) General geomorphometry, derivatives of altitude and descriptive statistics. *In:* Chorley, R.J. (ed.) *Spatial analysis in geomorphology.* London: Methuen.

Evans, I.S. (1987) A new approach to drumlin morphometry. *In:* Menzies, J. & Rose, J. (eds.) *Drumlin symposium*, p.119-130. Rotterdam, Balkema.

Evans, S. (1969) Glacier sounding in Polar regions : a symposium .1. The VHF radio echo technique. *Geographical Journal,* 135 (4)**:** 547-548.

Evans, S. & Smith, B.M.E. (1969) A radio echo equipment for depth sounding in Polar Ice sheets. *Journal of Physics E: Scientific Instruments,* 2 (2)**:** 131-136.

Everest, J.D., Bradwell, T. & Golledge, N. (2005) Subglacial landforms of the Tweed Palaeo-Ice Stream. *Scottish Geographical Journal* 121 (2): 163-173.

Everest, J.D. & Lawrence, D.J.D. (2006) Geological landscape character assessment, Nortumberland National Park and surrounding area. *British Geological Survey Commissioned Report*. CR/06/108N. 23pp.

Fahnestock, M., Abdalati, W., Joughin, I., Brozena, J. & Gogineni, P. (2001) High geothermal heat flow, basal melt, and the origin of rapid ice flow in central Greenland. *Science*, 294: 2338-2342. Doi 10.1126/sceince.1065370.

Farshad, F., Rieke, H. & Garber, J. (2001) New developments in surface roughness measurements, characterization, and modelling fluid flow in pipes. *Journal of Petroleum Science and Engineering,* 29 (2)**:** 139-150.

Feng, C.X., Wang, X.F. & Yu, Z.G. (2003) Neural networks modelling of honing surface roughness parameters defined by ISO 13565. *Journal of Manufacturing Systems,* 21 (5)**:** 395-408.

Feninat, F. E., Elouatik, S., Ellis, T.H., Sacher, E. & Stangel, I. (2001) Quantitative assessment of surface roughness as measured by AFM: application to polished human dentin. *Applied Surface Science*, 183: 205-215.

Fischer, T., Gemmer, M., Liu, L. & Su, B. (2012) Change-points in climate extremes in the Zhujiang River Basin, South China, 1961-2007. *Climatic Change*, 110: 783-799. Doi 10.1007/s10584-011-0123-8.

Fischer, U.H. & Hubbard, B.P.(2006) Borehole-based subglacial instrumentation. *In:* Knight, P. (ed.) *Glacier science and environmental change.* Oxford, Blackwell.

Fish, R.W. (1966) Navigational and instrument aids to air survey. *The Photogrammetric Record,* 5 (27)**:** 170-180.

Forsberg, R. & Skourup, H. (2005) Arctic Ocean gravity, geoid and sea-ice freeboard heights from ICESat and GRACE. *Geophysical Research Letters,* 32 (21)**:** -. L21502 Doi 10.1029/2005gl023711.

Fowler, A.C. (2010) Weertman, Lliboutry and the development of sliding theory. *Journal of Glaciology*, 56 (200): 965-972.

Fox, C.G. & Hayes, D.E. (1985) Quantitative methods for analysing the roughness of the seafloor. *Reviews of Geophysics,* 23 (1)**:** 1-48.
Frankel, K.L. & Dolan, J.F. (2007) Characterizing arid region alluvial fan surface roughness with airborne laser swath mapping digital topographic data. *Journal of Geophysical Research: Earth Surface,* 112 (F2). Doi 10.1029/2006jf000644.
Frolov, A.D. & Macheret, Y.Y. (1999) On dielectric properties of dry and wet snow. *Hydrological Processes,* 13 (12-13)**:** 1755-1760.
Fuchs, V., Swithinbank, C., Christensen, E.L., Mott, P.G., Evans, S., Gudmandsen, P. & Robin, G.D.Q. (1969) Glacier sounding in polar regions: a symposium: discussion. *The Geographical Journal,* 135 (4)**:** 559-563.
Fujita, S., Maeno, H., Uratsuka, S., Furukawa, T., Mae, S., Fujii, Y. & Watanabe, O. (1999) Nature of radio echo layering in the Antarctic ice sheet detected by a two-frequency experiment. *Journal of Geophysical Research: Solid Earth,* 104 (B6)**:** 13013-13024.
Gadelmawla, E.S. (2004) A vision system for surface roughness characterization using the grey level co-occurrence matrix. *NDT & E International,* 37 (7)**:** 577-588. Doi10.1016/j.ndteint.2004.03.004.
Gadelmawla, E.S., Koura, M.M., Maksoud, T.M.A., Elewa, I.M. & Soliman, H.H. (2001) Using the grey level histogram to distinguish between roughness of surfaces. *Proceedings of the Institution of Mechanical Engineers Part B - Journal of Engineering Manufacture,* 215 (4)**:** 545-553.
Gadelmawla, E.S., Koura, M.M., Maksoud, T.M.A., Elewa, I.M. & Soliman, H.H. (2002) Roughness parameters. *Journal of Materials Processing Technology,* 123**:** 133-145. .
Gades, A., Conway, H., Nereson, N., Naito, N. & Kadota, T. (2000) Radio echo-sounding through supraglacial debris on Lirung and Khumbu Glaciers, Nepal Himalayas. *In:* Nakawo, M., Raymond, C.F. & Fountain, A.G. (eds.) *Debris-covered glaciers.* Wallingford: International Association of Hydrological Sciences, publication no. 264.
Gades, A.M., Raymond, C.F., Conway, H. & Jacobel, R.W. (2000) Bed properties of Siple Dome and adjacent ice streams, West Antarctica, inferred from radio-echo sounding measurements. *Journal of Glaciology,* 46 (152)**:** 88-94
Glasser, N.F. (1995) Modelling the effect of topography on ice sheet erosion, Scotland. *Geografiska Annaler Series A, Physical Geography,* 77 (1-2)**:** 67-82.
Gogineni, S.P., Chuah, T., Allen, C., Jezek, K.C. & Moore, R.K. (1998) An improved coherent radar depth sounder. *Journal of Glaciology,* 44 (148)**:** 659-669
Gogineni, S.P., Tammana, D., Braaten, D., Leuschen, C., Akins, C., Legarsky, J., Kanagaratnam, P., Stiles, J., Allen, C. & Jezek, K.C. (2001) Coherent radar depth sounder measurements over the Greenland ice sheet. *Journal of Geophysical Research,* 106 (D24)**:** 33761-33772.
Goldstein, R.M., Engelhardt, H., Kamb, B. & Frolich, R.M. (1993) Satellite radar interferometry for monitoring ice-sheet motion - application to an Antarctic ice stream. *Science,* 262 (5139)**:** 1525-1530.
Gordon, J.E. (1981) Ice-scoured topography and its relationships to bedrock structure and ice movement in parts of Northern Scotland and West Greenland. *Geografiska Annaler Series A, Physical Geography,* 63 (1-2)**:** 55-65.
Gorlenko, O.A. (1981) Assessment of surface roughness parameters and their interdependence. *Precision Engineering*, 3 (2): 105-108. Doi 10.1016/0141-6359(81)90045-3.
Grohmann, C.H., Smith, M.J. & Riccomini, C. (2009) Surface roughness of topography: a multi-scale analysis of landform elements in Midland Valley, Scotland. *Proceedings of Geomorphometry,* Zurich, Switzerland, 31 August - 2 September
Gudmandsen, P. (1969) Airborne radio echo sounding of the Greenland Ice Sheet. *The Geographical Journal,* 135 (4)**:** 548-551.
Gudmundsson, G.H. (2003) Transmission of basal variability to a glacier surface. *Journal of Geophysical Research-Solid Earth,* 108 (B5). Doi 10.1029/2002jb002107

Gudmundsson, G.H., Adalgeirsdóttir, G. & Björnsson, H. (2003) Observational verification of predicted increase in bedrock-to-surface amplitude transfer during a glacier surge. *Annals of Glaciology*, 36: 91-96.
Gudmundsson, G.H. (2011) Ice-stream response to ocean tides and the form of the basal sliding law. *The Cryosphere*, 5: 259-270. Doi 10.5194/tc-5-259-2011
Guh, R.-S., Zorriassatine, F., Tannock, J.D.T. & O'Brien, C. (1999) On-line control chart pattern detection and discrimination - a neural network approach. *Artifical Intelligence in Engineering*, 13: 413-425.
Gupta, S., Collier, J.S., Palmer-Felgate, A. & Potter, G. (2007) Catastrophic flooding origin of shelf valley systems in the English Channel. *Nature,* 448 (7151)**:** 342-U5. Doi 10.1038/Nature06018.
Gurney, S.D., Popovnin, V.V., Shahgedanova, M. & Stokes, C.R. (2008) A glacier inventory for the Buordakh Massif, Cherskiy Range, northeast Siberia, and evidence for recent glacier recession. *Arctic Antarctic and Alpine Research,* 40 (1)**:** 81-88. Doi 10.1657/1523-0430(06-042)[Gurney]2.0.Co;2.
Hagen, J.O. & Sætrang, A. (1991) Radio-echo soundings of sub-polar glaciers with low-frequency radar. *Polar Research,* 9 (1)**:** 99-107.
Haldorsen, S. (1981) Grain-size distribution of subglacial till and its relation to glacial crushing and abrasion. *Boreas,* 10 (1)**:** 91-105.
Hall, R.M., Siney, P., Unsworth, A. & Wroblewski, B.M. (1997) The effect of surface topography of retrieved femoral heads on the wear of UHMWPE sockets. *Medical Engineering Physics,* 19 (8)**:** 711-719.
Hallet, B. (1979) A theoretical model of glacial abrasion. *Journal of Glaciology*, 23(89): 39-50.
Hallet, B. (1981) Glacial abrasion and sliding: their dependence on the debris concentration in basal ice. *Annals of Glaciology*, 2: 23-28.
Hammer, C.U. (1977) Past volcanism revealed by Greenland Ice Sheet impurities. *Nature,* 270 (5637)**:** 482-486.
Harbor, J., Sharp, M., Copland, L., Hubbard, B., Nienow, P. & Mair, D. (1997) Influence of subglacial drainage conditions on the velocity distribution within a glacier cross section. *Geology,* 25 (8)**:** 739-742.
Hargreaves, N.D. (1977) Polarization of radio signals in radio echo sounding of ice sheets. *Journal of Physics D, Applied Physics,* 10 (9)**:** 1285-1304.
Harrison, C.H. (1970) Reconstruction of subglacial reflief from radio echo sounding records. *Geophysics,* 35 (6)**:** 1099-&1115.
Harrison, W.D., Echelmeyer, K.A., Larsen, C.F. (1998) Measurement of temperature in a margin of Ice Stream B, Antarctica: implications for margin migration and lateral drag. *Journal of Glaciology*, 44: 615-624.
Hart, J.K. (1995) Subglacial erosion, deposition and deformation associated with deformable beds. *Progress in Physical Geography,* 19 (2)**:** 173-191.
Hart, J.K. (1997) The relationship between drumlins and other forms of subglacial glaciotectonic deformation. *Quaternary Science Reviews*, 16: 93-107.
Hart, J.K. & Rose, J. (2001) Approaches to the study of glacier bed deformation. *Quaternary International,* 81 (1)**:** 45-58.
Hart, J.K. & Smith, B. (1997) Subglacial deformation associated with fast ice flow, from the Columbia glacier, Alaska. *Sedimentary Geology,* 111 (1-4)**:** 177-197.
Hattersley-Smith, G. (1966) Results of radio echo sounding in Northern Ellesmere Island, 1966. *The Geographical Journal,* 135 (4)**:** 553-557.
Hättestrand, C., Goodwille, D. & Kleman, J. (1999) Size distribution of two cross-cutting drumlin systems in northern Sweden: a measure of selective erosion and formation time length. *Annals of Glaciology*, 28: 146-152.
Hättestrand, C. & Stroeven, A.J. (2002) A relict landscape in the centre of Fennoscandian glaciation: Geomorphological evidence of minimal Quaternary glacial erosion. *Geomorphology,* 44 (1-2)**:** 127-143. Pii S0169-555x(01)00149-0.
Hättestrand, C., Götz, S., Näslund, J-O., Fabel, D & Stroeven, A.P. (2004) Drumlin formation time: evidence from Northern and Central Sweden. *Geografiska Annaler*

Series A, Physical Geography, 86(2): 155-167. Doi 10.1111/j.0435-3676.2004.00221.x.
Hélière, F., Lin, C.C., Corr, H. & Vaughan, D. (2007) Radio echo sounding of Pine Island Glacier, West Antarctica: Aperture synthesis processing and analysis of feasibility from space. *IEEE Transactions on Geoscience and Remote Sensing,* 45 (8)**:** 2573-2582. Doi 10.1109/Tgrs.2007.891433.
Hempel, L. & Thyssen, F. (1992) Deep radio echo soundings in the vicinity of GRIP and GISP2 drill sites, Greenland. *Polarforschung,* 62 (1)**:** 11-16.
Herzfeld, U.C., Mayer, H., Feller, W. & Mimler, M. (2000a) Geostatistical analysis of glacier-roughness data. *Annals of Glaciology,* 30**:** 235-242.
Herzfeld, U.C., Stauber, M. & Stahl, N. (2000b) Geostatistical characterization of ice surfaces from ERS-1 and ERS-2 SAR data, Jakobshavn Isbræ, Greenland. *Annals of Glaciology,* 30**:** 224-234.
Herzfeld, U.C., Stosius, R. & Schneider, M. (2000c) Geostatistical methods for mapping Antarctic ice surfaces at continental and regional scales. *Annals of Glaciology,* 30**:** 76-82.
Hildes, D.H.D., Clarke, G.K.C., Flowers, G.E. & Marshall, S.J. (2004) Subglacial erosion and englacial sediment transport modelled for North American ice sheets. *Quaternary Science Reviews,* 23 (3-4)**:** 409-430. Doi 10.1016/j.quascirev.2003.06.005.
Hindmarsh, R.C.A. (1997) Deforming beds: Viscous and plastic scales of deformation. *Quaternary Science Reviews,* 16 (9)**:** 1039-1056.
Hindmarsh, R.C.A. (1998) Ice-stream surface texture, sticky spots, waves and breathers: the coupled flow of ice, till and water. *Journal of Glaciology,* 44 (148)**:** 589-614.
Hindmarsh, R.C.A. (1999) Coupled ice-till dynamics and the seeding of drumlins and bedrock forms. *Annals of Glaciology,* 28**:** 221-230.
Hindmarsh, R.C.A. (2000) Sliding over anisotropic beds. *Annals of Glaciology,* 30**:** 137-145.
Hindmarsh, R.C.A., Leysinger-Vieli, G.J.M.C., Raymond, M.J. & Gudmundsson, G.H. (2006) Draping or overriding: The effect of horizontal stress gradients on internal layer architecture in ice sheets. *Journal of Geophysical Research-Earth Surface,* 111 (F2). Doi 10.1029/2005jf000309.
Hindmarsh, R.C.A. & Stokes, C.R. (2008) Formation mechanisms for ice-stream lateral shear margin moraines. *Earth Surface Processes and Landforms,* 33 (4)**:** 610-626. Doi 10.1002/Esp.1665.
Hobbs, H. (1999) Origin of the Driftless Area by subglacial drainage - a new hypothesis. *In:* Mickelson, D.M. & Attig, J.W. (eds.) *Glacial processes: past and present.* Boulder, Colorado: Geological Society of America Special Paper 337.
Hoffman, E.G., Mccauley, C.J. & Hussain, M.I. (2000). *Shop reference for students and apprentices,* New York, Industrial Press Inc.
Holland, D.M., Jacobs, S.S. & Jenkins, A. (2003) Modelling the ocean circulation beneath the Ross Ice Shelf. *Antarctic Science,* 15 (1)**:** 13-23. Doi 10.1017/S0954102003001019.
Holmlund, P. (1986) Mikkaglaciaren: bed topography and response to 20th Century climate change. *Geografiska Annaler Series A, Physical Geography,* 68 (4)**:** 291-302.
Hooke, R.L. (2005) *Principles of glacier mechanics, second edition*. Cambridge University Press.
Hu, Z.M. & Dean, T.A. (2000) A study of surface topography, friction and lubricants in metalforming. *International Journal of Machine Tools & Manufacture,* 40 (11)**:** 1637-1649.
Hubbard, A. (1999) High-resolution modelling of the advance of the Younger Dryas ice sheet and its climate in Scotland. *Quaternary Research,* 52 (1)**:** 27-43.
Hubbard, B. & Hubbard, A. (1998) Bedrock surface roughness and the distribution of subglacially precipitated carbonate deposits: Implications for formation at Glacier de Tsanfleuron, Switzerland. *Earth Surface Processes and Landforms,* 23 (3)**:** 261-270.

Hubbard, A., Bradwell, T., Golledge, N., Hall, A., Patton, H., Sugden, D., Cooper, R. & Stoker, M. (2009) Dynamic cycles, ice streams and their impact on the extent, chronology and deglaciation of the British-Irish ice sheet. *Quaternary Science Reviews*, 28(7-8): 758-776. Doi 10.1016/j.quascirev.2008.12.026.

Hubbard, B., Siegert, M.J. & Mccarroll, D. (2000) Spectral roughness of glaciated bedrock geomorphic surfaces: Implications for glacier sliding. *Journal of Geophysical Research-Solid Earth,* 105 (B9)**:** 21295-21303.

Hubbard, T.D. & Reid, J.R. (2006) Analysis of flute forming conditions using ice sheet reconstructions and field techniques. *Geomorphology,* 74 (1-4)**:** 137-151. Doi 10.1016/j.geomorph.2005.07.013.

Hughes, R.A. (2003a) Carboniferous rocks and Quaternary deposits of the Appleby district (part of Sheet 30, England and Wales). *British Geological Survey Research Report*, RR/01/09.

Hughes, R.A. (2003b) Permain and Triassic rocks of the Appleby district (Sheet 30, England and Wales). *British Geological Survey Research Report*, RR/02/01.

Hughes, T. (1992) On the pulling power of the ice streams. *Journal of Glaciology*, 38 (128): 125-151.

Hulton, N.R.J. & Mineter, M.J. (2000) Modelling self-organization in ice streams. *Annals of Glaciology,* 30**:** 127-136.

Huybrechts, P. (1996) Basal temperature conditions of the Greenland ice sheet during the glacial cycles. *Annals of Glaciology,* 23**:** 226-236.

Huybrechts, P., Steinhage, D., Wilhelms, F. & Bamber, J. (2000) Balance velocities and measured properties of the Antarctic ice sheet from a new compilation of gridded data for modelling. *Annals of Glaciology,* 30**:** 52-60.

Iverson, N.R., Hanson, B., Hooke, R.L. & Jansson, P. (1995) Flow mechanism of glaciers on soft beds. *Science,* 267 (5194)**:** 80-81.

Iverson, N.R., Hooyer, T.S., Fischer, U.H., Cohen, D., Moore, P.L., Jackson, M., Lappegard, G. & Kohler, J. (2007) Soft-bed experiments beneath Engabreen, Norway: regelation infiltration, basal slip and bed deformation. *Journal of Glaciology,* 53 (182)**:** 323-340.

Jacka, T.H. 2006. Glacier composition, mechanics and dynamics. *In:* Knight, P. (ed.) *Glacier science and environmental change.* Oxford: Blackwell.

Jacobel, R.W., Scambos, T.A., Raymond, C.F. & Gades, A.M. (1996) Changes in the configuration of ice stream flow from the West Antarctic Ice Sheet. *Journal of Geophysical Research-Solid Earth,* 101 (B3)**:** 5499-5504.

Jansson, K.N. & Glasser, N.F. (2005) Palaeoglaciology of the Welsh sector of the British - Irish Ice sheet. *Journal of the Geological Society, London*, 162: 25-37. Doi 10.1144/0016-764901-009.

Johnson, M.R. & Smith, A.M. (1997) Seabed topography under the southern and western Ronne Ice Shelf, derived from seismic surveys. *Antarctic Science,* 9 (2)**:** 201-208.

Jonasson, M., Wihlborg, A. & Gunnarsson, L. (1998) Analysis of surface topography changes in steel sheet strips during bending under tension friction test. *International Journal of Machine Tools & Manufacture,* 38 (5-6)**:** 459-467.

Jones, C.W. & Leach, R.K. (2008) Adding a dynamic aspect to ampliude-wavelength space. *Measurement Science and Technology*, 19 005105. Doi 10.1088/0957-0233/19/5/005105.

Joughin, I., Abdalati, W. & Fahnestock, M. (2004) Large flucuations in speed on Greenland's Jakobshavn Isbræ glacier. *Nature*, 432: 608-610.

Joughin, I. (2006) Interferometric synthetic aperture radar (InSAR) study of the Northeast Greenland Ice Stream. *In:* Knight, P.G. (ed.) *Glacier science and environmental change.* Oxford: Blackwell.

Joughin, I., Gray, L., Bindschadler, R., Price, S., Morse, D., Hulbe, C., Mattar, K. & Werner, C. (1999) Tributaries of West Antarctic ice streams revealed by RADARSAT interferometry. *Science,* 286 (5438)**:** 283-286.

Joughin, I. & Tulaczyk, S. (2002) Positive mass balance of the Ross Ice Streams, West Antarctica. *Science,* 295 (5554)**:** 476-480.

Joughin, I., Tulaczyk, S., Bindschadler, R. & Price, S.F. (2002) Changes in west Antarctic ice stream velocities: Observation and analysis. *Journal of Geophysical Research - Solid Earth,* 117 (B11). Doi 10.1029/2001JB001029.

Joughin, I.R., Kwok, R. & Fahnestock, M.A. (1998) Interferometric estimation of three-dimensional ice-flow using ascending and descending passes. *IEEE Transactions on Geoscience and Remote Sensing,* 36 (1)**:** 25-37.

Kalpakjian, S. (1997). *Manufacturing processes for engineering materials,* Menlo Park, CA, Addison-Wesley.

Kamb, B. (1970) Sliding motion of glaciers - theory and observation. *Reviews of Geophysics and Space Physics,* 8 (4)**:** 673-728.

Kanagaratnam, P. (2002). *Airborne radar for high-resolution mapping of internal layers in glacial ice to estimate accumulation rate.* Department of Electrical Engineering and Computer Science, The University of Kansas [PhD thesis].

Karlsson, N.B., Rippin, D.M., Vaughan, D.G. & Corr, H.F.J. (2009) The interval layering of Pine Island Glacier, West Antarctica, from airborne radar-sounding data. *Annals of Glaciology* 50 (51): 141-146.

Kayton, M. & Fried, W.R. (1997). *Avionics navigation systems,* New York, Wiley.

King, E.C., Woodward, J. & Smith, A.M. (2007) Seismic and radar observations of subglacial bed forms beneath the onset zone of Rutford Ice Stream, Antarctica. *Journal of Glaciology* 53 (183): 665-672.

King, E.C., Hindmarsh, R.C.A. & Stokes, C.R. (2009) Formation of mega-scale glacial lineations observed beneath a West Antarctic ice stream. *Nature geoscience*, 2 (8): 585-588 Doi 10.1038/NGEO0581.

Kjær, K.H., Houmark-Nielsen, M. & Richardt, N. (2003) Ice-flow patterns and dispersal of erratics at the southwestern margin of the last Scandinavian Ice Sheet: signature of palaeo-ice streams. *Boreas,* 32 (1)**:** 130-148. Doi 10.1080/03009480310001074.

Kleman, J. (1990) On the use of glacial striae for reconstruction of paleo-ice sheet flow patterns. *Geografiska Annaler Series A, Physical Geography,* 72 (3-4)**:** 217-236.

Kleman, J. & Borgström, I. (1996) Reconstruction of palaeo-ice sheets: The use of geomorphological data. *Earth Surface Processes and Landforms,* 21 (10)**:** 893-909.

Knight, J. (2002) Glacial sedimentary evidence supporting stick-slip basal ice flow. *Quaternary Science Reviews,* 21 (8-9)**:** 975-983. Pii S0277-3791(01)00050-6

Knight, J. & Mccabe, A.M. (1997) Identification and significance of ice-flow-transverse subglacial ridges (Rogen moraines) in northern central Ireland. *Journal of Quaternary Science,* 12 (6)**:** 519-524.

Knight, P.G. (1999). *Glaciers,* Cheltenham, Stanley Thornes.

Knight, P.G. (ed.) 2006. *Glacier science and environmental change,* Oxford: Blackwell.

Koh, J.S., Kang, H., Choi, S.W. & Kim, H.O. (2002) Cigarette smoking associated with premature facial wrinkling: image analysis of facial skin replicas. *International Journal of Dermatology,* 41 (1)**:** 21-27.

Kovacs, A., Gow, A.J. & Morey, R.M. (1995) The in-situ dielectric-constant of polar firn revisited. *Cold Regions Science and Technology,* 23 (3)**:** 245-256.

Kozak, A., Kozak, R.A, Staudhammer, C.L. & Watts, S.B. (2008) *Introductory probability any statistics: applications for forestry and natural sciences.* CAB International, Oxford.

Krabbendam, M. & Bradwell, T. (2011) Lateral plucking as a mechanism for elongate erosional glacial bedforms: explaining megagrooves in Britain and Canada. *Earth Surface Processes and Landforms*, 36 (10): 1335-1349. Doi 10.1002/esp.2157.

Krajnik, P., Kopac, J. & Sluga, A. (2005) Design of grinding factors based on response surface methodology. *Journal of Materials Processing Technology,* 162**:** 629-636. Doi 10.1016/j.jmatprotec.2005.02.187.

Kumar, S., Chaudhury, K., Sen, P. & Guha, S.K. (2007) Quantitative analysis of surface micro-roughness alterations in human spermatozoa using atomic force microscopy. *Journal of Microscopy,* 227 (2)**:** 118-123.

Kupko, V.S., Lukin, I.V., Risto, V.A., Kovshov, S.B. & Kosenko, O.A. (2007) Linear and angular measurements: a primary standard equipment for measuring roughness parameters in the range from nanometers to millimeters. *Measurement Techniques,* 50 (11)**:** 1143-1148. Doi 10.1007/s11018-007-0213-1.

Lane, P.W. (2002) Generalized linear models in soil science. *European Journal of Soil Science*, 53: 241-251.

Lane, S.N. (2005) Roughness - time for a re-evaluation? *Earth Surface Processes and Landforms,* 30 (2)**:** 251-253. Doi 10.1002/Esp.1208.

Lavernhe, S., Quinsat, Y. & Lartigue, C. (2010) Model for the prediction of 3D surface topography in 5-axis milling. *International Journal of Advanced Manufacturing Technology*. Doi 10.1007/s00170-010-2686-3.

Le Brocq, A.M., Hubbard, A., Bentley, M.J. & Bamber, J.L. (2008) Subglacial topography inferred from ice surface terrain analysis reveals a large un-surveyed basin below sea level in East Antarctica. *Geophysical Research Letters,* 35 (16)**:** L16503. Doi 10.1029/2008gl034728.

Leysinger Vieli, G.J.-M.C. (2007) Three-dimensional flow influences on radar layer stratigraphy. *Annals of Glaciology,* 46**:** 22-28.

Leysinger Vieli, G.J.-M.C., Hindmarsh, R.C.A. & Siegert, M.J. (2007) Three-dimensional flow influences on radar layer stratigraphy. *Annals of Glaciology,* 46**:** 22-28.

Leysinger Vieli, G.J.-M.C. & Gudmundsson, G.H. (2010) A numerical study of glacier advance over deforming till. *The Cryosphere*, 4: 359-372. Doi 10.5194/tc-4-359-2010.

Li, P., Zheng, F. & Chang, J.T. (2009a) *Effects of surface texture on far field pattern of the reflector antenna*. Radar Conference, 2009 IET International, 20-22 April. p.1-4.

Li, W., Diao, Y.P., Wang, S.Y., Fang, G.P., Wang, G.C., Dong, X.J., Long, S.C. & Qiao, G.J. (2009b) New roughness parameter for the characterization of regularly textured or ordered patterned superhydrophobic surfaces. *Langmuir,* 25 (11)**:** 6076-6080. Doi 10.1021/La901073w.

Li, X., Sun, B., Siegert, M.J., Bingham, RG., Tang, X. Zhang, D., Cui, X. & Zhang, X. (2010) Characterization of subglacial landscapes by a two-parameter roughness index. *Journal of Glaciology*, 56 (199): 831-836. Doi 10.3189/002214310794457326.

Lillesand, T.M., Kiefer, R.W. & Chipman, J.W. (2004). *Remote sensing and image interpretation,* Hoboken, NJ, Wiley.

Lin, L.I.K. (2000) Total deviation index for measuring individual agreement with applications in laboratory performance and bioequivalence. *Statistics in Medicine,* 19 (2)**:** 255-270.

Ling, C.H. & Untersteiner, N. (1974) Calculation of roughness parameter of sea ice. *Journal of Geophysical Research,* 79 (27)**:** 4112-4114.

Liu, R. & Li, D.Y. (1999) Experimental studies on the tribological properties of pseudoelastic TiNi alloy with comparison to stainless steel 304. *Metallurgical and Material Transactions A,* 31 (11)**:** 2773-2783.

Livingstone, S.J., Ó Cofaigh, C. & Evans, D.J.A. (2008) Glacial geomorphology of the central sector of the last British-Irish Ice Sheet. *Journal of Maps* 2008: 258-377.

Livingstone, S.J., Ó Cofaigh, C. & Evans, D.J.A. (2010) A major ice drainage pathway of he last British-Irish Ice Sheet: the Tyne Gap, northern England. *Journal of Quaternary Science*, 25 (3): 254-370. Doi 10.1002/jqs.1341.

Livingstone, S.J., Evans, D.J.A., Ó Cofaigh, C., Davies, B.J., Merritt, J.W., Huddart, D., Mitchell, W.A., Roberts, D.H. & Yorke, L. (2012) Glaciodynamics of the central sector of the last British-Irish Ice Sheet in Northern England. *Earth-Science Reviews* 111(1-2): 25-55. Doi 10.1016/j.earscirev.2011.12.006.

Lou, M.S., Chen, J.C. & Li, C.M. (1998) Surface roughness prediction technique for CNC end-milling. *Journal of Industrial Technology,* 15 (1)**:** 2-6.

Lowe, H.F. & Spindloe, C. (2007) White light interfeometric profilometry of surface structured glas for high power laser microtargets. *Central Laser Facility annual report 2006/2007: 7. Target fabrication.* Target Fabrication Group, Central Laser

Facility, STFC, Rutherford Appleton Laboratory, HSIC, Didcot, Oxfordshire OX11 0QX.
Lythe, M.B. & Vaughan, D.G. (2001) BEDMAP: A new ice thickness and subglacial topographic model of Antarctica. *Journal of Geophysical Research-Solid Earth,* 106 (B6)**:** 11335-11351.
Maltman, A.J., Hubbard, B. & Hambrey, M.J. (2000) Deformation of glacial materials: introduction and overview. *Geological Society of London, Special Publications,* 176 (1)**:** 1-4.
Manes, C., Guala, M., Lowe, H., Bartlett, S., Egli, L. & Lehning, M. (2008) Statistical properties of fresh snow roughness. *Water Resources Research,* 44 (11). W11407 Doi 10.1029/2007wr006689.
Mark, D.M. (1975) Geomorphometric parameters: a review and evaluation. *Geografiska Annaler Series A, Physical Geography,* 57 (3/4)**:** 165-177.
Marshall, S.J. (2005) Recent advances in understanding ice sheet dynamics. *Earth and Planetary Science Letters*, 240: 191-204.
Massonnet, D. & Fiegl, K.L. (1998) Radar interferometry and its application to changes in the Earth's surface. *Reviews of Geophysics,* 36 (4)**:** 441-500.
Matejka, T. & Lewis, S.A. (1997) Improving research aircraft navigation by incorporating INS and GPS information in a variational solution. *Journal of Atmospheric and Oceanic Technology,* 14 (3)**:** 495-511.
Matheron, G. (1963) Principles of geostatistics. *Economic Geology,* 58**:** 1246-1266.
Mattia, F., Davidson, M.W.J., Le Toan, T., D'haese, C.M.F., Verhoest, N.E.C., Gatti, A.M. & Borgeaud, M. (2003) A comparison between soil roughness statistics used in surface scattering models derived from mechanical and laser profilers. *IEEE Transactions on Geoscience and Remote Sensing,* 41 (7)**:** 1659-1671. Doi 10.1109/Tgrs.2003.813359.
Maurer, T., Herrmann, L. & Stahr, K. (2010) Wind erosion characteristics of Sahelian surface types. *Earth Surface Processes and Landforms*. DOI 10.1002/esp.1975.
Mayer, C. & Siegert, M.J. (2000) Numerical modelling of ice-sheet dynamics across the Vostok subglacial lake, central East Antarctica. *Journal of Glaciology,* 46 (153)**:** 197-205.
Mayer, H. & Herzfeld, U.C. (2000) Structural glaciology of fast-moving Jakobshavn Isbræ, Greenland, compared to the surging Bering Glacier, Alaska, U.S.A. *Annals of Glaciology*, 30 (1): 243-249.
Mccarroll, D. & Nesje, A. (1993) The vertical extent of ice sheets in Nordfjord, Western Norway: measuring degree of rock surface weathering. *Boreas,* 22 (3)**:** 255-265.
Mccarroll, D. & Nesje, A. (1996) Rock surface roughness as an indicator of degree of rock surface weathering. *Earth Surface Processes and Landforms,* 21 (10)**:** 963-977.
Mcgrath, J. & Davis, C. (2004) Polishing pad surface characterisation in chemical mechanical planarisation. *Journal of Materials Processing Technology,* 153-54**:** 666-673. Doi 10.1016/j.jmatprotec.2004.04.094.
McKenzie, N.J. & Austin, M.P. (1993) A quantitative Australian approach to medium and small scale surveys based on soil stratigraphy and environmental correlation. *Geoderma*, 57: 329-355.
Mendeleev, V.Y. (2003) Empirical relations for height and spacing parameters of surface roughness. *Measurement Techniques,* 46 (7)**:** 662-666.
Menezes, P.L., Kishore & Kailas, S.V. (2008) Effect of surface roughness parameters and surface texture on friction and transfer layer formation in tin-steel tribo-system. *Journal of Materials Processing Technology,* 208 (1-3)**:** 372-382. Doi 10.1016/j.jmatprotec.2008.01.003.
Menezes, P.L., Kishore & Kailas, S.V. (2009a) Influence of roughness parameters and surface texture on friction during sliding of pure lead over 080 M40 steel. *International Journal of Advanced Manufacturing Technology,* 43 (7-8)**:** 731-743. Doi 10.1007/s00170-008-1756-2.
Menezes, P.L., Kishorea & Kailas, S.V. (2009b) Influence of surface texture and roughness parameters on friction and transfer layer formation during sliding of

aluminium pin on steel plate. *Wear,* 267 (9-10)**:** 1534-1549. Doi 10.1016/j.wear.2009.06.003.
Milana, J.P. & Maturano, A. (1999) Application of radio echo sounding at the arid Andes of Argentina: the Agua Negra Glacier. *Global and Planetary Change,* 22 (1-4)**:** 179-191.
Milledge, D.G., Lane, S.N. & Warburton, J. (2009) The potential of digital filtering of generic topographic data for geomorphological research. *Earth Surface Processes and Landforms,* 34**:** 63-74.
Militký, J. & Bajzik, V. (2003) Surface roughness of heat protective clothing textiles. *International Journal of Clothing Science and Technology,* 15 (3/4)**:** 358-267.
Mironchenko, V.I. (2005) On the ratio of surface roughness parameters. *Measurement Techniques,* 48(2)**:** 141-145.
Mironchenko, V.I. (2009) Linear and angular measurements: correlation of roughness parameters R_a and R_q with an optical method of measuring them. *Measurement Techniques,* 52 (4)**:** 354-359.
Mitchell, W.A. (1994) Drumlins in ice-sheet reconstructions, with reference to the Western Pennines, Northern England. *Sedimentary Geology,* 91 (1-4)**:** 313-331.
Mitchell, W.A. (2007) Reconstructions of the Late Devensian (Dimlington Stadial) British-Irish Ice Sheet: the role of the upper Tees drumlin field, north Pennines, England. *Proceedings of the Yorkshire Geological Society*, 56 (4): 221-234.
Mitchell, W.A. & Clark, C.D. (1994) The last ice sheet in Cumbria. IN: Boarman, J. & Walden, J. (Eds.) *Cumbria - field guide*. Quaternary Research Association. Oxford, pp. 4-14.
Mitchell, W.A. & Riley, J.M. (2006) Drumlin map of the Western Pennines and southern Vale of Eden, Northern England, UK. *Journal of Maps*, 2 (1): 10-16.
Montgomery, D.R. & Buffington, J.M. (1997) Channel-reach morphology in mountain drainage basins. *Geological Society of America Bulletin*, 109 (5): 596-611.
Moreau, J., Ghienne, J.F., Le Heron, D.P., Rubino, J.L. & Deynoux, M. (2005) 440 Ma ice stream in North Africa. *Geology,* 33 (9)**:** 753-756. Doi 10.1130/G21782.1.
Moutinho, I.M.T., Ferreira, P.J.T. & Figueiredo, M.L. (2007) Impact of surface sizing on inkjet printing quality. *Industrial & Engineering Chemistry Research,* 46**:** 6183-6188. Doi 10.1021/ie070356k.
Murray, T., Booth, A. & Rippin, D.M. (2007) Water-content of glacier-ice: limitations on estimates from velocity analysis of surface ground-penetrating radar surveys. *Journal of Environmental and Engineering Geophysics*, 12: 87-99. Doi 10.2113/JEEG12.1.87.
Murray, T., Corr, H., Forieri, A. & Smith, A.M. (2008) Contrasts in hydrology between regions of basal deformation and sliding beneath Rutford Ice Stream, West Antarctica, mapped using radar and seismic data. *Geophysical Research Letters,* 35 (12). L12504 Doi 10.1029/2008gl033681.
Najjar, D., Bigerelle, M. & Iost, A. (2003) The computer-based bootstrap method as a tool to select a relevant surface roughness parameter. *Wear,* 254**:** 450-460.
Näslund, J.O., Rodhe, L., Fastook, J.L. & Holmlund, P. (2003) New ways of studying ice sheet flow directions and glacial erosion by computer modelling - examples from Fennoscandia. *Quaternary Science Reviews,* 22 (2-4)**:** 245-258. Pii S0277-3791(02)00079-3.
Nelder, J.A. & Wedderburn, R.W.M.(1972) Generalized linear models. *Journal of the Roual Statistical Society, Series A (General)* 135 (3): 370-384.
Nereson, N.A., Raymond, C.F., Jacobel, R.W. & Waddington, E.D. (2000) The accumulation pattern across Siple Dome, West Antarctica, inferred from radar-detected internal layers. *Journal of Glaciology,* 46 (152)**:** 75-87.
Nitsche, F.O., Gohl, K., Larter, R.D., Hillenbrand, C.-D., Kuhn, G., Smith, J.A., Jacobs, S., Anderson, J.B. & Jakobsson, M. (2013) Paleo ice flow and subglacial meltwater dynamics in Pine Island Bay, West Antarctica. *The Cryosphere*, 7: 249-262.
Nolin, A.W., Fetterer, F.M. & Scambos, T.A. (2002) Surface roughness characterizations of sea ice and ice sheets: Case studies with MISR data. *IEEE Transactions on*

Geoscience and Remote Sensing, 40 (7)**:** 1605-1615. Doi 10.1109/Tgrs.2002.801581.
Nye, J.F. (1969) A calculation on sliding of ice over a wavy surface using a Newtonian viscous approximation. *Proceedings of the Royal Society of London Series A, Mathematical and Physical Sciences,* 311 (1506)**:** 445-467.
Nye, J.F. (1970) Glacier sliding without cavitation in a linear viscous approximation. *Proceedings of the Royal Society of London Series A, Mathematical and Physical Sciences,* 315 (1522)**:** 381-403.
Ó Cofaigh, C., Dowdeswell, J.A., Evans, J. & Larter, R.D. (2008) Geological constraints on Antarctic palaeo-ice-stream retreat. *Earth Surface Processes and Landforms,* 33**:** 513-525. Doi 10.1002/esp.1669.
Ó Cofaigh, C., Pudsey, C.J., Dowdeswell, J.A. & Morris, P. (2002) Evolution of subglacial bedforms along a paleo-ice stream, Antarctic Peninsula continental shelf. *Geophysical Research Letters,* 29 (8). Doi 10.1029/2001gl014488.
Ó Cofaigh, C. & Stokes, C.R. (2008) Reconstructing ice-sheet dynamics from subglacial sediments and landforms: introduction and overview. *Earth Surface Processes and Landforms,* 33 (4)**:** 495-502. Doi 10.1002/Esp.1672.
Oerlemans, J. (1982) A model of the Antarctic Ice Sheet. *Nature,* 297 (5867)**:** 550-553.
Oppenheimer, M. (1998) Global warming and the stability of the West Antarctic Ice Sheet. *Nature,* 393 (6683)**:** 325-332.
Oswald, G.K.A. & Gogineni, S.P. (2008) Recovery of subglacial water extent from Greenland radar survey data. *Journal of Glaciology,* 54 (184)**:** 94-106.
Ottesen, D., Dowdeswell, J.A., & Rise, L. (2005) Submarine landforms and the reconstruction of fast-flowing ice streams within a large Quaternary ice sheet: the 2500-km-long Norwegian-Svalbard margin (75°-80°N). *Geological Society of America Bulletin*, 117 (7-8): 1033-1050. Doi 10.1130/B25577.1.
Ottesen, D., Stokes, C.R., Rise, L. & Olsen, L. (2008) Ice-sheet dynamics and ice streaming along the coastal parts of northern Norway. *Quaternary Science Reviews,* 27 (9-10)**:** 922-940. Doi 10.1016/j.quascirev.2008.01.014.
Parrenin, F., Remy, F., Ritz, C., Siegert, M.J. & Jouzel, J. (2004) New modeling of the Vostok ice flow line and implication for the glaciological chronology of the Vostok ice core. *Journal of Geophysical Research-Atmospheres,* 109 (D20). D20102 Doi 10.1029/2004jd004561.
Paterson, W.S.B. (1994). *Physics of Glaciers,* Oxford, Butterworth-Heinemann.
Paterson, W.S.B. & Koerner, R.M. (1974) Radio echo sounding on four ice caps in Arctic Canada. *Arctic,* 27 (3)**:** 225-233.
Patrikar, R.A. (2004) Modelling and simulation of surface roughness. *Applied Surface Science,* 228 (1-4)**:** 213-220. Doi 10.1016/j.apsusc.2004.01.010.
Pattyn, F. (2003) A new three-dimensional higher-order thermomechanical ice sheet model: Basic sensitivity, ice stream development, and ice flow across subglacial lakes. *Journal of Geophysical Research-Solid Earth,* 108 (B8). 2382 Doi 10.1029/2002jb002329.
Pattyn, F., De Smedt, B., De Brabander, S., Van Huele, W.,, Agatova, A., Mistrukov, A. & Decleir, H. (2003) Ice dynamics and basal properities of Sofiyskiy glacier, Altai mountains, Russian, basedon on DGPS and radio-echo sounding surveys.
Pattyn, F., Nolan, M., Rabus, B. & Takahashi, S. (2005) Localized basal motion of a polythermal Arctic glacier: McCall Glacier, Alaska, USA. *Annals of Glaciology*, 40: 47-51.
Pawlus, P. & Śmieszek, M. (2005) The influence of stylus flight on change of surface topography parameters *Precision Engineering,* 29**:** 272-280.
Payne, A.J. (1998) Dynamics of the Siple Coast ice streams, West Antarctica: results from a thermomechanical ice sheet model. *Geophysical Research Letters,* 25 (16)**:** 3173-3176.
Payne, A.J. (1999) A thermomechanical model of ice flow in West Antarctica. *Climate Dynamics,* 15 (2)**:** 115-125.
Payne, A.J. & Vieli, A. 2006. Ice-flow models. *In:* Knight, P.G. (ed.) *Glacier Science and environmental change.* Oxford: Blackwell.

Peltonen, J., Jarn, M., Areva, S., Linden, M. & Rosenholm, J.B. (2004) Topographical parameters for specifying a three-dimensional surface. *Langmuir,* 20 (22)**:** 9428-9431. Doi 10.1021/La0400252.

Peters, M.E., Blankenship, D.D., Carter, S.P., Kempf, S.D., Young, D.A. & Holt, J.W. (2007) Along-track focusing of airborne radar sounding data from West Antarctica for improving basal reflection analysis and layer detection. *IEEE Transactions on Geoscience and Remote Sensing,* 45 (9)**:** 2725-2736. Doi 10.1109/Tgrs.2007.897416.

Petropoulos, G. & Pandazaras, C. (2003) Evaluating the real profile length in turning of carbon steels. *Industrial Lubrication and Tribology,* 55 (3)**:** 128-136. Doi10.1108/00368790310470967.

Petropoulos, G., Vaxevanidis, N.M. & Pandazaras, C. (2004) Modelling of surface finish in electro-discharge machining based upon statistical multi-parameter analysis. *Journal of Materials Processing Technology,* 155-156**:** 1247-1251. Doi 10.1016/j.matprotec.2004.04.189.

Pettersson, U. & Jacobson, S. (2003) Influence of surface texture on boundary lubricated sliding contacts. *Tribology International,* 36 (11)**:** 857-864. Doi 10.1016/S0301-679x(03)00104-X.

Phillips, E., Everest, J. & Diaz-Doce, D. (2010) Bedrock controls on subglacial landform distribution and geomorphological processes: evidence from the Late Devensian Irish Sea Ice Stream. *Sedimentary Geology*, 232 (3-4): 98-118.

Piotrowski, J.A. & Tulaczyk, S. (1999) Subglacial conditions under the last ice sheet in northwest Germany: ice-bed separation and enhanced basal sliding? *Quaternary Science Reviews,* 18 (6)**:** 737-751.

Plewes, L.A. & Hubbard, B. (2001) A review of the use of radio-echo sounding in glaciology. *Progress in Physical Geography,* 25 (2)**:** 203-236.

Pohl, M. & Stella, J. (2002) Quantitative CLSM roughness study on early cavitation-erosion damage. *Wear,* 252**:** 501-511.

Popov, V.L. & Dudko, O.K. (2004) Tribospectroscopy of surfaces with statistically random roughness. *Technical Research Letters,* 30 (2)**:** 148-150.

Press, W.H., Teukolsky, S.A., Vetterling, W.T. & Flannery, B.P. (2007). *Numerical recipes: The art of scientific computing,* Cambridge, Cambridge University Press.

Price, S.F. & Whillans, I.M. (2001) Crevasse patterns at the onset to Ice Stream B, West Antarctica. *Journal of Glaciology,* 47 (156)**:** 29-36.

Racoviteanu, A.E., Manley, W.F., Arnaud, Y. & Williams, M.W. (2007) Evaluating digital elevation models for glaciologic applications: An example from Nevado Coropuna, Peruvian Andes. *Global and Planetary Change,* 59 (1-4)**:** 110-125. Doi 10.1016/j.gloplacha.2006.11.036.

Rae, A.C., Harrison, S., Mighall, T. & Dawson, A.G. (2004) Periglacial trimlines and nunataks of the Last Glacial Maximum: the Gap of Dunloe, southwest Ireland. *Journal of Quaternary Science,* 19 (1)**:** 87-97.

Raja, J., Muralikrishnan, B. & Fu, S. (2002) Recent advances in separation of roughness, waviness and form. *Journal of the International Societies for Precision Engineering and Nanotechnology,* 26**:** 222-235.

Ramalu, M. (1999) Characterization of surface quality in machining of composites. *In:* Jahanmir, S., Ramulu, M. & Koshy, P. (eds.) *Machining of ceramics and composites*. Marcel Dekkerr, New York.

Ramasawmy, H. & Blunt, L. (2002) 3D surface topography assessment of the effect of different electrolytes during electrochemical polishing of EDM surfaces. *International Journal of Machine Tools & Manufacture,* 42**:** 567-574.

Rattas, M. & Piotrowski, J.A. (2003) Influence of bedrock permeability and till grain size on the formation of the Saadjarve drumlin field, Estonia, under an east-Baltic Weichselian ice stream. *Boreas,* 32 (1)**:** 167-177. Doi 10.1080/03009480310001849.

Raymond, C.F., Catania, G.A., Nereson, N. & Van der Veen, C.J. (2006) Bed radar reflectivity across the north margin of Whillans Ice Stream, West Antarctica, and implications for margin processes. *Journal of Glaciology,* 52 (176)**:** 3-10.

Rea, B.R., Evans, D.J.A., Dixon, T.S. & Whalley, W.B. (2000) Contemporaneous, localized, basal ice-flow variations: implications for bedrock erosion and the origin of p-forms. *Journal of Glaciology,* 46 (154)**:** 470-476.

Rémy, F.D., Shaeffer, P. & Legrésy, B. (1999) Ice flow physical processes derived from the ERS-1 high-resolution map of the Antarctica and Greenland ice sheets. *Geophysical Journal International,* 139 (3)**:** 645-656.

Retzlaff, R. & Bentley, C.R. (1993) Timing of stagnation of Ice Stream C, West Antarctica, from short-pulse radar studies of buried surface crevasses. *Journal of Glaciology,* 39 (133)**:** 553-561.

Rignot, E. (2001) Evidence for rapid retreat and mass loss of Thwaites Glacier, West Antarctica. *Journal of Glaciology*, 47(157): 213-222.

Rignot, E., Vaughan, D.G., Schmeltz, M., Dupont, T. & MacAyeal, D. (2002) Acceleration of Pine Island and Thwaites Glaciers, West Antarctica. *Annals of Glaciology*, 34 (1): 189-194.

Rignot, E. & Kanagaratnam, P. (2006) Changes in the velocity structure of the Greenland ice sheet. *Science,* 311 (5763)**:** 986-990. Doi 10.1126/science.1121381

Rignot, E. & Thomas, R.H. (2002) Mass balance of polar ice sheets. *Science,* 297 (5586)**:** 1502-1506.

Ripă, M., Tomescu, L., Hapenciuc, M. & Crudu, I. 2003. Tribological characterisation of surface topography using Abbott-Firestone curve. *National Tribology Conference, 24-26 September 2003.* The Annals of University "Dunărea de Jos" of Galati Fascicle VIII, tribology.

Rippin, D.M., Bamber, J.L., Siegert, M.J., Vaughan, D.G. & Corr, H.F.C. (2003) Basal topography and ice flow in the Bailey/Slessor region of East Antarctica. *Journal of Geophysical Research,* 108 (F1). Doi 10.1029/2003JF000039.

Rippin, D.M., Bamber, J.L., Siegert, M.J., Vaughan, D.G. & Corr, H.F.J. (2004) The role of ice thickness and bed properties on the dynamics of the enhanced-flow tributaries of Bailey Ice Stream and Slessor Glacier, East Antarctica. *Annals of Glaciology,* 39**:** 366-372.

Rippin, D.M., Bamber, J.L., Siegert, M.J., Vaughan, D.G. & Corr, H.F.J. (2006) Basal conditions beneath enhanced-flow tributaries of Slessor Glacier, East Antarctica. *Journal of Glaciology,* 52 (179)**:** 481-490.

Rippin, D.M., Vaughan, D.G., & Corr, H.F.J. (2011) The basal roughness of Pine Island Glacier, West Antactica. *Journal of Glaciology*, 57 (201): 67-76. Doi 10.3189/002214311795306574.

Robbe-Valloire, F. (2001) Statistical analysis of asperities on a rough surface. *Wear,* 249 (5-6)**:** 401-408.

Roberts, D.H. & Long, A.J. (2005) Streamlined bedrock terrain and fast ice flow, Jakobshavns Isbræ, West Greenland: implications for ice stream and ice sheet dynamics. *Boreas,* 34 (1)**:** 25-42. Doi 10.1080/03009480510012818.

Roberts, D.H., Long, A.J., Davies, B.J., Simpson, M.J. & Schnabel, C. (2009) Ice stream influence on West Greenland Ice Sheet dynamics during the Last Glacial Maximum. *Journal of Quaternary Science* 25: 850-864.

Robin, G.D.Q. (1969) Long-range radio echo flights over the Antarctic Ice Sheet. *The Geographical Journal,* 135 (4)**:** 557-559.

Robin, G.D.Q., Evans, S. & Bailey, J.T. (1969) Interpretation of radio echo sounding in polar ice sheets. *Philosophical Transactions of the Royal Society of London Series A, Mathematical and Physical Sciences,* 265 (1166)**:** 437-504.

Robin, G.D.Q., Swithinbank, C.W.M. & Smith, B.M.E. (1970). Radio echo exploration of the Antarctic Ice Sheet. *In:* International Symposium on Antarctic Glaciological Exploration, Hanover, New Hampshire 3-7 September 1968. International Association of Scientific Hydrology, 86: 97-115.

Rose, J. 1987. Drumlins as part of a glacier bedform continuum. *In:* Menzies, J. & Rose, J. (eds.) *Drumlin Symposium : proceedings of the Drumlin Symposium, first international conference on geomorphology, Manchester, 16-18 September 1985.* Rotterdam: Balkema.

Rose, K.E. (1979) Characteristics of ice flow in Marie Byrd Land, Antarctica. *Journal of Glaciology,* 24 (90)**:** 63-75.
Rudzit, Y.A. (1975) Accuracy of surface roughness parameter determinations. *Translated from Izmeritel'naya Teknika,* 1**:** 38-40.
Sacerdotti, F., Griffiths, B.J., Butler, C. & Benati, F. (2000) Surface topography in autobody manufacture - the state of the art. *Proceedings of the Institution of Mechanical Engineers Part B-Journal of Engineering Manufacture,* 214 (9)**:** 811-820.
Sakimoto, S.E.H., Frey, H.V., Garvin, J.B. & Roark, J.H. (1999) Topography, roughness, layering, and slope properties of the Medusae Fossae Formation from Mars Orbiter Laser Altimeter (MOLA) and Mars Orbiter Camera (MOC) data. *Journal of Geophysical Research-Planets,* 104 (E10)**:** 24141-24154.
Sandhäger, H. & Blindow, N. (2000) Surface elevation, ice thickness, and subglacial-bedrock topography of Ekstrom Ice Shelf (Antarctica) and its catchment area. *Annals of Glaciology,* 30**:** 61-68.
Schoof, C. (2002) Basal perturbations under ice streams: form drag and surface expression. *Journal of Glaciology,* 48 (162)**:** 407-416.
Schoof, C. (2003) The effect of basal topography on ice sheet dynamics. *Continuum Mechanics and Thermodynamics,* 15 (3)**:** 295-307. Doi 10.1007/s00161-003-0119-3.
Schoof, C. (2004a) Bed topography and surges in ice streams. *Geophysical Research Letters,* 31 (6). L06401 Doi 10.1029/2003gl018807.
Schoof, C. (2004b) On the mechanics of ice-stream shear margins. *Journal of Glaciology,* 50 (169)**:** 208-218.
Schoof, C. (2005) The effect of cavitation on glacier sliding. *Proceedings of the Royal Society A, Mathematical, Physical and Engineering Sciences,* 461 (2055)**:** 609-627. Doi 10.1098/rspa.2004.1350.
Schoof, C. (2006a) A variational approach to ice stream flow. *Journal of Fluid Mechanics,* 556**:** 227-251. Doi 10.1017/S0022112006009591.
Schoof, C. (2006b) Variational methods for glacier flow over plastic till. *Journal of Fluid Mechanics,* 555**:** 299-320. Doi 10.1017/S002211200609104.
Schoof, C. (2007) Pressure-dependent viscosity and interfacial instability in coupled ice-sediment flow. *Journal of Fluid Mechanics,* 570**:** 227-252. Doi 10.1017/S0022112006002874.
Schoof, C.G. & Clarke, G.K.C. (2008) A model for spiral flows in basal ice and the formation of subglacial flutes based on a Reiner-Rivlin rheology for glacial ice. *Journal of Geophysical Research-Solid Earth,* 113 (B5). B05204 Doi 10.1029/2007jb004957.
Sedlaček, M., Podgornik, B. & Vižintin, J. (2009) Influence of surface preparation on roughness parameters, friction and wear. *Wear,* 266 (3-4)**:** 482-487. Doi 10.1016/j.wear.2008.04.017.
Shabtaie, S. & Bentley, C.R. (1987) West Antarctic ice streams draining into the Ross Ice Shelf - configuration and mass balance. *Journal of Geophysical Research-Solid Earth and Planets,* 92 (B2)**:** 1311-1336.
Shabtaie, S., Whillans, I.M., Bentley, C.R. (1987) The morphology of Ice Streams A, B and C, West Antarctica, and their environs. *Journal of Geophysical Research*, 92: 8865-8883.
Shahgedanova, M., Popovnin, V., Aleynikov, A., Petrakov, D. & Stokes, C.R. (2007) Long-term change, interannual and intra-seasonal variability in climate and glacier mass balance in the central Greater Caucasus, Russia. *Journal of Glaciology,* 46**:** 355-361.
Shaw, R. 2007. An examination of novel roughness parameters to be used in conjunction with the HSE slips assessment tool (SAT). Health and Safety Executive, RR549.
Shepard, M.K., Campbell, B.A., Bulmer, M.H., Farr, T.G., Gaddis, L.R. & Plaut, J.J. (2001) The roughness of natural terrain: A planetary and remote sensing perspective. *Journal of Geophysical Research-Planets,* 106 (E12)**:** 32777-32795.

Shepherd, T., Bamber, J.L. & Ferraccioli, F. (2006) Subglacial geology in Coats Land, East Antarctica, revealed by airborne magnetics and radar sounding. *Earth and Planetary Science Letters,* 244 (1-2)**:** 323-335. Doi 10.1016/j.epsl.2006.01.068.
Shum, C.K., Ries, J.C. & Tapley, B.D. (1995) The accuracy and applications of satellite altimetry. *Geophysical Journal International,* 121 (2)**:** 321-336.
Siegert, M.J. (1999) On the origin, nature and uses of Antarctic ice-sheet radio-echo layering. *Progress in Physical Geography,* 23 (2)**:** 159-179. Doi 10.1177/030913339902300201.
Siegert, M.J. (2000) Antarctic subglacial lakes. *Earth-Science Reviews,* 50 (1-2)**:** 29-50.
Siegert, M.J. (2008) Antarctic subglacial topography and ice-sheet evolution. *Earth Surface Processes and Landforms,* 33 (4)**:** 646-660. Doi 10.1002/Esp.1670.
Siegert, M.J. & Dowdeswell, J.A. (1996) Spatial variations in heat at the base of the Antarctic ice sheet from analysis of the thermal regime bove subglacial lakes. *Journal of Glaciology*, 42 (142): 501-509.
Siegert, M.J., Dowdeswell, J.A., Gorman, M.R. & Mcintyre, N.F. (1996) An inventory of Antarctic sub-glacial lakes. *Antarctic Science,* 8 (3)**:** 281-286.
Siegert, M.J., Ellis-Evans, J.C., Tranter, M., Mayer, C., Petit, J.R., Salamatin, A. & Priscu, J.C. (2001) Physical, chemical and biological processes in Lake Vostok and other Antarctic subglacial lakes. *Nature,* 414 (6864)**:** 603-609.
Siegert, M.J. & Kwok, R. (2000) Ice-sheet radar layering and the development of preferred crystal orientation fabrics between Lake Vostok and Ridge B, central East Antarctica. *Earth and Planetary Science Letters,* 179 (2)**:** 227-235.
Siegert, M.J., Kwok, R., Mayer, C. & Hubbard, B. (2000) Water exchange between the subglacial Lake Vostok and the overlying ice sheet. *Nature,* 403 (6770)**:** 643-646.
Siegert, M.J. & Leysinger Vieli, G.J.-MC. (2007) Lake glacial history of the Ross Sea Sector of the West Antarctic Ice Sheet: evidence from englacial layering at Talos Dome, East Antarctica. *Journal of Environmental and Engineering Geophysics* 12: 63-67. Doi 10.2113/JEEG12.1.63.
Siegert, M.J., Payne, A.J. & Joughin, I. (2003) Spatial stability of Ice Stream D and its tributaries, West Antarctica, revealed by radio-echo sounding and interferometry. *Annals of Glaciology,* 37**:** 377-382.
Siegert, M.J., Pokar, M., Dowdeswell, J.A. & Benham, T. (2005a) Radio-echo layering in West Antarctica: a spreadsheet dataset. *Earth Surface Processes and Landforms,* 30 (12)**:** 1583-1591. Doi 10.1002/Esp.1238.
Siegert, M.J. & Ridley, J.K. (1998) Determining basal ice-sheet conditions in the Dome C region of East Antarctica using satellite radar altimetry and airborne radio-echo sounding. *Journal of Glaciology,* 44 (146)**:** 1-8.
Siegert, M.J., Taylor, J. & Payne, A.J. (2005b) Spectral roughness of subglacial topography and implications for former ice-sheet dynamics in East Antarctica. *Global and Planetary Change,* 45 (1-3)**:** 249-263. Doi 10.1016/j.gloplacha.2004.09.008.
Siegert, M.J., Taylor, J., Payne, A.J. & Hubbard, B. (2004) Macro-scale bed roughness of the Siple Coast ice streams in West Antarctica. *Earth Surface Processes and Landforms,* 29 (13)**:** 1591-1596. Doi 10.1002/Esp.1100.
Simpson, R.A. (1976) Surface-roughness estimation at three points on the lunar-surface using 23-cm monostatic radar. *Journal of Geophysical Research,* 81 (23)**:** 4407-4416.
Siska, P.P. & Hung, I.K. (2004). Advanced digital terrain analysis using roughness-dissectivity parameters in GIS. *In:* Proceedings of the 2004 ESRI international user conference, 2004 San Diego, California. ESRI Press.
Small, D., Holecz, F., Meier, E., Nüesch, D. & Barmettler, A. (1997). Geometric and radiometric calibration of RADARSAT images. *In:* Proceedings of Geomatics in the era of RADARSAT, 1997 Ottawa, Canada. p.24-30.
Smith, A.M. (2007) Subglacial bed properties from normal-incidence seismic reflection data*. Journal of Environmental and Engineering Geophysics,* 12: 3-13. Doi 10.2113/JEEG12.1.3.

Smith, M.J. & Clark, C.D. (2005) Methods for the visualization of digital elevation models for landform mapping. *Earth Surface Processes and Landforms,* 30**:** 885-900.
Smith, M.J., Dunlop, P. & Clark, C.D. 2006a. An overview of subglacial bedforms in Ireland, mapped from digital elevation data. *In:* Knight, P. (ed.) *Glacier science and environmental change.* Oxford: Blackwell.
Smith, M.J., Rose, J. & Booth, S. (2006b) Geomorphological mapping of glacial landforms from remotely sensed data: An evaluation of the principal data sources and an assessment of their quality. *Geomorphology,* 76 (1-2)**:** 148-165. Doi 10.1016/j.geomorph.2005.11.001.
Smith, M.L. (1999) The analysis of surface texture using photometric stereo acquisition and gradient space domain mapping. *Image and Vision Computing,* 17 (14)**:** 1009-1019.
Smith, M.W., Cox, N.J. & Bracken, L.J. (2007) Applying flow resistance equations to overland flows. *Progress in Physical Geography,* 31 (4)**:** 363-387. Doi 10.1177/0309133307081289.
Smith, S.L., Elfick, A.P.D. & Unsworth, A. (1999) An evaluation of the tribological performance of zirconia and CoCrMo femoral heads. *Journal of Materials Science,* 34**:** 5159-5162.
Spagnolo, M., Clark, C.D. & Hughes, A.L.C. (2012) Drumlin relief. *Geomorphology*, 153-154: 179-191. Doi 10.1016/j.geomorph.2012.02.023.
Spragg, R.C. & Whitehouse, D.J. (1970) A new unified approach to surface metrology. *Proceedings of the Institute of Mechanical Engineers,* 185**:** 697-707.
Staines, K.E.H. (2009) *The glacial geomorphology of the tweed valley and surrounding area, eastern British Isles*. Masters thesis, Durham University. Available at Durham E-Theses Online: http://etheses.dur.ac.uk/2032/
Steichen, T.J. & Cox, N.J. (1998) Concordance correlation coefficient. *Stata Technical Bulletin*, 43: 35-39.
Steichen, T.J. & Cox, N.J. (2002) A note on the concordance correlation coefficient. *The Stata Journal*, 2 (2)**:** 183-189.
Steinhage, D., Nixdorf, U., Meyer, U. & Miller, H. (1999) New maps of the ice thickness and subglacial topography in Dronning Maud Land, Antarctica, determined by means of airborne radio-echo sounding. *Annals of Glaciology,* 29**:** 267-272.
Steinhage, D., Nixdorf, U., Meyer, U. & Miller, H. (2001) Subglacial topography and internal structure of central and western Dronning Maud Land, Antarctica, determined from airborne radio echo sounding. *Journal of Applied Geophysics,* 47 (3-4)**:** 183-189.
Stephenson, S.N. & Bindschadler, R.A. (1988) Observed velocity fluctuations on a major Antarctic ice stream. *Nature,* 334 (6184)**:** 695-697.
Stewart, H., Bradwell, T. & Stoker, M. (2011) *Ice streaming and ice-sheet re-advances in SE Scotland and NE England: new evidence from multibeam echosounder data*. British Geological Survey (Unpublished exhibition poster). URI: http://nora.nerc.ac.uk/id/eprint/16440.
Stokes, C.R. & Clark, C.D. (1999) Geomorphological criteria for identifying Pleistocene ice streams. *Annals of Glaciology,* 28**:** 67-74.
Stokes, C.R. (2001) *The geomorphology of palaeo-ice streams: indentification, characterisation and implications for ice stream functioning.* Unpublished PhD Thesis, Department of Geography, University of Sheffield.
Stokes, C.R. & Clark, C.D. (2001) Palaeo-ice streams. *Quaternary Science Reviews,* 20 (13)**:** 1437-1457.
Stokes, C.R. & Clark, C.D. (2002) Are long subglacial bedforms indicative of fast ice flow? *Boreas,* 31 (3)**:** 239-249.
Stokes, C.R. & Clark, C.D. (2003a) The Dubawnt Lake palaeo-ice stream: evidence for dynamic ice sheet behaviour on the Canadian Shield and insights regarding the controls on ice-stream location and vigour. *Boreas,* 32 (1)**:** 263-279. Doi 10.1080/03009480310001155.
Stokes, C.R. & Clark, C.D. (2003b) Laurentide ice streaming on the Canadian Shield: A conflict with the soft-bedded ice stream paradigm? *Geology,* 31 (4)**:** 347-350.

Stokes, C.R. & Clark, C.D. (2006). What can the 'footprint' of a palaeo-ice stream tell us? Interpreting the bed of the Dubawnt Lake Ice Stream, Northern Keewatin, Canada. *In:* Knight, P.G. (ed.) *Glacier science and environmental change.* Oxford: Blackwell.

Stokes, C.R., Clark, C.D., Lian, O.B. & Tulaczyk, S. (2007) Ice stream sticky spots: A review of their identification and influence beneath contemporary and palaeo-ice streams. *Earth-Science Reviews,* 81 (3-4)**:** 217-249. Doi 10.1016/j.earscirev.2007.01.002.

Stokes, C.R., Clark, C.D., Lian, O.B. & Tulaczyk, S. (2006a) Geomorphological map of ribbed moraines on the Dubawnt Lake palaeo-ice stream bed: a signature of ice stream shut-down? *Journal of Maps*, v2006 1-9.

Stokes, C.R., Clark, C.D. & Winsborrow, M.C.M. (2006b) Subglacial bedform evidence for a major palaeo-ice stream and its retreat phases in Amundsen Gulf, Canadian Arctic Archipelago. *Journal of Quaternary Science* 21(4): 399-412. Doi 10.1002/jqs.991.

Stokes, C.R., Lian, O.B., Tulaczyk, S. & Clark, C.D. (2008) Superimposition of ribbed moraines on a palaeo-ice-stream bed: implications for ice stream dynamics and shutdown. *Earth Surface Processes and Landforms*, 33: 593-609. Doi 10.1002/esp.1671.

Storrar, R. & Stokes, C.R. (2007) A glacial geomorphological map of Victoria Island, Canadian Arctic. *Journal of Maps*, v2007: 191-210.

Stoudt, M.R. & Hubbard, J.B. (2009) Fundamental relationships between deformation-induced surface roughness, critical strain localisation and failure in AA5754-O. *Philosophical Magazine,* 89 (27)**:** 2403-2425.

Stover, J.C. (1995). *Optical scattering: measurement and analysis,* Washington, SPIE - The International Society for Optical Engineering.

Suh, A.Y. & Polycarpou, A.A. (2003) Effect of molecularly thin lubricant on roughness and adhesion of magnetic disks intended for extremely high-density recording. *Tribology Letters,* 15 (4)**:** 365-376.

Suh, A.Y., Polycarpou, A.A. & Conry, T.F. (2003) Detailed surface roughness characterization of engineering surfaces undergoing tribological testing leading to scuffing. *Wear,* 255**:** 556-568. Doi 10.1016/S0043-1648(03)00224-2.

Sul, Y.-T., Byron, E.-S.E.-S. & Jeong, Y.Y. (2004) Biomechanical measurements of calcium-incorporated oxidized implants in rabbin bone: effect of calcium surface chemistry of a novel implant. *Clinical implant dentistry and related research,* 6 (2)**:** 101-110.

Sul, Y.-T., Johansson, C., Byon, E. & Albrektsson, T. (2005) The bone response of oxidized bioactive and non-bioactive titanium implants. *Biomaterials,* 26**:** 6720-6730. Doi 10.1016/j.biomaterials.2005.04.058.

Swithinbank, C.W.M. (1954) Ice streams. *Polar Record*, 7: 185-186.

Swithinbank, C.W.M. (1969) Airborne radio echo sounding by the British Antarctic Survey. *The Geographical Journal,* 135 (4)**:** 551-553.

Swithinbank, C.W.M. (1983) Towards an inventory of the great ice sheets. *Geografiska Annaler Series A, Physical Geography,* 65 (3/4)**:** 289-294.

Tarasov, L. & Peltier, W.R. (2004) A geophysically constrained large ensemble analysis of the deglacial history of the North American ice-sheet complex. *Quaternary Science Reviews,* 23 (3-4)**:** 359-388. Doi 10.1016/j.quascirev.2003.08.004.

Taylor, J., Siegert, M.J., Payne, A.J. & Hubbard, B. (2004) Regional-scale bed roughness beneath ice masses: measurement and analysis. *Computers & Geosciences,* 30 (8)**:** 899-908. Doi 10.1016/j.cageo.2004.06.007.

Theakstone, W.H. & Jacobsen, F.M. (1997) Digital terrain modelling of the surface and bed topography of the Glacier Austre Okstindbreen, Okstindan, Norway. *Geografiska Annaler Series A, Physical Geography,* 79 (4)**:** 201-214.

Thomas, R.H. (1979) The dynamics of marine ice sheets. *Journal of Glaciology*, 24: 167-177.

Thomas, T.R. (1981) Characterization of surface roughness. *Journal of the American Society for Precision Engineering,* 3 (2)**:** 97-104.

Thomas, T.R., Rosen, B.G. & Amini, N. (1999) Fractal characterisation of the anisotropy of rough surfaces. *Wear,* 232 (1)**:** 41-50.
Thompson, W.R. & Squyres, S.W. (1990) Titan and other icy satellites: dielectric properties of constituent materials and implications for radar sounding. *Icarus,* 86**:** 336-354.
Thorsteinsson, T., Raymond, C.F., Gudmundsson, G.H., Bindschadler, R.A., Vornberger, P. & Joughin, I. (2003) Bed topography and lubrication inferred from surface measurements on fast-flowing ice streams. *Journal of Glaciology,* 49 (167)**:** 481-490.
Tillard, S. & Dubois, J.C. (1995) Analysis of GPR data-wave-propagation velocity determination. *Journal of Applied Geophysics,* 33 (1-3)**:** 77-91.
Tobacco, I.E., Bianchi, C., Chiappini, M., Passerini, A., Zirizzotti, A. & Zuccheretti, E. (1999) Latest improvements for the radio echo sounding system of the Italian radar glaciological group and measurements in Antarctica. *Annali Di Geofisica,* 42 (2)**:** 271-276.
Ulmeanu, M., Serghei, A., Mihailescu, I.N., Budau, P. & Enachescu, M. (2000) C-Ni amorphous multilayers studied by atomic force microscopy. *Applied Surface Science,* 165**:** 109-115.
Urbini, S., Vittuari, L. & Gandolfi, S. (2001) GPR and GPS data integration: examples of application in Antarctica. *Annali Di Geofisica,* 44 (4)**:** 687-702.
Van der Veen, C.J. (1999) *Fundamentals of Glacier Dynamics*. Balkema, Rotterdam.
Van der Veen, C.J., Ahn, Y., Csatho, B.M., Mosley-Thompson, E. & Krabill, W.B. (2009) Surface roughness over the northern half of the Greenland Ice Sheet from airborne laser altimetry. *Journal of Geophysical Research-Earth Surface,* 114. F01001 Doi 10.1029/2008jf001067.
Van der Veen, C.J., Krabill, W.B., Csatho, B.M. & Bolzan, J.F. (1998) Surface roughness on the Greenland ice sheet from airborne laser altimetry. *Geophysical Research Letters,* 25 (20)**:** 3887-3890.
Vaughan, D.G. (2005) How does the Antarctic ice sheet affect sea level rise? *Science,* 308. Doi 10.1126/science.1113708.
Vaughan, D.G. (2006) The Antarctic Ice Sheet. *In:* Knight, P.G. (ed.) *Glacier science and environmental change.* Oxford: Blackwell.
Vaughan, D.G., Corr, H.F.J., Doake, C.S.M. & Waddington, E.D. (1999) Distortion of isochronous layers in ice revealed by ground-penetrating radar. *Nature,* 398 (6725)**:** 323-326.
Vermeulen, M., Scheers, J., Demare, C. & Decooman, B. (1995) 3D-characterization of EBT-steel sheet surfaces. *International Journal of Machine Tools & Manufacture,* 35 (2)**:** 273-280.
Wager, A.C. (1982) Mapping the depth of a valley glacier by radio echo sounding. *British Antarctic Survey Bulletin,* 51**:** 111-123.
Walford, M.E.R. & Harper, M.F.L. (1981) The detailed study of glacier beds using radio-echo techniques. *Geophysical Journal of the Royal Astronomical Society,* 67 (2)**:** 487-514.
Weber, J.R. & Andrieux, P. (1970) Radar soundings on the Penny Ice Cap, Baffin Island. *Journal Of Glaciology,* 9 (55)**:** 49-54.
Webster, R. & Oliver, M.A. (2000) *Geostatistics for environmental scientists,* New York, John Wiley & Sons.
Weertman, J. (1962) Catastrophic glacier advances. IASH Publication. 58 (Symposium at Obergurgl 1962 - *Variations in the regime of existing glaciers*), 31-39.
Welch, B.C. & Jacobel, R.W. (2003) Analysis of deep-penetrating radar surveys of West Antarctica, US-ITASE 2001. *Geophysical Research Letters,* 30 (8). 1444 Doi 10.1029/2003gl017210.
Wennerberg, A., Hallgren, C., Johansson, C. & Danelli, S. (1998) A histomorphometric evaluation of screw-shaped implants each prepared with two surface roughnesses. *Clinical Oral Implants Research,* 9 (1)**:** 11-19.
Weisberg, S. (2005) *Applied linear regression*. Wiley, New Jersey.

Whillans, I.M. (1976) Radio-echo layers and recent stability of West Antarctic Ice Sheet. *Nature,* 264 (5582)**:** 152-155.
Whillans, I.M., Bentley, C.R. & van der Veen, C.J. (2001) Ice streams B and C. IN: Alley, R.D., Bindschadler, R. (Eds.) *The West Antarctic Ice Sheet: behaviour and environment*. Antarctic Research Series, 77: 257-281. American Geophysical Union, Washington.
Whitehouse, D.J. (1974) The measurement and analysis of surfaces. *Tribology International,* 7**:** 249-259.
Whitehouse, D.J. (1994). *Handbook of Surface Metrology,* Bristol, Institute of Physics Publishing Ltd.
Whitehouse, D.J. (2009) A new look at surface metrology. *Wear,* 266**:** 560-565. Doi 10.1016/j.wear.2008.04.058.
Wilhelms, F. (2005) Explaining the dielectric properties of firn as a density-and-conductivity mixed permittivity (DECOMP). *Geophysical Research Letters,* 32 (16). L16501 Doi 10.1029/2005gl022808.
Williams, J. (2005) *Engineering Tribology*. Cambridge University Press, Cambridge.
Winebrenner, D.P., Smith, B.E., Catania, G.A., Conway, H.B. & Raymond, C.F. (2003) Radio-frequency attenuation beneath Siple Dome, West Antarctica, from wide-angle and profiling radar observations. *Annals of Glaciology,* 37**:** 226-232.
Winsborrow, M.C.M. (2007). *Exploring controls on the location of Laurentide palaeo-ice streams.* PhD, Department of Geography, The University of Sheffield [PhD thesis].
Winsborrow, M.C.M., Clark, C.D. & Stokes, C.R. (2010) What controls the location of ice streams? *Earth-Science Reviews*, 103: 45-49 Doi 10.1016/j.earthscirev.2010.07.003.
Wolski, M., Podsiadlo, P. & Stachowiak, G.W. (2010) Applications of the variance orientation transform method to the multiscale characterization of surface roughness and anisotropy. *Tribology International*, 43 (11): 2203-2215. Doi 10.1016/j.triboint.2010.07.006.
Woodward, J. & Burke, M.J. (2007) Applications of ground-penetrating radar to glacial and frozen materials. *Journal of Environmental and Engineering Geophysics,* 12 (1)**:** 69-85.
Xiao, L., Rosen, B.G. & Amini, N. (2004) Surface lay effect on rough friction in roller contact. *Wear,* 257 (12)**:** 1301-1307. Doi 10.1016/j.wear.2003.09.006.
Yang, K. & Jeang, A. (1994) Statistical surface roughness checking procedure based on a cutting tool wear model. *Journal of Manufacturing Systems,* 13 (1)**:** 1-8.
Yoshida, I. & Tsukada, T. (2006) Uncertainty of wavelength limitation due to stylus tip radius for engineering surface texture based on wavelength and amplitude by FFT. *Wear*, 261: 1225-1231.
Young, D.A., Blankenship, D.D. & Holt, J.W. (2007). Subglacial roughness of the West Antarctic Ice Sheet, in Antarctica: a keystone in a changing world. *In:* Cooper, A.K. & Raymond, C.R., eds. 10th International Symposium on Antarctic Earth Sciences, 2007 University of California. U.S. Geological Survey and the National Academies, 1-4.
Young, D.A., Kempf, S.D., Blankenship, D.D., Holt, J.W. & Morse, D.L. (2008) New airborne laser altimetry over the Thwaites Glacier catchment, West Antarctica. *Geochemistry Geophysics Geosystems,* 9. Q06006 Doi 10.1029/2007gc001935.
Zeng, W., Jiang, X. & Blunt, L. (2009) Surface characterisation-based tool wear monitoring in peripheral milling. *International Journal of Advanced Manufacturing Technology,* 40 (3-4)**:** 226-233. Doi 10.1007/s00170-007-1352-x.
Zheng, B. & Agresti, A. (2000) Summarizing the predictive power of a generalized linear model. *Statistics in Medicine*, 19: 1771-1781.
Zipin, R.B. (1990) Analysis of the R_k surface roughness parameter proposals. *Journal of the American Society for Precision Engineering,* 12 (2)**:** 106-108.
Zwally, H.J., Abdalati, W., Herring, T., Larson, K., Saba, J. & Steffen, K. (2002a) Surface melt-induced acceleration of Greenland ice-sheet flow. *Science,* 297 (5579)**:** 218-222.

Zwally, H.J., Giovinetto, M.B., Li, J., Cornejo, H.G., Beckley, M.A., Brenner, A.C., Saba, J.L. & Yi, D. (2005) Mass changes of the Greenland and Antarctic ice sheets and shelves and contribution to sea-level rise: 1992-2002. *Journal of Glaciology,* 51 (175)**:** 509-527.

Zwally, H.J. & Li, J. (2002) Seasonal and interannual variations of firn densification and ice-sheet surface elevation at the Greenland summit. *Journal of Glaciology*, 48 (161): 199-207.